DEVELOPMENT AND VALIDATION OF MATHEMATICAL MODELS OF THE HUMAN CARDIOVASCULAR SYSTEM

MAHA IBRAHEAM MAJEED AL-DAHAN

Thesis submitted for the
Degree of Doctor of Philosophy

The City University, London
Department of Systems Science

1984

TO

[redacted]

for his patience and
encouragement during
the preparation of
this thesis

My parents,

for providing the
necessary incentive
for this study

and to
my daughter, [redacted]
for being so patient.

CONTENTS

ACKNOWLEDGEMENTS

I gratefully acknowledge and express my sincere gratitude to my principal supervisor, Dr. E. R. Carson, Director of Research Centre for Measurement and Information in Medicine, for his excellent supervision, support and understanding.

I am very grateful to Professor L. Finkelstein, Dean of the School of Electrical Engineering and Applied Physics, for his invaluable guidance, helpful comments and support.

[redacted]

[redacted]

ABSTRACT

This thesis describes the development and validation of mathematical models of the human cardiovascular system suitable for the study of short-term haemodynamic effects.

The basis of the model development is a large-scale mathematical representation of the controlled circulatory system which is capable of investigating short-term dynamics resulting from the administration of drugs which have rapid effects upon the heart and blood vessels. This model comprised a 19th order representation of the uncontrolled circulatory dynamics, so that overall, with neural control and pharmacokinetic and local pharmacodynamic models added, it was of 61st order with 178 parameters. A comprehensive and systemic programme of validation has been undertaken upon these models. Principal features of this validation programme include: investigating the nature of the sources of data used in specifying model parameters and initial values of model variables, in particular identifying the magnitude of uncertainty associated with such data; performing a series of empirical tests, examining the ability of the model to reproduce the principal features of response observed in dynamic experimental data corresponding to a wide range of physiological and pharmacological investigation; and using the results of such validation tests to highlight areas of structural uncertainty in the model, specifically relating to the representation of neural control mechanisms.

Whilst such large-scale mathematical models have substantial heuristic potential, more compact representations are required if such models are to find potential clinical application. The associated problems of model reduction are therefore discussed.

The result of this model reduction process is a smaller model which includes an 8-segment representation of the uncontrolled circulatory dynamics. The development of this reduced form is fully described, as is the programme of model validation which parallels that performed upon the original large-scale model. Particular emphasis is placed on the role of this more compact model to test alternative hypotheses regarding the neural control of peripheral resistance.

The programme of work described in this thesis constitutes an exemplar of the role of validation and the processes by which it is implemented in the context of large-scale physiological systems.

CHAPTER 1

INTRODUCTION

Mathematical models are now widely used as important investigative tools in the analysis of complex problems in physiology and medicine. Such models can be used to serve a wide variety of purpose ranging from testing hypotheses regarding the nature and structure of physiological control systems to their use in predicting patient response to therapy and thus potentially constituting an important aid to clinical decision making.

The nature of the modelling process is becoming increasingly well understood and the importance of model validation within the overall process is becoming both more clearly defined and more widely appreciated. Nevertheless, there is still the need for further development, particularly with regard to the validation of complex, large-scale models of correspondingly complex physiological systems.

The cardiovascular system is one which exhibits a variety of forms of complexity, for instance in terms of its structural complexity as well as in terms of the number of control systems which are involved in the maintenance of normal circulatory function. Whilst this system has received a great deal of attention from many physiologists and clinicians as well as, increasingly, from control and biomedical engineers, there are still many aspects of its function which are not clearly understood.

In seeking to increase the knowledge-base regarding the cardiovascular system, mathematical models have a vital role to perform, particularly since they provide the means by which alternate hypotheses, for example regarding the neural control of heart rate, can be assessed in quantitative terms.

The work described in this thesis takes as its basis a large-scale mathematical model of the controlled circulatory system which was originally developed in order to investigate the short-term dynamics resulting from the administration of drugs which have rapid effects upon the heart and the blood vessels (Pullen, 1976). This model incorporated representations of circulatory dynamics, the neural control of circulatory variables/parameters together with pharmacokinetic and local pharmacodynamic models such that overall pharmacodynamic effects

could be investigated. Although some initial validation studies were carried out by Pullen, the nature of his research investigation was such that it did not set out to include a full and rigorous programme of model validation. It is this process of model validation, performed both upon the large-scale model initiated by Pullen as well as on a variety of developments and reductions of this model form, which is the core of the work to be described in the subsequent chapters.

1.1 AIMS

The aims of the work described in the earlier chapters of the thesis are directed towards carrying out a comprehensive and rigorous investigation of the validity of the model developed by Pullen. This model comprised a 19th order representation of the uncontrolled circulatory dynamics, so that overall, with neural control and pharmacokinetic and local pharmacodynamic models added, it was of 61st order with 178 parameters. Three specific aspects of this validation study were as follows:

(i) to investigate the nature of the sources of data used in specifying model parameters and initial values of model variables, in particular identifying the magnitude of uncertainty associated with such data;

(ii) to perform a series of empirical tests, examining the ability of the model to reproduce the principal features of response observed in dynamic experimental data corresponding to a wide range of physiological and pharmacological investigation; and

(iii) to use the results of such validation tests to highlight areas of structural uncertainty in the model, specifically relating to the representation of neural control mechanisms.

Following on from this the programme of work described sets out to examine the procedures by which complex models can be reduced in order to render them more tractable and capable of being simulated on smaller computers.

The final chapters are then aimed at examining the validity of a reduced model of the cardiovascular system which incorporates an 8th order representation of the uncontrolled circulatory dynamics. The specific aspects of this validation study are the same as that for the

full model with the addition of testing alternative hypotheses regarding the neural control of peripheral resistance.

1.2 ORGANISATION OF THE THESIS

Chapter 2 provides a description in systemic terms of aspects of cardiovascular physiology relevant to the models which are to be developed in subsequent chapters. The nature of the modelling process in relation to physiological systems is described and a critical review is presented of some earlier important models of the cardiovascular system.

In Chapter 3, a comprehensive description is given of the large-scale pulsatile mathematical model of the cardiovascular system developed originally by Pullen (1976). This model comprises a 19th order representation of the uncontrolled circulatory dynamics together with sub-models representing the neural control of circulatory variables and parameters and pharmacokinetics and local pharmacodynamic effects of vasoconstrictive and vasodilitative drugs.

Chapters 4 - 7 are concerned with the validation of this large-scale model. In Chapter 4 the general framework of model validity and model validation which is to be employed is outlined. Chapter 5 focusses on the nature of the information incorporated into the model, examining the validity of parameter values and initial conditions (steady state values) of the variables, highlighting the uncertainty associated with much anatomic and physiological measurement and the need for enhanced experimental design.

Chapter 6 describes the validation of the complete model, examining its responses to a range of dynamic tests including blood volume changes, orthostasis, the Valsalva manoeuvre and short-term drug effects.

In Chapter 7, a programme of sensitivity analysis performed upon the completed model is presented to complete the validation study of the 19-segment model.

Given the uncertainty associated with the full-model due to the limited availability of experimental data, approaches to model reduction are considered in order to render the model more tractable. This review of the model reduction process, together with proposals for obtaining a simpler realisation, is reported in Chapter 8.

Chapter 9 describes the development of such a reduced model, this form containing an 8-segment representation of the circulatory dynamics. To this are added simple realisations of the thermoregulatory and body fluid sub-systems, thereby increasing the model's potential to investigate the nature of circulatory-related effects. In this chapter modifications to the neural control model are described, including specifically the effects of volume receptors.

In Chapter 10, the validity of this reduced model is considered involving a programme which parallels that described in Chapters 6 and 7. Model responses are compared with empirical data on blood volume changes and a full programme of sensitivity analysis is described.

Overall conclusions from the research programme, together with recommendations for future work, are given in Chapter 11.

CHAPTER 2

A SYSTEMS APPROACH TO CARDIOVASCULAR PHYSIOLOGY

This chapter provides a systemic view of cardiovascular physiology revealing the complexity of the processes under investigation and their essentially control system nature.

Having presented an overall systems model of the cardiovascular system, the role of mathematical models in the analysis of complex physiological mechanisms is defined. The chapter concludes with a brief critical review of some of the more important models which have been developed as aids to the understanding of cardiovascular physiology.

2.1 A SYSTEMS VIEW OF CARDIOVASCULAR PHYSIOLOGY

The human heart and blood vessels are a complex closed-loop system which can be considered to be the transport system of the body. It distributes to the cells the oxygen and metabolic fuels which are involved in physico-chemical processing.

Cells produce an output of work, carbon dioxide, heat and secretions indispensable for life. In addition, cells excrete the unwanted end products of metabolism.

The body must maintain an appropriate balance between metabolic activity, and the rates of delivery and removal of the biochemical substances from the cells (Figures 2.1 - 2.3). The distribution of blood flow to different parts of the body is a function of the local demands, and these depend on the factors mentioned above.

From a systems point of view, the cardiovascular system is a regulatory system, whose main objective is the control of blood pressure and the flow of blood to act as a general transport system. The cardiovascular system may therefore be divided into two interacting subsystems:

(i) controlled subsystem

(ii) controlling subsystem.

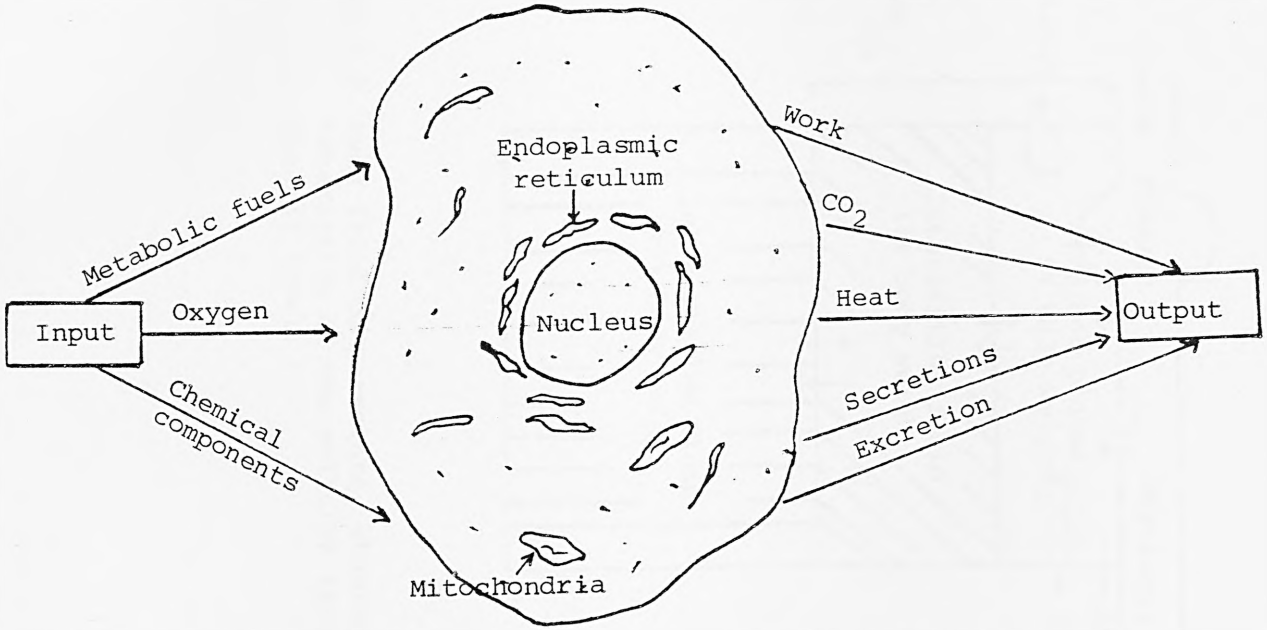

Figure 2.1 Logistics of metabolism

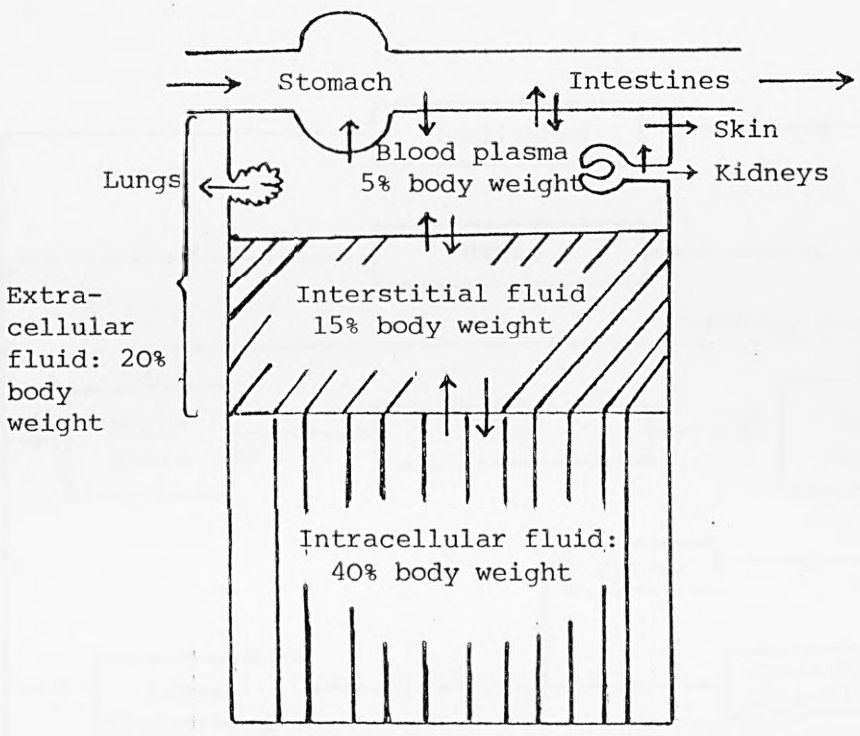

Figure 2.2 Body fluid compartments, showing the functional interaction of the cellular level with the haemodynamic level.

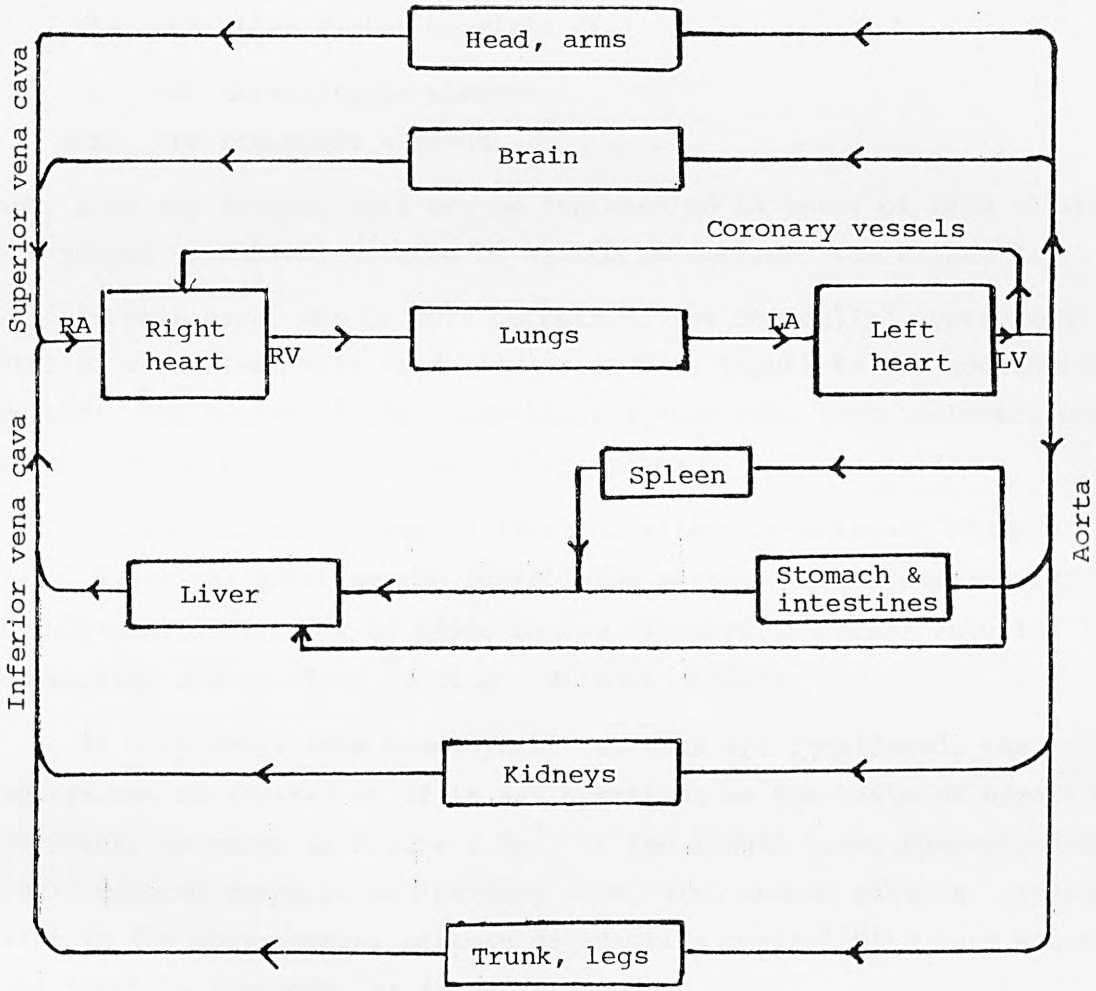

Figure 2.3 Scheme of the human circulation

The controlling system consists of the brain and neuro-endocrine systems. This is analogous to a computer which controls an industrial machine or plant (controlled system).

The controlling system consists of:

(i) neural section (vasomotor centres, medullary and cardiac)
(ii) hormonal section (endocrine glands) which operates on the heart and the blood vessels.

The controlled system consists of:

(i) the haemodynamic element
(ii) the transport element

and, like any system, this may be represented in terms of sets of input and output variables, related by system parameters (see Figure 2.4).

In this case, one or more outputs of the controlled system (controlled variables) will feed back to provide inputs to the controlling system. The output of the controlling system will then influence one or more properties of the controlled system.

In general, the system is affected either by external changes (e.g. exercise) entering the controlling system (termed command forcing by Milhorn (1966)), or by disturbances (internal changes) entering the controlled system (load forcing - Milhorn (1966)).

If only short-term haemodynamic effects are considered, the system can be treated as if it was operating on the basis of negative feedback, as shown in Figure 2.5a. In the longer term, however, hormonal control needs to be included along with neural effects, giving rise to the more complex picture of adaptive control with both negative and positive feedback, as shown in Figure 2.5b.

A more detailed systems view of cardiovascular physiology as it relates to short-term effects is given in Chapter 3.

2.2 MATHEMATICAL MODELLING IN BIOLOGY AND MEDICINE

The development of mathematical models provides a means of quantifying the behaviour and properties of complex processes such as occur in biology and medicine. As in other fields, mathematical models in biology and medicine are formulated on the basis of current knowledge about the system. This basis may be empirical, theoretical, or a

combination of empirical and theoretical knowledge. In general, as much theoretical, a priori knowledge should be incorporated in the formulation process as is consistent with the purpose of the model. Available theories (and data) reflect the stage of development of the particular area of research or application. As the field develops through increased availability of data, an increased theoretical basis for model formulation will normally result (Carson et al, 1983).

Mathematical models can be classified in accordance with the way in which they represent the system, that is into behavioural (or functional) models and structural (or physical) models.

Behavioural or functional models are models which simply represent behaviour (or function), relating input and output variables without any of the characteristics of the equations corresponding to any aspects of the system structure.

Structural models mirror, in the form of equations relating input and output, the structure of the system. There is a one-to-one correspondence between features of the system and features of the equation. The models may therefore be termed isomorphic.

Empirical models are behavioural only. Theoretical models may be isomorphic, but structural information may be lost in mathematical transformations or reductions of the model (Finkelstein and Carson, 1979; Carson et al, 1983).

Given the complex nature of biological systems, the types of mathematical model which have been employed to describe such processes cover the spectrum of approaches which are typically available to the control engineer - deterministic and stochastic models, linear and non-linear models, lumped and distributed models. Again, as to which should be applied in a particular situation must depend upon the particular physiological processes being examined and the level of scrutiny required.

The form and detail of a mathematical model and the processes by which it is derived are principally determined by the purposes for which it is desired. Classically, models can be categorised as being descriptive, predictive and explanatory. For complex processes such as the cardiovascular system, specific purposes for modelling could include:

(i) testing hypotheses regarding mechanisms by which cardiovascular variables are controlled

(ii) estimating inaccessible circulatory parameters

(iii) prediction of the behaviour of the cardiovascular system following drug administration or physiological stimulus.

A methodology appropriate for modelling complex physiological systems has been reported in a number of recent publications, including Carson et al (1983) and Leaning et al (1982a; b).
The basic outlining of this modelling approach is shown in Figure 2.6. The inter-related components are: modelling objectives or purposes, the laws, theory and data relevant to the model, model formulation, identification and model validation, the overall processing being essentially iterative in nature.

The three distinct components of model formulation are: conceptualisation; mathematical realisation; solution to give required relations between variables of interest. At any stage additional data may be required. In conceptualisation, assumptions of aggregation, abstraction and idealisation are necessary consistent with the model's purpose in order that it shall be tractable. Having produced an appropriate conceptual model, equations are then constructed either describing the overall relations contained within the functional model or providing a detailed description of the physico-chemical processes involved.

Within the model, the relevant variables are commonly connected through complex relations, e.g. differential equations. Model solution involves obtaining the required explicit relations between variables and/or parameters, often by computer implementation. In some cases model structure and parameter values may be known a priori. Often, however, there is uncertainty in the structure of the model and/or its parameters. In this situation, solution is not possible directly and identification of the model from input/output data must be carried out.

Model validation involves assessing the extent to which a model is well-founded, tractable and fulfils the purposes for which it is formulated. It is an integral component of the modelling process, being firmly embedded within all its stages rather than merely being an activity which is carried out once model identification has been completed. Model validation is treated in more detail in Chapter 5.

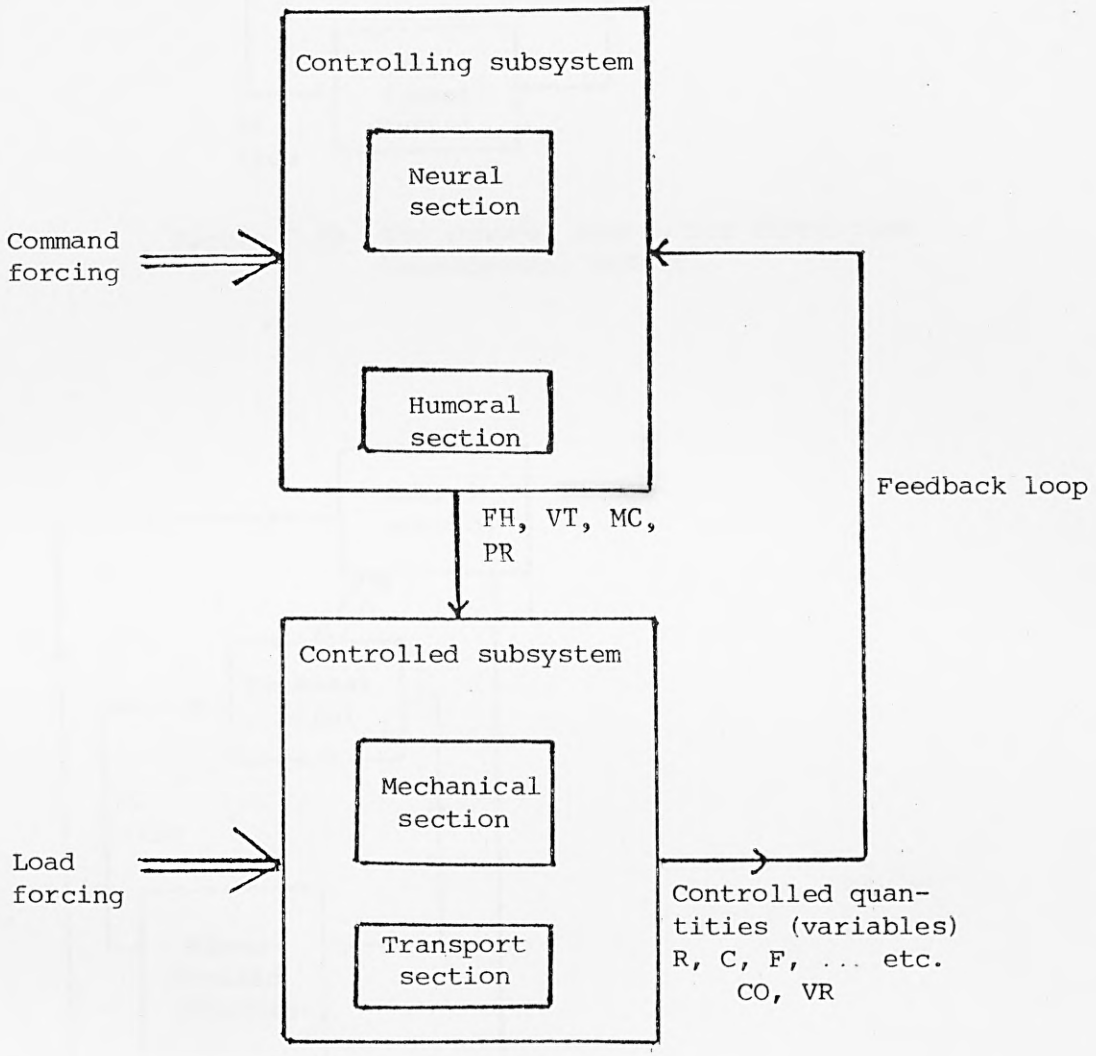

Figure 2.4 The cardiovascular system as a feedback control system

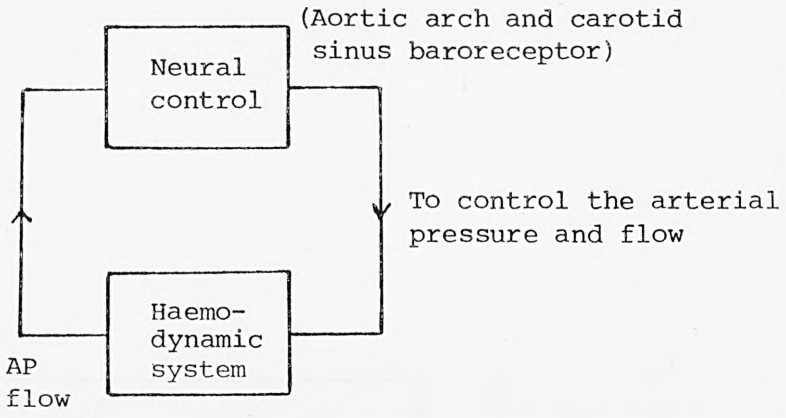

Figure 2.5a The control system for short-term haemodynamic effect.

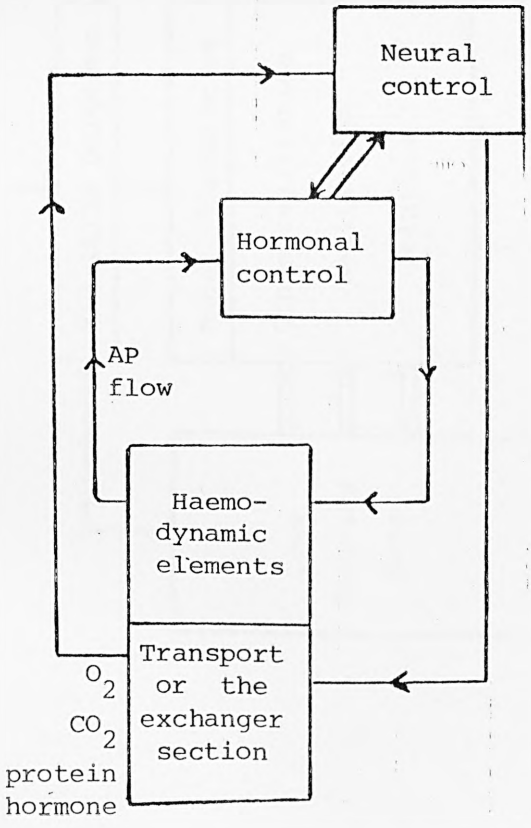

Figure 2.5b The adaptive control for long-term haemodynamic effects.

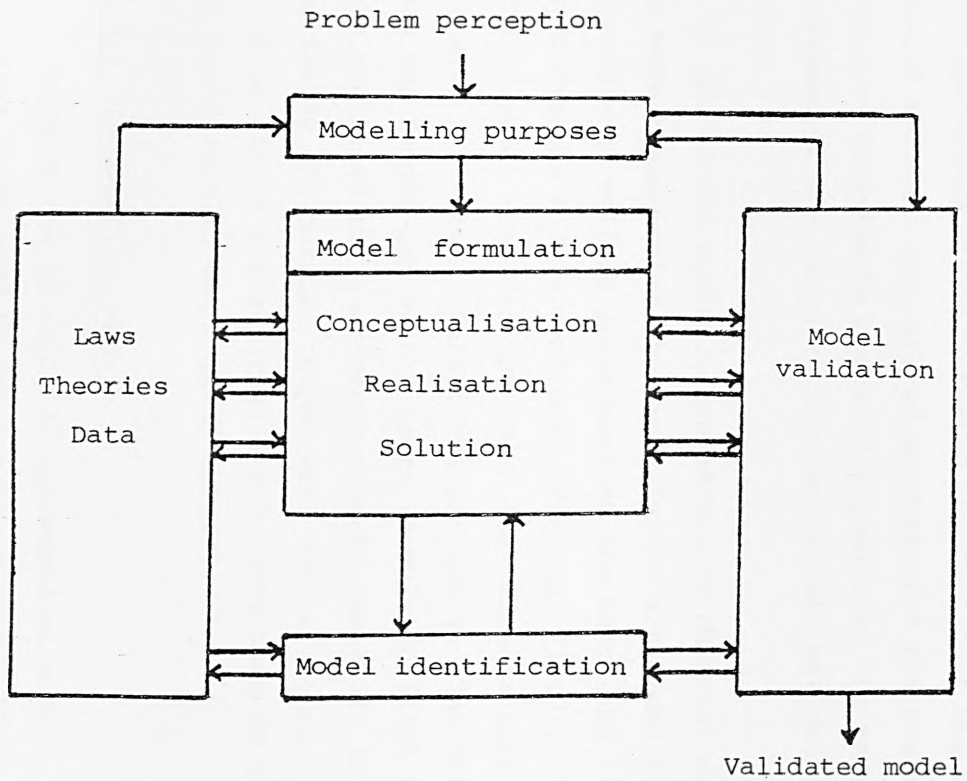

Figure 2.6 The modelling process.

2.3 A REVIEW OF MODELS OF THE CARDIOVASCULAR SYSTEM

In this section a brief historical review is given of some of the models which have been used in cardiovascular research. The review is not exhaustive but rather is intended to illustrate some of the more important developments which have been made in relation to physical aspects of the heart and circulation.

Let us first consider some models that have aided the basic operation of the circulatory system. In the seventeenth century William Harvey (1628) inferred the fact that the heart propels blood around a closed circuit and demonstrated the passage of blood from arteries to veins by means of a ligature. He showed that the continual movement of the blood within its circuit was caused by the beat of the heart.

One of the earliest approaches to physical modelling was the study of wave transmission phenomena in the aorta and its large arterial branches as well as properties of the heart and circulation using hydrodynamic models mentioned by Schwan (1969). It was pointed out that the arterial wave did not reach the veins, a fact which he attributed to wave reflection against the periphery. The next significant advance was the famous law of the heart formulated first by Starling (1866-1927) who explained the phenomenon whereby the heart is able to balance automatically the cardiac output with venous return. Hence, within physiological limits the external stroke work done by the heart is proportional to end-diastolic ventricular volume.

2.3.1 Uncontrolled Models

Turning now to explicit mathematical models, one of the earliest was that formulated by Van Harreveld et al (1949; 1951) using a resistive-capacitive electrical analogue. This model represented the mean flow and the mean pressures at the outlet and inlet of the heart, together with their changes when the system parameters vary. In this analogue form resistance to blood flow is represented by the resistance in the electrical circuit, the capacity for blood storage is represented by the charge capacity, and the blood pressure is represented by voltage.

This model of Van Harreveld, like all the other work carried out in this period, described the steady state behaviour of cardiovascular

systems without taking into account the effects of neural or hormonal control.

Guyton (1955) used graphical techniques for determining mean cardiac output, venous return and atrial pressure for both normal and abnormal conditions. In this method curves of venous return and cardiac output are drawn against the right atrial pressure (cardiac-response curves and venous return curves). The intersection of venous return and cardiac output determines the operating point, thereby satisfying Starling's law.

In 1959 Grodins proposed a more sophisticated resistive-capacitive model to describe steady state behaviour. In this Starling's law was represented by a linear relationship between end-diastolic ventricular volume and stroke work. The model consisted of 23 simultaneous equations. This may thus be regarded as the next level of complexity in the development of cardiovascular models in terms of compartmental structure.

Noordergraaf et al (1963; 1964) used an electrical analogue model of the systemic arterial tree, in which the pressure-flow relationships in the peripheral vascular bed were assumed to be linear even in the stationary state. The model consists of 113 segments, but the only measurements made were the magnitude and phase of the input impedance of a single artery and of the entire systemic arterial tree.

Dick and Rideout (1965) developed a four-compartment model representing the major elements of the arterial tree. They used time-varying compliance of the left ventricular compartment to represent the pumping action of the heart.

Beneken (1965) simulated an 8-segment model representing the two ventricles of the heart, two for pulmonary arteries and veins, two for the systemic arteries and two for the systemic veins. The mechanical properties included in the model were: the contractility of the vessels and the elasticity of the heart chambers. The model was simulated on an analogue computer and was uncontrolled but included the time-varying compliances of both ventricular segments. He investigated the effect of perturbing the parameter corresponding to the properties of the contractile elements.

2.3.2 Models of the Cardiovascular System Including Neural Control

The next development was the inclusion of the neural control of the heart and blood vessels. This allowed the control and stability of the system to be studied over longer time periods and under conditions of changing environment. There are two kinds of controlled haemodynamic models: firstly, pulsatile models suitable for investigating short-term (i.e. less than 5 minutes) haemodynamic effects (Section 2.3.2.1); secondly, non-pulsatile models for studying long-term effects (Section 2.3.2.2).

2.3.2.1 Pulsatile haemodynamic models

Beneken and DeWit (1967) developed a 19-segment model of the cardiovascular system. This consisted of 4 heart chambers, a 7-segment systemic arterial tree, 6 segments to represent systemic veins, and a 2-segment pulmonary tree. All the 4 heart segments have time-varying compliances and the neural control of heart rate, myocardial contractility, peripheral resistance and venous tone are included. The models of the two baroreceptors (carotid sinus and aortic arch) which send pressure information to the central nervous system are based on Katona's studies on dogs (1965; 1967). In these, the relationship between arterial pressure and heart rate was examined, the net effect at the brain of all the baroreceptor impulses being considered as a single input signal to the model. The model responses were shown to agree well with a range of circulatory responses over short periods of time.

Pullen (1976) based his model structure on that of Beneken and DeWit (1967), and on Hyman's (1970) "bang-bang" models of neural control. These were developed in a study of the cardiac arrhythmias. In addition, Pullen's model makes use of the method of Beneken and Rideout (1968) known as "multiple modelling" to represent the transport of chemical substances in the bloodstream. Pullen introduced an algebraic method for modelling the local effects of cardiovascular active drugs. This model is discussed in detail in Chapter 3.

2.3.2.2 Non-pulsatile models

Guyton et al (1972) developed a non-pulsatile lumped parameter model of the uncontrolled circulation to which was added a large number of short- and long-term control mechanisms. In this model some of the

control and haemodynamic systems operate with very short time constants of the order of 0.005 min (e.g. in the haemodynamic circuit), while others operate with longer time constants as high as 57,600 min (e.g. describing ventricular hypertrophy). The model, used to study overall circulatory behaviour, yields responses which agree adequately with the results from equivalent physiological experiments.

The non-pulsatile control model of the cardiovascular system developed by Boyers et al (1972) was used to study the normal responses to change of posture, blood loss, transfusion and autonomic blockade. The model can simulate the steady state responses of the cardiovascular system to stresses ranging in duration from a few seconds to many hours, and can also be used to study the regulation of interstitial fluid and total blood volumes. The model, which consists of the heart, large arteries, peripheral circulation and the central blood volume (pulmonary reserve), was also used to investigate the effects of the ganglionic blocking agent Arfonad on the circulatory response to a large transfusion of blood. The results from all the tests agreed closely with the observed measurements .

Noriaki et al (1979) produced a large-scale model of the overall regulation of body fluids to consider problems concerning body fluid distribution and fluid therapy. This model consists of the following subsystems: circulation, respiration, renal function, and intra- and extra-cellular fluid spaces.

Dickinson et al (1971) developed a mathematical model and computer simulation of systemic haemodynamics (MACMAN) to be used particularly for teaching purposes. The model is based upon Starling's law of the heart (which describes its performance) and includes neural control via the arterial baroreceptor feedback loop. This model was designed in such a way that it could easily be used by the student to simulate a variety of circulatory effects (e.g. the effects of vasoconstrictor or vasodilator drugs, myocardial infarction, pericardial tamponade, positive pressure ventilation, and haemorrhage or transfusion).

2.4 CONCLUSION

In this chapter, the structure and functioning of the human cardiovascular system has been set within a systemic framework. The role of mathematical models in the analysis of complex physiological systems

has been examined and a brief, but critical, review of some of the more important cardiovascular system models has been presented.

In Chapter 3, the pulsatile model of the human cardiovascular system developed by Pullen and others (Pullen, 1976; Leaning et al, 1983) is described in detail, this being the model, the validity of which is assessed in Chapters 5 and 6.

CHAPTER 3

A 19-SEGMENT PULSATILE MATHEMATICAL MODEL OF THE HUMAN CARDIOVASCULAR SYSTEM

3.1 INTRODUCTION

Having reviewed a number of models of the cardiovascular system in the previous chapter, the present chapter will be devoted to a description of a comprehensive, cybernetic, pulsatile mathematical model developed by Pullen (Pullen, 1976; Pullen and Finkelstein, 1977; Leaning et al, 1982a). Its function was to examine short-term blood dynamics, particularly those observed following the administration of rapidly acting drugs.

This model is the vehicle for the validation studies which follow in Chapters 4 and 5. It is also used in Chapter 6 to focus upon the need for new experiments with which to provide anatomical and physiological data with which to validate cardiovascular models in general.

The three major sections of the model - circulatory fluid dynamics, neural control and pharmacokinetics/pharmacodynamics - are described in the following sections. The total set of all the symbols adopted is given in Appendix I, with a complete listing of all the model equations being given in Appendix II.

3.2 MODEL OF THE CIRCULATORY FLUID MECHANICS

3.2.1 The Basic Structure and Equations

Blood flow through the complex network of vessels in the circulatory system may be described accurately by a very large set of simultaneous non-linear partial differential equations. To avoid computational unwieldiness, a simplified 19-segment fluid mechanics model, based on the approach of Beneken and DeWit (1967), is used (Figure 3.1). A diagrammatic representation of this model is shown in Figure 3.2. Each segment is an elastic reservoir with lumped hydrodynamic parameters representing the distributed properties of the appropriate collection of blood vessels.

General equations characterising a typical segment are derived considering two typical segments connected together, as shown in

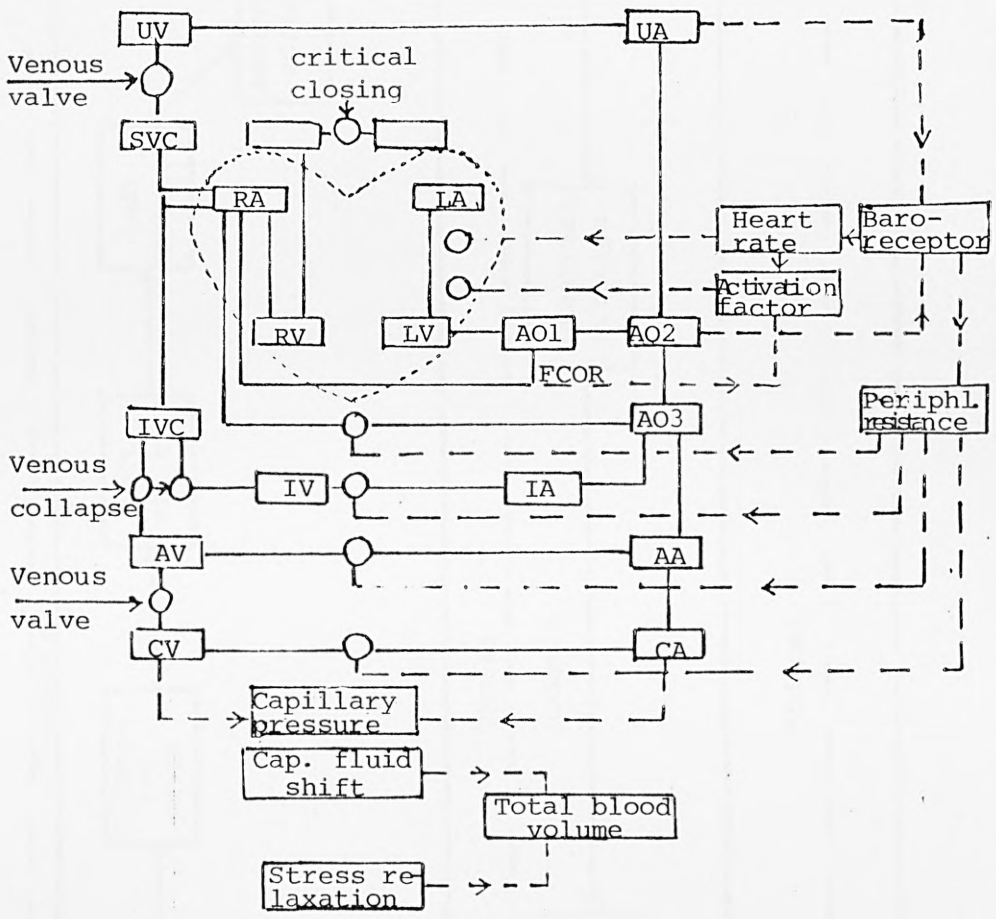

Figure 3.1 Block diagram of the cardiovascular model. The continuous lines interconnecting these blocks (segments) denote the flow path; the control aspects are identified in separate blocks; and the broken lines denote the sensor locations and sites on which the control mechanisms operate. (Beneken and DeWit, 1967)

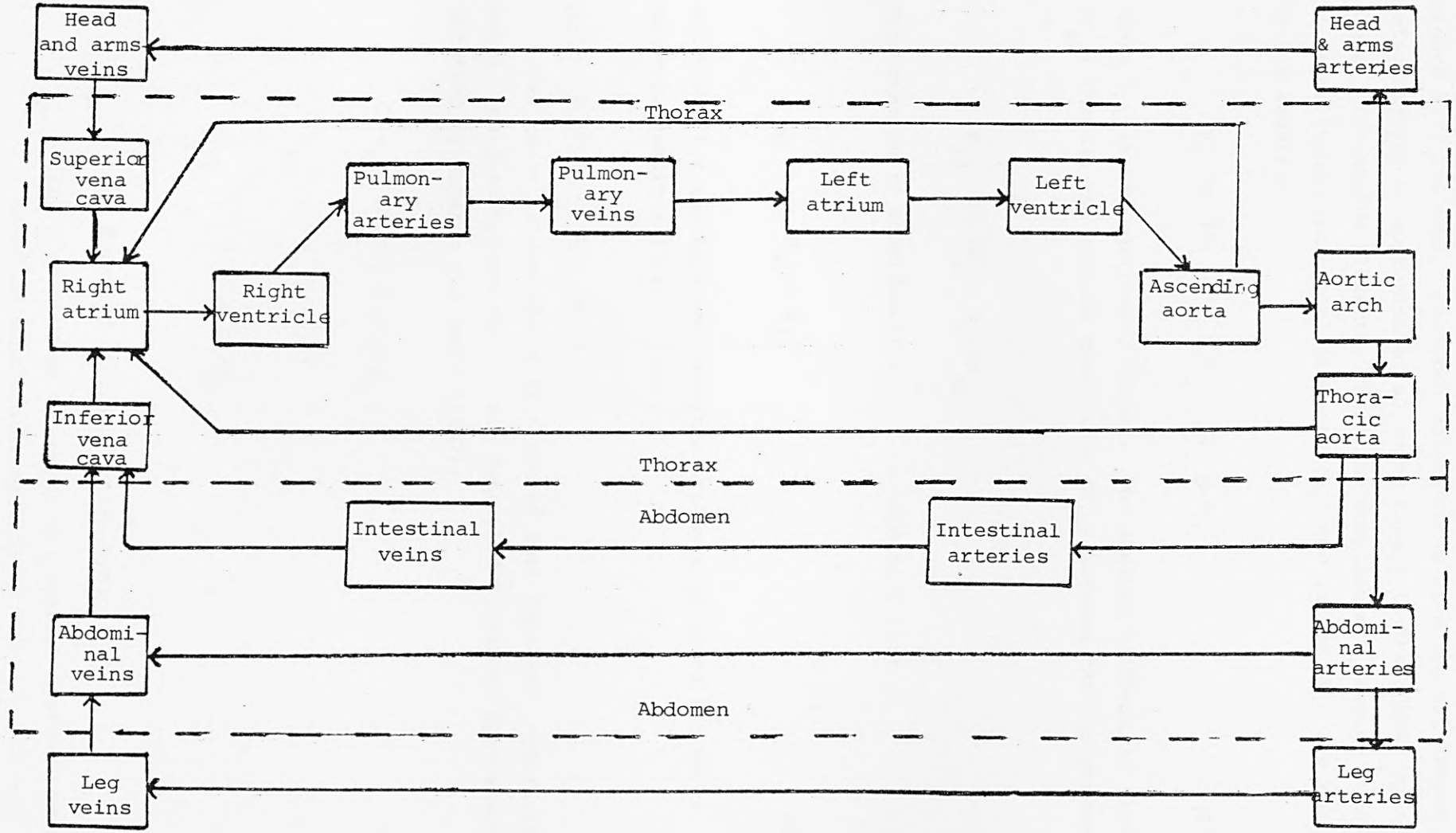

Figure 3.2 Interconnection of segments in the circulatory fluid mechanics model of Beneken and DeWit (1967)

Figure 3.3. The static pressure-volume curve of a typical lumped parameter segment is approximated as being linear in the normal operating range. In passive elements, where the compliance C_1 can be considered to be constant, transmural pressure (P_1) and volume (V_1) are related by the equation

$$P_1 = (V_1 - V_{U1})/C_1 , \quad V_1 \geq V_{U1} \tag{3.1}$$

where V_{U1} is the unstressed volume. The laminar Poisseuille flow (F_{12}) through the viscous resistance (R_{12}) between the two segments is

$$F_{12} = (P_1 - P_2)/R_{12} \tag{3.2}$$

From continuity considerations, it is necessary that

$$\frac{dV_1}{dt} = F_{01} - F_{12} \tag{3.3}$$

Equations for the nineteen segments are derived using the above general equations (3.1) - (3.3).

3.2.2 A model of the heart

The heart is considered as a set of four separate undirectional pumps. Cardiac hydromechanics are described by linear approximations obtained by Beneken and DeWit (1967):

$$T_{AS} = 0.1 + 0.09T_H \tag{3.4}$$

$$T_{AV} = T_{AS} - 0.04 \tag{3.5}$$

$$T_{VS} = 0.16 + 0.2T_H \tag{3.6}$$

where

T_{AS} = the duration of the aterial systole

T_{AV} = the time between the onset of aterial systole and the onset of ventricular systole

T_{VS} = the duration of ventricular systole

T_H = the heart period

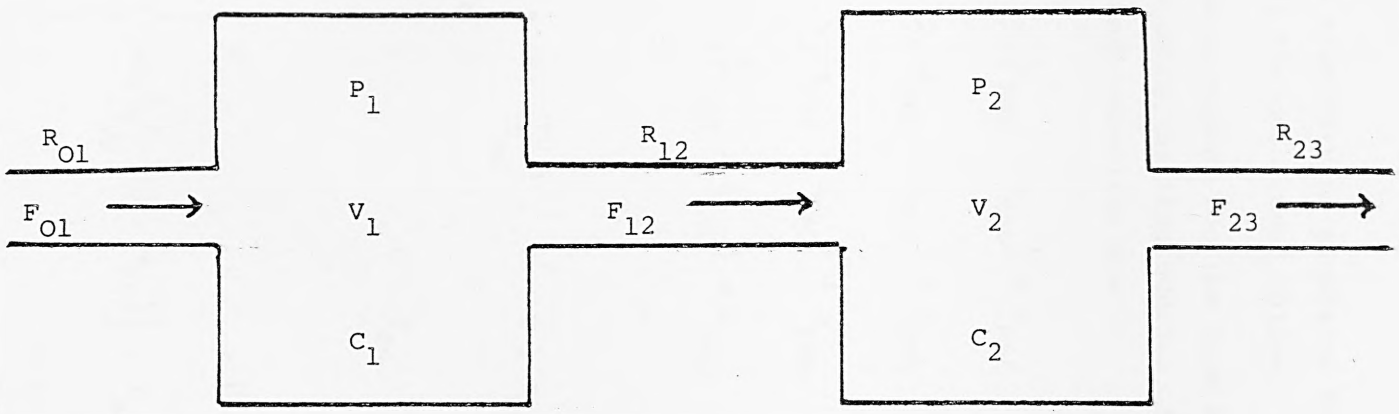

Figure 3.3 Two typical adjoining lumped parameter segments.

Assuming a normal heart rate of 75 bpm, the heart period (T_H) is 0.8 secs; and T_{AS} = 0.172 secs, T_{AV} = 0.132 secs, T_{VS} = 0.32 secs.

The pumping action of the heart is described by the equation relating pressure and volume

$$P = a(t)\left[V - V_U\right] \tag{3.7}$$

where a(t) is the time-varying elastance function (reciprocal compliance) and V_U is the unstressed volume.

The elastance functions for the four heart chambers are given by equations derived using the time courses of the four elastances shown in Figure 3.4. These equations are

$$a_{RA} = x_3\left(a_{RAS} - a_{RAD}\right) + a_{RAD} \tag{3.8}$$

$$a_{RV} = x_5\left(a_{RVS} - a_{RVD}\right) + a_{RVD} \tag{3.9}$$

$$a_{LA} = x_3\left(a_{LAS} - a_{LAD}\right) + a_{LAD} \tag{3.10}$$

$$a_{LV} = x_5\left(a_{LVS} - a_{LVD}\right) + a_{LVD} \tag{3.11}$$

where

$$x_3 = \begin{cases} \sin\left(\frac{\pi U}{T_{AS}}\right), & 0 < U \leq T_{AS} \\ 0, & 0 \geq T_{AS} \end{cases} \tag{3.12}$$

$$x_5 = \begin{cases} 0, & U \leq T_{AV} \\ \sin\left[\frac{\pi}{T_{VS}}\left(U - T_{AV}\right)\right], & T_{AV} < U < \left(T_{AV} + T_{VS}\right) \\ 0, & U \geq \left(T_{AV} + T_{VS}\right) \end{cases} \tag{3.13}$$

and the suffices D and S for elastance values denote minimum and maximum values given by

$$a_D = P_D/(V_D - V_U) \; ; \quad a_S = P_S/(V_S - V_U) \tag{3.14}$$

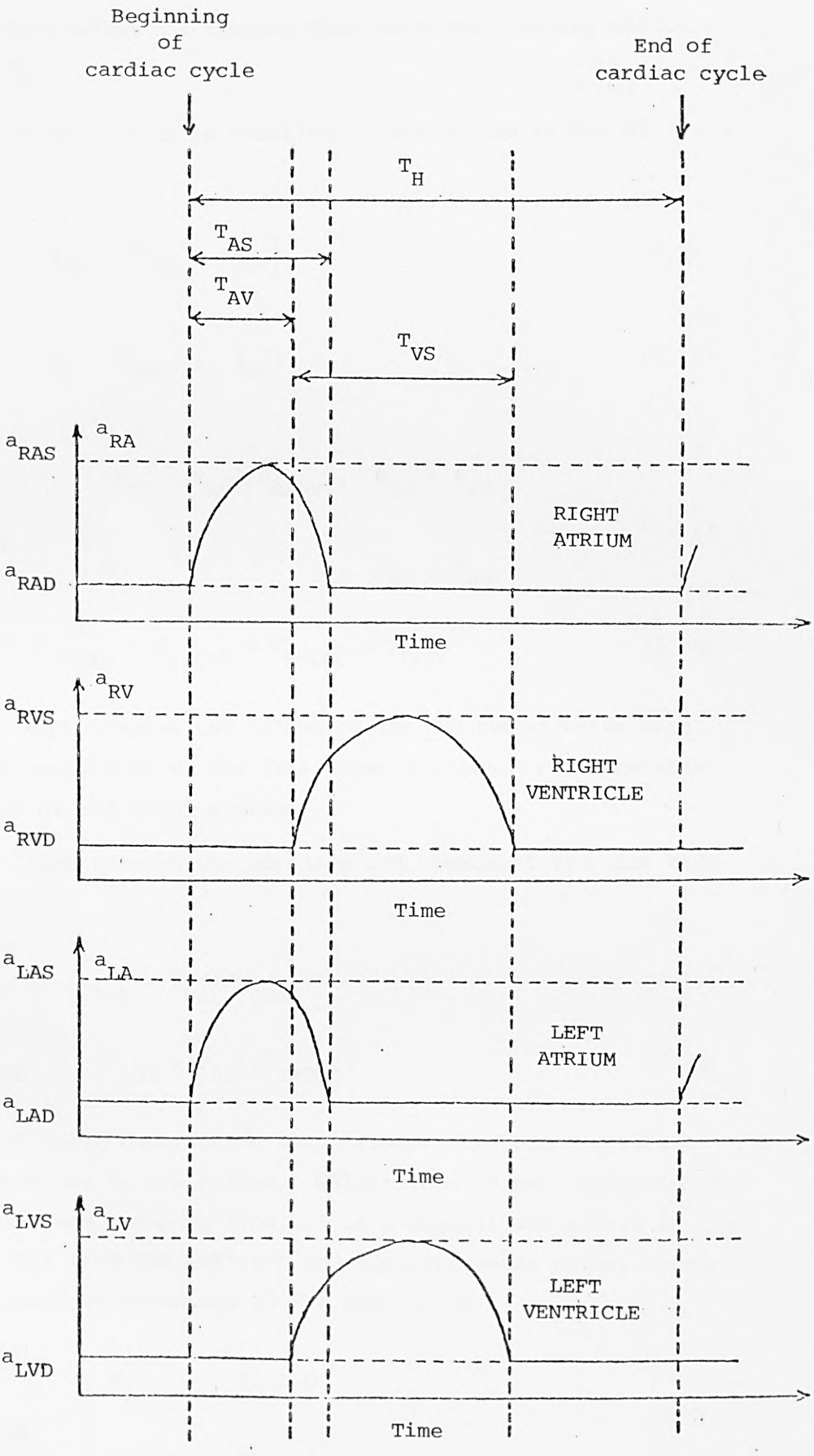

Figure 3.4 Elastances of the four heart chambers.

with the variable U being the elapsed time measured from the cardiac cycle ($0 \leq U \leq T_H$).

The Atria. The right atrium is modelled by the following set of equations:

$$P_{RA} = a_{RA}(t)\left[V_{RA} - V_{URA}\right] \tag{3.15}$$

$$\frac{dV_{RA}}{dt} = F_1 - F_{RARV}\ , \quad V_{RA} \geq 0 \tag{3.16}$$

$$F_{RARV} = \begin{cases} \left(P_{RA} - P_{RV}\right)/R_{RARV}\ , & P_{RA} > P_{RV} \\ 0 \qquad\qquad\qquad\ , & P_{RA} \leq P_{RV} \end{cases} \tag{3.17}$$

$$F_1 = F_{SVCRA} + F_{IVCRA} + F_{BRONC} + F_{COR} \tag{3.18}$$

Equation (3.17) approximates the action of the tricuspid valve with R_{RARV} being the resistance of the fully opened valve. F_1 represents the total inflow of the right atrium.

The basic flows through the coronary and bronchial vascular beds are given by

$$F_{COR} = \left(P_{AO1} - P_{RA}\right)/R_{COR} \tag{3.19}$$

$$F_{BRONC} = \left(P_{AO3} - P_{RA}\right)/R_{BRONC} \tag{3.20}$$

The right atrial inlet contraction which assists the pumping action introduces resistance to the inflow. Whilst this is negligible in the case of bronchial and coronary flow, it is a significant effect in the case of blood flow from the inferior and superior venae cavae, represented in the model by equations (3.21) and (3.22).

$$F_{IVCRA} = \begin{cases} F_9 & F_9 \geq 0 \\ 0.1\ F_9\ , & F_9 < 0 \end{cases} \tag{3.21}$$

$$F_{SVCRA} = \begin{cases} F_{10} & , \quad F_{10} \geq 0 \\ 0.1\, F_{10}, & F_{10} < 0 \end{cases} \tag{3.22}$$

where F_9 and F_{10} are the respective flows assuming no contraction.

For the left atrium, the equations are

$$P_{LA} = a_{LA}(t)\left[V_{LA} - V_{ULA}\right] \tag{3.23}$$

$$\frac{dV_{LA}}{dt} = F_{PVLA} - F_{LALV}, \quad V_{LA} \geq 0 \tag{3.24}$$

$$F_{LALV} = \begin{cases} \left(P_{LA} - P_{LV}\right)/R_{LALV}, & P_{LA} > P_{LV} \\ 0 & , \quad P_{LA} \leq P_{LV} \end{cases} \tag{3.25}$$

This takes into consideration the action of the mitral valve, the resistance of which fully opened is R_{LALV}.

The left atrial inlet contraction modifies the inlet flow to

$$F_{PVLA} = \begin{cases} F_3 & F_3 \geq 0 \\ 0.1\, F_3, & F_3 < 0 \end{cases} \tag{3.26}$$

where F_3 is the outflow with no contraction.

The Ventricles. The basic equations for the ventricles are:

$$P_{RV} = a_{RV}(t)\left[V_{RV} - V_{URV}\right] \tag{3.27}$$

$$\frac{dV_{RV}}{dt} = F_{RARV} - F_{RVPA}, \quad V_{RV} \geq 0 \tag{3.28}$$

$$P_{LV} = a_{LV}(t)\left[V_{LV} - V_{ULV}\right] \tag{3.29}$$

$$\frac{dV_{LV}}{dt} = F_{LALV} - F_{LVAO1}, \quad V_{LV} \geq 0 \tag{3.30}$$

Equations for the outflows from the ventricles are obtained from those used by Beneken and DeWit (1967) for the pulmonary and aortic

valves. These equations are

$$P_{RV} - P_{PA} = R_{RVPA}F_{RVPA} + L_{RV}\frac{dF_{RVPA}}{dt} + \frac{\rho}{2}\left(\frac{F_{RVPA}}{2A^2_{PA}}\right)^2, \quad F_{RVPA} \geq 0 \qquad (3.31)$$

$$P_{LV} - P_{AO1} = R_{LVAO1}F_{LVAO1} + L_{LV}\frac{dF_{LVAO1}}{dt} + \frac{\rho}{2}\left(\frac{F_{LVAO1}}{2A^2_{AO1}}\right)^2, \quad F_{LVAO1} \geq 0 \qquad (3.32)$$

The first term on the right-hand side of each equation represents pressure drop caused by viscous properties of blood; the second term accounts for the inertia of the blood column; and the third term represents the pressure drop due to the fact that the cross-sectional area of the outflow vessel is much smaller than that of the corresponding ventricle.

The equations for the outflows are

$$\frac{dF_{RVPA}}{dt} = \frac{P_{RV} - P_{PA} - R_{RVPA}F_{RVPA} - \left(\frac{\rho}{2A^2_{PA}}\right)F^2_{RVPA}}{L_{RV}}, \quad F_{RVPA} \geq 0 \qquad (3.33)$$

$$\frac{dF_{LVAO1}}{dt} = \frac{P_{LV} - P_{AO1} - R_{LVAO1}F_{LVAO1} - \left(\frac{\rho}{2A^2_{AO1}}\right)F^2_{LVAO1}}{L_{LV}}, \quad F_{LVAO1} \geq 0 \qquad (3.34)$$

3.2.3 A Model of the Systemic Arteries

For a typical arterial segment, inertia effects, wall viscoelasticity, geometric and elastic taper are taken into account. The equations used by Beneken and DeWit (1967) to describe a typical arterial segment are:

$$P_1 - P_2 = R_{12}F_{12} + L_{12}\frac{dF_{12}}{dt} \qquad (3.35)$$

$$\frac{dV_2}{dt} = F_{12} - F_{23}, \quad V_2 \geq 0 \qquad (3.36)$$

$$P_2 = \frac{1}{C_2}\left(V_2 - V_{U2}\right) + R'_2\frac{dV_2}{dt} \qquad (3.37)$$

where R'_2 is equivalent to wall viscosity, the reciprocal of C_2 is

equivalent to wall elasticity, and $C_2R_2' = 0.04$.

3.2.4 A Model of the Systemic Vascular Beds

The resistances of the vascular beds are represented by lumped arterio-venous resistances. Thus the equations derived for blood flow are typified by that given below for flow through the bronchial vascular bed:

$$F_{BRONC} = \left(P_{AO3} - P_{RA}\right)/R_{BRONC} \tag{3.38}$$

3.2.5 A Model of the Systemic Veins

Unlike the arteries, veins are highly compliant, collapsible, large-capacity vessels with low transmural pressures, and non-linear modelling has to be applied. When a venous segment collapses and volume becomes less than the unstressed volume V_U, the compliance increases to 20 times its normal value C_N.

Equations for a typical venous segment are:

$$P_2 = \left(V_2 - V_{U2}\right)/C_2 \tag{3.39}$$

where

$$C_2 = \begin{cases} C_{2N} , & V_2 > V_{U2} \\ 20\, C_{2N} , & V_2 \leq V_{U2} \end{cases} \tag{3.40}$$

$$\frac{dV_2}{dt} = F_{12} - F_{23} , \quad V_2 \geq 0 \tag{3.41}$$

Due to the increase in resistance as a result of a venous segment collapsing, the flow is given by

$$F_{23} = K_A\left(P_2 - P_3\right)r^4 \tag{3.42}$$

where K_A is a constant and r is the radius of the connecting vessel. The volume V_2 is given by

$$V_2 = K_B r^2 \tag{3.43}$$

where K_B is a constant.

$$F_{23} = K_C(P_2 - P_3)V_2^2 \tag{3.44}$$

where $K_C = K_A/K_B^2$.

If it is assumed that $F_{23} = \dfrac{P_2 - P_3}{R_{23}}$ when $V_2 = V_{U2}$ then

$$K_C = \frac{1}{R_{23}V_{U2}^2} \quad \text{and} \quad F_{23} = \frac{(P_2 - P_3)V_2^2}{R_{23}V_{U2}^2} \tag{3.45}$$

Venous valves. The venous valve situated between the segments representing leg veins and abdominal veins obstructs back flow completely. This valve is represented by the following equation:

$$F_{CVAV} = \begin{cases} F_8 , & F_8 > 0 \\ 0 , & F_8 \leq 0 \end{cases} \tag{3.46}$$

where F_8 is the flow assuming no valve is present. Similarly, for the valve between head and arm veins and the superior vena cava

$$F_{UVSVC} = \begin{cases} F_5 , & F_5 > 0 \\ 0.667F_5 , & F_5 \leq 0 \end{cases} \tag{3.47}$$

3.2.6 A Model of the Pulmonary Circulation

The pulmonary circulation is represented by two lumped parameter segments: pulmonary arteries and pulmonary veins. The equations for the pulmonary arteries (after Beneken and DeWit, 1967) are

$$P_{PA} = (V_{PA} - V_{UPA})/C_{PA} \tag{3.48}$$

$$\frac{dV_{PA}}{dt} = F_{RVPA} - F_{PAPV} , \quad V_{PA} \geq 0 \tag{3.49}$$

$$F_{PAPV} = \begin{cases} (P_{PA} - P_{PV})/R_{LUNG} , & P_{PV} > P_{CC} \\ (P_{PA} - P_{CC})/R_{LUNG} , & P_{PV} \leq P_{CC} \end{cases} \tag{3.50}$$

The flow in the pulmonary vascular bed is dependent on the value of the pulmonary venous pressure relative to a critical closing pressure (P_{CC}) which is about 7 torr.

The pulmonary veins are represented by a segment which has equations similar to those for the systemic veins segment described in section 3.2.5 with the addition of the atrial inlet contraction as described by equation (3.26).

3.2.7 A Model of Respiration

Cyclic respiration is introduced into the model to illustrate the respiratory variation of blood pressure, heart rate, etc. and also to demonstrate the action of the respiratory pump.

Considering the time courses of the respiratory variables, as shown in Figure 3.5, the intrathoracic pressure (P_{TH}) and the intra-abdominal pressure (P_{ABD}) are:

$$P_{TH} = K_1 + (K_2 - K_1)\sin\left(\frac{\pi y_1}{T_{IE}}\right) \tag{3.51}$$

$$P_{ABD} = K_3 + (K_4 - K_3)\sin\left(\frac{\pi y_1}{T_{IE}}\right) \tag{3.52}$$

where T_{IE} = the inhalation-exhalation duration and

$$y_1 = \begin{cases} y_2 \ , & 0 \leq y_2 \leq T_{IE} \\ 0 \ , & T_{IE} \leq y_2 \leq T_R \end{cases} \tag{3.53}$$

with T_R being the respiratory period.

These pressures being defined by equations (3.51) and (3.52) are introduced into the equations defining flows across the thoracic or abdominal boundaries.

3.2.8 A Model of Orthostasis

Gravity effects on the columns of blood in the cardiovascular system are included in the model by employing the approach used by Snyder and Rideout (1969). Effective hydrostatic pressure differences are represented by pressure generators included between various segments. The hydrostatic pressure difference is given by

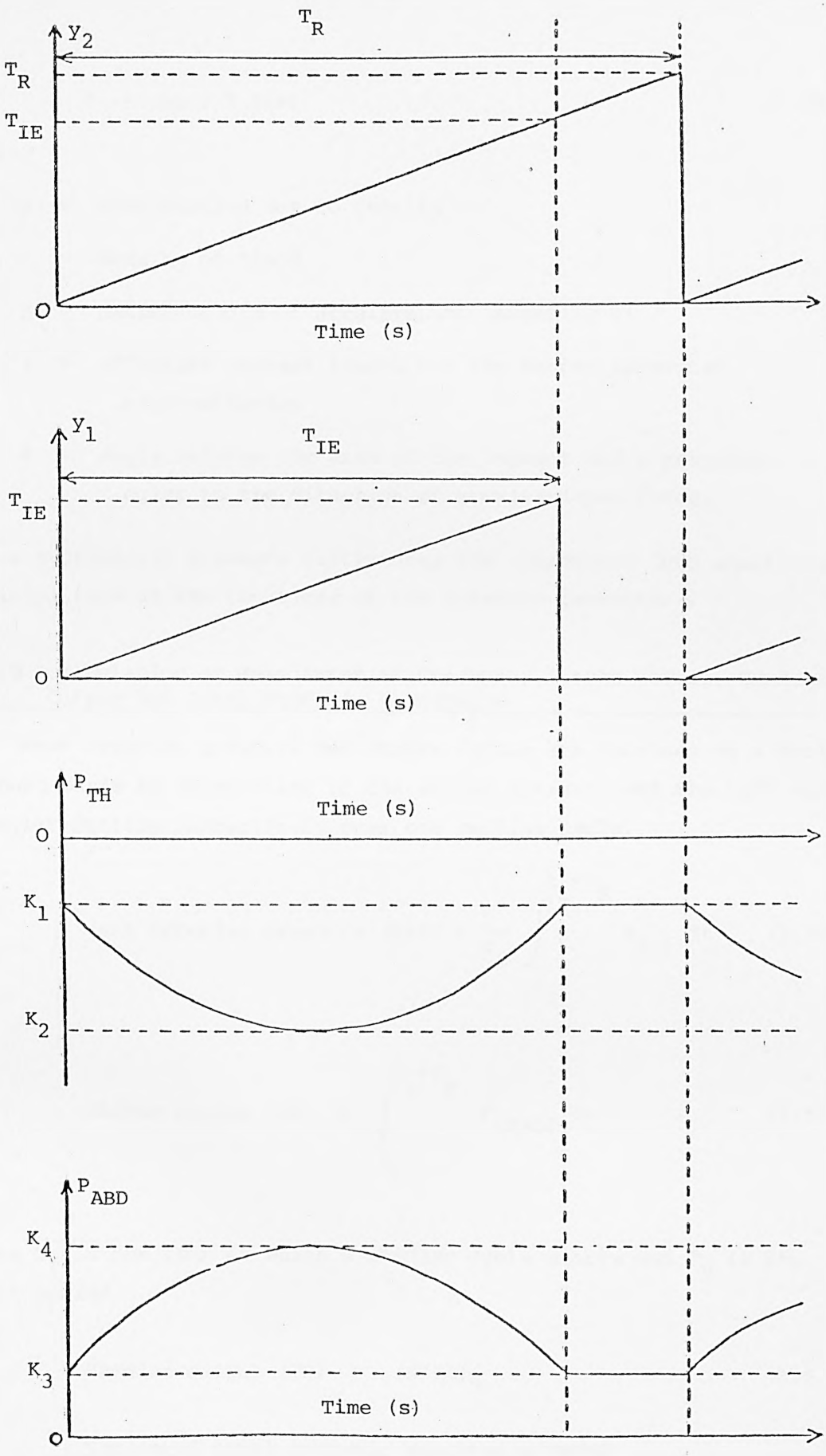

Figure 3.5 Time courses of variables in the cyclic respiration model.

$$G = ng\,\rho\,\ell\,\sin\phi \tag{3.54}$$

where

g = acceleration due to gravity

ρ = density of blood

n = number of g's of acceleration (normally 1)

ℓ = effective segment length for the lumped parameter representation

ϕ = angle between the axis of the segment and a perpendicular to the direction of gravitational force.

These hydrostatic pressure differences are introduced into equations defining flow at the locations of the pressure generators.

3.2.9 Calculation of Mean Arterial Pressure, Stroke Volume, Cardiac Output and Total Systemic Resistance

Mean arterial pressure and stroke volume are obtained on a beat-by-beat basis by integration of the aortic pressure and the left ventricular outflow respectively over one cardiac cycle.

$$\text{Mean arterial pressure (MAP)} = \frac{1}{T_H}\int_{t_1}^{t_1+T_H} P_{AO1}\,dt \tag{3.55}$$

$$\text{Stroke volume (SV)} = \int_{t_1}^{t_1+T_H} F_{LVAO1}\,dt \tag{3.56}$$

where t_1 is the time at which a cardiac cycle starts and T_H is the heart period

$$\text{Cardiac output (CO)} = (SV)/T_H \tag{3.57}$$

$$\text{Estimated total systemic resistance (ETSR)} = (MAP)/(CO) \tag{3.58}$$

3.3 MODEL OF NEURAL CONTROL

Fluid mechanical modelling is based essentially on physical laws. However, modelling based on physical laws is not applicable to the complete Central Nervous System (CNS) and, therefore, empirical models have to be developed that represent neural control of the cardiovascular system. Such models, based on the data obtained from physiological experiments, have been included for baroreceptors (which monitor blood pressure in certain main arteries and send information to the CNS) and CNS control of heart rate, peripheral resistance, myocardial contractility and venous tone. These models are based upon the work of Katona et al (1967) and Hyndman (1970). Further development of these models has resulted in the incorporation of:

(i) separate aortic arch and carotid sinus baroreceptors,

(ii) pulsatile baroreceptor dynamics,

(iii) adaption of the controllers to the 19-segment circulatory fluid mechanics model.

The neural control model consists of 11 first order differential equations and 23 algebraic equations. Non-linearities arise due to the unidirectional rate sensitivity of the baroreceptors and the "bang-bang" action of the controllers. The mathematical formulation is illustrated by considering the baroreceptor model and that for the CNS control of heart rate.

3.3.1 The Baroreceptor System

Baroreceptors, forming a part of short-term negative feedback mechanisms, monitor blood pressure in certain main arteries and transmit information to the CNS.

The output function (B_2) of a baroreceptor is given by a linear combination of a dynamic estimate (S_C) of the positive pressure derivative (S_A) and the dynamic mean pressure estimate (S_B), together with a threshold pressure below which firing of the baroreceptor does not occur. A further constraint is incorporated to ensure a positive firing rate. The equations for each baroreceptor area are thus as follows;

$$S_A = \begin{cases} \frac{dP}{dt} , & \frac{dP}{dt} > 0 \\ 0 , & \frac{dP}{dt} \leq 0 \end{cases} \qquad (3.59)$$

$$\frac{dS_B}{dt} = (P - S_B)/\tau_1 \tag{3.60}$$

$$\frac{dS_C}{dt} = (S_A - S_C)/\tau_2 \tag{3.61}$$

$$S_D = S_B + K_C S_C - K_D \tag{3.62}$$

$$B_2 = \begin{cases} S_D \ , & S_D > 0 \\ 0 \ , & S_D \leq 0 \end{cases} \tag{3.62}$$

where K_D is the threshold pressure below which firing does not occur and K_C is the average contribution of the positive pressure derivative term over one cardiac cycle. K_C is estimated by assuming that the average value of $K_C S_C$ over one cycle is 60, i.e.

$$\frac{1}{T_H}\int_{t_1}^{t_1+T_H} K_C S_C dt = 60 \text{ giving } K_C = \frac{60T_H}{\int_{t_1}^{t_1+T_H} S_C dt} \tag{3.64}$$

For normal heart rate and blood pressure, the value of K_C thus calculated is approximately 1.0.

The effective input for the central nervous system is assumed to be a static function of the output of the aortic arch baroreceptor (B_{AO2}) and the carotid sinus baroreceptor (B_{UA}) and is given by

$$B = B_{UA} + (1 - \alpha)B_{AO2} \tag{3.65}$$

where α is assumed to be 0.7.

A block diagram representation of an individual baroreceptor model and of the linear combination of such models is given in Figure 3.6.

3.3.2 Central Nervous Control of Heart Rate

A two-region dynamic model is adopted for the CNS control of heart rate, one for blood pressures above normal and the other for pressures below normal. For elevated blood pressures, the CNS input function B

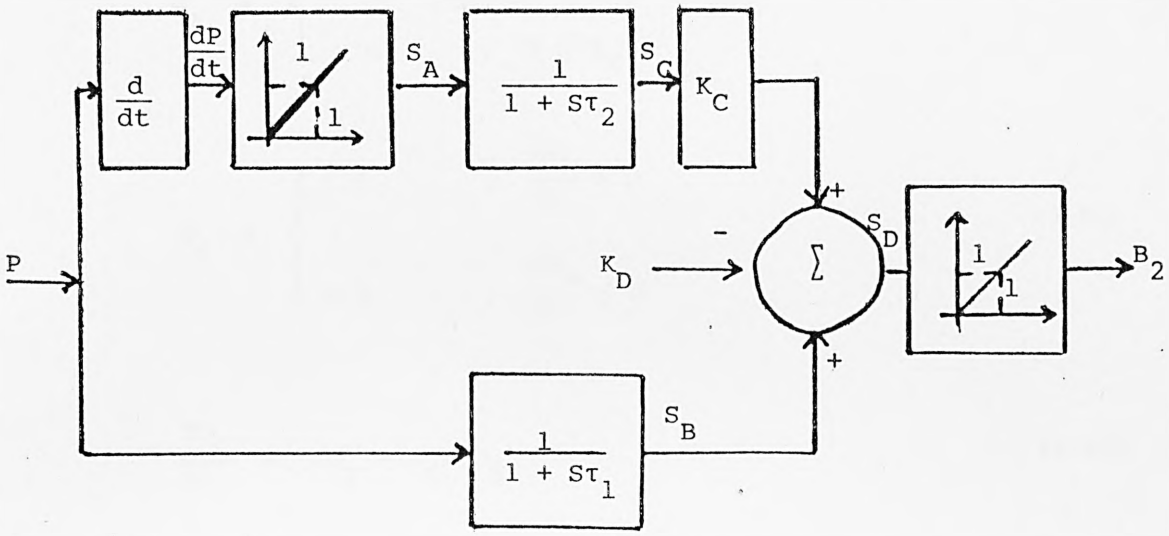

Figure 3.6(a) Block diagram of an individual baroreceptor model.

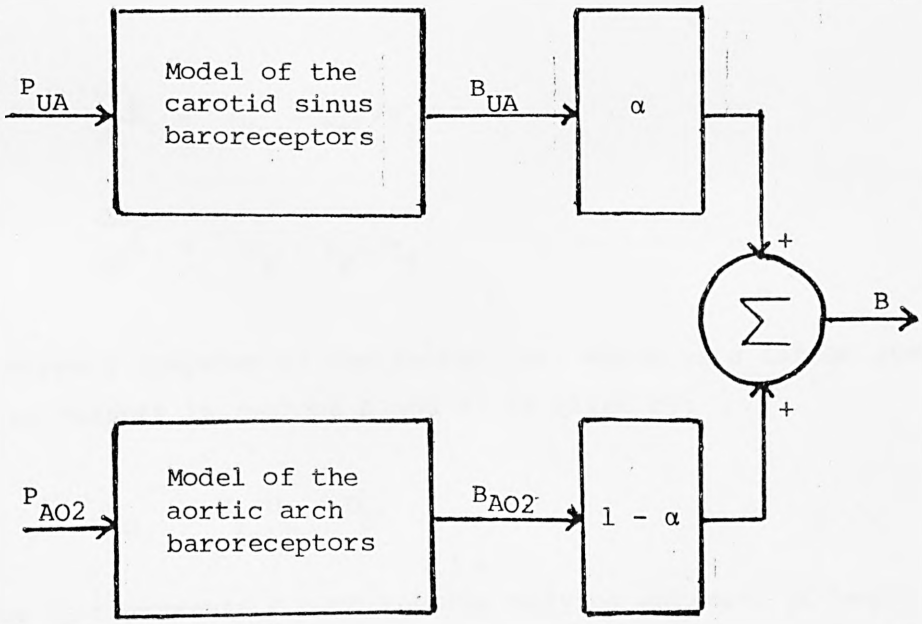

Figure 3.6(b) Linear combination of baroreceptor outputs to give the C.N.S. input function.

is greater than a threshold value K_E and the dynamics of this region (region A) are approximated by a first-order system, described by the following equations:

$$U_A = \begin{cases} (B - K_E) & , \quad B > K_E \\ 0 & , \quad B \leq K_E \end{cases} \tag{3.66}$$

$$U_B = \begin{cases} 1.5 & , \quad \frac{dU_A}{dt} > 0 \\ 4.5 & , \quad \frac{dU_A}{dt} \leq 0 \end{cases} \tag{3.67}$$

$$\frac{dU_C}{dt} = (U_A - U_C)/U_B \tag{3.68}$$

For the other region (region B), the dynamics are approximated by a second-order system described by the following equations:

$$U_D = \begin{cases} K_E & , \quad B > K_E \\ 0 & , \quad B \leq K_E \end{cases} \tag{3.69}$$

$$\frac{dU_E}{dt} = (U_D - U_E)/\tau_3 \tag{3.70}$$

$$\frac{dU_F}{dt} = (U_E - U_F)/\tau_4 \tag{3.71}$$

The overall response of the controller, which is a linear combination of the outputs in regions A and B, is given by:

$$U_G = K_F(U_C + U_F) \tag{3.72}$$

where U_G represents a continuously varying estimate of heart period for use in the next cardiac cycle, subject to the following constraint (limiting the heart rate (f_H) to a range $30 \leq f_H \leq 200$ bpm):

$$U_H = \begin{cases} 2.0 \ , & U_G \geq 2.0 \\ U_G \ , & 0.3 < U_G < 2.0 \\ 0.3 \ , & U_G \leq 0.3 \end{cases} \qquad (3.73)$$

A block diagram of the heart rate controller is given in Figure 3.7.

3.4 MODEL OF PHARMACOKINETICS

The pharmacokinetics model represents the injection, transport and action of a single drug. This model can thus be combined with those of circulatory fluid mechanics and neural control.

3.4.1 Drug Transport

The "multiple modelling" technique of Beneken and Rideout (1968) is used to represent the transport of a chemical substance in the bloodstream. A slave 19-segment transport model is coupled to the main 19-segment blood circulation model so that, for each segment, transport flow is proportional to concentration in the transport model multiplied by volume flow in the circulation model.

Equations characterising a typical segment are derived, from Figure 3.8, as follows. Concentration is mass per unit volume and is given by

$$\omega = m/v \qquad (3.74)$$

The mass inflow to segment 1 is $\omega_{01} F_{01}$ and the mass outflow is $\omega_{12} F_{12}$ where

$$\omega_{01} = \begin{cases} \omega_0 \ , & F_{01} > 0 \\ \omega_1 \ , & F_{01} \leq 0 \end{cases} \qquad \omega_{12} = \begin{cases} \omega_1 \ , & F_{12} > 0 \\ \omega_2 \ , & F_{12} \leq 0 \end{cases} \qquad (3.75)$$

The rate of change of mass in segment 1 is given by

$$\frac{dm_1}{dt} = \omega_{01} F_{01} - \omega_{12} F_{12} \ , \ m_1 \geq 0 \qquad (3.76)$$

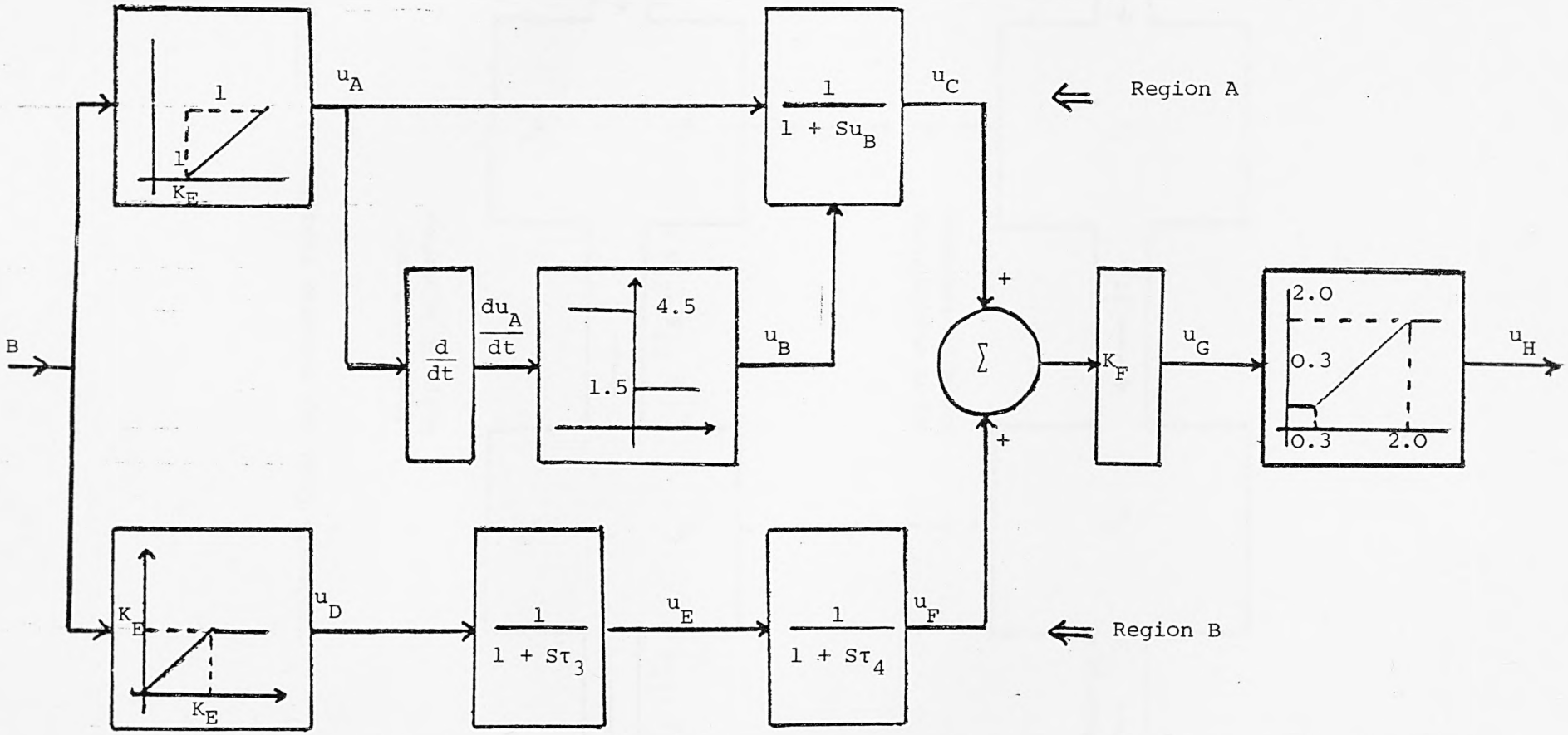

Figure 3.7 Block diagram of the heart rate controller based on the model of Katona et al (1967)

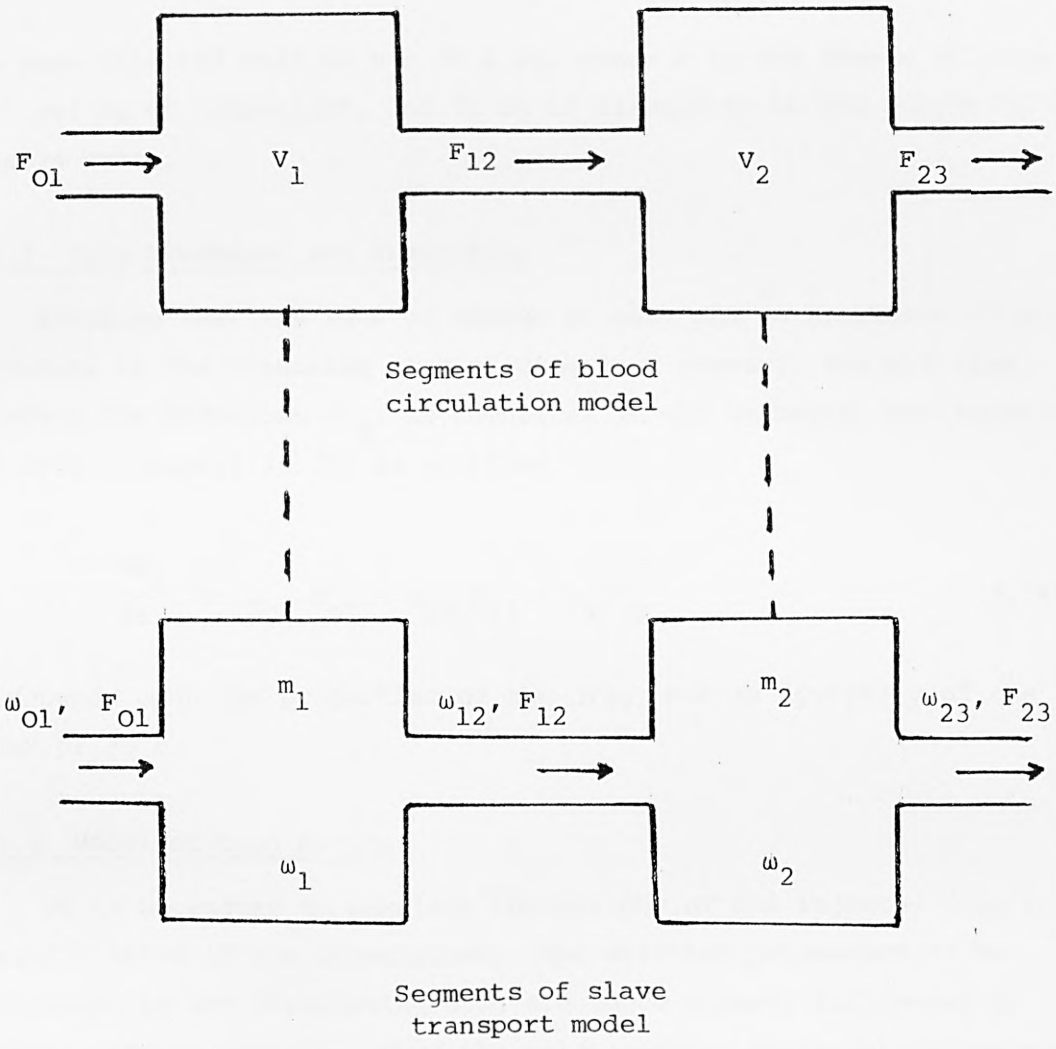

Figure 3.8 Two typical segments for drug transport.

3.4.2 Drug Injection

If the mass of drug contained in an injection is M, then injection into segment 1 at time t_I may be modelled by a Dirac delta function δ, thus modifying equation (3.76) to become:

$$\frac{dm_1}{dt} = M\delta(t - t_I) + \omega_{01} F_{01} - \omega_{12} F_{12} \qquad (3.77)$$

The mass injected will be $M = 70\ \Delta\ \mu g$, where Δ is the dosage of drug (μg) per kg of bodyweight, and 70 kg is assumed to be the weight of an average human.

3.4.3 Drug Breakdown and Absorption

Assuming that the rate of change of mass due to breakdown is proportional to the remaining mass of drug in a segment, and the time constant for breakdown (τ_B) is identical in all segments, the equation for drug transport (3.76) is modified to:

$$\frac{dm_1}{dt} = \omega_{01} F_{01} - \omega_{12} F_{12} - m_1/\tau_B \qquad (3.78)$$

τ_B depends upon the properties of the drug, but is typically of the order of 30 s.

3.4.4 Model of Drug Action

It is necessary to simulate the actions of the injected drug at specific sites in the circulation. The selected parameters to be influenced by the circulating drug are those already influenced by central nervous control. Thus the relationship, representing the combined neural and humoral influences on a general circulatory parameter (R), is:

$$R = R_N \sigma_N \sigma_D \qquad (3.79)$$

where R_N is the normal value of R, σ_N corresponds to neural control action which is equal to 1.0 in the absence of neural control and deviates from 1.0 when neural control is present, and σ_D corresponds to drug action which is equal to 1.0 in the absence of drug action and deviates from 1.0 when drug action is present.

If σ_N is regarded as constant and if R and drug concentration (ω) change in the same direction, then

$$\sigma_D = 1 + K\omega \tag{3.80}$$

where K is a positive constant. If R and ω change in opposite directions, then

$$\sigma_D = \frac{1}{1 + K\omega} \tag{3.81}$$

Drug effect on heart rate. This is achieved by modifying the rate controller output (equation (3.68)) to become:

$$U_G = K_F \sigma_H (U_C + U_F) \tag{3.82}$$

where σ_H depends upon drug concentration.

$$\sigma_H = \begin{cases} 1 + \sigma_2 \omega_{RA} & , \text{ bradycardia} \\ 1/(1 + \sigma_2 \omega_{RA}) & , \text{ tachycardia} \end{cases} \tag{3.83}$$

where σ_2 is a constant which determines the sensitivity of the heart period to changes in drug concentration.

Drug effect on peripheral resistance. The drug action variable, σ, multiplies the normal values of arterio-venous resistance in the bronchial, intestinal, abdominal, leg and head vascular beds in the model. For example:

$$\sigma_{BRONC} = \begin{cases} 1 + \sigma_1 \omega_{AO3} & , \text{ vasoconstriction} \\ 1/(1 + \sigma_1 \omega_{AO3}) & , \text{ vasodilatation} \end{cases} \tag{3.84}$$

where σ_1 determines the sensitivity of arterio-venous resistances to changes in drug concentration.

Drug effect on myocardial contractility. The drug action variable, σ, multiplies the normal systolic elastances in all four heart chambers. The multiplier, σ_{RA}, for the right atrium is, for example, given by the

following equation:

$$\sigma_{RA} = \begin{cases} 1 + \sigma_3 \, \omega_{RA} & , \text{ positive inotropy} \\ 1/(1 + \sigma_3 \, \omega_{RA}) & , \text{ negative inotropy} \end{cases} \tag{3.85}$$

where the empirical constant σ_3 determines the sensitivity of the individual systolic elastances to changes in drug concentration and is assumed to be the same for each heart chamber.

Drug effect on venous properties. Unstressed volumes and compliances of venous segments are modified in the following manner:

$$V_{U2} = V_{U2N}/\sigma_U \quad \text{and} \quad C = C/\sigma_C \tag{3.86}$$

σ_U and σ_C represent the effects of the drug on the unstressed volume and compliance, respectively, and depend on the drug concentration in the venous segments as follows:

$$\sigma_U = \begin{cases} 1 + \sigma_4 \, \omega_V & , \text{ venoconstriction} \\ 1/(1 + \sigma_4 \, \omega_V) & , \text{ venodilatation} \end{cases} \tag{3.87}$$

$$\sigma_C = \begin{cases} 1 + \sigma_5 \, \omega_V & , \text{ venoconstriction} \\ 1/(1 + \sigma_5 \, \omega_V) & , \text{ venodilatation} \end{cases} \tag{3.88}$$

where σ_4 and σ_5 determine the sensitivity of the venous unstressed volume and venous compliance, respectively, to changes in drug concentration.

The total pharmacokinetics model consists of 19 first order differential equations and 53 algebraic equations and, in combination with the fluid mechanics and neural control models, gives an overall model which is satisfactory for the study of short-term pharmacokinetics, i.e. in which the major dynamics are complete within 2 or 3 minutes.

3.5 DIGITAL COMPUTER IMPLEMENTATION OF THE MODEL

The complete model consists of 61 first order differential equations and 159 algebraic equations. A complete listing of these equations is given in Appendix II, adopting the nomenclature contained in Appendix I. Figure 3.9 shows the signal flow between the various subsystems in the complete model and shows the various interacting control loops.

Examination of the differential equations of the model revealed the property of time-varying stiffness in the equation system. This property enabled a fixed step-length Euler integration method to be used with truncation and rounding errors kept at an acceptably low level. A simulation in FORTRAN IV required approximately 56 seconds of CDC 7600 execution time for the independent variable t to reach 100 seconds in the solution.

3.6 CONCLUSION

The development of a detailed, pulsatile, mathematical model of the human cardiovascular system suitable for the study of short-term haemodynamics and pharmacodynamics has been described. In the chapters which follow the validity of the model will be examined using data both from physiological tests and drug studies. It will be shown that a complex model such as this does have a role in the prediction of short-term effects as well as constituting a test-bed for examining hypotheses relating to the control of circulation.

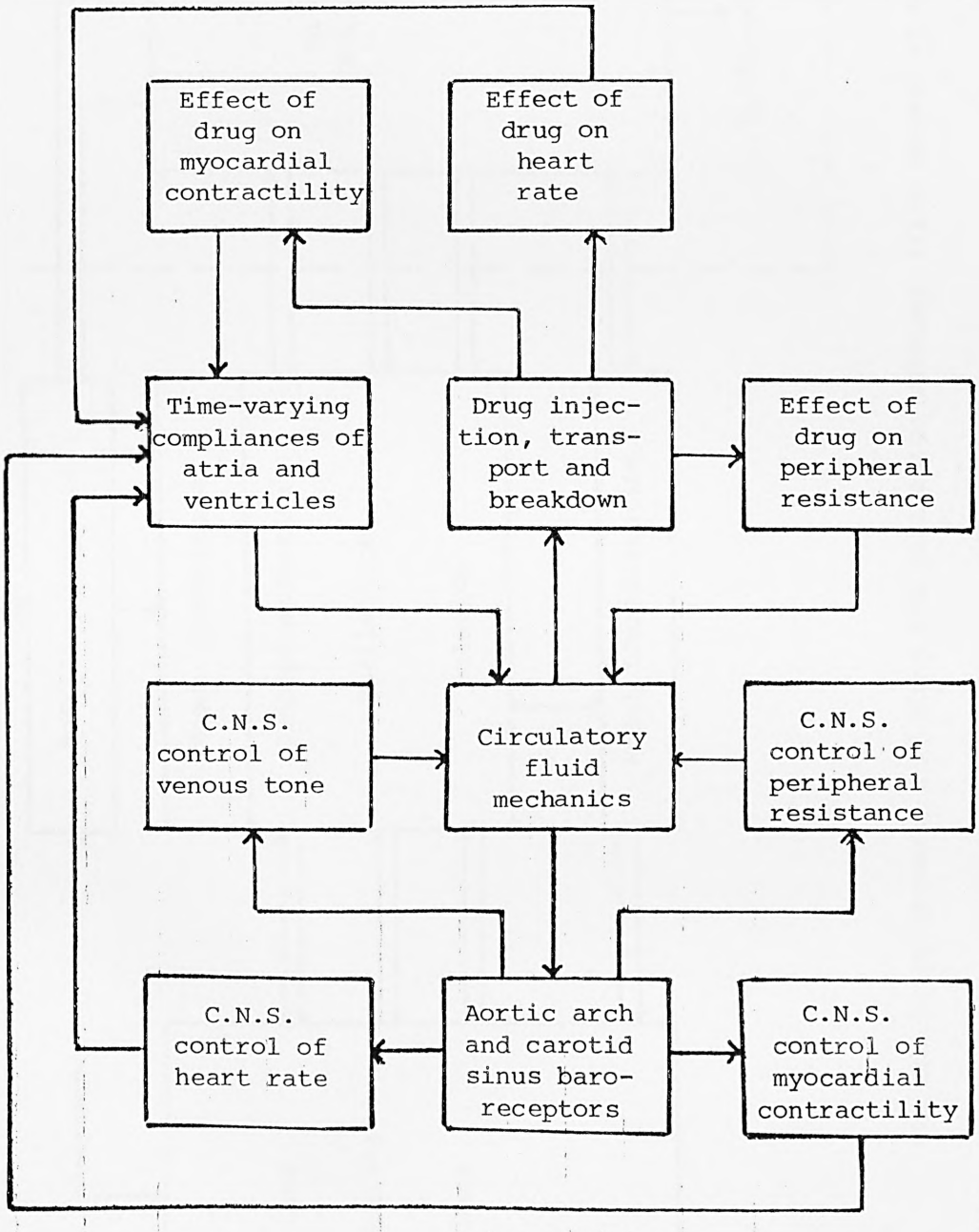

Figure 3.9 Interactions between sub-systems in the model.

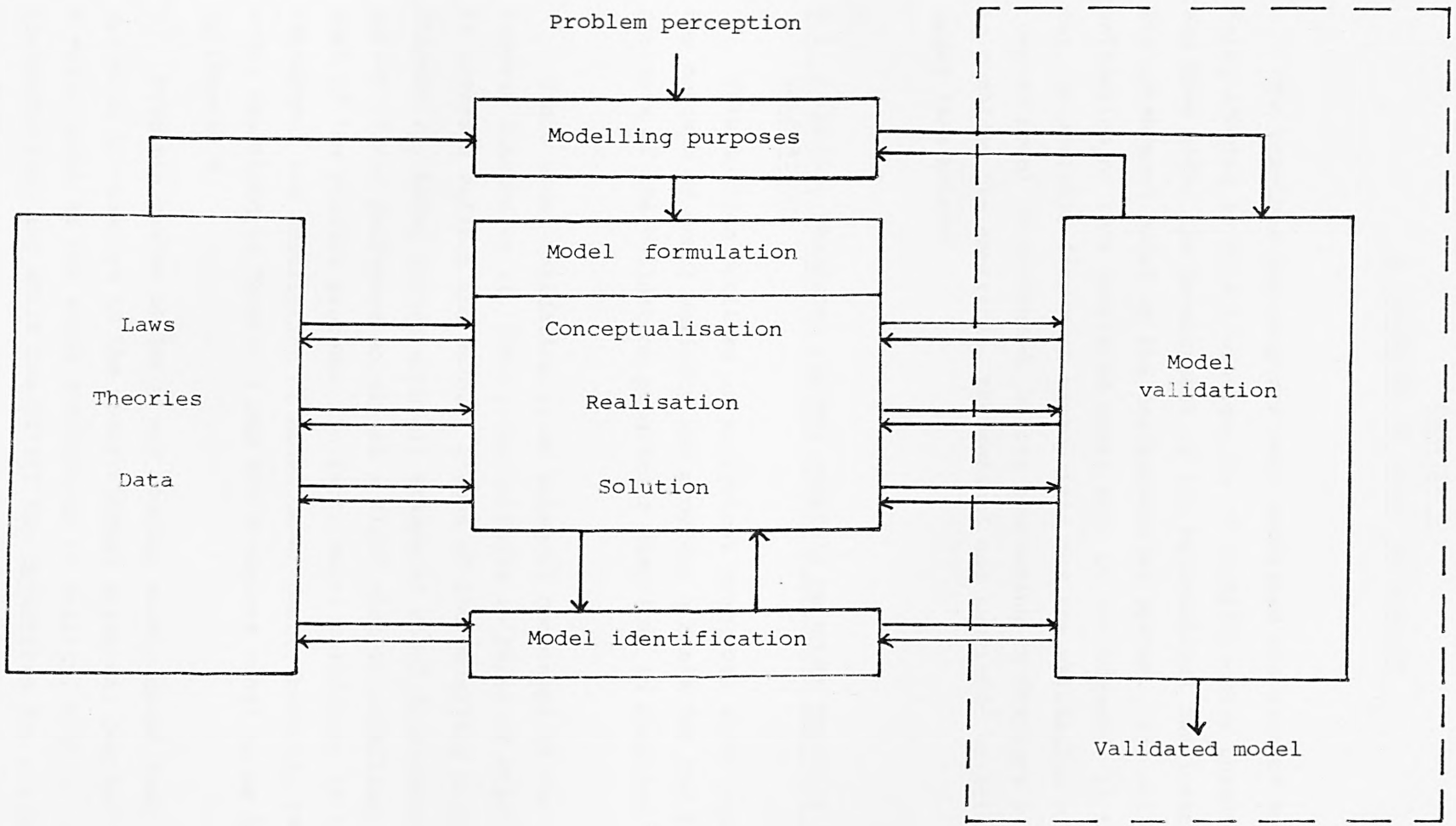

The modelling process, including the validation strategy (from Carson et al (1983)).

CHAPTER 4

A FRAMEWORK OF MODEL VALIDATION

The previous two chapters have explained the systems approach being adopted in this investigation of cardiovascular physiology, and have shown the development of the mathematical realisation of the 19-segment model of the cardiovascular system. The validity and validation of this completed model will be considered. In this chapter, an analytic framework appropriate for the validation of this complex model is presented, before proceeding in Chapters 5, 6 and 7 to consider the empirical, theoretical and heuristic validity of the model (see below).

4.1 A GENERAL FRAMEWORK FOR THE ANALYSIS OF MODEL VALIDITY AND VALIDATION

This section outlines an analytical framework which explains the concept of model validity and provides a basis for the rational analysis of the validation programmes described in Chapters 5, 6 and 7.

Since model validation is an integral component of the modelling process (Carson et al, 1983), the criteria in terms of which validity is assessed reflect the several stages of the modelling process (see Chapter 2), being joined with all stages of model development. Validation is not performed solely as a final step in modelling, but is part of the overall process. In fact, model validation is included throughout the description of model development, both the 19-segment model described in Chapter 3 and the 8-segment model to be described in Chapter 9.

From his review of large and complex models drawn from a wide spectrum of examples in the observational sciences, Leaning defined a valid model as one which corresponds to reality, with no structural contradictions and which can fulfil the objectives for which it has been developed (Leaning, 1980).

Traditionally, model validation has mainly been treated as concerning only the determination of the empirical accuracy of a model. Such a treatment omits any assessment of important aspects such as the

role of the model in improving understanding and in suggesting new experiments and applications. These aspects are particularly relevant in the case of complex models such as the cardiovascular model under consideration here.

Validity should be regarded as a multidimensional concept reflecting the following (Carson et al, 1983; Leaning, 1980; Leaning et al, 1983a, b):

(i) Model objectives (which determine the range of application)

(ii) Current theories and experimental test data relating to the particular system of interest, together with other relevant knowledge. (The nature of measurement scales, direct and indirect measurement, uncertainty in data.)

Validity is assessed in terms of a number of criteria as explained below.

4.2 VALIDITY CRITERIA

The validity criteria, classed as internal and external criteria, express the various ways in which the validity of complex physiological models, such as that of the human cardiovascular system described in this thesis, is assessed (Carson et al, 1983; Leaning, 1980; Leaning et al, 1983a, b).

4.2.1 Internal Validity Criteria

These consist of tests which do not require reference to theories, data, etc., outside the model; they are prerequisite or necessary criteria. They are:

4.2.1.1 Consistency: which requires that the model contains no logical, mathematical or conceptual contradiction and should be complete.

4.2.1.2 Algorithmic: which requires that the algorithm for solution or simulation is appropriate and leads to accurate solution.

4.2.2 External Validity Criteria

These refer to modelling purposes, theories and data and include:

4.2.2.1 Empirical validity: which requires that the model (its structure and parameters) and its behaviour agree with empirical data over the range of application to the necessary level of resolution and/or data uncertainty. In Chapter 6, the empirical validity of the 19-segment cardiovascular model is examined in terms of its ability to reproduce response features and fit the time courses of experimental test data.

4.2.2.2 Theoretical validity: requires that the model is consistent with accepted theories or models.

These two criteria (4.2.2.1 and 4.2.2.2) should be applied at any stage within the modelling process in a recursive manner. In other words, they can be applied from the basic relationships used in the model. Assessment is carried out both qualitatively and quantitatively, as described below.

4.2.2.3 Progmatic validity: which is assessed by testing the extent to which the model satisfies the objectives of the use to which it is to be put, and whether the objectives have been met (particularly relevant with clinical models for prediction).

4.2.2.4 Heuristic validity: which assesses the potential of the model for scientific explanation, discovery and hypothesis testing.

4.3 MODEL VALIDATION PROCEDURES

The procedures to be used in validating the completed model essentially depend on the theoretical identifiability of the model.

4.3.1 Simple (Theoretically Identifiable) Models

Models where all the unknown parameters can be estimated using formal identification techniques, that is models which are theoretically identifiable, can be regarded as simple models in contrast to the complex forms such as the representation of the cardiovascular system (Carson et al, 1983; Cobelli et al, 1984). Whilst such models usually have a relatively simple structure, this class does, in fact, include all models where there is no mismatch between the structure postulated and the measurements which are available for model identification. The

validation strategy for this class of model involves assessment in terms of both numerical and statistical criteria arising from the identification procedures and also examination of the plausibility of the model in relation to current physiological thinking.

4.3.2 Complex (Theoretically Unidentifiable) Models

In contrast, complex models, such as that of the cardiovascular system, are those where not all the unknown parameters can be estimated using formal identification techniques (theoretically unidentifiable models). This class includes models which are linear but of high order with only a small number of variables accessible to direct measurement and models which incorporate non-linear, distributed or stochastic effects for which formal identification procedures are not generally available. Such models are essentially incomplete as there must be a very high degree of uncertainty with respect to both structure and parameters. Validation and experimental determination of structure and parameters are necessarily closely inter-related in such cases (Cobelli et al, 1984). The approach to be adopted involves first seeking to enhance the testability of the model through model simplification, improved experimental design, and model decomposition. If the testability cannot be increased to the stage where the model becomes theoretically identifiable, the validation procedure should continue by way of adaptive fitting (Carson et al, 1983). This involves, first, seeking a set of parameter values in the model such that the model response for one input/output experiment, say corresponding to a normal physiological condition, adequately matches the corresponding experimental test data. If this parameter set is not plausible, another must be sought that is within the physiologically feasible range. If this can be achieved, then the model can be said to be trained on this input/output experiment.

The model incorporating these parameter values is then tested against all other input/output experiments corresponding to the normal physiological situation and other relevant data. This testing by computer simulation should include the examination of model predictions for a wide range of test signals corresponding to both physiological and abnormal conditions. In all these tests the model must match the experimental data if it is to be deemed empirically valid in terms of the criteria described below. If further parameter adaption is needed in adequately matching the model to one of the experiments in

this test set, it will, of course, be necessary to go back and examine the effect of such parameter changes on all tests previously carried out. This test programme involves examining the effects of a single input upon a large number, if not all, of the system variables as well as examining the effects of input variation on individual variables.

Assessment of the empirical validity of the model in terms of model fit over this test set of responses is carried out using qualitative and quantitative feature matching and time course prediction. Normal and abnormal physiological responses are generally characterised by the presence or absence of certain dynamic features, and therefore a qualitative assessment of their occurrence or non-occurrence in the model response is a necessary component of the validation process. Such features may be simple, for example a rise or fall in one or more variables following the application of a stimulus, or complex, for example a biphasic or oscillatory response pattern.

The next step involves quantifying these distinctive qualitative features. This requires setting up an appropriate measure of distance between the features as predicted by the model and those seen in the available experimental test data: this distance being regarded as an error function which should be reduced to an adequate level if the model is to be valid.

Following these stages of qualitative and quantitative feature evaluation, ideally the whole time course of the model prediction should be examined against both the corresponding experimental test data and independent information from subsystem and unit process studies.

Having carried out the adaptive fitting procedures outlined earlier and having obtained a model fit that is deemed adequate, it is now necessary to examine the plausibility of the model. This involves examining both structure and parameters in relation to a number of factors such as model complexity, sensitivity of model outputs to uncertainty in model parameters (see Chapter 7) and the plausibility of the parameter values for any particular model structure.

4.4 PROBLEMS OF VALIDATING THE 19-SEGMENT MODEL OF THE HUMAN CARDIOVASCULAR SYSTEM

The central objective of modelling the human cardiovascular system, as explained in Chapter 3, was to produce a pulsatile mathematical model and computer simulation of the controlled cardiovascular system of a normal, resting, conscious, average human suitable for the study of short-term haemodynamics (1 - 3 minutes) and to use it for investigations of short-term pharmacodynamics. The complete model consists of 61 first order differential equations and 159 algebraic equations. Figure 4.1 shows the signal flows between the submodels and the various interacting control loops.

Given this complexity of model structure, the following particular difficulties arise in model validation:

4.4.1 Availability of Data

There is a lack of theory and/or data concerning portions of the structure and the behaviour of the system. In part this stems from difficulty in making measurements of anatomical parameters (see Chapter 5). Equally, many of the variables and parameters are unobservable and so validation has largely to be based upon overall input-output data.

4.4.2 Inter-relation of Model Structure and Behaviour

In examining the model, certain patterns of features of dynamic behaviour have been found to be closely linked to particular control strategies and model sub-structures included in the representation of the overall cardiovascular system (Leaning et al, 1982). This further highlights the need, when validating the complete model, to place emphasis first on the existence of qualitative characteristics in the model response and system data, as outlined in Section 4.3.2.

4.5 CONCLUSIONS

An analytical framework has been presented for model validation showing that validity is a multidimensional concept, closely related to the modelling objectives, and the nature of system data. Validity is essentially concerned with the representation of the system by the model within the domain of application.

An outline of the model validation process has been described in

this chapter. The degree to which validation can be achieved is critically dependent upon the availability of adequate data. The lack of such data is the major problem in validating large-scale models of complex systems, as evidenced in this particular study of the cardiovascular system.

In the chapter which follows, the availability of data on the 178 parameters of the 19-segment cardiovascular model will be considered, examining in particular the uncertainty in such data.

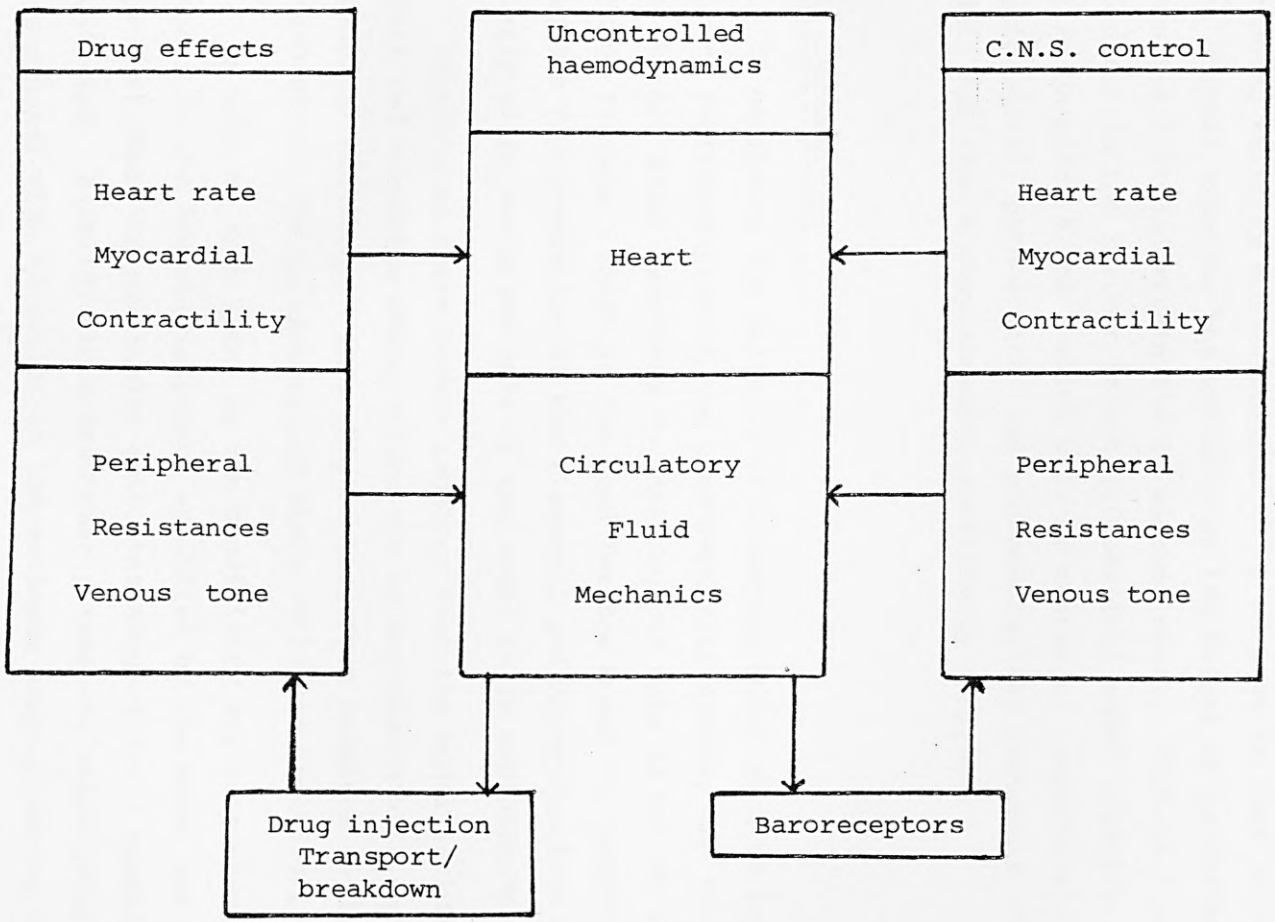

Figure 4.1 Interaction between subsystems in the 19-segment model of the human cardiovascular system.

CHAPTER 5

THE VALIDITY OF THE ESTIMATES OF PARAMETERS AND VARIABLES INCORPORATED WITHIN THE 19-SEGMENT MODEL

Having in the previous chapter outlined the general framework for model validity and validation to be adopted in this investigation, this chapter examines the validity of the values of parameters and variables included within the 19-segment model. This is a necessary precursor to the further investigations into model validity carried out in Chapters 6 and 7 which will be concerned respectively with physiological, pathological and pharmacological responses of the model, and then a comprehensive sensitivity analysis.

5.1 INTRODUCTION

In examining the validity of a complex model such as the 19-segment representation of the cardiovascular system, the fitting of the overall model responses to input/output data is not an adequate form of testing. There is the need for the model to constitute an adequate representation at the elemental and sub-system levels, particularly since the prime role of the model is in explanation.

Validity at these levels requires that the model includes parameters and variables whose values are in accordance with current physiological knowledge. This chapter therefore examines in detail the values of all the parameters and state variables included in the model.

As will be seen later in the sensitivity analysis carried out in Chapter 7, the overall responses exhibited by the model are critically dependent upon the particular estimates adopted for a number of the parameters. Equally, there are other parameters where uncertainty is less crucial with variation in the estimate adopted having little overall influence in changing the patterns of response to a number of physiological tests.

In this chapter, the aim is to focus upon existing knowledge of the parameters incorporated in the model, highlighting particular areas of uncertainty. The values used in the model should in general be in agreement with data, such as they are, as reported in the physiological and anatomical literature; and give rise to patterns of

overall behaviour in the model which are in general agreement with the corresponding experimental data (where this assessment of behaviour patterns involves more than just considerations of model fit to data as discussed in the previous chapter).

As will be seen, considerable uncertainty exists concerning many of the anatomical and physiological parameters, with apparently substantial differences between values reported by different research groups. Beneken (1965) has attributed this, in part, to variation in measurement techniques, but also suggests that some of the parameter values in the literature may have been chosen primarily for their ability to reproduce physiologically observed patterns of behaviour, leaving uncertainty as to whether such values are truly anatomical or physiological.

Parameter	Symbol	Physiological units	SI units
Pressure	P	torr	0.133 kPa
Volume	V	cm^3	1×10^{-3} ℓ
Flow	F	$cm^3\ s^{-1}$	1×10^{-3} ℓ s^{-1}
Time	t	s	1 s
Resistance	R	torr cm^{-3} s	133 kPa ℓ^{-1} s
Compliance	C	$torr^{-1}\ cm^3$	7.518×10^{-3} kPa^{-1} ℓ
Elastance	a	torr cm^{-3}	133 kPa ℓ^{-1}
Inertance	L	torr $cm^{-3}\ s^2$	133 kPa $\ell^{-1}\ s^2$

Table 5.1 Conversion table from physiological units to SI units

5.2 PARAMETERS AND VARIABLES OF THE 19-SEGMENT MODEL OF THE HUMAN CARDIOVASCULAR SYSTEM

Simulation of the overall model requires knowledge of 178 parameters and the initial conditions of 61 state variables. In this section the sources of information are examined in order to gain insight as to the confidence that can be attached to the adopted parameter and state variable values. The units adopted in the model are largely those currently employed in physiological practice. Table 5.1 lists

these physiological units together with their correspondence to SI units.

5.2.1 Parameters

Within the circulatory component of the model, the required parameters describe the anatomical and mechanical properties of the arteries, veins and heart chambers represented as lumped segments. Whilst the majority of these parameters can be treated as constants, the ventricular and atrial elastances, characterising the pumping action of the circulation, are functions of time.

The majority of these parameters cannot be measured directly, and furthermore do not correspond exactly to those parameters for which normal ranges are reported in the literature. Pullen (1976) based the parameter values incorporated in the circulatory model largely on those used by Beneken and DeWit (1967) and Hyndman (1970). Examining the values used by Beneken, which were reported in his 1965 paper, there is no specification of normal or reference range or any other measure of uncertainty. This leads to the need for sensitivity analyses, as will be reported in Chapter 7.

The parameters for the neural sub-system of the model are based on the empirical models fitted to data from dog experiments (Katona et al, 1967) since such sub-system studies cannot be performed on human subjects.

The parameters required to describe the local drug effects in the pharmacokinetic model are also not, in general, readily available. The values incorporated into the overall model depended upon the use of the "multiple modelling" technique of Beneken and Rideout (1968) and upon data obtained by Hughes (1971) from studies on conscious dogs using the same drug doses as adopted in the overall human model.

Having made these general comments, the sources of information for the adopted parameter estimates in the human cardiovascular system model can now be considered in detail, grouped according to the type of parameter.

5.2.1.1 Unstressed volume

As can be seen from Table 5.2, all the values of unstressed volume (V_U) incorporated into the circulatory model are those assumed by Beneken and DeWit (1967) which in turn were taken from Beneken (1965).

Unstressed volume, V_U	Model value (mℓ)	Beneken and DeWit value (mℓ)
V_{URA}	30.0	30.0
V_{URV}	0.0	0.0
V_{UPA}	50.0	50.0
V_{UPV}	460.0	460.0
V_{ULA}	30.0	30.0
V_{ULV}	0.0	0.0
V_{UAO1}	53.0	53.0
V_{UAO2}	61.0	61.0
V_{UUA}	114.0	114.0
V_{UUVN}	552.0	552.0
V_{UAO3}	59.0	59.0
V_{UIA}	17.0	17.0
V_{UIVN}	607.0	607.0
V_{UAA}	58.0	58.0
V_{UAVN}	305.0	305.0
V_{UCA}	63.0	63.0
V_{UCVN}	257.0	257.0
V_{UIVC}	488.0	488.0
V_{USVC}	488.0	488.0

Table 5.2 Parameter values for unstressed volumes

Unstressed volume is derived from the pressure/volume relationship:

$$P = \frac{1}{C}(V - V_U) \qquad \text{if } V > V_U$$
$$P = 0 \qquad \text{if } V \leq V_U \tag{5.1}$$

where P is the transmural pressure in the segment, C is the compliance

of the segment and V is the segmental volume. This means that unstressed volume is a parameter derived from the values of transmural pressure, compliance and volume which, in turn, is calculated as the product of the length of that arterial/venous segment and its average cross-sectional area.

For example, in calculating the unstressed volume of the pulmonary arteries (V_{UPA}), Beneken (1965) assumed a value of 17 torr for P_{PA}, regarding this as a value which had general physiological acceptance. The sources of the assumed values of compliance are given in Section 5.2.1.2. The value of C_{PA} adopted was 4.3 $torr^{-1}$ cm^3 $(33 \times 10^{-9}$ kg^{-1} $m^4 s^2)$, this being derived from Noordergraaf (1963), Noordergraaf et al (1963), and Westerhof et al (1965). The value of pulmonary arterial volume (V_{PA}) was taken as 120 cm^3, the product of cross-sectional area $\pi \times 1.3^2$ cm^2 and length of segment 23 cm. This results in:

$$V_{UPA} = 120 - 4.3 \times 17 = 50 \text{ cm}^3 \ (= 50 \text{ ml}) \qquad (5.2)$$

No indication is provided as to uncertainty associated with these measures. Assuming an inherent uncertainty of $\pm$ 10% in the values of length, area, pressure and compliance, generally within the range of experimental error, the possible range of value for V_{UPA} would be from 12 - 88 ml. A similar pattern of uncertainty applies to the estimates of all the other segmental unstressed volumes.

5.2.1.2 Compliance

The values of compliance incorporated into the circulatory model, together with values reported in sources used as the basis for these model estimates, are listed in Table 5.3.

The compliance of each segment is calculated from the corresponding values of pressure and volume. Considerable uncertainty arises with such estimates, however, as can clearly be seen from Table 5.3, where it should be noted that all these sources refer to models of the circulatory system rather than the original experimental data. In part this is attributable to differences in specification of the various segments, with those included in the model (as based on the work of Beneken and DeWit, 1967) not corresponding exactly to the anatomical definition of the blood vessel or vessels used by the investigators, whose results are included in Table 5.3. Furthermore,

Compliance C	Model value ($torr^{-1}$ cm^3)	Values in published sources as listed below ($torr^{-1}$ cm^3)
C_{PA}	4.3	4.3^{A}
C_{PVN}	8.4	8.4^{A}, 25.0^{E}
C_{AO1}	0.28	$(0.0702, 0.067)^{B}$, 0.28^{A}, 0.2^{C}, $(6.92 \times 10^{-5}, 6.92 \times 10^{-5})^{D}$
C_{AO2}	0.29	$(0.039, 0.069)^{B}$, 0.29^{A}, 0.2^{C}, $(4.42 \times 10^{-5}, 8.58 \times 10^{-5})^{D}$
C_{UA}	0.33	0.33^{A}, 0.278^{C}
C_{UVN}	9.4	9.4^{A}
C_{AO3}	0.29	$(0.079, 0.033, 0.03)^{B}$, 0.29^{A}, $(0.147, 0.147)^{C}$, $(7.8 \times 10^{-5})^{D}$
C_{IA}	0.06	0.06^{A}
C_{IVN}	10.6	10.6^{A}
C_{AA}	0.21	$(0.027, 0.024, 0.021)^{B}$, 0.21^{A}, $(0.1, 0.69, 0.182)^{C}$, $(5.76 \times 10^{-5}, 5.7 \times 10^{-5}, 5.76 \times 10^{-5})^{D}$
C_{AVN}	5.1	5.1^{A}
C_{CA}	0.12	0.12^{A}, 0.182^{C}
C_{CVN}	4.8	4.8^{A}
C_{IVCN}	8.3	8.3^{A}
C_{SVCN}	8.3	8.3^{A}

Table 5.3 Parameter values for compliance of the segments of the circulatory model. (Published sources are: A - Beneken and DeWit (1967); B - Westerhof et al (1969); C - Brubakk and Aaslid (1978); D - Noordergraaf et al (1963); E - Beneken (1965).

Westerhof et al (1969) and Noordegraaf et al (1963) specify the circulatory system in a less aggregated form so that two or three of their segments in series correspond to one segment of the present model. The compliance values of these two or three segments from those sources are shown in parenthesis in Table 5.3. It is also interesting to note differences in value quoted by Beneken in 1965 and by Beneken and DeWit in 1967. For example, the compliance of the pulmonary veins is given as 25.0 and 8.4 $torr^{-1}$ cm^3, respectively. This apparent inconsistency might be due to the former value incorporating the compliance of the left atrium.

As with other parameters, there is a general dearth of experimental data on human subjects, with the majority of experimental investigations having been performed upon dogs and other animals either *in vivo* (e.g. Pedley, 1980) or *in vitro* (e.g. Cox, 1975). One exception is the work of Hayashi et al (1980) who have examined the stiffness and elastic behaviour of human intracranial and extracranial arteries. Thus, given the dangers involved in extrapolation from non-human data, the compliance parameters used in the model have to an extent been adopted for their ability to yield appropriate physiological patterns of overall model response.

5.2.1.3 Resistance

All the values of resistance (R) incorporated into the circulatory model are listed in Table 5.4, together with other model values reported in the literature including those on which the adopted values in this study were based.

As discussed in Beneken (1965), the pressure drop across the fully-opened cardiac valves is a quadratic function of the flow through the valves. Under normal conditions, however, this pressure drop is so small that a linear approximation - resistance - provides an adequate description of this pressure drop/flow relationship. Beneken assumed a pressure drop across an open valve of 0.25 torr for the mean flow and a cardiac output of 84.0 $m\ell\ s^{-1}$, leading to

$$R_{SV2\ RV} = R_{RVPA} = R_{PVLV} = R_{LVAO} = \frac{0.25}{84.0} = 3.0 \times 10^{-3}\ torr\ m\ell^{-1}\ s,$$

where in the terminology of the Beneken model SV2 is the systemic venous segment and AO is the aorta. The same values of resistance are used in the 19-segment model described in this current thesis for R_{RARV}, R_{LALV}, R_{LVAO1} and R_{RVPA}, as shown in Table 5.4.

Resistance R	Model value (torr cm^3 s)	Values in published sources as listed below (torr cm^3 s)
R_{RARV}	0.003	0.003^{E}
R_{RVPA}	0.003	0.003^{E}
R_{LUNG}	0.11	0.11^{A}
R_{PVLA}	0.007	0.007^{A}, 0.003^{E}
R_{LALV}	0.003	0.003^{E}
R_{LVAO1}	0.003	0.003^{E}
R_{COR}	12.0	12.0^{A}
R_{AO2}	3.10×10^{-5}	3.10×10^{-5} A, $(7.3 \times 10^{-5}, 17.0 \times 10^{-5})^{B}$, $(2.0 \times 10^{-4}, 7.2 \times 10^{-5}, 13.9 \times 10^{-5})^{D}$
R_{UA}	0.047	0.047^{A}
R_{AO3}	0.0009	0.0009^{A}, $(0.000298, 0.00121, 0.00173)^{B}$, $(0.0004, 0.0004)^{C}$, $(0.00037, 0.00037, 0.00037)^{D}$
R_{HEAD}	6.0	6.0^{A}
R_{UA}	0.226	0.226^{A}, 40×10^{-3} C
R_{BRONC}	12.0	12.0^{A}
R_{AA}	0.012	0.012^{A}, $(0.00216, 0.00269, 0.00339)^{B}$, 10×10^{-3} C, $(0.00068, 0.00068, 0.00068)^{D}$
R_{INT}	2.3	2.3^{A}
R_{IV}	0.166	0.166^{A}
R_{ABD}	57.0	57.0^{A}
R_{CA}	0.18	0.18^{A}, 40×10^{-3} C
R_{AV}	0.595	0.595^{A}
R_{LEG}	15.0	15.0^{A}

Table 5.4 (continued overleaf)

Resistance R	Model value (torr cm^3 s)	Values in published sources as listed below (torr cm^3 s)
R_{CV}	0.3	0.3[A]
R_{IVC}	0.015	0.015[A]
R_{SVC}	0.06	0.06[A]
R_{IA}	0.0014	0.0014[A]

Table 5.4 Parameter values for resistance to flow in the circulatory model. (Published sources are: A - Beneken and DeWit (1967); B - Westerhof et al (1969); C - Brubakk and Aaslid (1978); D - Noordergraaf et al (1963); E - Beneken (1965)).

Examining the model data presented in Table 5.4, substantial differences occur in the values adopted by the several research groups. For instance, more than four-fold differences occur in the values of R_{AO2}, R_{AO3} and R_{uA}. As with the parameters discussed in the previous two sections, these discrepancies are partly attributable to differences in definition of the segments in the aggregated representations of the circulatory system. Once again, there is a general dearth of experimental data on the resistance of arterial and venous segments.

5.2.1.4 Inertance

The model includes inertance parameters for eight of its segments. The values adopted, together with other published model values, are depicted in Table 5.5.

Similar comments apply here as for resistance and compliance with a near total absence of experimental data, compounded yet again by the different anatomical specification adopted in the segmental representation of the circulatory system as compared with normal anatomical practice. As can be seen from Table 5.5, all the values adopted in the 19-segment model were taken directly from those used by Beneken and DeWit (1967).

5.2.1.5 Segmental lengths

The values of length of each of the segments included in the model are listed in Table 5.6. Table 5.7 includes data used by Westerhof et al (1969) in his model relating to anatomical lengths of vessels together with associated values of elastic properties.

Comparison of the data on length presented in these two Tables indicates differences, in part due to difference in the anatomical specification of the vessels between the models, and also due to the fact that Westerhof et al further sub-divide some of the arteries and veins, giving rise for example to the two rows of data in Table 5.7 corresponding to the ascendens aorta.

Problems of measurement of blood vessel length. Given the geometrical complex of the circulatory system, a major problem arises in specifying the end points of each vessel (Caro et al, 1974). This leads to difficulty in assessing the validity of the values of segmental length included in the 19-segment model of the circulation as detailed below (Salman, 1981; Webster, 1980):

Inertance L	Model value (torr cm^{-3} s^2)	Values in published sources as listed below (torr cm^{-3} s^2)
L_{RV}	0.00018	0.00018[A]
L_{LV}	0.00022	0.00022[A]
L_{UA}	0.014	0.014[A], 0. 013[C]
L_{AO2}	0.00043	0.00043[A], (0.0004, 0.000857)[B], 0.0008[C], (0.00036, 0.00072)[D]
L_{IA}	0.0027	0.0027[A]
L_{AA}	0.014	0.014[A], (0.0035, 0.0039, 0.00446)[B], 0.006[C], (0.00186, 0.00186, 0.00186)[D]
L_{CA}	0.031	0.031[A], 0.013[C]
L_{AO3}	0.0038	0.0038[A], (0.0013, 0.0029, 0.0031)[B], (0.0004, 0.0004)[C], (0.00137, 0.00137, 0.00137)[D]

Table 5.5 Parameter values for inertance (L) of the segments of the circulatory model. (Published sources are: A - Beneken and DeWit (1967); B - Westerhof et al (1969); C - Brubakk and Aaslid (1978); D - Noordergraaf et al (1963)

Length	Model value x 10^{-2} m
ℓ_{AO2UA}	19.5
ℓ_{AO2AO3}	10.0
ℓ_{UVSVC}	18.0
ℓ_{AO3IA}	8.0
ℓ_{AO3AA}	16.0
ℓ_{IVCIV}	8.0
ℓ_{AACA}	48.0
ℓ_{IVCAV}	16.0
ℓ_{AVCV}	48.0
ℓ_{IVCRA}	10.0
ℓ_{SVCRA}	1.5
ℓ_{AO3RA}	10.0

Table 5.6 Parameter values of the length of various segments of the circulatory model.

Name of the artery	Length ℓ (cm)	Compliance C ($torr^{-1}$ cm^3)	Inertance L (torr cm^{-3} s^2)	Resistance R (torr cm^3 s)
Ascendens aorta	2.0	0.0702	0.00023	2.45×10^{-5}
" "	2.0	0.067	0.00024	2.69×10^{-5}
Aortic arch	2.0	0.039	0.0004	7.3×10^{-5}
	3.9	0.069	0.000857	17.0×10^{-5}
Thoracic aorta	5.2	0.079	0.0013	0.000298
" "	5.2	0.033	0.0029	0.00121
" "	5.2	0.03	0.0031	0.00173
Abdominal aorta	5.3	0.027	0.0035	0.00216
" "	5.3	0.024	0.0039	0.00269
" "	5.3	0.021	0.00446	0.00339
Aorta iliaca common	5.8	0.009	0.0107	0.0183
Aorta iliaca externa	5.8	0.0051	0.017	0.0472
Aorta iliaca externa	2.5	0.0023	0.0075	0.0203

Table 5.7 Data for a subject with a height of 175 cm and weight of 75 kg (Westerhof et al, 1969)

(i) ℓ_{AO2UA} (effective length from aortic arch to head and arm arteries)

The value included in the model is 19.5×10^{-2} m. This distance, however, can only be measured on the right side of the body because anatomically there is only one brachiocephalic trunk (measured as 3.4×10^{-2} m). On the left side the left subclavian (to the arm) and left common carotid (to the head) emerge directly from the aortic arch, in which case the distance between them is zero, as shown in Figure 5.1a.

(ii) ℓ_{AO2AO3} (effective length from aortic arch to thoracic aorta).

Anatomically it is impossible to define such a distance since the end of the arch is also the start of the thoracic aorta.

(iii) ℓ_{UVSVC} (effective length from the head and arm veins to superior vena cava)

Anatomically this length is ambiguous since there are two sets of veins in each side of the head and in the arms, and hence the end points of this segment are ill-defined.

(iv) ℓ_{AO3IA} (effective length from the thoracic aorta to intestinal arteries)

Once more there is uncertainty since anatomically there are three intestinal arteries. These are

(a) the coeliac artery ($\simeq 1 \times 10^{-2}$ m),

(b) the superior mesenteric artery ($\simeq 5.9 \times 10^{-2}$ m),

(c) the inferior mesenteric artery ($\simeq 5 \times 10^{-2}$ m),

these measures being as given in Westerhof et al (1969). Using other data contained in this same source, the distance from the thoracic aorta to the end of the coeliac artery is $(2.5 + 1.0) \times 10^{-2} = 3.5 \times 10^{-2}$ m; that from the thoracic aorta to the end of the superior mesenteric artery is $(2.5 + 1.5 + 5.9) \times 10^{-2} = 9.9 \times 10^{-2}$ m; and the distance from the thoracic aorta to the inferior mesenteric artery is $(2.5 + 1.5 + 5.3 + 5.0) = 14.3 \times 10^{-2}$ m.

(v) ℓ_{AO3AA} (effective length from the thoracic aorta to the abdominal arteries)

Anatomically it is not realistic to think in terms of such a distance because the start of the abdominal aorta coincides with the end

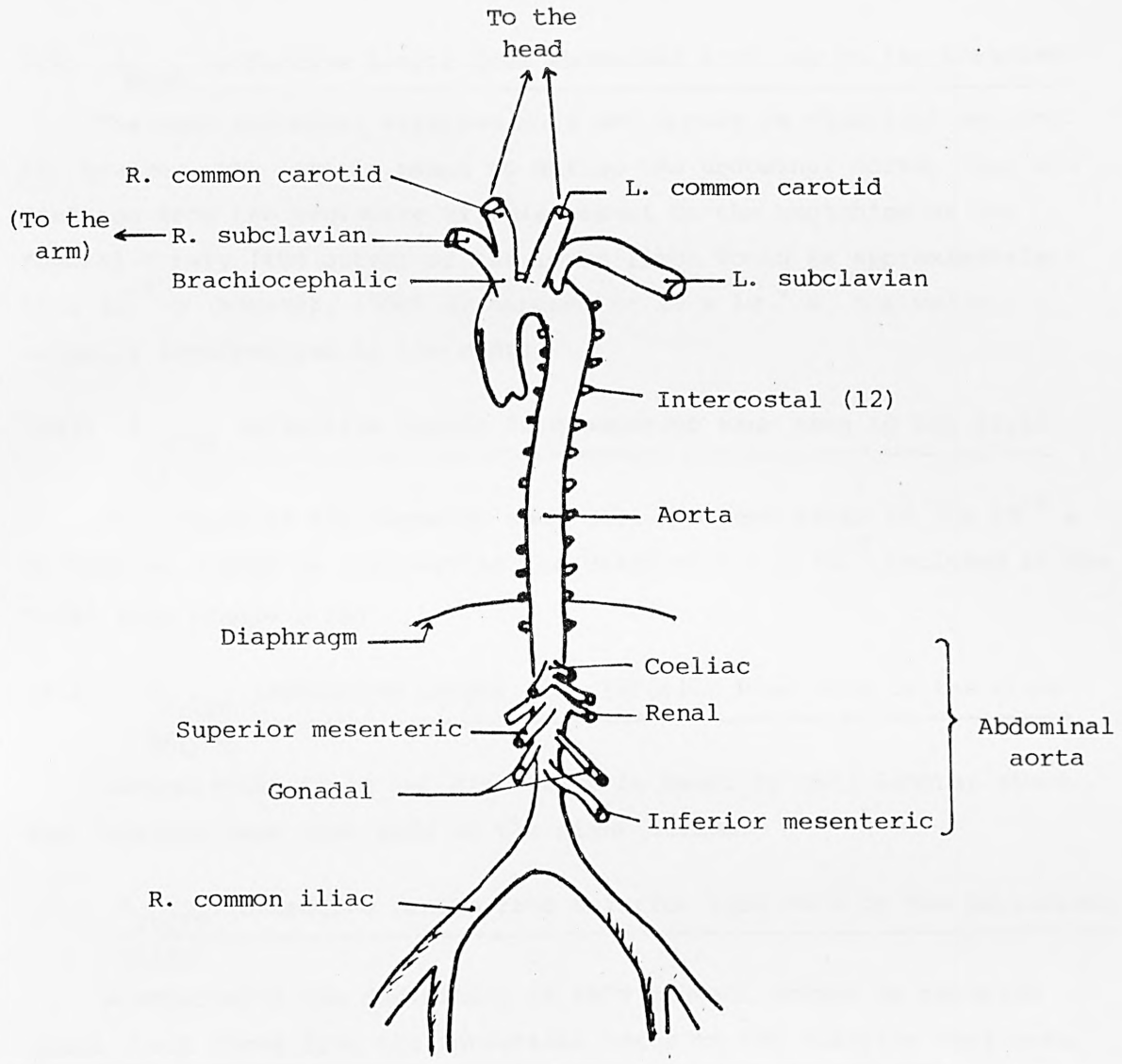

Figure 5.1a Main branches of the aorta

of the thoracic aorta. If, on the other hand, this distance is meant to correspond to that from the end of the thoracic aorta to the end of the abdominal aorta, its value would, according to Westerhof et al (1969), be equal to 15.9 x 10^{-2} m, which is approximately equal to the value used in the model.

(vi) ℓ_{AACA} (effective length from abdominal arteries to leg arteries)

The term abdominal arteries does not appear in classical anatomy. If, however, the term is meant to define the abdominal aorta, then the distance from the beginning of this vessel to the beginning of the femoral artery (the artery of the lower limb) would be approximately 12 x 10^{-2} m (Webster, 1980) as opposed to 48 x 10^{-2} m, the value actually incorporated in the model.

(vii) ℓ_{SVCRA} (effective length from superior vena cava to the right atrium)

The length of the superior vena cava has been given as 7 x 10^{-2} m by Webster (1980) in contrast to the value of 1.5 x 10^{-2} included in the model (see Figure 5.1b).

(viii) ℓ_{IVCRA} (effective length from inferior vena cava to the right atrium

Anatomically it is not clear what is meant by this length, since the inferior vena cava ends at the right atrium.

(ix) ℓ_{IVCIV} (effective length from inferior vena cava to the intestinal veins)

Anatomically the definition of this segment should be reversed since blood flows from the intestinal veins to the inferior vena cava. A similar comment applies to ℓ_{AO3IA}, but there is a further anatomical query since these veins do not drain directly into the inferior vena cava and, in addition, each vein drains via a different route.

(x) ℓ_{AVCV} (effective length from the abdominal veins to the leg veins)

The direction of flow is from leg veins to abdominal veins. The distance between the femoral vein (leg vein) and the inferior vena cava is specified by Webster (1980) as approximately (4 - 5) x 10^{-2} m. The model adopts a value of 48 x 10^{-2} m.

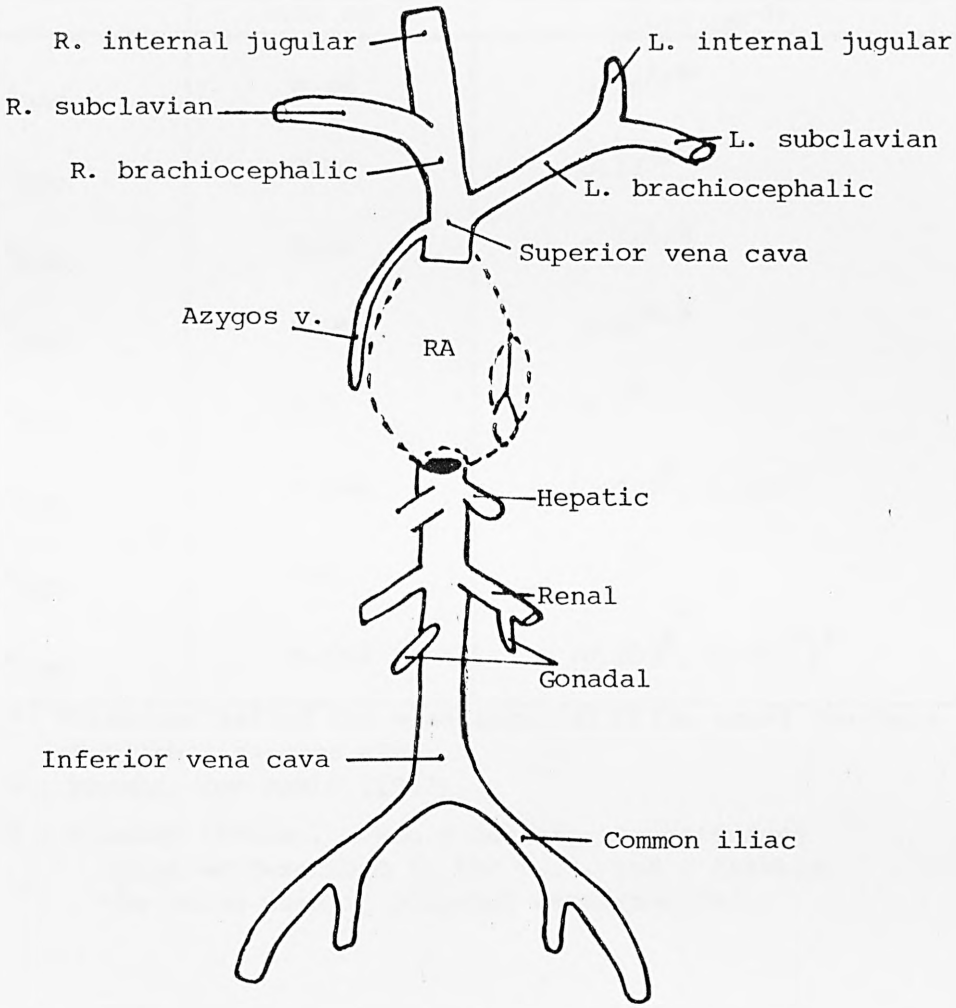

Figure 5.1b Vena cavae and main tributaries

5.2.1.6 Elastances

The values of the diastolic and systolic elastances of the heart chambers incorporated in the model are listed in Table 5.8, together with values used in other models reported in the literature.

Elastance (a)	Model value (torr cm^{-3})	Values in published sources (torr cm^{-3})
a_{LAS}	0.28	$0.28^{A,B}$
a_{LAD}	0.12	$0.12^{A,B}$
a_{RAS}	0.15	$0.15^{A,B}$
a_{RAD}	0.05	$0.05^{A,B}$
a_{RVS}	0.3	0.3^{B}
a_{RVD}	0.046	$(0.027^{E}, 0.025^{C})^{B}$
a_{LVS}	1.5	1.5^{B}
a_{LVD}	0.067	$(0.053^{E}, 0.052^{C})^{B}$

Table 5.8 Parameter values for elastance (a) of the heart chambers. (Published sources are:
A - Beneken and DeWit (1967)
B - Beneken (1965a), where E denotes the estimated value as described in the text, and C denotes the value used in computer measurements)

The method adopted by Beneken (1965a) for estimating the values of elastance is illustrated by considering the elastance of the right ventricle during systole, a_{RVS}. In this case the right ventricular end-systolic pressure is assumed to be 24 torr and the end-systolic volume equal to the difference between the end-diastolic and stroke volumes (150 - 70 = 80 mℓ), so $a_{RVS} = \frac{24}{80} = 0.3$ torr $m\ell^{-1}$.

5.2.1.7 Normal thoracic and abdominal pressures

These two parameters are set at P_{THN} = - 4.0 torr and P_{ABDN} = + 4.0 torr in the model. These values are identical to those adopted by Rushmer (1976).

5.2.1.8 Cross-sectional area

The model includes values of two parameters of cross-sectional area corresponding to the pulmonary artery and the ascending aorta. The values used in the model are listed below with, in parenthesis, values reported by Patel et al (1964).

$$A_{PA} = 1.539 \times 10^{-4} \ m^2 \ (6.33 \times 10^{-4} \ m^2)$$

$$A_{AOl} = 1.539 \times 10^{-4} \ m^2 \ (6.4 \times 10^{-4} \ m^2)$$

There is thus a consistent fourfold discrepancy between these values. Furthermore the values adopted in the model appear to deviate substantially from the values cited in Guyton (1981) which are shown below in Table 5.9.

Segment	Cross-sectional area $\times 10^{-4}$ (m^2)
Aorta	2.5
Small arteries	20
Arterioles	40
Capillaries	2500
Venules	250
Small veins	80
Venae cavae	8

Table 5.9 Cross-sectional areas of the vessels of each type (Guyton, 1981)

5.2.1.9 Heart period

The value included in the model, TH(O) = 0.8264 s, is the same as that reported in Guyton (1981) for a normal, healthy, young adult.

5.2.1.10 Pharmacokinetic parameters

The values of the pharmacokinetic parameters used in the model are shown in Table 5.10.

The value of mass of drug included in the model was based by Pullen on data obtained from Hughes (1971). These data resulted from

Parameter		Model value
M	Mass of drug	70 μg
σ_1	Constant defining the sensitivity of the arterio venous resistance to change in drug concentration	400 mℓ μg^{-1}
σ_2	Constant defining the sensitivity of the heart period to change in drug concentration	50 mℓ μg^{-1}
σ_3	Constant defining the sensitivity of the individual systolic elastance to change in drug concentration	50 mℓ μg^{-1}

Table 5.10 Pharmacokinetic parameters

the injection of 1 μg kg^{-1} of noradrenaline and isoprenaline into conscious dogs. This value is, however, at variance with information provided by Kyriakou (1980). He reported results obtained by injecting a mass of approximately 3 μg of noradrenaline into a 70 kg human subject, corresponding to a dose per kilogram of 0.042 μg.

The sensitivity coefficients σ_1, σ_2 and σ_3 (for effects on peripheral resistance, heart rate and myocardial contractility, respectively) were determined by Pullen (1976) in an approximate manner using the following procedure:

(i) The average values of segmental concentrations obtained in the test involving the injection of a neutral substance into the head and arms veins segment were used as a rough guide to the average values likely to occur in the investigation of drug effects. The average concentration figures assumed by Pullen were:

ω_1 = 0.0025 μg $m\ell^{-1}$ for the vascular beds

ω_2 = 0.005 μg $m\ell^{-1}$ for the heart

ω_3 = 0.025 μg $m\ell^{-1}$ for the venous segment into which the injection is made.

(ii) He then assumed that the arteriovenous resistance in a vascular bed doubled on average in drug-induced vasoconstriction so that

$\sigma_1\omega_1 = 1$, giving

$$\sigma_1 = \frac{1}{0.0025} = 400 \text{ m}\ell\ \mu g^{-1}$$

(iii) He assumed that heart rate on average increased by 25% in drug-induced tachycardia so that

$$\sigma_2\omega_2 = 0.25, \text{ from which}$$

$$\sigma_2 = \frac{0.25}{0.005} = 50 \text{ m}\ell\ \mu g^{-1}$$

(iv) He finally assumed that the systolic elastance on average increased by 25% in drug-induced positive inotropy so that

$$\sigma_3\omega_2 = 0.25, \text{ giving}$$

$$\sigma_3 = \frac{0.25}{0.005} = 50 \text{ m}\ell\ \mu g^{-1}$$

The gross approximations and assumptions in this procedure were justified by Pullen (1976) on the basis of there being considerable variability in the human population and that, in the pharmacological literature, it is frequently only directions of change that are of interest. Considerable uncertainty, however, is clearly associated with these values.

5.2.1.11 Other parameters

All the other parameters fall into two categories. The first is those which are functions of parameters discussed in the foregoing sections whose uncertainty will be related to the basic uncertainties in its constituents according to the form of the functional relationship. The second is those which are constant whose values are chosen on the basis of yielding adequate overall model responses in simulation.

5.3 VARIABLES

The overall model contains 61 state variables together with an additional 112 variables which are computed during the simulation. The basis for the adopted values of the 61 state variables is as follows:

5.3.1 Volume

The values of volume adopted for the nineteen segments of the circulatory model are listed in Table 5.11. In a number of instances these values approximate closely to the model values adopted by

Beneken. These are also shown in Table 5.11.

State variable	Model value (mℓ)	Other published values (mℓ)
V_{RA}	153.63	80[B]
V_{RV}	132.32	125[B]
V_{PA}	114.86	120[A], 119[B]
V_{PV}	536.52	514[B], 630[A]
V_{LA}	104.02	80[B]
V_{LV}	131.27	125[B]
V_{AO1}	81.233	82[B]
V_{AO2}	90.243	91[B]
V_{UA}	146.39	147[B]
V_{UV}	546.85	597[B]
V_{AO3}	88.157	89[B]
V_{IA}	22.552	23[B]
V_{IV}	597.54	649[B]
V_{AA}	77.249	78[B]
V_{AV}	290.32	315[B]
V_{CA}	74.33	75[B]
V_{CV}	271.05	295[B]
V_{IVC}	534.00	530[B]
V_{SVC}	542.37	530[B]

Table 5.11 State variables corresponding to volumes of the segments of the circulatory model. (Published sources are: A - Beneken (1965); B - Beneken and DeWit (1967))

From systematic searching there is a general paucity of reported values of volume which correspond to the segmental configuration adopted in the model. Published data from experimental studies tend to relate to the aggregation of a number of segments, as evidenced by the values presented in Table 5.12.

Segments	Data (mℓ)	Percentage of the total blood volume
Pulmonary circuit	550 - 650[A] mℓ 440 mℓ[B]	10 - 12%[A] 8.8 - 15%[C]
Heart	400 - 600[A] mℓ 360 mℓ[B]	8 - 11%[A] 5%[C]
Systemic capillaries	200 - 250[A] mℓ	4 - 5%[A]
Arteries	500 - 700[A] mℓ	10 - 12%[A] 13%[C]
Veins	3500 - 4000[A] mℓ	60 - 70%[A]

Table 5.12 The distribution of blood volume in a recumbent 70 kg man, where total blood volume is 5.5 litres, that is 8% of body weight (Folkow et al 1971). (Published sources are: A - Folkow et al (1971); B - Mountcastle (1974); C - Guyton (1959))

5.3.2 Blood Flow

The initial values of the eight variables representing blood flow (F_{RVPA}, F_{LVAO1}, F_{AO1AO2}, F_{AO2UA}, F_{AO2AO3}, F_{AO3IA}, F_{AO3AA}, F_{AACA}) in the model simulation are derived from the corresponding values of pressure and the components of vessel impedance. Experimental data are confined to blood flow through body organs, as illustrated by the data presented in Table 5.13 and so no direct comparison is possible.

5.3.3 Variables and Parameters of the Neural Control Model

The neural control model for the 19-segment model of the circulation is based essentially on the work of Katona et al (1967). This had involved the development of a highly simplified empirical configuration of model in which the net effect at the brain of all the baroreceptor impulses was characterised by a single "input function". In the representation adopted by Pullen (1976), the Katona model was modified to provide separate components for the aortic arch and carotid sinus baroreceptors. The Pullen model also included an adaptation of the central nervous control of heart rate as postulated by Katona.

Organ	Weight (kg)	Blood flow (mℓ/min)	
		Total	Per 100 g tissue
Brain	1.5	750[A]	50
Heart	0.3	150[A] 250[B]	50
Liver	1.5	1500[A] 1300[B]	100
Kidneys (2)	0.3	1200[A]	400
Skeletal muscle	25.0	750[A] 1000[B]	3
Other organs	40.0	650[A]	1.5

Table 5.13 Approximate distribution of cardiac output of 5.0 ℓ/min in man at rest
(Published sources are: A - Lippold et al (1979); B - Folkow et al (1971))

Given the empirical nature of the neural control model, little theoretical basis exists for the values to be adopted for these neural control variables. Those values adopted here were largely taken from Katona et al (1967). Equally, any uncertainty in the parameters of the neural control model can only be assessed on the basis of sensitivity analysis, as described in Chapter 7.

Data for parameters and variables relating to the control of peripheral resistance, myocardial contractility and venous tone are based on results obtained by Hyndman (1970), who incorporated structures corresponding to bang-bang or on-off control. Again, sensitivity analysis provides the only means of assessing the effects of uncertainty in the parameters of these control loops.

5.4 THE NEED FOR ENHANCED EXPERIMENTAL DESIGN

The programme of model validation requires first that the representation of the cardiovascular system be an adequate description of the

behaviour exhibited by normal human subjects. Once this objective has been achieved, the further extent of the domain of validity can be examined by investigating model behaviour for various pathological conditions. Examining model behaviour, however, requires the provision within the model of appropriate values of the many parameters, together with initial conditions for the model variables. What is apparent from the foregoing sections is that, in general, adequate data from anatomical and physiological experiments are not available. This applies both in the case of normal, healthy young adults and also in the case of pathological effects and effects due to aging, as will be considered further in Chapter 6.

Having classified in the earlier sections of this chapter the parameter and initial values of variables of the model required for its implementation, it is clear that there is not only a dearth of specific values but, more important, a lack of data specifying "normal" or "reference" ranges. Where experimental data are available they have often been the result of animal experiments and hence uncertainty must exist regarding their transferability to the human subject. Given this paucity of data and hence uncertainty in the parameter values incorporated in the model, there must as a result be uncertainty in the output responses of the model. The model will thus be limited as to its predictive capability, if not its heuristic potential. The effects of uncertainty will be more crucial in some parameter estimates than in others and this will be highlighted in the sensitivity analysis presented in Chapter 7.

These deficiencies in anatomical and physiological data raise several questions. Why have such measurements not been made? Is it because they have not been required particularly in conventional anatomical investigations - or is it that the measurements are intrinsically not capable of being made, given the state of the art of measurement technology?

In the case of the lengths of the blood vessels, one complicating factor is that the definition of the segments of the circulatory subsystem of the model does not correspond to the standard anatomical classification of the arteries and veins. In discussions with anatomists, this has tended to obscure the real problem, namely the absence of adequate data, particularly on ranges of size of vessel. It is, however, reasonably clear that the absence of data at least in part

reflects the fact that anatomists have not in general been exposed to the needs of dynamic modellers with their requirement for precise quantitative measures. There is clearly a need for a dialogue with the community of anatomists, highlighting the need for and role of reliable accurate anatomical measurements in dynamic investigations of the cardiovascular system such as being described in this thesis. Specifically, there is, first, the need to resolve the question of what segmentation should be adopted for the circulatory system. Secondly, for the agreed set of circulatory segments, there is the need for precise and accurate measures of lengths and cross-sectional areas of the blood vessels. Such data should include data on the ranges of these measures for specific classes of human subject, by age, sex, in relation to height of the subject. The pursuit of such information would appear to offer the prospect of new lines of research within anatomy, providing motivation to seek ways of overcoming the difficulties of measurement which undoubtedly exist. Equally for the dynamic modeller there is the need to reconsider the segmentation of the circulatory system with a view to aligning it more closely with anatomical practice.

The second major area where better experimental data are required is in relation to the elastic properties of the blood vessels. These parameters are derived from measures of pressure and volume, in the latter case this often being obtained from the integral of flow measurement (between two segments of the circulatory system). There is therefore the need for improved measurement of pressure and flow, particularly using non-invasive techniques as the number of sites where measurement can be made directly on living subjects is clearly limited. A recent review of techniques available for the measurement of blood flow in man is given in Roberts (1982).

The most difficult area for measurement is clearly that of the neural activity where direct approaches will clearly be highly restricted in human studies for the foreseeable future. Whilst some additional data may be obtained from animal experiments, progress will depend upon the use of model-based measurement with the animal studies providing information for the refinement of appropriate models.

The final area where increased and more accurate data are required relates to the pharmacokinetic and pharmacodynamic components of the model. More measures are needed both for the concentration of drug in different sites following injection, as well as the more-readily accessible measures of overall system response to drug stimulus. Again, it can be hoped that dynamic modelling studies such as that described in this thesis can highlight the need for dynamic measurement and thus help to bring about enhanced experimental design.

5.5 CONCLUSIONS

This chapter has focussed upon the availability of experimental measures of parameters and variables included in the overall cardiovascular system model. Examination of the validity of the values incorporated in the model constitute an important part of the overall programme of validation, a part that needs to be considered before examining the validity of model responses to physiological and other stimuli.

From the descriptions presented in Sections 5.2 and 5.3, it is clear that the availability of experimental measures on human studies is severely limited. Many of the parameter values cited in the literature correspond either to experiments performed upon animals or to other modelling (as opposed to experimental) investigations. As a result, the uncertainty of parameter values included in the model gives rise to uncertainty in its predictive validity, although not necessarily diminishing its heuristic potential. Consequently there is a vital requirement to carry out a comprehensive programme of sensitivity analysis upon the model. This analysis, which will be described in Chapter 7, will also serve to provide more information as to the ranges of parameter values occurring in "normal" human populations, ranges which, in the absence of direct experimental evidence, have been based upon personal communication with experienced clinicians.

This chapter has highlighted the need for enhanced experimental design. For example, it would appear that a dialogue should take place with anatomists indicating the need for improved measures of lengths and cross-sectional areas of blood vessels, both as to specific values and to "normal" or "reference"ranges. It appears that these dynamic modelling studies have exposed the need for measurements not conventionally required. As such, this interdisciplinary investigation can assist in indicating new directions for anatomical research.

In terms of the overall programme of model validation, this chapter, examining the validity of the values of parameters and variables included within the cardiovascular system model, has constituted a necessary precursor to the further investigations into model validity which will be described in the next two chapters. Chapter 6 examines the validity of physiological, pathological and pharmacological responses of the completed model, whilst Chapter 7 details a comprehensive programme of sensitivity analysis.

CHAPTER 6

VALIDATION OF THE COMPLETE 19-SEGMENT MODEL

6.1 INTRODUCTION

In Chapter 5, as a first stage in considering the validity of the 19-segment model, the availability of data defining values of model parameters and variables was considered. It was shown that there was, in general, a paucity of data on human subjects and that, moreover, available data tended to be sparse so that, for example, the ranges of parameter values for a "normal" population could not be specified with any degree of confidence. This uncertainty in available data gives rise to uncertainty in the predictive validity of the model.

In this chapter the validity of the model is considered further, focussing on the empirical validity (see Section 4.2.2.1) of the complete form, drawing upon data from physiological and pharmacodynamic experiments. The aims are to demonstrate the potentialities and limitations of this model as a representation of a normal subject in relation to short-term haemodynamics with their associated rapid neural control, ignoring the other important mechanisms for long-term cardiovascular control such as hormonal and other chemical effects. Assessment of the empirical validity of the model is carried out using data and criteria appropriate to the domain of application.

Before proceeding to consider dynamic responses of the model, its steady state conditions are examined since physiologically plausible values of measurable circulatory variables in the steady state constitute a necessary condition for the model to be valid. The assessment is described in Section 6.2.

The model is then subjected to a number of standard physiological tests and the resultant haemodynamic changes are compared with those obtained from corresponding human studies. The four types of test performed, which are described in Sections 6.3 - 6.6, respectively, are:

(i) Valsalva manoeuvre,

(ii) blood volume changes,

(iii) postural changes,

(iv) drug effects.

This programme of model testing builds upon and extends the preliminary studies on the validation of the 19-segment model reported by Pullen (1976). A full account of the validity of the model, in qualitative and quantitative terms, is presented, and more generally the role of the validation process within the overall development of a complex model is described. The problems which emerged in obtaining adequate experimental data for validation are discussed.

In addition to examining model validity in relation to normal subjects, the domain of applicability is extended by examining data corresponding to diabetic patients and an athlete. Hypotheses are generated, in quantitative terms, for parametric changes within the dynamic processes of the circulation and its control which could account for the observed, abnormal patterns of response (see Sections 6.3 and 6.5).

The drug effects which are discussed in Section 6.5 include both short-term vasodilatation and vasoconstriction effects.

6.2 STEADY STATE CONDITIONS

Before considering the model responses to standard physiological tests performed upon the cardiovascular system, it is necessary to examine the steady state conditions of the 19-segment model as a representation of a recumbent, resting human subject.

Examination of available sources of literature reveals considerable variation in the normal (steady state) values given to major circulatory variables such as mean arterial pressure, systolic and diastolic pressures, stroke volume, cardiac output, heart rate and estimated total systemic resistance.

This variation may, in part, reflect natural variability within the human population, but is also a reflection of the experimental measurement procedures adopted which give rise to measurement uncertainty. For example, Mancia et al (1983) have reported that the effect of a clinician making measurement of systolic and diastolic blood pressures within the first five minutes of a period of consultation with a patient can result in values which differ substantially from true steady-state resting levels. The observed ranges of the measurement errors due to these emotional/anxiety effects for the groups of subjects studied were 4 - 75 torr for systolic pressure and 1 - 36 torr for diastolic pressure.

These effects were shown to be unrelated to age, sex, baseline blood pressure or the values of blood pressure measured at a later time during a doctor/patient consultation. This important component of error needs to be taken fully into account when measuring blood pressure by the cuff method.

Direct measurements of cardiac function in man are not generally possible since they would require surgical intervention. As a result, the two methods commonly used to measure cardiac output are the oxygen Fick method and the indicator dilution method. Uncertainty must be considered in each case due both to direct measurement error and also the effect of disturbances, such as changing patterns of respiratory function.

Table 6.1 lists the steady state values of major circulatory variables of the 19-segment model, together with ranges of experimental data drawn from a number of sources.

The steady state values of the model lie within the overall ranges given in Table 6.1, although the values of systolic, mean and diastolic arterial pressure are at the upper end of the ranges which would be expected in clinical practice (Bourdillon, 1981). (This point is also considered in the context of the 8-segment reduced model in Section 9.5.) In the model, mean arterial pressure (MAP) is obtained on a beat-by-beat basis by integration of the aortic pressure over one cardiac cycle. On the other hand, in standard clinical practice, MAP is calculated using the empirically derived equation:

$$MAP = \frac{1}{3}\left(PMAX - PMIN\right) + PMAX \qquad (6.1)$$

One component of any discrepancy between model-derived and experimental values of MAP could reflect pressure difference between the location of the measured value (bracheal artery) and the model-derived value corresponding to the ascending aorta, although this component of error is likely to be small. The high value of arterial pressure in the model is probably a consequence of the high left ventricular pressure together with uncertainties in the neural control sub-model (Leaning, 1981). Nevertheless, the model responses of these variables do provide a generally satisfactory representation of the steady state.

Variable	Model response	Data on normal human subjects	Overall range
Mean arterial pressure (MAP) (torr)	109.1	(96.0 - 100.0)^{A} and 110.0^{A} (for elderly subjects), (73.3 - 110.0)^{B}, 106.6^{D}, (95.0 - 103.0)^{E}, 92.0^{J}	(73.3 - 110.0)
Systolic pressure (PMAX) (torr)	130.9	120.0^{A,C,I}, 140.0^{D}, (100.0 - 150.0)^{B}, (110.0 - 130.0)^{F}, 125.0^{G}, (110.0 - 135.0)^{K1}, (105.0 - 128.0)^{K2}	100.0 - 150.0
Diastolic pressure (PMIN) (torr)	90.8	80.0^{A,C}, (60.0 - 90.0)^{B}, 90.0^{D}, 70.0^{I}, (60.0 - 80.0)^{F}, 75.0^{J}, (66.0 - 77.0)^{K1}, (61.0 - 73.0)^{K2}	60.0 - 90.0
Stroke volume (SV) (ml)	69.6	70.0^{C,G,J,K}, 77.0^{B}, 60.0^{F}	60.0 - 77.0
Cardiac output (CO) (ml s^{-1})	84.6	100.0^{B}, 66.6^{F}, 83.3^{C,G,J}	66.6 - 100.0
Heart rate (FH) (bpm)	72.9	75.0^{B,G,K}, (60.0 - 100.0)^{H}, 70.0^{C}, 72.0^{J}	60.0 - 100.0
Estimated total systemic resistance (ETSR) (torr s ml^{-1})	1.29	All calculated as $ETSR = \frac{MAP}{CO}$	

Table 6.1 Steady state values of variables of the 19-segment model and corresponding available data on normal human subjects drawn from the following sources: A - Guyton, 1981; B - Mountcastle, 1974; C - Keele et al, 1982; D - Rushmer, 1976; E - Bourdillon, 1981; F - Lippold et al, 1979; G - Hawker, 1979; H - Handbook of Physiology, 1965; I - Ganong, 1975; J - Vander et al, 1980; K - Weller et al, 1979 (K_1 - for men and K_2 for women of age 20).

In the sections which follow, qualitative and quantitative comparisons will be made between dynamic responses of the 19-segment model and corresponding experimental data for a number of standard physiological tests.

6.3 THE EFFECTS OF VALSALVA MANOEUVRE

The first of the physiological tests used to examine the validity of the mathematical model was the Valsalva manoeuvre. This manoeuvre (VM) is designed to raise intrathoracic pressure sufficiently to reduce significantly blood flow into the right heart during a prescribed time interval. It is thus a useful test of validity of the integrity of the cardiovascular reflexes in the model.

6.3.1 The Processes of the Valsalva Manoeuvre

The manoeuvre described by Valsalva (e.g. Lippold et al., 1979) consisted of a forced expiration against a closed glottis and was meant to clear the Eustachian tubes. The response to the manoeuvre can be considered to consist of four phases. There is an immediate rise in the arterial blood pressure with an elevation of both systolic and diastolic pressures. The rise lasts for a few heart beats and is proportional to the rise in intrathoracic pressure (Sharpey-Schafer, 1965). The reduction in the venous return is followed by a decrease in stroke volume, so the systemic systolic, mean, and pulse pressures begin to fall (the second phase). The reduced pulse pressure stimulates baroreceptor activity, and tachycardia and peripheral vasoconstriction result. The tachycardia increases progressively for the first ten seconds of this phase (Arenson, 1978). There is then a diversity in the patterns of response, with some subjects exhibiting a continuation of increasing tachycardia whilst others remain stable for the rest of this phase.

Forced expiration can, typically, be maintained only for between 10 and 25 seconds. At the end of this period there is a sudden release of intrathoracic pressure (the third phase). The loss of transmural aortic pressure support results in a further drop in mean systemic arterial pressure. The rush of blood through the heart in the face of a raised peripheral resistance causes an upward surge of arterial pressure (the fourth phase). The systolic pressure rapidly rises above the control (pre-stimulus) level, as also usually does the diastolic pressure.

As a consequence the pulse pressure is greater than it was at the beginning of the manoeuvre. This pulse exhibits an overshoot before returning to the resting level. There is a baroreceptor response to the raised pulse pressure which results in the characteristic bradycardia and peripheral vessel dilatation. The venous return increases as blood rushes back into the heart and cardiac output rises sharply, the effect being a large rise in arterial pressure.

The quantitative dynamic effects of a Valsalva manoeuvre on the blood pressure and heart rate of a normal human subject (in which the intrathoracic pressure rises by approximately 40 torr) are shown in Figures 6.1a - 6.1c. The principal qualitative features of the response to the manoeuvre are shown in Figures 6.2 (taken from Flessas et al, 1970) and 6.3 (from Arenson, 1978).

6.3.2 Model Response to the Valsalva Manoeuvre

The Valsalva manoeuvre is simulated in the 19-segment model by setting the intrathoracic and intra-abdominal pressures to +40 torr for a period of 12 seconds. Figure 6.4 shows the model responses of arterial pressure, stroke volume, cardiac output, heart rate and estimated total peripheral resistance.

In general there is qualitative agreement between the model responses of these variables and the experimental data shown in Figures 6.1 - 6.3. There are, however, a number of discrepancies which are as follows:

(i) In the first phase of the manoeuvre, blood pressure rises in both model response and all the data shown in Figures 6.1 - 6.3.The model heart rate response is in agreement with the data of Beneken and DeWit (1967) and Flessas et al (1970) with an initial decrease in value. On the other hand, the data of Arenson (1978) show no such decrease, but rather an immediate increase in heart rate.

(ii) In the data of Flessas et al (1970) and Sharpey-Schafer (1965) during the second phase, there is first a decrease in blood pressure followed, after a few seconds, by a rise due to peripheral vasoconstriction. The pulse pressure, however, is still less than at the beginning of the manoeuvre. The model response, however,indicates a continuing fall in blood pressure until the end of the period of forced expiration, thus revealing an inadequacy in the central nervous control

(a)

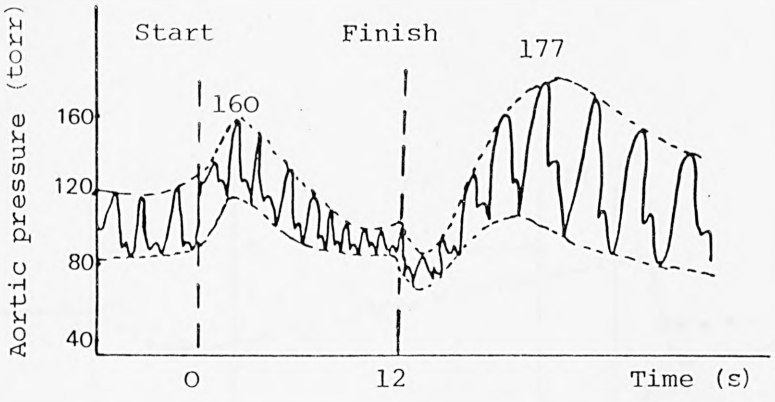

(b)

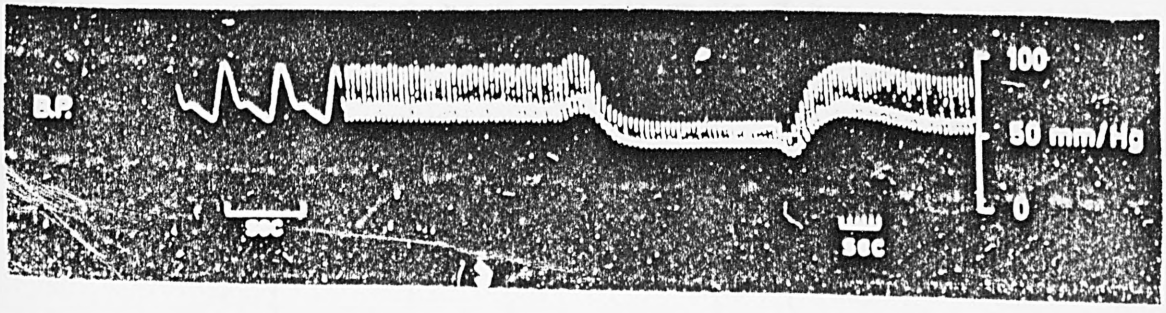

Figure 6.1 Effects of a Valsalva manoeuvre on the arterial pressure in man: (a) from Sharpy-Schafer (1965); (b) from Bushman (1981).

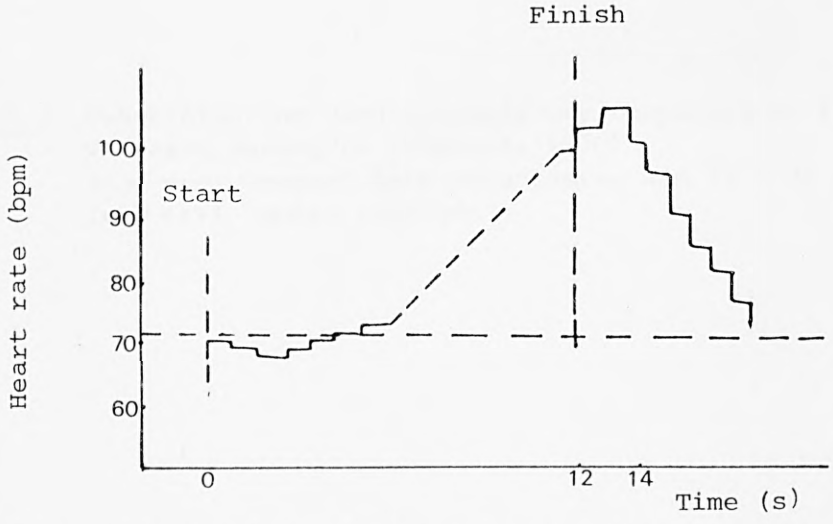

Figure 6.1c Effects of a Valsalva manoeuvre on the heart rate in man (from Beneken and DeWit, 1967)

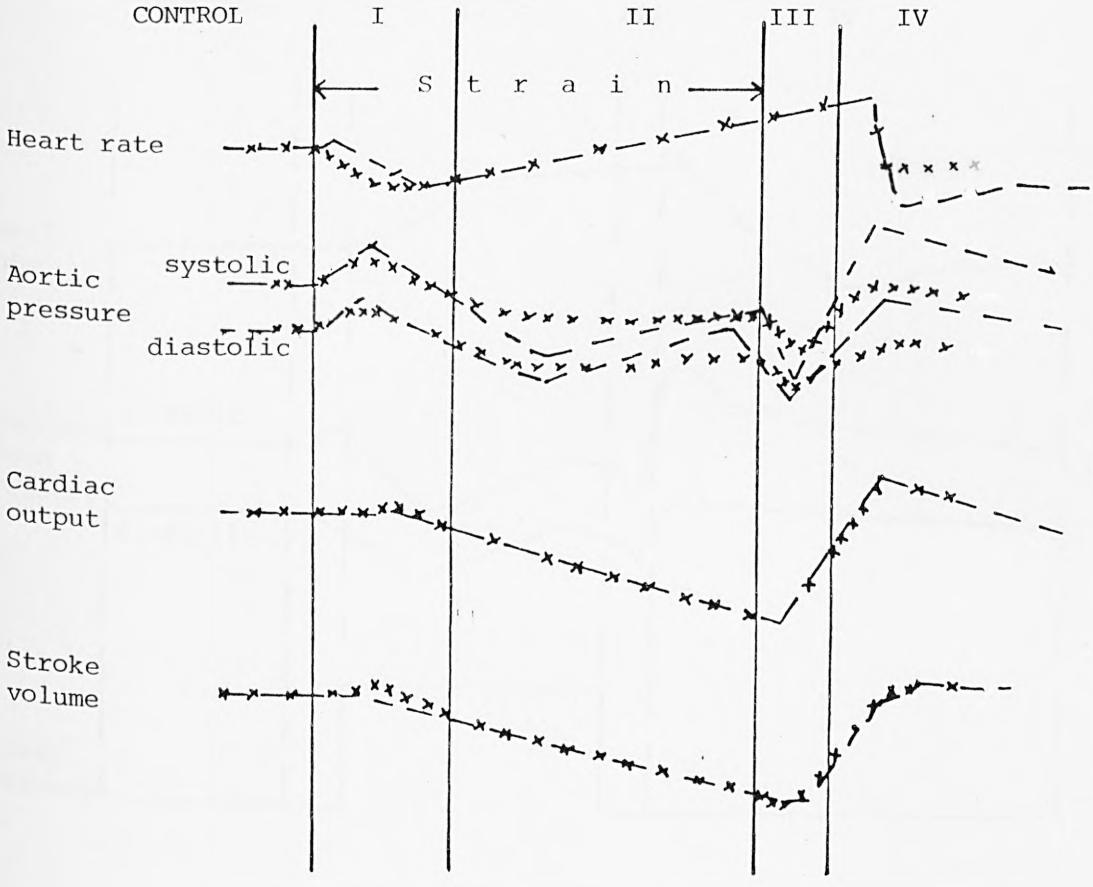

Figure 6.2 Describing the cardiocirculatory responses to the Valsalva manoeuvre (Flessas, 1970)
(– – – –) normal male volunteers, age 22 - 32 years;
(x x x x x x) model response

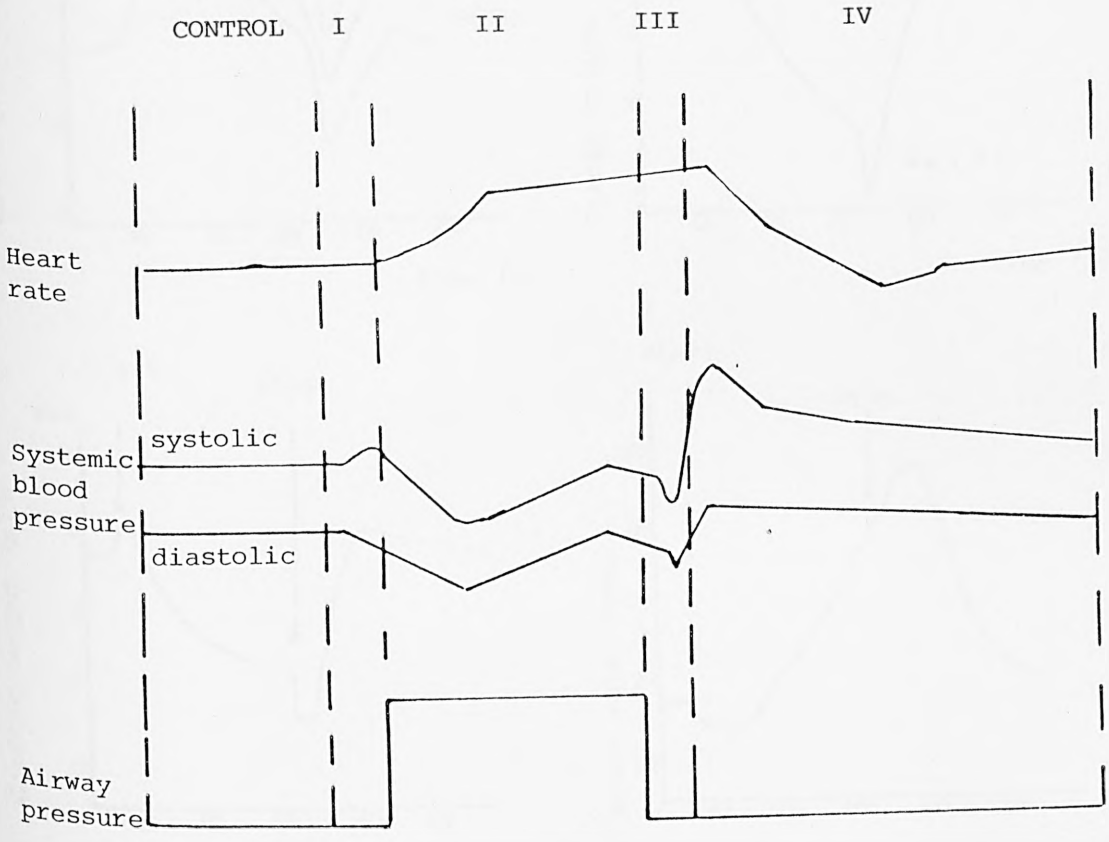

Figure 6.3 A schematic representation of the normal four phases of the Valsalva manoeuvre (Arenson, 1978).

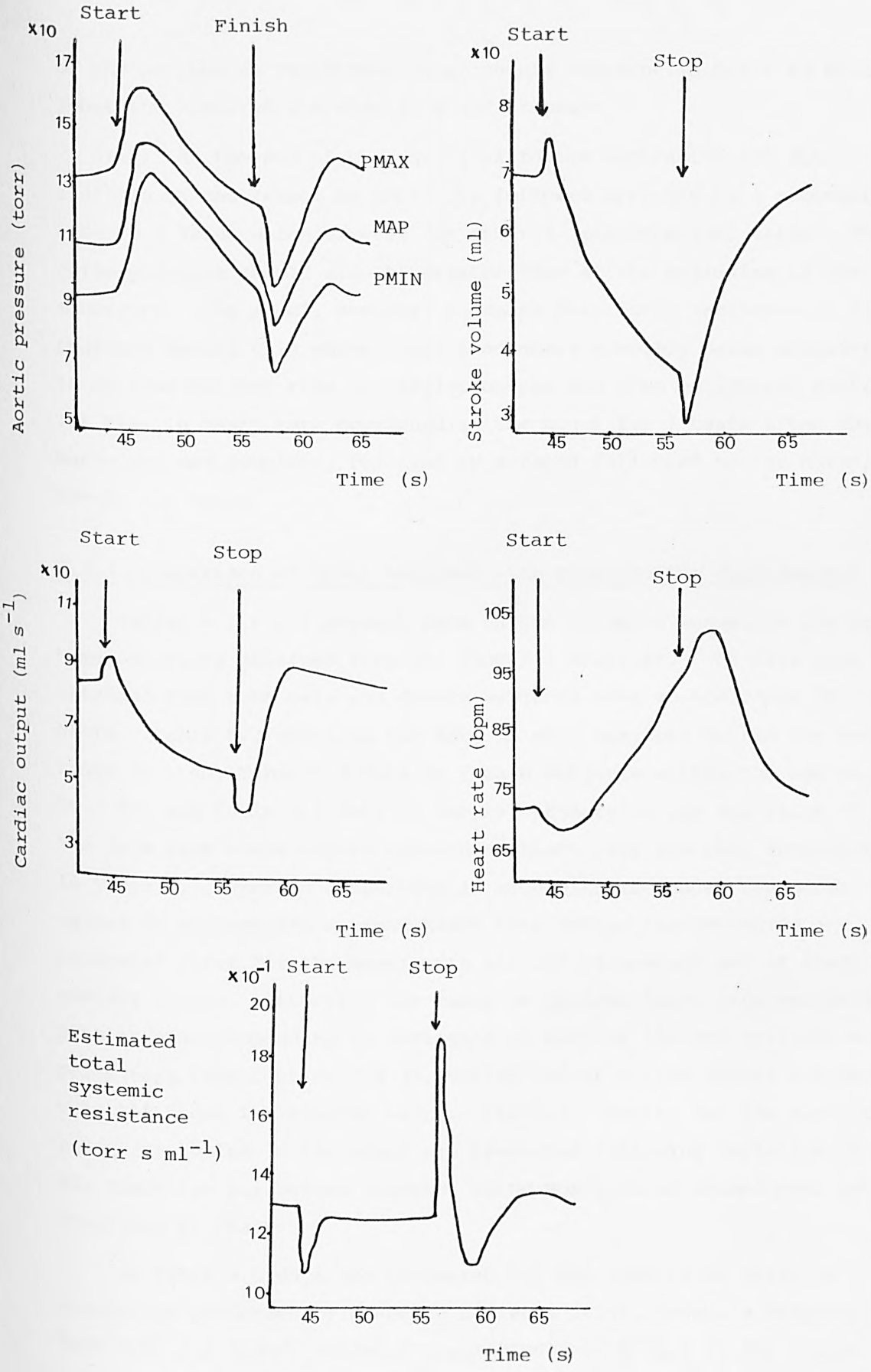

Figure 6.4 The dynamics in a Valsalva manoeuvre. The manoeuvre starts at t = 44 sec, with $P_{TH} = P_{ABD} = +40$ torr, and stops at t = 56 sec, with P_{TH} and P_{ABD} returning to normal values of -4 torr and +4 torr, respectively.

of the peripheral resistance which should increase in order to bring about the observed increase in blood pressure.

(iii) At the end of the period of forced expiration the data indicate an undershoot in pressure, followed directly by a substantial rise to a value which exceeds the control (pre-stimulus) value. The pulse pressure should also be greater than at the beginning of the manoeuvre. The model, however, produces only small increases in blood pressure during this phase, this inadequacy possibly being attributable to an insufficient rise in cardiac output and also peripheral resistance. The rise in heart rate continued in the model for 3 beats after the manoeuvre was complete, followed by a rapid fall back to the normal level.

6.3.3 Comparison of Model Response with Quantitative Experimental Data

Tables 6.2 - 6.4 present data on the Valsalva manoeuvre for normal human subjects obtained from St. Thomas's Hospital. The data were obtained from both male and female subjects over an age range 20 - 80 years. Table 6.2 contains the data on male subjects within the age range 20 - 40, Table 6.3 data on female subjects within the age range 20 - 40, and Table 6.4 data on female subjects in the age range 40 - 80. The data from these tables concerning heart rate are then summarised in Table 6.5, where a comparison is made with the model response. The values of minimum and maximum heart rate during the manoeuvre are presented first for the model with all its parameters set at their nominal values. Secondly, the range of maximum heart rate values is presented corresponding to variation of each of the ten critical model parameters (see Section 7.4.3), varied one at a time within a range of $\pm$ 15% about its nominal value. Finally, results for the maximum heart rate value in the model are presented following variation of all these ten parameters together using Monte Carlo techniques, as described in Chapter 7.

In Table 6.6 data are presented for the results of Valsalva manoeuvres performed by diabetic patients at St. Thomas's Hospital. Both male and female subjects are included with ages in the range 21 - 40 years. In order to simulate these data it was necessary to incorporate parameter changes reflecting the ways in which diabetic patients differ from normal subjects regarding the functioning of the cardiovascular system. One of the major effects which is believed to

Patient's No.	Sex	Age	Pre-stimulus heart rate (bpm)	Heart rate during the Valsalva manoeuvre	
				Low heart rate	High heart rate
1	M	40	53.6	43.47	79.47
2	M	39	84.25	54.29	115.38
3	M	38	59.9	59.11	84.50
4	M	38	54.49	43.79	100.84
5	M	37	70.21	45.45	110.09
6	M	36	69.58	45.28	92.30
7	M	35	86.41	60.91	108.10
8	M	35	65.23	50.20	89.55
9	M	35	55.3	48.00	75.94
10	M	34	82.00	41.81	122.44
11	M	32	55.62	49.38	93.75
12	M	32	82.33	53.81	129.03
13	M	31	63.9	52.63	94.48
14	M	30	67.74	56.87	84.50
15	M	28	90.5	67.03	131.86
16	M	27	64.34	44.94	103.44
17	M	27	73.03	66.29	95.23
18	M	26	76.08	63.82	102.56
19	M	25	89.22	49.38	120.0
20	M	25	53.04	50.47	79.84
21	M	25	64.85	54.79	81.08
22	M	24	55.33	46.51	87.59
23	M	24	69.92	56.07	85.71
24	M	24	68.3	55.55	109.09
25	M	23	67.3	104.34	52.17
26	M	22	75.2	64.17	92.30
27	M	22	68.0	59.88	81.40
Range	M	20 - 40	53.6 - 90.5	41.81 - 67.03	75.94 - 131.86

Table 6.2 Valsalva manoeuvre on normal male subjects aged 20 - 40 (St. Thomas's Hospital)

Patient's No.	Sex	Age	Pre-stimulus heart rate (bpm)	Heart rate during the Valsalva manoeuvre	
				Low heart rate	High heart rate
1	F	40	76.01	67.03	97.56
2	F	40	93.1	74.53	106.19
3	F	37	78.67	58.82	105.26
4	F	36	63.55	56.07	99.17
5	F	35	56.81	43.47	86.33
6	F	33	67.3	56.60	88.88
7	F	32	68.36	55.29	82.75
8	F	32	77.69	58.25	120.0
9	F	31	67.39	52.63	111.11
10	F	31	69.64	52.86	96.0
11	F	30	57.0	41.66	72.70
12	F	29	68.12	64.86	91.60
13	F	28	64.98	58.25	116.50
14	F	28	81.61	68.18	108.1
15	F	28	70.96	52.17	126.31
16	F	28	76.37	52.17	117.64
17	F	28	64.45	43.95	95.23
18	F	28	73.96	64.51	107.14
19	F	27	75.16	62.5	110.09
20	F	27	56.14	41.66	83.91
21	F	27	70.17	41.09	110.09
22	F	27	63.03	60.91	73.43
23	F	26	68.98	52.40	88.23
24	F	25	79.5	65.57	116.5
25	F	24	59.8	47.43	101.69
26	F	23	74.71	63.49	102.56
27	F	23	75.3	65.57	80.53
28	F	22	67.63	46.87	125.0
29	F	22	67.09	52.63	116.5
30	F	21	58.46	44.6	112.14
Range	F	21 - 40	56.14 - 93.1	41.09 - 74.53	72.70 - 126.31

Table 6.3 Valsalva manoeuvre test on normal female subjects aged 20 - 40 (St. Thomas's Hospital)

Patient's No.	Sex	Age	Pre-stimulus heart rate (bpm)	Heart rate during the Valsalva manoeuvre	
				Low heart rate	High heart rate
1	F	78	69.89	59.7	112.14
2	F	73	66.97	59.11	75.0
3	F	73	79.71	53.3	112.14
4	F	69	72.14	58.25	110.09
5	F	67	76.54	60.3	97.56
6	F	64	59.79	49.58	86.9
7	F	59	64.95	61.5	80.0
8	F	59	83.51	71.4	111.1
9	F	56	70.06	60.0	107.14
10	F	54	66.6	57.69	78.43
11	F	51	79.0	67.41	105.2
12	F	51	55.9	41.8	98.36
13	F	46	66.53	64.51	118.8
14	F	44	65.8	60.3	76.4
15	F	44	75.28	61.22	108.1
Range	F	40 - 80	55.90 - 79.71	41.8 - 71.4	75.0 - 118.8

Table 6.4 Valsalva manoeuvre test on normal female subjects aged 40 - 80 (St. Thomas's Hospital)

(a)

Number of patients	Sex	Age	Pre-stimulus range of heart rate (bpm)	Post-stimulus heart rate (bpm)	
				Range of minimum value	Range of maximum value
27	M	20 - 40	53.60 - 90.50	41.81 - 67.03	75.94 - 131.86
30	F	20 - 40	56.14 - 93.10	41.09 - 74.53	72.72 - 126.31
15	F	40 - 80	55.90 - 79.71	41.80 - 71.40	75.00 - 118.80
Model response			72.9	68.0	92.0

(b)

	Pre-stimulus range of heart rate (bpm)	Post-stimulus range of peak heart rate (bpm)
Empirical data for patients aged 20 - 80 years	53.60 - 93.10	72.72 - 131.86
Model response following perturbation of each ten critical parameters one at a time by ± 15% from their nominal values	67.98 - 80.33	84.50 - 107.80
Model response following perturbation of all the ten parameters together using the Monte Carlo approach	67.50 - 80.33	84.50 - 107.80

Table 6.5 Heart rate variation following the Vslsalva manoeuvre: (a) Empirical data showing range of pre-stimulus values and range of maximum and minimum post-stimulus values; (b) Empirical and model heart rate responses indicating the sensitivity of the model response to parameter variation.

Patient's No.	Sex	Age	Pre-stimulus heart rate (bpm)	Heart rate during the Valsalva manoeuvre	
				Min. heart rate	Max. heart rate
1	F	21	81.05	62.82	103.44
2	M	27	92.25	71.85	117.6
3	M	28	114.14	102.56	125.0
4	F	28	93.7	79.47	107.1
5	F	29	89.2	85.7	100.8
6	F	30	90.2	84.5	100.8
7	F	32	97.8	99.17	130.4
8	M	32	86.3	82.19	110.09
9	F	33	76.4	60.3	102.5
10	F	33	87.65	79.47	117.64
11	F	36	89.1	80.0	100.0
12	F	38	89.8	77.4	99.17
13	F	39	89.0	88.88	96.0
14	M	39	89.9	83.33	105.26
15	F	40	94.8	67.03	130.4
Range		21 - 40	76.4 - 114.14	60.3 - 102.56	96.0 - 130.4

Table 6.6a Experimental data on heart response to the Valsalva manoeuvre in diabetic patients

Compliance of arterial and venous segments	Pre-stimulus heart rate	Post-stimulus heart rate (maximum and minimum values)	
		Minimum value	Maximum value
Nominal (normal) values	72.9	68.0	92.0
All increased by 30%	87.66	80.33	107.6
All increased by 50%	95.13	87.16	118.2

Table 6.6b Model simulation of Valsalva manoeuvre examining the hypothesis of variation of compliance in diabetic patients.

occur in diabetic patients is a change in compliance of the arteries and veins, so that in effect a diabetic population of a given age range corresponds in this respect to an older normal population. It was this hypothesis that was tested using the model. Unfortunately, however, it was difficult to establish the extent to which change in compliance would occur in such a diabetic population, as reported in Table 6.6a. Two hypotheses were, therefore, tested. In the first case it was assumed that the compliance of all the arterial and venous segments would increase by 30% as compared to the nominal values, and in the second case that the increase was 50%. The results of model simulation for both these cases are given in Table 6.6b; these results correspond to pre-stimulus heart rate together with the minimum and maximum values of heart rate occurring during the Valsalva manoeuvre.

Comparison of these features of model and data indicate that the change of compliance by either 30% or 50% does lead to model results which are compatible with the observed data, whilst attempting to represent diabetic patients using a "normal" model results in a failure to match the observed peak heart rate value.

6.4 BLOOD VOLUME CHANGES

The second physiological test of the validity of the model involves examining its response to blood volume changes, both haemorrhage and transfusion.

6.4.1 Haemorrhage

Two sets of model responses following haemorrhage have been obtained. The first simulation, described by Pullen (1976), involved the sudden removal of 500 ml of blood from the model segment representing the head and arms veins. The results of this are shown in Figure 6.5. The second simulation corresponded to a typical blood donation and a comparison of model response and experimental data is given in Section 6.4.2.

Before considering the responses shown in Figure 6.5, it is appropriate to examine the dynamic physiological processes which occur as a result of a haemorrhage.

In general, haemorrhage results in a decrease of mean systemic filling pressure and consequently a decrease in venous return. As a

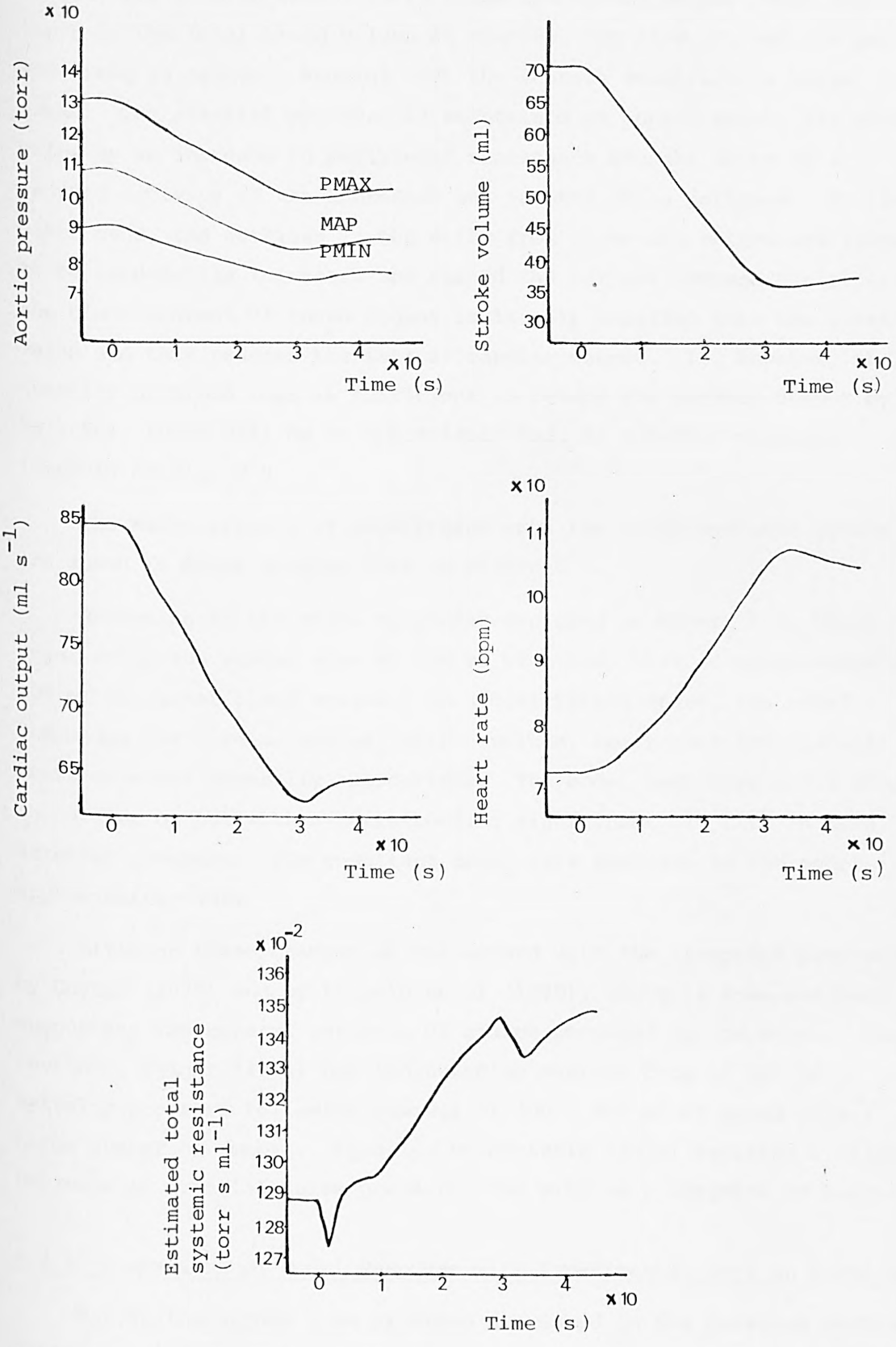

Figure 6.5 Dynamics following the sudden removal of 500 ml of blood from the segment representing the head and arms veins at t = 0 sec.

result, the cardiac output falls below its normal value. When one-tenth of the total blood volume is removed, the flow through the gut and limbs is reduced, showing that the vessels constrict in these areas. The arterial pressure is maintained at approximately its normal value by an increase in peripheral resistance brought about by a reduced activity of the depressor and carotid sinus reflexes. On the other hand, the outflows in the veins from liver and spleen are found to be temporarily increased and exceed the inflows through the arteries; the blood content of these organs is largely expelled into the great veins and this reduces the fall in cardiac output. If, however, the quantity of blood lost is sufficient to reduce the cardiac output by 30 - 50%, there will be an appreciable fall in arterial pressure (Lippold et al, 1979).

The major effects of haemorrhage upon the cardiovascular system are shown in block diagram form in Figure 6.6.

Returning to the model responses depicted in Figure 6.5, these result from the sudden loss of 500 ml of blood, that is approximately 10% of the total blood volume. In a qualitative sense, the model responses for cardiac output, stroke volume, heart rate and systemic resistance are generally appropriate. The model indicates a 23% drop in cardiac output with a corresponding significant 22% fall in mean arterial pressure. The resultant heart rate increase in the model is approximately 43%.

Although these changes do not accord with the viewpoint proposed by Guyton (1979) and by Lippold et al (1979), there is some evidence supporting the general patterns of change produced by the model. For instance, Wright (1955) has indicated an average drop of 10% in systolic pressure following removal of 400 - 500 ml of blood from a large number of donors. Equally, Mountcastle (1974) reported a slight decrease in arterial pulse pressure even with small degrees of haemorrhage.

6.4.2 Comparison of Model Response with Experimental Data on Blood Loss

Unlike the sudden loss of blood discussed in the previous section, experimental data on heart rate and systolic and diastolic arterial pressures are available following the removal of 420 ml of blood from donors (normal human subjects). Data from two subjects, obtained during a blood donor session at Moor House (North East Thames Region, DHSS), are shown in Table 6.7. The blood was removed over a period

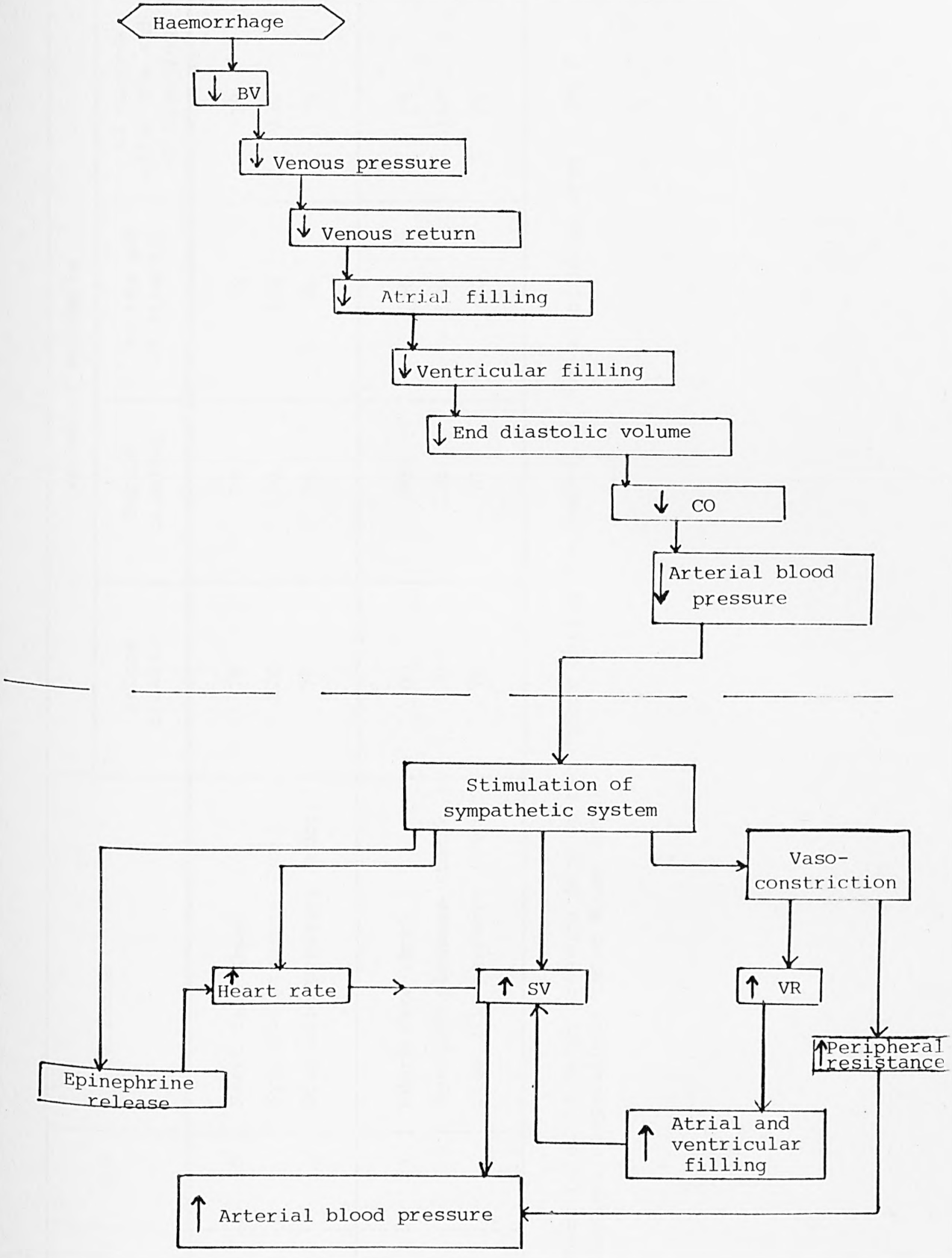

Figure 6.6 Block diagram showing the effects of haemorrhage on the cardiovascular system and the associated responses of the nervous system. (Note: ↑ = increase, and ↓ = decrease)

Donor's No.	Age	Variable	Values of variables			
			Before bleeding	During bleeding	At the end of bleeding	10 minutes after the end of bleeding
(1)	30	Heart rate (bpm)	78	78	78	78
		Systolic pressure (torr)	120	140	150	130
		Diastolic pressure (torr)	75	75	80	75
(2)	24	Heart rate (bpm)	60	60	56	58
		Systolic pressure (torr)	120	120	120	120
		Diastolic pressure (torr)	70	70	70	70

Table 6.7 Heart rate and blood pressure data on two donors during the removal of 420 ml of blood over 5 and 8 minutes, respectively (Moor House data)

varying from 5 - 8 minutes. Heart rate was measured as the pulse in the radial artery at the wrist and arterial pressure was measured using a sphygmanometer.

In the case of the first donor, an increase of systolic pressure by 25% was observed without any change in the heart rate. On the other hand, the second donor exhibited a constant systolic pressure, but heart rate decreased by 7% (4 beats per minute). The possibility of error in the pressure measurements needs to be considered, however, as discussed in Section 6.2.

A further set of experimental data was obtained from six donors (normal human subjects) at the North East Thames Regional Blood Transfusion Centre. The results obtained during and following the loss of 420 ml of blood are shown in Figure 6.7. The data on heart rate, index of stroke volume and index of cardiac output were obtained by transcutaneous aortovelography (TAV), a non-invasive Doppler ultrasound technique for measuring mainstream flow velocity in the aorta (Light et al, 1980). (Note that the technique yields not the stroke volume and cardiac output measures themselves, but rather values which are directly proportional to the variables, hence the prefix "index of" (Light et al, 1980).) Using TAV, beat-to-beat changes in stroke volume and the manner of left ventricular ejection were followed throughout a blood transfusion in six supine donors. Quantitative measurements of mainstream flow velocity were obtained from the highest Doppler shift present in the back-scattered signal. Direction-resolving signal processing and an on-line spectral analyser-recorder, providing immediate hard copy spectral recordings with grey scale on relatively inexpensive paper, are important features of the instrumentation. Such recordings indicate when the signals picked up are adequate and give visual discrimination between aortic signals and artefacts (Light et al, 1980).

Figure 6.7a shows the raw (unfiltered) data comprising beat-to-beat changes in index of stroke volume, index of cardiac output and heart rate obtained using the microprocessor-based TAV evaluator. This provides first, 3-point analysis by triangular approximation and, secondly, beat-to-beat analysis of these variables as shown in Figures 6.8a and 6.8b. Figure 6.7b presents the same data after removal of the high frequency noise using a recursive averaging filter (see Section 6.5.3.1). The arterial pressure was measured during the test using a cuff sphygmanometer.

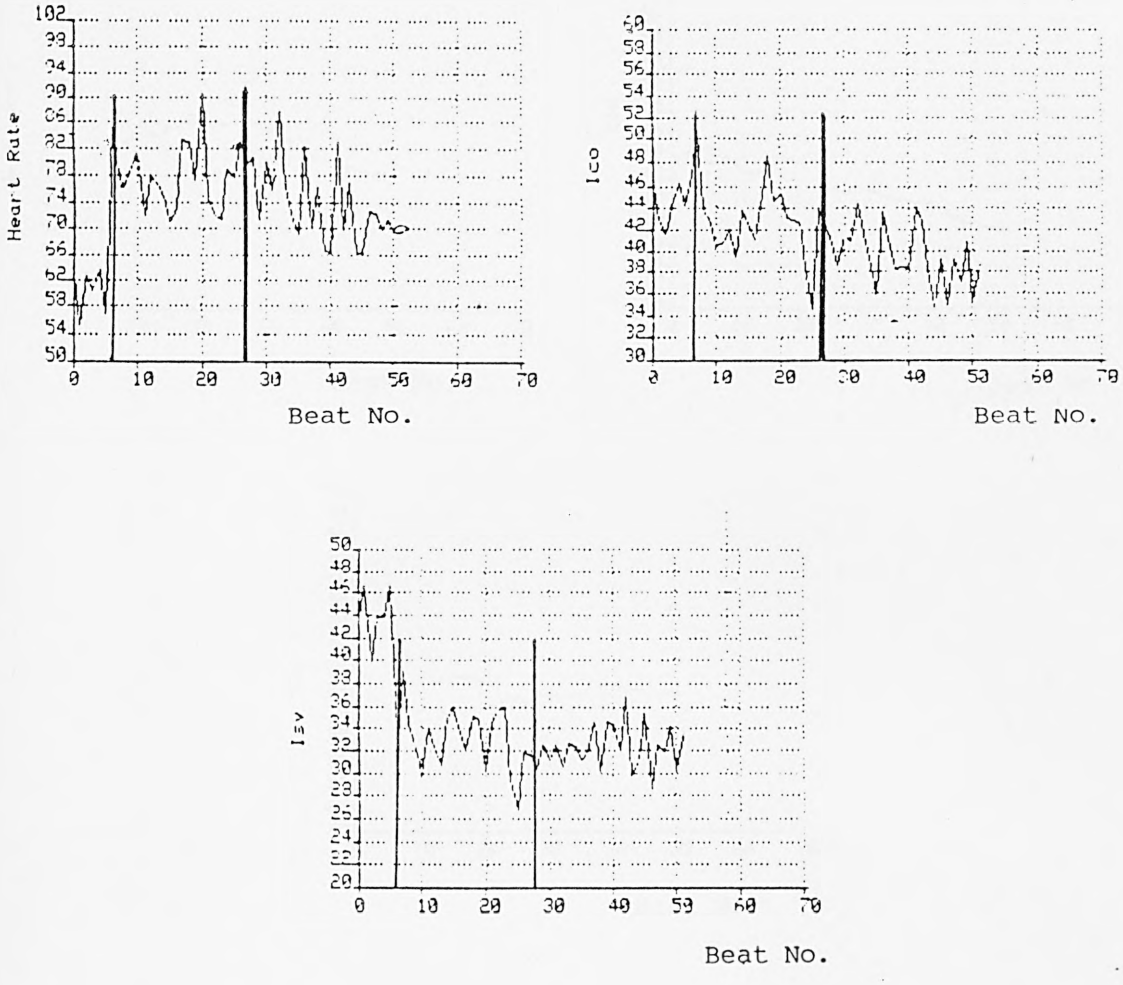

Figure 6.7a1 Raw data from subject BD1G(3) for the three variables as indicated during and following the loss of 420 ml of blood. The vertical lines indicate the times at which the bleeding starts and the end of bleeding.

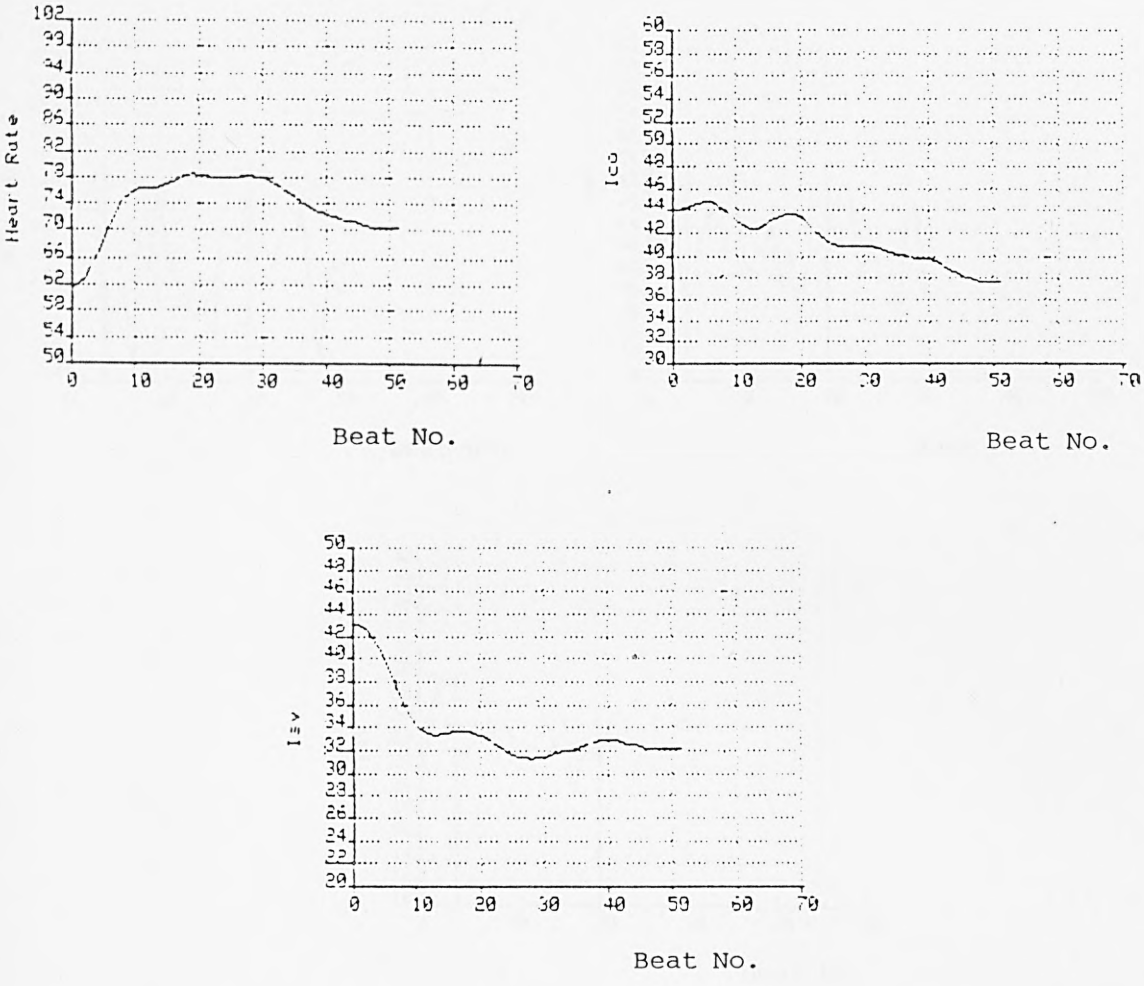

Figure 6.7b1 Filtered form of the data depicted in Figure 6.7a1 obtained using a recursive averaging filter.

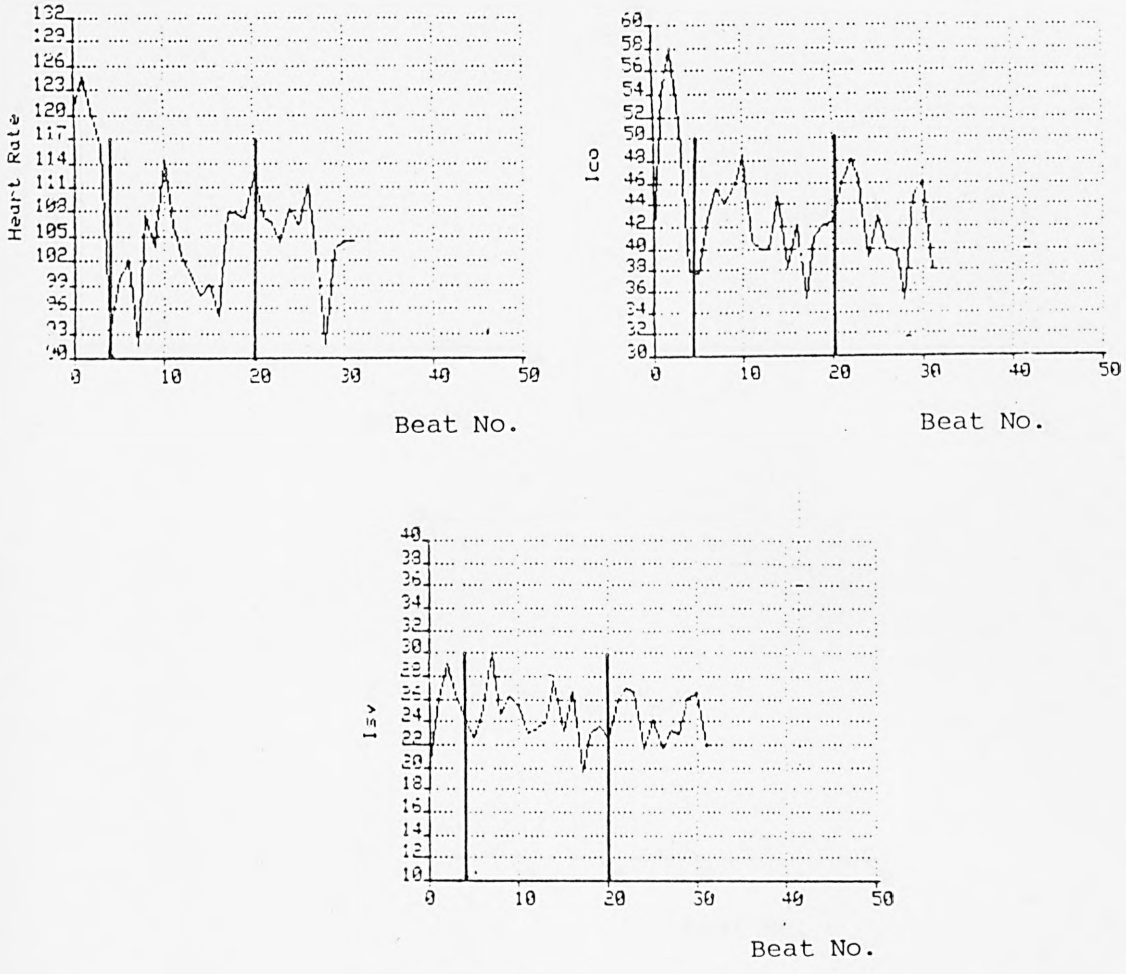

Figure 6.7a2 Raw data from subject BD2J(4) for the three variables as indicated during and following the loss of 420 ml of blood. The vertical lines indicate the times at which the bleeding starts and the end of bleeding.

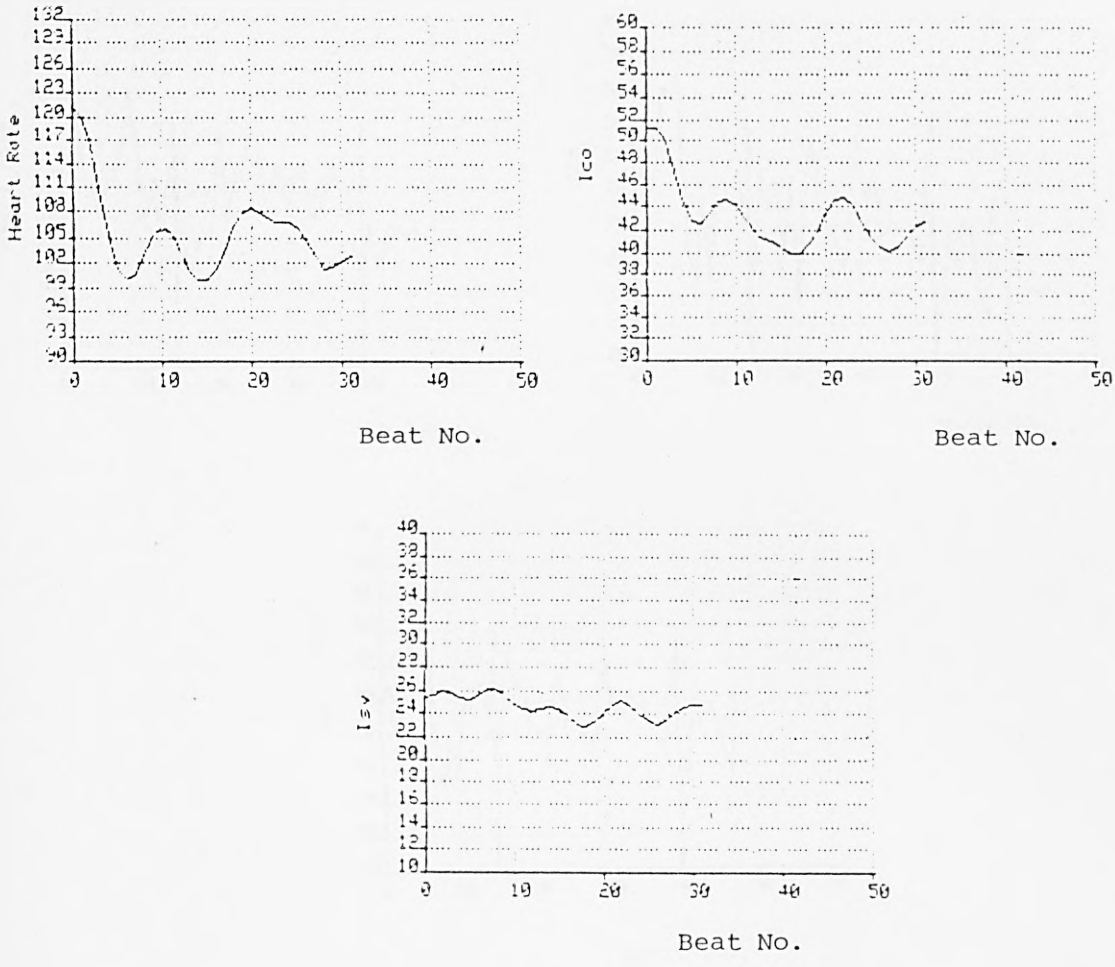

Figure 6.7b2 Filtered form of the data depicted in Figure 6.7a2 obtained using a recursive averaging filter.

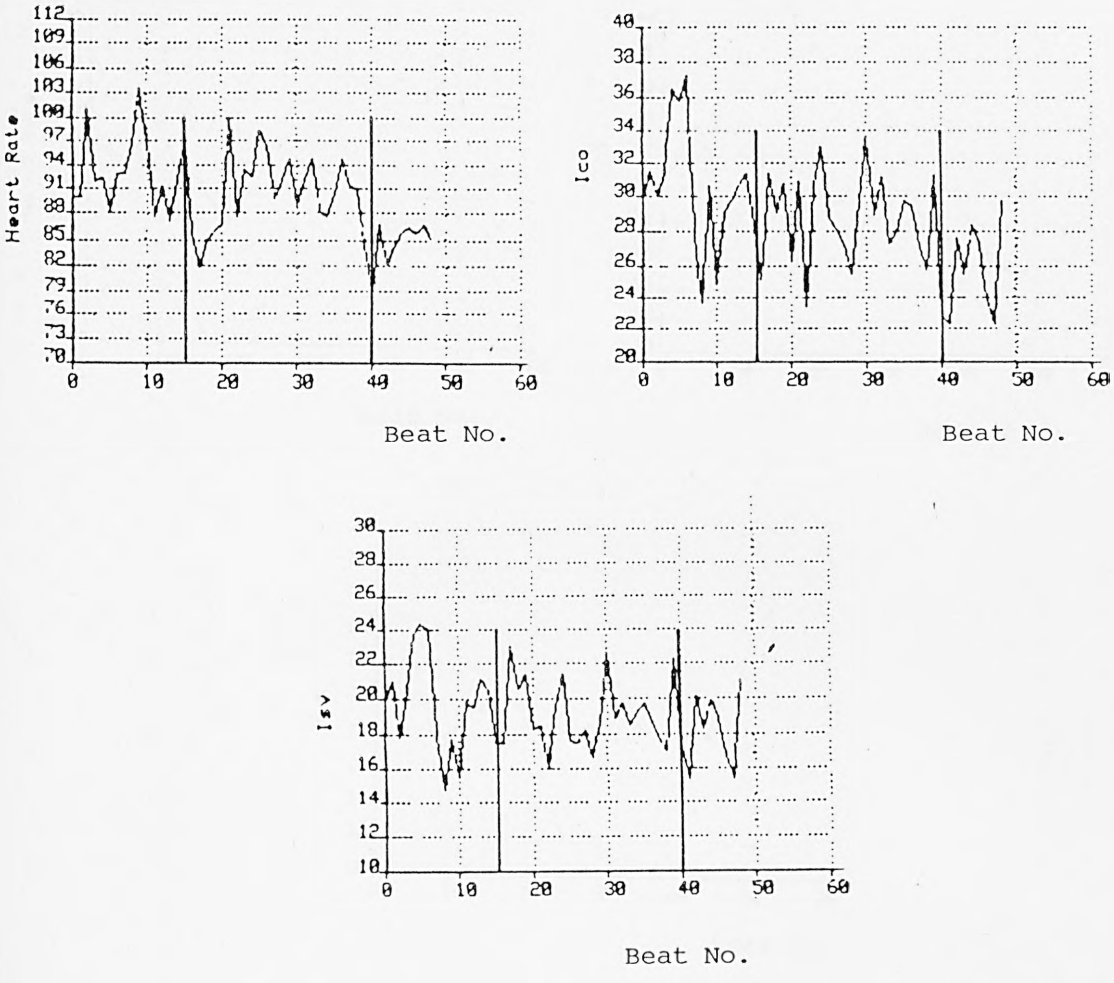

Figure 6.7a3 Raw data from subject BD5E(6) for the three variables as indicated during and following the loss of 420 ml of blood. The vertical lines indicate the times at which the bleeding starts and the end of bleeding.

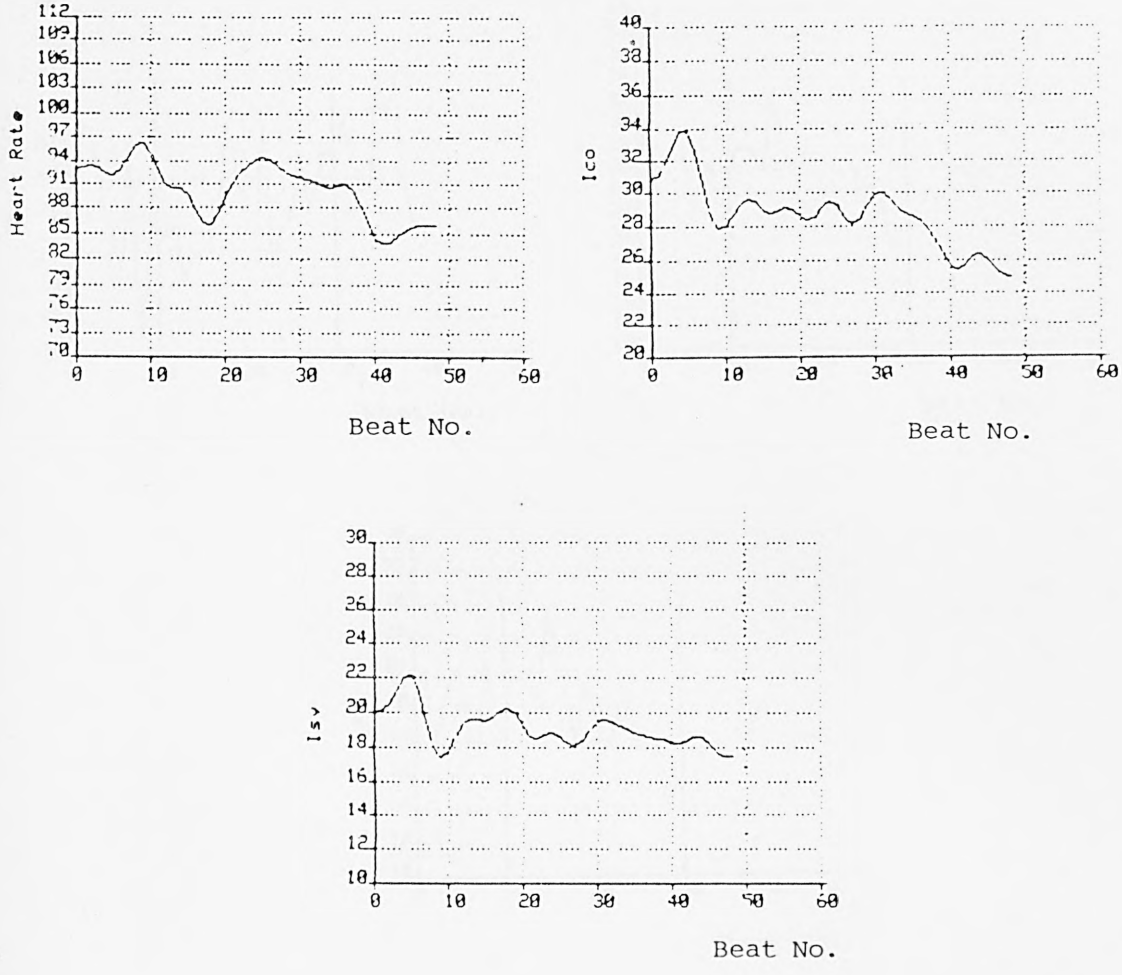

Figure 6.7b3 Filtered form of the data depicted in Figure 6.7a3 obtained using a recursive averaging filter.

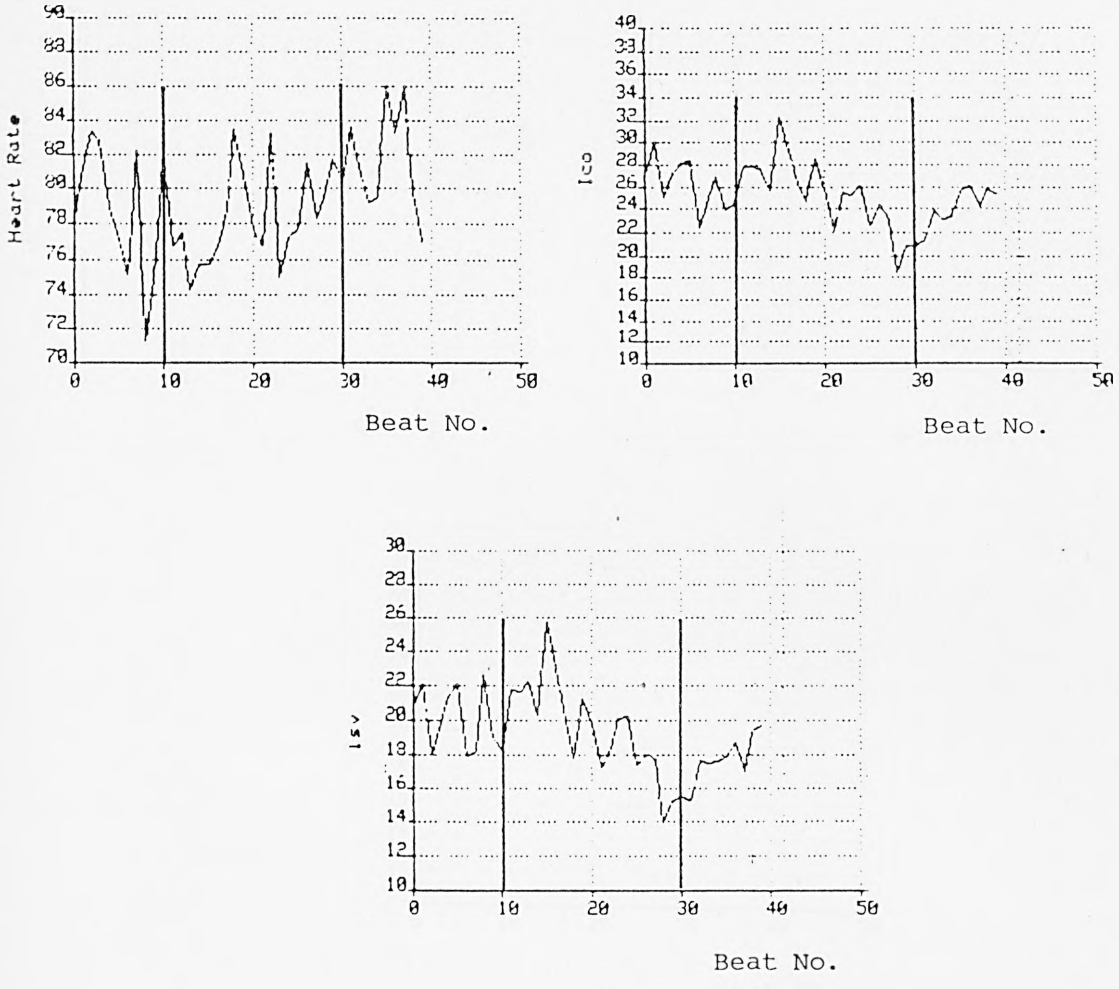

Figure 6.7a4 Raw data from subject BD6F(7) for the three variables as indicated during and following the loss of 420 ml of blood. The vertical lines indicate the times at which the bleeding starts and the end of bleeding.

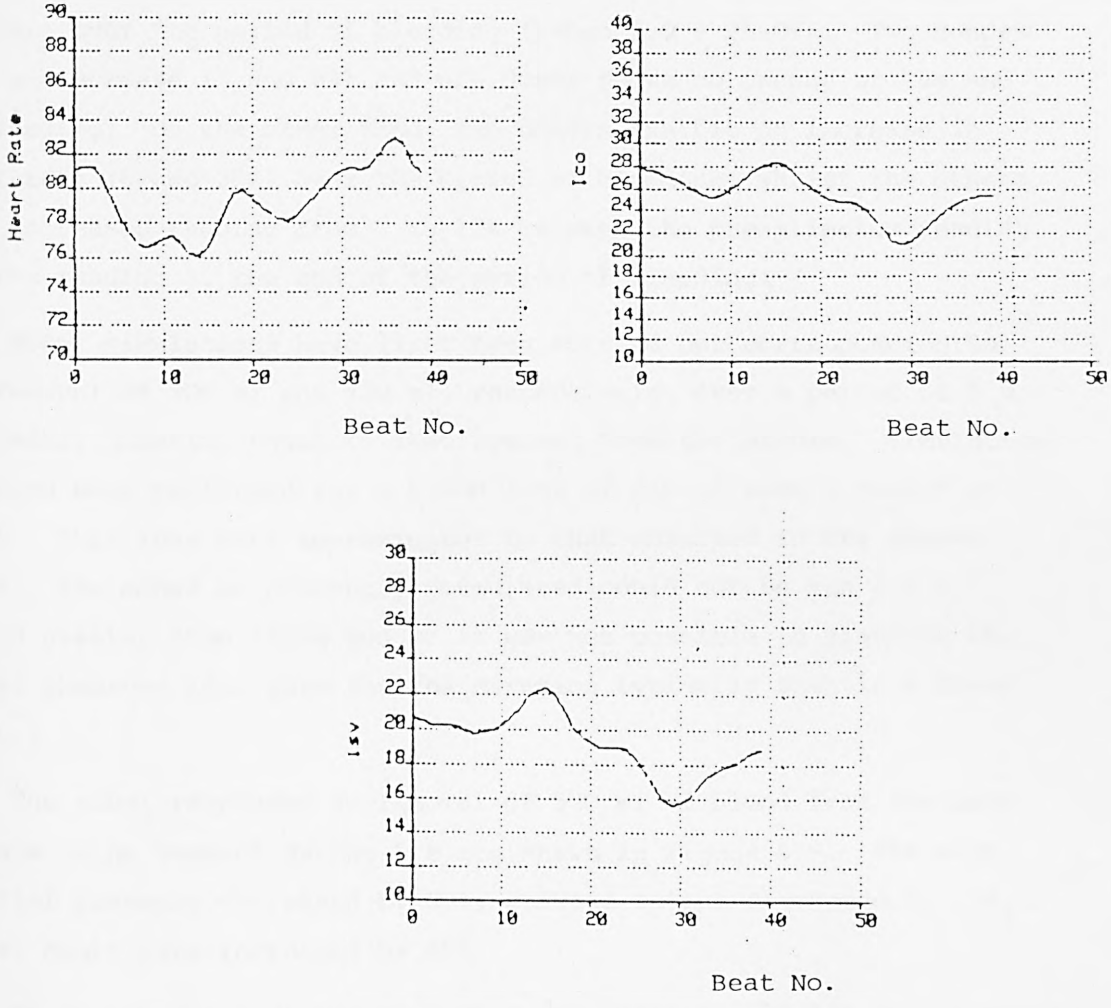

Figure 6.7b4 Filtered form of the data depicted in Figure 6.7a4 obtained using a recursive averaging filter.

The different patterns of response from the donors are presented in Table 6.8. In three subjects there is a decrease in arterial pressure over the period of bleeding (range 3.0 - 25.0%). Two donors show an increase (5 and 6%) and one donor shows no change at the end of bleeding. On the other hand, two donors exhibit an increase in heart rate (6 and 36%) over the period of bleeding, whilst the others show decreases ranging from 2 to 12% between the pre-stimulus reading and the reading at the end of the period of bleeding.

Model simulations have first been carried out corresponding to the removal of 500 ml and 420 ml, respectively, over a period of 5 s, the latter quantity equal to that removed from the donors. Simulation has also been performed for a blood loss of 210 ml over a period of 150 s. This loss rate approximates to that observed in the donors. (Note: the model as presently formulated could not be run for a period greater than 150 s and so it was not possible to simulate the actual observed loss rate for the duration typically seen in a blood donor.)

The model responses to removal of 500 ml of blood from the head and arm veins segment during 5 s are shown in Figure 6.9. The mean arterial pressure decreased by 28%, cardiac output decreased by 31%, whilst heart rate increased by 65%.

These results indicate that there is still an insufficient increase in systemic resistance to prevent this substantial decrease in arterial pressure. Similar effects are seen with the loss of 420 ml of blood over the same 5-second period.

The model was then used to simulate the removal of 210 ml of blood over 150 seconds. This results in decreases of systolic, mean and diastolic pressures by 10, 10 and 7%, respectively, due to a 12% decrease in cardiac output. Heart rate is increased by 16%, as shown in Figure 6.10.

The variability of response seen in the eight donors whose results were listed in Tables 6.7 and 6.8 is summarised in Table 6.9a and Figure 6.11. In contrast to the textbooks (e.g. Mountcastle, 1974) which suggest little change in mean arterial pressure following the loss of 10% of blood volume, these eight subjects exhibit substantial variability with the change in mean arterial pressure over 5 minutes ranging from -25% to +15%. The model exhibits only the single mode of response, namely a decrease in blood pressure (as shown in Table 6.9b),

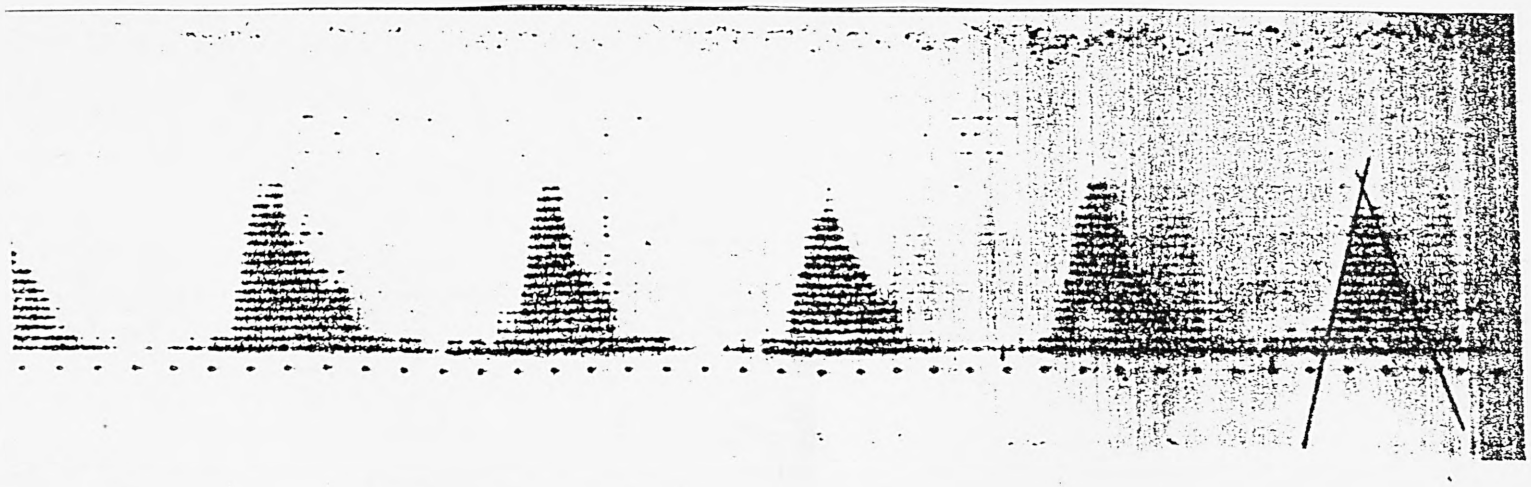

Figure 6.8a 3-point analysis by triangular approximation using transcutaneous aortovelography (TAV).

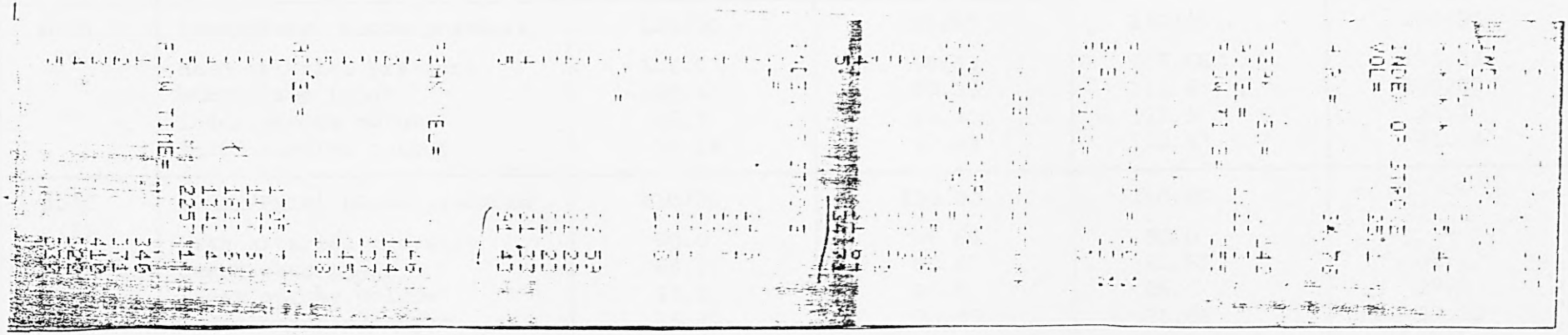

Figure 6.8b 3-point analysis by triangular approximation and beat-to-beat analysis of the heart rate and indices of cardiac output and stroke volume.

Donor's No.	Variables	Pre-stimulus values	Start of bleeding	End of bleeding	Sample values of variables taken during the 10-min period following the end of bleeding
BD1G (3)	(PMAX/PMIN) blood pressure	145/95	115/70	110/70	115/70
	Mean arterial pressure	111.66	85.00	83.33	85.00
	Heart rate (bpm)	60.87	85.13	82.87	70.41
	Index stroke volume	43.5	33.1	31.9	32.47
	Index cardiac output	44.07	46.92	44.01	37.87
BD2J (4)	(PMAX/PMIN) blood pressure	125/90	125/85	130/95	130/90
	Mean arterial pressure	101.6	98.33	106.66	103.33
	Heart rate (bpm)	120.4	93.29	112.6	100.87
	Index stroke volume	25.5	24.3	22.6	24.4
	Index cardiac output	51.14	37.83	42.43	41.04
BD3C (5)	(PMAX/PMIN) blood pressure	110/80	130/80	110/80	-
	Mean arterial pressure	90.0	96.66	90.0	-
	Heart rate (bpm)	84.76	82.81	82.67	81.32
	Index stroke volume	25.2	25.6	26.0	27.5
	Index cardiac output	35.31	35.35	35.86	37.22
BD5E (6)	(PMAX/PMIN) blood pressure	120/80	112/88	110/80	108/78
	Mean arterial pressure	93.33	96.0	90.0	88.0
	Heart rate (bpm)	89.46	96.6	79.04	86.07
	Index stroke volume	20.25	17.5	17.3	18.0
	Index cardiac output	30.2	28.15	22.8	25.77

Table 6.8 (continued overleaf)

Continued overleaf

Donor's No.	Variables	Pre-stimulus values	Start of bleeding	End of bleeding	Sample values of variables taken during the 10-min period following the end of bleeding
BD6F (7)	(PMAX/PMIN) blood pressure	125/70	125/70	120/80	127/75
	Mean arterial pressure	88.33	88.33	93.33	92.33
	Heart rate (bpm)	75.9	81.65	80.38	82.42
	Index stroke volume	19.45	18.2	15.5	18.75
	Index of cardiac output	24.52	24.73	20.75	25.38
BD7H (8)	(PMAX/PMIN) blood pressure	148/85	140/80	128/90	140/95
	Mean arterial pressure	106.0	100.0	102.66	110.0
	Heart rate (bpm)	82.61	82.39	75.68	82.94
	Index stroke volume	19.8	21.5	16.2	20.3
	Index cardiac output	27.27	29.47	20.43	28.17

Table 6.8 Effects of removal of 420 ml of blood from six donors (Regional Blood Transfusion Centre data)

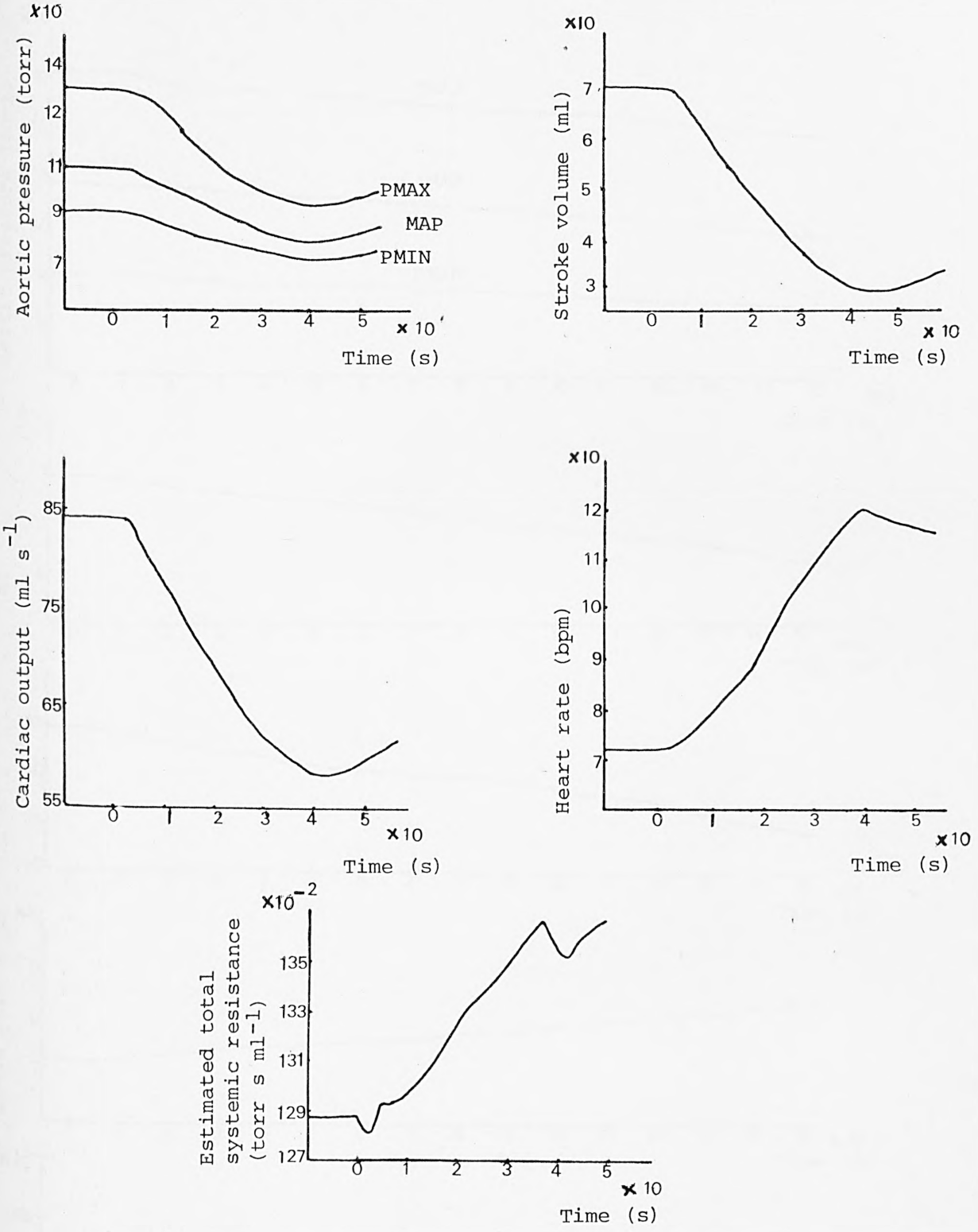

Figure 6.9 Dynamics following the removal of 500 ml of blood from the head and arms veins segment during 5 s at t = 0 s.

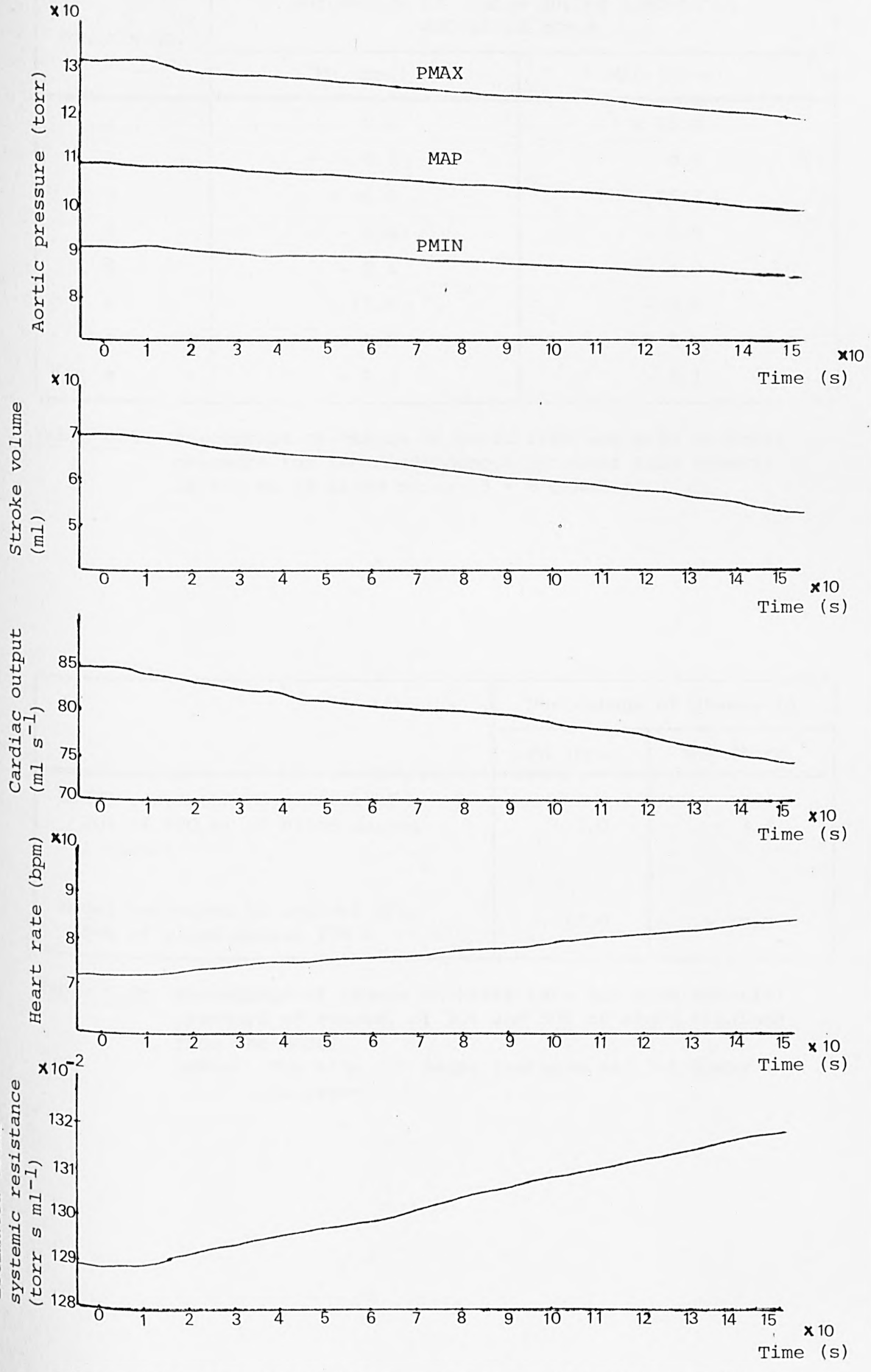

Figure 6.10 Dynamics following the removal of 210 ml of blood over 150 s from the head and arms veins segment.

Donor's No.	Percentage of change during removal of 420 ml of blood	
	FH (bpm)	MAP (torr)
1	0.0	+ 15.0
2	- 6.7	0.0
3	+ 36.0	- 25.3
4	- 6.4	+ 4.9
5	- 2.4	0.0
6	- 11.6	- 3.5
7	+ 5.9	+ 5.6
8	- 8.3	- 3.1

Table 6.9a Percentage of change of heart rate and mean arterial pressure for the eight donors obtained from removal of 420 ml of blood during 5 - 8 minutes

	Percentage of change in	
	FH (bpm)	MAP (torr)
Model responses to removal of 20% of 420 ml of blood during 1 minute	+ 5.0	- 3.4
Model responses to removal of 50% of blood during 150 s	+ 17.0	- 10.0

Table 6.9b Percentage of change in heart rate and mean arterial pressure of removal of 20% and 50% of blood obtained from the model
(Note: The sign (+) means increase and (-) means decrease)

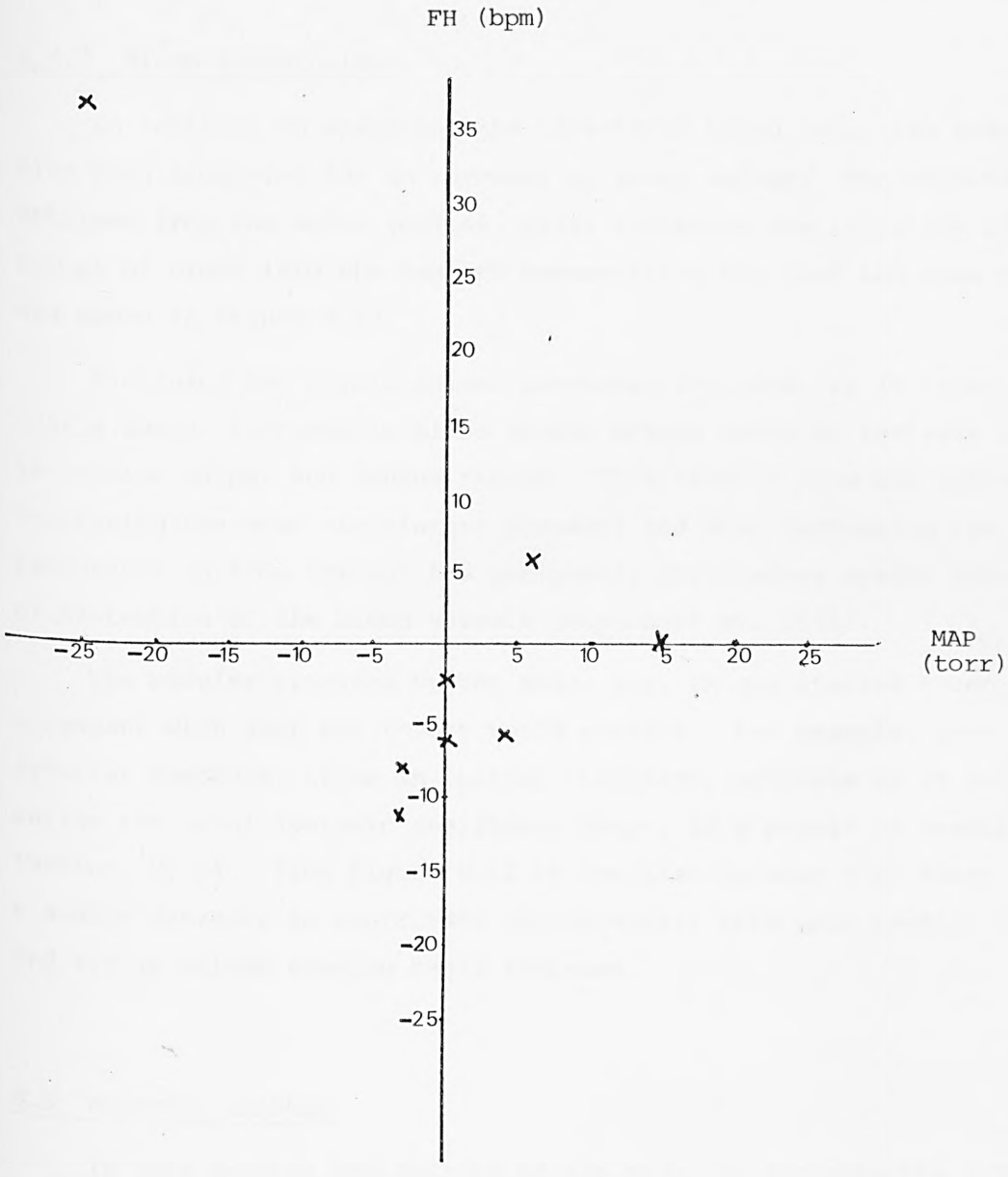

Figure 6.11 The variability of the responses of eight donors, as listed in Table 6.9a, for the heart rate and mean arterial pressure.

but one which is significantly greater than expected on the basis of "textbook information".

6.4.3 Blood Transfusion

In addition to examining the effects of blood loss, the model has also been simulated for an increase in blood volume. The results obtained from the model (Pullen, 1976) following the injection of 500 ml of blood into the segment representing the head and arms veins are shown in Figure 6.12.

Examining the physiological processes involved, it is known that a sudden increase in blood volume brings sbout an increase both in cardiac output and venous return. This results from the infusion increasing the mean circulatory pressure and also decreasing the resistance to flow through the peripheral circulatory system because of distention of the blood vessels (Guyton et al. 1958).

The results produced by the model are, in qualitative terms, in agreement with what the theory would predict. For example, mean arterial pressure, after an initial transient, exhibits an 8% increase, whilst the total systemic resistance drops, as a result of vessel distention, by 5%. From Figure 6.12 it can also be seen that there is a sudden decrease in heart rate (bradycardia) with both cardiac output and stroke volume showing rapid increase.

6.5 POSTURAL CHANGES

In this section the ability of the model to describe the effects of postural changes tests is examined. The model results are compared both with empirical data obtained from experiments performed upon volunteer subjects and also with references data obtained from human studies.

The results of such model testing are particularly important in the assessment of model validity. The circulatory dynamics are most stable when the subject is lying down since many of the arteries and veins are horizontally oriented at or near heart level. In contrast, when the subject is tilted, either head up or down, many of the arteries and veins are oriented vertically, or near vertically, and large hydrostatic pressures are produced by the long, uninterrupted columns of blood.

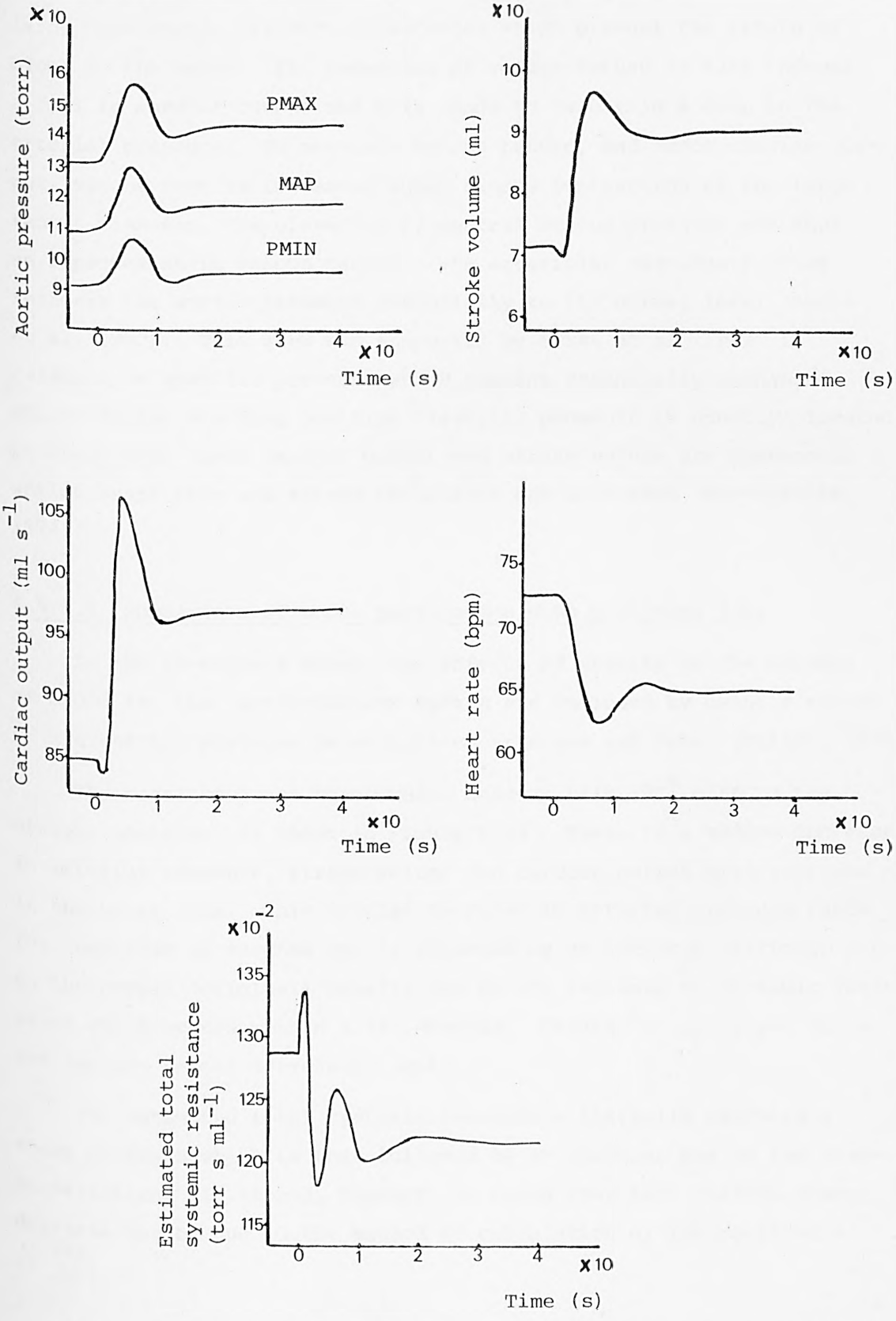

Figure 6.12 Dynamics following the sudden injection of 500 ml of blood into the segment representing the head and arms veins at t = 0 s.

6.5.1 Head-Up Tilt

A passive tilt from a recumbent to an upright position leads to large hydrostatic pressure differences which prevent the return of blood to the heart. The reduction of venous return in turn induces a fall in cardiac output and this tends to result in a drop in the arterial pressure. To maintain venous return, and hence cardiac output, venous tone is increased which causes contraction of the large venous channels, the elevation of central venous pressure and thus an improvement in venous return. The arteriolar vasoconstriction restores the aortic pressure essentially to its normal level (Keele et al, 1982). This view was supported by Borst et al (1982) in relation to systolic pressure which remains essentially unchanged, whilst in the standing position diastolic pressure is usually elevated by about 10%. Both cardiac output and stroke volume are decreased, whilst heart rate and system resistance are increased (Mountcastle, 1974).

6.5.1.1 Comparison of model performance with published data

In the 19-segment model, the effects of gravity on the columns of blood in the cardiovascular system are included by using a series of hydrostatic pressure generators to arteries and veins (Pullen, 1976).

The model response to a sudden head-up tilt (90^{o} tilt to the upright position) is shown in Figure 6.13. There is a sudden decrease in arterial pressure, stroke volume and cardiac output with increase in the heart rate. This initial decrease in arterial pressure lasts for less than 10 seconds and is followed by an increase (although not to the normal (original) level), due to the increase in systemic resistance which occurs within a few seconds. Cardiac output rises for a few seconds before decreasing again.

The estimated total systemic resistance initially exhibits a sharp decrease which is then followed by an increase due to the vasoconstriction. It should, however, be noted that this initial sharp decrease may be due to the method of calculation of the resistance $\left(= \frac{MAP}{CO}\right)$.

Figure 6.13 shows the mean arterial pressure drop by 7% without a subsequent return to the initial value. The fall in cardiac output is limited to approximately 6%, which is rather less than the 20 - 27%

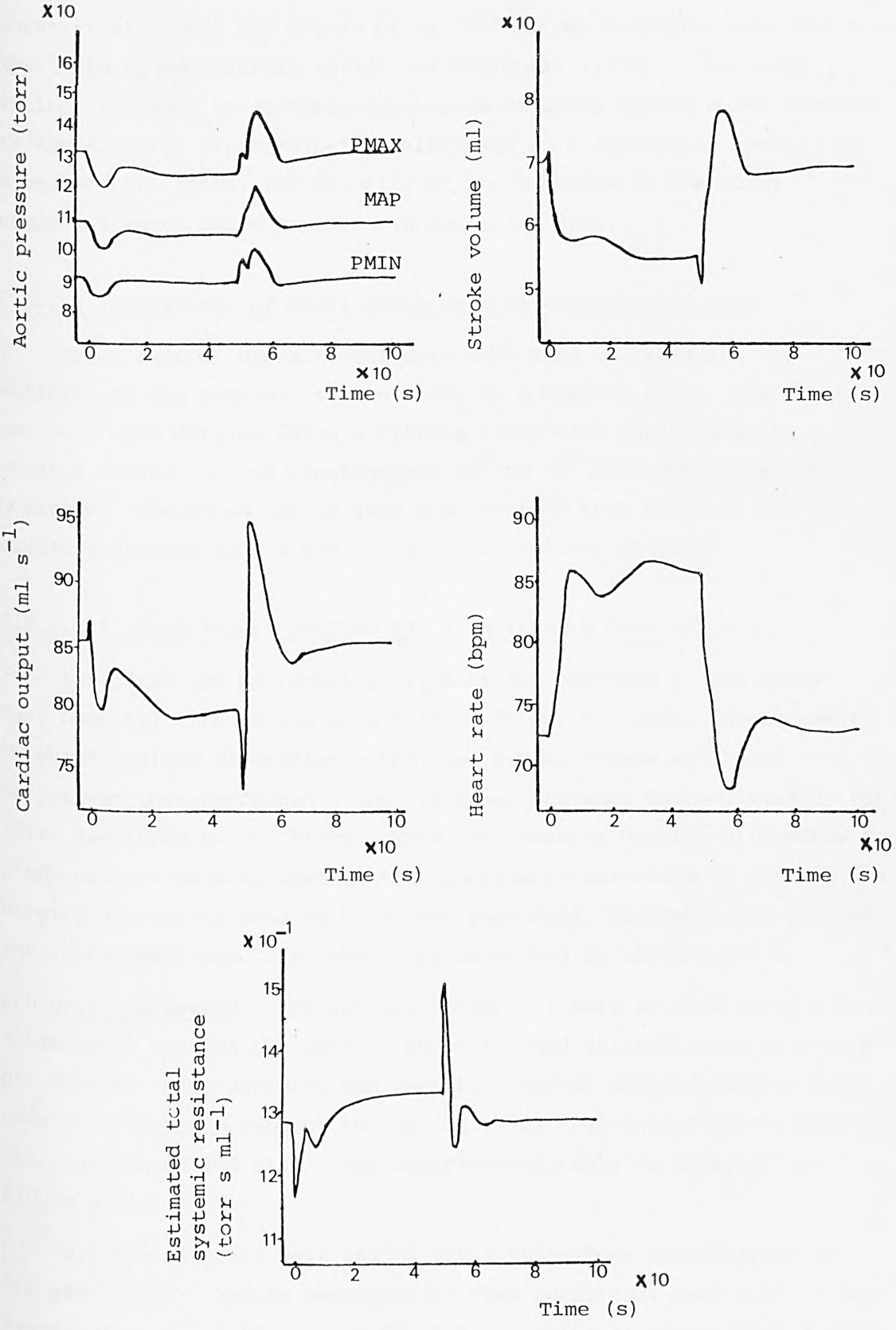

Figure 6.13 Dynamics following a head-up tilt ($\phi = 90^{o}$) at t = 0 s, and a return to recumbency ($\phi = 0^{o}$) at t = 50 s.

fall revealed in published data and depicted in Table 6.10. The increase in heart rate in the model is within the range given by Borst et al (1982) and Boyers et al (1972), but is higher than the range specified by Mountcastle (1974) and McClintic (1978). The insufficient increase in systemic resistance produced by the model results in the arterial pressure being maintained at a sub-normal level. In a qualitative sense, the majority of the features of the model responses match those reported in published data.

6.5.1.2 Comparison of model response with experimental data

Three sets of experimental data were used in examining the validity of the response of the model to a head-up tilt. The first two sets were derived using a tilting table with subjects being rotated through angles ranging from 20^{o} to 70^{o} from the recumbent position. The third set of data was obtained from subjects who suddenly changed from a horizontal to a vertical position.

6.5.1.2.1 Experiments carried out at Northwick Park Hospital

The first set of experimental data was obtained at Northwick Park Hospital through the good offices of Mr. H. Light. Measurements by which indices of cardiac output and stroke volume and heart rate could be derived were performed using the transcutaneous aortovelography apparatus (TAV) developed by Mr. Light. This non-invasive Doppler ultrasound technique was the same as used in the experiments described in Section 6.4.1. Varying degrees of head-up tilt were performed, together with studies involving head-down tilt, which are described in Section 6.5.2.

Subjects and methods. Seven male volunteers were studied using a tilting table which enables the subject to be rotated (tilted) at a rate of 6^{o} per second. Foot supports and antislip (DYCEM) mattress strips were used to attach the subject to the table and thus ensure both a comfortable and controlled tilt. The experimental table is depicted in Figure 6.14.

All the subjects were fasted for a three-hour period prior to the experiment. Before measurements were performed, each subject lay recumbent on the table for at least ten minutes to ensure that a pre-stimulus steady state was achieved. Readings were then obtained intermittently during a one-minute period using the TAV non-invasive Doppler ultrasound technique with the subject in this recumbent position prior

Variable	Model response	Data
Mean arterial pressure	- 7%	Little change[B], -2%[E]
Systolic pressure	- 6.7%	No change [A,B,E]
Diastolic pressure	- 6.3%	+ 10%[A]
Heart rate	+ 14 bpm	+(15 - 30)%[A,E], 30%[E] +(5 - 10)bpm[B,D], 15 bpm[G]
Stroke volume	- 20%	-(10 - 50)%[B,D,E]
Cardiac output	- 6%	-27%[C], 20%[B,D], 20 - 30%[F,G]
Systemic resistance	+ 4%	+ 20%[B]

Table 6.10 The effects of head-up tilt on the model variables compared with the data from the following sources:
A - Borst et al, 1982; B - Mountcastle, 1974;
C - Keele et al, 1982; D - McClintic, 1978;
E - Boyers et al, 1972; F - Guyton, 1981;
G - Rushmer, 1976.

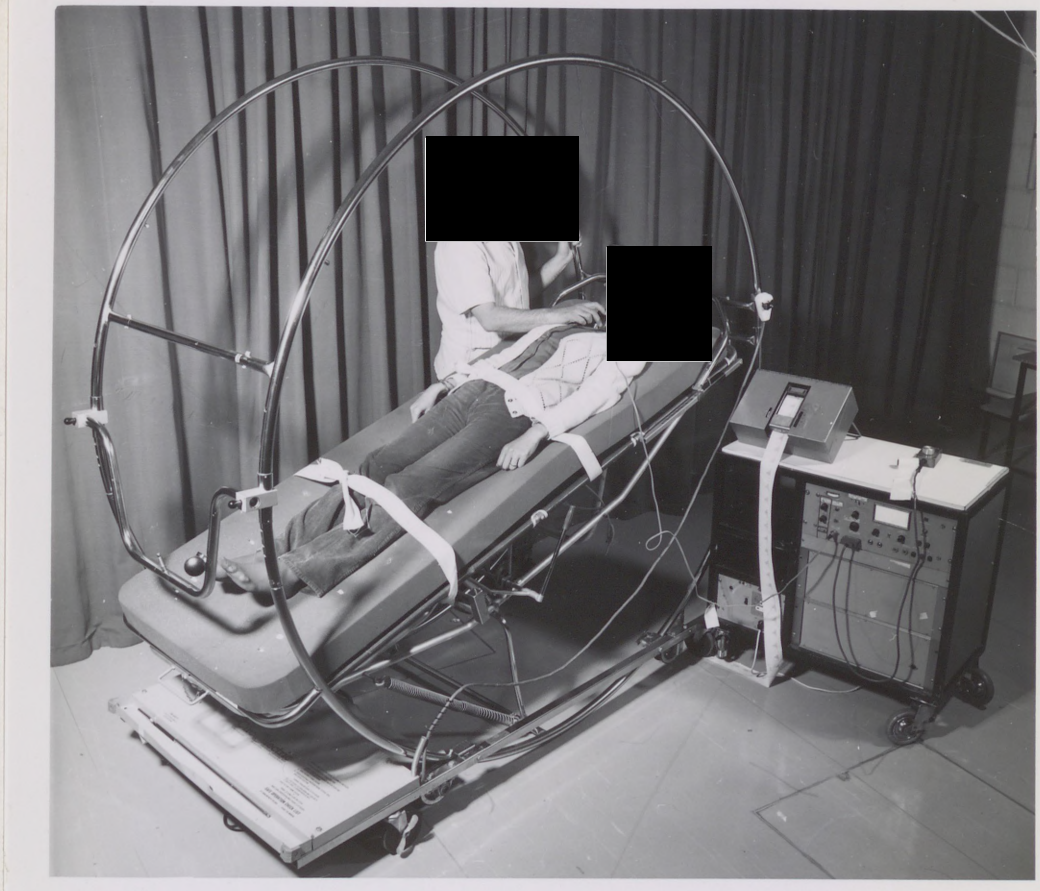

(a)

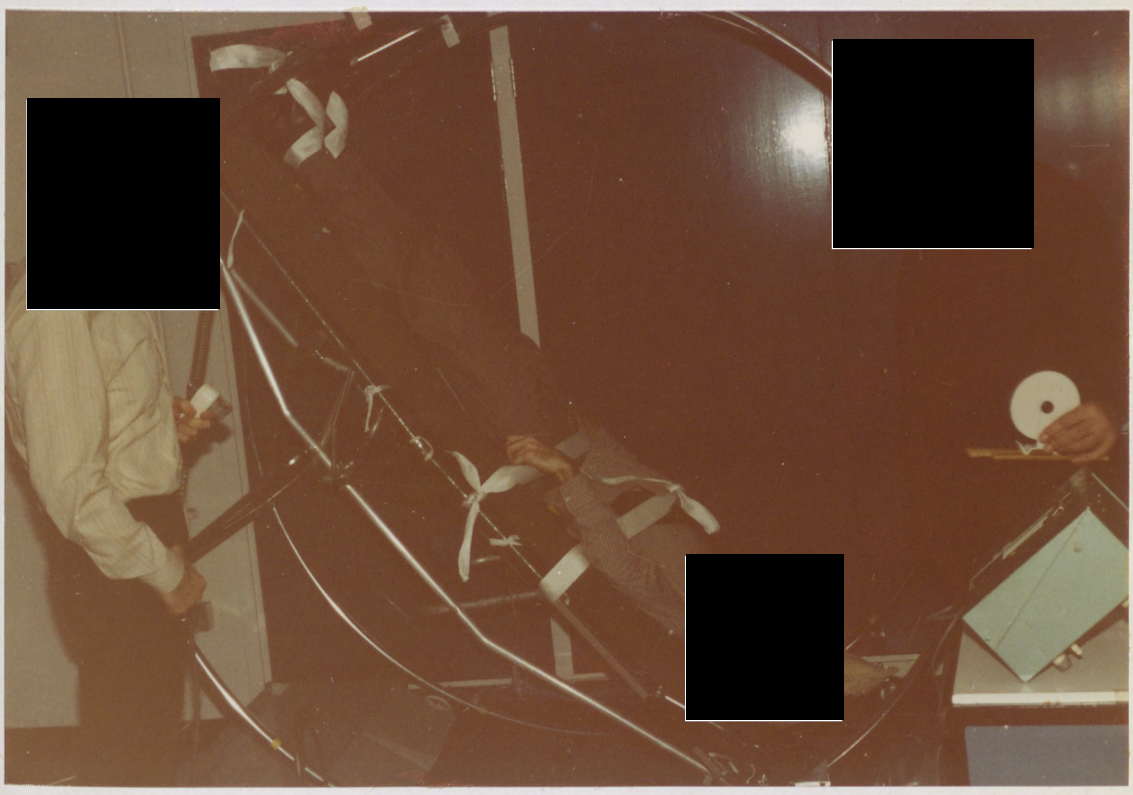

(b)

Figure 6.14 Experimental configuration for head-up and head-down tilt.

to the start of the tilt. The transducer was located over the aortic arch.

Up to six consecutive experiments were then performed on each subject. The three head-up experiments involved rotation from the horizontal position through 20^{o}, 45^{o} and 60^{o}, respectively. Once the rotation had been completed, the subject remained in the inclined position for 150 seconds before being rotated back to the horizontal position. Measurements were taken during the rotation to the inclined position, during the rest in this position, during the return to the horizontal and at rest post-stimulus in the horizontal position for a further 90 seconds.

Having regained a steady-state, the next experiment was performed using a similar measurement protocol.

Similar experiments were performed with head-down tilts of 20^{o}, 45^{o} and 60^{o}. In general, these experiments involved some discomfort for the subject, particularly in the case of the 60^{o} tilt. In some cases difficulty was experienced in trying to locate an adequate signal for measurement purposes and thus there are some gaps in the results as discussed in Section 6.5.2. Experiments which were successfully completed are indicated in Table 6.11.

Following painstaking analysis of the traces obtained from the TAV measurements, values of heart rate and indices of cardiac output and stroke volume were obtained prior to, and after each tilt. These are shown in Table 6.12a, b and c for head-up tilts of 20^{o}, 45^{o} and 60^{o}, respectively. Also shown are the percentage changes in mean post-stimulus variable values as compared to the mean pre-stimulus values.

In Figure 6.15a, the raw measurements obtained from subject A during a 45^{o} head-up tilt are shown for the three variables. It can be clearly seen that these data exhibit high frequency "noise" or beat-to-beat variability. In order to be able to examine the principal features of the response to the stimulus, low pass filtering was employed. Two approaches were examined. In the first a fast Fourier transform (FFT) was used to produce the amplitude frequency responses shown in Figure 6.15b. Frequencies higher than 20 Hz were then removed (an empirical definition of "noise") and the time-domain responses re-constituted. Comparison of these (Figure 6.15c) with the originals presented in Figure 6.15a revealed that a number of significant features (as perceived visually) appeared to be missing. This approach

Subject		Age (years)	Weight (kg)	+20° tilt	-20° tilt	+45° tilt	-45° tilt	+60° tilt	-60° tilt
Code	Initials								
A	N.S.	32	76	✓	✓	✓	✓	✓	✓
B	C.P.	24	76.2	✓	✓	✓	✓	-	✓
C	J.O.	28	88.9	✓	✓	✓	✓	✓	✓
D	R.L.	27	63.5	-	✓	✓	✓	✓	✓
E	E.N.	30	80	-	-	✓	✓	✓	✓
G	M.B.	29	65	-	-	✓	✓	-	✓
K	M.D.	29	57.15	✓	-	✓	✓	-	✓

Table 6.11 List of the subjects investigated, their age and body weight and the range of tilt experiments to which they were subjected (indicated by ✓)

Subject code		Recumbency	Mean	+ 20° tilt	Mean	% change	Recumbency	Mean
A	FH	68.92, 70.33, 74.67, 73.94, 80	73.57	87.88, 91.6, 87.62, 76.89, 81.24	85.04	+ 15.5	74.08, 73.9, 77.1, 81.67, 78.5	77.05
	ICO	28.95, 27.68, 24.24, 27.98, 34.06	28.58	23.23, 22.14, 24.3, 23.02, 24.26	23.39	- 18	24.21, 26.94, 25.6, 23.64, 25.09	25.09
	ISV	25.2, 23.6, 19.5, 22.7, 25.5	23.3	15.9, 14.5, 16.6, 18.0, 17.9	16.58	- 28.8	19.6, 21.9, 19.9, 17.4, 19.2	19.6
B	FH	70.58, 65.7, 57.61, 54.32, 63.11	62.27	58.96, 66.55, 65.51, 67.69, 70.35	65.81	+ 5.6	59.84, 66.65, 62.04, 62.55, 64.4	63.1
	ICO	26.05, 25.67, 24.65, 25.16, 23.23	24.95	25.2, 28.25, 28.94, 28.7, 30.8	28.37	+ 13.7	29.54, 29.86, 29.4, 27.34, 28.56	28.94
	ISV	22.1, 23.4, 25.7, 27.8, 22.1	24.2	25.7, 25.5, 26.5, 25.4, 26.3	25.88	+ 6.9	29.6, 26.9, 28.4, 26.2, 26.6	27.6
C	FH	57.93, 60, 61.09, 61.72, 58.83	59.91	65.39, 60.16, 59.8, 69.86, 54.76	61.99	+ 3.4	58.98, 59.56, 60.4, 56.96, 60.4	59.26
	ICO	34.38, 37.8, 37.97, 39.86, 38.33	37.67	31.5, 34.16, 31.61 35.02, 30.27	32.51	- 13.69	34.4, 32.64, 30.35, 31.64, 31.84	32.17
	ISV	35.6, 37.8, 37.3, 38.8, 39.1	37.7	28.9, 34.1, 31.7, 30.1, 33.2	31.6	- 16.1	35, 32.9, 30.2, 33.3, 31.6	32.6

Table 6.12a continued overleaf

Subject code		Recumbency		+ 20° tilt		% Change	Recumbency	
			Mean		Mean			Mean
K	FH	49.06, 45.46, 46.42, 46.77, 47.71	47.08	47.06, 47.46, 52.27, 47.16, 47.76	48.34	+ 2.6	50.41, 46.78, 46.71, 63.12, 56.75	52.75
	ICO	17.31, 15.39, 20.12, 18.71, 17.45	17.79	19.88, 20.8, 21.17, 18.63, 19.31	19.95	+ 12	20.41, 20.02, 19.35, 25.92, 22.49	21.63
	ISV	21.2, 20.3, 26, 24, 21.9	22.68	25.3, 26.3, 24.3, 23.7, 24.3	24.78	+ 9.2	24.3, 25.7, 24.9, 24.6, 23.8	24.66

Table 6.12a Values of heart rate and indices of cardiac output and stroke volume obtained before the tilt, in the inclined position and in the restored horizontal position. Five sample values from consecutive heart beats are listed, together with the mean of these five values in each case. The percentage change in each variable in the inclined position as compared to the pre-stimulus horizontal state is also given.

Subject code		Recumbency	Mean	+ 45° tilt	Mean	% change	Recumbency	Mean
A	FH	68.04, 75.31, 69.74, 68.43, 73.05	70.9	85.28, 88.18, 87.13, 87.13, 86.35	86.73	+ 22	75.09, 73.22, 74.71, 74.9, 74.71	74.52
	ICO	26.42, 25, 25.19, 25.7, 30.43	26.54	14.76, 18.25, 20.63, 18.83, 16.73	17.84	- 32.7	23.96, 27.31, 25.03, 23.65, 25.4	25.07
	ISV	23.3, 19.9, 21.7, 22.5, 25	22.48	10.4, 12.4, 14.2, 13, 11.6	12.32	- 45	19.1, 22.4, 20.1, 18.9, 20.4	20.18
B	FH	67.47, 74.96, 70.18, 71.33, 71.5	71.09	87.78, 87.03, 87.03, 86.78, 89.59	87.64	+ 23	73.32, 79.43, 72.97, 72.79, 67.18	73.13
	ICO	28.89, 29.47, 28.8, 30.89, 30.44	29.69	32.27, 30.36, 32.2, 34.16, 30.27	31.85	+ 7.2	30.03, 30.29, 28.35, 32.39, 31.6	30.53
	ISV	25.7, 23.6, 24.6, 26, 25.5	25.08	22.1, 20.9, 22.2, 23.6, 20.3	21.82	- 12.9	24.6, 22.9, 23.3, 26.7, 28.2	25.14
C	FH	68.15, 67.55, 65.52, 66.81, 67.4	67.09	71.81, 69.61, 65.99, 66.56, 63.91	67.57	+ 0.7	66.8, 58.46, 59.73, 60.08, 61.04	61.22
	ICO	36.6, 38.45, 33.6, 34.99, 41.75	37.08	26.45, 24.8, 25.43, 23.83, 21.84	24.47	- 34	33.69, 32.64, 31.87 31.47, 30.8	32.09
	ISV	32.2, 34.2, 30.8, 31.4, 37.2	33.16	22.1, 21.4, 23.2 21.5, 20.5	21.74	- 34.4	30.3, 33.5, 32, 31.4, 30.3	31.5
D	FH	79.69, 77.66, 60.24, 55.23, 72.17	69	83.57, 91.53, 90.18, 84.2, 82.38	86.37	+ 25	89.16, 88.65, 81.81, 89.42, 85.44	86.89
	ICO	31.62, 30.14, 23.79, 24.32, 27.81	27.54	25.63, 29.23, 22.56, 26.12, 25.49	25.81	- 6.2	28.09, 27.75, 30.66, 31.13, 27.82	29.09
	ISV	23.8, 23.3, 23.7, 26.4, 23.1	24.1	18.4, 19.2, 15, 18.6, 18.6	17.96	- 25	18.9, 18.8, 22.5, 20.9, 19.5	20.12

Table 6.12b continued overleaf

Subject code		Recumbency	Mean	+ 45° tilt	Mean	% change	Recumbency	Mean
E	FH	79.69, 75.37, 72.34, 77.27, 75.18	75.97	77.81, 81.77, 88.92, 87.14, 83.11	83.75	+ 10.2	75.79, 81.73, 72, 80.21, 75.04	76.95
	ICO	35.57, 38.98, 35.04, 34.6, 38.04	36.45	27.6, 30.9, 28.1, 29.24, 28.24	28.82	- 20	34.05, 36.15, 37.05, 31.33, 35.54	34.82
	ISV	26.8, 31, 29.1, 26.9, 30.4	28.8	21.3, 22.7, 19, 20.1, 20.4	20.7	- 28	27, 26.5, 30.9, 23.4, 28.4	27.24
G	FH	66.14, 62.7, 71.77 60.84, 69.75	66.24	81.84, 79.06, 75.3, 78, 79.06	78.65	+ 18.7	67.54, 70.87, 65.08 72.3, 68.1	68.78
	ICO	33.6, 30.4, 32.86, 32.8, 36.96	33.3	18.39, 19.9, 24.6, 21.5, 23.29	21.53	- 35	27.2, 28.3, 26.4, 29.4, 22.6	26.78
	ISV	30.5, 29.1, 27.5, 32.4, 31.8	30.26	13.5, 15.2, 19.7 16.6, 17.7	16.54	- 45	24.2, 24, 24.4 24.4, 28.7	25.14
K	FH	43.12, 48.54, 47.62, 48.31, 53.67	48.25	65.47, 72.1, 71.75, 71.81, 63.14	68.85	+ 42.6	46.23, 42.86, 46.12, 51.56, 44.8	46.31
	ICO	21.4, 23.61, 20.6, 22.19, 22.62	22.08	19.72, 24.2, 19.3, 22.59, 19.03	20.96	- 5.1	18.38, 18.96, 22.12, 25.05, 19.49	20.8
	ISV	29.8, 29.2, 26, 27.6, 25.3	27.58	18.1, 20.1, 16.1, 18.9, 18.1	18.26	- 33.7	23.9, 26.6, 28.8, 29.1, 26.1	26.9

Table 6.12 b Values of heart rate and indices of cardiac output and stroke volume obtained before the tilt, in the inclined position and in the restored horizontal position. Five sample values from consecutive heart beats are listed, together with the mean of these five values in each case. The percentage change in each variable in the inclined position as compared to the pre-stimulus horizontal state is also given.

Subject code		Recumbency	Mean	+ 60° tilt	Mean	% change	Recumbency	Mean
A	FH	75.87, 72.75, 70.7, 78.44, 82.98	76.15	111.25, 100.53, 106.93, 102.23, 105.07	105.2	+ 38	77.28, 75.16, 67.73, 70.59, 73.69	72.89
	ICO	23.21, 21.88, 21.05, 19.8, 27.24	22.63	18.96, 16.77, 13.44, 14.76, 14.48	15.68	- 30.7	27.56, 26.74, 23.69, 25.25, 23.3	25.31
	ISV	18.4, 18, 17.9, 15.1, 19.7	17.82	10.2, 10, 7.5, 8.7, 8.3	8.94	- 49.8	21.4, 21.3, 21, 21.5, 19	20.8
C	FH	60.89, 61.56, 64.33, 72.91, 65.16	64.97	76.02, 75.45, 76.41, 68.75, 72.72	73.87	+ 13.6	52.54, 59.13, 66.19, 63.26, 60.69	61.36
	ICO	41.05, 38.06, 37.55, 43.99, 40.8	40.29	29.74, 26.36, 25.9, 25.9, 29.49	27.47	- 31	30.77, 33.11, 35.67 35.03, 34.37	33.79
	ISV	40.5, 37.1, 35, 36.2, 37.6	37.28	23.5, 21, 20.3, 22.6, 24.3	22.34	- 40	32.1, 33.6, 32.3, 33.2, 34	33.00
D	FH	79.21, 50.76, 74.5, 81.37, 80.27	73.26	87.65, 87.65, 84, 91.36, 86.9	87.51	+ 19	77.97, 84.34, 65.83, 83.39, 80.05	78.32
	ICO	23.24, 18.21, 27.61, 31.29, 27.45	25.56	20.73, 24.61, 19.91, 17.48, 19.29	20.4	- 20	23.97, 16.26, 24.43, 24.48, 20.17	21.86
	ISV	17.6, 21.5, 22.2 23, 20.5	20.96	14.2, 16.8. 14.2, 11.5, 13.3	14.0	- 33	18.4, 20.2, 22.3, 17.6, 15.1	18.72

Table 6.12c continued overleaf

Subject code		Recumbency	Mean	+ 60° tilt	Mean	% change	Recumbency	Mean
E	FH	68.12, 75.2, 68.12, 66.62, 71.31	69.87	83.28, 96.76, 87.09, 87.09, 88.6	88.56	+ 26.7	83.79, 80.9, 96.83, 81.55, 75.5	83.71
	ICO	27.2, 32.82, 31.02, 30.68, 33.26	30.99	22.57, 20.56, 21.84, 23.4, 24.41	22.55	- 27	37.42, 32.76, 36.55, 35.17, 33.39	35.06
	ISV	24, 26.2, 27.3, 27.6, 28	26.62	16.3, 12.8, 15, 16.1, 16.5	15.34	- 42	26.8, 24.3, 22.6, 25.9, 26.5	25.22

Table 6.12c Values of heart rate and indices of cardiac output and stroke volume obtained before the tilt, in the inclined position and in the restored horizontal position. Five sample values from consecutive heart beats are listed, together with the mean of these five values in each case. The percentage change in each variable in the inclined position as compared to the pre-stimulus horizontal state is also given.

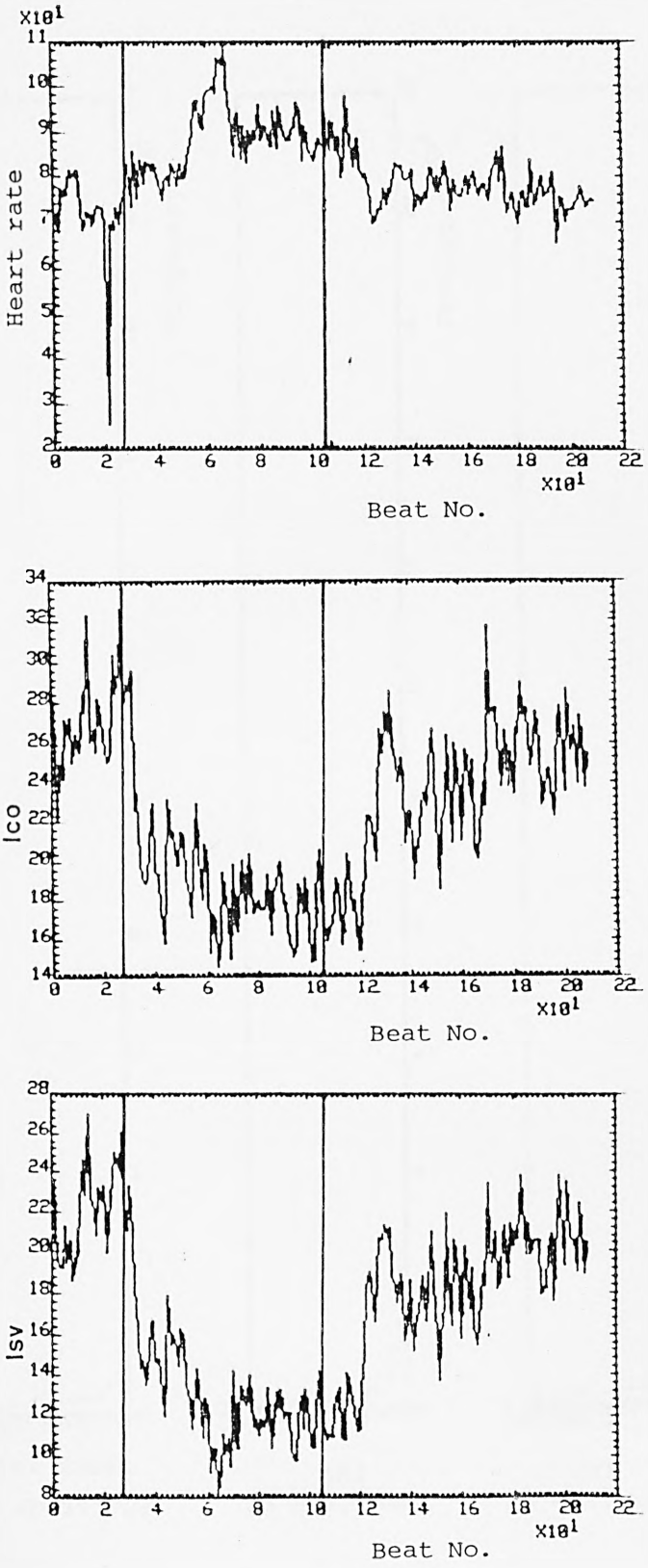

Figure 6.15a Raw data obtained from subject A for the three variables as indicated during a 45° head-up tilt. The vertical lines indicate the times at which the tilt to the inclined position and the return to the horizontal began.

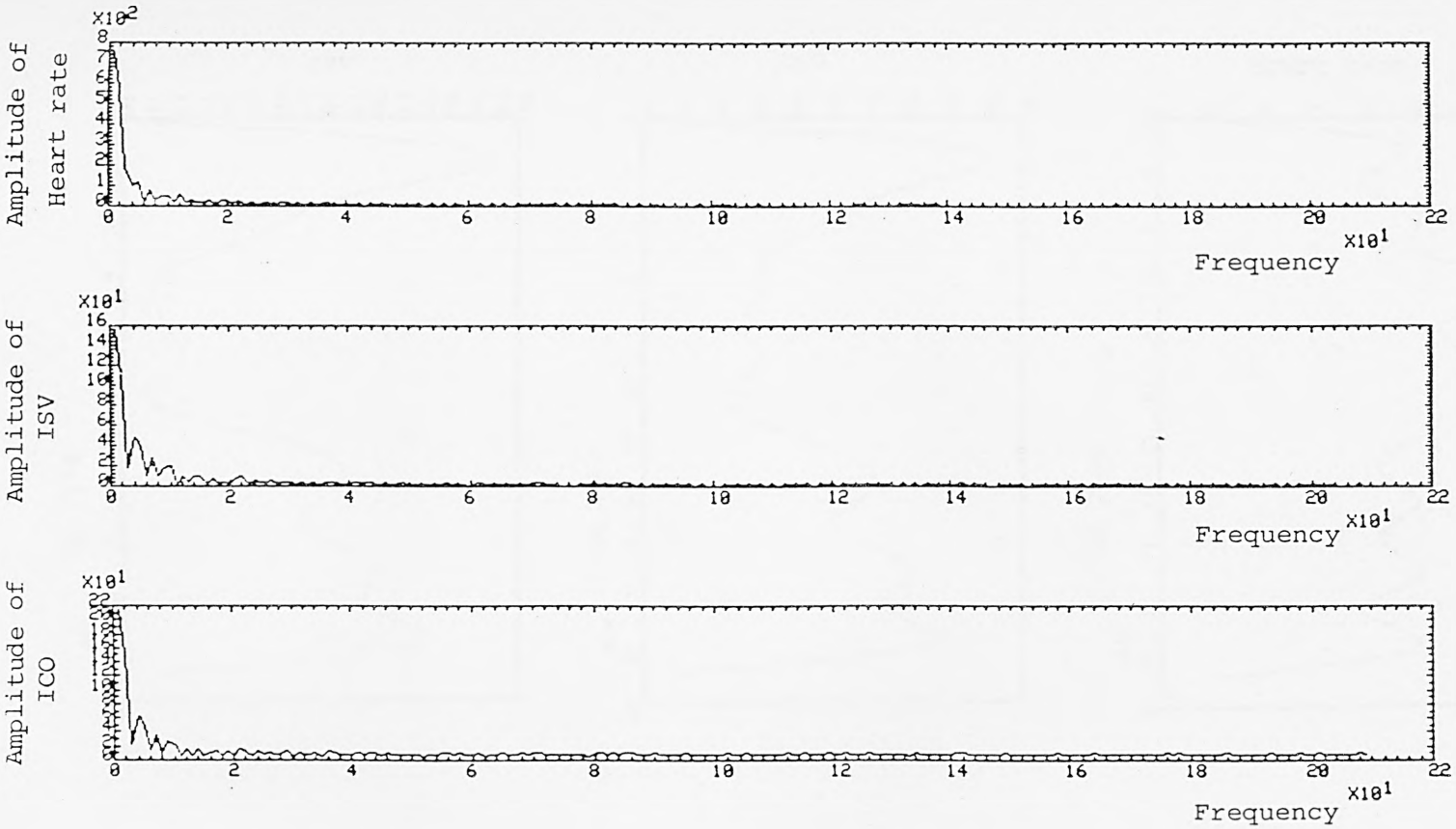

Figure 6.15b Amplitude frequency response of the raw data depicted in Figure 6.15a.

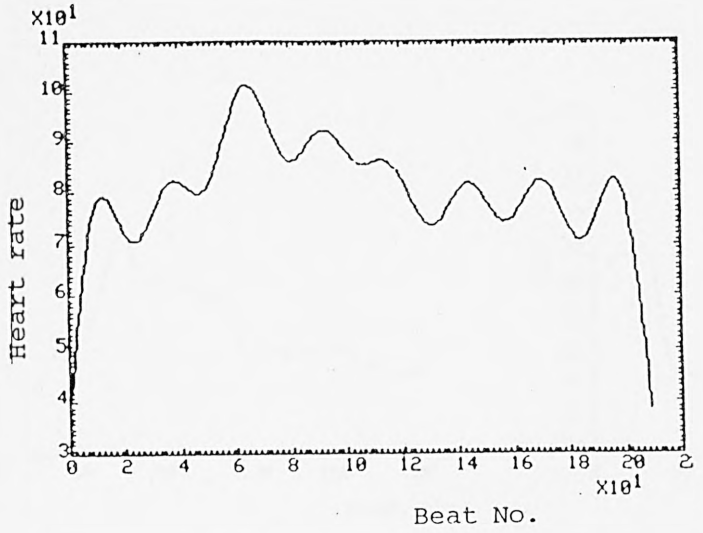

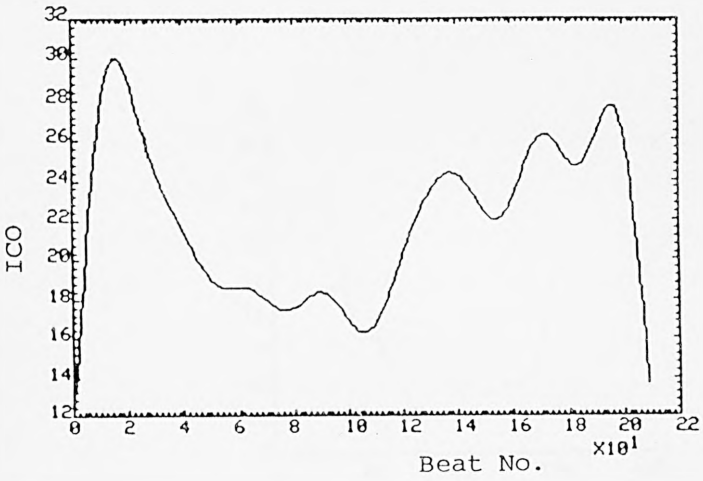

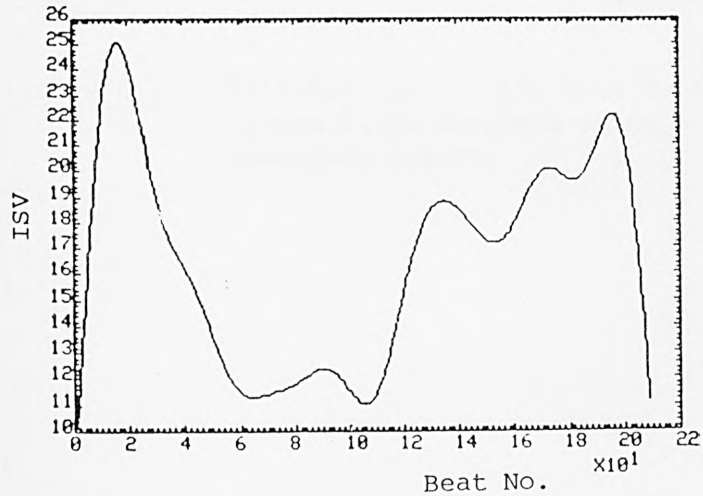

Figure 6.15c Reconstituted version of the raw data shown in Figure 6.15a from which frequencies greater than 20 Hz have been removed.

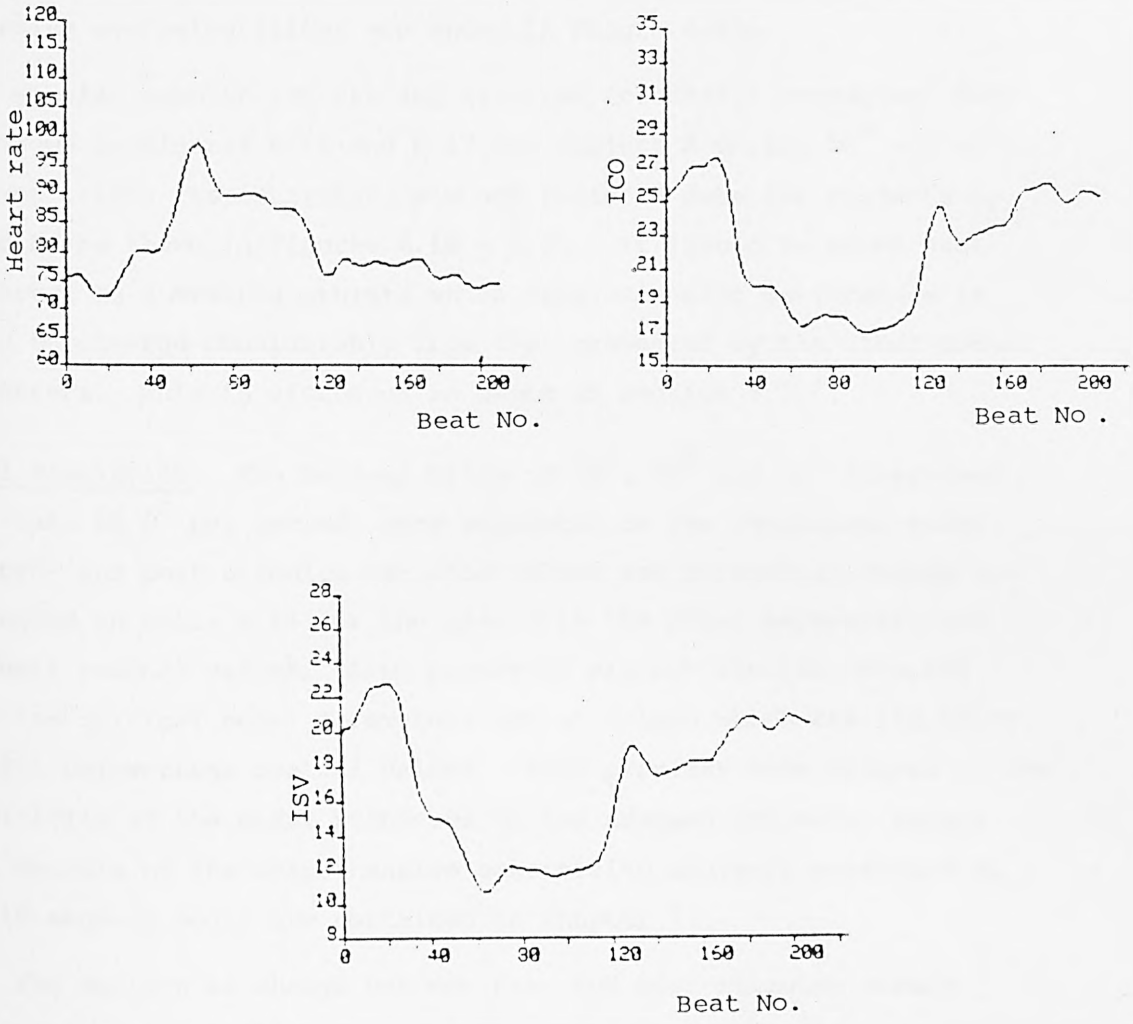

Figure 6.15d Filtered form of the data depicted in Figure 6.15a obtained using a recursive averaging filter.

to filtering was therefore replaced by a simple averaging filter (averaging three consecutive values). The results of using this recursive averaging filter are shown in Figure 6.15d.

Similar results for raw and filtered (recursive averaging) data are shown in Figures 6.16 and 6.17 for subject A during 20^{o} and 60^{o} head-up tilts, respectively. Raw and filtered data for subjects G, E and K are shown in Figures 6.18 - 6.21. It should be noted that subject K is a trained athlete whose cardiovascular performance is found to diverge considerably from that presented by the other normal volunteers. This is discussed in depth in Section 6.5.4.

Model simulation. The head-up tilts of 20^{o}, 45^{o} and 60^{o} (performed at a rate of 6^{o} per second) were simulated on the 19-segment model. The pre- and post-stimulus variable values and percentage change are presented in Table 6.13 for the case with the model parameters set at their nominal values. Also presented are the results obtained with ten critical model parameters set at values which are 15% above and 15% below these nominal values. This provides some measure of the sensitivity of the model responses to the assumed parameter values. Full details of the comprehensive sensitivity analysis performed on the 19-segment model are contained in Chapter 7.

The pattern of change between pre- and post-stimulus steady state values for model and normal subjects can be clearly seen in Figures 6.22 - 6.24 (the pre- and post-stimulus values are connected by straight lines). The principal changes are summarised in Table 6.14.

In the four subjects on whom the 20^{o} head-up tilt was performed, the effect of the tilt was a percentage increase in heart rate ranging from 3 - 16%, as shown in Table 6.14. By comparison the model, incorporating nominal parameter values, yielded a 7% increase. With the ten critical model parameters respectively increased and decreased by 15% from their nominal values, the percentage increase in heart rate was 3% and 8%.

Although the model response is in accord with these experimental data, it should be noted that conflicting data were obtained by Tuckman et al (1966). In this case a 20^{o} head-up tilt experiment was performed upon eight subjects. Of these, two exhibited heart rate increases of 10% and 22%, one exhibited no effective change, whilst the other five showed decreases ranging from 1% - 10%.

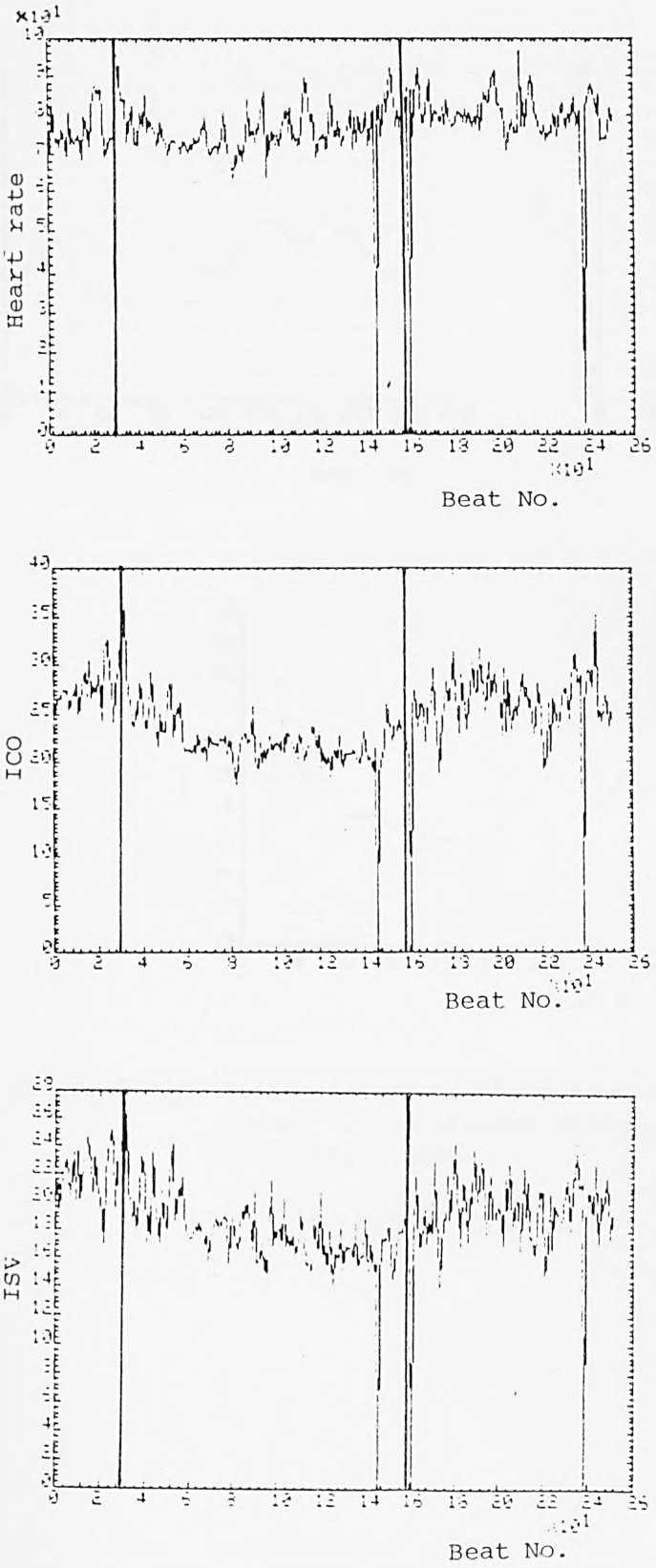

Figure 6.16a Raw data obtained from subject A for the three variables as indicated during a 20° head-up tilt. The vertical lines indicate the times at which the tilt to the inclined position and the return to the horizontal began.

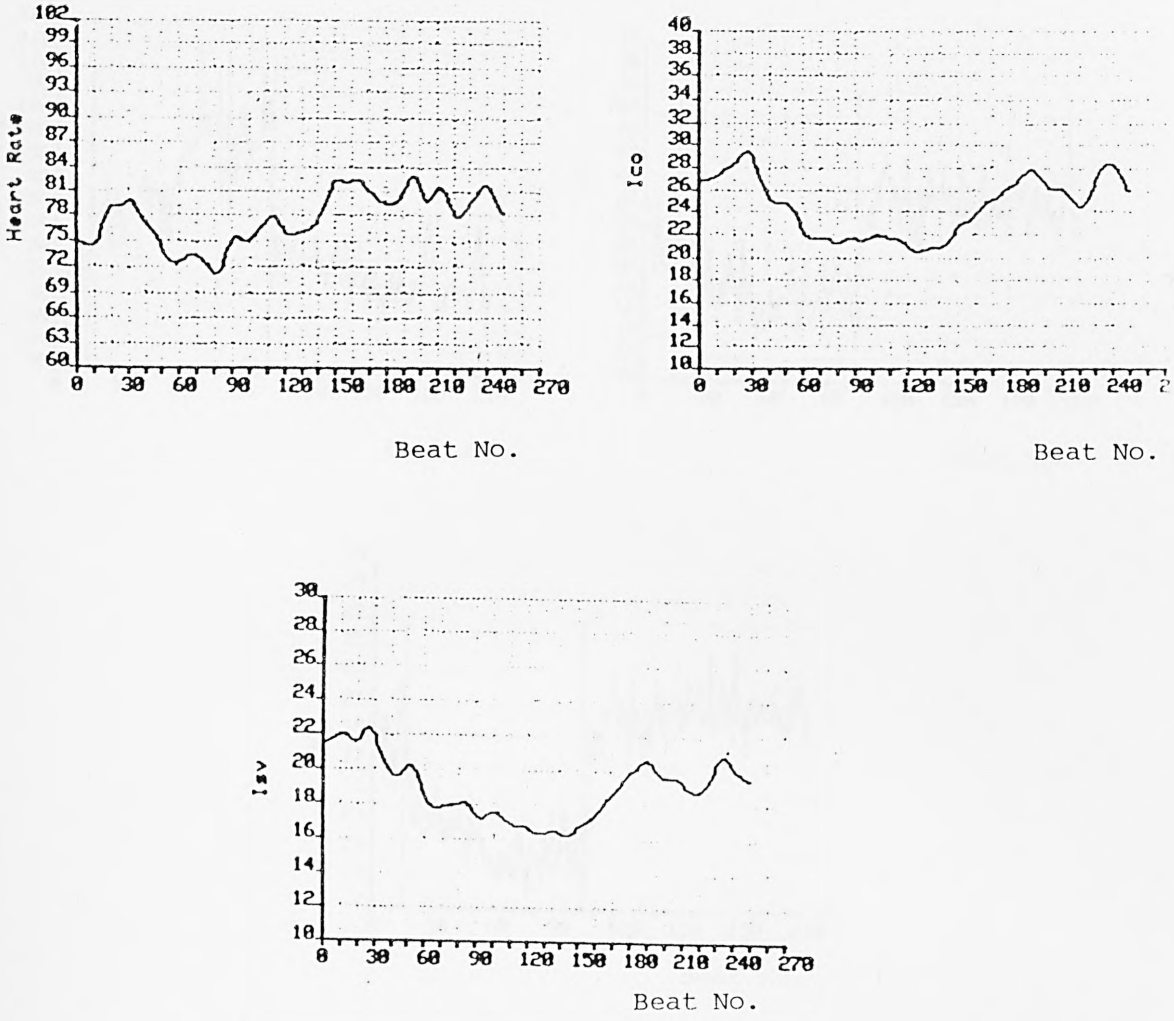

Figure 6.16b Filtered form of the data depicted in Figure 6.16a obtained using a recursive averaging filter.

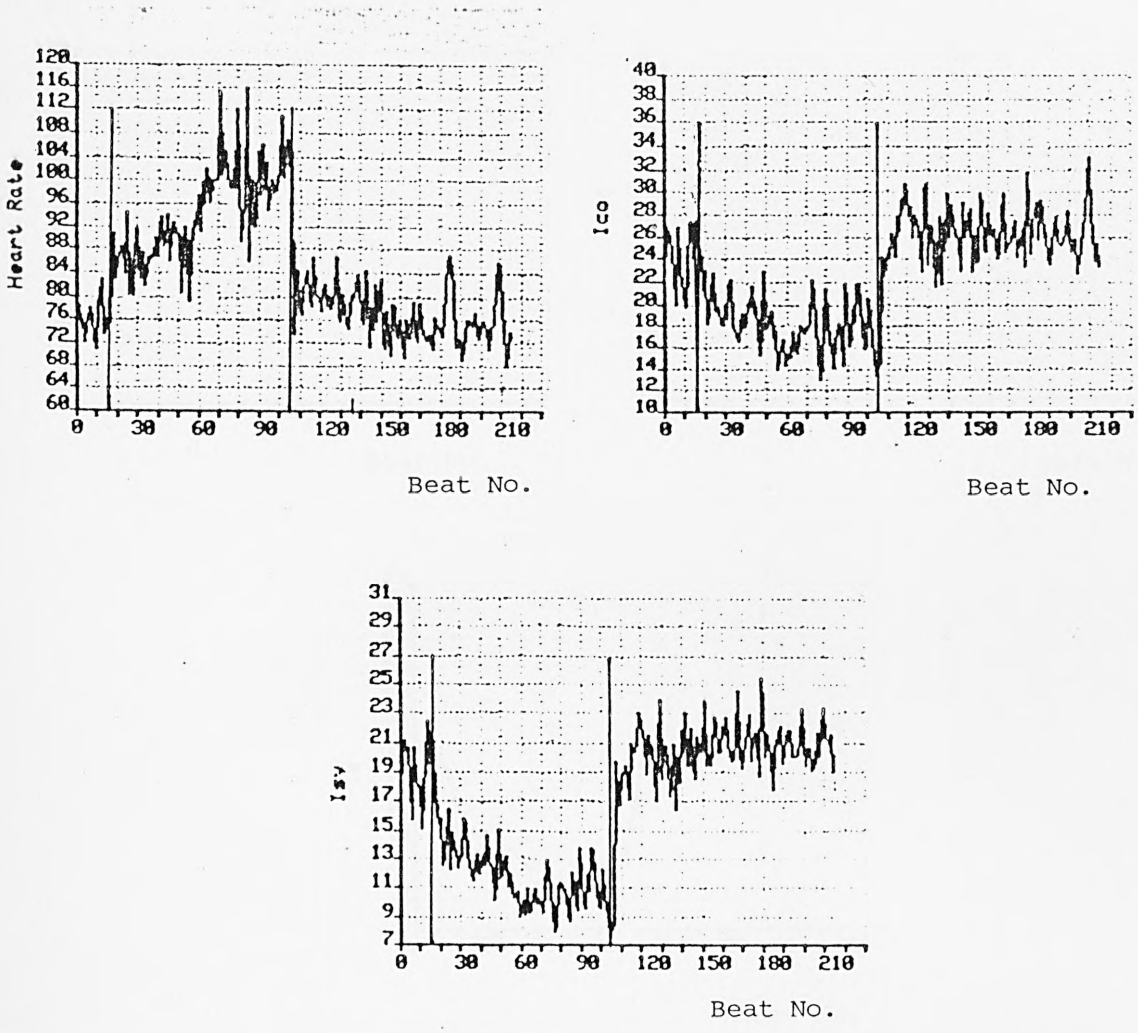

Figure 6.17a Raw data obtained from subject A for the three variables as indicated during a 60° head-up tilt. The vertical lines indicate the times at which the tilt to the inclined position and the return to the horizontal began.

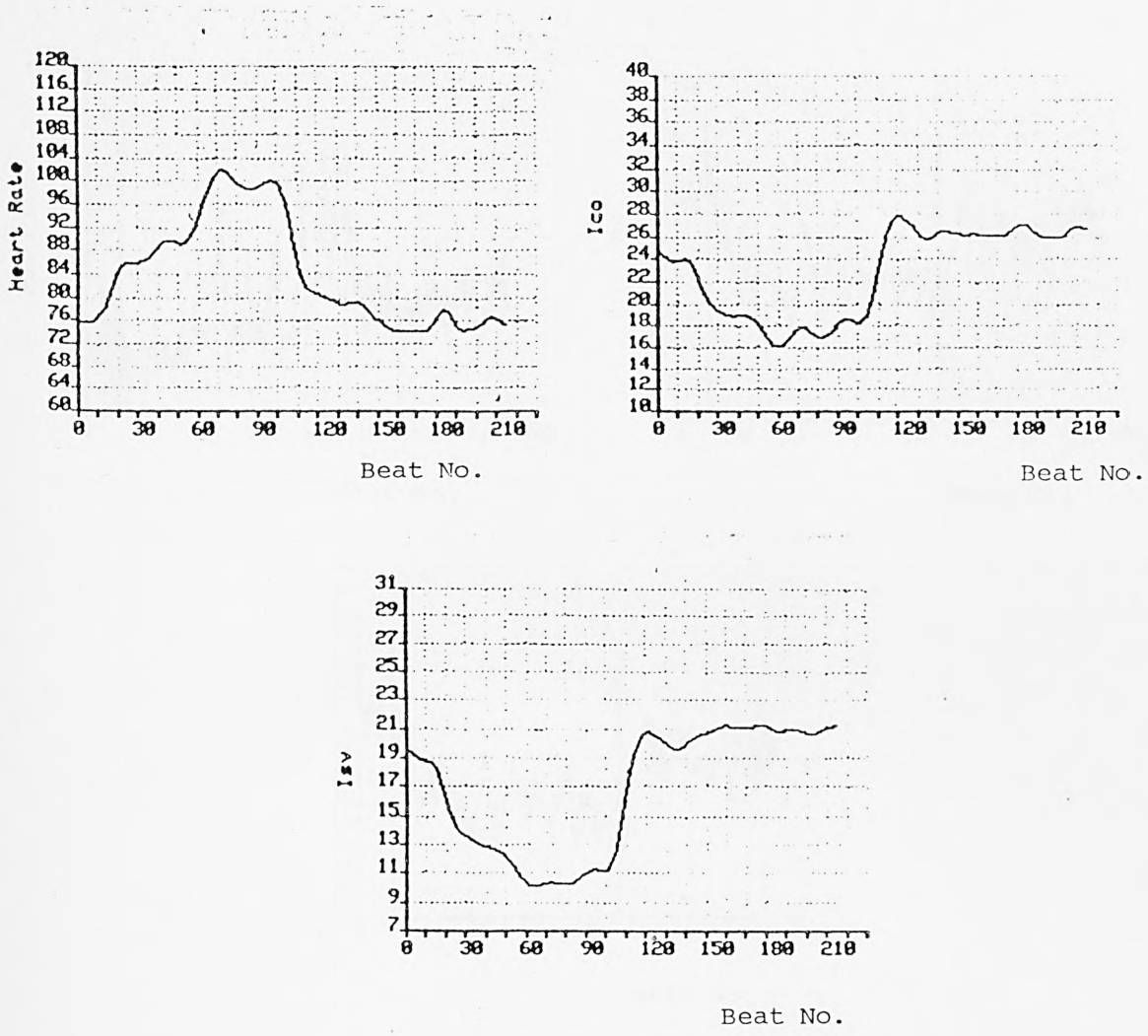

Figure 6.17b Filtered form of the data depicted in Figure 6.17a obtained using a recursive averaging filter.

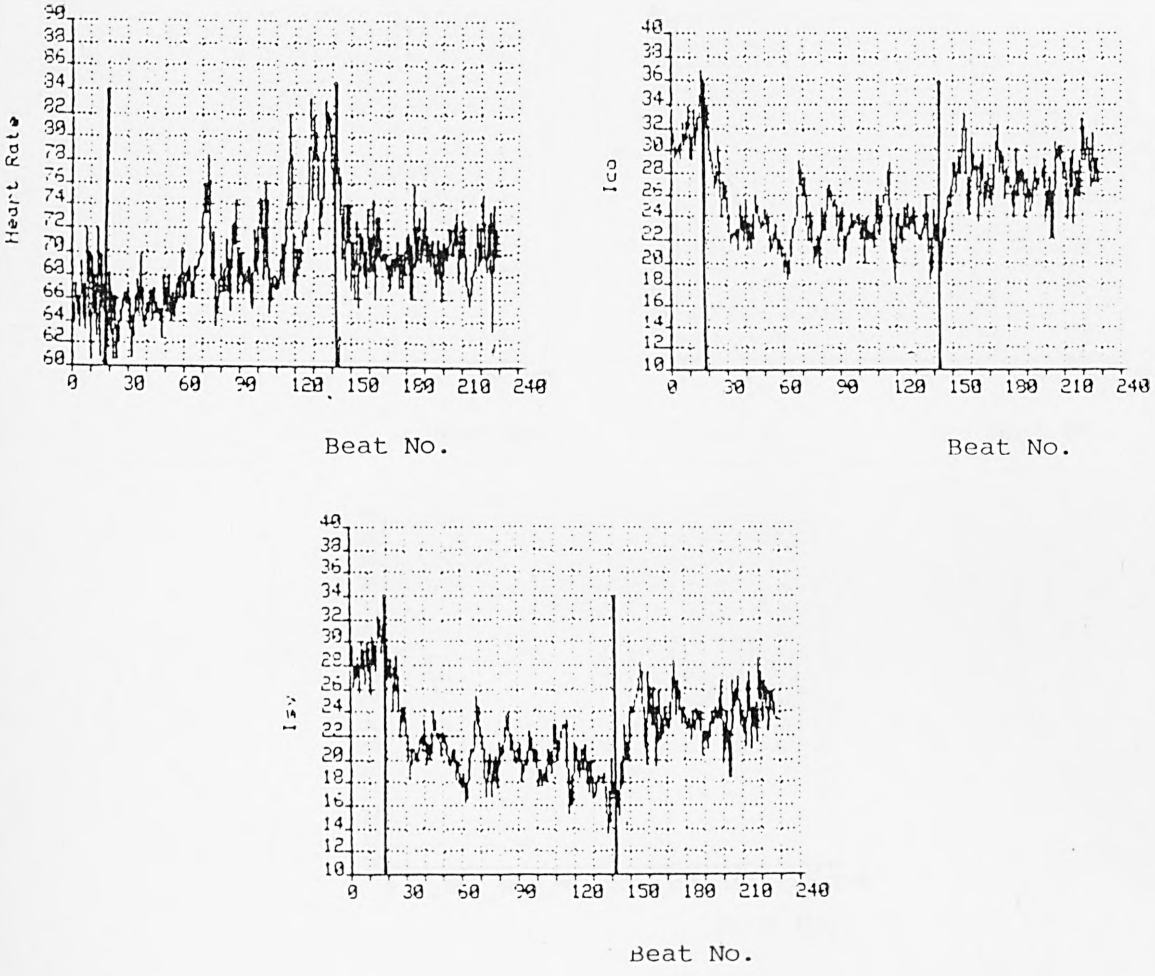

Figure 6.18a Raw data obtained from subject G for the three variables as indicated during a 45° head-up tilt. The vertical lines indicate the times at which the tilt to the inclined position and the return to the horizontal began.

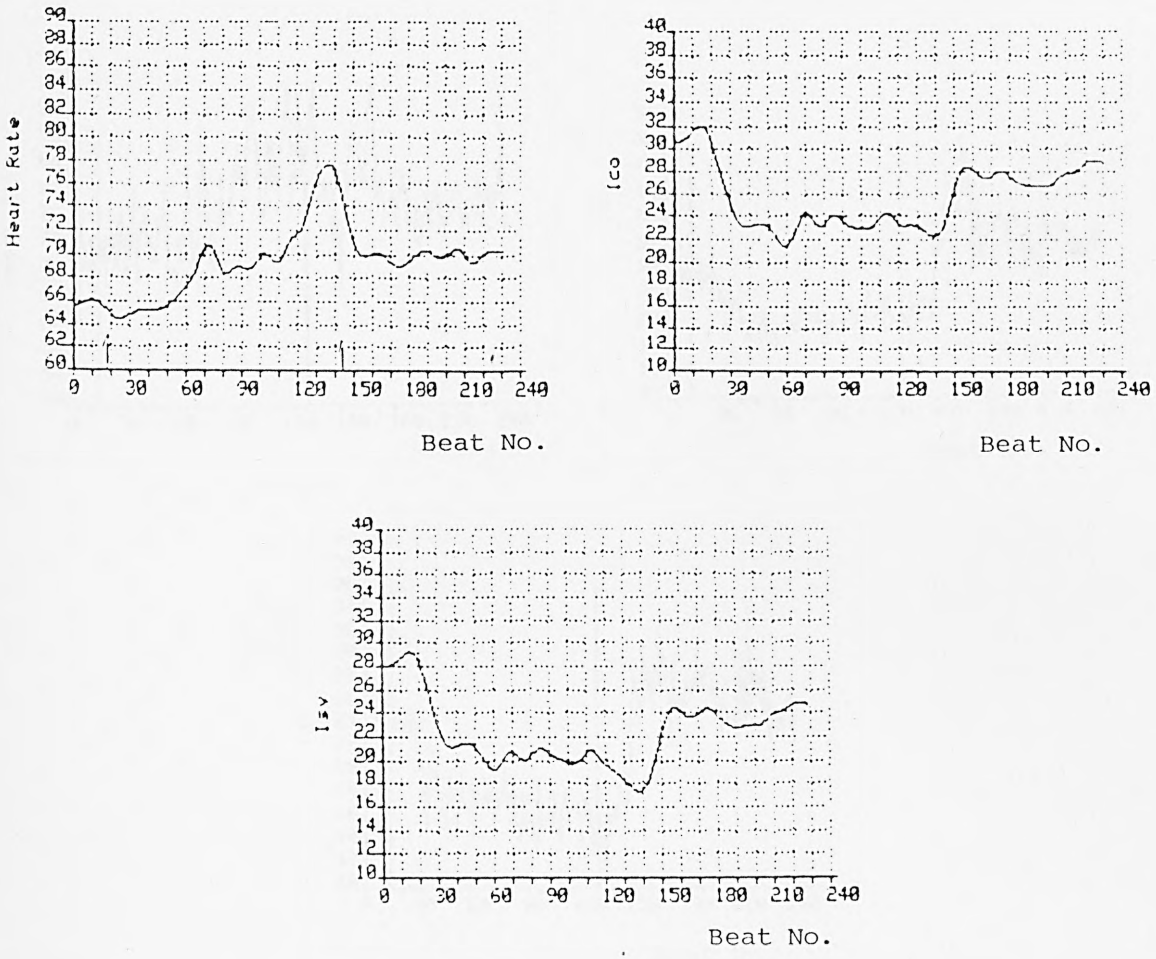

Figure 6.18b Filtered form of the data depicted in Figure 6.18a obtained using a recursive averaging filter.

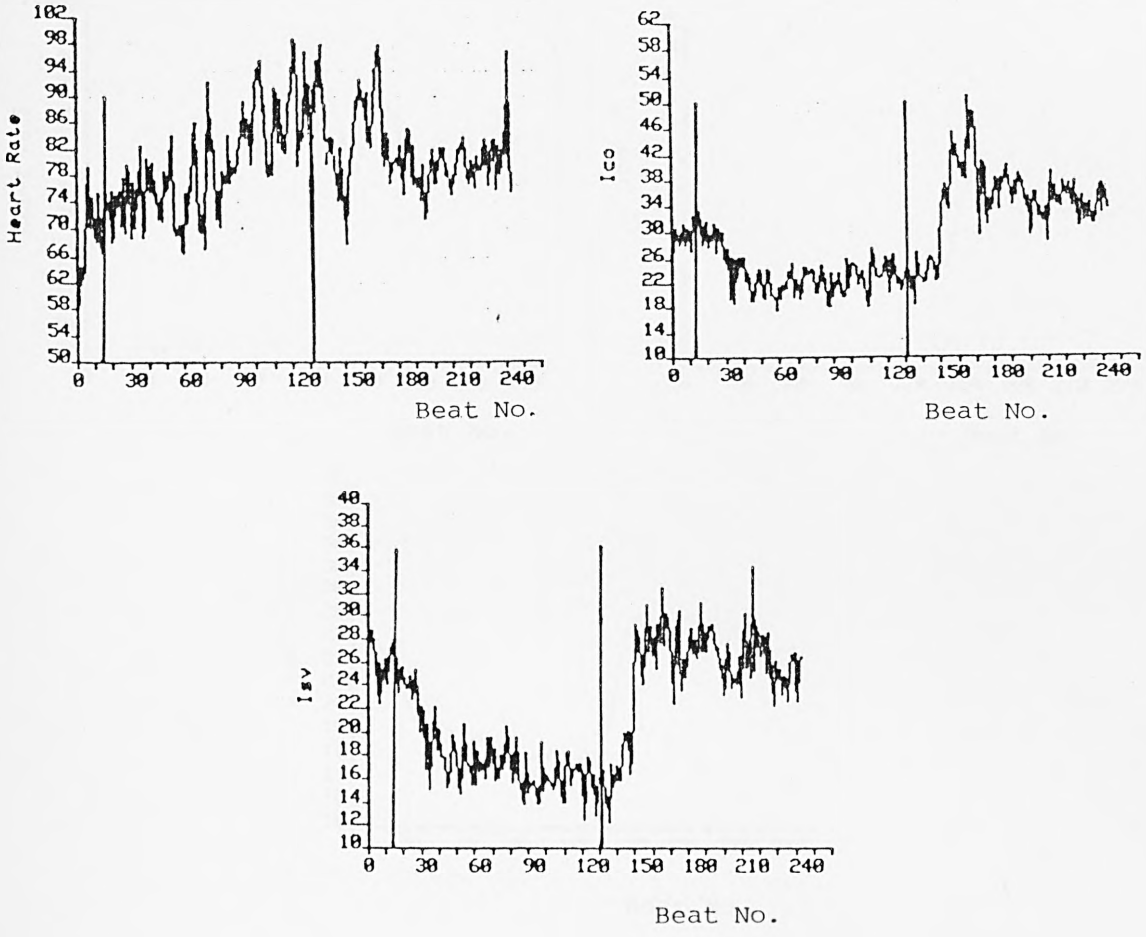

Figure 6.19a Raw data obtained from subject E for the three variables as indicated during a 60° head-up tilt. The vertical lines indicate the times at which the tilt to the inclined position and the return to the horizontal began.

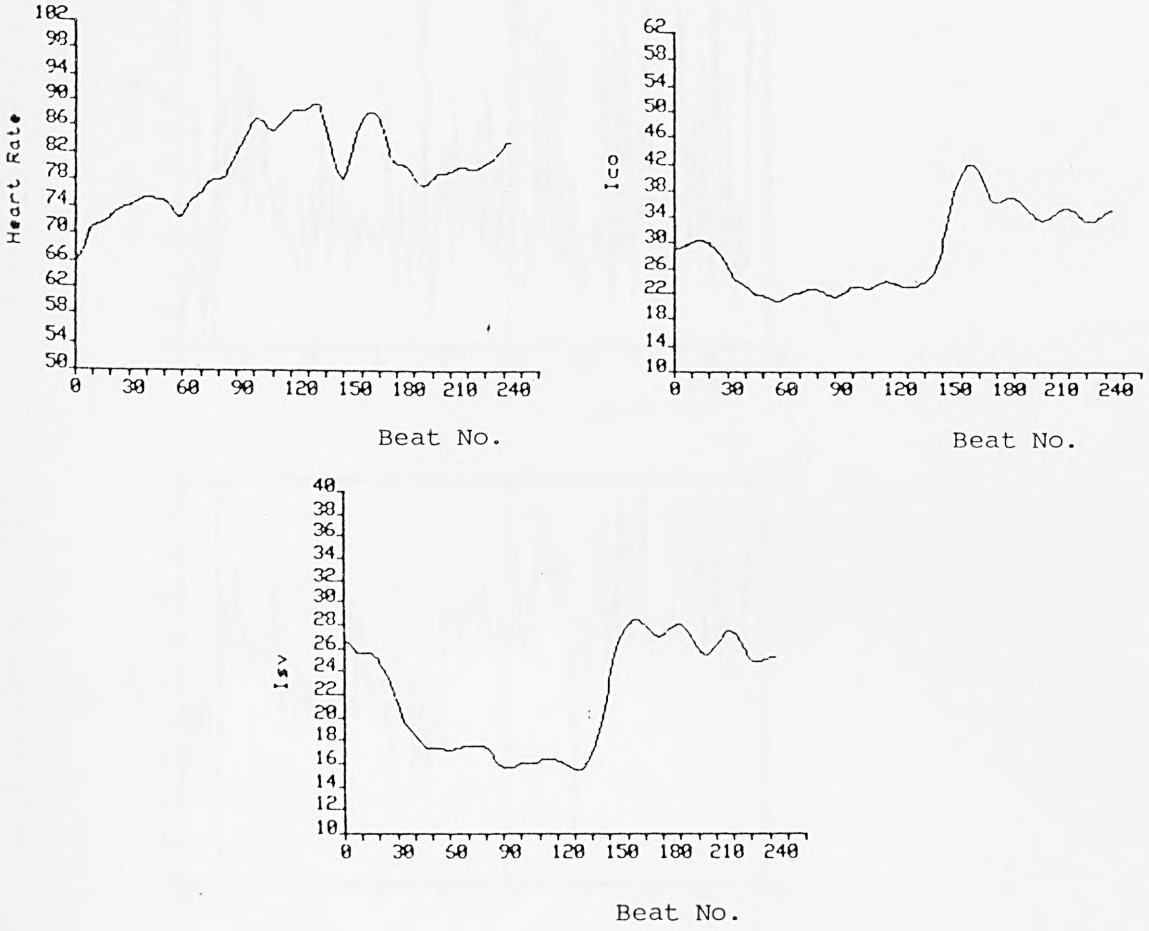

Figure 6.19b Filtered form of the data depicted in Figure 6.19a obtained using a recursive averaging filter.

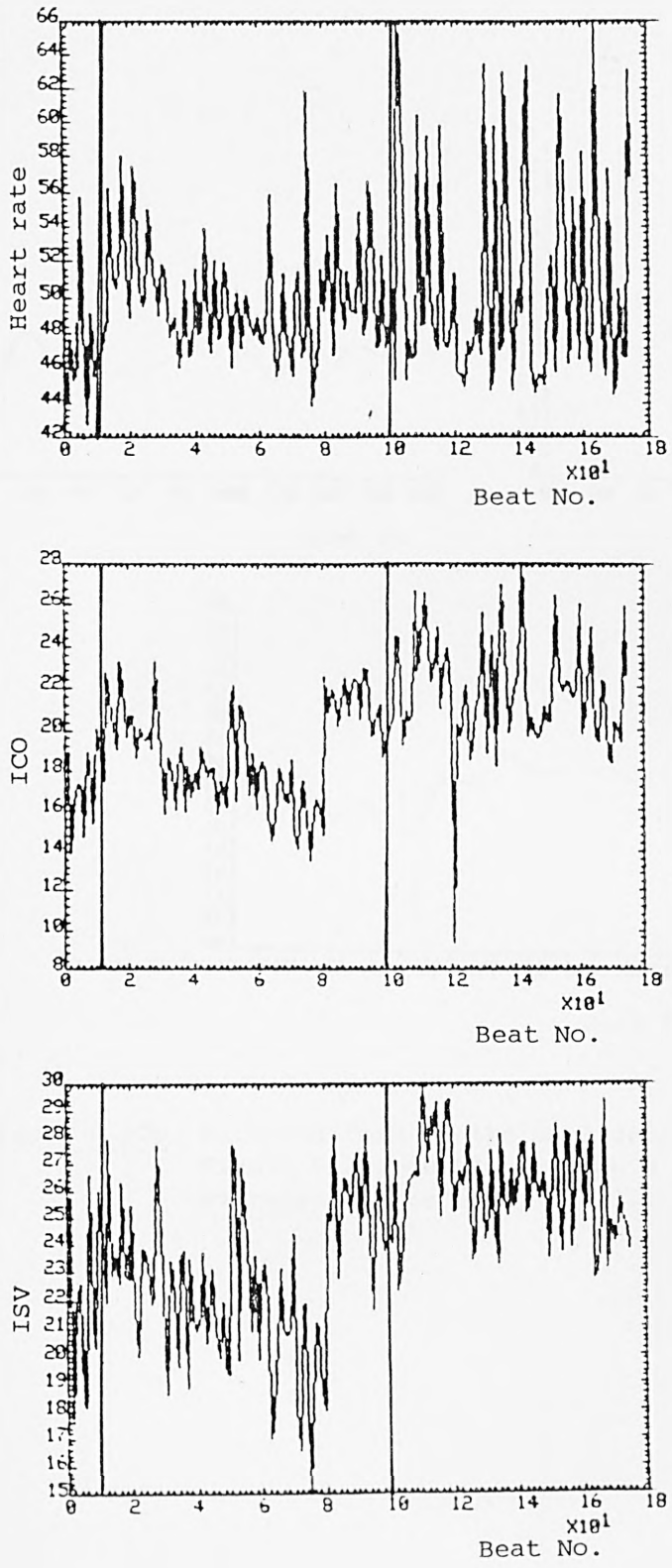

Figure 6.20a Raw data obtained from subject K for the three variables as indicated during a 20° head-up tilt. The vertical lines indicate the times at which the tilt to the inclined position and the return to the horizontal began.

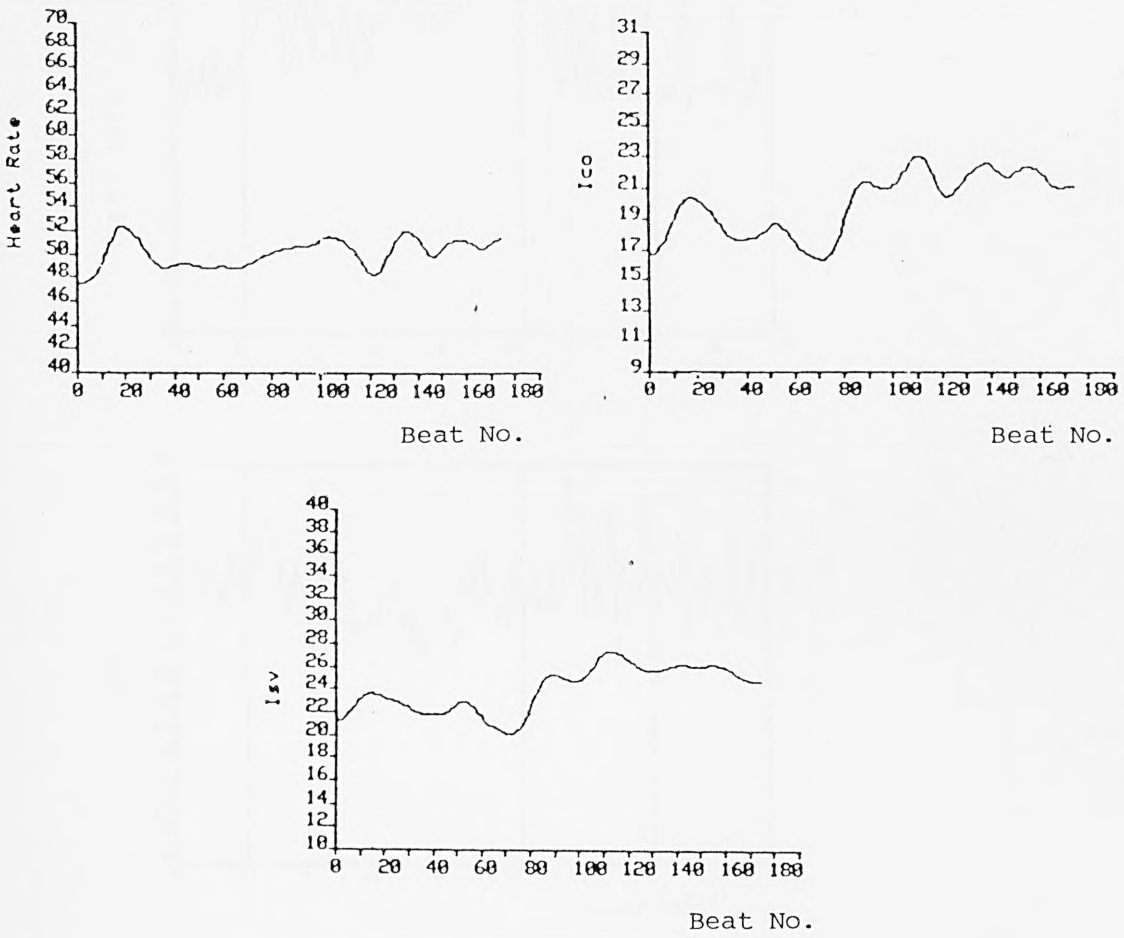

Figure 6.20b Filtered form of the data depicted in Figure 6.20a obtained using a recursive averaging filter.

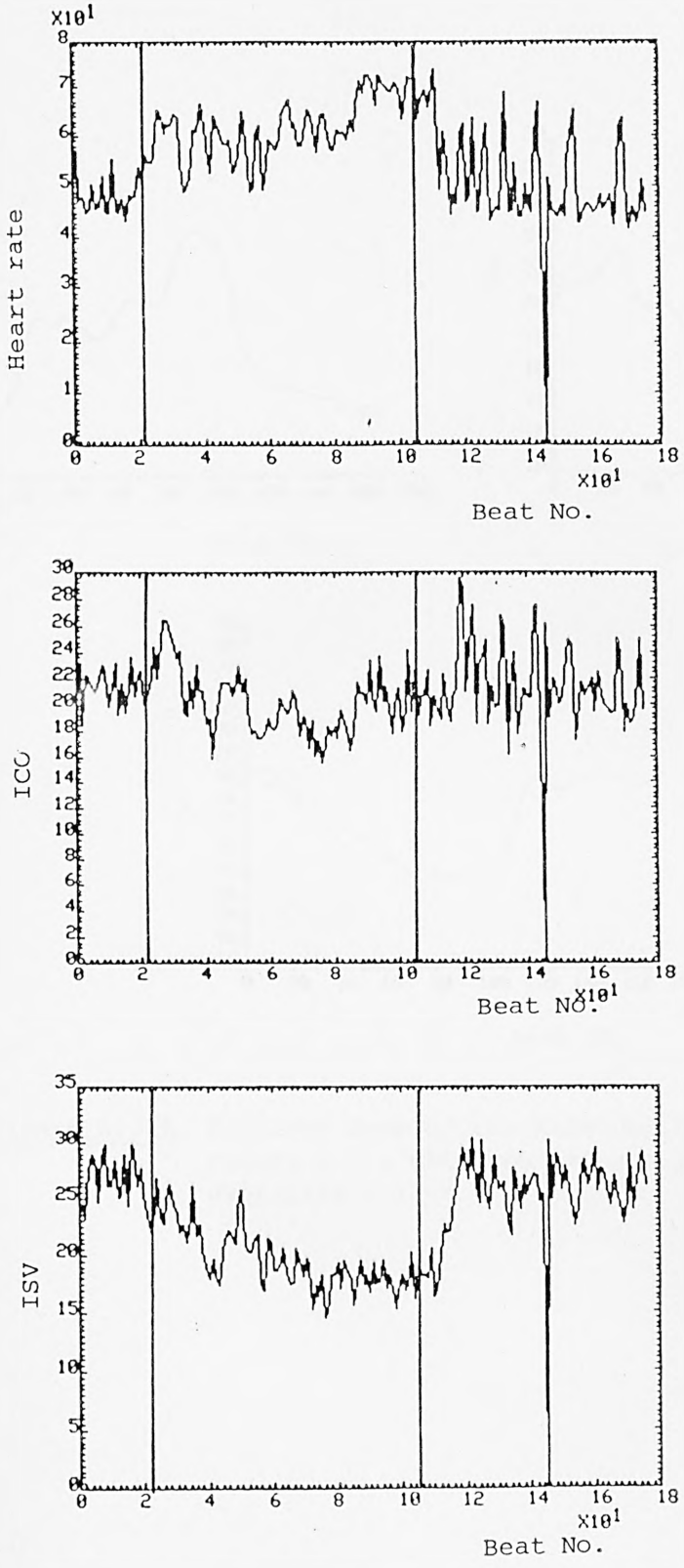

Figure 6.21a Raw data obtained from subject K for the three variables as indicated during a 45° head-up tilt. The vertical lines indicate the times at which the tilt to the inclined position and the return to the horizontal began.

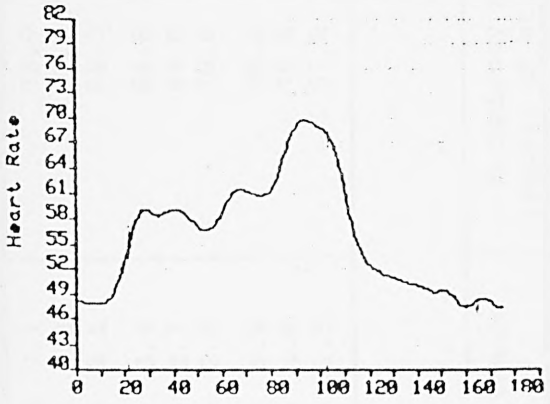

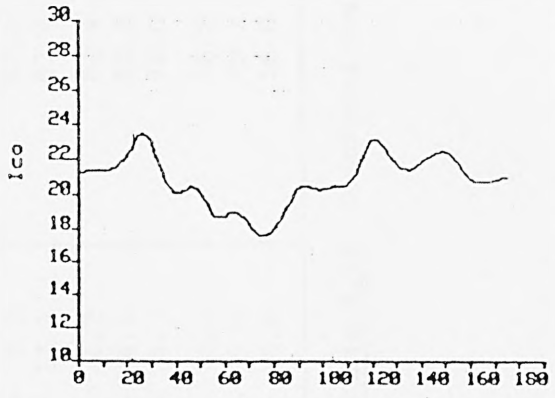

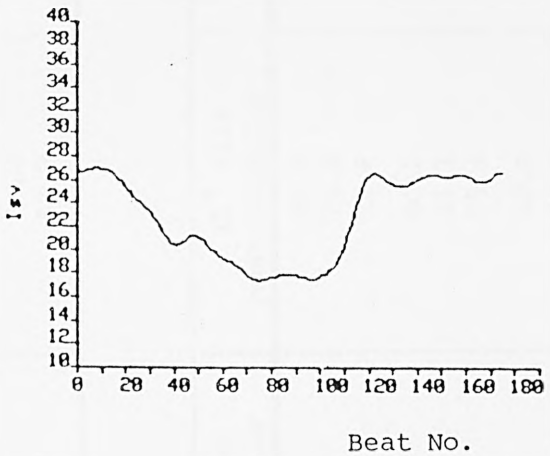

Figure 6.21b Filtered form of the data depicted in Figure 6.21a obtained using a recursive averaging filter.

(a)

Parameter values	Variable	Recumbency pre-stimulus	+ 20° tilt post-stimulus	% change	Recumbency after removal of stimulus
Nominal value	FH	72.8	78.0	+ 7.1	72.9
+ 15% change		70.0	72.0	+ 2.8	67.0
- 15% change		81.0	87.6	+ 8.1	81.0
Nominal value	CO	84.8	81.9	- 3.4	84.6
+ 15% change		88.0	85.6	- 2.7	89.0
- 15% change		78.6	76.6	- 2.5	78.6
Nominal value	SV	69.2	63.0	- 8.9	69.4
+ 15% change		74.8	71.2	- 4.8	79.8
- 15% change		59.0	52.2	- 11.5	57.8

(b)

Parameter values	Variable	Recumbency pre-stimulus	+ 45° tilt post-stimulus	% change	Recumbency after removal of stimulus
Nominal value	FH	72.8	81.4	+ 11.8	72.9
+ 15% change		70.0	76.8	+ 9.7	67.0
- 15% change		81.0	91.8	+ 13.3	83.4
Nominal value	CO	84.4	80.8	- 4.2	84.4
+ 15% change		88.0	84.1	- 4.4	89.0
- 15% change		79.0	75.4	- 4.5	78.0
Nominal value	SV	69.4	59.0	- 14.9	56.8
+ 15% change		75.0	65.9	- 12.0	79.2
- 15% change		58.8	49.6	- 15.6	56.8

Table 6.13 continued overleaf

(c)

Parameter values	Variable	Recumbency pre-stimulus	+ 60° tilt post-stimulus	% change	Recumbency after removal of stimulus
Nominal value	FH	72.8	84.9	+ 16.6	73.0
+ 15% change		70.0	79.2	+ 13.0	77.6
- 15% change		81.0	93.8	+ 15.8	83.0
Nominal value	CO	84.6	79.4	- 6.1	84.4
+ 15% change		88.0	83.0	- 5.6	89.0
- 15% change		78.9	74.8	- 5.1	77.4
Nominal value	SV	69.4	56.3	- 18.8	69.2
+ 15% change		74.9	63.0	- 15.8	79.6
- 15% change		58.9	48.0	- 18.5	56.4

Table 6.13 Model responses to (a) 20°, (b) 45°, and (c) 60° head-up tilts. Values of heart rate, cardiac output and stroke volume are given first with all parameters set at their nominal values and then with the ten critical parameters (as defined in Chapter 7) changed by + 15% and - 15%, respectively.

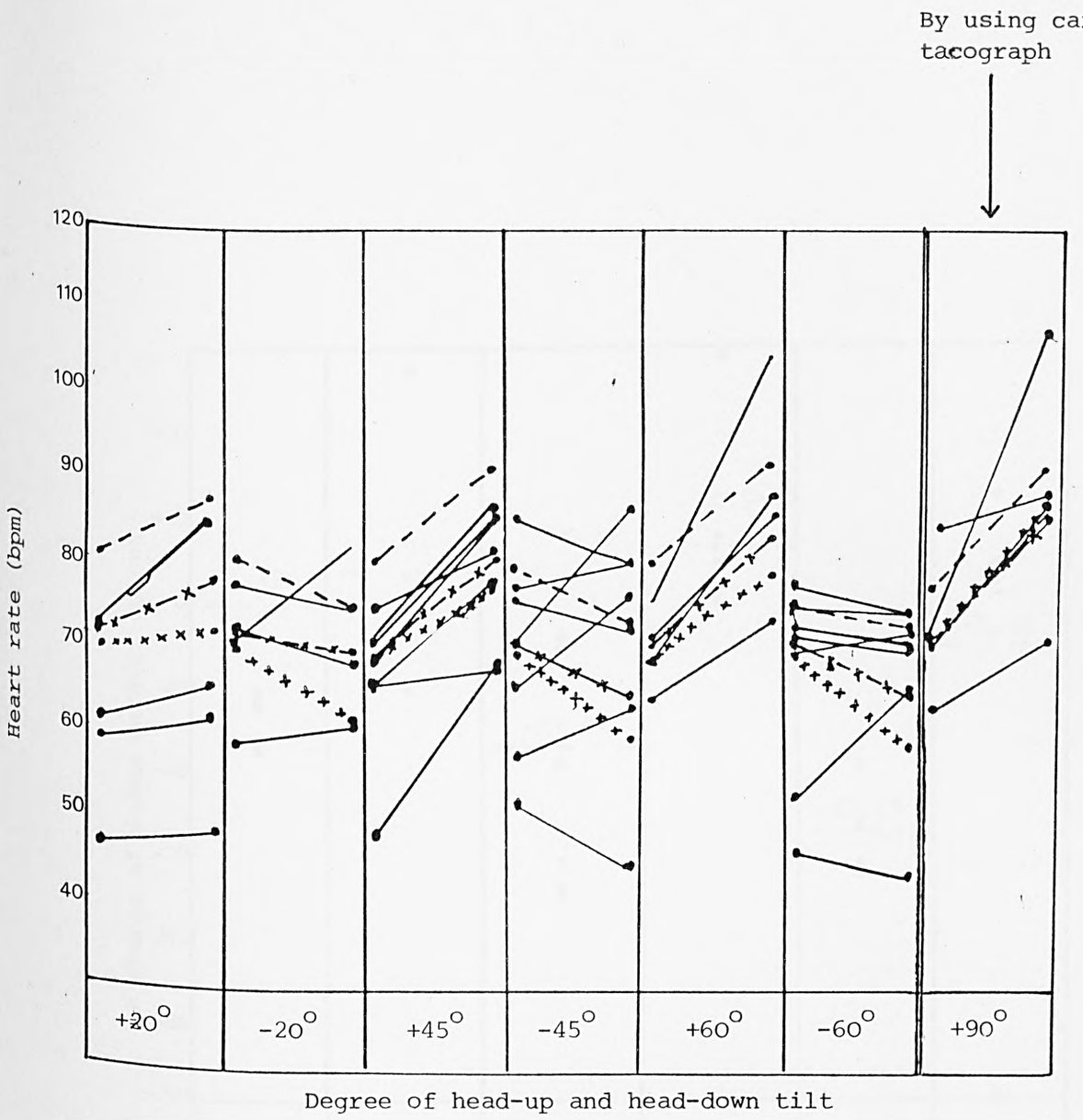

Figure 6.22 Change in heart rate following different degrees of head-up and head-down tilt. (-X-X-) represents the model response with all parameters set at their nominal values, (- - -) model response with -15% change in the ten critical parameter values, and (x x x x x) with +15% change in the ten critical parameter values.

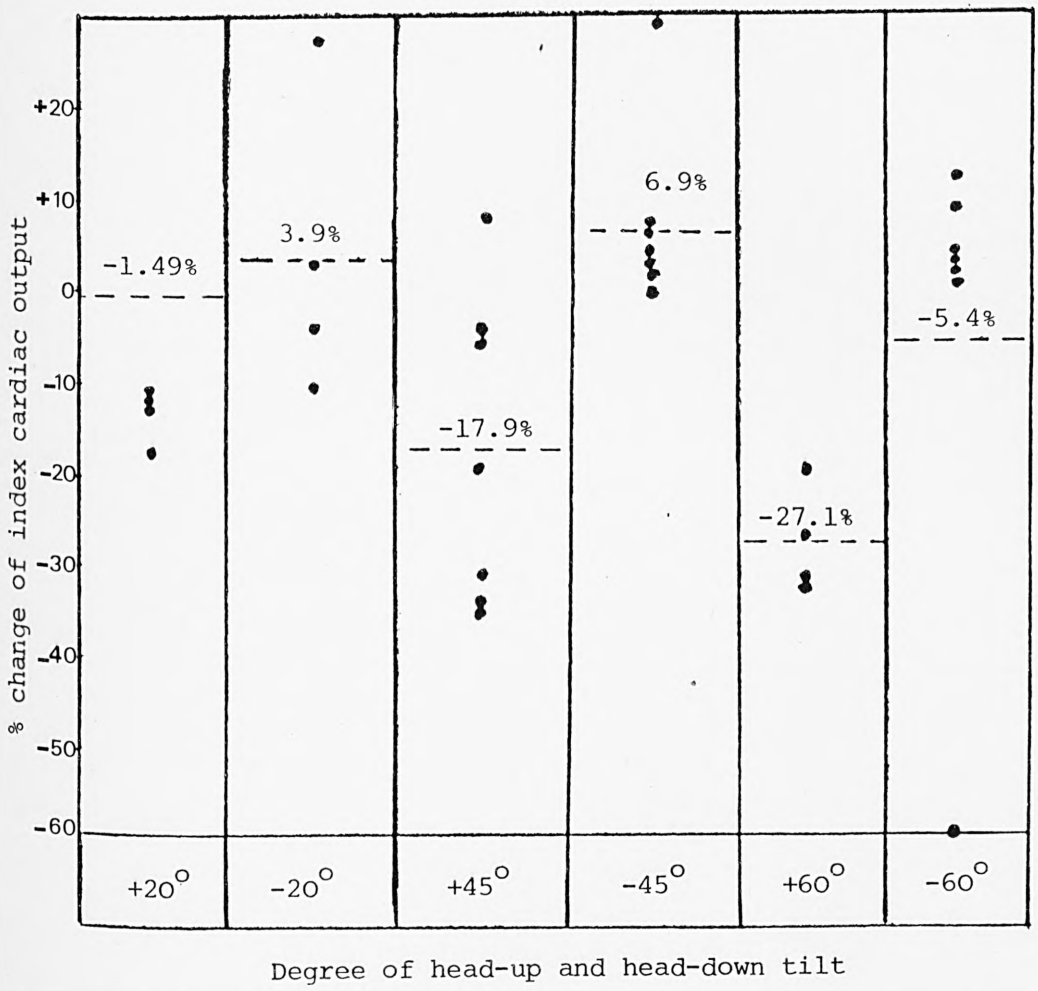

Figure 6.23a Percentage change in index of cardiac output following different degrees of head-up and head-down tilt.

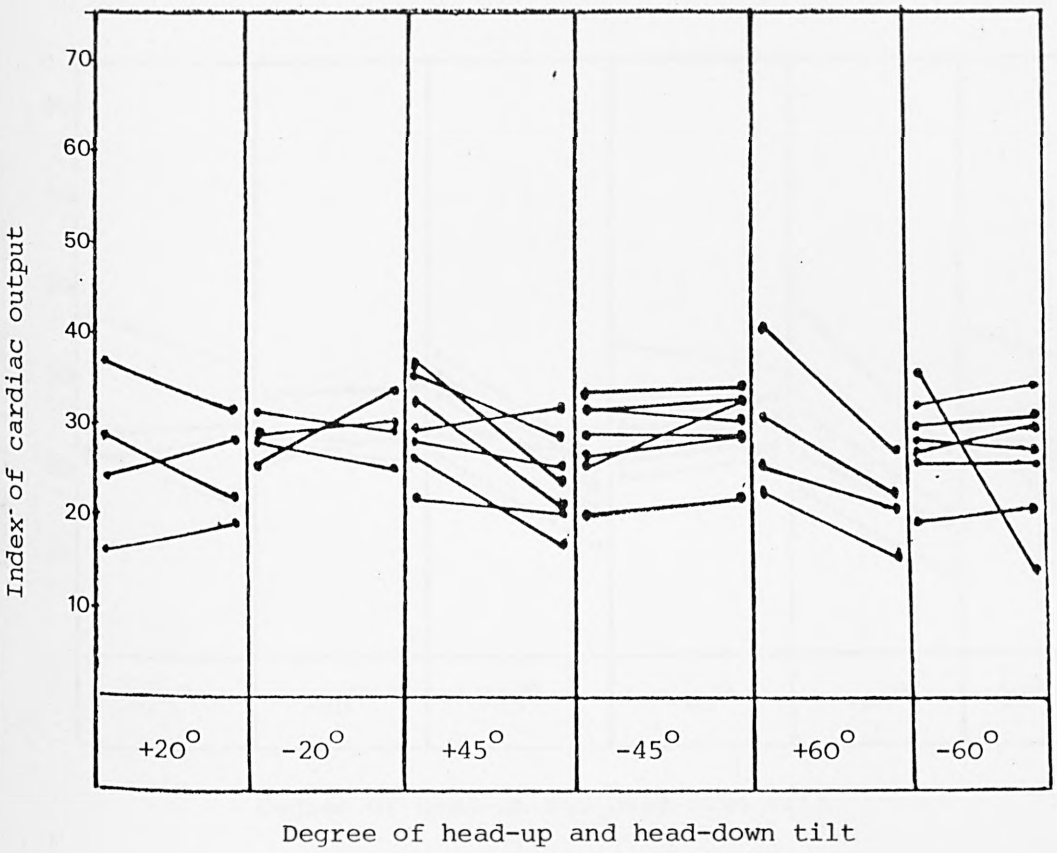

Figure 6.23b Change in index of cardiac output following different degrees of tilt.

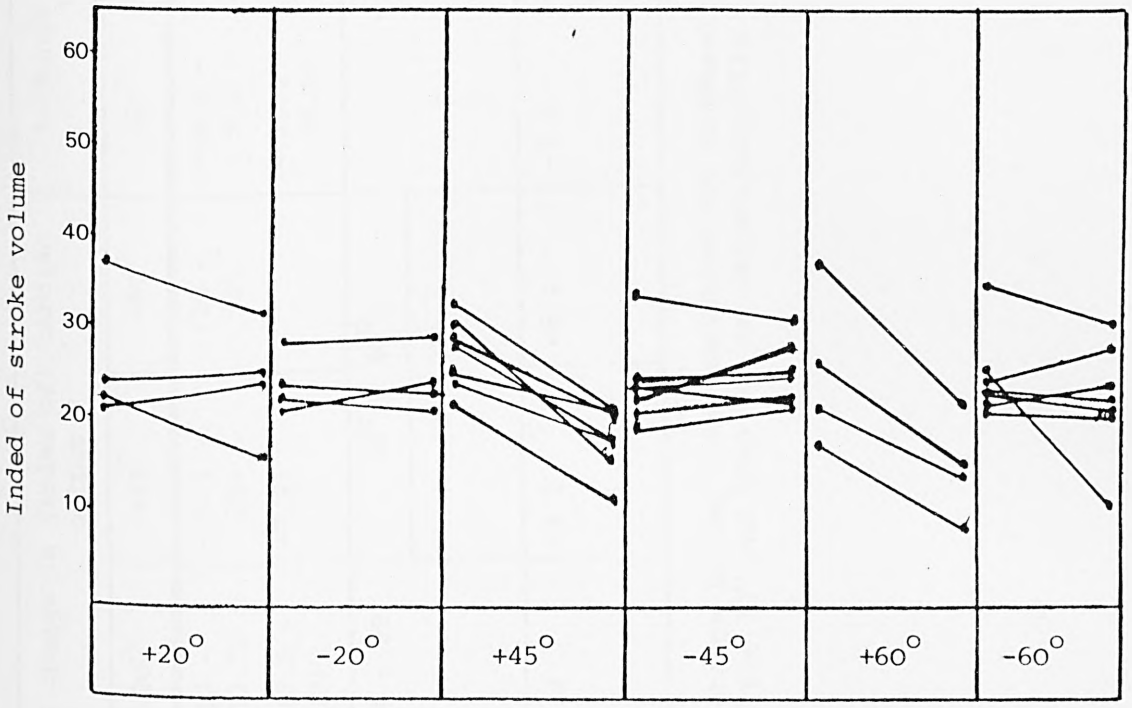

Figure 6.24 Change in index stroke volume following different degrees of tilt.

	% change in heart rate from supine to the tilt position			% change in (index of) cardiac output			% change in (index of) stroke volume		
Empirical data (Northwick Park)	$+20^{\circ}$	$+45^{\circ}$	$+60^{\circ}$	$+20^{\circ}$	$+45^{\circ}$	$+60^{\circ}$	$+20^{\circ}$	$+45^{\circ}$	$+60^{\circ}$
	+(2.6 - 15.5)	+(0.7 - 42.6)	+(13.6 - 38)	+(12 - 13.7) -(13.6 - 18)	-(5.1 - 35) +7.2	-(20 - 31)	+(6.9 - 9.2) -(16.1 - 28.8)	-(12.9 - 45)	-(33 - 49.8)
Data from Tuckman et al (1966)	+(9.7 - 22) -(1.4 - 9.7)	40° - 60° +(2.8 - 63.9)		-(9 - 29)	40° - 60° -(2 - 35)		-	40° - 60° -	
Model response	+7.1 (2.8 - 8.1)	+11.8	+16.6	-3.4	-4.2	-6.1	-8.9	-14.9	-18.8

Table 6.14 Comparison of the range of percentage change in the three variables for different degrees of head-up tilt. Note that Tuckman et al presented data for 20° and then for an unspecified tilt within the range 40° - 60° head-up.

In Figures 6.25 - 6.27, values of the three variables are presented for each of the subjects for 20^{o}, 45^{o} and 60^{o} head-up tilt (these are the post-stimulus steady state values of the variables). The corresponding results obtained from model simulation are also depicted. Also shown are the results (experimental and model) for the head-down tilt perturbations which are described in Section 6.5.2. The correlation coefficients for head-up tilt for the three variables for each of the subjects and the model are tabulated in Table 6.15, indicating general agreement between model and experimental data.

6.5.1.2.2 Experiments carried out at St. Thomas's Hospital

The second set of experimental data was obtained from St. Thomas's Hospital, where a 70^{o} head-up tilt was performed on nine normal subjects (five male, four female, age range 20 - 32 years). Values of heart rate and arterial pressure were measured pre- and post-stimulus and these are listed in Table 6.16.

In all cases, the heart rate increases, the mean increase being with a range from 9% - 62%. Of the nine subjects, eight exhibited an increase in arterial pressure ranging from 7% - 16%. On the other hand, in one subject arterial pressure decreased by 3%.

The model response indicated a 17% increase in heart rate, but a 3% decrease in arterial pressure. These values were obtained with the parameters set at their nominal values and with the 70^{o} rotation achieved over a period of one minute, this being approximately the time required in the experiment. (Note that whereas in the experiments performed at Northwick Park Hospital the table was rotated (motor-driven) at a constant 6^{o} per second, the table at St. Thomas's Hospital was hand-cranked and hence the rotation was somewhat variable.)

6.5.1.2.3 Heart rate variability and response to 90^{o} head-up tilt

The third set of experimental data was obtained in tests carried out at The City University on four normal subjects, including three who were subjects of the head-up experiments described in Section 6.5.1.2.1. The purpose of the experiment was two-fold. The first was to examine the response to a sudden change from the recumbent position to standing, and secondly to examine the inherent beat-to-beat variability in heart rate occurring in a normal recumbent individual. The motivation for this second aim arose from the degree of "noise"

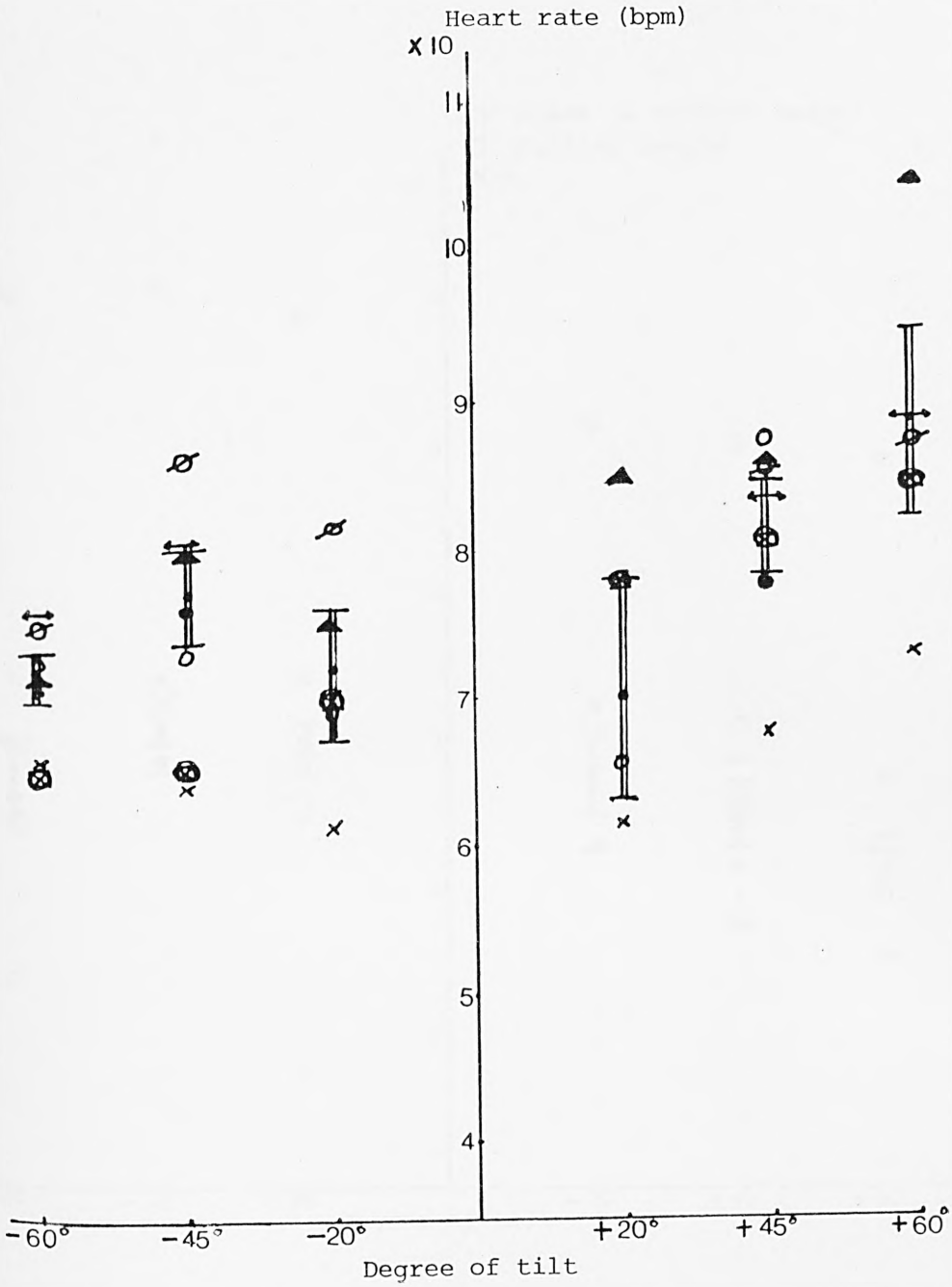

▲ - Subject A

o - Subject B

x - Subject C

⌀ - Subject D

↔ - Subject E

● - Subject G

H - Mean value for the subjects, with standard error of the mean

⊗ - Model response

Figure 6.25 The effects of different degrees of tilt on the heart rate for six subjects and the model response.

▲ - Subject A

o - Subject B

x - Subject C

ø - Subject D

↔ - Subject E

● - Subject G

⊗ - Model response for cardiac output

H - Mean value for the subjects, with standard error of the mean

Figure 6.26 The effects of different degrees of tilt on index cardiac output or cardiac output for six subjects and the model response.

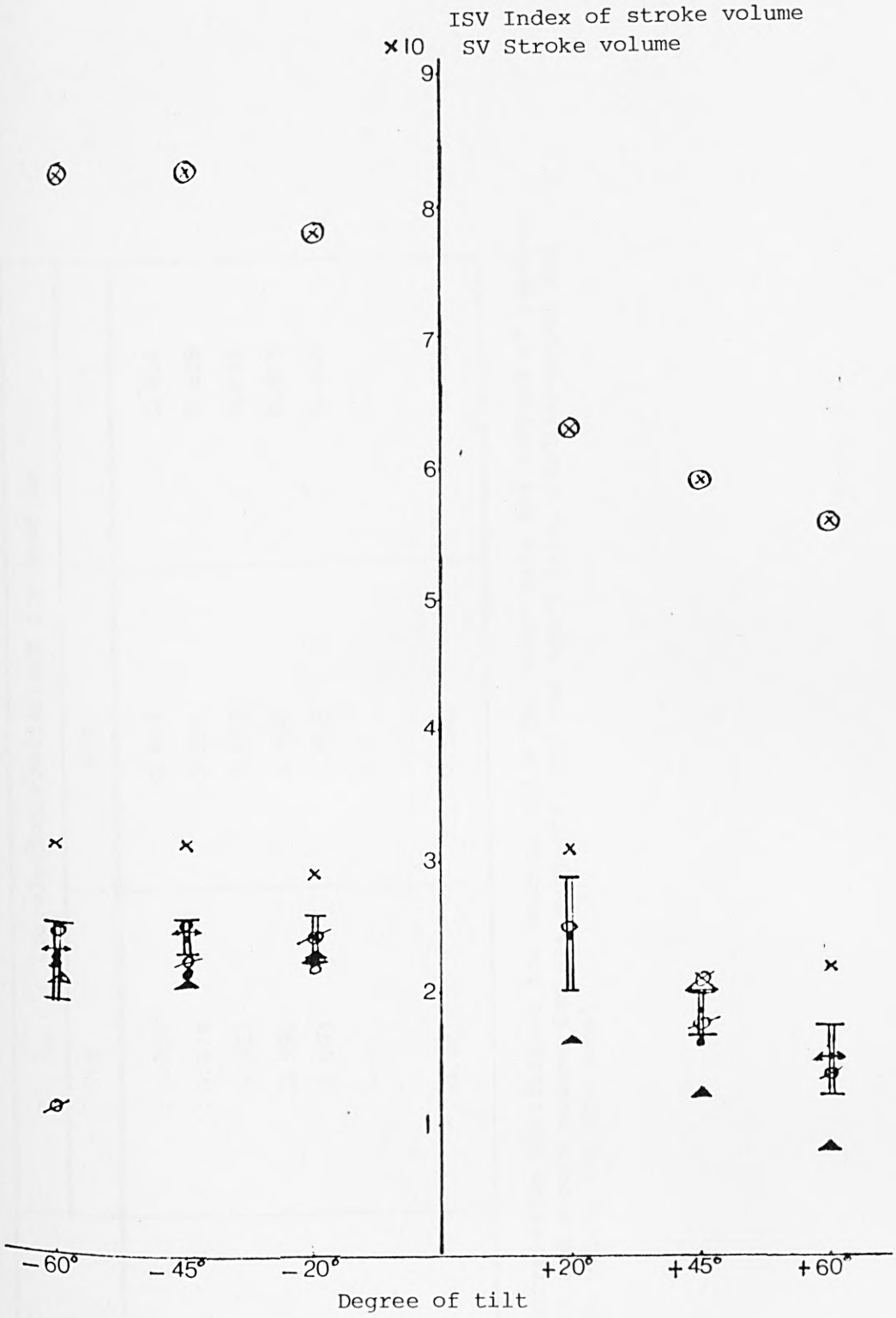

▲ - Subject A
O - Subject B
X - Subject C
⌀ - Subject D
↔ - Subject E
● - Subject G
⊗ - Model response for stroke volume
H - Mean value for the subjects, with standard error of the mean

Figure 6.27 The effects of different degrees of tilt on index stroke volume or stroke volume for six subjects and the model response.

Subject	Correlation coefficient for head up		
	FH	ICO	ISV
A	0.955	0.854	0.814
B	0.974	0.952	0.899
C	0.953	0.892	0.856
D	0.990	0.966	0.965
E	0.993	0.965	0.958
G	1.0	1.0	1.0
Model	0.941	0.925	0.911

Table 6.15 The correlation coefficient for head-up tilts for heart rate and indices of cardiac output and stroke volume for six subjects, and the heart rate, cardiac output and stroke volume for the model.

Subject No.	Sex	Age	Pre-stimulus		Post-stimulus 70° head-up tilt		% change FH	% change MAP
			FH (bpm)	MAP (torr)	FH (bpm)	MAP (torr)		
1	M	32	54.0	85.0	64.0	94.6	+ 18.5	+ 11.2
2	F	21	85.4	70.6	93.2	82.0	+ 9.0	+ 16.1
3	M	24	54.4	70.0	88.2	81.3	+ 62.0	+ 16.1
4	F	24	38.6	73.66	48.6	85.0	+ 25.0	+ 15.3
5	F	23	53.0	79.3	65.0	86.0	+ 22.0	+ 8.4
6	F	29	64.0	86.3	89.0	83.3	+ 39.0	- 3.4
7	M	29	76.0	83.0	85.0	94.3	+ 11.0	+ 13.6
8	M	27	73.8	94.3	105.2	103.3	+ 42.0	+ 9.5
9	M	23	62.0	99.66	75.0	107.0	+ 20.0	+ 7.3
Model response			72.8	109.1	85.5	105.3	+ 17.4	- 3.4

Table 6.16 Experimental data on heart rate (FH) and mean arterial pressure (MAP) for nine normal subjects prior to and after a 70° head-up tilt. Model-derived data are also shown.

evidenced in the heart rate data obtained from the experiments carried out at Northwick Park Hospital.

Experimental data were obtained using a Hewlett-Packard fetal monitor-cardiotocograph (model 8040A), which features a wide beam pulsed Doppler ultrasound transducer (see Figure 6.28a). Using this apparatus a continuous recording of the heart rate of each of the subjects in the recumbent position was taken over a period of ten minutes. At the end of this time the subject made the sudden transition from the supine to the standing position whilst the recording of heart rate was continued. An example of the heart rate trace obtained for one of the subjects is presented in Figure 6.28b. This includes the transition from recumbent to standing position as well as showing heart rate variability in both positions.

Figure 6.29 a - d shows the histogram of heart rate variability for each of the four subjects. In each case the lower panel indicates the distribution in the recumbent position (taken from the heart rate recording over a period of 109.2 seconds), whilst the top panel indicates the distribution in the standing position (taken from the heart rate recording over a period of 109.2 seconds).

A comparison of the change of heart rate exhibited by each of the four subjects during the sudden postural change from recumbent to standing position with the model response is presented in the final column of Figure 6.22. From this it can be seen that the direction of change in heart rate is the same both for the model and all the normal subjects.

6.5.2 The Circulatory Effects of a Head-down Tilt

In order to examine further the validity of the 19-segment model, its response to a head-down tilt was examined. The principal features of the model response following a 90^{o} head-down tilt and subsequent return to recumbency as discussed by Pullen (1976) are depicted in Figure 6.30.

It should be noted, however, that the use of such tests in assessing model validity is restricted by the paucity of suitable experimental data. Indeed, comparatively little appears to be known regarding the physiology associated with this inverted position. This lack of knowledge may be attributed to the apparent unimportance of the position, which was almost never assumed except by children or

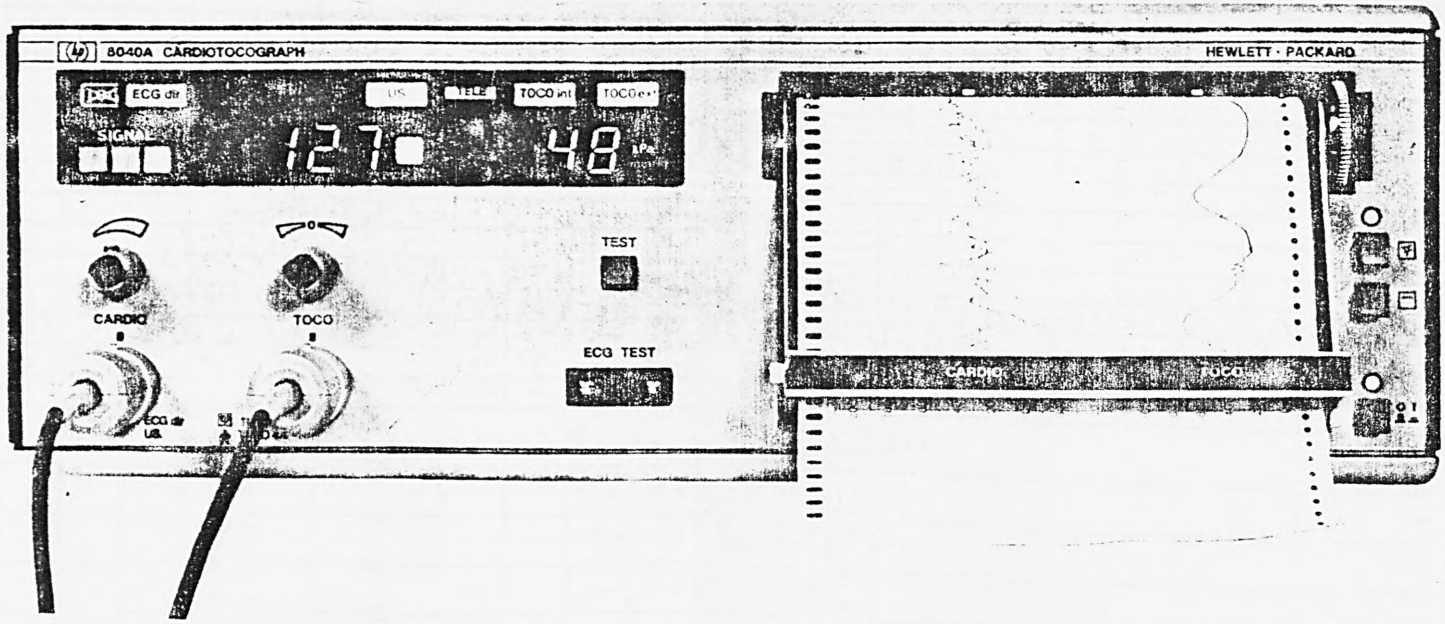

Figure 6.28a Foetal monitor cardiotocograph (model 8040A) used in measuring the heart rate.

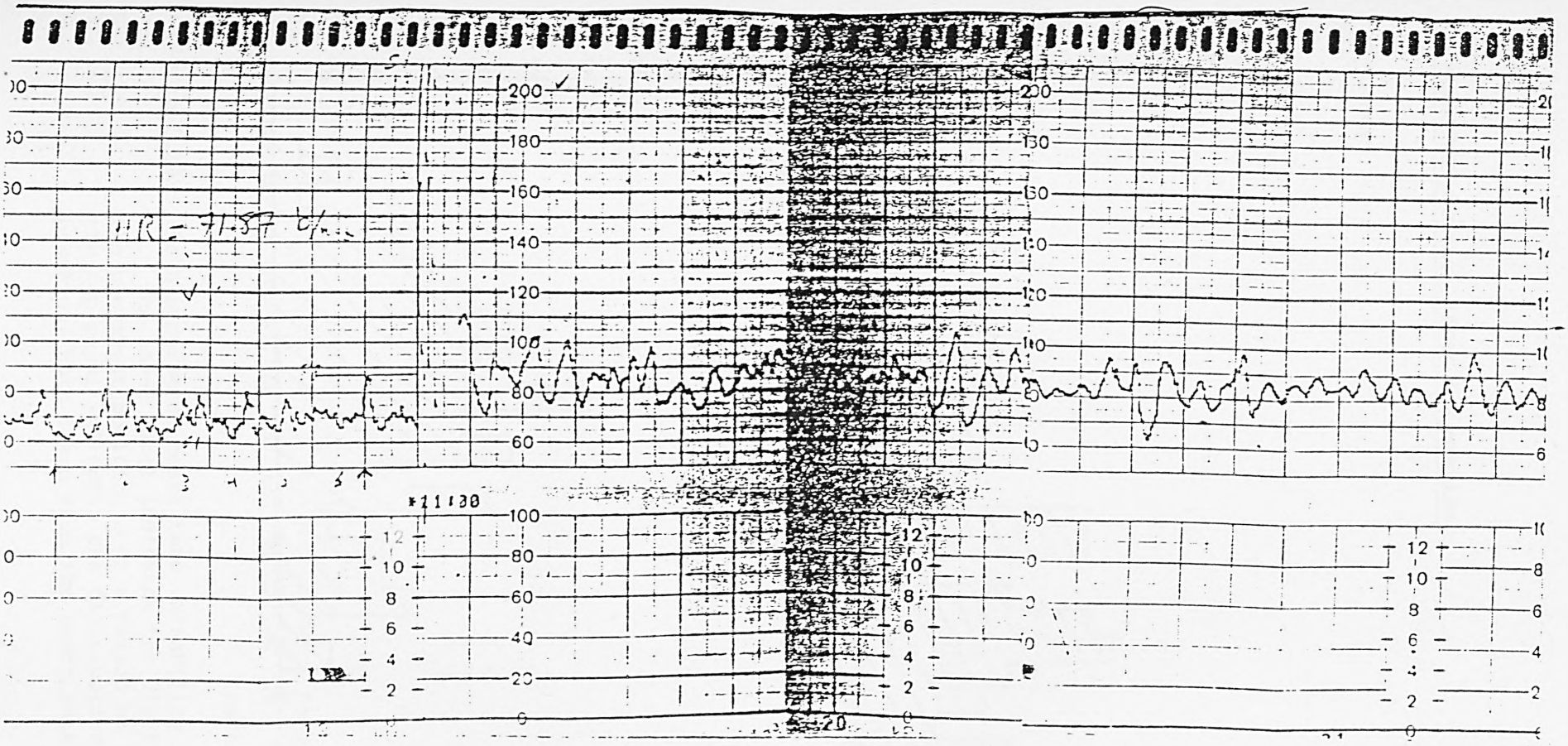

Figure 6.28b One of the four records of heart rate changes from recumbent position to standing position using the foetal monitor cardiotocograph.

In standing position after few minutes

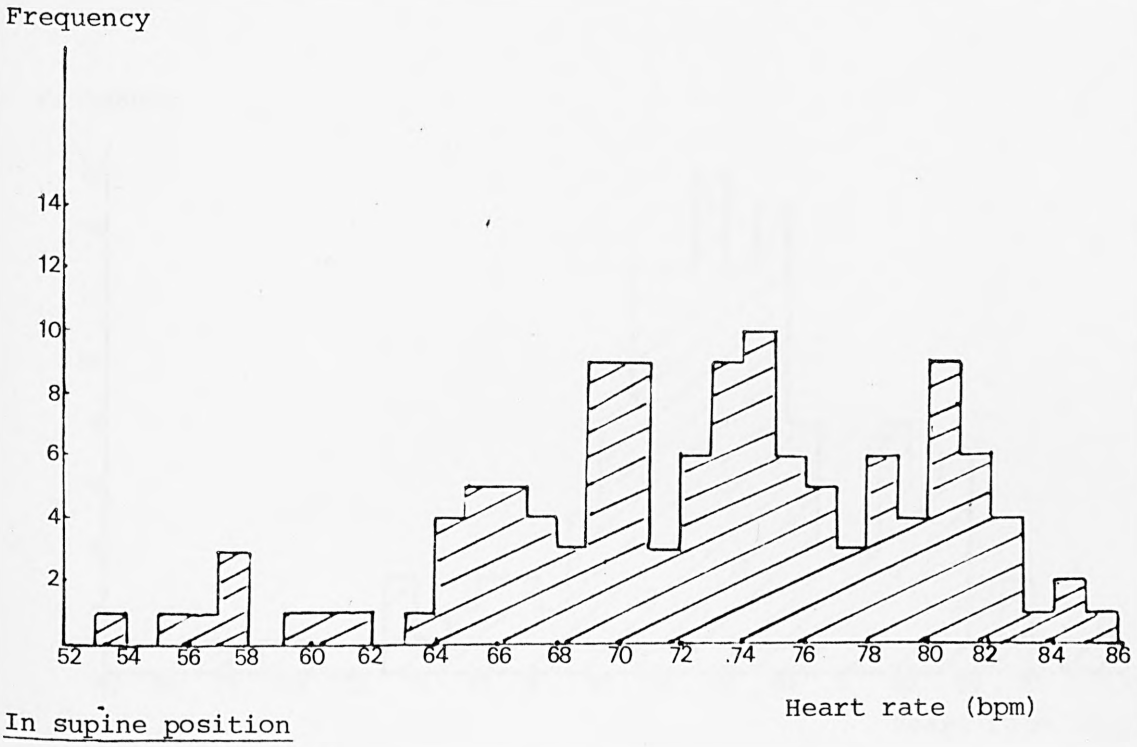

In supine position

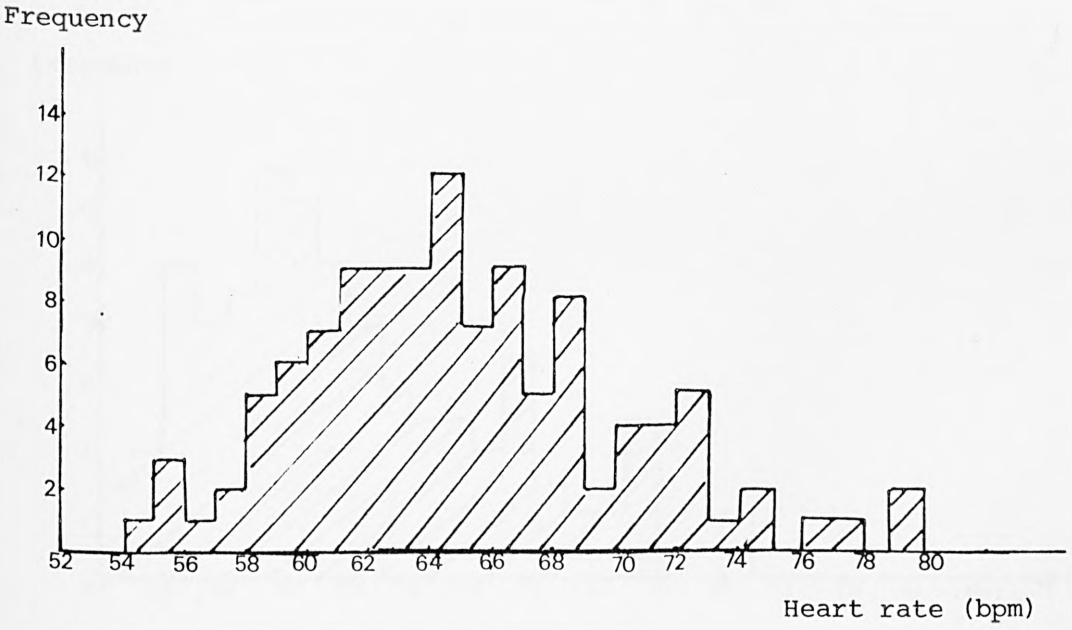

Figure 6.29a The histogram of heart rate variability for subject AC. The lower panel indicates the distribution in the recumbent position over a period of 109.2 s, and the top panel indicates the distribution in the standing position, both taken from the heart rate record.

In standing position

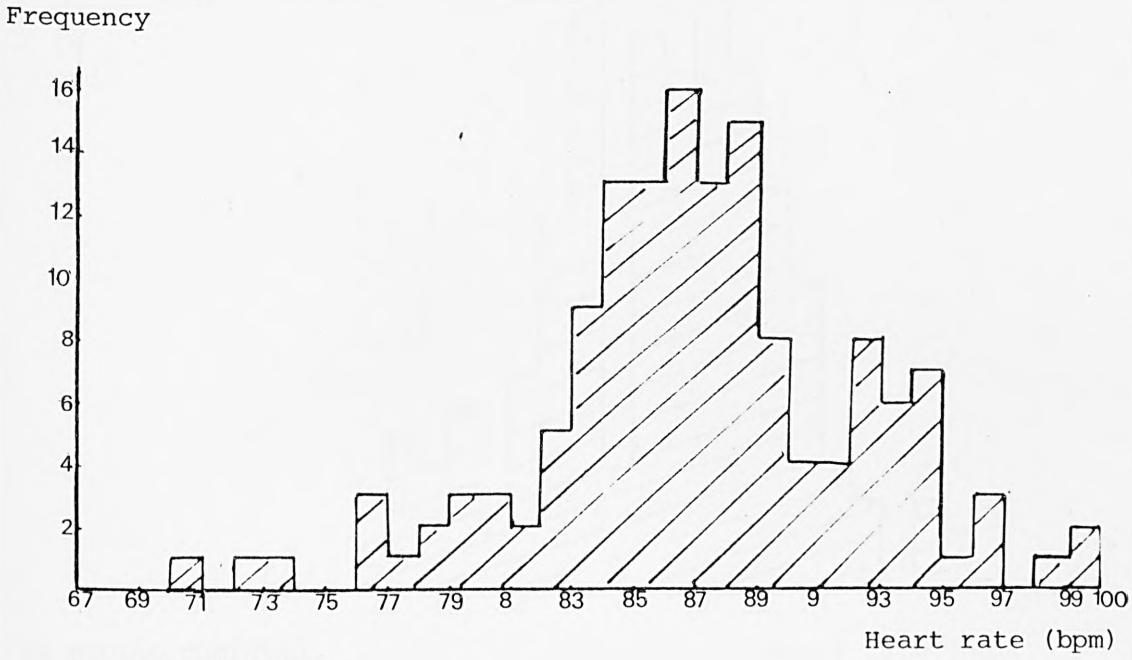

In supine position

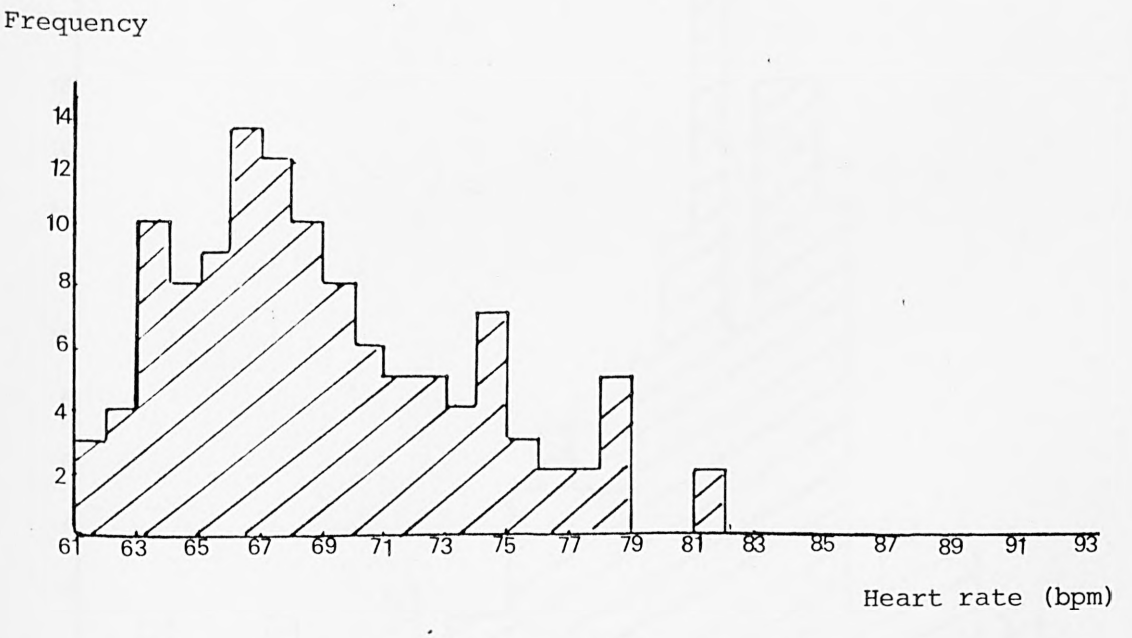

Figure 6.29b The histogram of heart rate variability for subject BN. The lower panel indicates the distribution in the recumbent position over a period of 109.2 s, and the top panel indicates the distribution in the standing position, both taken from the heart rate record.

In standing position

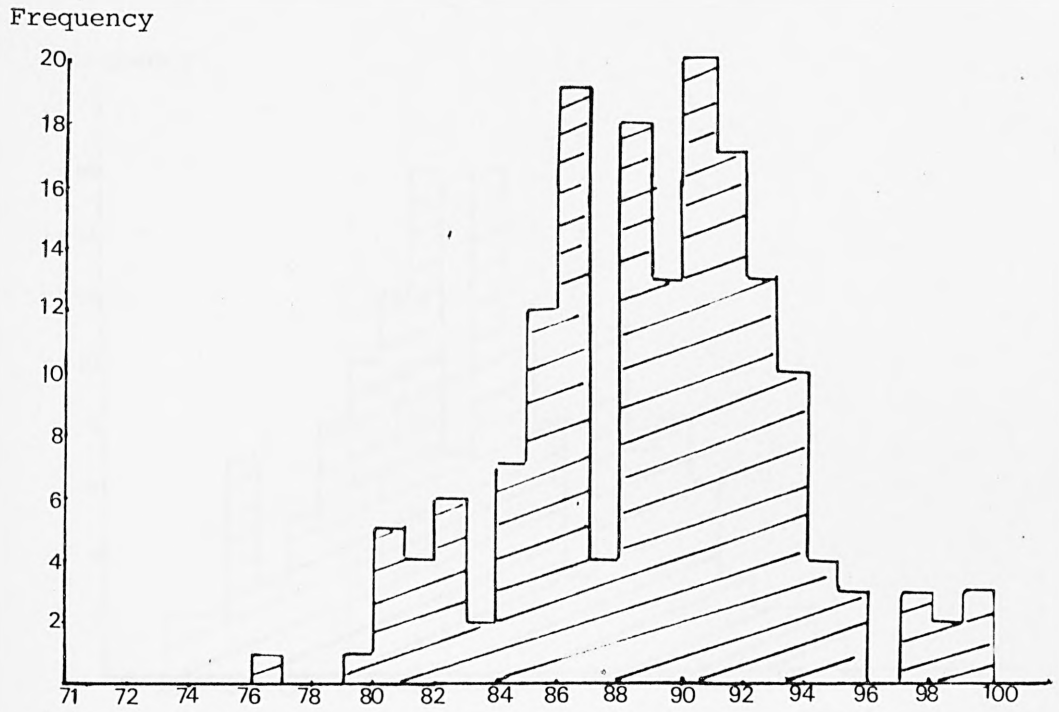

In supine position

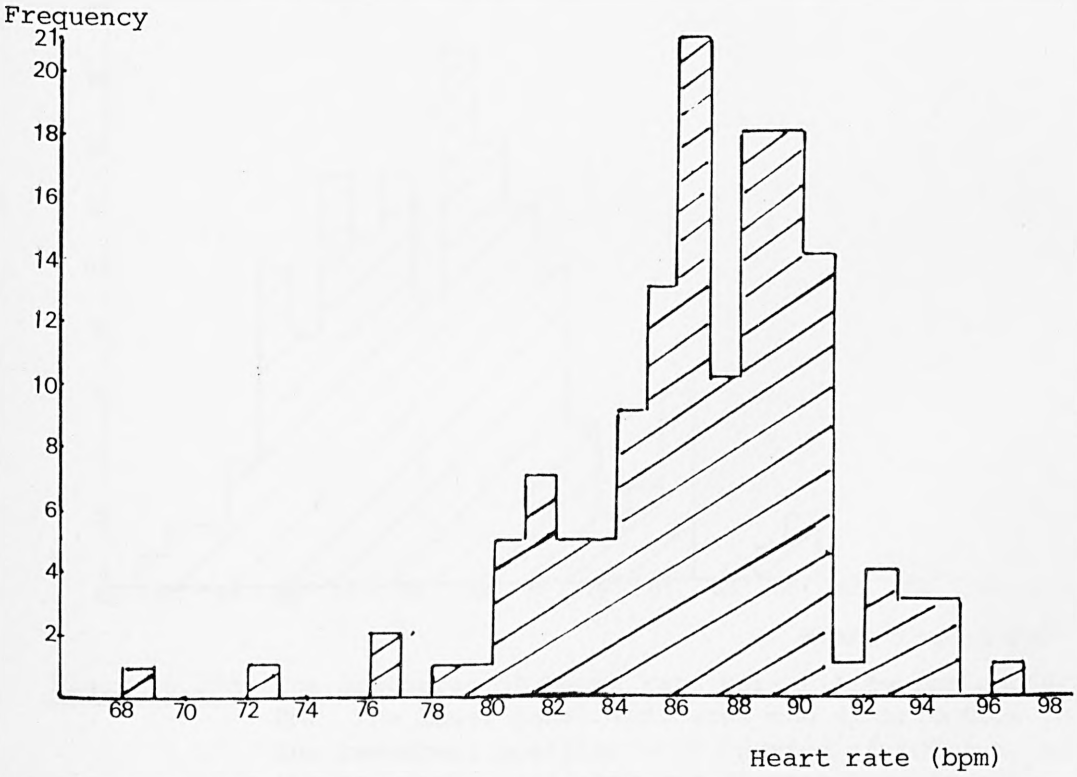

Figure 6.29c The histogram of heart rate variability for subject CR. The lower panel indicates the distribution in the recumbent position over a period of 109.2 s, and the top panel indicates the distribution in the standing position, both taken from the heart rate record.

In standing position

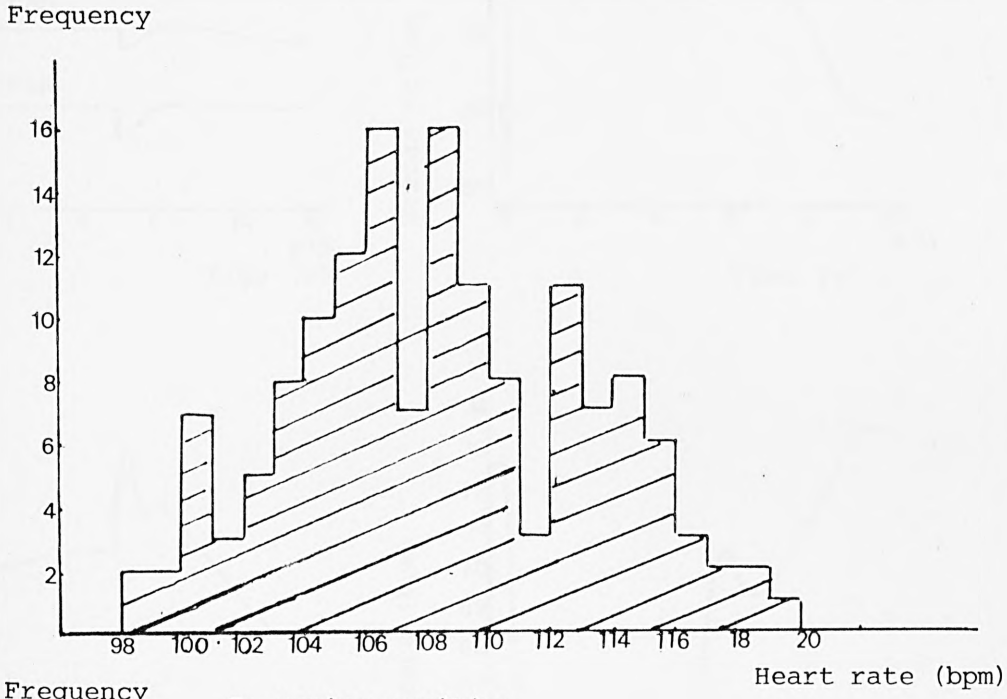

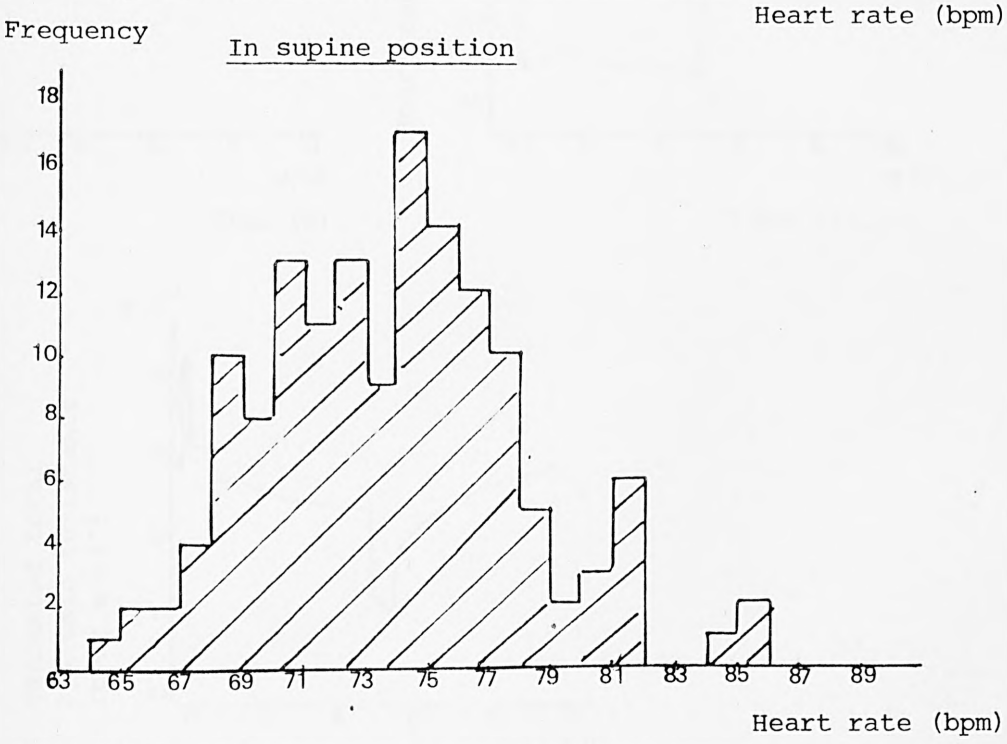

Figure 6.29d The histogram of heart rate variability for subject DM. The lower panel indicates the distribution in the recumbent position over a period of 109.2 s, and the top panel indicates the distribution in the standing position, both taken from the heart rate record.

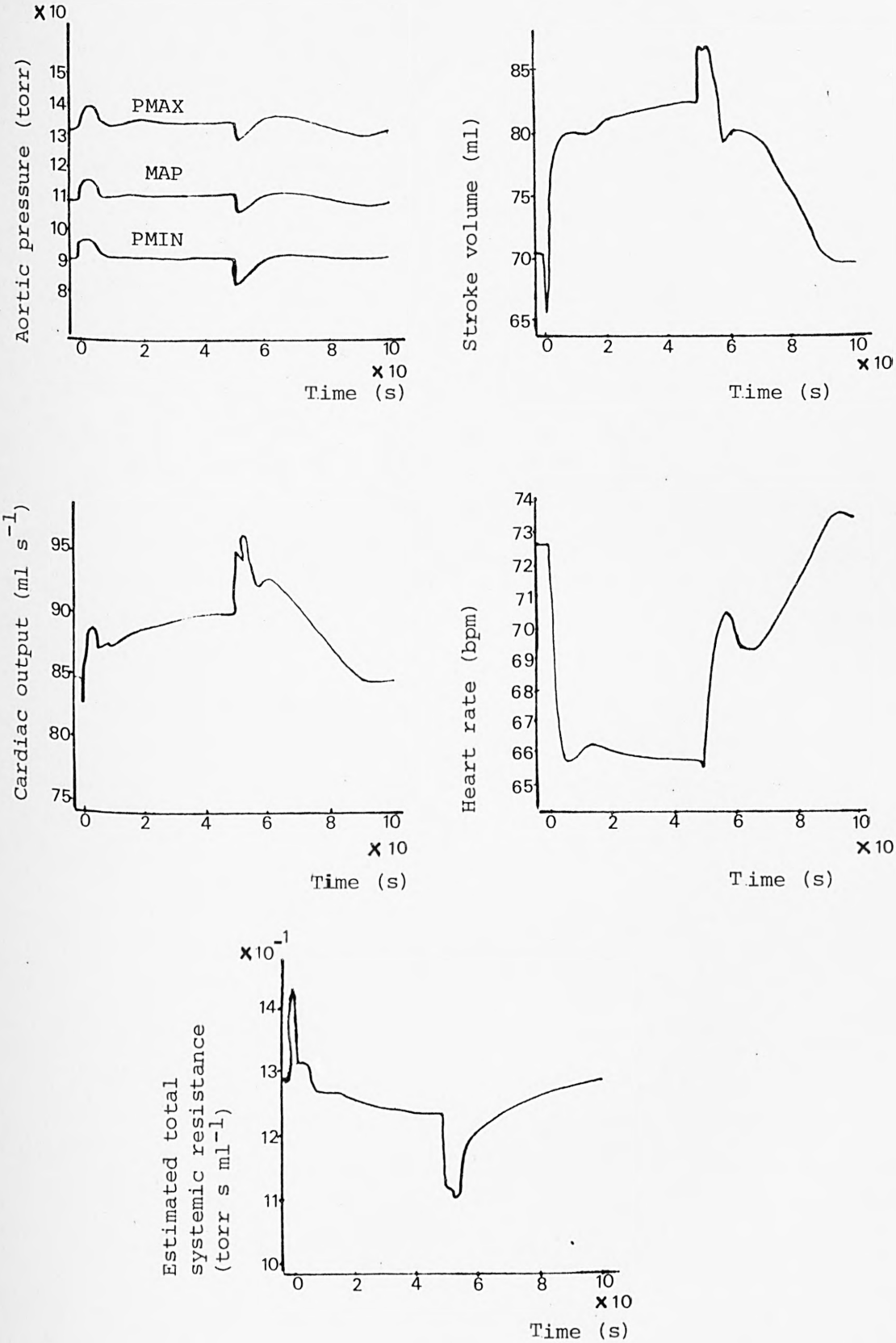

Figure 6.30 Dynamics following a head-down tilt (ϕ = -90°) at t = 0 s, and a return to recumbency (ϕ = 0°) at t = 50 s.

acrobats, or in the case of less severe head-down tilt in the treatment of certain orthopaedic conditions. With the development of air warfare, however, the action of all types of centrifugal and gravitational force upon human physiology became important (Wilkins et al, 1950). Nevertheless, such data as are available tend more to be associated with chronic rather than acute effects of head-down tilt and to consider degrees of tilt very much less than are needed to test the validity of the model. Typical data in this category relate to 24-hour studies of a 5 - 6° head-down tilt such as could be associated with space flight (Nixon et al, 1979; Srinivasan et al, 1982).

According to the limited information available, it has been found that stroke volume and cardiac output are increased by greater venous return (due to the effect of gravity). Conversely, the head-down position reportedly causes an increase in carotid, brachial and radial arterial pressures in normal man and anaesthetised dogs, accompanied by decreased femoral and abdominal aortic pressures (Abel et al, 1963). Wilkins et al (1950) indicate an immediate change in arterial pressure, followed by a brief stable plateau for two or three pulse beats, when the subject was tilted 75° down from horizontal, as shown in Figure 6.31a and b. The first shift in pressure was assumed to be due to the passive hydrostatic effect of the new position. After a few beats a gradual slight decline in the pressure occurred in femoral and brachial arteries.

The heart rate increased towards the normal value after the initial decrease. This is considered further in Section 6.5.3.1.2.

6.5.2.1 Comparison of model response with experimental data

Two sets of experimental data were used in examining the validity of the model responses to head-down tilts. These involved a series of head-down tilts over a range of angles from 20° to 75°. In addition, the model response to a 90° head-down tilt is considered although no corresponding experimental data are available.

6.5.2.1.1 Experiments carried out at Northwick Park Hospital

In a manner identical to that described in Section 6.5.1.2.1, measurements by which heart rate and indices of cardiac output and stroke volume could be derived were performed using transcutaneous aortovelography. Using the tilt table, head-down tilts of 20°, 45° and 60° were carried out,

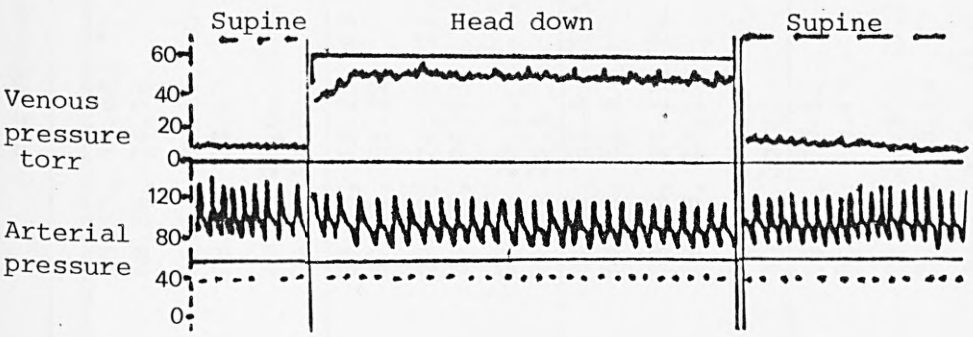

Figure 6.31a Optical (Hamilton) record of internal jugular venous pressure (upper tracing) and brachial arterial pressure (middle tracing) in a normal subject. The interrupted horizontal line below indicates seconds. At the first heavy vertical line the subject was tilted quickly into the inverted (75°) position and, at the second, back to the horizontal.

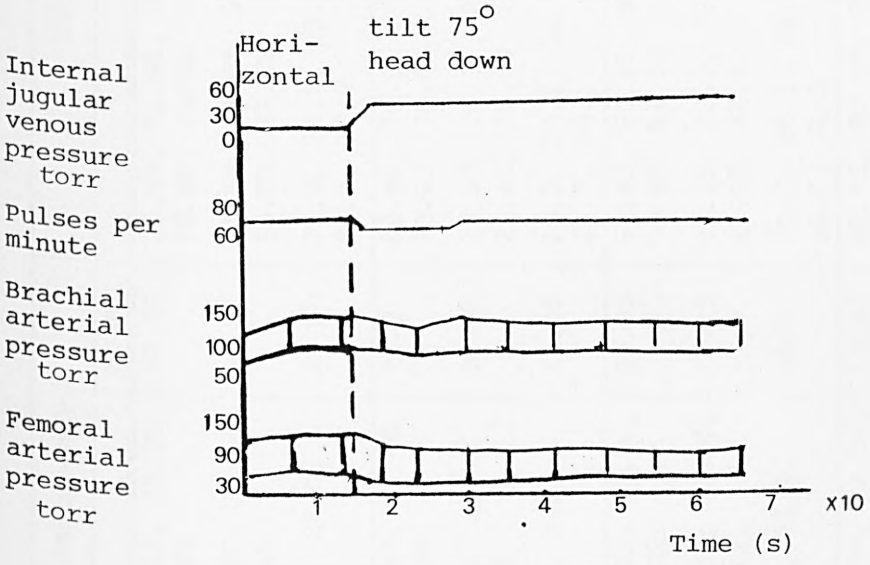

Figure 6.31b Graph of internal jugular venous pressure, pulse rate, brachial arterial pressure and femoral arterial pressure in a normal subject. At the vertical interrupted line he was tilted into an inverted position (75°).

Subject code		Recumbency		- 20° tilt		% change	Recumbency	
			Mean		Mean			Mean
A	FH	78.75, 86.63, 72.38, 74.72, 74.32	77.36	75.48, 71.95, 74.26, 78.69, 74.86	75.05	- 2.98	78.37, 76.64, 73.4, 68.86, 74.78	74.41
	ICO	27.81, 28.97, 33.74, 34.18, 29.35	30.81	27.54, 28.97, 29.31, 30.38, 32.32	29.7	- 4.86	26.83, 30.16, 30.66, 28.27, 27.17	28.61
	ISV	21.2, 20.1, 28.0, 27.4, 23.7	24.08	21.9, 24.2, 23.7, 23.2, 25.9	23.78	- 1.2	20.5, 23.6, 25.1, 24.6, 21.8	23.12
B	FH	73.46, 80.48, 73.46, 71.73, 70.39	73.9	69.58, 70.9, 65.06, 70.23, 70.4	69.23	- 6.3	58.68, 58.23, 63.49, 69.31, 68.22	63.58
	ICO	30.7, 27.43, 29.7, 28.39, 25.3	28.3	23.37, 27.27, 26.95, 25.41, 23.56	25.31	-10.5	23.33, 24.35, 23.53, 24.27, 28.93	24.88
	ISV	25.1, 20.5, 24.3, 23.8, 21.6	23.06	20.2, 23.1, 24.9, 21.7, 20.1	22.0	- 4.59	23.9, 25.1, 22.2, 21.0, 25.4	23.52
C	FH	65.21, 60.73, 57.26, 57.04, 59.06	59.86	61.43, 62.85, 60.48, 60.85, 61.34	61.72,	+ 3.1	54.28, 51.6, 55.18, 53.62, 52.5	53.75
	ICO	30.34, 28.73, 30.02, 30.73, 26.12	29.19	31.39, 29.9, 28.99, 27.07, 31.9	30.2	+ 3.4	28.59, 27.13, 26.36, 27.19, 28.13	27.89
	ISV	27.9, 28.4, 31.5, 32.3, 26.5	29.3	30.7, 28.5, 28.8, 26.7, 31.2	29.36	+ 0.2	31.6, 31.5, 28.7, 30.4, 32.1	31.15
D	FH	70.19, 64.59, 72.01, 83.38, 72.01	72.43	81.75, 83.58, 84.04, 81.75, 80.65	82.35	+13.6	68.23, 72.51, 74.31, 80.48, 69.49	73.0
	ICO	24.22, 25.04, 28.46, 29.8, 26.28	26.76	33.18, 34.06, 34.81, 34.68, 34.22	34.19	+27.7	27.5, 26.55, 29.53, 26.78, 26.14	27.3
	ISV	20.7, 23.3, 23.7, 21.4, 21.9	22.2	24.4, 24.5, 24.8, 25.4, 25.5	24.9	+12.0	24.2, 22.0, 23.8, 20.0, 22.6	22.5

Table 6.17a Values of heart rate and indices of cardiac output and stroke volume obtained before the tilt, in the inclined position and in the restored horizontal position. Five sample values from consecutive heart rates are listed, together with the mean of these five values in each case. The percentage change in each variable in the inclined position as compared to the pre-stimulus horizontal state is also given.

Subject code		Recumbency	Mean	- 45° tilt	Mean	% change	Recumbency	Mean
A	FH	84.1, 95.03, 82.15, 91.45, 77.34	86.01	79.29, 81.74, 81.74, 83.14, 76.18	80.41	- 6.5	76.1, 67.98, 69.27, 70.94, 70.6	70.97
	ICO	31.97, 25.34, 28.65, 29.75, 25.34	28.21	25.01, 27.56, 30.9, 29.88, 28.62	28.39	+ 0.63	20.69, 21.42, 19.96, 21.13, 20.53	20.74
	ISV	22.8, 16, 20.9, 19.5, 19.7	19.78	18.9, 20.2, 22.7, 21.6, 22.5	21.18	+ 7.0	16.3, 18.9, 17.3, 17.9, 17.4	17.56
B	FH	75.33, 81.98, 75.89, 76.46, 73.7	76.67	75.34, 73.72, 72.74	73.93	- 3.5	74.53, 70.76, 71.09, 66.19, 62.31	68.97
	ICO	27.65, 30.55, 35.11, 32.11, 30.68	31.22	30.95, 32.13, 29.6	30.89	- 1.05	28.36, 27.11, 26.64, 27.84, 33.04	28.6
	ISV	22, 22.4, 27.8, 25.2, 25	24.48	24.6, 26.2, 24.4	25.06	+ 2.3	22.8, 23, 22.5, 25.3, 31.8	25.08
C	FH	57.2, 54.12, 60.28, 60.52, 58.07	58.03	64.27, 64.27, 62.02, 65.82, 66.84	64.73	+ 11.5	52.87, 52.87, 53.16 56.04, 57.76	54.54
	ICO	33.27, 32.82, 34.2, 35.33, 30.75	33.27	31.84, 33.2, 33.7, 36.58, 35.11	34.08	+ 2.4	29.79, 30.6, 32.54 33.86, 32.19	31.79
	ISV	34.9, 36.4, 34, 35, 31.8	34.42	29.7, 31, 32.6, 33.3, 31.5	31.62	- 8.1	33.8, 34.7, 36.7, 36.3, 33.4	34.98
D	FH	71.29, 73.01, 76.25, 74.37, 65.62	72.1	88.53, 86.49, 86, 89.58, 84.08	86.93	+ 20.0	78.9, 80.16, 86.59, 80.8, 77.29	80.74
	ICO	26.38, 25.35, 27.89, 24.28, 23.31	25.44	33.34, 33.17, 31.45, 34.95, 30.84	32.75	+ 28.7	29.1, 27.72, 27.28, 27.04, 22.84	26.79
	ISV	22.2, 20.8, 21.9, 19.6, 21.3	21.16	22.6, 23, 21.9, 23.4, 22	22.58	+ 6.7	22.1, 20.7, 18.9, 20.1, 17.7	19.9

Table 6.17b continued overleaf

Subject code		Recumbency	Mean	- 45° tilt	Mean	% change	Recumbency	Mean
E	FH	78.04, 76.46, 76.27, 78.04, 79.06	77.57	79.01, 81.56, 81.78, 83.82, 78.39	80.91	+ 4.3	72.32, 76.9, 72.14, 67.48, 70.14	71.79
	ICO	33.96, 30.58, 28.69, 29.92, 33.04	31.23	38.92, 36.54, 32.67, 31.85, 27.96	33.58	+ 7.5	34.51, 27.59, 26.27, 27.79, 29.73	29.17
	ISV	26.1, 24, 22.6, 23, 25.1	24.16	29.6, 26.9, 24, 22.8, 21.4	24.94	+ 3.2	28.6, 21.5, 21.8, 24.7, 25.4	24.4
G	FH	65.16, 66.77, 69.1, 67.22, 62.69	66.18	73.27, 77.66, 79.57, 80.65, 73.68	76.96	+ 16.2	69.65, 73.24, 71.48, 65.81, 66.7	69.37
	ICO	26.5, 27.63, 25.46 28.01, 26.61	26.84	27.84, 27.95, 29.24, 30.12, 27.15	28.46	+ 6.0	28.3, 30.65, 29.42, 27.52, 27.44	28.66
	ISV	24.4, 24.8, 22.1, 25, 25.5	24.36	22.8, 21.6, 22, 22.4, 22.1	22.18	- 8.9	24.4, 25.1, 24.7, 25.1, 24.7	24.8
K	FH	52.33, 47.9, 54.53, 52.28, 60.04	53.01	43.36, 50.3, 44.68, 46.38, 50.97	45.72	- 13.7	45.3, 49.37. 51.37, 52.8, 50.18	48.11
	ICO	19.5, 21.39, 19.27, 21.56, 23.82	20.5	21.29, 21.82, 20.33 20.33, 22.92, 21.8	21.5	+ 4.8	20.8, 20.32, 23.01 20.73, 24.47	21.46
	ISV	22.4, 26.8, 21.2, 24.7, 23.8	23.25	29.5, 26, 27.3, 29.6, 25.7	28.35	+ 21.9	27.6, 24.7, 26.9 23.6, 29.3	26.85

Table 6.17b Values of heart rate and indices of cardiac output and stroke volume obtained before the tilt, in the inclined position and in the restored horizontal position. Five sample values from consecutive heart beats are listed, together with the mean of these five values in each case. The percentage change in each variable in the inclined position as compared to the pre-stimulus horizontal state is also given.

Subject code		Recumbency	Mean	- 60° tilt	Mean	% change	Recumbency	Mean
A	FH	73.1, 69.07, 74.89, 71.77, 74.29	72.62	73.6, 67.17, 71.97, 73.6, 71.97	71.66	- 1.3	68.41, 75.46, 80.22, 71.76, 73.02	73.77
	ICO	24.39, 24.3, 30.4, 24.25, 26.5	25.9	27.72, 20.71, 24.9, 24.69, 30.35	25.67	- 0.88	23.84, 21.42, 20.91, 22.73, 20.56	21.89
	ISV	20, 21.1, 24.4, 20.3, 21.4	21.4	22.6, 18.5, 20.3, 20.1, 25.3	21.46	+ 0.28	20.9, 17, 15.6, 19, 16.9	17.88
B	FH	68.04, 75.26, 74.89, 71.05, 67.58	71.36	74.74, 68.36, 76.62, 70.25, 72.09	72.41	+ 1.47	71.29, 67.64, 65.75 66.9, 67.2	67.75
	ICO	28.47, 25.28, 24.36, 28.34, 26.22	26.5	33.06, 28.95, 29.38, 29.74, 28.78	29.98	+ 13.00	28.66, 26.7, 27.03, 26.35, 26.47	27.04
	ISV	25.1, 20.2, 19.5, 23.9, 23.3	22.4	26.5, 25.4, 23, 25.4, 24	24.86	+ 10.9	24.1, 23.7, 24.7, 23.6, 23.6	23.94
C	FH	51.36, 53.15, 54.4, 54.47, 56.89	54.1	70.65, 71.81, 64.12, 64.96, 58.46	66.00	+ 21.9	53.51, 54.49, 56.72, 57.58, 51.8	54.82
	ICO	30.49, 29.79, 34.2, 33.09, 33.17	32.15	37.06, 37.72, 34.62, 34.56, 30.12	34.82	+ 8.3	31.2, 31.41, 30.36, 30.86, 30.29	30.82
	ISV	35.6, 33.6, 37.7, 36.5, 35	35.68	31.5, 31.5, 32.4, 31.9, 30.9	31.64	- 11.3	35, 34.6, 32.1, 32.2, 35.1	33.8
D	FH	77, 77.8, 84.7, 79.7, 75.4	78.2	55.54, 76.01, 79.2, 81.79, 83.84	75.28	- 3.7	78.18, 80.27, 67.01, 69.65, 68.07	72.63
	ICO	35.3, 37.5, 33.3, 36.0, 35.0	35.8	11.71, 17.02, 14.94, 12.77, 14.52	14.19	- 60.0	21.45, 25.4, 22.38 27.56, 29.23	25.2
	ISV	27.3, 26.5, 23.6, 27.1, 27.9	26.6	12.7, 13.4, 11.3, 9.4, 10.4	11.4	- 57.0	16.5, 19, 20, 23.7, 25.8	21.00

Table 6.17c continued overleaf

Subject code		Recumbency	Mean	- 60° tilt	Mean	% change	Recumbency	Mean
E	FH	75.3, 76.05, 75.67, 78.4, 77.01	76.49	76.97, 71.55, 76.97, 79.58, 74.89	75.99	- 0.65	72.92, 73.45, 74.52, 72.23, 73.09	73.24
	ICO	27.96, 28.73, 30.63, 30.13, 31.59	29.8	30.29, 31.82, 29.39, 30.68, 28.54	30.24	+ 1.4	33.17, 26.81, 31.61, 31.17, 32.94	31.14
	ISV	22.3, 22.7, 24.3, 23.1, 24.6	23.4	23.6, 26.7, 23.3, 23.1, 22.9	23.92	+ 2.2	27.3, 21.9, 25.5, 25.9, 27	25.52
G	FH	74.31, 70.16, 73.76, 74.12, 72.87	73.0	68.52, 72.25, 69.61, 69.3, 76.59	71.25	- 2.3	No signal	
	ICO	22.02, 27.83, 26.81, 29.66, 31.02	27.46	25.32, 23.16, 26,8, 28.5, 28.48	26.4	- 3.8		
	ISV	17.8, 23.8, 21.8, 24, 25.5	22.58	22.2, 19.2, 23.2, 24.7, 22.3	22.3	- 1.15		
K	FH	43.3, 45.17, 43.3, 63.2, 40.05	47.0	44.87, 42.64, 45.33, 48.05, 43.38	44.89	- 4.48	46.66, 48.94, 46.68, 48.54, 49.82	48.13
	ICO	15.94, 18.11, 16.07, 33.34, 14.35	19.56	18.24, 22.61, 19.9, 19.71, 21.39	20.37	+ 4.1	20.63, 20.81, 20.5, 23.29, 22.79	21.6
	ISV	22.1, 24.1, 22.3, 31.6, 21.5	24.3	24.4, 31.8, 26.2, 24.6, 29.6	27.32	+ 12.4	26.5, 25.5, 26.4, 28.8, 27.4	26.92

Table 6.17c Values of heart rate and indices of cardiac output and stroke volume obtained before the tilt, in the inclined position and in the restored horizontal position. Five sample values from consecutive heart beats are listed, together with the mean of these five values in each case. The percentage change in each variable in the inclined position as compared to the pre-stimulus horizontal state is also given.

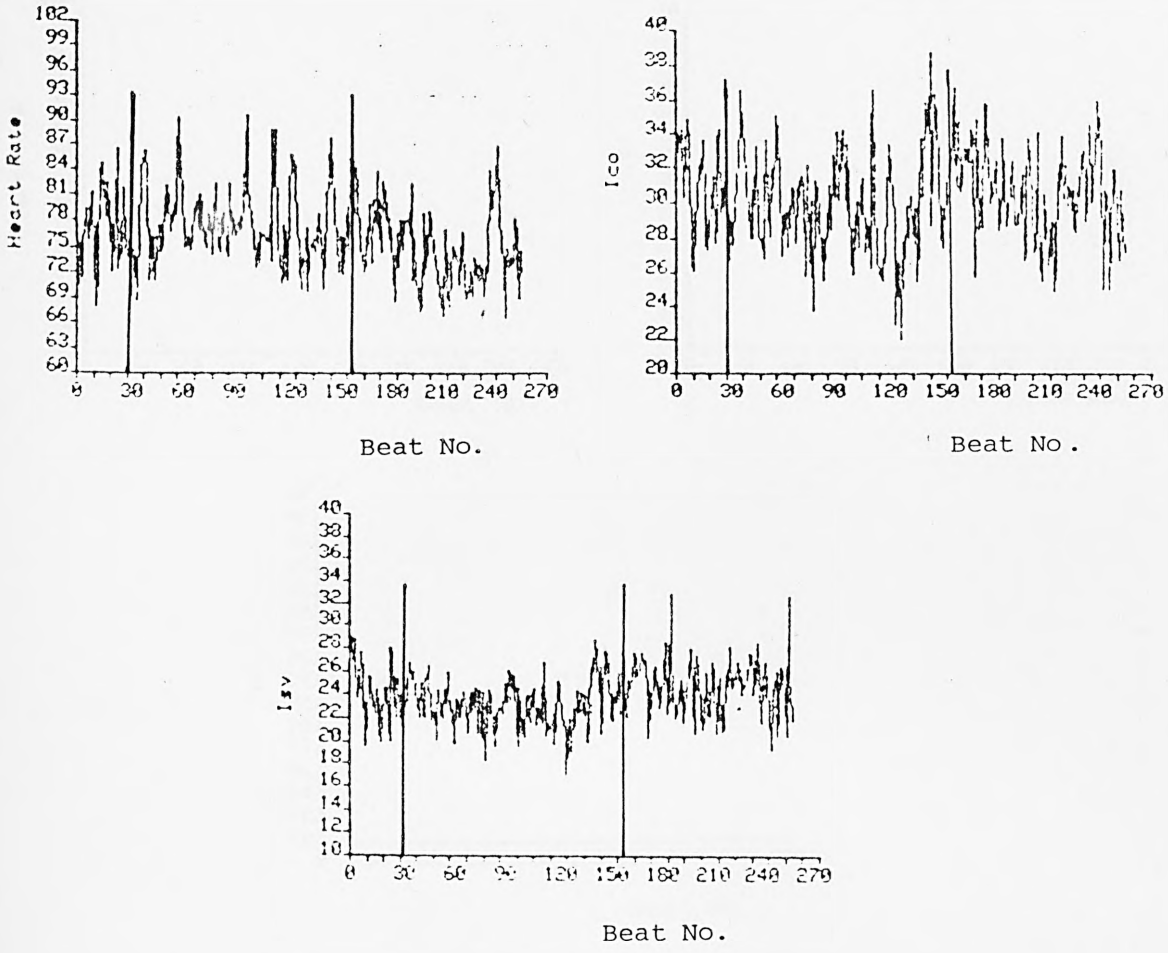

Figure 6.32a Raw data obtained from subject A for the three variables as indicated during a 20° head-down tilt. The vertical lines indicate the times at which the tilt to the inclined position and the return to the horizontal began.

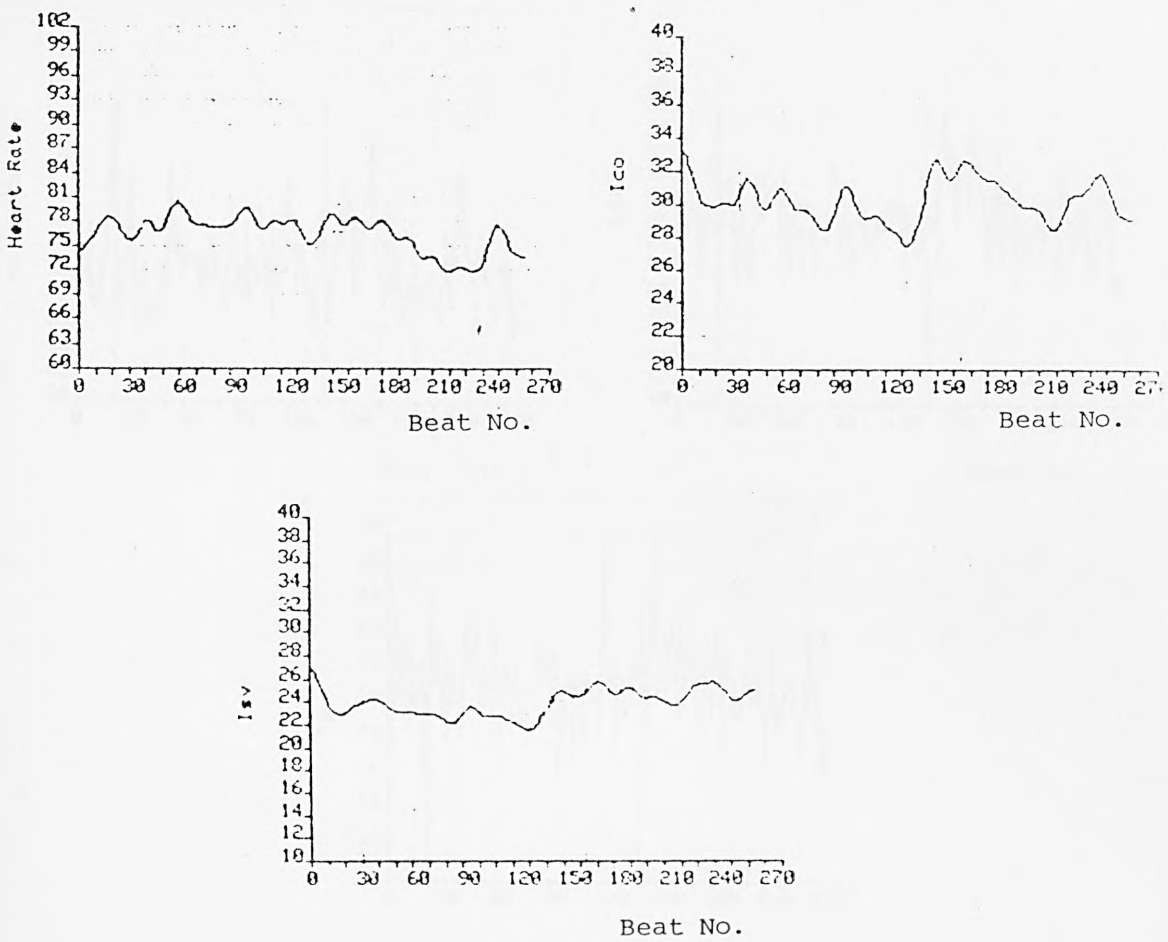

Figure 6.32b Filtered form of the data depicted in Figure 6.32a obtained using a recursive averaging filter.

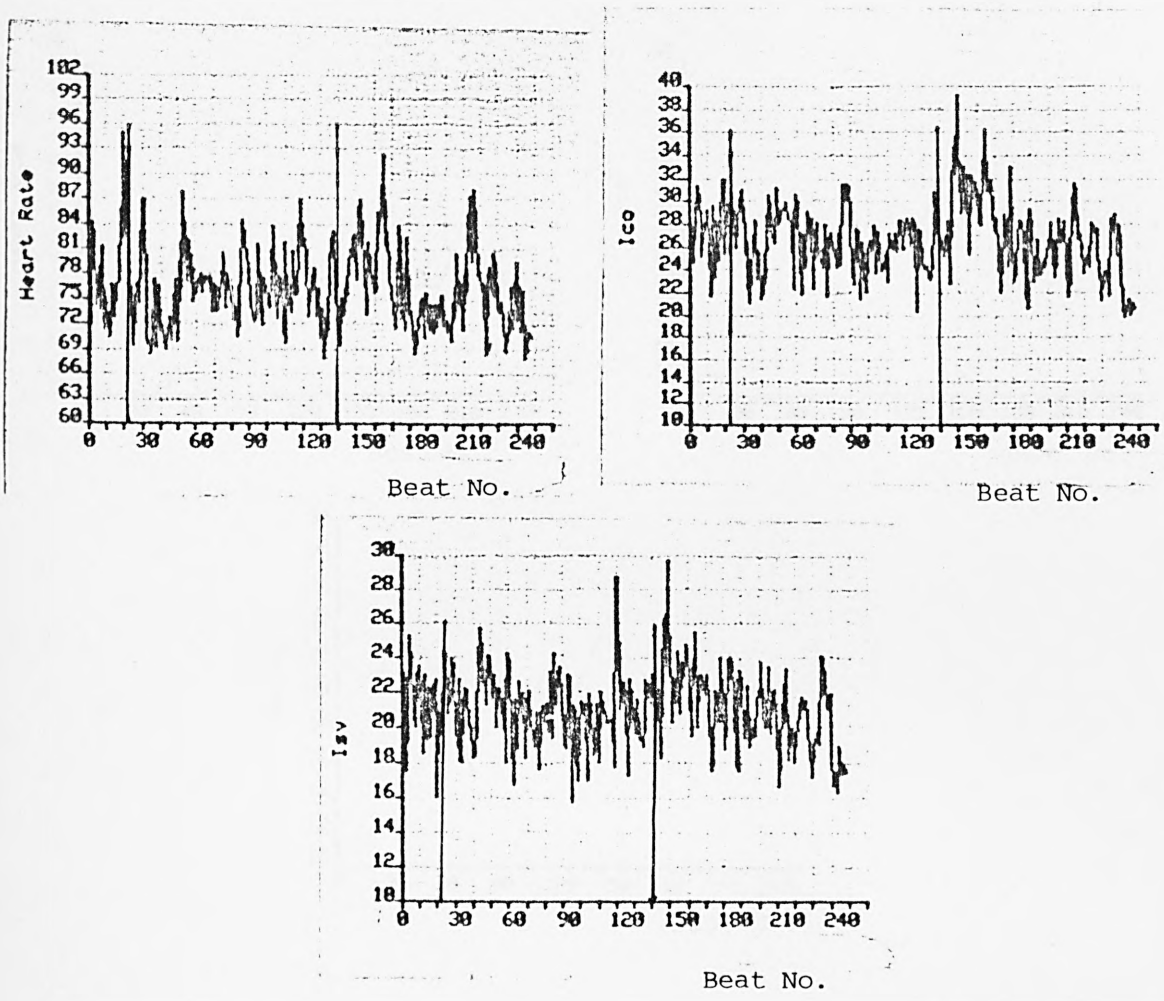

Figure 6.33a Raw data obtained from subject A for the three variables as indicated during a 45° head-down tilt. The vertical lines indicate the times at which the tilt to the inclined position and the return to the horizontal began.

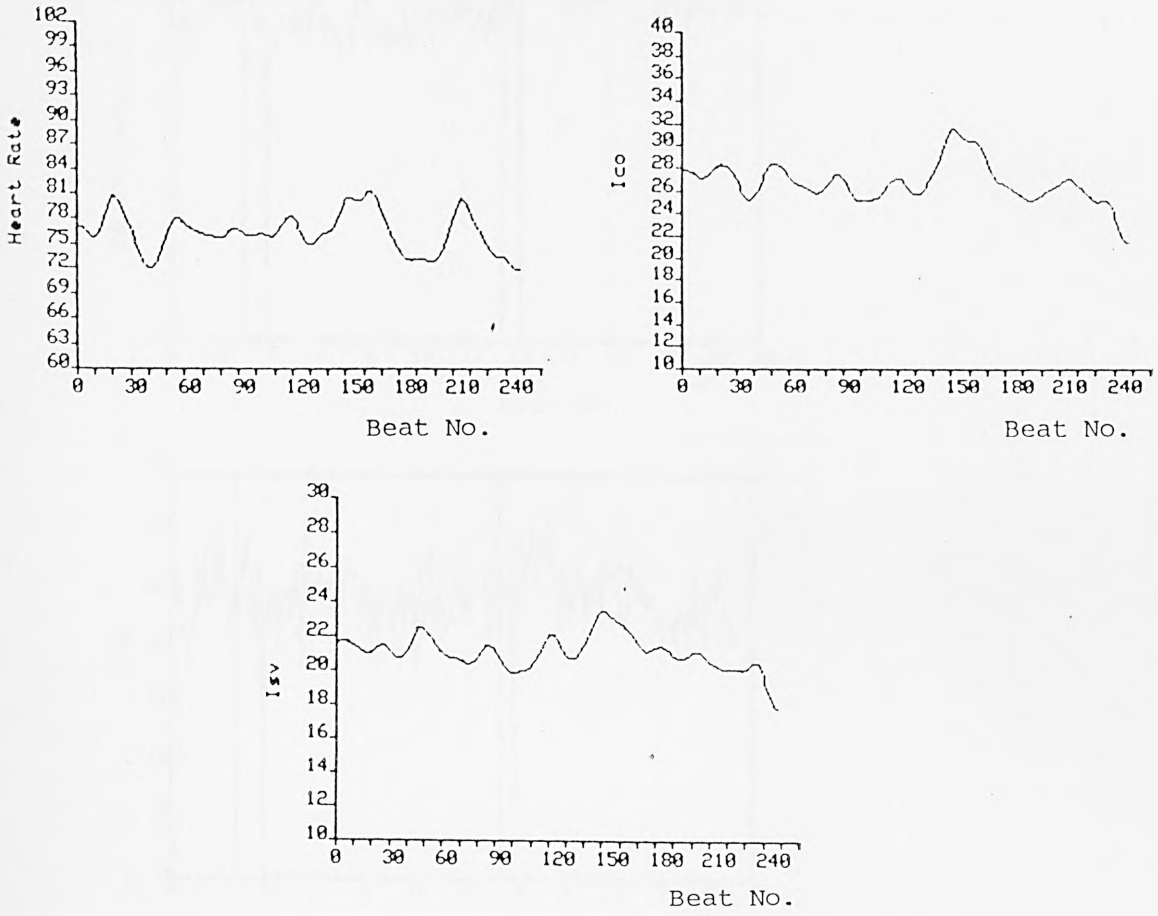

Figure 6.33b Filtered form of the data depicted in Figure 6.33a obtained using a recursive averaging filter.

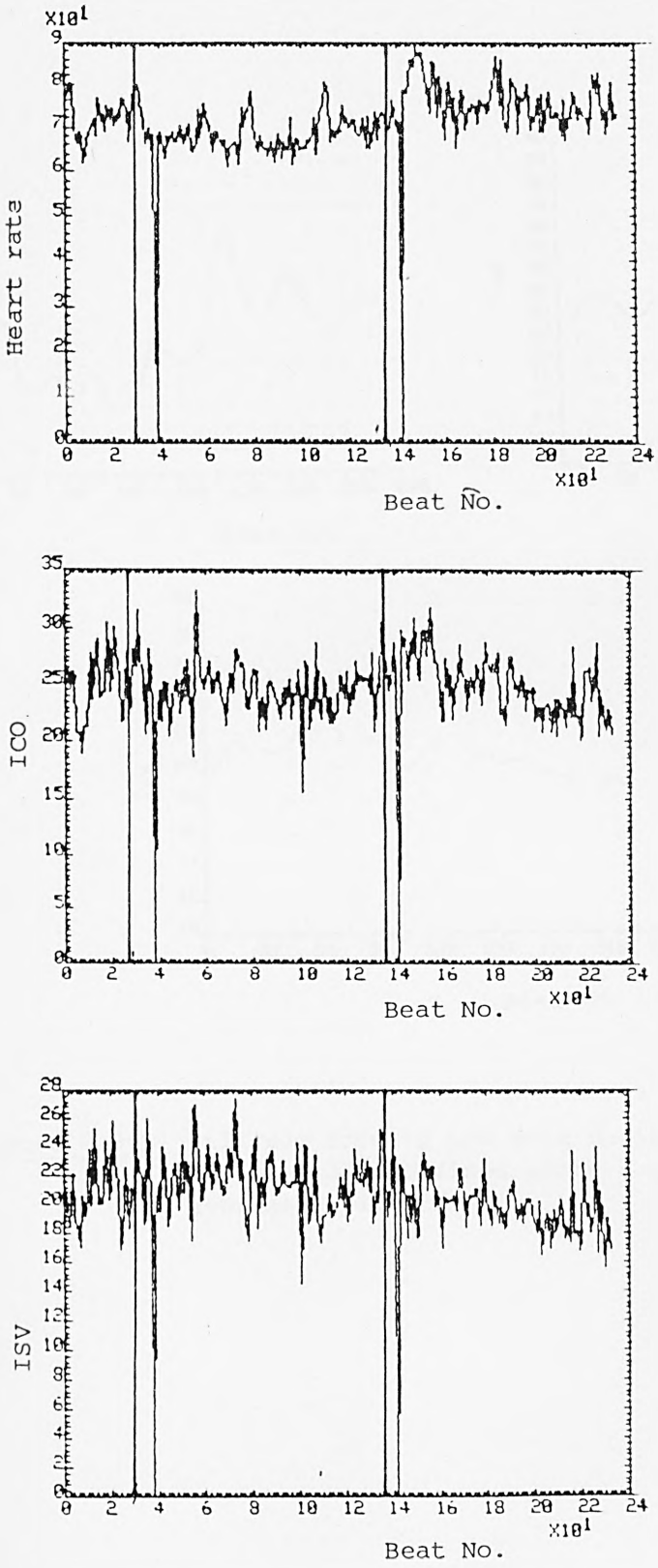

Figure 6.34a Raw data obtained from subject A for the three variables as indicated during a 60° head-down tilt. The vertical lines indicate the times at which the tilt to the inclined position and the return to the horizontal began.

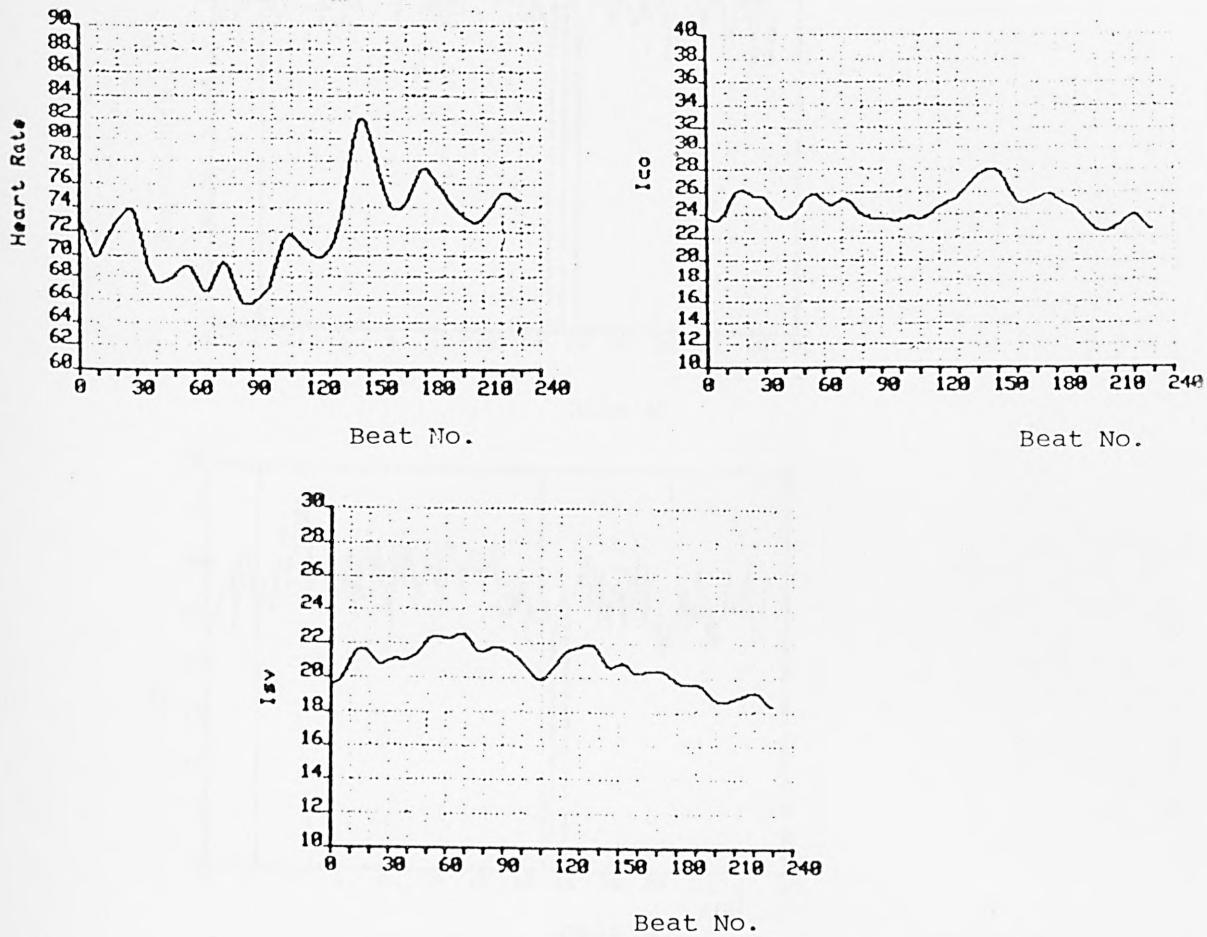

Figure 6.34b Filtered form of the data depicted in Figure 6.34a obtained using a recursive averaging filter.

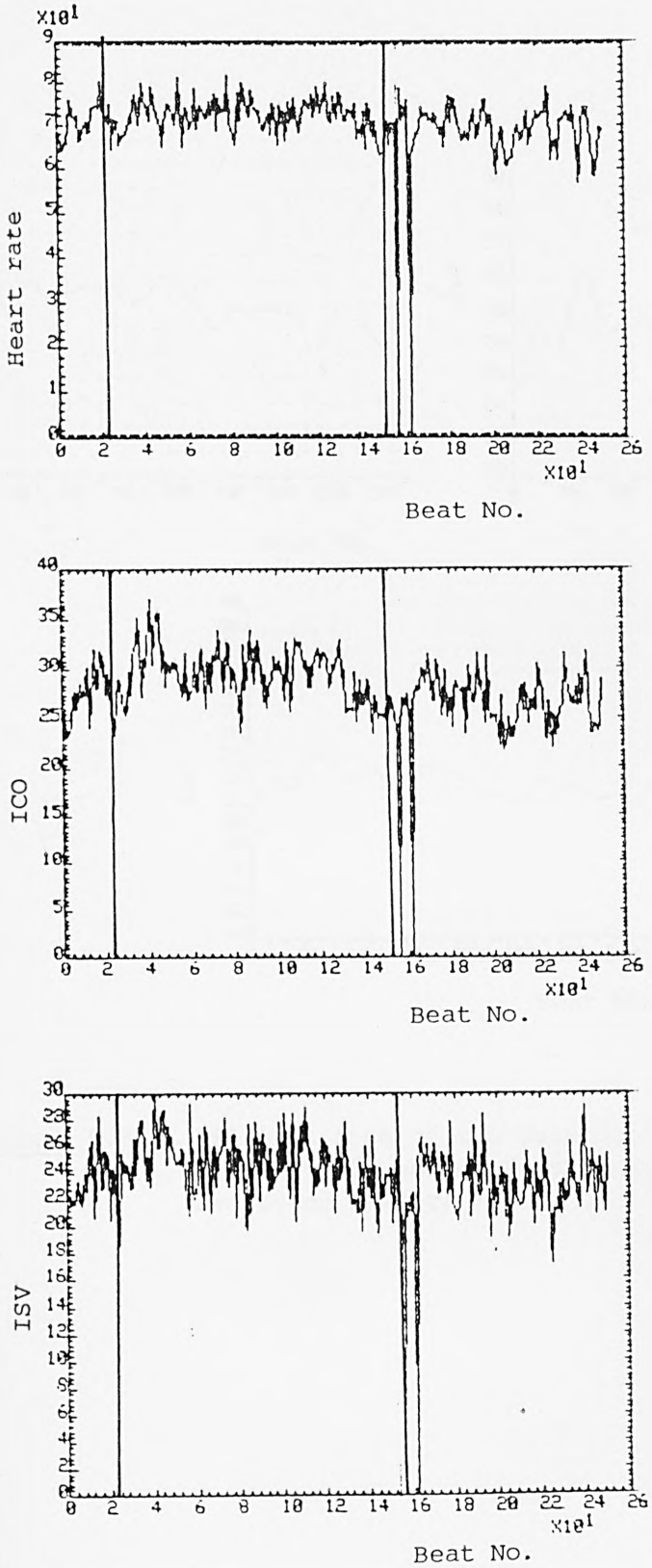

Figure 6.35a Raw data obtained from subject B for the three variables as indicated during a 20° head-down tilt. The vertical lines indicate the times at which the tilt to the inclined position and the return to the horizontal began.

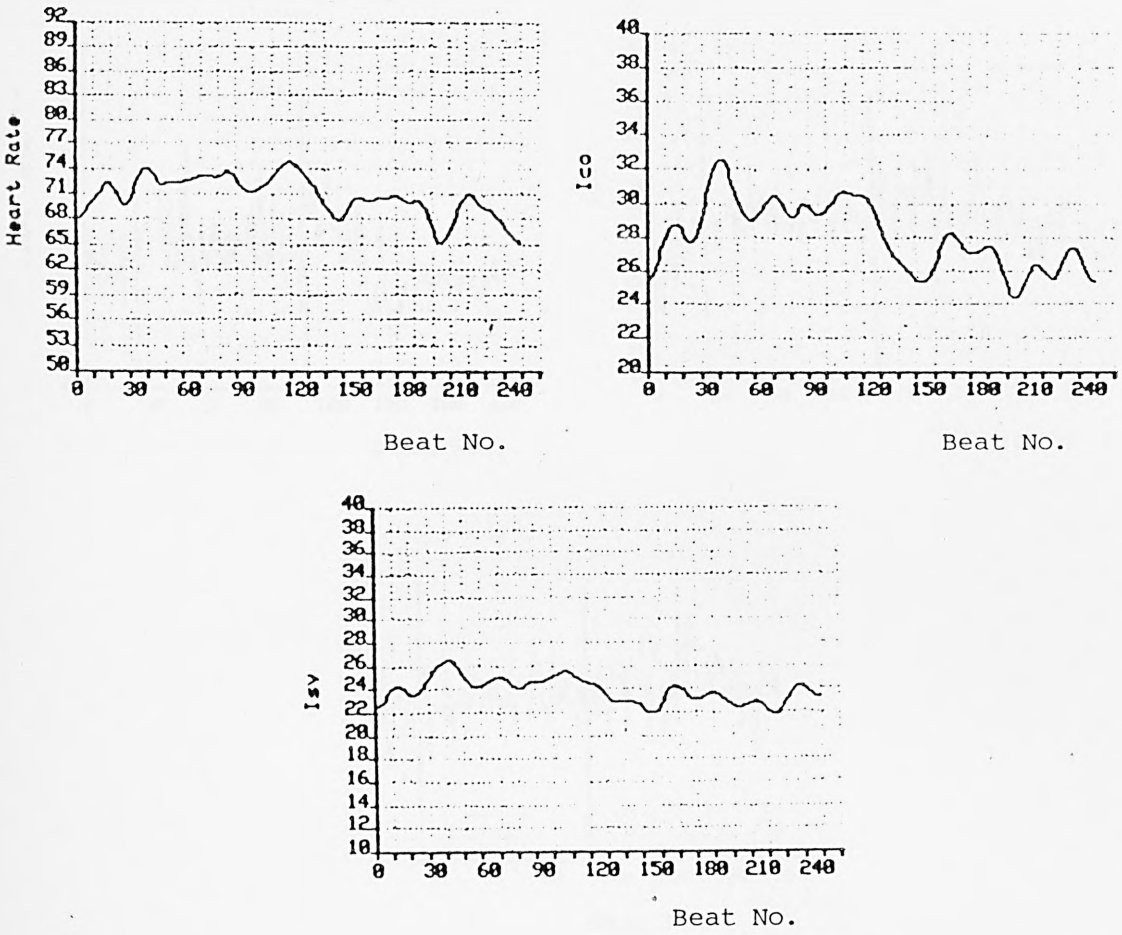

Figure 6.35b Filtered form of the data depicted in Figure 6.35a obtained using a recursive averaging filter.

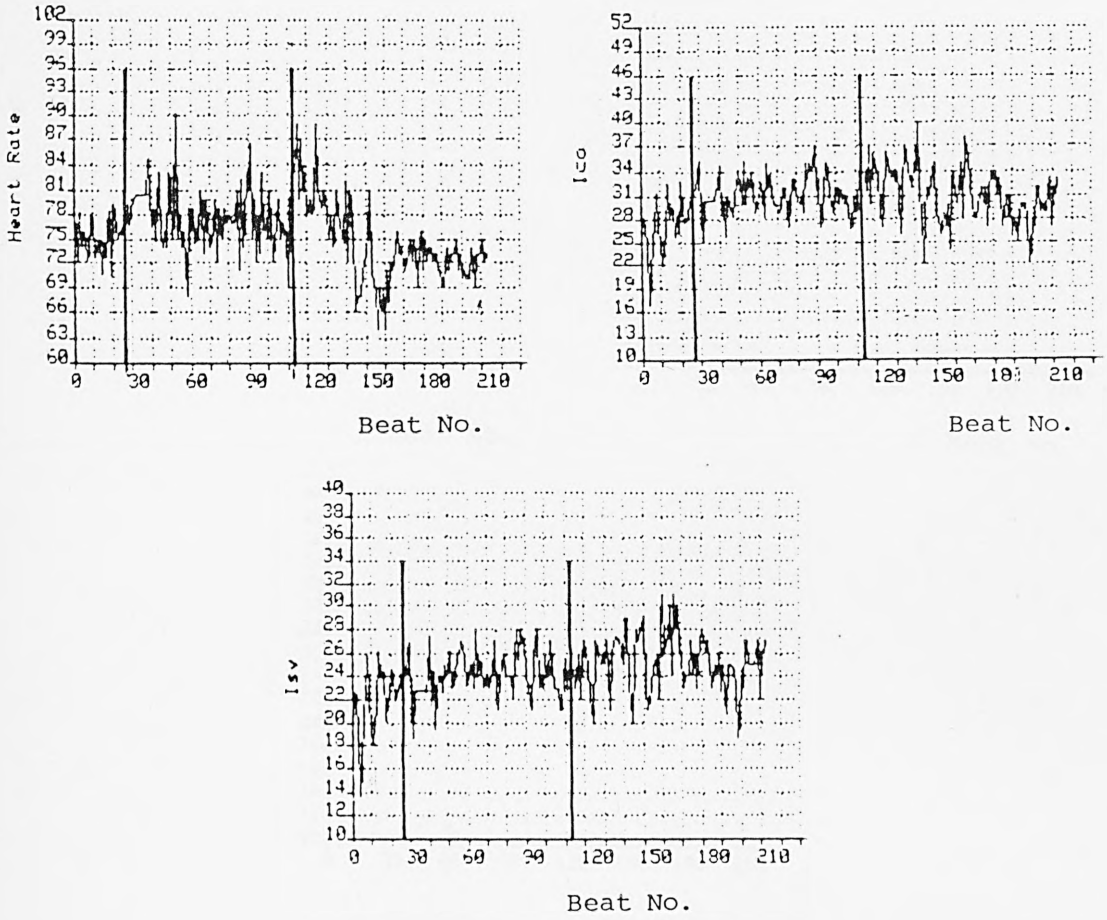

Figure 6.36a Raw data obtained from subject E for the three variables as indicated during a 60° head-down tilt. The vertical lines indicate the times at which the tilt to the inclined position and the return to the horizontal began.

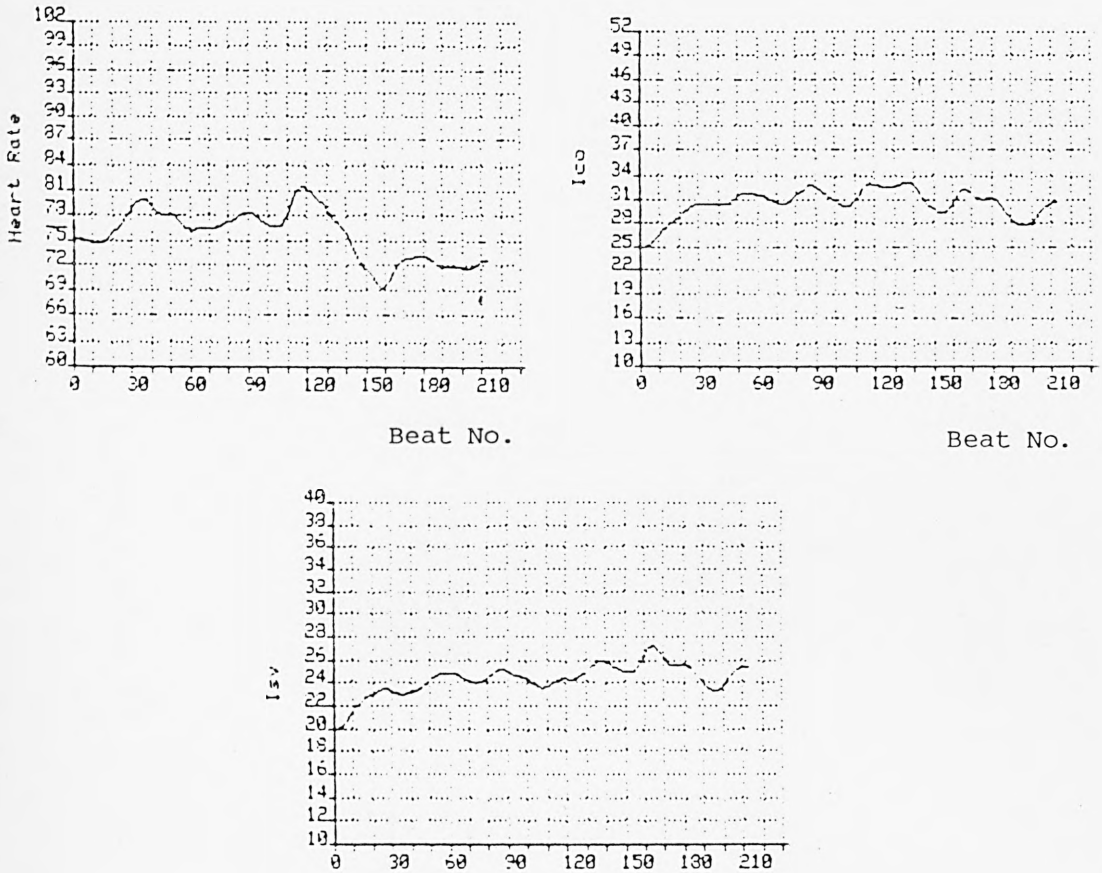

Figure 6.36b Filtered form of the data depicted in Figure 6.36a obtained using a recursive averaging filter.

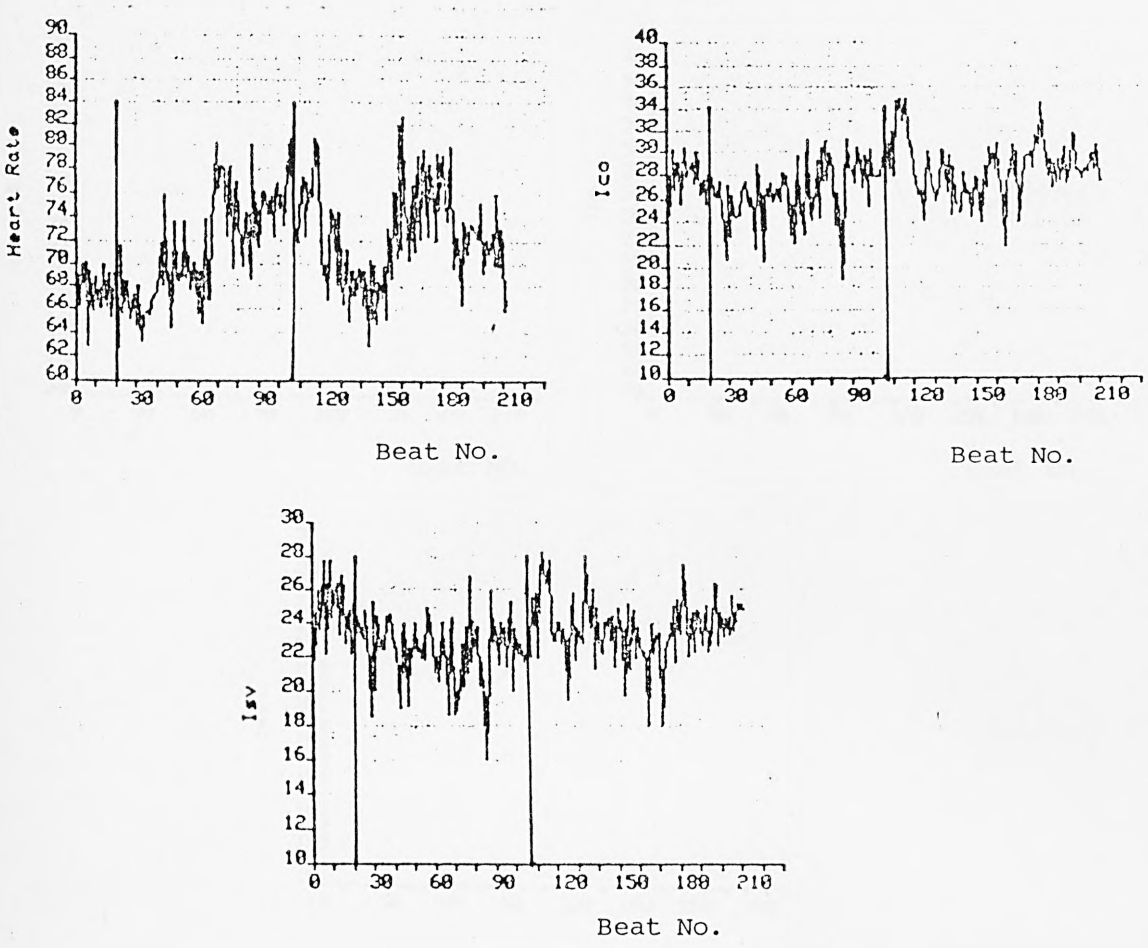

Figure 6.37a Raw data obtained from subject G for the three variables as indicated during a 45° head-down tilt. The vertical lines indicate the times at which the tilt to the inclined position and the return to the horizontal began.

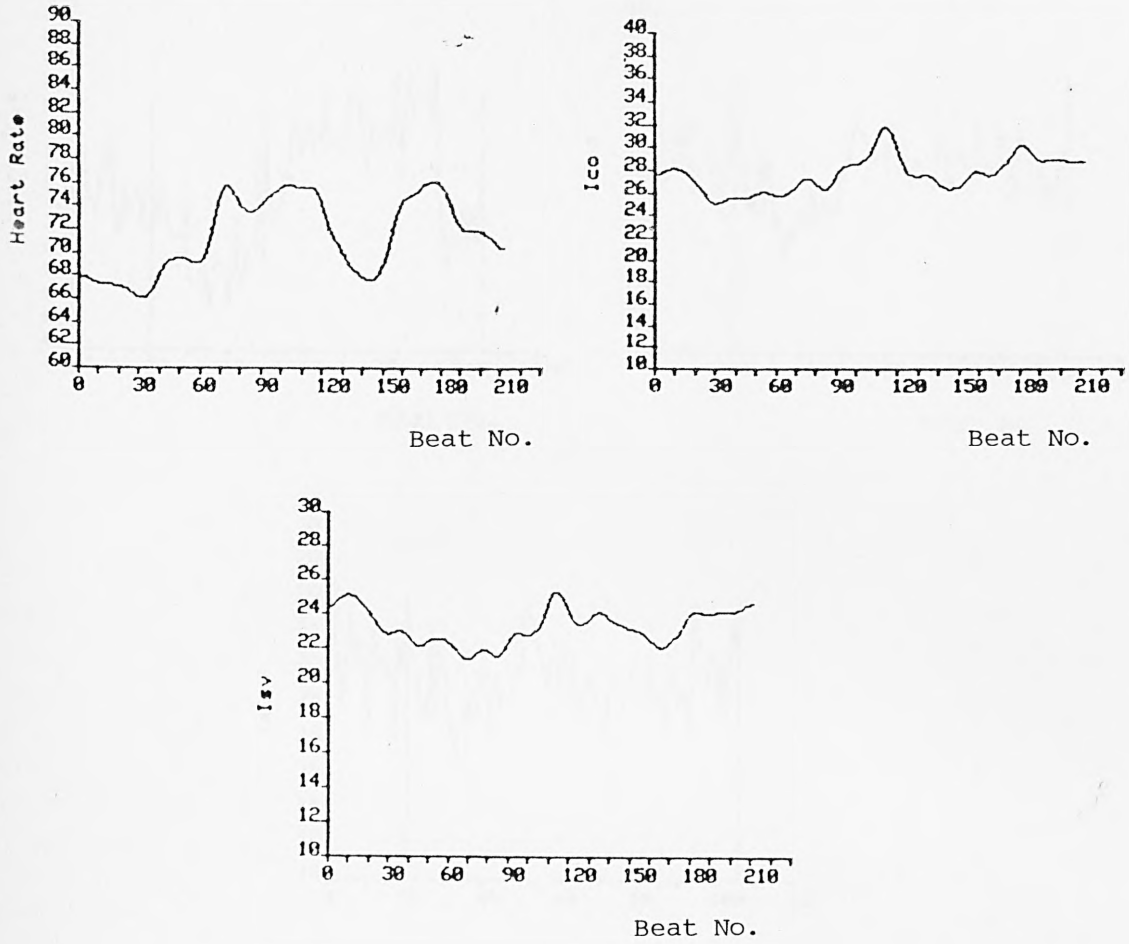

Figure 6.37b Filtered form of the data depicted in Figure 6.37a obtained using a recursive averaging filter.

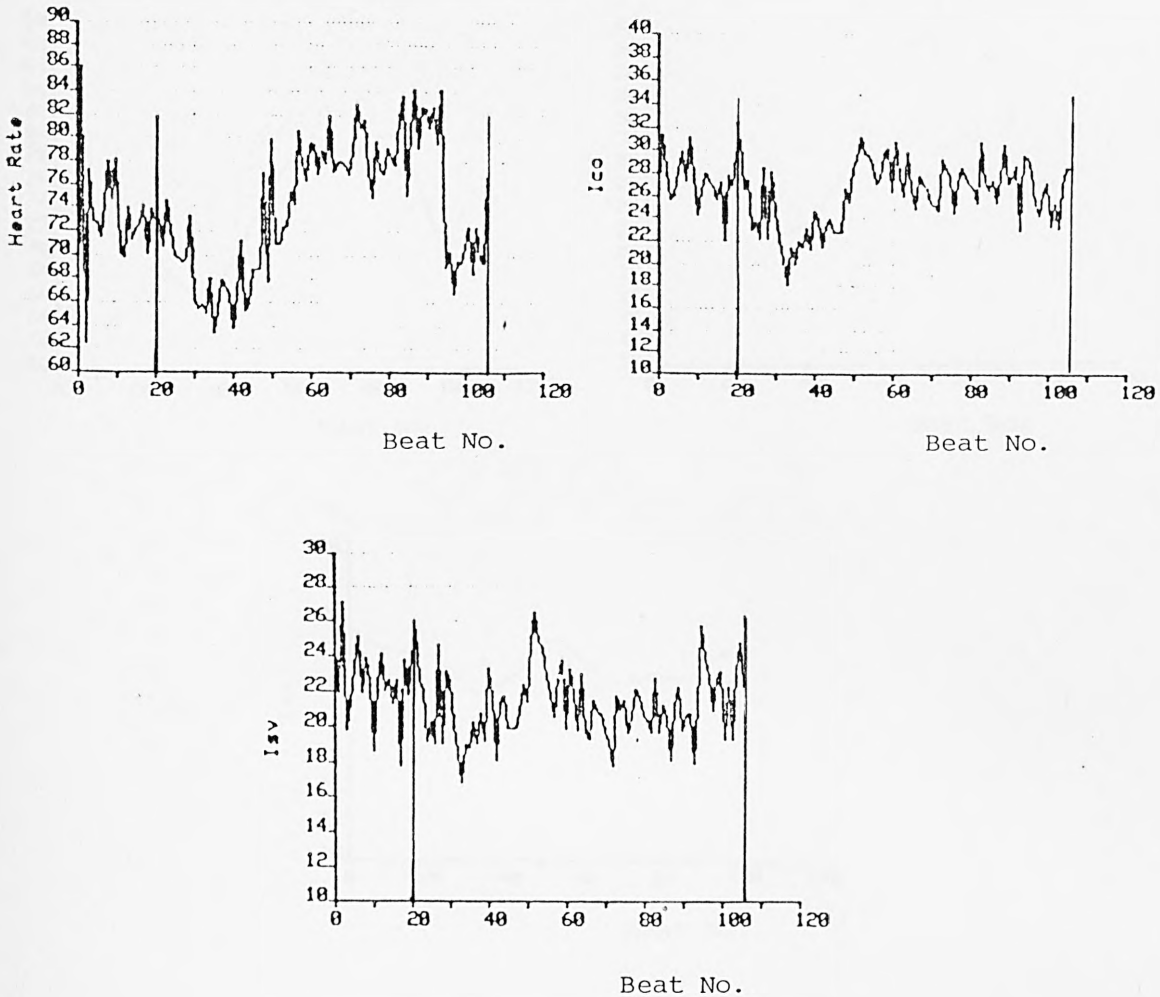

Figure 6.38a Raw data obtained from subject G for the three variables as indicated during a 60° head-down tilt. The vertical lines indicate the times at which the tilt to the inclined position and the return to the horizontal began.

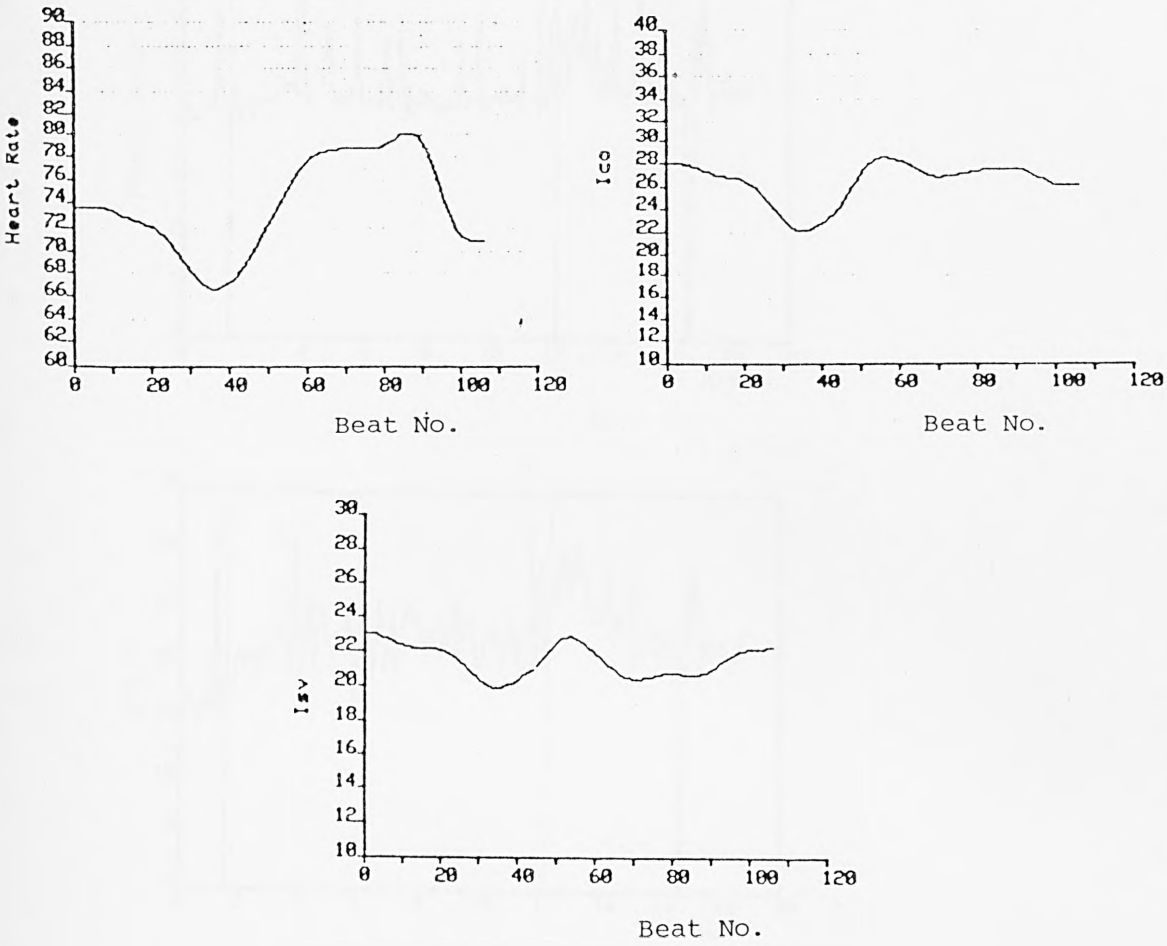

Figure 6.38b Filtered form of the data depicted in Figure 6.38a obtained using a recursive averaging filter.

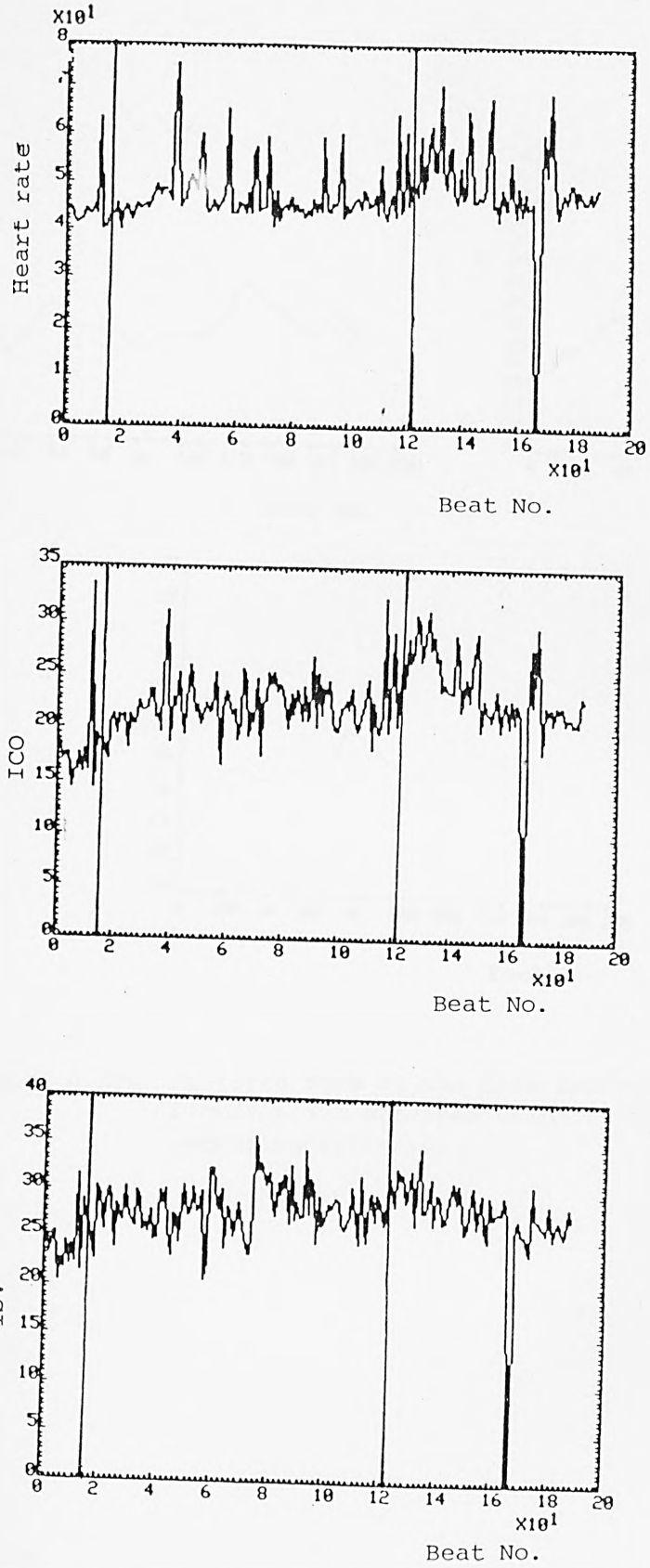

Figure 6.39a Raw data obtained from subject K for the three variables as indicated during a 60° head-down tilt. The vertical lines indicate the times at which the tilt to the inclined position and the return to the horizontal began.

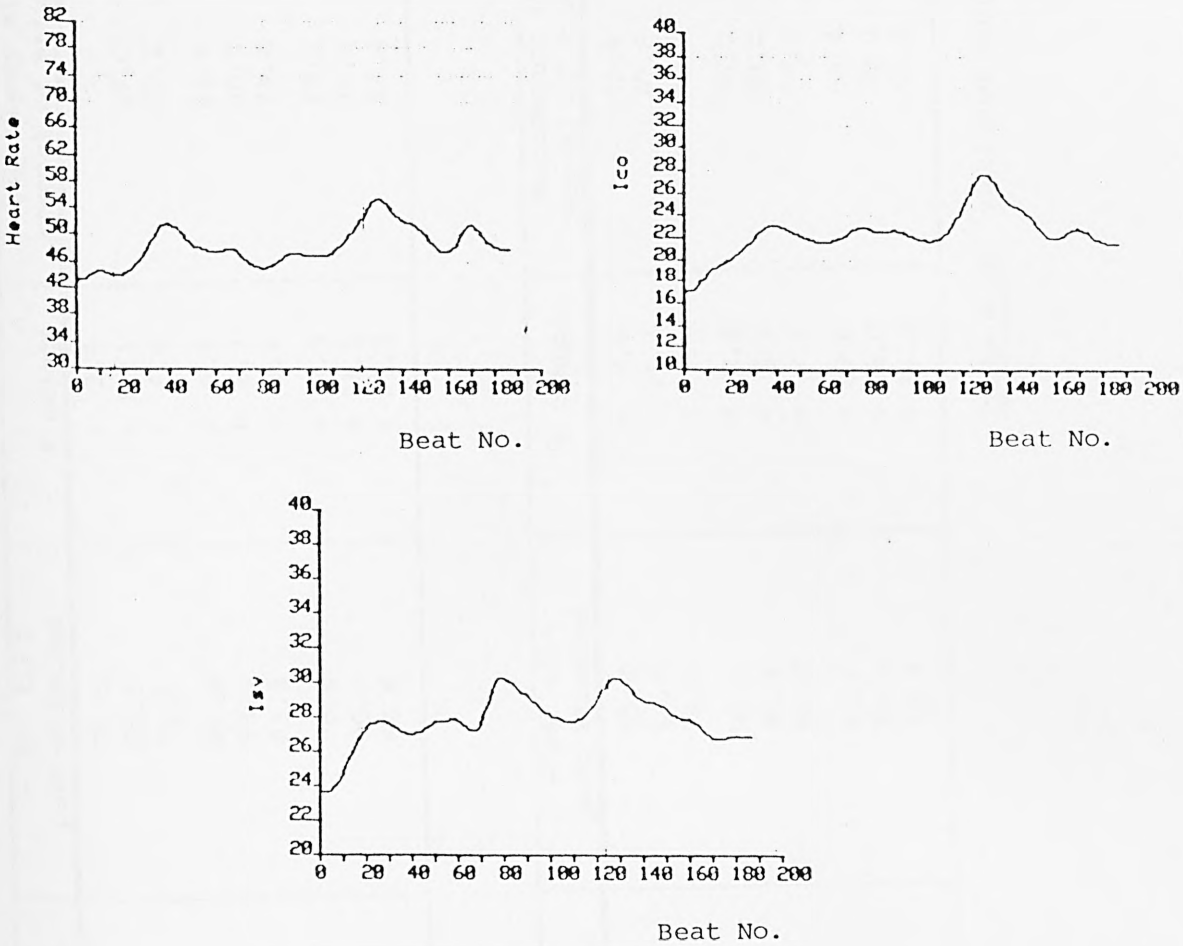

Figure 6.39b Filtered form of the data depicted in Figure 6.39a obtained using a recursive averaging filter.

(a)

Parameter values	Variable	Recumbency pre-stimulus	- 20° tilt post-stimulus	% change	Recumbency after removal of stimulus
Nominal value	FH	72.8	70.0	- 3.8	75.4
+ 15% change		70.0	62.2	- 11.1	67.0
- 15% change		81.0	75.6	- 6.6	82.2
Nominal value	CO	84.4	89.0	+ 5.4	84.4
+ 15% change		88.0	93.9	+ 6.7	88.9
- 15% change		78.8	83.9	+ 6.4	78.8
Nominal value	SV	69.2	78.6	+ 13.5	69.2
+ 15% change		74.6	90.4	+ 21.1	79.0
- 15% change		58.6	66.6	+ 13.6	57.4

(b)

Parameter values	Variable	Recumbency pre-stimulus	- 45° tilt post-stimulus	% change	Recumbency after removal of stimulus
Nominal value	FH	72.8	65.8	- 9.6	73.4
+ 15% change		70.0	60.0	- 14.2	67.8
- 15% change		81.0	74.0	- 8.6	82.4
Nominal value	CO	84.4	91.0	+ 7.8	85.0
+ 15% change		88.0	96.2	+ 9.3	89.0
- 15% change		78.9	84.6	+ 7.2	79.2
Nominal value	SV	69.4	82.6	+ 19.0	69.4
+ 15% change		74.9	96.0	+ 28.0	79.0
- 15% change		58.8	68.4	+ 16.3	57.8

Table 6.18 continued overleaf

(c)

Parameter values	Variable	Recumbency pre-stimulus	- 60° tilt post-stimulus	% change	Recumbency after removal of stimulus
Nominal value	FH	72.8	65.8	- 9.6	73.0
+ 15% change		70.0	59.9	- 14.4	67.0
- 15% change		81.0	74.0	- 8.6	81.0
Nominal value	CO	84.6	90.6	+ 7.0	84.6
+ 15% change		88.0	96.0	+ 9.0	89.0
- 15% change		78.8	83.8	+ 6.3	79.9
Nominal value	SV	69.6	82.8	+ 18.9	69.6
+ 15% change		74.4	96.6	+ 29.8	79.2
- 15% change		58.6	67.6	+ 15.3	58.4

Table 6.18 Model responses to (a) 20°, (b) 45°, and (c) 60° head-down tilts. Values of heart rate, cardiac output and stroke volume are given first with all parameters set at their nominal values and then with the ten critical parameters (as defined in Chapter 7) changed by + 15% and - 15%, respectively.

Subject	Correlation coefficient for head down		
	FH	ICO	ISV
A	- 0.924	- 0.907	- 0.911
B	- 0.937	- 0.953	- 0.947
C	- 0.939	- 0.949	- 0.941
D	- 0.917	- 0.784	- 0.797
E	- 0.985	- 0.981	- 0.986
G	- 0.983	- 0.983	- 0.99
Model	- 0.919	- 0.932	- 0.937

Table 6.19 The correlation coefficient for head-down tilts for heart rate and indices of cardiac output and stroke volume for six subjects, and the heart rate, cardiac output and stroke volume for the model.

the tilting rate being 6^{o} per second. The experimental situation is shown in Figure 6.14b.

In Tables 6.17a - c, values of heart rate and indices of cardiac output and stroke volume are listed, these being obtained before and after the tilts of 20^{o}, 45^{o} and 60^{o}, respectively. Also shown are the percentage changes in mean post-stimulus values as compared to the mean pre-stimulus values.

Corresponding simulations of the model were performed for each degree of tilt. The model was run first with all parameters set at their nominal values and then with ten critical parameters first increased by 15% and then decreased by 15%.

In Figures 6.32 - 6.39 both raw and filtered (by recursive averaging) data are presented, paralleling the presentation of head-up data described in Section 6.5.1.2.1. Those data shown in Figures 6.32 - 6.34 correspond to subject A during head-down tilts of 20^{o}, 45^{o} and 60^{o}, respectively. Raw and filtered data for subjects B, E, G (45^{o} and 60^{o}) and K are shown in Figures 6.35 - 6.39.

Returning to the summaries of these data which are presented in Figures 6.22 - 6.27, it is clear that different patterns of response can be observed in these head-down tilts. Some of the normal volunteers exhibit an increase in heart rate and indices of stroke volume and cardiac output whilst others exhibit a decrease. Examining the responses of the model, including allowable changes in the values of the critical parameters, only a single mode of response can be reproduced, namely a decrease in heart rate and increase in both stroke volume and cardiac output, as shown in Table 6.18. Values of correlation coefficients both for the normal subjects and for the model are presented in Table 6.19.

6.5.2.1.2 Data from Wilkins et al (1950)

The second set of experimental data is taken from the responses of four subjects to 75^{o} head-down tilting, as described by Wilkins et al (1950). These data, for heart rate, stroke volume and cardiac output are presented in Table 6.20.

Simulation of the 19-segment model for the corresponding perturbation resulted in the responses shown in Figure 6.40 for aortic pressure and heart rate. In the model the heart rate decreased after

the tilting and remained stably at the new level. In the data of Wilkins et al, however, the heart rate decreases for a period of approximately 15 seconds, followed by a return towards (occasionally reaching) the original resting level, as shown in Figures 6.31 and 6.40. Table 6.21 summarises the post-stimulus changes exhibited by the model for the variables heart rate, stroke volume, cardiac output and mean arterial pressure.

6.5.2.1.3 90^{o} head-down tilt

The simulation by the 19-segment model of a sudden 90^{o} head-down tilt, as described by Pullen (1976), is shown in Figure 6.30. Blood pressure initially rises followed by a return almost to the normal level since the rise in blood pressure is limited by reflex of the peripheral vasodilatation, bradycardia, venodilatation and negative inotropy. In the case of the heart rate, the model exhibits a sudden decrease in heart rate, lasting for approximately 5 seconds. A rise is then observed which is then followed by a slight decrease until the end of the tilt, this decrease being approximately 10%.

In terms of cardiac output, the model indicates a 6% rise which is little different from the increase observed when simulating a 75^{o} head-down tilt, as described in the previous section. In both cases, however, the figure was substantially less than the increases observed in the four subjects of the study of Wilkins et al (1950) (range 25.6 - 37.5%), as presented in Table 6.20. In part, this discrepancy is a direct mirror of the discrepancy in the change in stroke volume. The model responses (both 75^{o} and 90^{o} head-down tilts) result in increases of approximately 16%, whilst the data indicate increases ranging from 27 to 79%.

Differences between the data of Wilkins et al (1950) and the model responses to 75^{o} and 90^{o} head-down tilt, with respect to heart rate and arterial pressure, may be due to the fact that the stroke volume and cardiac output in the model increase very little, as indicated in Tables 6.20 and 6.21.

6.5.2.1.4 Comparison of results

In Table 6.22 the comparison between the empirical data, those of Wilkins et al (1950) and the model responses is shown for different degrees of tilt.

Subject	Recumbent			75° head down					
	Heart rate (bpm)	Stroke volume (ml)	Cardiac output (ml/sec)	Heart rate (bpm)	%	Stroke volume (ml)	%	Cardiac output (ml/sec)	% change
M.D.	85	37	53.3	87	+ 2.3	50	+ 35	71.6	+ 34.3
F.G.	91	43	66.6	71	-21	77	+ 79	91.6	+ 37.5
W.T.	69	61	69.97	66	- 4.3	84	+ 37	93.29	+ 33.3
G.S.	76	51	64.97	76	0	65	+ 27	81.63	+ 25.6

Table 6.20 The effect of 75° head-down tilt on heart rate, stroke volume and cardiac output for normal subjects (Wilkins et al, 1950).

Variables	Pre-stimulus	Post-stimulus 75° head down	% change
Heart rate (bpm)	72.9	65.69	- 9.8
Stroke volume (ml)	69.6	82.58	+ 18.6
Cardiac output (ml s^{-1})	84.6	90.41	+ 6.8
Mean arterial pressure (torr)	109.1	110.7	+ 1.4

Table 6.21 The percentage change in heart rate, stroke volume, cardiac output and mean arterial pressure in the model from pre- to post-stimulus 75° head-down tilt.

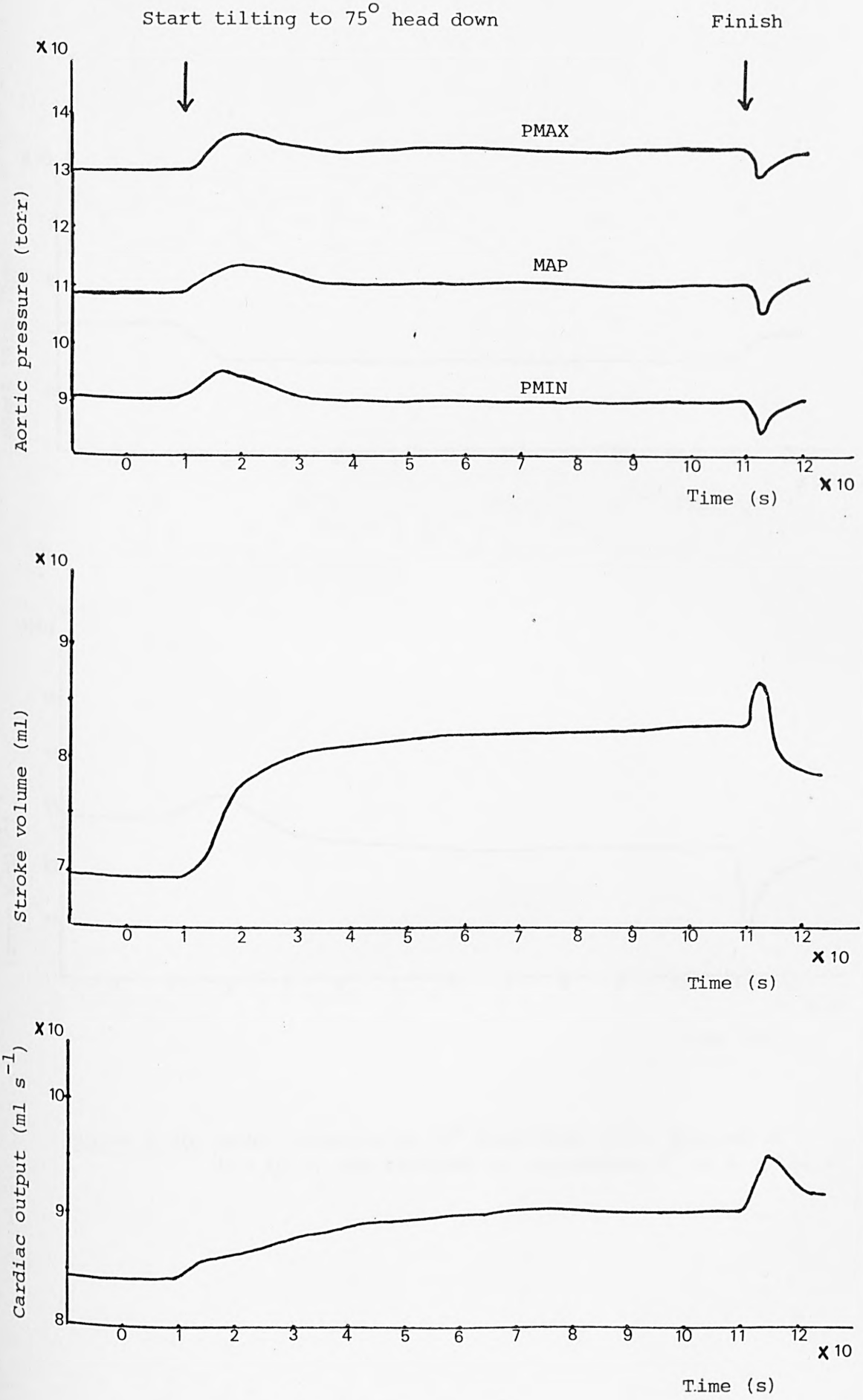
Start tilting to 75° head down
Finish
X 10
14
13
12
11
10
9
PMAX
MAP
PMIN
Aortic pressure (torr)
0 1 2 3 4 5 6 7 8 9 10 11 12
X 10
Time (s)
X 10
9
8
7
Stroke volume (ml)
0 1 2 3 4 5 6 7 8 9 10 11 12
X 10
Time (s)
X 10
10
9
8
Cardiac output (ml s-1)
0 1 2 3 4 5 6 7 8 9 10 11 12
X 10
Time (s)

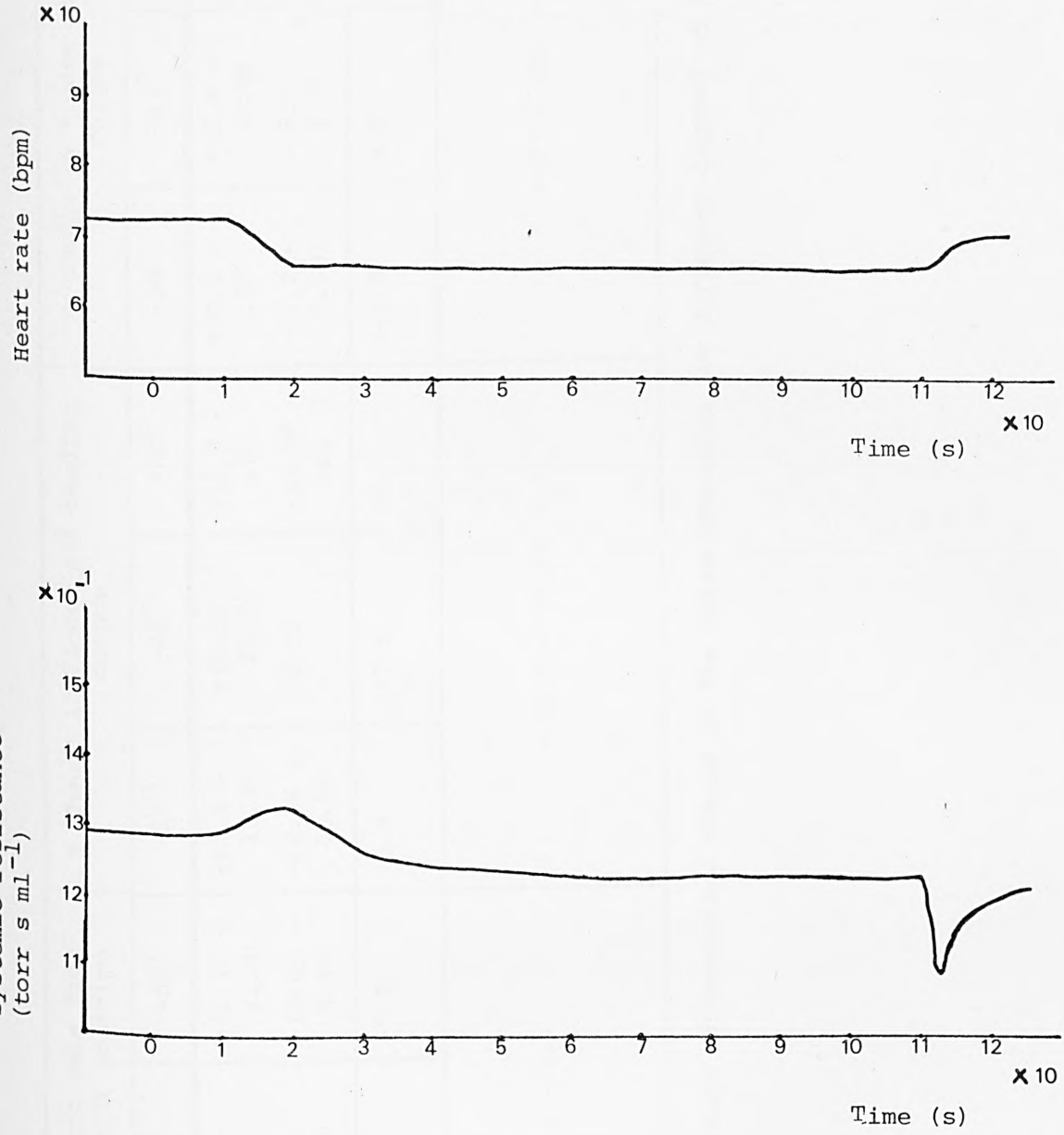

Figure 6.40 Model response to 75° head-down tilt, started at t = 10 s, and returned to recumbency 0° at t = 110 s.

	% change in heart rate from supine to the tilt position			% change in (index of) cardiac output			% change in (index of) stroke volume		
	-20^{o}	-45^{o}	-60^{o}	-20^{o}	-45^{o}	-60^{o}	-20^{o}	-45^{o}	-60^{o}
Empirical data (Northwick Park)	+(3.1 - 13.6) -(2.98 - 6.3)	+(4.3 - 20) -(3.5 - 13.7)	+(1.47 - 21.9) -(0.65 - 4.48)	+(3.4 - 27.7) -(4.86 - 10.5)	+(0.63 - 28.7) -1.05	+(1.4 - 13) -(0.88 - 60)	+(0.2 - 12) -(1.2 - 4.59)	+(2.3 - 21.9) -(8.1 - 8.9)	+(0.28 - 12.4) -(1.15 - 57)
Model response	-3.8	-9.6	-9.6	+5.4	+7.8	+7	+13.5	+19	+18.9
Data from Wilkins et al 1950 (to -75^{o})	+(2.3), -(4.3 - 21)			+(25.6 - 37.5)			+(27 - 79)		

Table 6.22 Comparison of the range of percentage change in the three variables for different degrees of head-down tilt.

One feature common to the empirical results obtained at Northwick Park and the data of Wilkins et al (1950) is the two distinct patterns of heart rate response which are observed. In some subjects there is an increase in this variable, whilst others exhibit a decrease. It should be noted, however, that the increase in heart rate in the one subject of the Wilkins et al data is only 2.3% which could possibly be attributed to the inherent variability of this variable. Nevertheless it is clear that further investigation is required, since the changes seen in the subjects who took part in the Northwick Park study were greater than could be accounted for in terms of variability alone.

It should be noted, however, that the experimental procedure is such that it is very difficult to ensure that all the subjects are receiving similar stresses and stimuli. Thus it is possible, for instance, that differences between individuals in the time taken for a steady state to be re-established, in either recumbent or tilted position, may have given rise to apparent differences in physiological response.

6.5.3 Study of a Trained Athlete

In the data presented in the previous section, it was observed that subject K exhibited low values of heart rate and indices of cardiac output and stroke volume. This can be seen in Table 6.12 (a and c) for 20^{o} and 45^{o} head-up tilt and in Table 6.17 (b and c) for 45^{o} and 60^{o} head-down tilts. These low values were to be expected since it had been discovered that this subject was a trained (marathon) runner. Given that the responses of such a subject are significantly different from those of a normal population (as evidenced by the responses of the other subjects tested), there is the need to examine, critically, the nature of these differences.

6.5.3.1 The physiology

In general, athletes tend to have slower heart rates, larger blood volumes, higher ventricular filling pressures, larger ventricular dimensions and larger stroke volumes than sedentaty individuals when examined in equally relaxed and recumbent states (Rushmer, 1976). In athletes, the myocardium is more developed, as are other muscles. Isometric muscle contraction will lead to an increase in the size of cardiac muscle fibres as well as the specific skeletal muscles, and the size of

the chambers is also increased to a greater extent than the thickness of the walls (Williams, 1962).

More specific information has been provided by Tunstall-Pedoe (1983). He has stated that the athlete's heart is physiologically larger with an above-normal stroke volume, which at rest, therefore, can beat much more slowly than average and still maintain an adequate resting cardiac output - a condition known as athlete's bradycardia.

This bradycardia has recently been found to be either partly an intrinsic property of the size of the heart or, as is more likely, due to the athlete's heart being less sensitive to the normal sympathetic chronotropic bombardment. Tunstall-Pedoe also reported an increase in left ventricular wall thickness as well as increases in diastolic volume and total left ventricular mass in endurance athletes (such as marathon runners).

Some clinicians have indicated that the blood volume of an athlete might be 30 - 40% greater than that of a corresponding normal subject, this enlargement being for the required athletic work. Such changes can bring about a 50% increase in stroke volume (Williams, 1962). As stroke volume increases, pulse rate drops, as seen in subject K or as indicated in his paper by Williams, where the resting pulse rate was seen to be 60 beats per minute or commonly less. Williams also indicated that variations in the resting heart rate between individual athletes could be attributed in part to sinus arrhythmia.

The data presented in Table 6.23 show that the type of exercise undertaken has an important bearing on the degree of bradycardia attained (Grande et al, 1965). Table 6.24 shows that the heart volume for long-distance runners is increased by less than 20%, although it should be noted that the values given are not related to body size (Grande et al, 1965).

6.5.3.2 Model simulation

In order to test possible mechanisms underlying the differences in response seen in subject K, a number of model simulations were carried out in which parameters were set at non-normal values, representing the various hypotheses under test.

The first hypothesis tested was that the difference in the short-term studies was attributable to an increase in blood volume in the athlete.

Sport	Subject No.	Mean heart rate/min	SD
Various sports	198	50	*
Middle-distance runners	16	63	11.8
Long-distance runners	15	61	16.1
Marathon runners	28	57	7.3
Various sports (well trained)	107	50	5.6
Long-distance runners (very well trained)	10	43	4.8
Light sports	47	61	12.1

Table 6.23 The resting heart rate in trained sportsmen (Grande et al, 1965). (American Physiological Society)

* The published data do not allow computation of the SD.

Subject No. and activity	Mean volume (ml)	Range
67 normals	790	490 - 1080
86 swimmers, football players, tennis players	876	605 - 1130
66 skiers, rowers, long-distance runners, swimmers	923	645 - 1180

Table 6.24 Heart volume estimated from areas of heart shadow in two Teleoroentgenograms taken of the thorax at 90^{o} angle (Grande et al, 1965).

Table 6.25 represents the responses of the 19-segment model with a 40% increase in the blood volume of the cardiovascular system. Heart rate falls by 20% from its steady state value with an increase in stroke volume of 74% and cardiac output by 39%, as shown in the table. The aortic pressure, however, is higher than would be expected clinically.

The second hypothesis to be examined was that of a decrease in the arterial compliance. The effects of a 30% change in this parameter on the main variables are shown in Table 6.26. The results shown here are generally, in a qualitative sense, what would be expected by a clinician, as were the majority of the results shown in Table 6.25 (Tunstall-Pedoe, 1983). The value of aortic pressure is less with this assumption of decreased compliance than it was with increased volume. The changes in stroke volume and cardiac output are less with this second assumption, markedly so in the case of stroke volume (15% as opposed to 74%).

Having examined the effects of these two hypotheses individually, simulations were then carried out with various combinations of increase in blood volume and decrease of compliance. The principal results are presented in Tables 6.27 - 6.31.

Table 6.27 shows the changes in the main variables (mean arterial pressure, stroke volume, cardiac output, heart rate, systolic and diastolic pressure) due to an increase in the total cardiovascular system volume by 40% and a decrease in the compliance, first for both arterial and venous segments, and secondly only for the arterial segments. For these two cases, the heart rate decreased by 33% and 32%, respectively, but the systolic pressure rose sharply by 35% and 32%, respectively, due to an increase in stroke volume by 111% and 100%, respectively. Again, the aortic pressure is unacceptably high.

Next, the effects of decreasing the arterial compliance by 30% are considered, together with increasing volume, first increasing the volume of all the arteries and veins by 20%, and secondly by increasing only the volume of the heart chambers by 20%. The results are shown in Table 6.28.

For these two cases, stroke volume increased by 63% and 27%, respectively, causing a drop in the heart rate by 26% and 18%, respectively, as compared to the steady state values. On the other hand, the systolic pressures increased by 21% and 10%, respectively.

Variable	+ 40% change in the blood volume of all the cardiovascular system
MAP	125.1
SV	120.9
CO	117.5
FH	58.27
PMAX	154.5
PMIN	95.71

Table 6.25 The effect of changing the blood volume on the aortic pressure, stroke volume, cardiac output and heart rate.

Variable	- 30% change in arterial compliance
MAP	109.7
SV	80.23
CO	84.06
FH	62.86
PMAX	138.7
PMIN	81.4

Table 6.26 The effects of a decrease in arterial compliance by 30% on the main variables.

Variable	+ 40% change in the blood volume of all the vascular system and the heart chamber with	
	- 30% change in arterial and venous compliance	- 30% change in the arterial compliance
MAP	128.6	126.5
SV	147.1	139.3
CO	119.3	115.5
FH	48.6	49.78
PMAX	177.1	172.5
PMIN	81.6	81.5

Table 6.27 The model responses following decrease of arterial and venous compliance first, and decrease of arterial compliance alone.

Variable	- 30% change in the arterial compliance with	
	+ 20% change in blood volume of the cardio-vascular system	+ 20% change in volume of the heart chamber
MAP	120.8	113.2
SV	114.0	88.23
CO	102.4	88.27
FH	53.8	60.0
PMAX	159.0	144.3
PMIN	82.38	82.4

Table 6.28 The effects of increasing the volume of the cardio-vascular system, or the heart chamber only, decreasing the arterial compliance by 30%.

Variable	(1) + 30% change of the heart chamber volume (2) - 30% change of the arterial compliance	
	$P_{139} = 1.0$	$P_{137} = 68.0$
MAP	113.5	103.8
SV	94.5	76.8
CO	87.3	83.9
FH	55.39	65.55
PMAX	146.3	131.6
PMIN	80.7	76.87

Table 6.29 The model responses after increasing the volume of the heart chamber by 30% and decreasing arterial compliance by 30% with given different values to the parameters ($P(137) = 80.0 = K_{18}$ threshold constant in neural control, and $P(139) = 1.5 = K_{14}$ constant in neural control).

Variable	(1) + 30% change in the heart chamber volume (2) - 50% change in arterial compliance (with another change in)					
		P(137) = 70.0	P(137) = 70.0 P(139) = 1.3	P(137) = 68.0 P(139) = 1.3	P(139) = 2.0	P(137) = 68.0 P(139) = 1.3 All (a) = -30%
MAP	112.2	104.8	104.9	103.3	112.1	102.1
SV	94.9	85.75	87.9	85.9	90.0	83.72
CO	86.06	82.75	82.38	81.69	86.8	80.63
FH	54.37	57.9	56.2	57.05	57.34	57.78
PMAX	153.9	142.7	143.6	141.2	152.0	139.1
PMIN	71.6	68.7	67.3	66.62	73.05	66.17

Table 6.30 The model responses after increasing the heart chamber volume by 30%, decreasing the arterial compliance by 50%, and also by changing the nominal values of P(137) and P(139) and by decreasing the elastance by 30%.

Variable	(1) + 30% change of the heart chamber volume (2) - 30% change of the arterial compliance
	P(137) = 68, P(139) = 1.3 All (a) change by - 30%
MAP	101.9
SV	80.9
CO	80.82
FH	59.9
PMAX	136.2
PMIN	68.9

Table 6.31 The model responses after 30% increase in the heart chamber volume, 30% decrease in the arterial compliance and also changing all the elastance by - 30% and both P(137) = 68 and P(139) = 1.3.

Although the patterns of blood pressure shown in both these cases are less extreme than those shown in Table 6.27, there is still uncertainty as to whether blood pressure patterns exhibited by athletes are in any way abnormal, and hence it is difficult to make judgement between the results shown in Table 6.28.

Other degrees of change in blood volume and compliance were then investigated in order to examine ways in which the rise in pressure might be reduced, whilst at the same time preserving the athlete's bradycardia.

Table 6.29 shows the model responses following an increase in heart volume by 30% and decrease in the arterial compliance by 30%, together with examining the effect of changing the nominal values of two of the parameters defining neural control. The two were P(137), which is one of the ten critical parameters, and P(139). Both of these have an effect upon pressure and heart rate, as can be seen from the results of the sensitivity analysis described in Chapter 7.

From the results presented it can be seen that the effect of changing P(137) from its nominal value of 80 to 68, whilst keeping P(139) at its nominal value, gives a realistic pressure with a 10% increase in stroke volume and a 1% decrease in cardiac output. With P(137) kept at its nominal values and P(139) reduced from 1.5 to 1.0, however, the systolic pressure is still clinically high, but, again, it is not clear as to whether such a change might occur in an athlete.

In Table 6.30, results are presented corresponding to the assumption that the arterial compliance is decreased by 50%, whilst retaining the 30% increase in heart chamber volume, together with various combinations of value of P(137) and P(139). Again, the problem arises of interpretation of the values of pressure obtained, given the inadequate understanding of the underlying physiology.

Also examined is the effect of decreasing all the elastances by 30%. The results in this case are shown in the final column of Table 6.30.

The final case examined involved a 30% increase in heart chamber volume, 30% decrease in arterial compliance and 30% decrease in elastance. The results are presented in Table 6.31.

In Figure 6.41, a comparison is given between the data obtained from the tilt experiments on subject K and the model responses as a

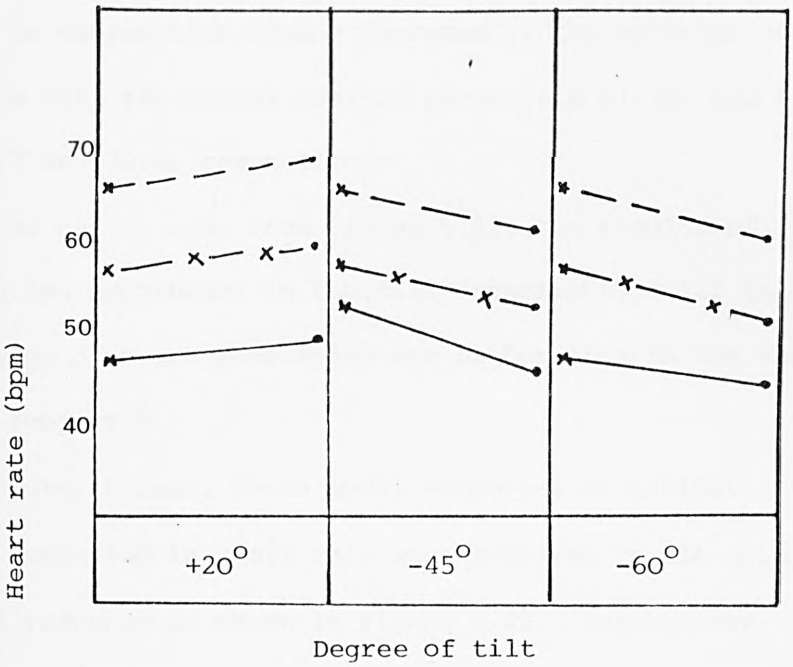

Figure 6.41 Comparison between the response of subject K (——) to 20° head-up tilt and 45° and 60° head-down tilt, and the results of two hypotheses: (a) (- - - -) the model response with change (+30% in the volume of the heart chamber, -30% in the arterial compliance, and P(137) = 68.0); (b) (—x—x) the model response with change (+30% volume of the heart chamber, -50% of the arterial compliance and P(139) = 1.3, P(137) = 70.0).

result of including, in turn, two hypotheses describing the difference between an athlete and a normal subject. The first involved a 30% increase in the volume of the heart chambers and a decrease in the arterial compliance by 30% with the neural control parameter P(137) set at a value of 68.0. The second again involved an increase in the heart volume by 30%, but this time in conjunction with a decrease in the arterial compliance of 50% with the neural control parameters P(139) and P(137) set to 1.3 and 70.0, respectively.

As can be seen from Figure 6.41, the results of applying these two hypotheses in the tilt experiments still leads to patterns of heart rate which are higher than in the response from subject K.

Nevertheless, these model responses do exhibit a significant reduction in heart rate when compared to the original model response as shown in Figure 6.22. Furthermore, on the evidence of the information provided in Table 6. 23, the heart rate responses with the second hypothesis are well within the range of heart rate given for comparable athletes (43 - 61 beats per minute), although this simulation does result in a low value of diastolic pressure.

In order to make further assessment of the model behaviour in seeking to explain differences between normal subjects and athletes, there is the need for information on many more of the key physiological variables. Some limited results have been obtained from a study carried out at St. Bartholomew's Hospital by Dr. Tunstall Pedoe and his colleagues in the Department of Cardiology. These results were obtained from three subjects who underwent the tilt experiments described earlier (subjects

D, G and K), one of these, subject K, being the athlete. Table 6.32 presents the results of echocardiographic measurement, blood volume and chest X-ray measurements of transverse cardiac diameter/transverse chest diameter. The results for subjects D and G were mostly within normal limits. For subject K (the athlete), however, some of the echocardiographic measurements and blood volumes were above normal limits, the echo stroke volume being 107.8 ml while the normal range is 55 - 95 ml (see Figure 6.42 - Tunstall Pedoe (1984)).

Further data are still needed, however, in order to proceed further with the process of model validation . Nevertheless, the hypotheses which have been tested appear, at least in part, to characterise the observed differences between the two groups of subjects.

6.6 DRUG EFFECTS

In Section 3.4, a brief presentation of the pharmacokinetic model was given. This included representations of the injection, transport and action of a single drug. In this section an examination is carried out into the validity of the cardiovascular model in relation to its ability to describe and predict the dynamic effects observed following injection of drugs whose short-term action is upon specific components of the cardiovascular system.

Again as in other aspects of model validation, considerable difficulties were encountered in obtaining suitable experimental data. Much of the assessment of model validity had therefore to be based upon

(a)

	K	D	G
CXR	0.135/0.29 m	0.12/0.29 m	0.12/0.30 m
ECG	Normal	Partial RBBB	Normal
Longest R-R	1.2 s	0.64 s	0.88 s
Blood volume	5.261 ml	4.480 ml	5.558 ml
Weight (kg)	57.2	72.6	66.0
Blood volume/kg	92.0	72.6	84.2

(b)

Measured data	K	D	G	Normal ranges
Left atrial diameter	0.0305	0.0229	0.0333	0.019 - 0.038 m
Aortic root diameter	0.0314	0.0324	0.0314	0.02 - 0.037 m
Aortic valve excursion	0.0219	0.0171	-	0.016 - 0.026 m
Mitral valve closure rate	0.23	0.13	0.13	0.05 - 0.12 m/s
Mitral valve excursion	0.0314	0.0286	0.019	0.02 - 0.025 m
End diastolic diameter	0.0505	-	0.0476	0.035 - 0.056 m
End systolic diameter	0.0276	-	0.0381	0.025 - 0.041 m
LV post. wall thickness	0.0105	-	0.0076	0.006 - 0.011 m
Interventricular septum	0.0095	-	0.0076	0.006 - 0.011 m
Right ventricular diameter	0.0171	-	0.0238	0.007 - 0.023 m
LV stroke volume	107.76	-	-	55 - 95 ml

Table 6.32 Results of blood volume, chest X-ray and the echocardiographic measurements for the three subjects

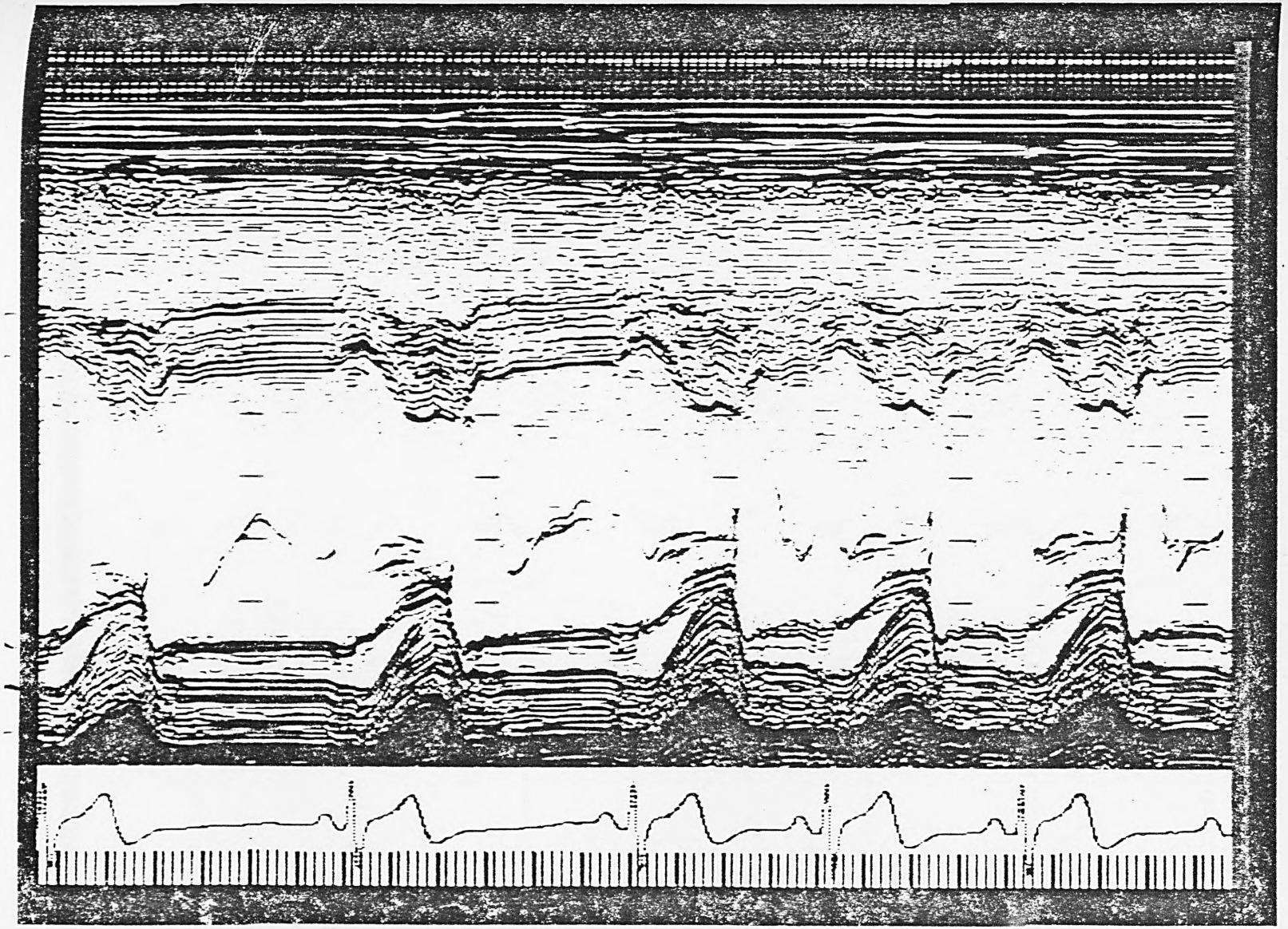

Figure 6.42a The echo of left ventricle for subject K.

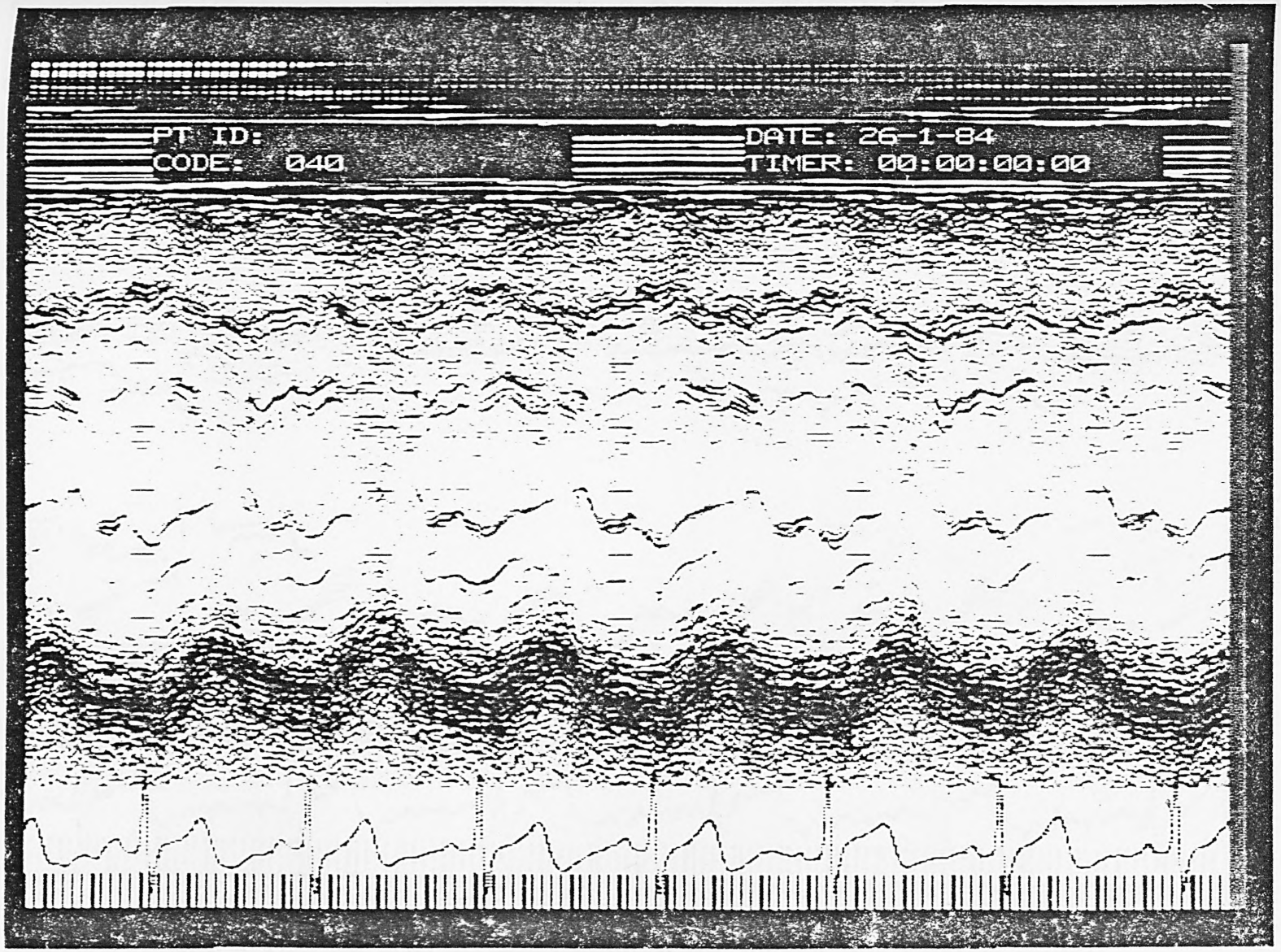

Figure 6.42b The echo of left ventricle for subject D (LV view not measurable - Tunstall-Pedoe, 1984).

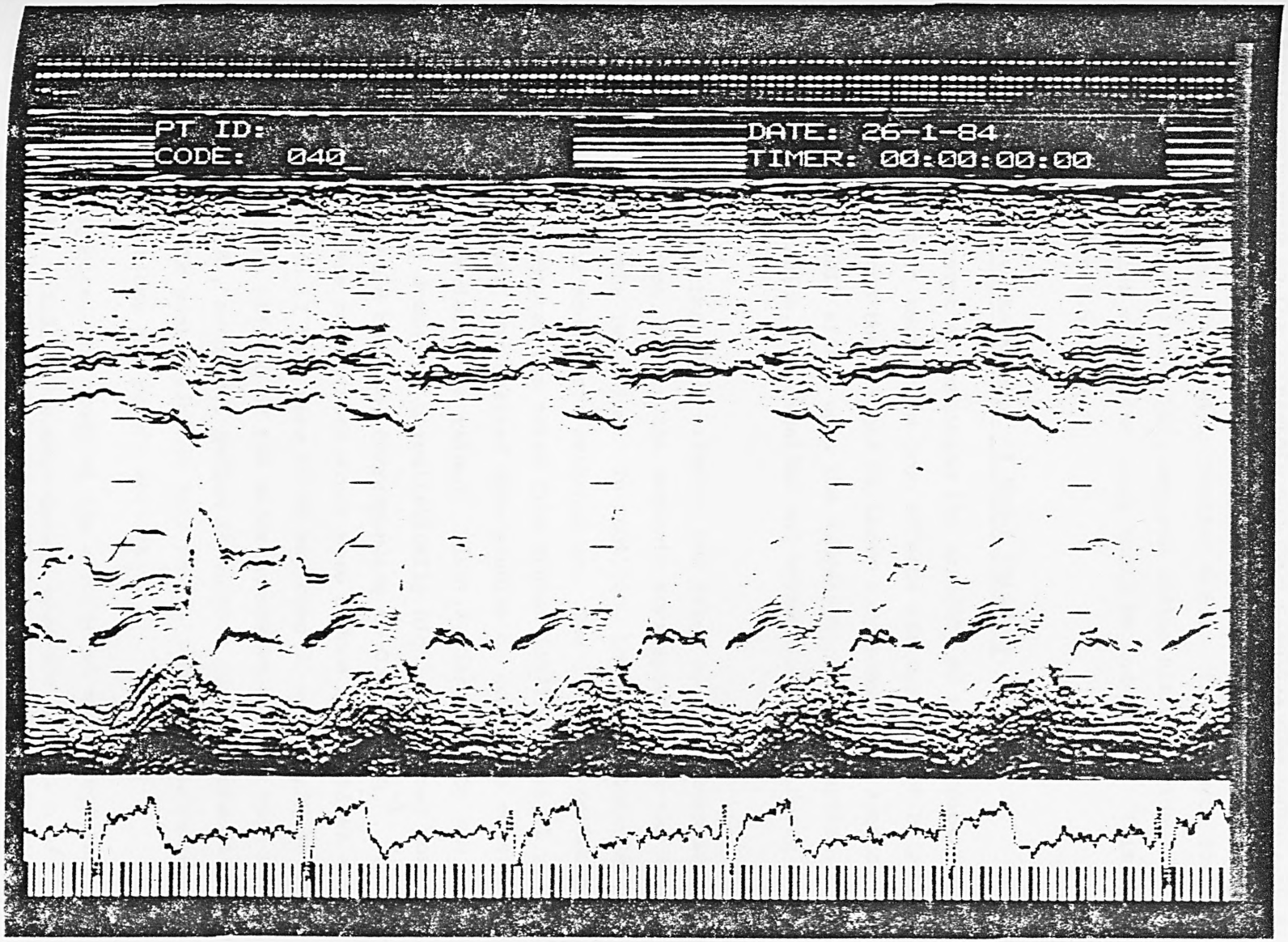

Figure 6.42c The echo of left ventricle for subject G.

results published in the literature and upon clinical assessment, on a qualitative basis, of the patterns of response yielded by the model. These approaches are described in Section 6.6.1. The one drug for which experimental data were obtained was sodium nitroprusside, and in this case a fuller validation study could be undertaken. This is reported in Section 6.6.2.

6.6.1 A Qualitative Assessment of Model Validity

The first attempt at examining the validity of the cardiovascular model in relation to short-term drug effects was carried out by Pullen (1976). He simulated the effects of three sympathomimetic agents, that is drugs having their effect upon the sympathetic nervous system. The three were methoxamine, isoprenaline and noradrenalin, all being related to adrenalin.

In simulating these drug effects, two sites of administration were adopted for injection, namely the segments corresponding to the head and arm veins and the leg veins. In addition, the appropriate local drug effects in the model were switched on. The dosage of noradrenalin and isoprenaline adopted was taken from Hughes (1971), namely 1 $\mu g\ kg^{-1}$. This figure, however, was derived from studies on conscious dogs. Two criticisms can immediately be raised. First, Kyriakou (1980) has indicated that the dosage is unrealistically high. A typical dose for a 70 kg subject would be 3 µg, corresponding to 0.042 $\mu g\ kg^{-1}$. Furthermore, such drugs are rarely used since more modern alternatives are available, and even if they were to be employed it would only be to counteract the side effects of the major anaesthetic drugs such as: nitrous oxide (OP8), morphine, sodium thiopentan plus phenobarbitone (barbiturates). As such, clinical data on the effects of noradrenalin and isoprenaline alone are rarely available.

As a consequence, the study of the effects of such drugs in relation to model validity focusses merely upon the direction of change of key physiological variables induced by intravenous injection of these agents.

The principal features of the simulation results are shown in Table 6.33, together with the corresponding features for human subjects as described in standard pharmacological texts (e.g. Goodman et al, 1965). These features are simply the dominant direction of change following drug administration of systolic, mean and diastolic arterial

Drug	Human or model	Systolic arterial pressure	Mean arterial pressure	Diastolic arterial pressure	Cardiac output	Heart rate	Total peripheral resistance
Methoxamine	Human	+	+	+	0 or -	-	+
	Model	+	+	+	-	-	+
Noradrenaline	Human	+	+	+	0 or -	-	+
	Model without venoconstriction	+	+	+	-	+	+
	Model with venoconstriction	+	+	+	-	-	+
Sodium nitroprusside	Human	-	-	-	+	+	-
	Model	-	-	-	+	+	-
Isoprenaline	Human	-	-	-	+	+	-
	Model	-	-	-	+	+	-

Table 6.33 General features of the responses in the model and the human to intravenous injection of methoxamine, noradrenaline, sodium nitroprusside and isoprenaline.

pressures, cardiac output, heart rate and total peripheral resistance. In addition to methoxamine, isoprenaline and noradrenalin, the patterns of change are also given for sodium nitroprusside which will be considered in quantitative terms in Section 6.6.1.3.

The drugs considered have either vasoconstrictive or vasodilatative effects. In terms of the model representation, simulation can be performed with their effects being restricted to the blood vessels only or else affecting both heart chambers and blood vessels.

6.6.1.1 Vasoconstrictive drugs - effects on blood vessels only

The drug of this category considered was methoxamine, whose pharmacological effects are almost exclusively those characteristic of α-receptor stimulation (Goodman et al, 1965). The outstanding effect produced by this drug is an increase in blood pressure due mainly to an increase in peripheral resistance (vasoconstriction). The drug has virtually no stimulatory action on the heart and lacks β-receptor action on smooth muscle. Cardiac output is usually decreased, and the reflex of bradycardia is produced through the baroreceptors.

The model response, including vasoconstriction of the blood vessels only, is shown in Figure 6.43. Comparing features of this response with pharmacological data indicates, as presented in Table 6.33, that the model, in this qualitative sense, is a valid representation of these short-term effects, as evidenced by the matching of model and data features for the principal physiological variables.

6.6.1.2 Vasoconstrictive drugs - effects on both heart chambers and blood vessels

Noradrenalin was chosen as the representative drug of this category. Its overall effect is to raise both systolic and diastolic pressures, and since cardiac output is decreased, this must be brought about by strong constricting action upon the peripheral vessels. The heart usually beats more slowly (bradycardia), this being due to the large rise in arterial pressure and strong stimulation of baroreceptors in the aortic arch and carotid sinuses (Lippold et al, 1979).

The model is simulated by "switching on" vasoconstriction, tachycardia and positive inotropy and setting the value of $\sigma_1 = 400$, $\sigma_2 = 50$ and $\sigma_3 = 50$ (see Section 3.4).

The model produces a 9.9% increase in mean arterial pressure with

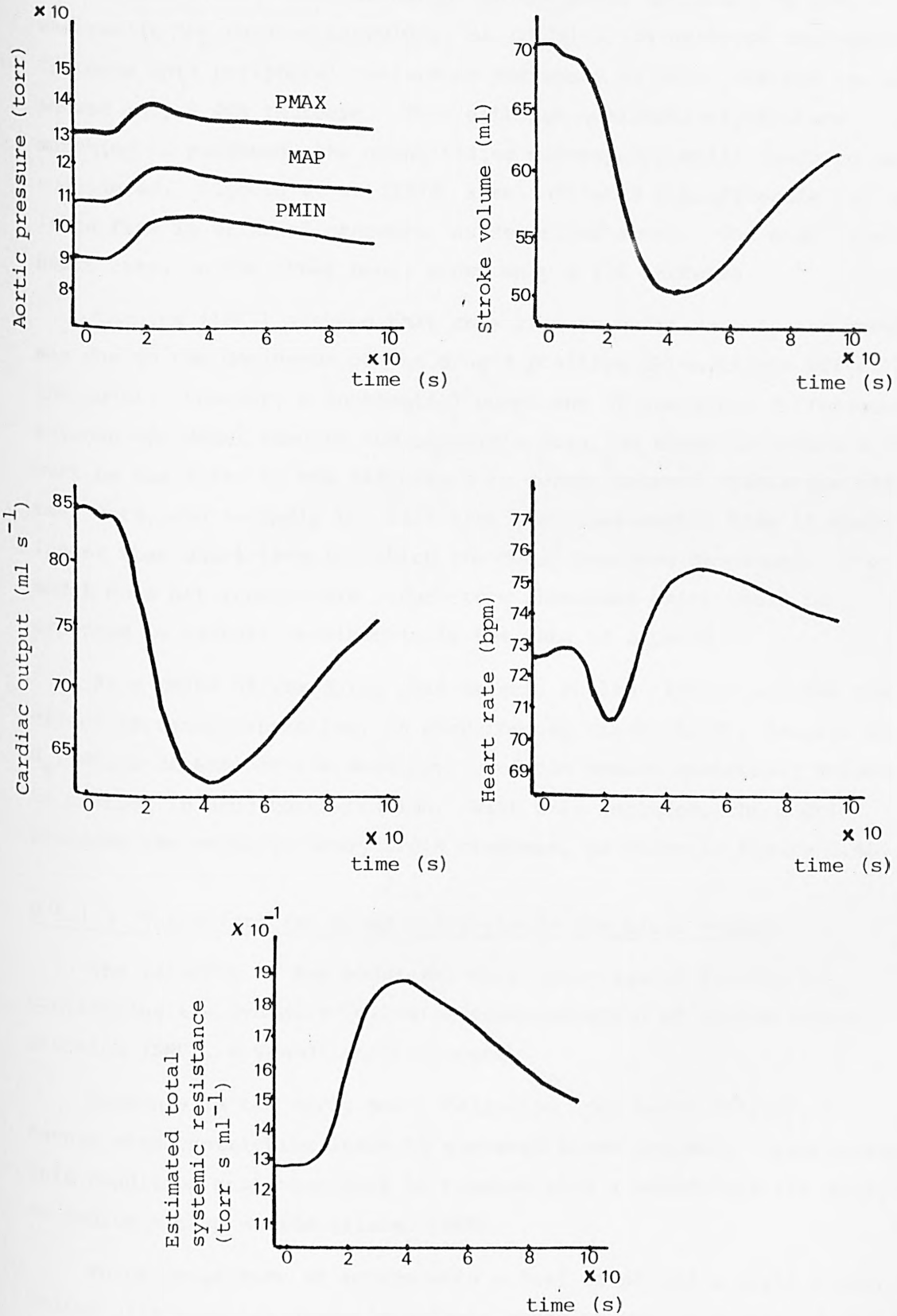

Figure 6.43 Injection of methoxamine into the head and arms veins segment at t = 0 s (σ_1 = 400, σ_2 = 0, σ_3 = 0).

the diastolic pressure showing a larger increase of approximately 14% (see Figure 6.44). Cardiac output in the model decreased by 23%, whereas in the data of Lippold et al (1979) a 33% decrease was evident. In these data peripheral resistance increased by 100%, whereas the model showed only a 40% increase. Thus,although qualitatively feature matching is produced, the quantitative discrepancy still needs to be considered. Lippold et al (1979) also indicates a bradycardia due to the large rise in arterial pressure, as described above. The model response of heart rate, on the other hand, shows only a 17% increase.

Leaning (1981) assumed that this rise in heart rate in the model was due to the dominance of the drug's positive chronotropic effect in the model. However, a substantial component of the large differences between the model results and Lippold's data, as shown in Figure 6.45, must be due first to the difference in dosage between simulation and test data, and secondly the fact that the experimental time is much longer than short-term for which the model has been developed. The model does not incorporate longer-term phenomena which would be expected to feature prominently in the data of Lippold.

As a means of remedying this defect, Pullen (1976) included the effect of venoconstriction, as described by Green (1972), denoted by σ_4, which determines the sensitivity of the venous unstressed volume to changes in drug concentration. With this included, the model produced the required bradycardia response, as shown in Figure 6.46.

6.6.1.3 Vasodilatative drugs - effects on the blood vessels

The validity of the model was then investigated further by considering the dynamics following administration of sodium nitroprusside (SNP), a vasodilatative agent.

Commonly in the early hours following open heart surgery, a severe vasoconstriction leads to elevated blood pressure (hypertension). This condition must therefore be treated with a vasodilatative drug, such as sodium nitroprusside (Slate, 1980).

These drugs have an action with a fast onset and a rapid decay. Sodium nitroprusside directly relaxes vascular smooth muscle, decreasing the resistance of the vascular bed and increasing venous capacitance. The local action of sodium nitroprusside is therefore simulated by setting the arterio-venous resistance sensitivity coefficient (σ_1) to the normal value and setting the remaining sensitivity coefficients

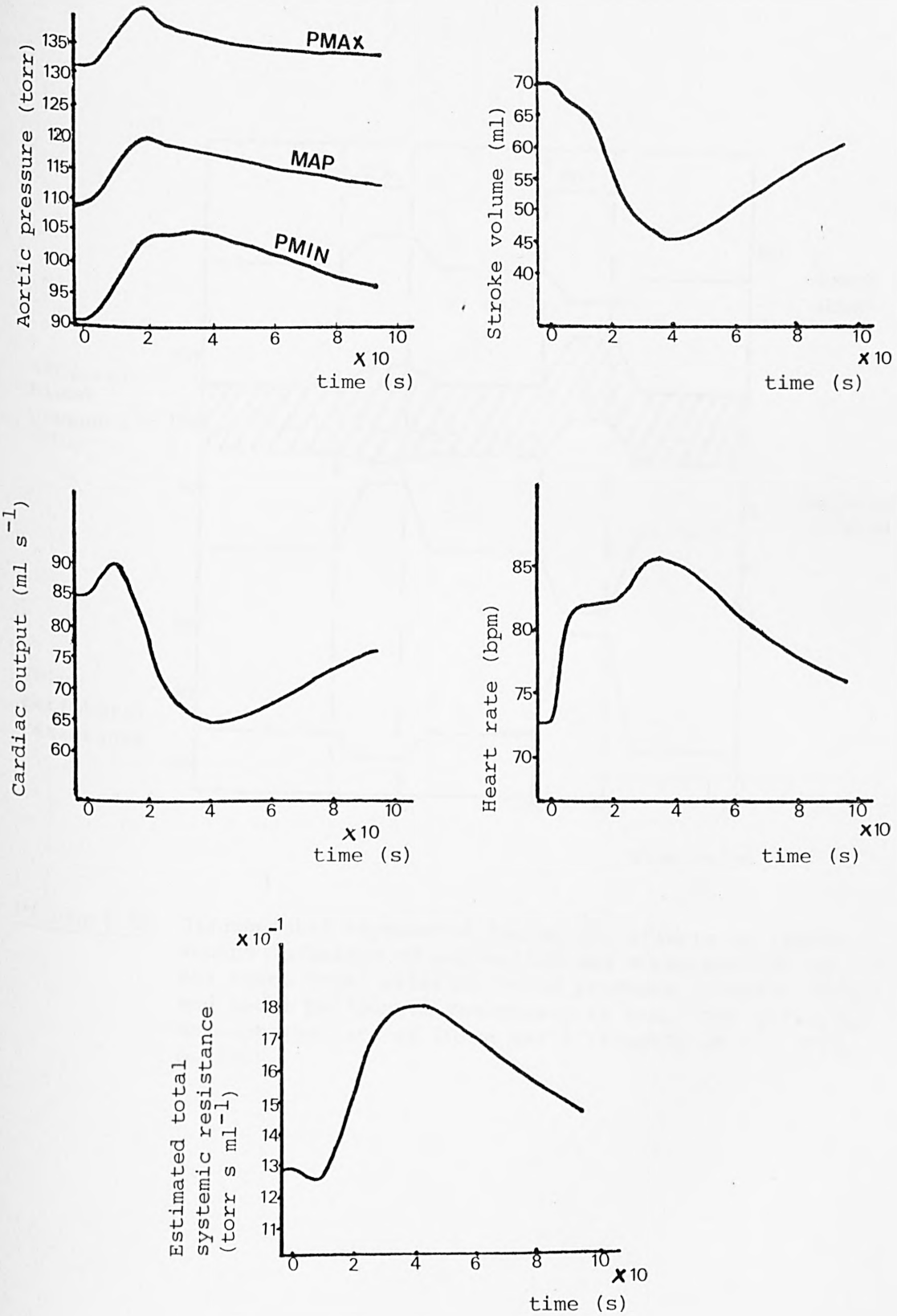

Figure 6.44 Noradrenaline injection into the head and arms veins segment at t = 0 (σ_1 = 400, σ_2 = 50, σ_3 = 50, σ_4 = 0).

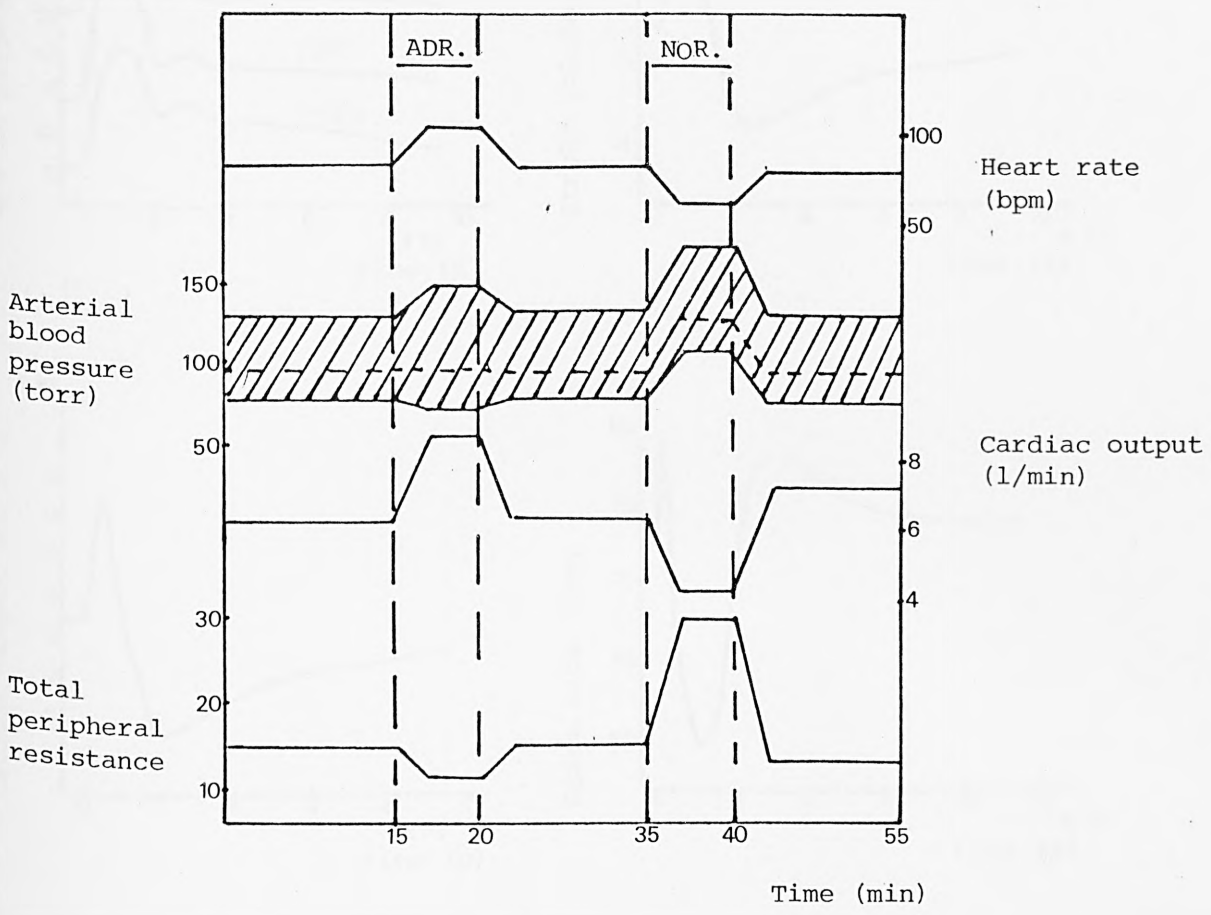

Figure 6.45 Diagrammatic representation of the effects of intravenous infusions of adrenaline and noradrenaline on the heart rate, arterial blood pressure, cardiac output and total peripheral resistance in man. The infusions were at the rate of 10 mg min^{-1} (Lippold et al, 1979, p. 232).

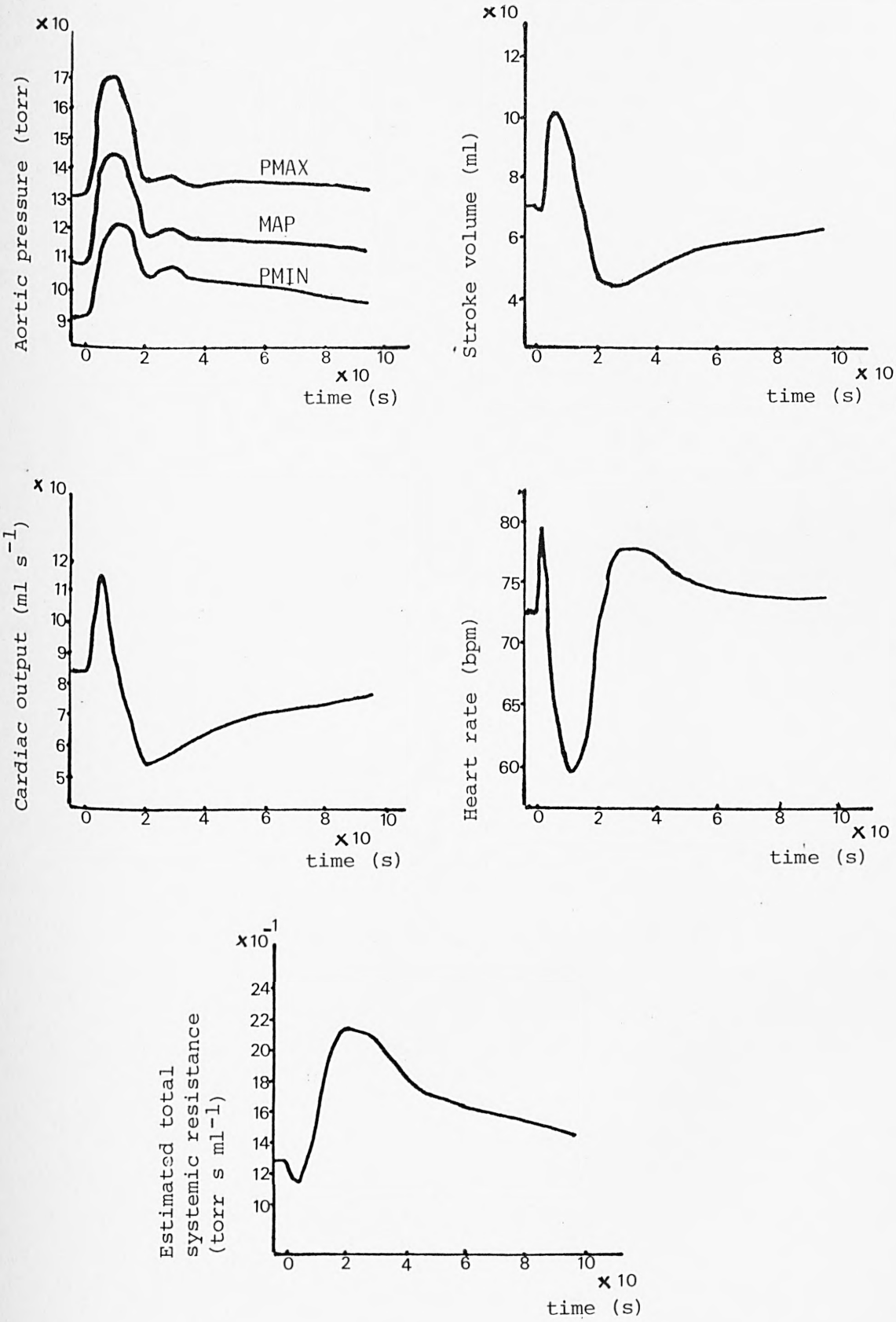

Figure 6.46 Noradrenaline injection into the head and arms veins segment at t = 0 (σ_1 = 400, σ_2 = 10, σ_3 = 50, σ_4 = 10).

to zero (σ_2, σ_3). (This is the switching on of vasodilatation in the computer program.) The normal intravenous dosage of SNP infused into the head and arm veins model segment is 210 µg for a 70 kg patient (Cole, 1982), as shown in Figure 6.47, which also includes a simulation of a 70 µg/70 kg dosage. Clinically, sodium nitroprusside is administered as a continuous infusion.

As a first simulation, for comparison with the drug studies reported in the earlier section, the sodium nitroprusside was given as a single injection. With a dosage of 210 µg/70 kg, the heart rate increased by approximately 44%, as shown in Figure 6.47. This drug administration is thus clearly unrepresentative of clinical practice and thus, as would be expected, produces a heart rate change much in excess of typical figures given in relevant textbooks. Wang et al (1977), in experiments performed on dogs, typically found an increase in heart rate change of 2% for a dosage in the range 4 - 10 µg/kg/min. However, the same test repeated for the more realistic continuous infusion of 210 µg/70 kg over a period of 60 s, as shown in Figure 6.48, still results in a 45% decrease in the arterial pressure, causing a large increase in heart rate.

Since σ_1 appears to alter the degree of change in peripheral resistance, and hence arterial pressure, simulations were performed for various values of this parameter, as shown in Figure 6.49. In each case the dose was 210 µg/70 kg over the 60 s period. Table 6.34 shows the percentage change in mean arterial pressure, stroke volume, cardiac output, heart rate and estimated total systemic resistance in each case. From these results it can be seen that with σ_1 = 100, the pattern of response obtained is qualitatively in accord with clinical expectation.

Table 6.34 also shows that with σ_1 set at 100, the model produces a decrease of approximately 16% in mean arterial pressure, whilst cardiac output and heart rate increased by 20% and 6%, respectively. By comparison, Wang et al (1977), albeit in dog experiments, found a 26 - 32% decrease in arterial pressure with a 2% increase in heart rate. It should also be noted that the dosage employed in these experiments differed from that used in the model simulation, as described above.

In a qualitative sense, the model, overall, was found to provide an adequate representation of the expected patterns of response (Cole, 1982 and Slate, 1983).

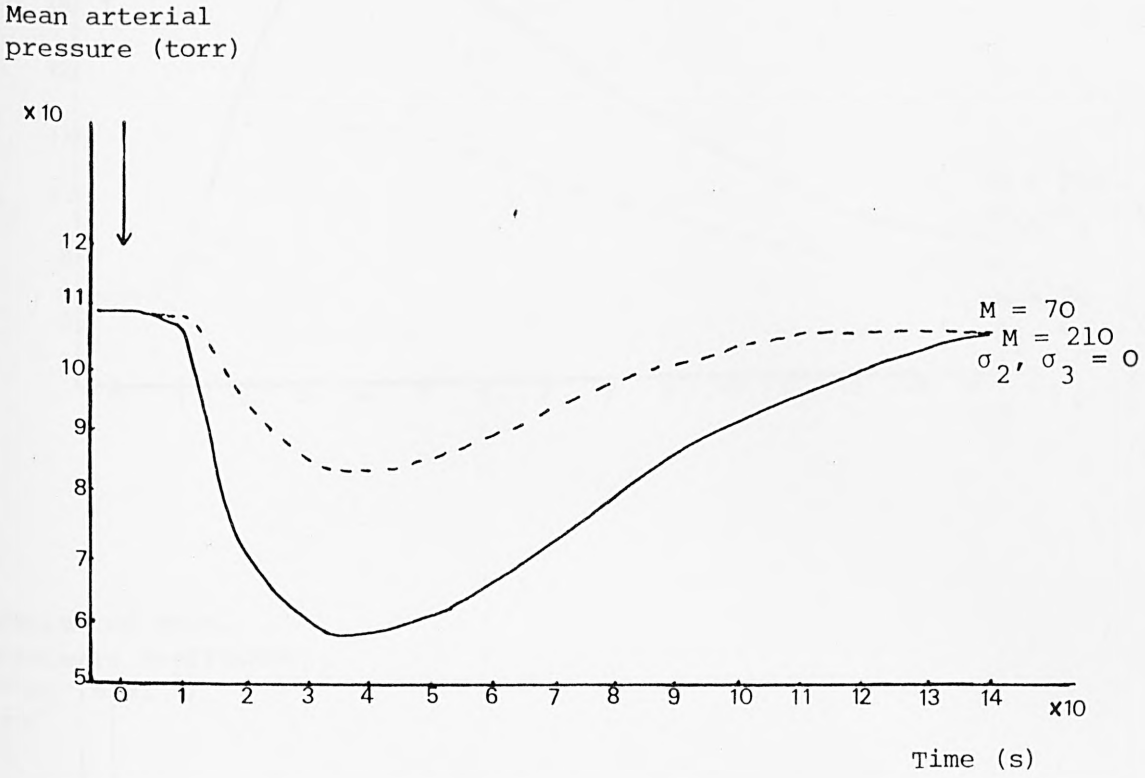

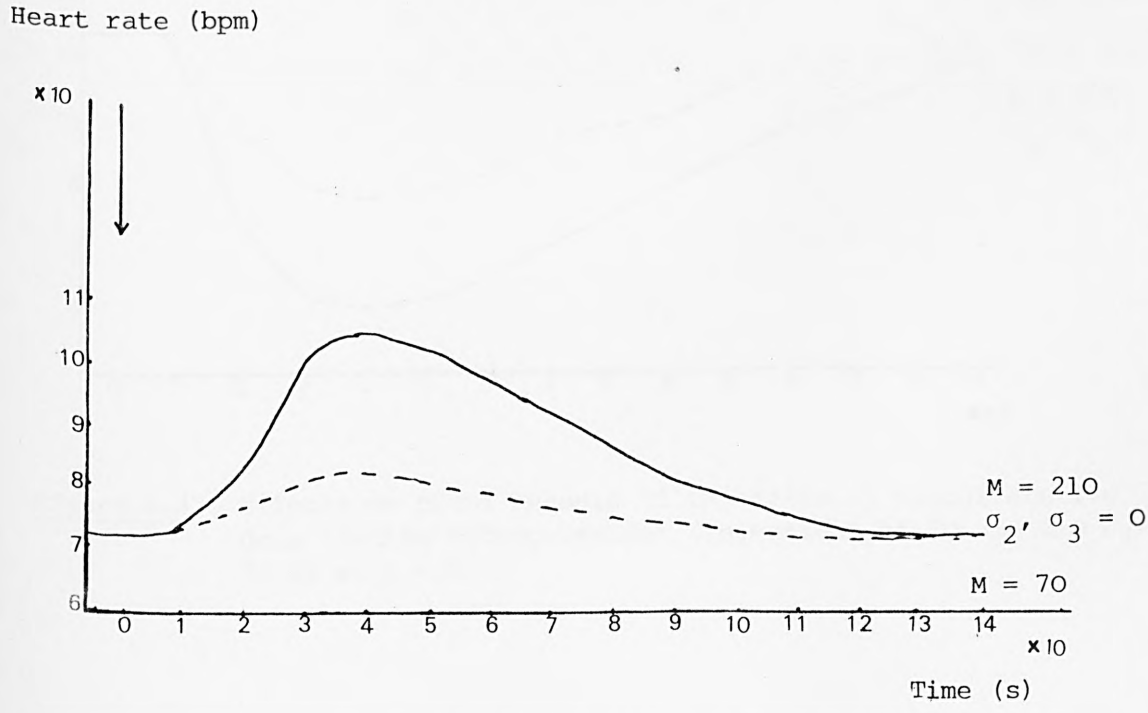

Figure 6.47 continued overleaf

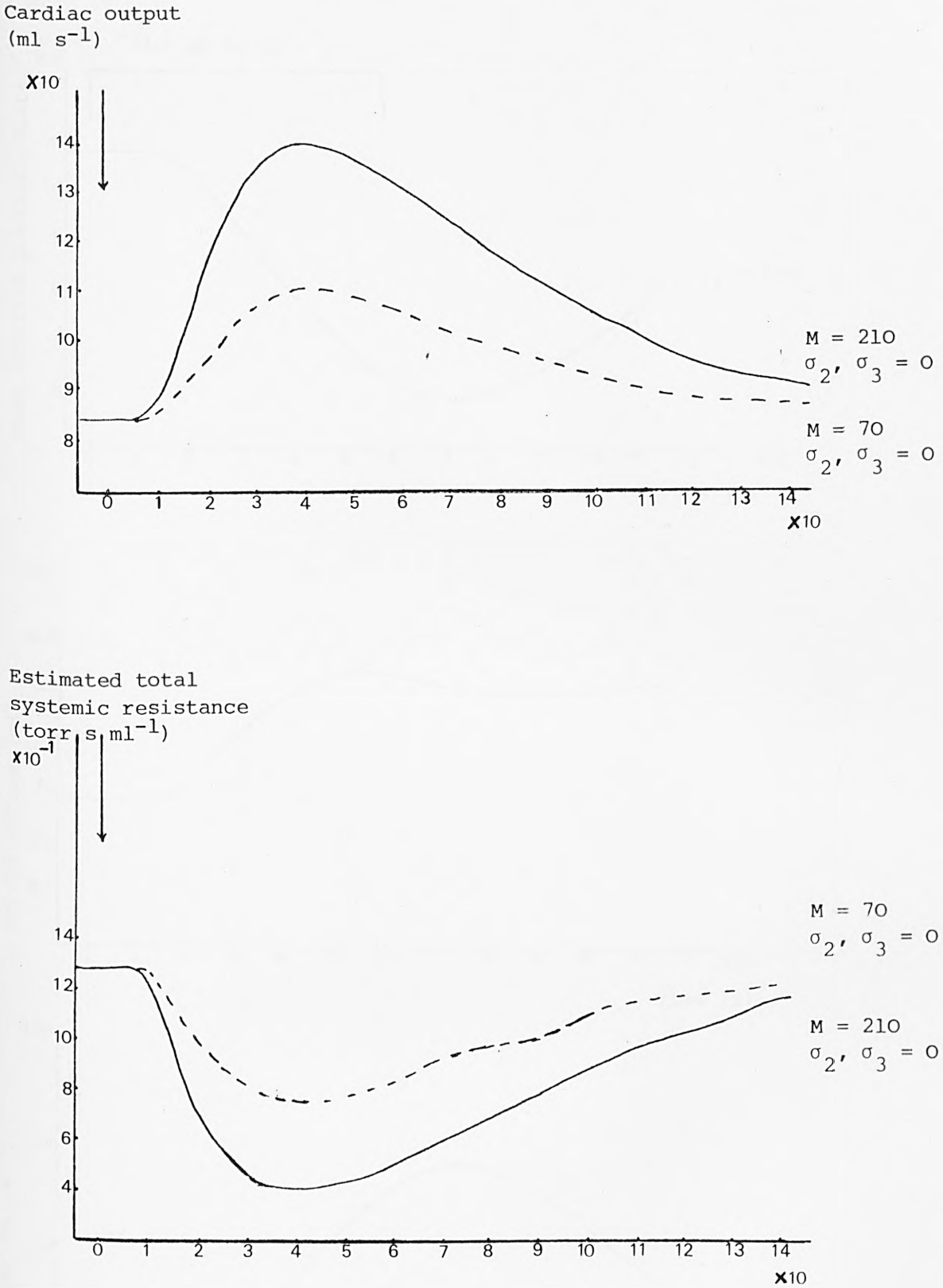

Figure 6.47 Effects on blood vessels of injection of vasodilatative drug (sodium nitroprusside) (injections of 70 and 210 µg/ 70 kg at t = 0.

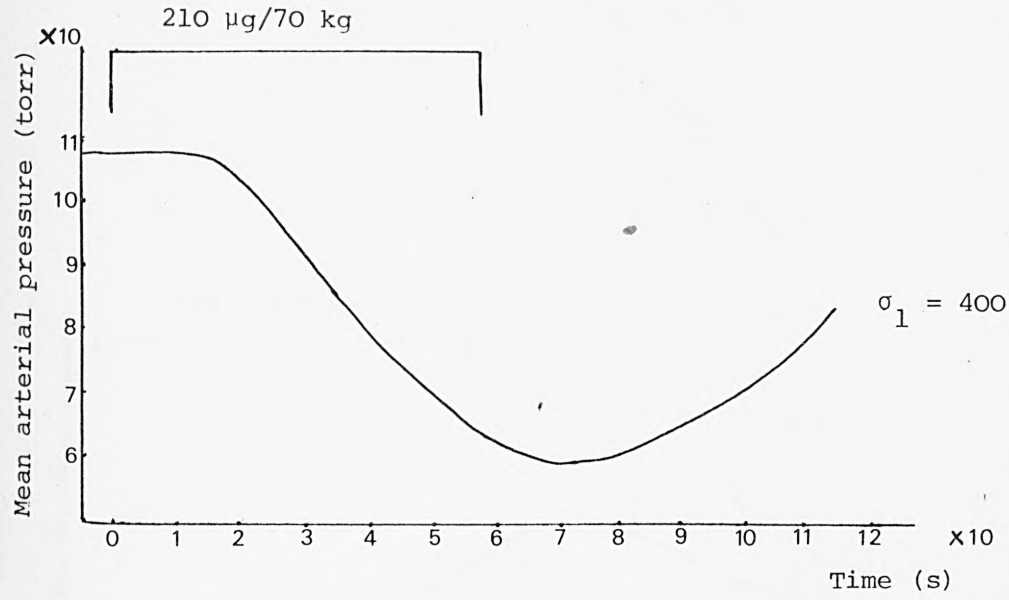

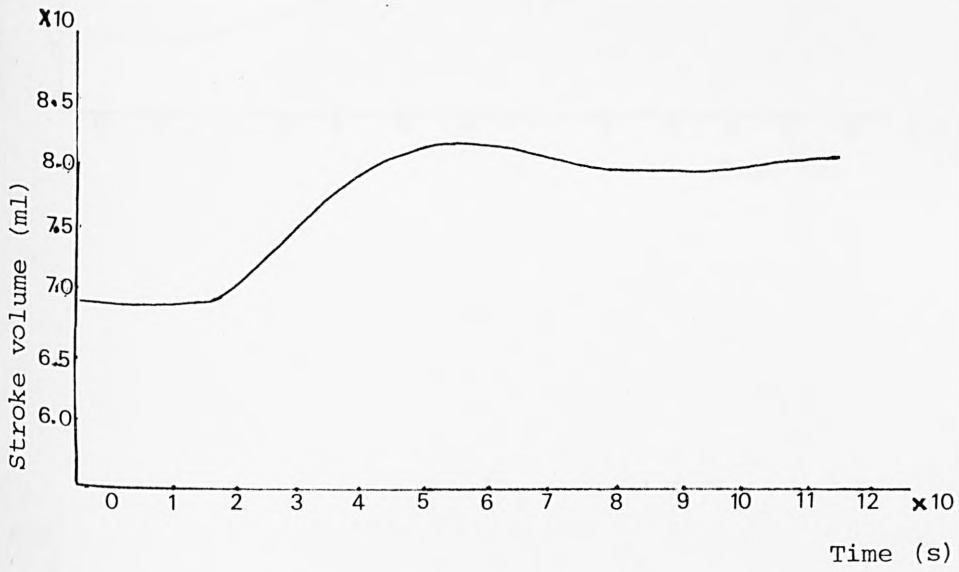

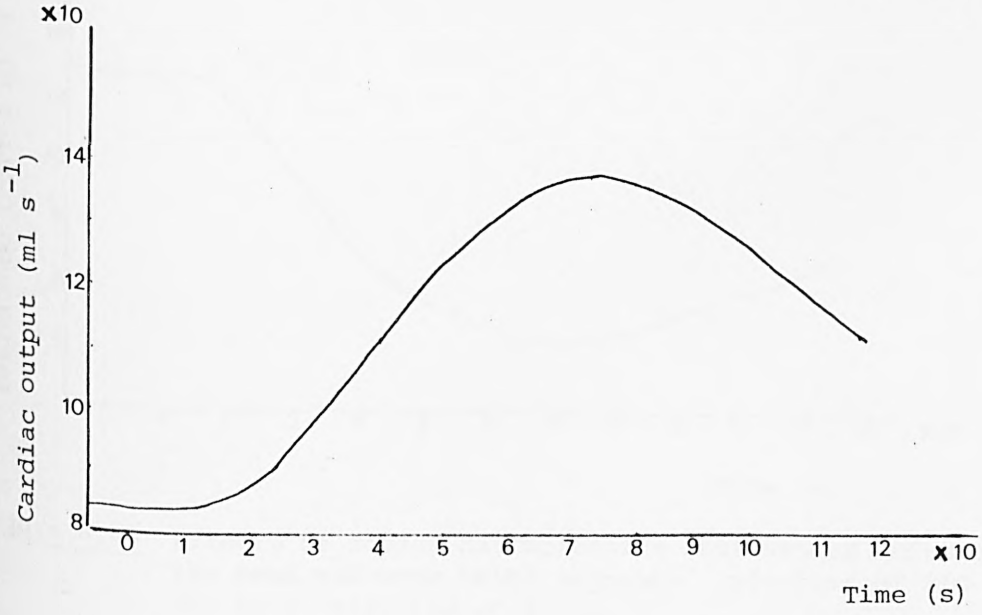

Figure 6.48 continued overleaf

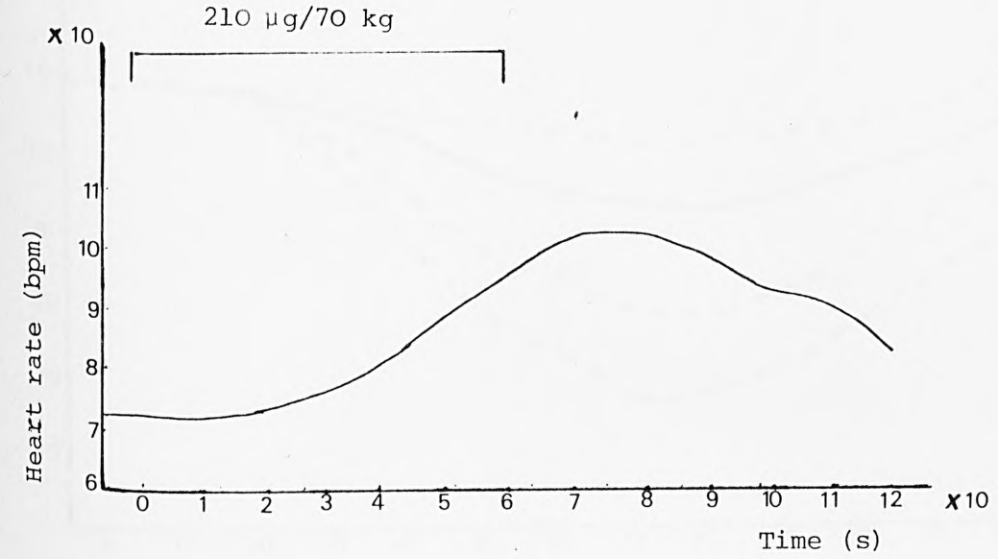

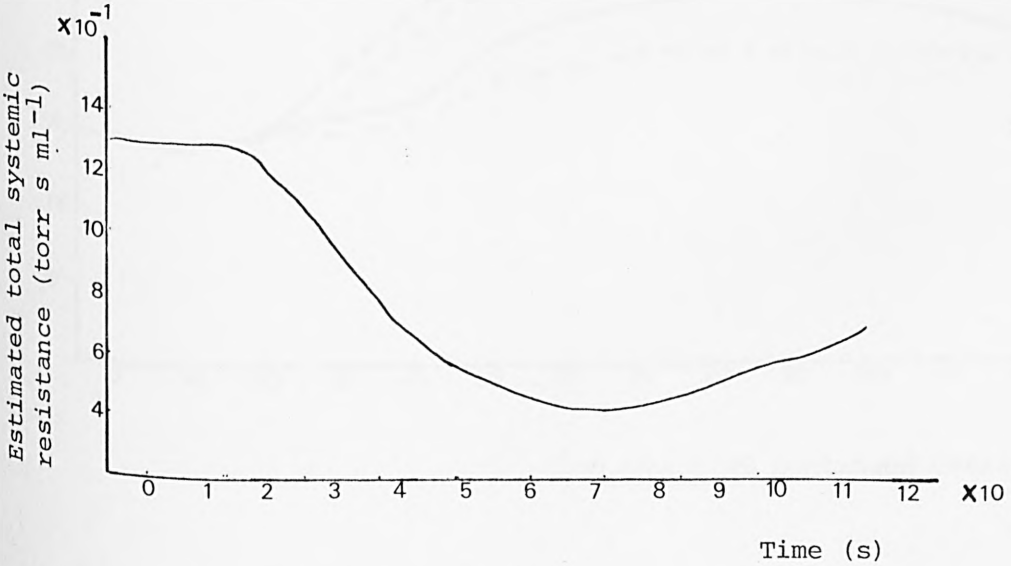

Figure 6.48 Effects of sodium nitroprusside intravenous infusion into the head and arms veins segment; injection of 210 µg/70 kg for 60 s, starting at t = 0.

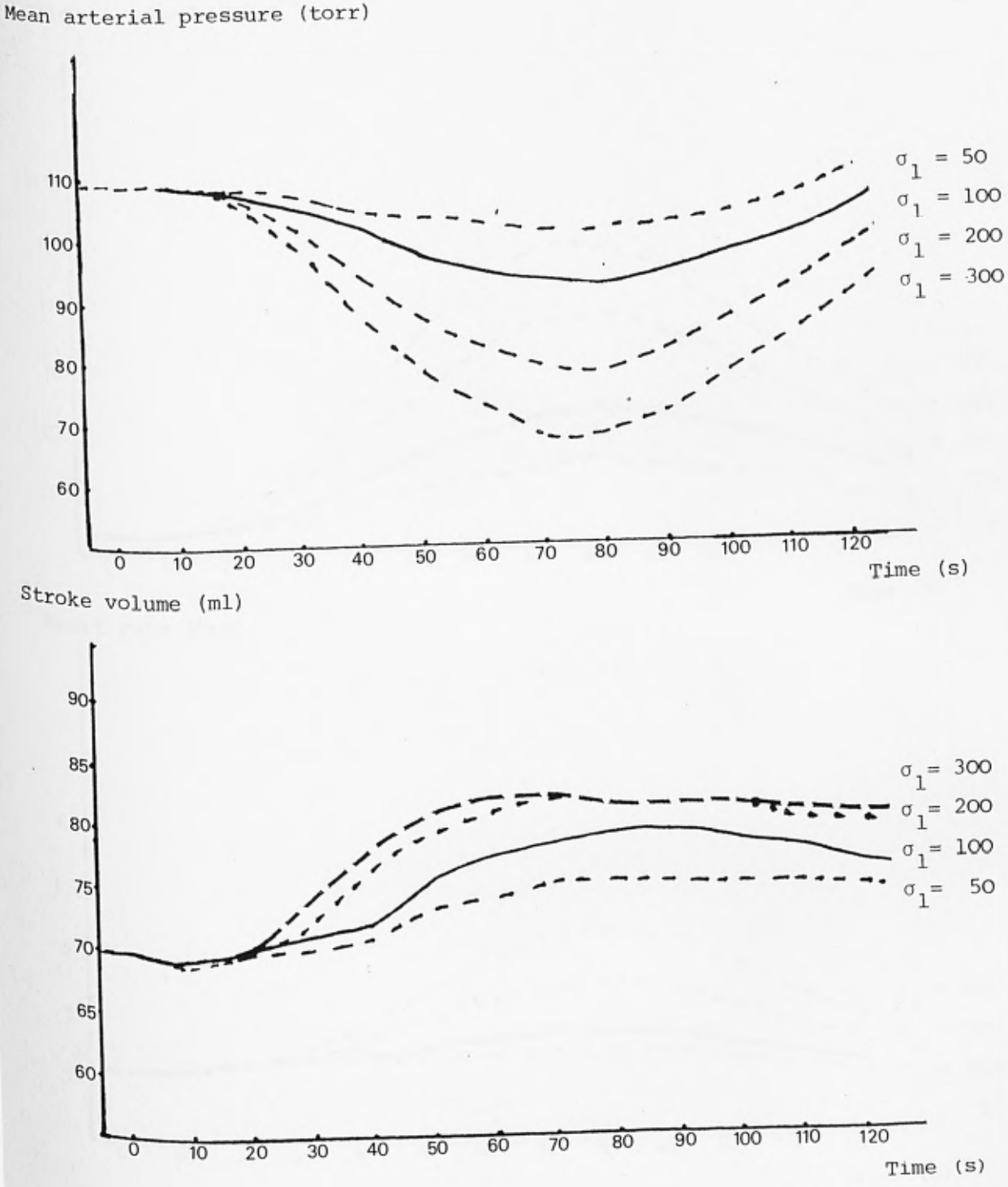

Figure 6.49 continued overleaf

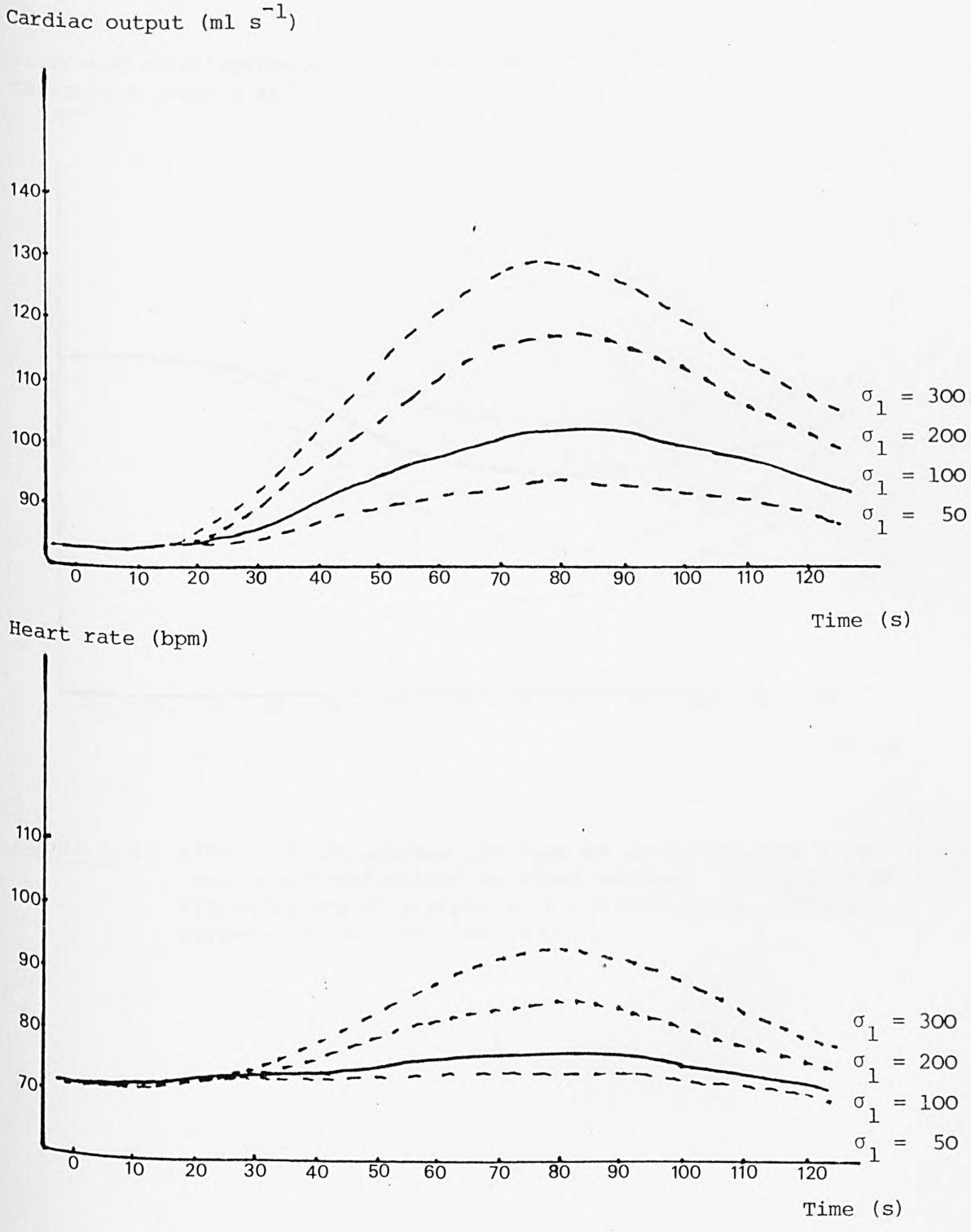

Figure 6.49 continued overleaf

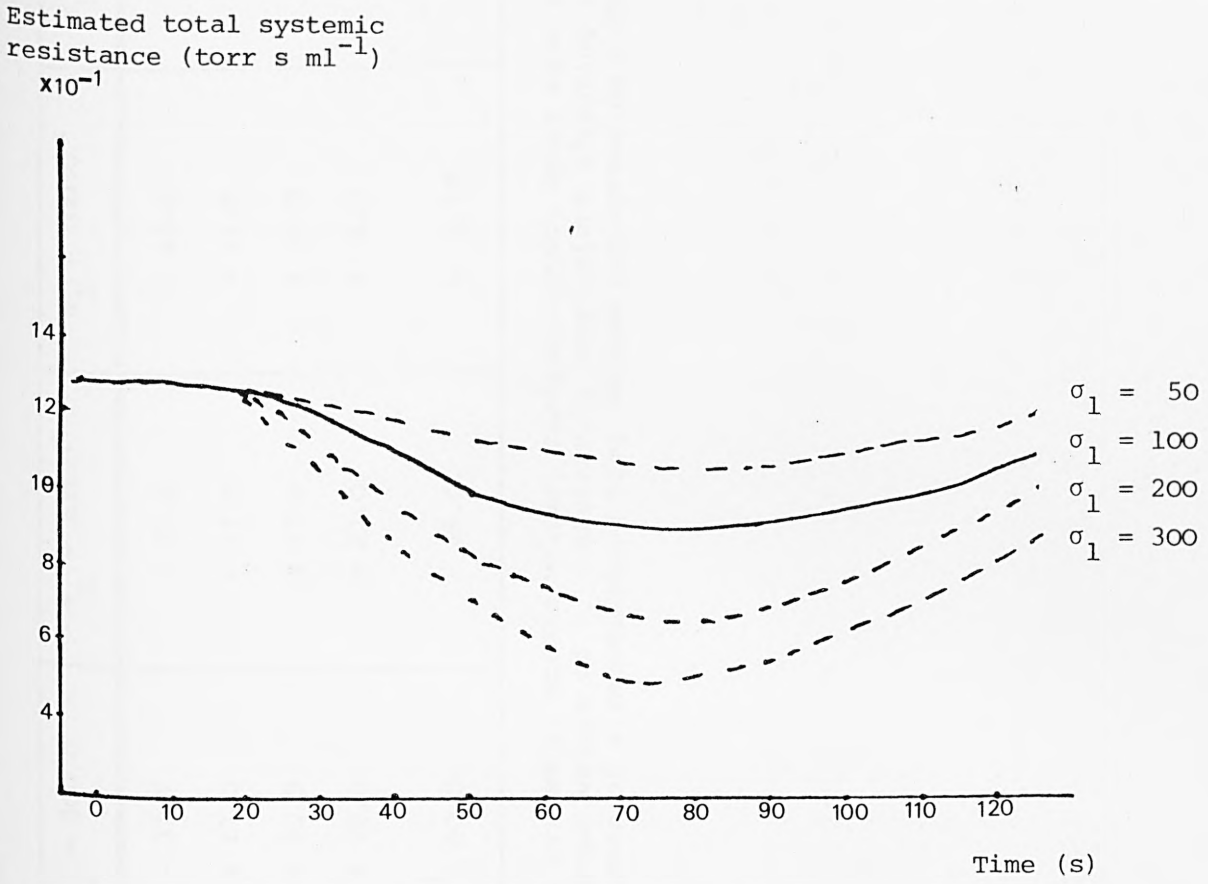

Figure 6.49 Effect of intravenous infusion of vasodilatative drug (sodium nitroprusside) on blood vessels. Injections of 210 µg/kg for 60 s start at t = 0 with given different values σ_1 = 50, 100, 200, 300.

% change in	σ_1 = 400.0	σ_1 = 300.0	σ_1 = 200.0	σ_1 = 100.0	σ_1 = 50.0
Mean arterial pressure	- 45.0	- 37.7	- 28.6	- 15.8	- 7.0
Stroke volume	+ 17.0	+ 17.0	+ 17.0	+ 12.8	+ 7.0
Cardiac output	+ 6.0	+ 50.9	+ 37.9	+ 20.0	+ 10.0
Heart rate	+ 39.0	+ 29.0	+ 17.0	+ 6.0	+ 1.9
Estimated total system resistance	- 67.0	- 60.0	- 48.0	- 0.29	- 17.0

Table 6.34 Percentage change of the mean arterial pressure, stroke volume, cardiac output, heart rate and estimated total systemic resistance due to different values of σ_1 (sensitivity coefficient affecting the peripheral resistance) following intravenous infusion of a vasodilating drug (Sodium Nitroprusside - SNP).

6.6.1.4 Vasodilatative drugs - effects on the heart and blood vessels

In contrast to sodium nitroprusside, which has its effect only on the blood vessels, isoprenaline affects both the blood vessels and the heart. Its action is to produce a relaxation of smooth muscle, for example vasodilatation, and, more important therapeutically, dilatation of the bronchioles (Lippold et al, 1979). The action of the drug on the β-receptors also brings about an increase in the force of contraction of the heart muscle and an increase in heart rate.

The co-operative interaction of these effects on blood vessels and the heart produced by isoprenaline, as a representative member of this group of vasodilatative drugs, is shown in Figure 6.50. Figure 6.51 shows the dynamics produced by the model following an injection of isoprenaline into the head and arms veins segment at time t = 0, where the local actions of isoprenaline are simulated by setting σ_1, σ_2 and σ_3 to their normal values and "switching on" vasodilatation, tachycardia and positive inotropy in the computer program. The model has been simulated for a range of dosages (50, 70, 98 and 210 µg/70 kg) due to uncertainty in the dose typically administered to patients. In his earlier study, Pullen (1976) had chosen a single dosage of 70 µg/70 kg. Over the range of dosage examined, the model produces responses due to the interaction of effects on blood vessels and heart which are in general agreement with published information (Goodman et al, 1965).

In Figure 6.52, the relationships between the main variables (mean arterial pressure, heart rate, cardiac output and estimated total systemic resistance) and the drug dosage are presented. An increase in dosage results in increases in heart rate and cardiac output, but decreases in arterial pressure, and estimated total systemic resistance due to the vasodilatation.

6.7 CONCLUSIONS

This chapter has reported studies aimed at examining the empirical validity of the complete non-linear 19-segment model of the cardiovascular system. As such it complements the results presented in the previous chapter in assessing the overall validity of the model.

The steady state of the model is consistent with results expected for a subject at the upper end of the normal range in terms of mean

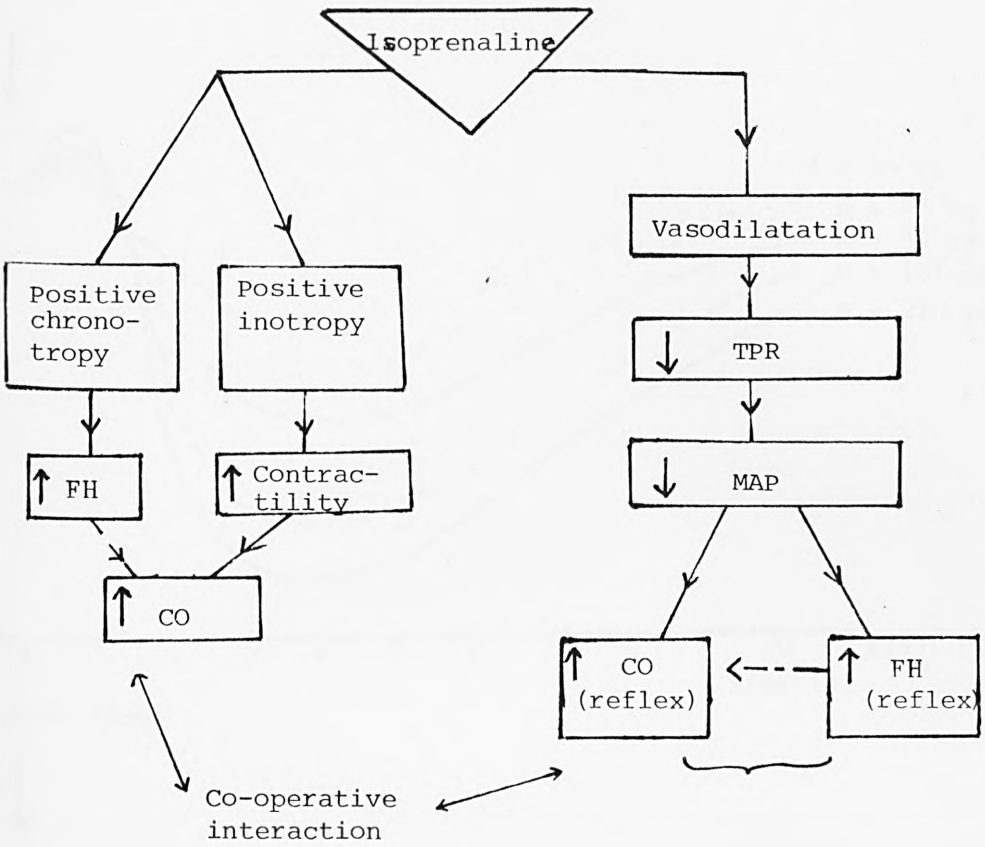

Figure 6.50 The action of isoprenaline on the heart and blood vessels. (Note: ↑ = increase; ↓ = decrease)

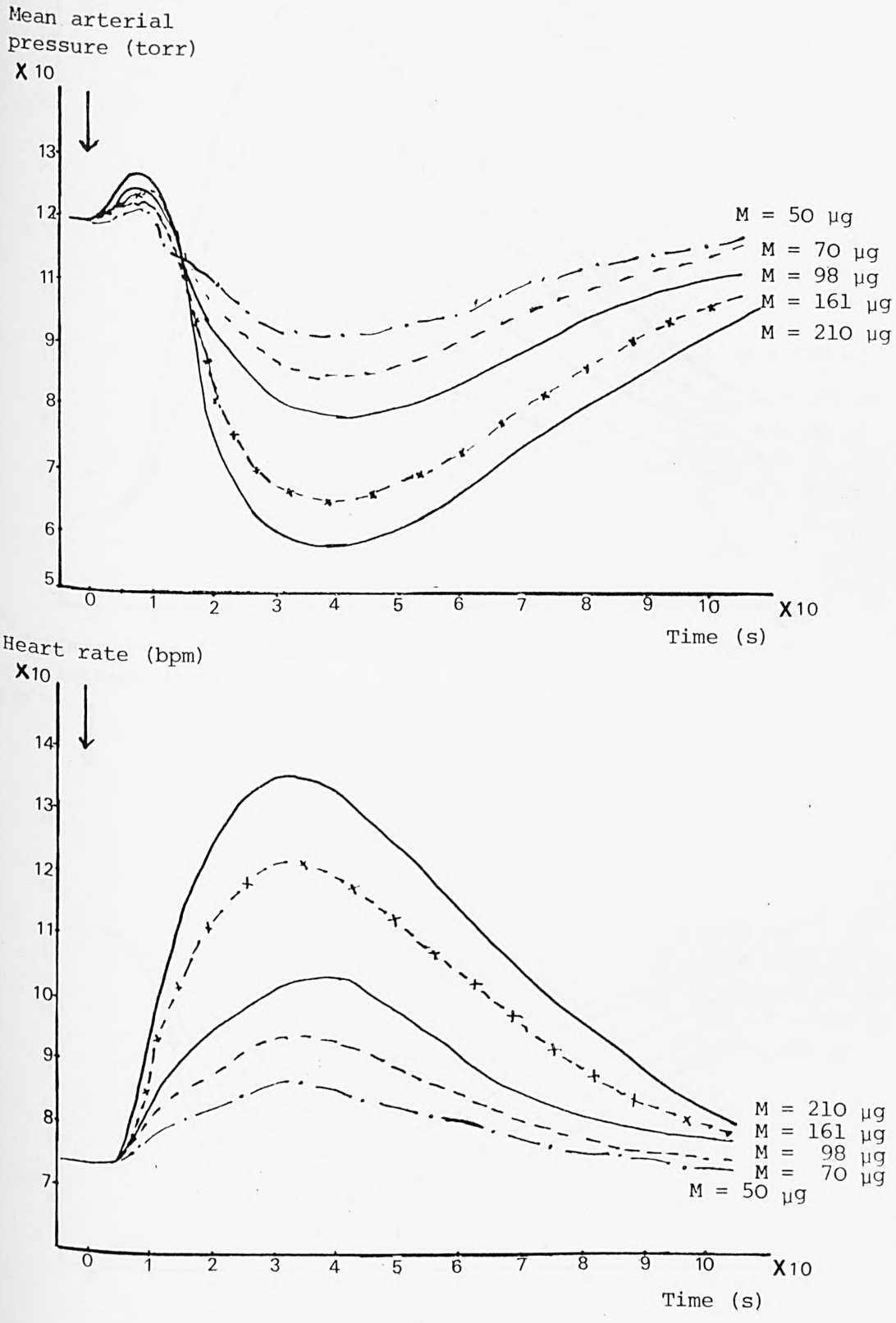

Figure 6.51 continued overleaf

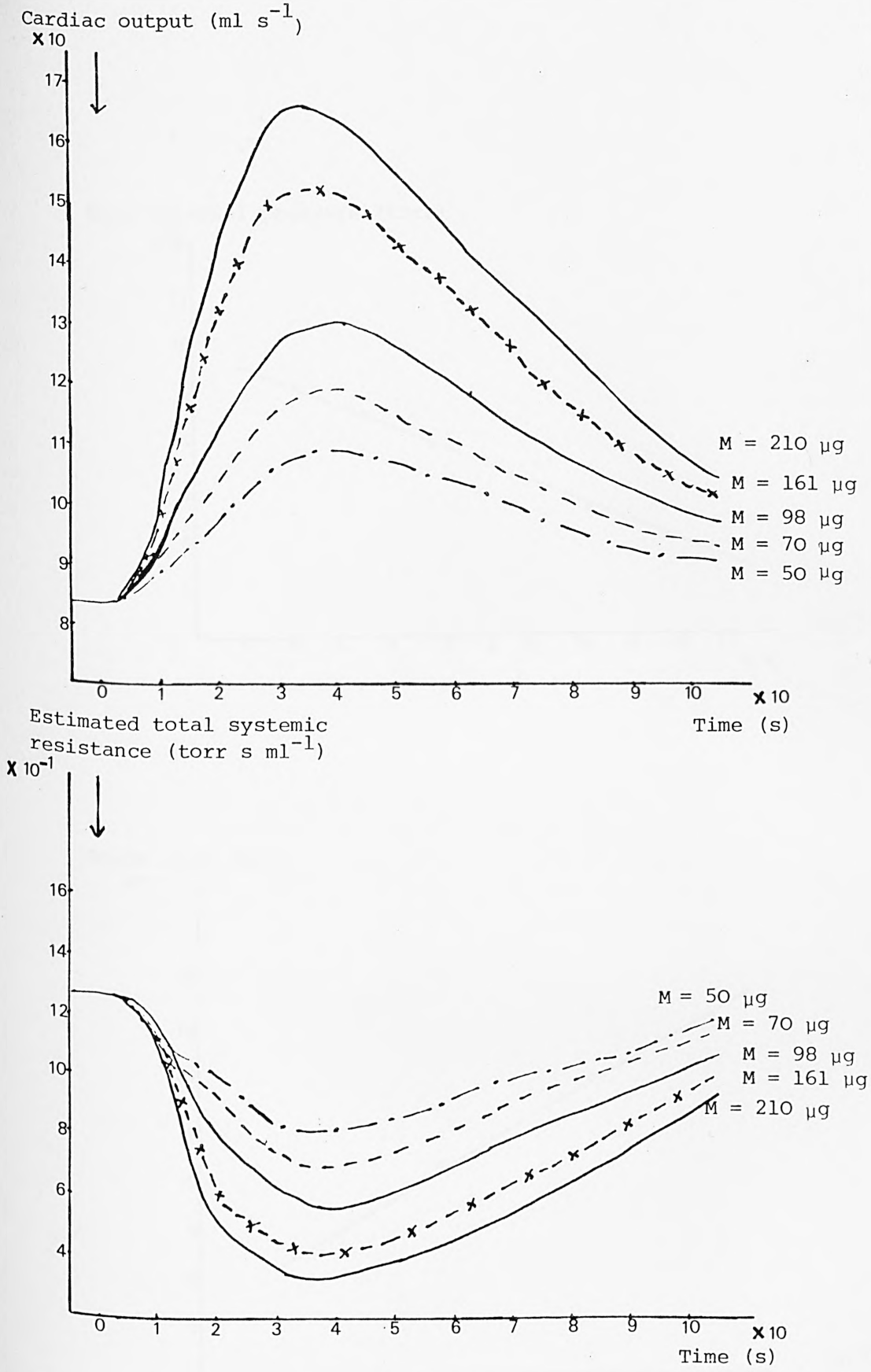

Figure 6.51 Effect on heart and blood vessels of injection of vasodilatation drug (isoprenaline) into the head and arms veins segment at t = 0 for different dosages to 70 kg body weight.

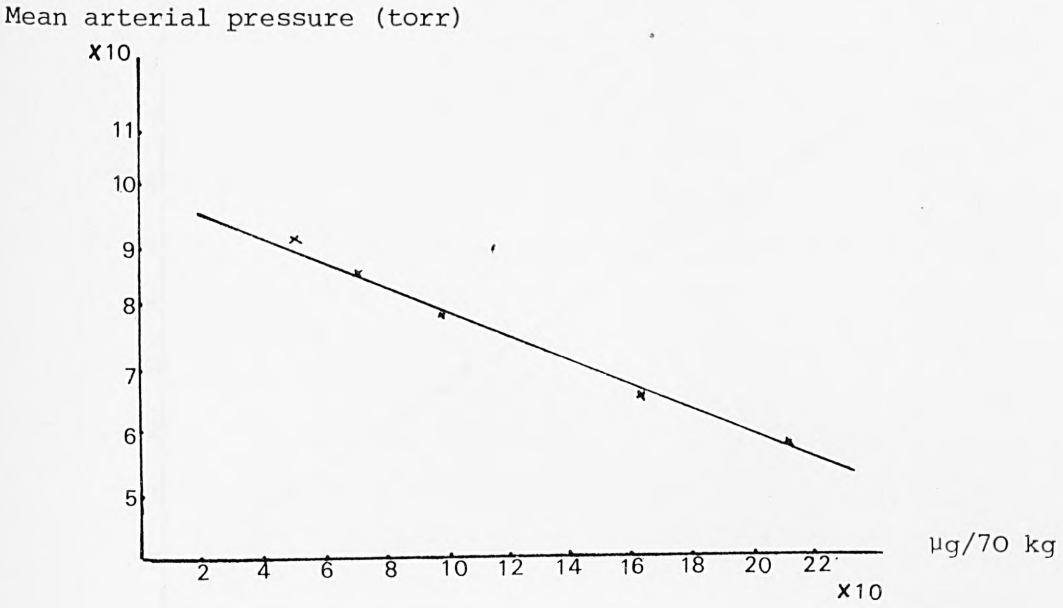

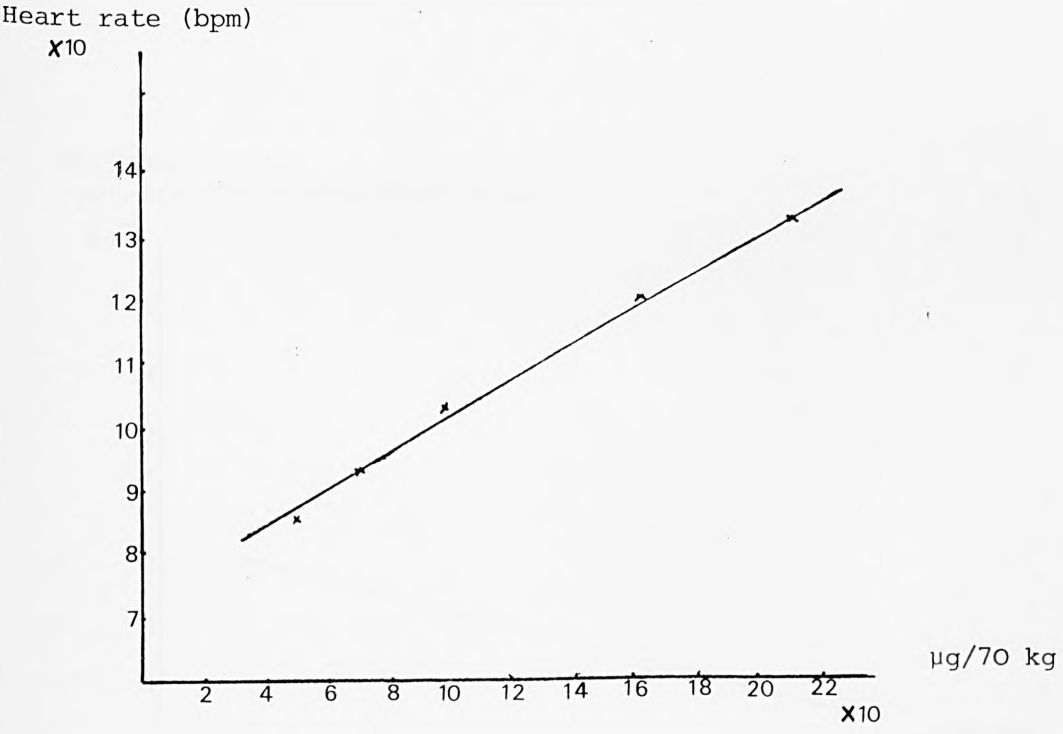

Figure 6.52 continued overleaf

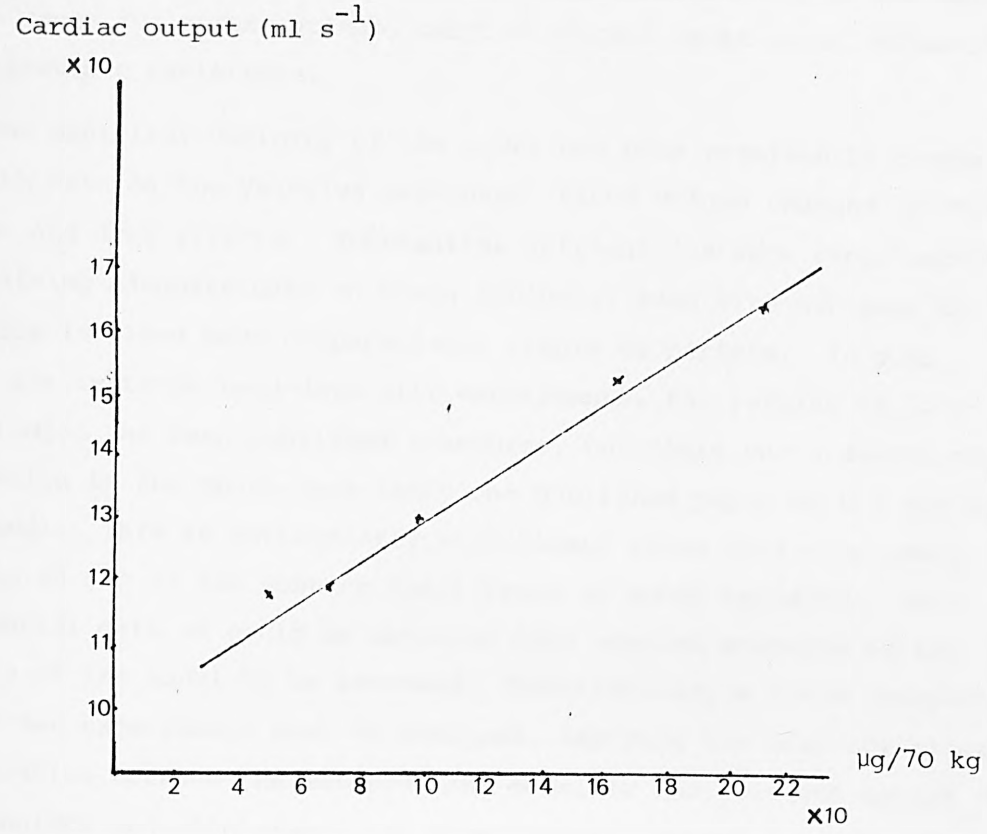

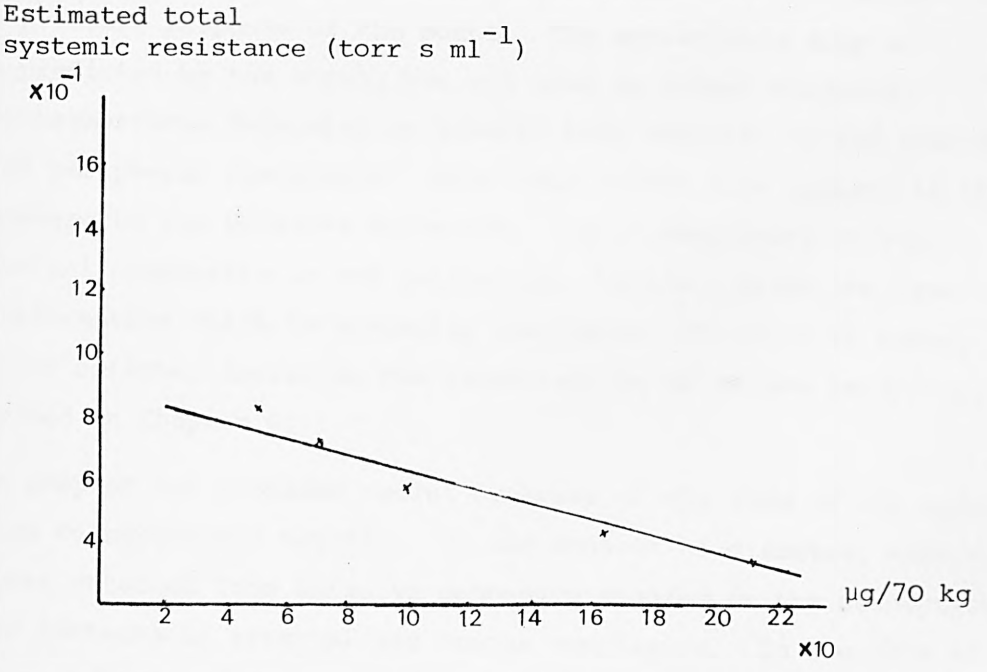

Figure 6.52 The relationship between the mean variables and the different dosages of the vasodilatative drug (isoprenaline) which affects both the heart and blood vessels 40 s after the injection at t = 0.

arterial pressure, systolic and diastolic pressures, and in the middle of the range for stroke volume, cardiac output, heart rate, estimated total systemic resistance.

The empirical validity of the model has been examined by comparison with data on the Valsalva manoeuvre, blood volume changes, postural changes and drug effects. Substantial difficulties were experienced in obtaining adequate data on human subjects, even although many of the tests involved were comparatively simple to perform. In some cases, for instance head-down tilt experiments, the results of long-term studies had been published elsewhere, but there was a dearth of information in the short-term (only one published paper on the subject was found). This is particularly significant since this experiment constituted one of the most critical tests of model validity. Such experimental data as could be obtained have enabled measures of the validity of the model to be assessed. Nevertheless, a clear conclusion is that new experiments must be designed, implying the need for close collaboration between the mathematical modeller and relevant groups of physiologists and clinicians. In this context, appropriate dynamic mathematical models serve a vital function in identifying those tests which are critical from the standpoint of model validity.

The empirical validity of the model, in relation to short-term dynamics, is supported by much of the available experimental data, although a number of defects have been highlighted as evidenced by the arterial pressure response of the model. The appreciable drop in pressure predicted by the model, but not seen in normal subjects, following haemorrhage indicates an insufficient response in the neural control of peripheral resistance. This same defect also appears in the model response to the Valsalva manoeuvre. Model deficiency in such neural control components is not unexpected, however, given the restricted information which is currently available. Attempts to remedy the observed defects, including the incorporation of volume receptors, are described in Chapter 9.

This chapter has provided useful examples of the role of the model in relation to hypothesis testing. In the context of diabetes, encouraging results were obtained from Valsalva manoeuvre studies on the assumption of altered patterns of arterial and venous compliance. In the case of the response of a trained athlete, the model provides a useful test-bed for examining the hypotheses of altered heart volume, total blood volume

and compliance. Further experimental data are needed before anything more than a preliminary judgement can be made.

The general lack of data referred to above is particularly apparent in the case of drug studies. Thus, although the model response to the drugs as described in Section 6.6 appears to be adequate in a qualitative sense, there is a general lack of hard quantitative information. Again, though, the model highlights the nature of the additional experiments which are required .

The procedures adopted and results presented in this chapter and in Chapter 5 are important ingredients of the process of model validation. The final component is that of a full-scale sensitivity analysis, examining the sensitivity of the model's responses to the assumed values of model parameters. This analysis is presented in Chapter 7.

CHAPTER 7

SENSITIVITY ANALYSIS OF THE 19-SEGMENT CARDIOVASCULAR MODEL

7.1 INTRODUCTION

In Chapter 6, the validity of the 19-segment cardiovascular system model was assessed in relation to empirical data obtained from physiological, pathological and pharmacological studies. As a further stage in testing the validity of this model, it has been subjected to a programme of sensitivity analysis which is described in this chapter. This analysis, which involves assessment of the sensitivity of the behaviour of the model to variation of the parameters, is always an important step in the validation of large theoretically unidentifiable models such as the cardiovascular model in question where the values of many of the parameters are uncertain.

This chapter briefly outlines the nature of sensitivity analysis and its particular role in assessing the validity of large physiological models such as that of the cardiovascular system. The results of applying this analysis, including the use of Monte-Carlo simulation, are presented, enabling the most uncertain parameters to be identified and their effects upon model performance to be quantified.

7.2 SENSITIVITY ANALYSIS

The techniques of sensitivity analysis permit investigation of the effects on overall model behaviour of small changes in model structure, parameters, or inputs (including initial conditions).

7.2.1 Sensitivity Coefficients and Equations

Consider the dynamic model, M:

$$\dot{\underline{x}} = f(\underline{x}, \underline{p}; \; t, \underline{u}) \qquad (7.1)$$

where $\underline{u}$ is an input vector and there are n state variables x_j, $j = 1, \ldots, n$ and m parameters p_r, $r = 1, \ldots, m$.

The dependency of state variable x_j on parameter p_r is represented by the "sensitivity coefficient" C_r^j:

$$C_r^j = \frac{dx_j}{dp_r} = C_r^j(\underline{x}, \underline{p}; t, \underline{u}) \qquad (7.2)$$

For M, there are n x m sensitivity coefficients, all time-varying. The dynamic responses of the sensitivity coefficients can be determined analytically or by simulation from the "sensitivity equations". Differentiating (7.1) with respect to p_r, and the j^{th} state variable, x_j, gives:

$$\frac{d}{dp_r}\left(\frac{dx_j}{dt}\right) = \frac{d}{dp_r}\left(f_j(\underline{x}, \underline{p})\right)$$

Therefore

$$\dot{C}_r^j = \frac{df_j(\underline{x}, \underline{p})}{dp_r} + \sum_{i=1}^{n} C_r^i \frac{\partial f_j(\underline{x}, \underline{p})}{\partial x_i} \qquad (7.3)$$

In total, there are n x m sensitivity equations whose solution requires the prior solution of (7.1) for x(t). Further details of this classical approach to sensitivity analysis are contained in Tomović (1963). In practice,the sensitivity equations can be solved analytically for linear models, and by numerical integration for some small non-linear models. However, for complex non-linear models, such as that of the cardiovascular system, the determination of the dynamic sensitivity coefficients is intractable by this method. This can be seen clearly by considering one of the 19 segments of the cardiovascular model described in Chapter 3, say the right atrium.

Example

This segment is shown in Figure 7.1 and rewriting in Section 3.2.2 defines the rate of change of the volume of this segment as:

$$\frac{dV_{RA}}{dt} = F_1 - F_{RARV}, \quad V_{RA} \geq 0 \qquad (7.4)$$

where F_{RARV} is the flow from right atrium to right ventricle and F_1 is given by

$$F_1 = F_{SVCRA} + F_{IVCRA} + F_{BRONC} + F_{COR} \qquad (7.5)$$

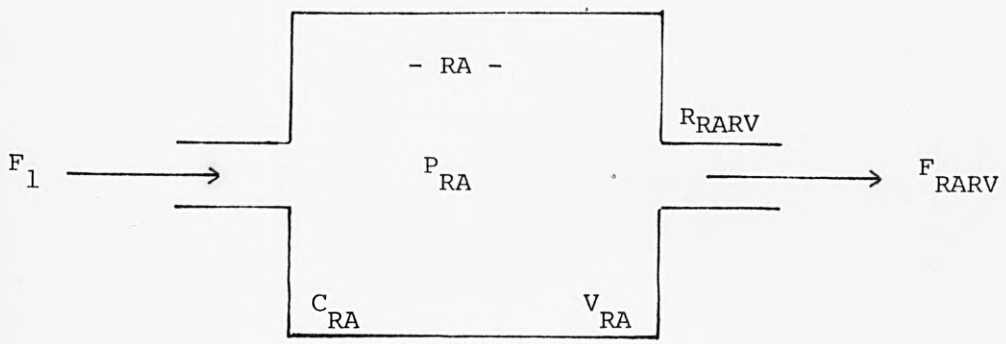

Figure 7.1 The right atrium segment.

$$F_{RARV} = \begin{cases} F_2 , & F_2 > 0 \\ 0 , & F_2 \leq 0 \end{cases} \tag{7.6}$$

where

$$F_2 = \frac{P_{RA} - R_{RV}}{R_{RARV}} \tag{7.7}$$

Differentiating (7.4) with respect to any parameter p yields

$$\frac{d^2 V_{RA}}{dt\ dp} = \frac{dF_1}{dp} - \frac{dF_{RARV}}{dp} \tag{7.8}$$

Replacing $\frac{dV_{RA}}{dp}$ by the sensitivity coefficient C,

$$\dot{C} = \frac{dF_1}{dp} - \frac{dF_{RARV}}{dp} \tag{7.9}$$

Substituting for F_1 and F_{RARV} in (7.9) using (7.5) - (7.7):

$$\dot{C} = \frac{d}{dp}\left[F_{SVCRA} + F_{IVCRA} + F_{BRONC} + F_{COR}\right] - \frac{d}{dp}\left[\frac{P_{RA} - P_{RV}}{R_{RARV}}\right] \tag{7.10}$$

Further substitution can be carried out using the relations defined in Chapter 3 which are re-stated below:

$$F_{SVCRA} = K_5 F_{10} \tag{7.11}$$

$$F_{IVCRA} = K_5 F_9 \tag{7.12}$$

$$F_{BRONC} = \frac{P_{AO3} - P_{RA} - G_{AO3RA}}{R_{BRONC} \cdot q_4 \cdot \sigma_{BRONC}} \tag{7.13}$$

$$F_{COR} = \frac{P_{AO1} - P_{RA}}{R_{COR}} \tag{7.14}$$

$$P_{RA} = a_{RA}\left(V_{RA} - V_{uRA}\right) \tag{7.15}$$

$$P_{RV} = a_{RV}\left(V_{RV} - V_{uRV}\right) \tag{7.16}$$

Equation (7.10) thus becomes:

$$\dot{C} = K_5 \frac{dF_{10}}{dp} + K_5 \frac{dF_9}{dp} + \frac{d}{dp}\frac{\left[P_{AO3} - P_{RA} - G_{AO3RA}\right]}{R_{BRONC}.q_4.\sigma_{BRONC}} + \frac{d}{dp}\frac{\left[P_{AO1} - P_{RA}\right]}{R_{COR}}$$

$$- \frac{d}{dp}\left[\frac{a_{RV}\left(V_{RA} - V_{uRA}\right)}{R_{RARV}}\right] + \frac{d}{dp}\left[\frac{a_{RV}\left(V_{RV} - V_{uRV}\right)}{R_{RARV}}\right] \qquad (7.17)$$

The complexity of (7.17) serves to emphasize the practical difficulty which would arise in applying this approach to the complete 19-segment cardiovascular model with its 178 parameters.

7.2.2 Perturbation Method

An alternative, yet simple, method is to obtain the approximate sensitivity coefficients by perturbing each parameter p_r by a small amount Δp_r:

$$C_r^j = \frac{\Delta x_j(t)}{\Delta p_r}, \text{ where } \Delta x_j(t) = x_j(p_r + \Delta p_r, t) - x_j(p_r, t) \qquad (7.18)$$

The place of perturbation methods within the spectrum of approaches available for the determination of sensitivity coefficients can be seen in the classification shown in Figure 7.2.

Sensitivity analysis varies the parameters sequentially out along the axes of parameter space from their nominal position. It, therefore, leaves many directions uncovered. In Monte-Carlo simulations all the parameters are varied randomly in an attempt to cover more regions of the parameter space surrounding the nominal value.

7.2.3 Monte-Carlo Simulation

In Monte-Carlo simulation, the model is simulated a large number of times with a different set of model parameters (or initial conditions, inputs, etc.) each time. The values of the parameters are given by:

$$p_r = p_{r_o} + \Delta p_r(k) \qquad r = 1, \ldots, m$$

where $\Delta p_r(k)$ is the random value of a variation for the k^{th} simulation

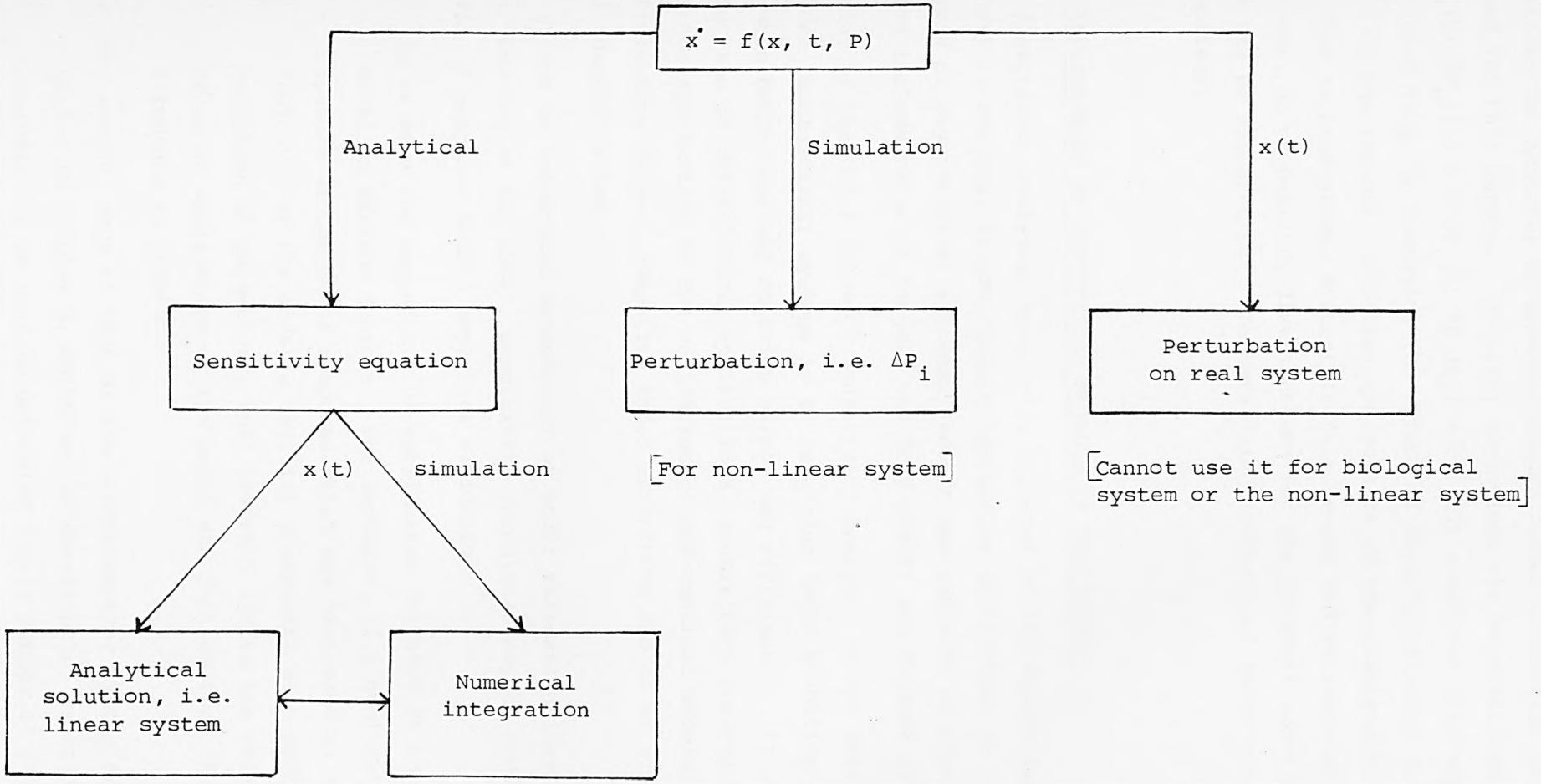

Figure 7.2 Classification of methods to determine the sensitivity coefficient, where x is a variable, P is a parameter, and t is time.

drawn from a probability distribution. On most computers there are facilities for interval or gaussian random number generation which can be used for this purpose. Usually, variations are uncorrelated (i.e. $E\{\Delta\beta_r(k).\Delta\beta_r(\ell)\} = E\{\Delta\beta_r(k).\Delta\beta_s(k)\} = 0$), but sometimes they may be correlated (e.g. in assessing the effect of correlated noise disturbances on the inputs). Finally, the results of the simulations can be presented as histograms, statistics (e.g. means and variance-covariance matrices), or probability distributions for the relevant model variables. These may be compared with the data using statistical techniques if appropriate.

7.3 APPLICATIONS OF SENSITIVITY METHODS IN PHYSIOLOGY

Sensitivity analysis, originally employed in the design and analysis of physical systems, is now finding increasing application in the analysis of physiological systems. Recent applications to physiological systems include those of Bendall and Gray (1978) and Bogumil (1980).

One of the chief roles of sensitivity analysis in the design of physical (engineering) systems is in assessing their stability in order that when built they may function safely and efficiently. In contrast, in the case of physiological applications, sensitivity analysis finds its major application in the validation of mathematical models, in discriminating between competing model structures and as an aid to model identification.

Within an integrated methodology of model validation (Leaning, 1980; Leaning et al, 1982), sensitivity techniques may be used for a variety of purposes within empirical validation:

(i) To examine the dependency of qualitative features of the model on various factors. For instance, if a qualitative feature of the model response which has been used as an indicator of the model's validity disappears with slight variation of parameters, this severely limits the valid range of application of the model and implies that the structure is invalid.

(ii) For models, such as that of the cardiovascular system described in Chapter 3, which are unidentifiable, sensitivity analysis can be used to determine likely ranges of parameter uncertainty.

(iii) To trace through uncertainties in initial conditions, inputs, structure, and model parameters on to the overall response of the model. The range of model responses can then be re-tested to see if they satisfy empirical validation criteria (e.g. feature or time series comparisons),

(iv) To determine a parameter sensitivity matrix to generate new search directions in parameter space for model parameter estimation.

(v) To determine optimal variables and times for measurement points in order to estimate a certain parameter (i.e. experimental design).

The role of sensitivity analysis in validating the large-scale model of the cardiovascular system is described in the following section.

7.4 SENSITIVITY ANALYSIS OF THE 19-SEGMENT CARDIOVASCULAR SYSTEM MODEL

Section 7.2.1 showed the difficulties with using the sensitivity equation method for this complex nonlinear cardiovascular model. Hence, other methods must be adopted to study the sensitivity of this model.

7.4.1 Dynamic Coefficient Approach to Sensitivity Analysis

The technique employed on the 19-segment cardiovascular model involved perturbing the parameters of the model within a limited range (see Section 7.4.3) and examining the resulting response of the model. The sensitivity of the model can then be described in terms of one of the following measures:

(i) Dynamic coefficient $= \frac{\Delta x}{x} = \frac{x' - x}{x}$ which is a function of time, where x is the normal value of the variable in question, and x' is the new value of this variable after the parameter p has been changed by an incremental value, Δp.

(ii) Sensitivity coefficient $= \frac{\Delta x}{\Delta p} \simeq \frac{dx}{dp}$ if Δp is small.

(iii) Relative sensitivity coefficient $= \frac{\Delta x/x}{\Delta p/p}$.

7.4.2 Application of the Dynamic Coefficient Approach to the 19-segment Cardiovascular Model

The dynamic coefficient approach can be employed in the sensitivity analysis of the model, for example, if x is one of the variables such as the mean arterial pressure (MAP) or the cardiac output (CO).

The dynamic coefficients for the variables x_1, x_2, x_3 would thus be given by $\frac{x_1' - x_1}{x_1}$, $\frac{x_2' - x_2}{x_2}$ and $\frac{x_3' - x_3}{x_3}$.

If the variable is the mean arterial pressure, x = MAP, x' = MAP', then the dynamic coefficient is $\frac{MAP' - MAP}{MAP}$.

During the Valsalva manoeuvre, for example, $\frac{\Delta x}{x}$ varies.

The dynamic coefficients for MAP and CO corresponding to a 10% variation in R_{RARV} are shown in Figure 7.3. From this it can be seen that the sensitivity varies over the duration of the Valsalva manoeuvre with peaks in the responses indicating times at which the dynamic coefficients have locally maximum values. Difficulty arises in interpreting such responses physiologically (Bushman, 1980) and therefore this approach has not been developed further.

7.4.3 Perturbation Approach to Sensitivity Analysis of the 19-segment Cardiovascular Model

The approach which was therefore adopted was that of examining the response of the model following parameter perturbation, as has already been outlined in Section 7.2.2. Each parameter was varied within a limited range. This range was chosen such as to yield the range of values of physiological variables seen in a population of normal individuals. The parameters were varied one at a time.

An example of this approach as applied to the analysis of a pharmacokinetic system appears in Bendall and Gray (1978). The effect of perturbation of a single parameter on the time response of the percentage of the drug absorbed, assuming a second-order model of pharmacokinetics, is shown in Figure 7.4.

Each parameter, however, should be thought of as a random quantity whose expectation appears in the equation of the model but whose exact value fluctuates in some random manner (Gold, 1977).

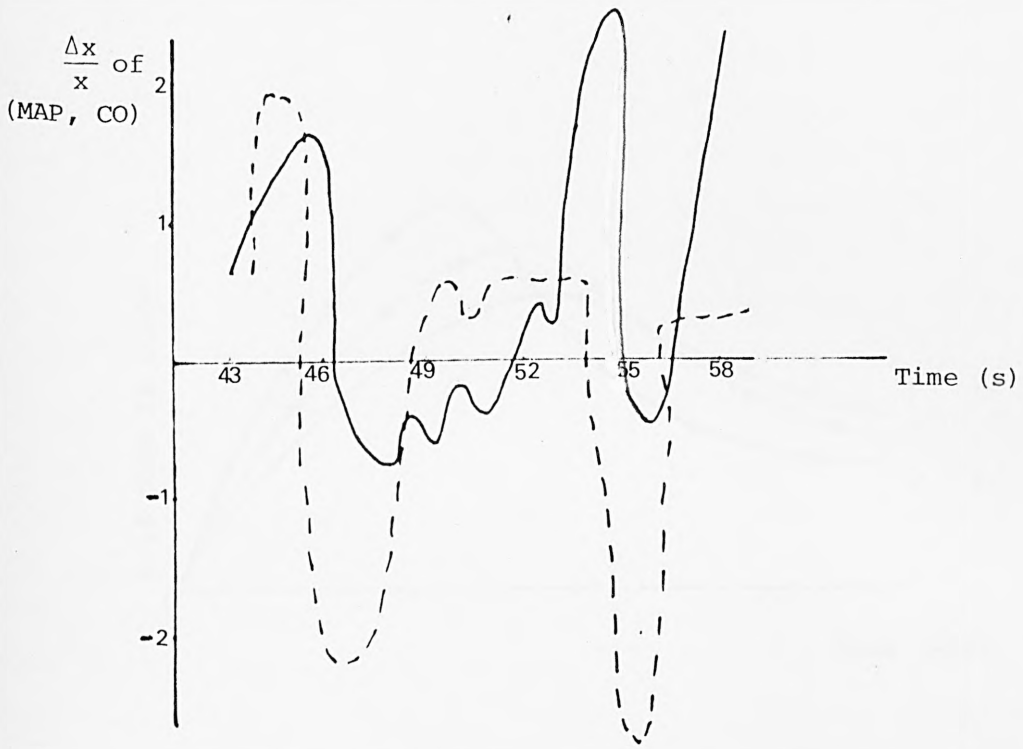

Figure 7.3 Plot of the dynamic coefficients of mean arterial pressure (MAP) (straight line) and cardiac output (CO) (dotted line) against time, by changing the parameter (R_{RARV}) 10% during the Valsalva manoeuvre simulation.

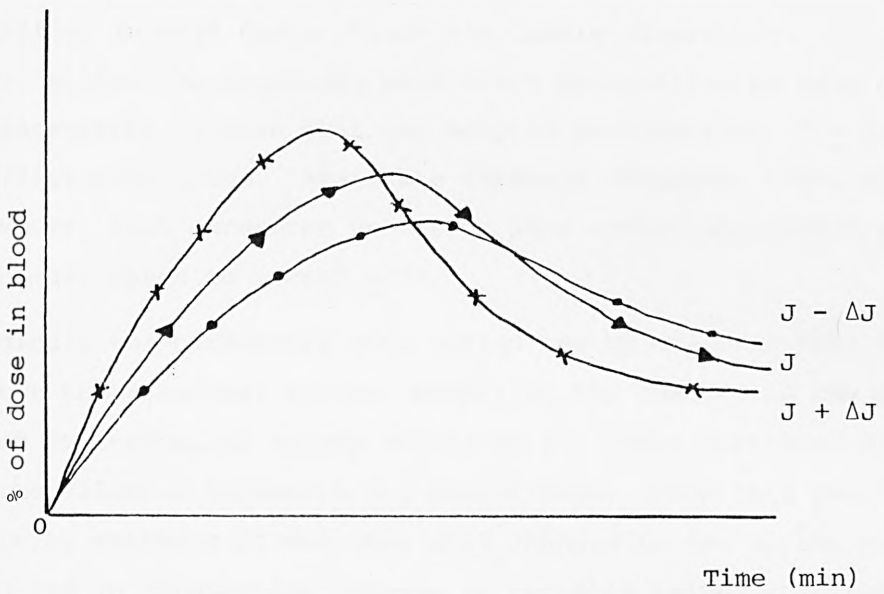

Figure 7.4 Graph showing the deviations of the response of a second-order system resulting from perturbation of a parameter (J) about its mean value.
(Normal value, J = ▲; J + ΔJ = + ; J - ΔJ = •)
(Bendall and Gray, 1978)

The investigation commenced by varying the 178 parameters by a nominal $\pm$ 10% about their mean values, and examining the effect of this perturbation on seven representative variables during a number of physiological tests. These were mean arterial pressure (MAP), stroke volume (SV), cardiac output (CO), estimated total systemic resistance (ETSR), heart rate (FH), and systolic and diastolic pressures (PMAX, PMIN), being measured in the steady state and during the Valsalva manoeuvre, and during orthostasis.

In response to variation by $\pm$ 10%, whilst for a few of the parameters there were significant changes in the steady state values of these variables, in most cases change was barely detectable. This implied that either the responses were truly insensitive to many of the model parameters or else that the adopted perturbation of $\pm$ 10% was not sufficiently large. Available evidence (Bushman, 1980) suggested, however, that parameter variation in a normal population was unlikely in most cases to exceed $\pm$15%.

Accordingly the parameters were varied one by one over this range of $\pm$15% about their nominal values, examining the changes in the pre-stimulus and post-stimulus steady states of the seven variables listed above for the Valsalva manoeuvre and haemorrhage. From this phase of the sensitivity analysis it was seen that changes in ten of the parameters resulted in substantial changes in variable values together with marginal effects in the case of a number of the other parameters. The ten critically sensitive parameters from the full set of 178 are listed in Table 7.1.

Since the true values of these ten parameters are not known, model responses with them varied one at a time by $\pm$30% and $\pm$50% about nominal values were examined. These more extreme parameter perturbations would probably correspond to pathological conditions. A representative set of results (from the total of 1260 sets of model responses) is shown in Figures 7.5 - 7.7.

The effects on model response of varying all the parameters representing the lengths of veins and arteries within the circulatory system together by $\pm$15% were also examined. This study was carried out on simulations of the Valsalva manoeuvre and haemorrhage in terms of pre- and post-stimulus steady state values of the seven variables, as specified above. In each case the results obtained were essentially insensitive to these parameter perturbations.

Parameter in computer program	Parameter in mathematical model	Nominal value	Interpretation
p(7)	P_{THN}	-4.0 torr	Normal thoracic pressure
p(29)	a_{RAS}	0.15 torr ml^{-1}	Elastance value of the right atrium during systole
p(30)	a_{RAD}	0.05 torr ml^{-1}	Elastance value of the right atrium during diastole
p(31)	V_{URA}	30.0 ml	Unstressed volume of the right atrium
p(32)	R_{RARV}	0.003 torr s ml^{-1}	Resistance of the fully opened tricuspid valve
p(34)	a_{RVS}	0.3 torr ml^{-1}	Elastance value of right ventricle during systole
p(45)	V_{UPV}	460.0 ml	Unstressed volume of the pulmonary veins
p(53)	a_{LVS}	1.5 torr ml^{-1}	Elastance value of the left ventricle during systole
p(133)	K_{16}	0.7	Constant controlling the relative contribution of the aortic arch and carotid sinus baroreceptors to the overall central nervous input function (B)
p(137)	K_{18}	80.0	Threshold constant in neural control model

Table 7.1 The ten most sensitive model parameters

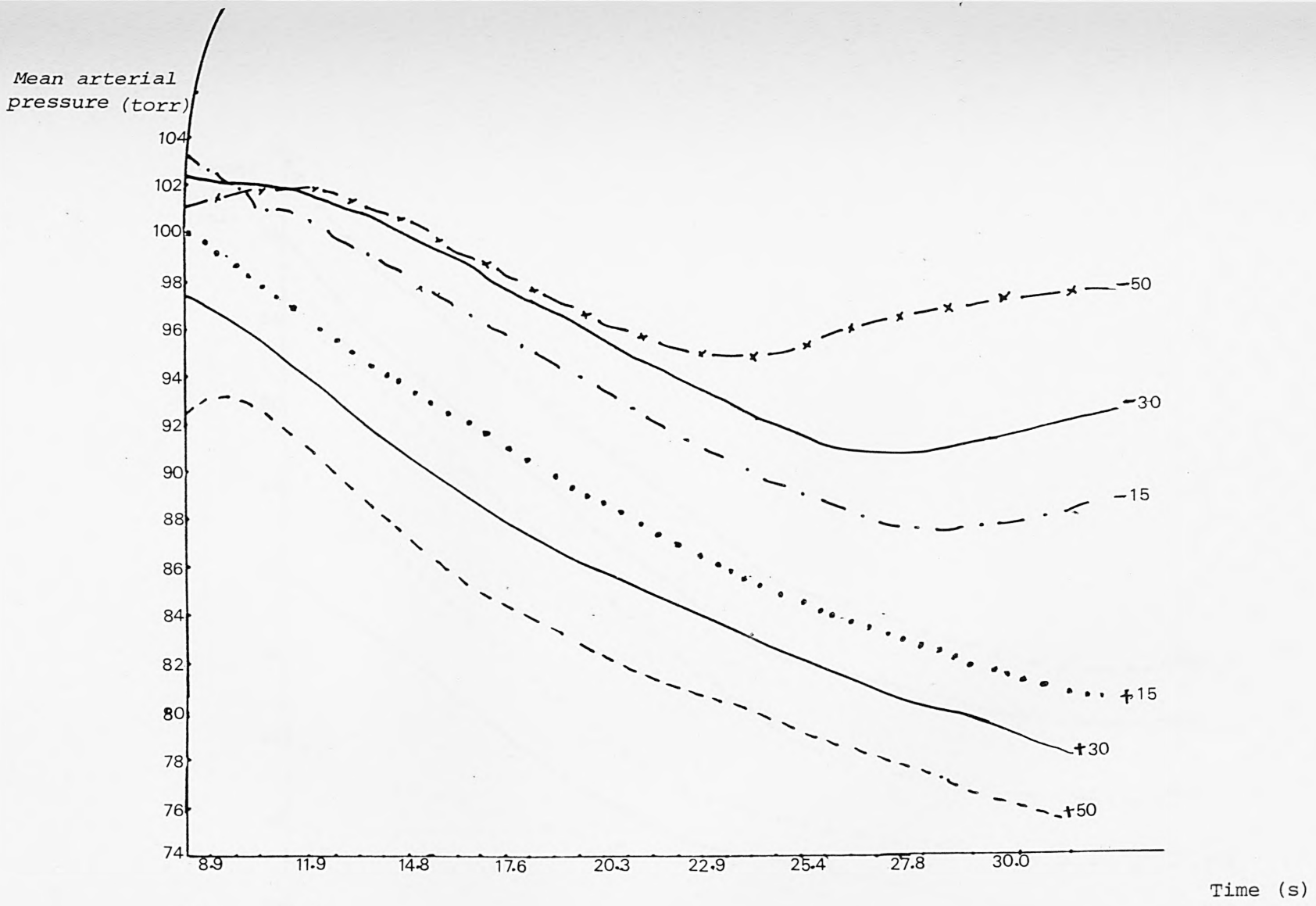

Figure 7.5a

Figure 7.5a-d The effects on model response of varying P(45), the unstressed volume, of the pulmonary veins by ±15, ±30 and ±50% about the nominal value, following a loss of 500 ml of blood.

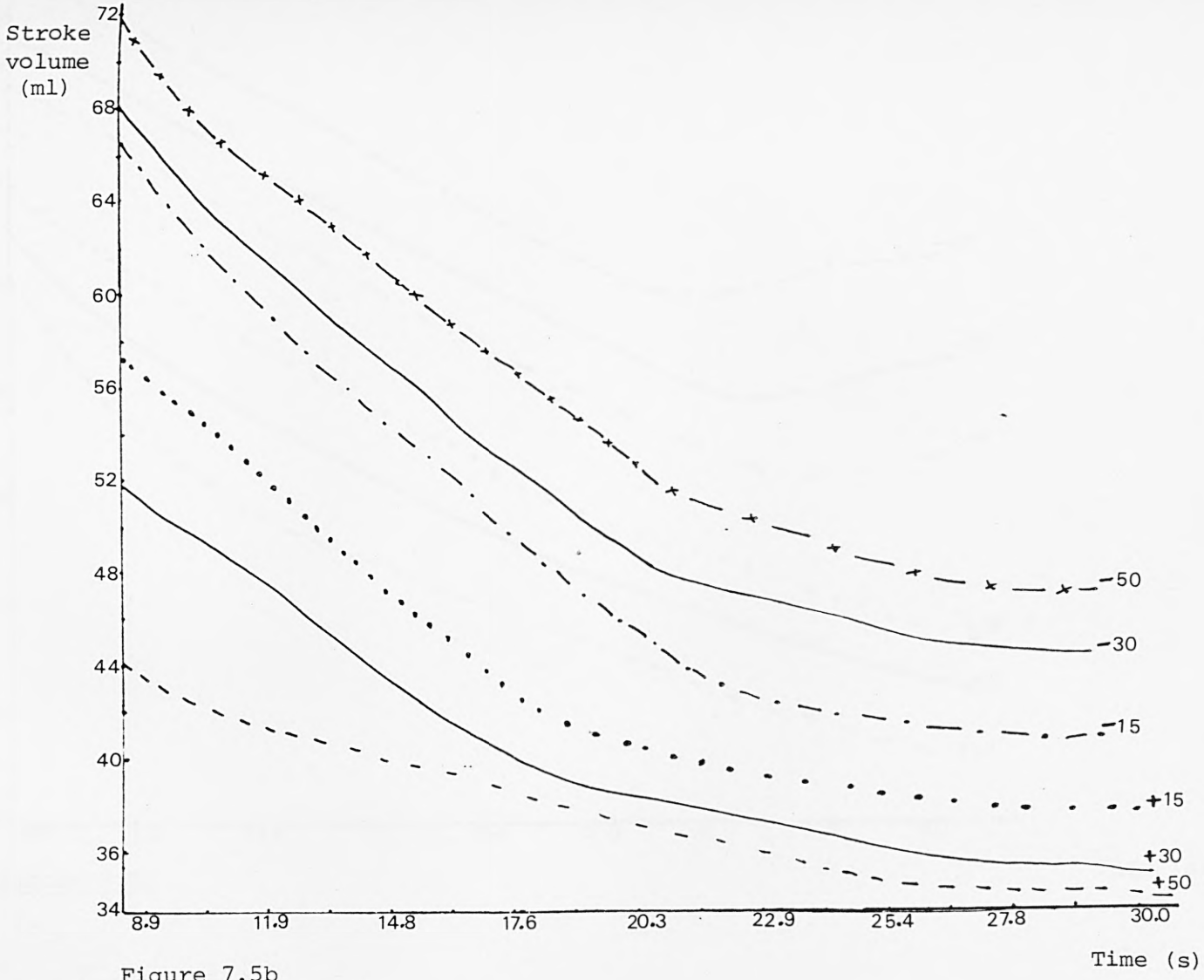
Stroke volume (ml)
72
68
64
60
56
52
48
44
40
36
34
8.9
11.9
14.8
17.6
20.3
22.9
25.4
27.8
30.0
Time (s)
-50
-30
-15
+15
+30
+50

Figure 7.5b

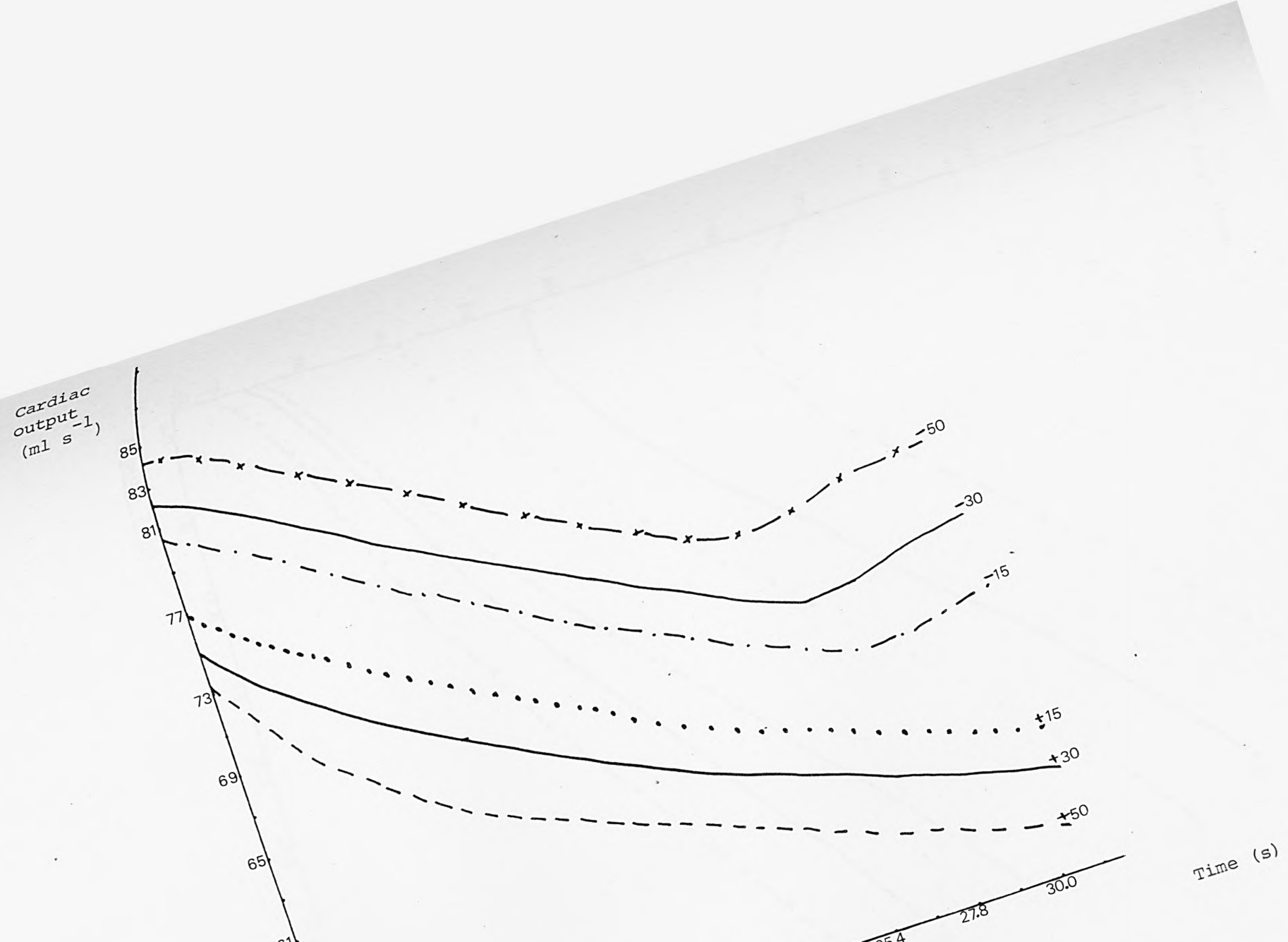
Cardiac output (ml s⁻¹)
85
83
81
77
73
69
65
50
30
15
15
30
50
Time (s)
27.8
30.0

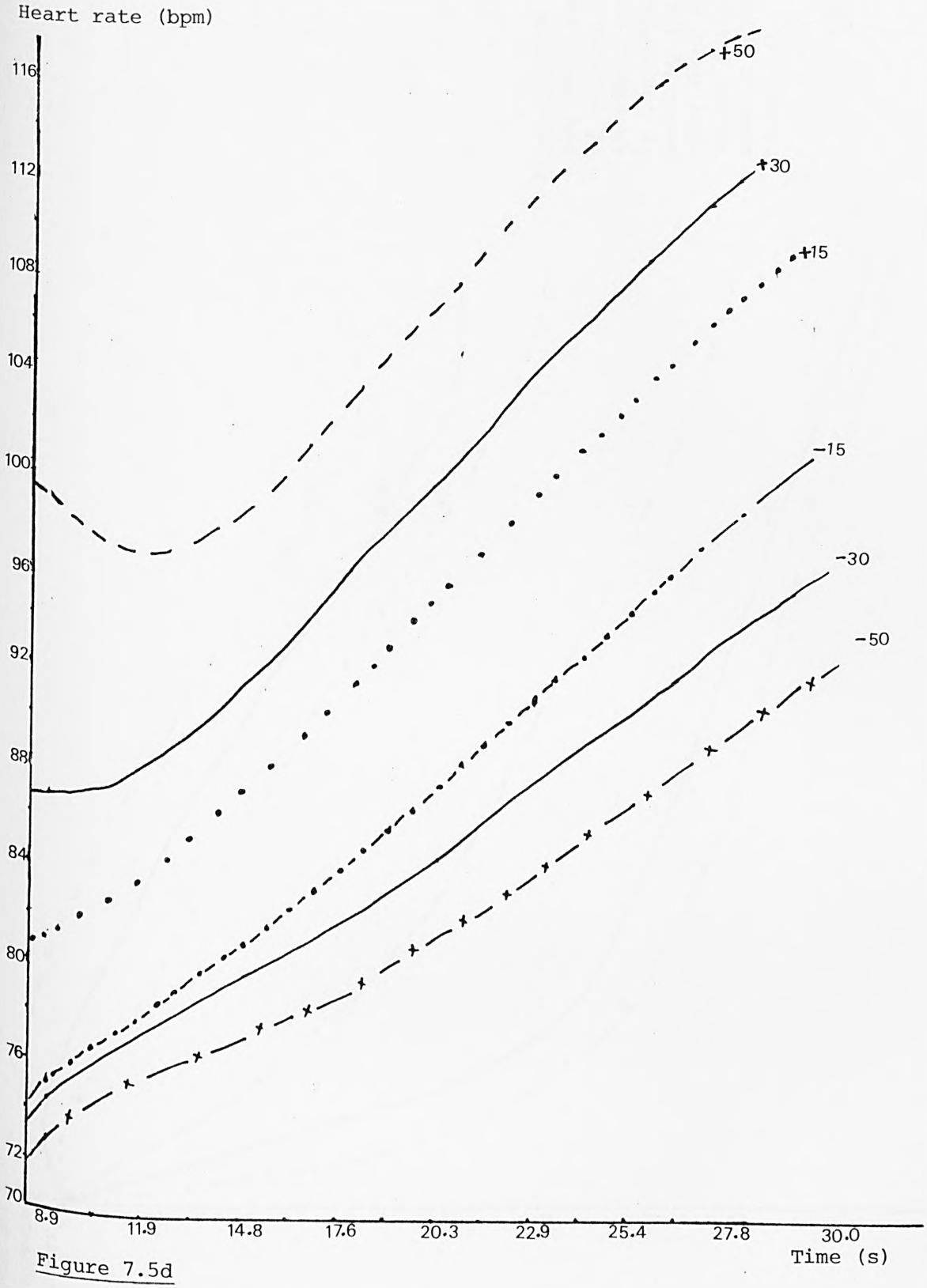
Heart rate (bpm)
116
112
108
104
100
96
92
88
84
80
76
72
70
+50
+30
+15
-15
-30
-50
8.9
11.9
14.8
17.6
20.3
22.9
25.4
27.8
30.0
Time (s)

Figure 7.5d

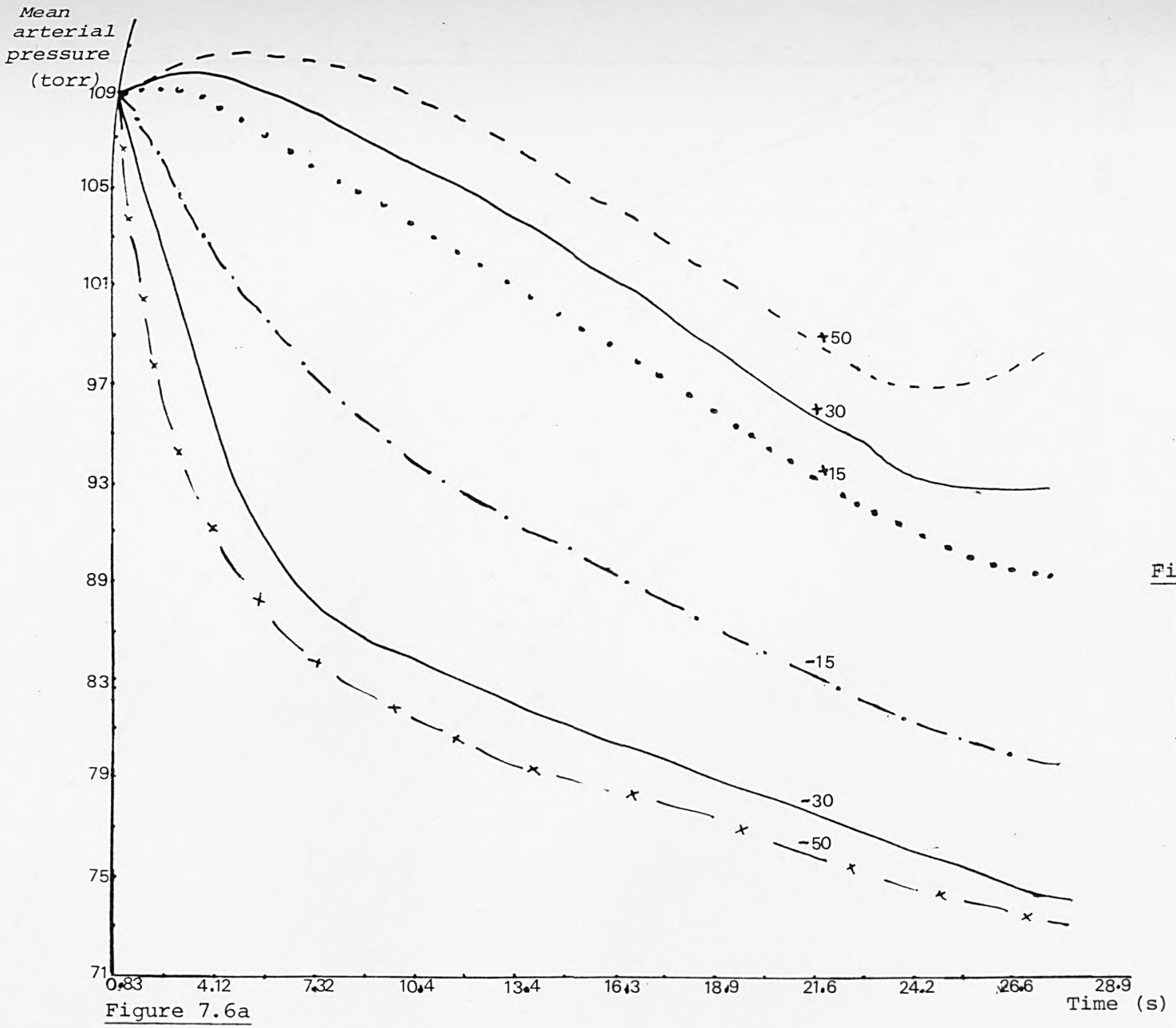

Figure 7.6a

Figure 7.6a-d The
The model response of varying P(137) threshold constant in the neural cont model by ±15, ±30 ±50% about the nomi value, following a loss of 500 ml of blood.

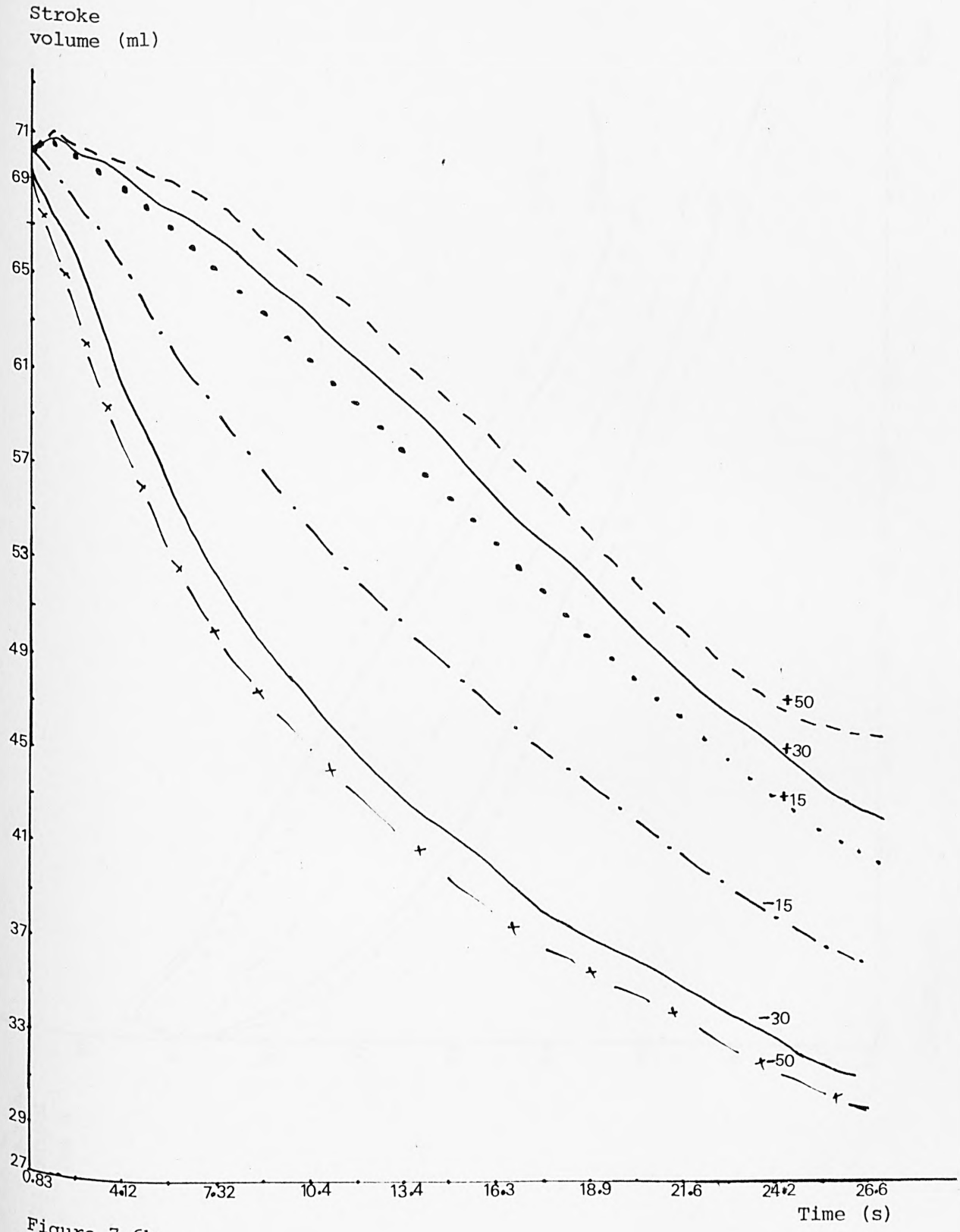
Stroke
volume (ml)
71
69
65
61
57
53
49
45
41
37
33
29
27
+50
+30
+15
-15
-30
-50
0.83
4.12
7.32
10.4
13.4
16.3
18.9
21.6
24.2
26.6
Time (s)

Figure 7.6b

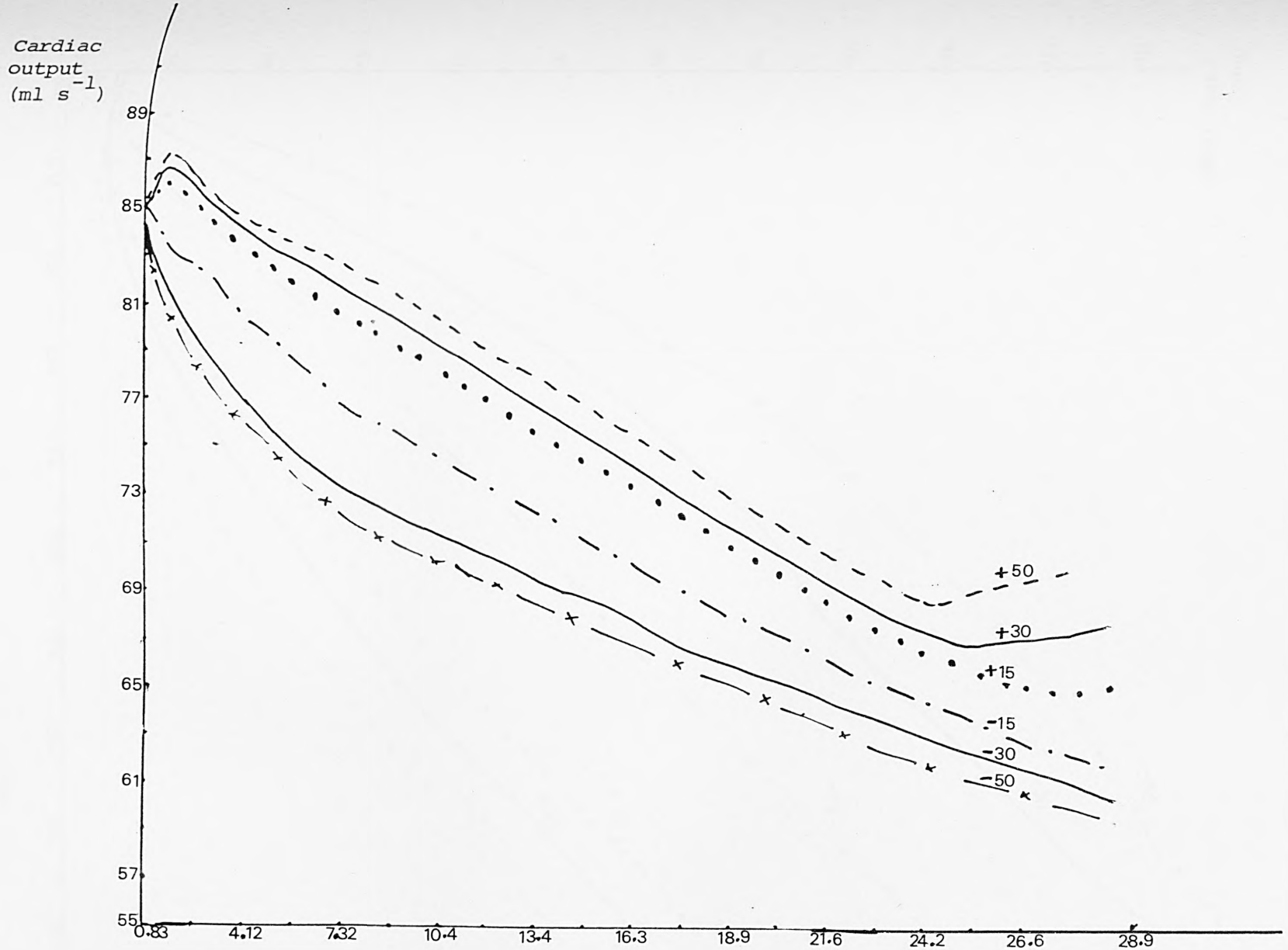
Cardiac output (ml s-1)
89
85
81
77
73
69
65
61
57
55
0.83
4.12
7.32
10.4
13.4
16.3
18.9
21.6
24.2
26.6
28.9
Time (s)
+50
+30
+15
-15
-30
-50

Figure 7.6c

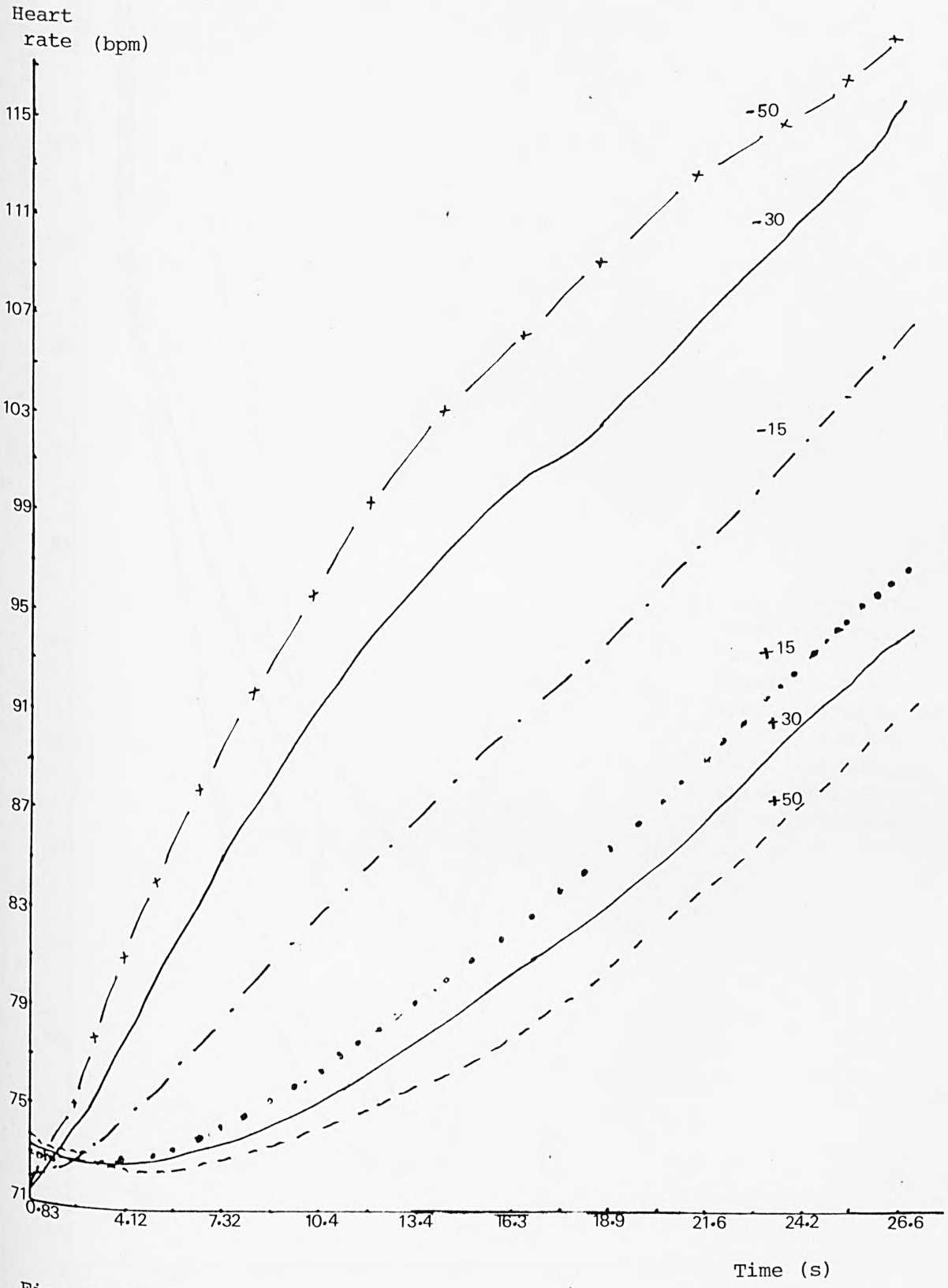
Heart rate (bpm)
115
111
107
103
99
95
91
87
83
79
75
71
-50
-30
-15
+15
+30
+50
0·83
4·12
7·32
10·4
13·4
16·3
18·9
21·6
24·2
26·6
Time (s)

Figure 7.6d

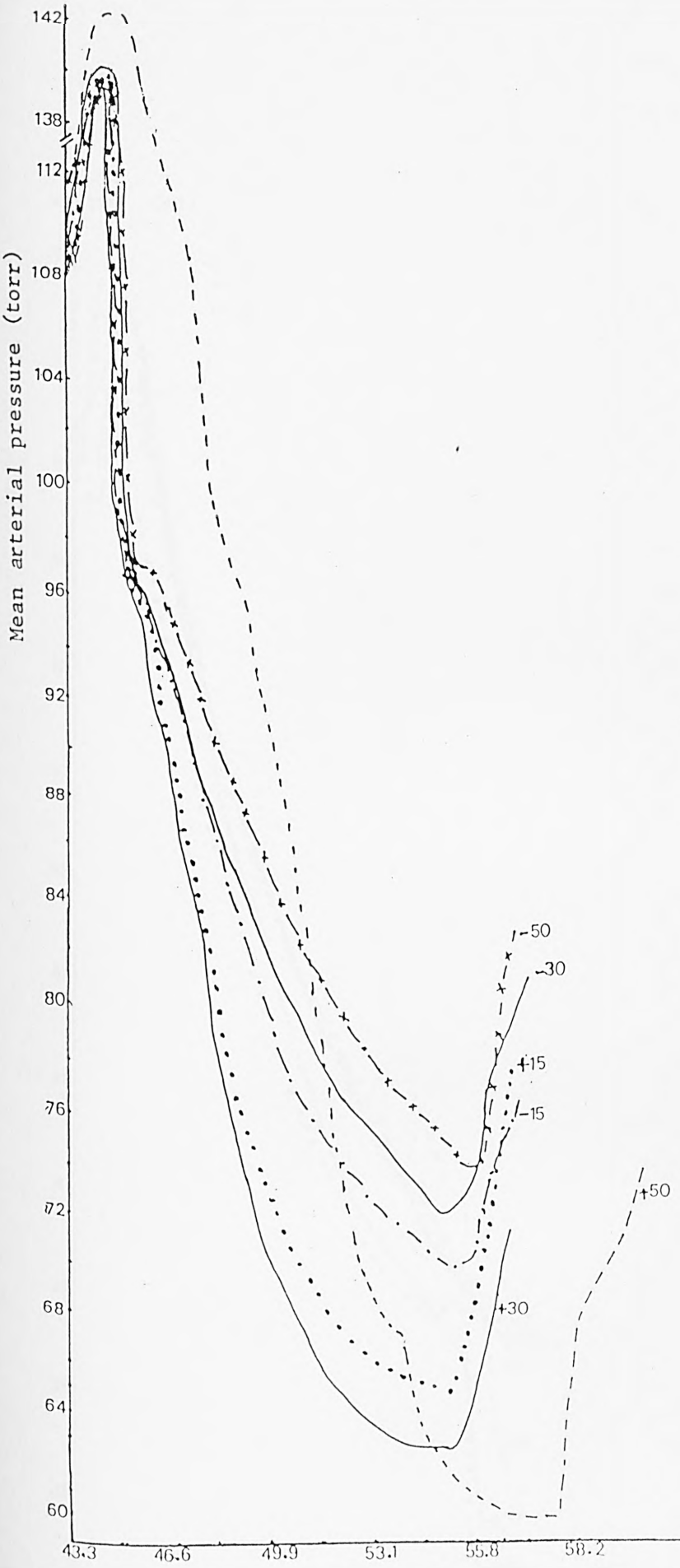

Figure 7.7a-d The model response of varying P(133), constant in the neural control model, by ±15, ±30 and ±50% about the nominal value during the Valsalva manoeuvre.

Figure 7.7a

Figure 7.7 continued overleaf

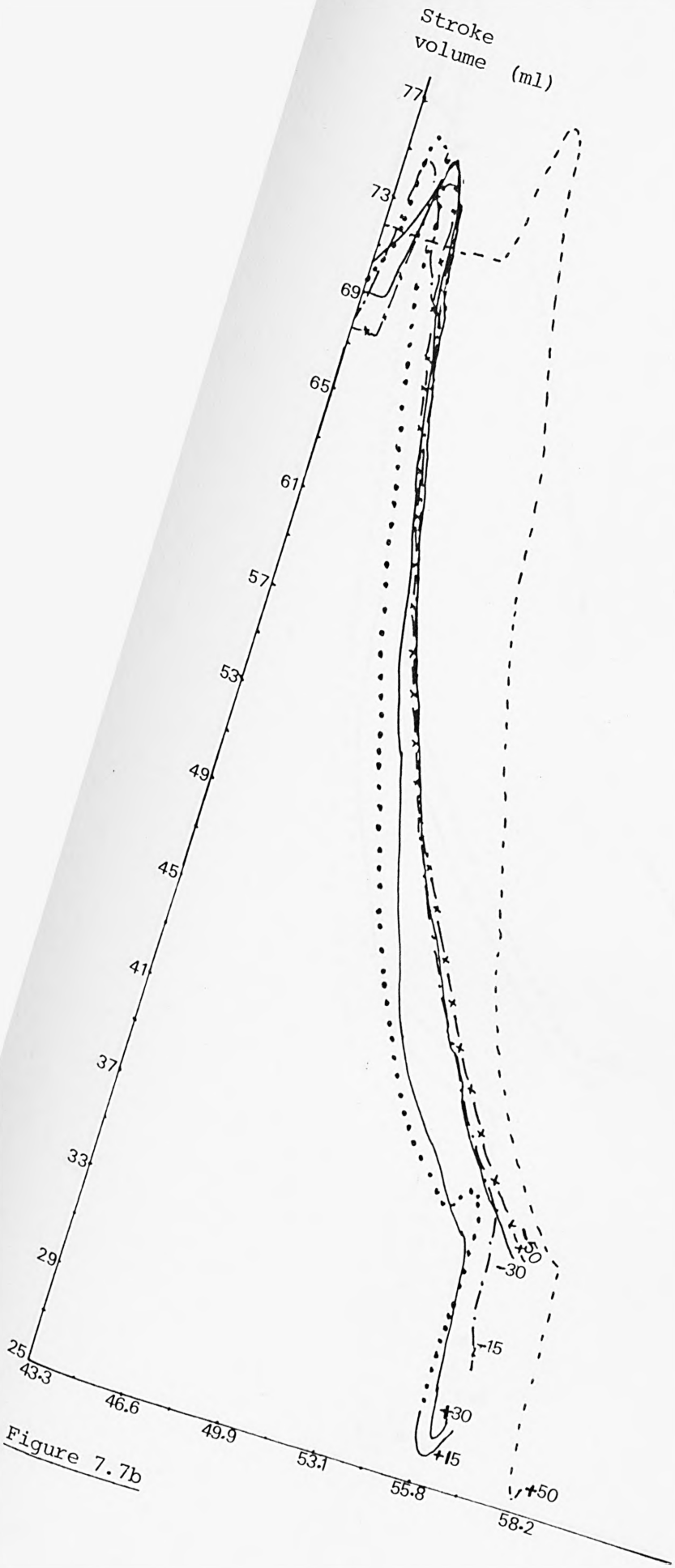
Stroke volume (ml)
77
73
69
65
61
57
53
49
45
41
37
33
29
25
43.3
46.6
49.9
53.1
55.8
58.2
-50
-30
-15
+30
+15
+50

Figure 7.7b

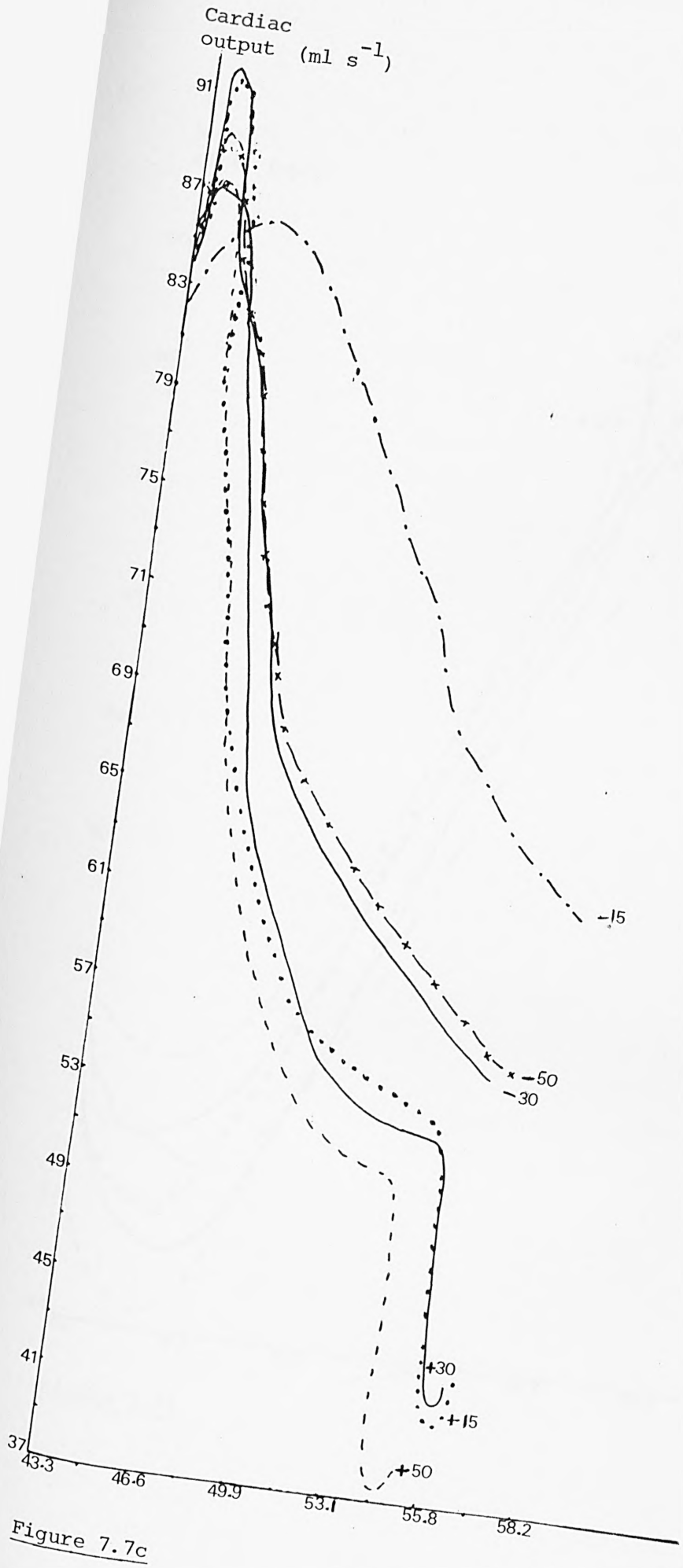
Cardiac output (ml s^{-1})
91
87
83
79
75
71
69
65
61
57
53
49
45
41
37
43.3
46.6
49.9
53.1
55.8
58.2
Time (s)
-15
-50
-30
+30
+15
+50

Figure 7.7c

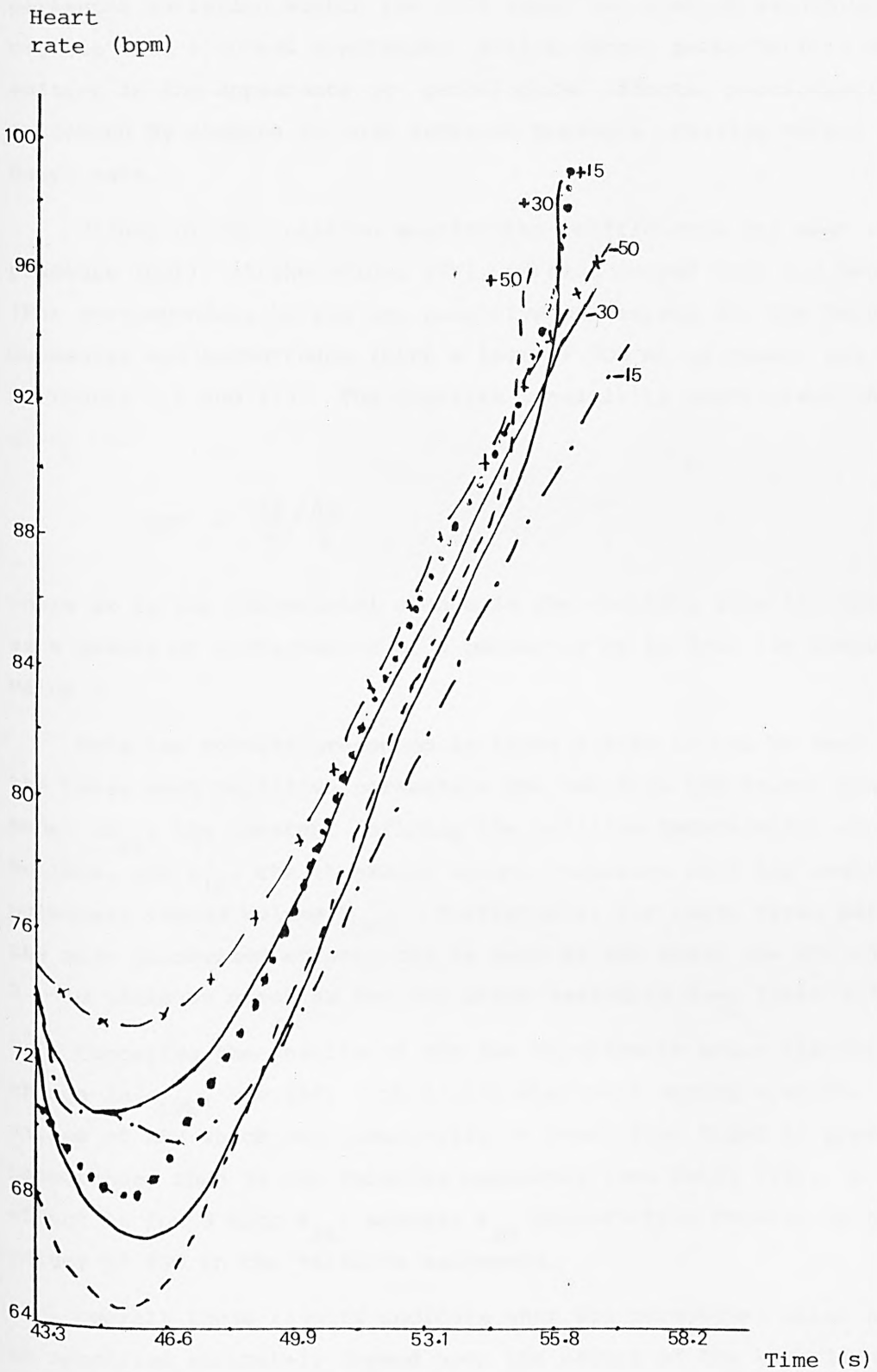
Heart
rate (bpm)
100
96
92
88
84
80
76
72
68
64
+15
+30
+50
-50
-30
-15
43.3
46.6
49.9
53.1
55.8
58.2
Time (s)

Figure 7.7d

The overall results of this analysis supported the assumption that parameter variation within the ±15% about the nominal values was compatible with a normal population, whilst larger perturbations were resulting in the appearance of pathological effects, particularly as evidenced by changes in mean arterial pressure, cardiac output and heart rate.

Values of the relative sensitivity coefficients for mean arterial pressure (MAP), stroke volume (SV), cardiac output (CO) and heart rate (FH) corresponding to the ten sensitive parameters for the Valsalva manoeuvre and haemorrhage (with a loss of 500 ml of blood) are listed in Tables 7.2 and 7.3. The relative sensitivity coefficient (RSC) is given by:

$$RSC = \frac{\Delta x}{x} \Big/ \frac{\Delta p}{p}$$

where Δx is the incremental change in the variable from its value x as a result of perturbation of a parameter by Δp from its nominal value p.

From the results presented in these Tables it can be seen that the three most sensitive parameters are two from the neural control model (K_{16}, the constant defining the relative baroreceptor contributions, and K_{18}, the threshold value), together with the unstressed pulmonary venous volume V_{UPV}. Furthermore, for these three parameters the most pronounced effects can be seen in MAP where the RSC values are 2 - 10 times as great as for the other variables (see Table 7.3).

Comparing the results of the two experiments being simulated, change in a_{LVS}, the left ventricular elastance during systole, produces values of RSC which are numerically at least four times as great in haemorrhage than in the Valsalva manoeuvre (see Table 7.4). A similar effect is found with K_{16}, whereas K_{18} perturbation results in higher values of RSC in the Valsalva manoeuvre.

Overall these results indicate that the parameters which need to be specified accurately depend upon the nature of the experiment being performed.

It should be noted that the confidence interval of the neural control parameters K_{16} and K_{18} and the unstressed volume of the pulmonary veins is very large. This means that the model response is invariant to large

Parameter in computer program	Parameter in mathematical model	RSC for MAP	RSC for SV	RSC for CO	RSC for FH
p(7)	P_{THN}	0.07058	0.1754	0.1149	-0.1307
p(29)	a_{RAS}	0.2666	0.3333	4.91228	-0.3986
p(30)	a_{RAD}	-0.00784	-0.1929	-0.0835	-0.56209
p(31)	V_{URA}	0.01568	-0.10526	-0.04179	0.02614
p(32)	R_{RARV}	0.01568	-0.10526	-0.04179	-0.4836
p(34)	a_{RVS}	0.3058	0.7719	0.2194	-0.4575
p(45)	V_{UPV}	-0.1568	0.7719	-0.2298	-0.0653
p(53)	a_{LVS}	0.23529	0.666	0.2298	-0.4248
p(133)	K_{16}	0.2666	0.5614	0.2507	-0.3137
p(137)	K_{18}	0.4705	0.9649	0.1358	-0.5882

Table 7.2 Relative sensitivity coefficients evaluated for the four variables MAP, SV, CO and FH corresponding to +15% parameter perturbation in the simulation of sudden removal of 500 ml of blood. The post-stimulus steady state values of the four variables with the parameters at their nominal values were: MAP = 87.6 torr; SV = 37.39 ml; CO = 64.78 ml s^{-1}; FH = 104 bpm.

Parameter in computer program	Parameter in mathematical model	RSC for MAP	RSC for SV	RSC for CO	RSC for FH
p(7)	P_{THN}	-0.129	-0.099	-0.044	0.082
p(29)	a_{RAS}	-0.036	-0.058	0.0069	0.061
p(30)	a_{RAD}	-0.026	-0.055	0.0103	0.061
p(31)	V_{URA}	-0.051	-0.073	0.025	0.0916
p(32)	R_{RARV}	-0.0486	-0.0716	0.0346	0.098
p(34)	a_{RVS}	-0.083	-0.144	0.0138	0.157
p(45)	V_{UPV}	-0.102	-0.338	-0.228	0.115
p(53)	a_{LVS}	-0.0776	-0.0462	-0.053	0.0049
p(133)	K_{16}	-0.284	-0.175	0.201	-0.0158
p(137)	K_{18}	0.872	1.229	0.548	-0.589

Table 7.3 Relative sensitivity coefficients evaluated for the four variables MAP, SV, CO and FH corresponding to +15% parameter perturbation in the simulation of the Valsava manoeurve. The values of the variables 52s after the start of the manoeuvre with the parameters at their nominal values were: MAP = 71.29 torr; SV = 44.67 ml; CO = 57.78 ml s^{-1}; FH = 80 bpm.

Parameter in mathematical model	RSC for MAP in haemorrhage	RSC for MAP in Valsalva manoeuvre
a_{RAS}	0.2666	-0.036
a_{RAD}	-0.00784	0.026
a_{RVS}	0.3058	-0.083
a_{LVS}	0.23529	-0.0776

(a)

Parameter in mathematical model	RSC for CO in haemorrhage	RSC for CO in Valsalva manoeuvre
a_{RAS}	4.91228	0.0069
a_{RAD}	-0.0835	0.0103
a_{RVS}	0.2194	0.0138
a_{LVS}	0.2298	-0.053

(b)

Table 7.4 Comparison of relative sensitivity coefficients of (a) mean arterial pressure (MAP), and (b) cardiac output (CO) in the simulation of haemorrhage and Valsalva manoeuvre following perturbation of elastance parameters.

changes in these parameters, and, since many of their values cannot be determined by direct measurement (see Chapter 5), they are highly uncertain (Leaning, 1980).

Whilst in carrying out the sensitivity analysis as described above parameter perturbations amounted to ±15%, there is still uncertainty as to whether this represented an adequate range, even although from discussions with clinical colleagues it was assumed to be reasonable. Furthermore, the analysis described so far has only examined effects following perturbation of the parameters one at a time. In order to investigate possible effects resulting from parameter interaction a Monte-Carlo simulation was carried out effectively increasing coverage of the multidimensional parameter space, again though limiting parameter perturbation to the range ±15% about the nominal values. These results are presented in the following section.

7.4.4 Monte-Carlo Simulation

As described in Section 7.2.3, Monte-Carlo simulation provides a means of examining the effects of variation in a number of model parameters simultaneously, as opposed to considering the effects of varying one parameter at a time as outlined in Section 7.4.3. In the simulations presented here, the effects of simultaneous variation of the ten most sensitive model parameters as defined earlier were examined. In each of the simulations, all of the parameters were set at particular values lying within a ±15% range about their nominal values. The perturbation from the nominal value was determined for each of the parameters in turn using a random number generator assuming that all values within the respective ±15% ranges were equi-probable (that is, a rectangular probability density

distribution was assumed in perturbing each variable). Repeated simulations were carried out in order to provide an adequate coverage of the effects of multiple parameter perturbations within their respective ranges. The model was tested for change in steady values as well as the dynamic responses to haemorrhage (loss of 500 ml of blood) and the Valsalva manoeuvre. Results corresponding to the four variables mean arterial pressure (MAP), stroke volume (SV), cardiac output (CO) and heart rate (FH) are shown in the tables and figures which follow.

Table 7.5 lists the parameter values corresponding to thirteen simulations using the Monte-Carlo approach. The steady state values of the key physiological variables for each of these simulations are presented in Figure 7.8, and for MAP, CO and FH in histogram form in Figures 7.9 - 7.11. The minimum values of MAP, CO and SV, together with the maximum values of FH in each of six of these simulations following the sudden removal of 500 ml of blood, are shown in Figure 7.12. These extremum values occurred approximately 30 seconds after the sudden blood loss (see Figure 7.13) for some of the time courses of these variables). In a similar manner, Figure 7.14 shows values of the same four variables in eight Monte-Carlo simulations of the Valsalva manoeuvre, the values being those obtained at the end of the manoeuvre.

Run No.	1	2	3	4	5	6	7	8	9	10	11	12	13
p(7)	-3.987	-4.378	-3.570	-3.961	-4.355	-3.544	-3.936	-4.327	-3.519	-3.91	-3.835	-4.01	-4.197
p(29)	0.142	0.167	0.148	0.128	0.1534	0.133	0.158	0.138	0.164	0.144	0.13	0.15	0.169
p(30)	0.049	0.043	0.052	0.047	0.056	0.051	0.045	0.054	0.049	0.043	0.057	0.0572	0.0571
p(31)	28.657	30.763	32.86	25.97	28.07	30.184	32.28	34.39	27.5	29.6	33.08	31.19	29.301
p(32)	0.0027	0.0029	0.003	0.0031	0.0033	0.0025	0.0027	0.0028	0.003	0.0031	0.0026	0.0034	0.0033
p(34)	0.32	0.273	0.316	0.27	0.313	0.266	0.31	0.263	0.306	0.260	0.299	0.298	0.297
p(45)	472.4	526.76	443.06	497.37	413.68	467.98	522.29	438.59	492.9	409.2	504.0	470.6	437.38
p(53)	1.466	1.594	1.722	1.4	1.528	1.656	1.334	1.462	1.59	1.718	1.524	1.706	1.439
p(133)	0.609	0.618	0.627	0.637	0.646	0.656	0.665	0.674	0.684	0.693	0.745	0.735	0.726
p(137)	90.72	89.866	89.01	88.16	87.3	86.453	85.6	84.74	83.89	83.04	82.121	76.95	71.78

Table 7.5 Parameter values corresponding to thirteen simulation runs of the model using Monte-Carlo techniques

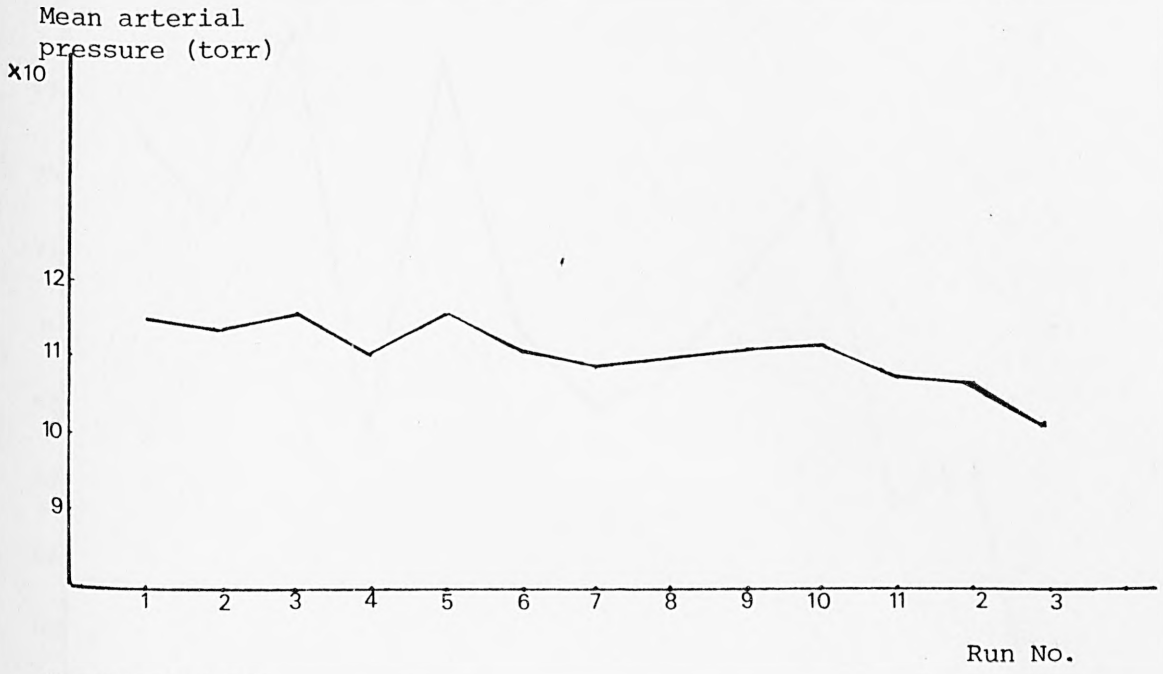

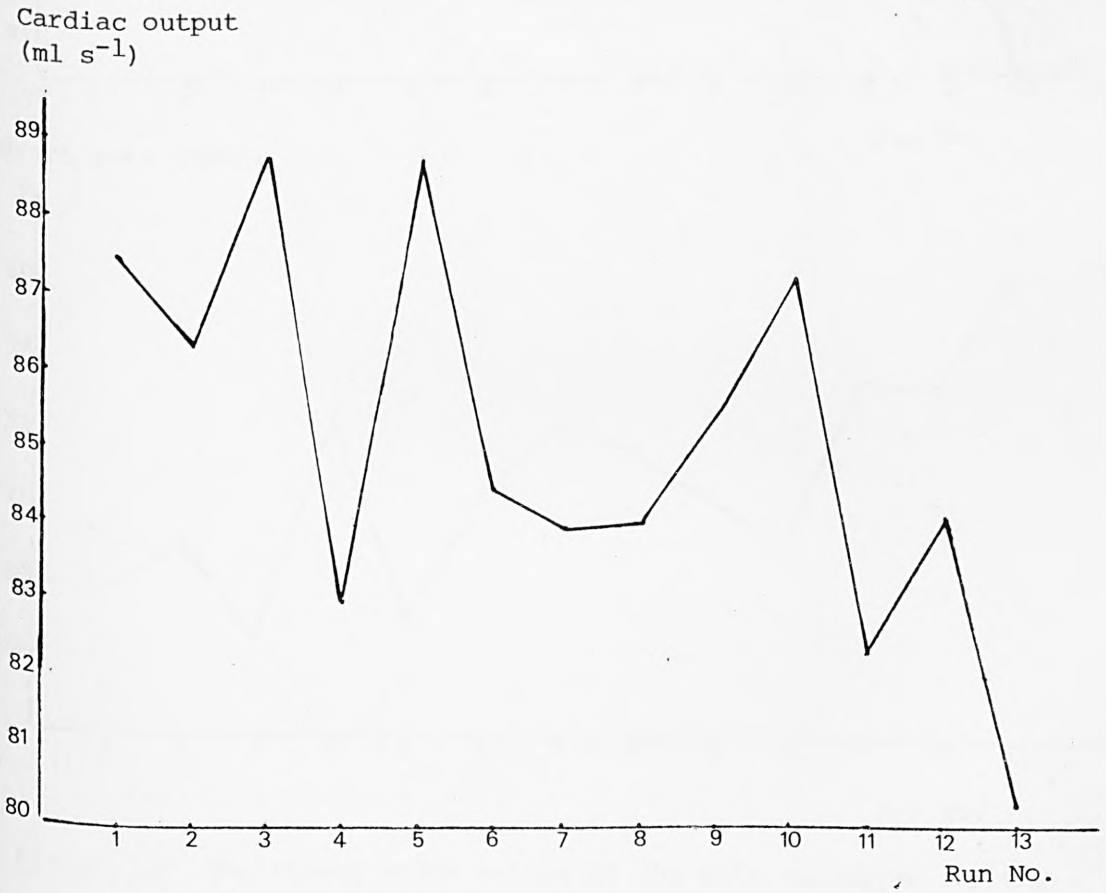

Figure 7.8 continued overleaf

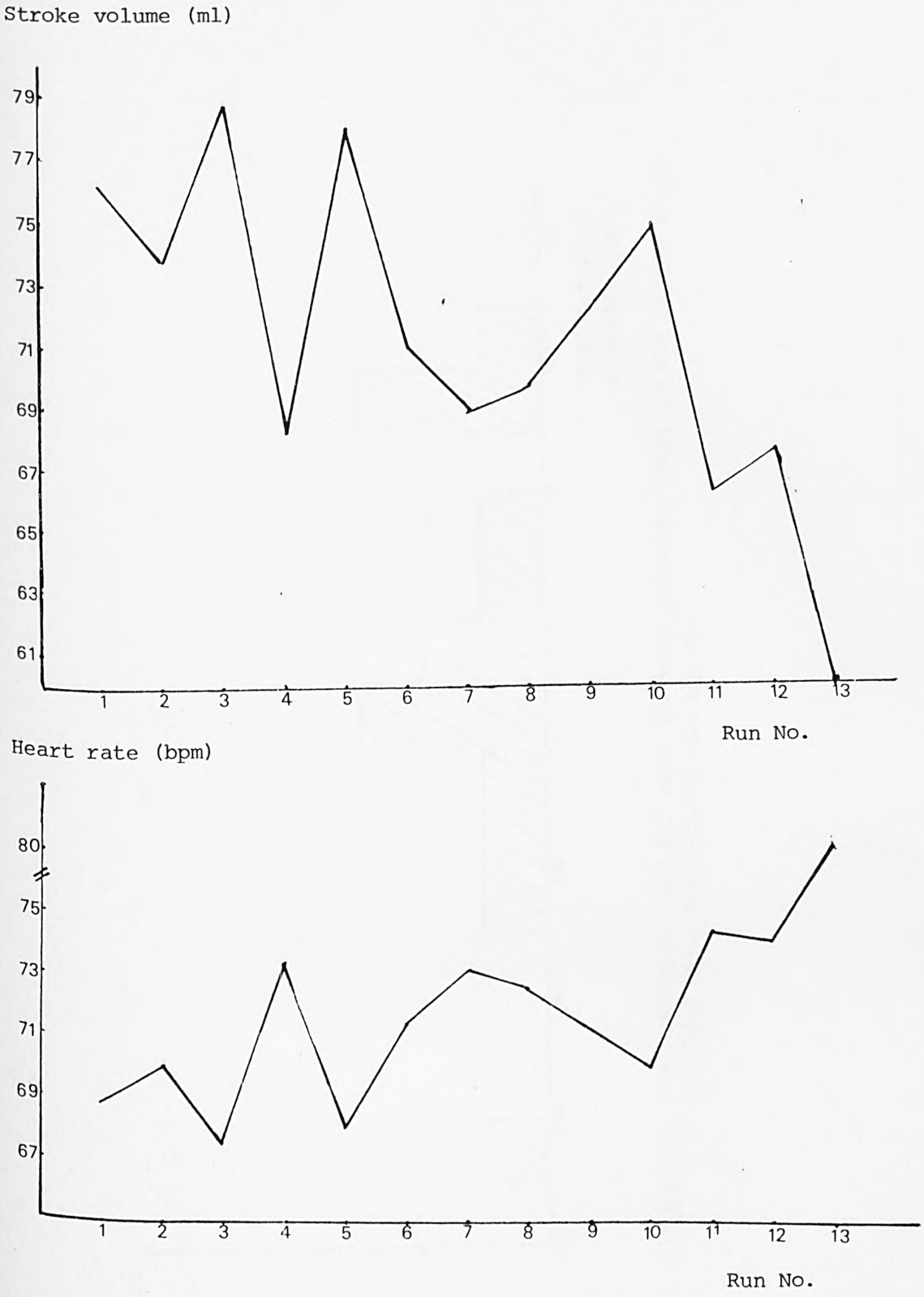

Figure 7.8 The steady state values of the main variables for the 13 simulations using the Monte-Carlo approach, with parameter values as specified in Table 7.5.

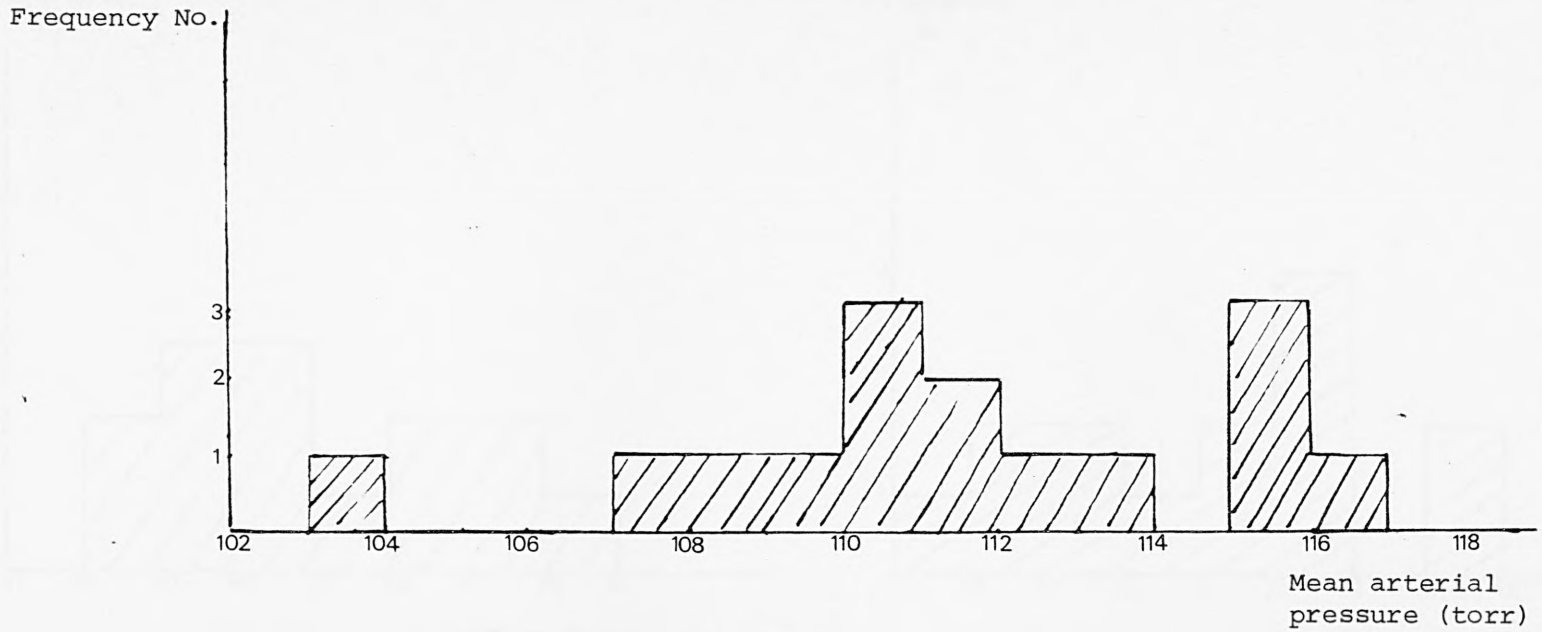

Figure 7.9 The histogram form for mean arterial pressure (MAP) in the steady state obtained from Monte-Carlo simulation.

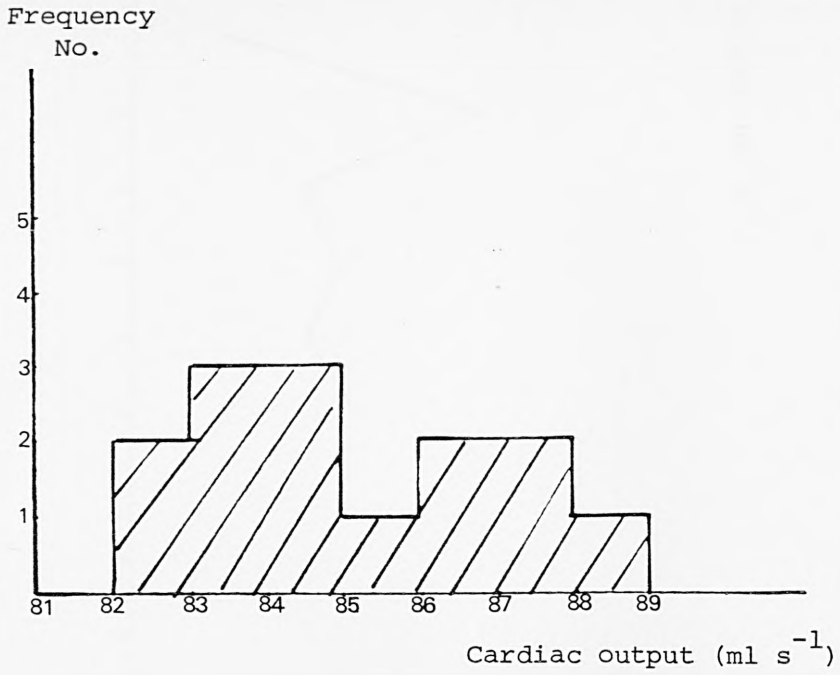

Figure 7.10 The histogram form for cardiac output (CO) in the steady state obtained from Monte-Carlo simulation.

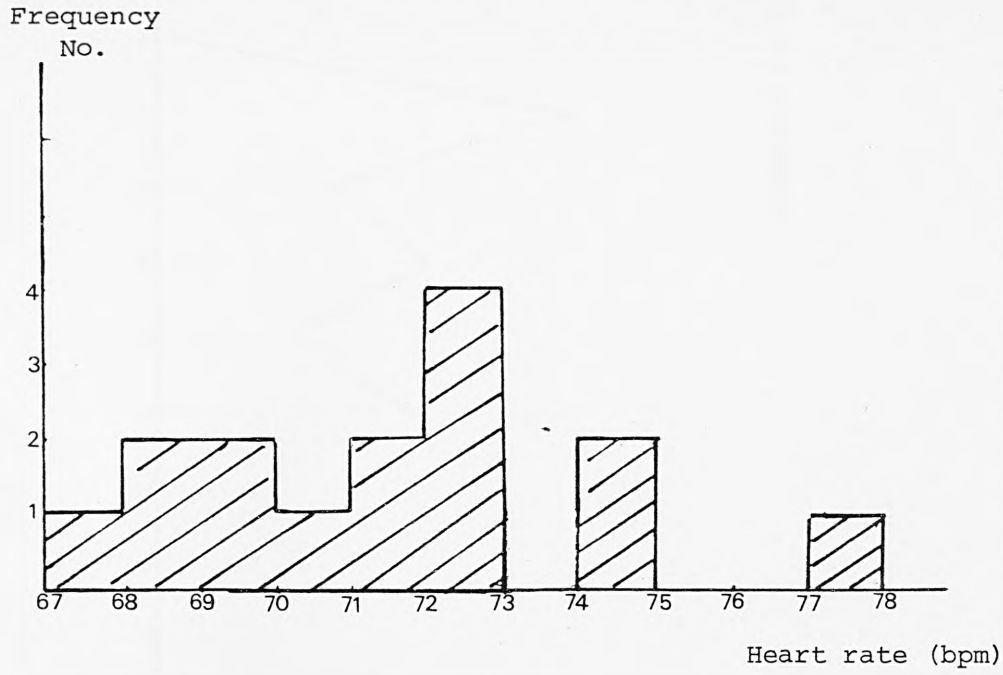

Figure 7.11 The histogram form for heart rate (FH) in the steady state obtained from Monte-Carlo simulation.

Mean arterial pressure
(torr)

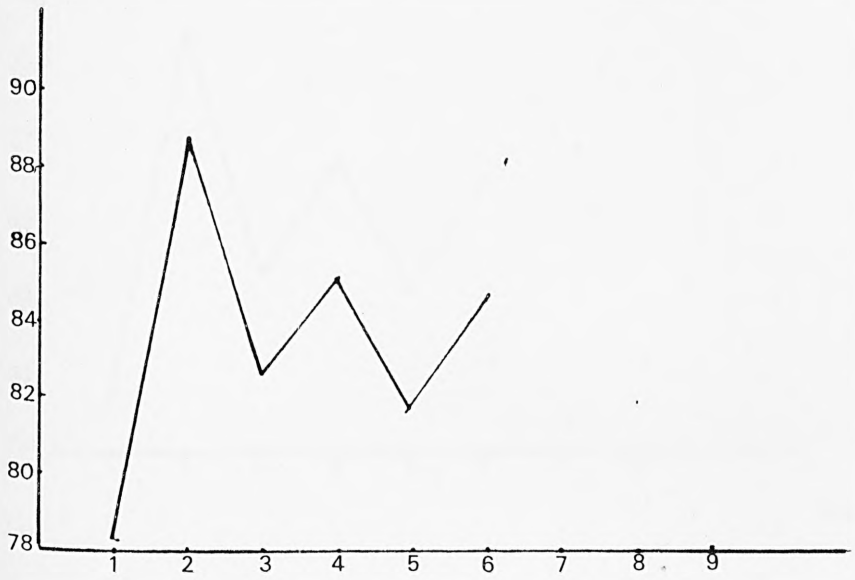

Run No.

Cardiac output (ml s^{-1})

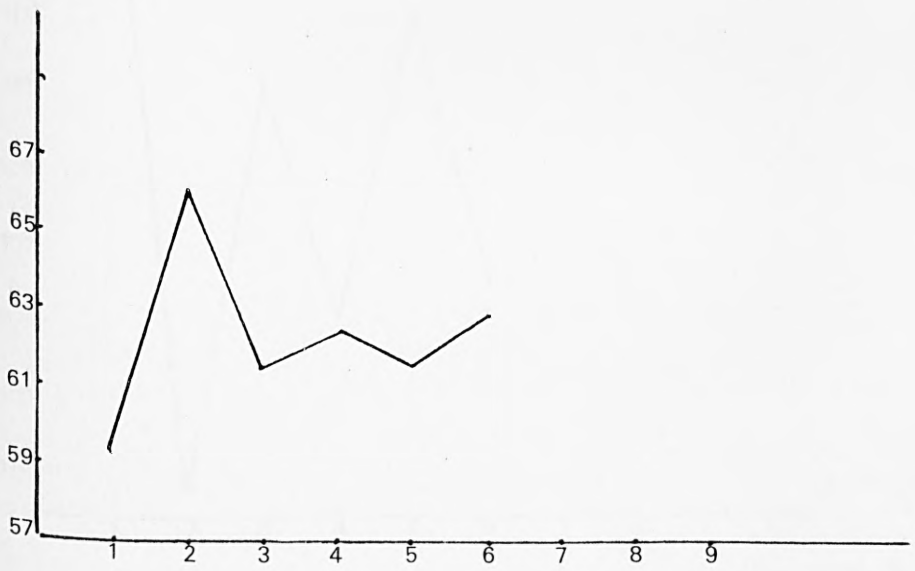

Run No.

Figure 7.12 continued overleaf

Stroke volume (ml)

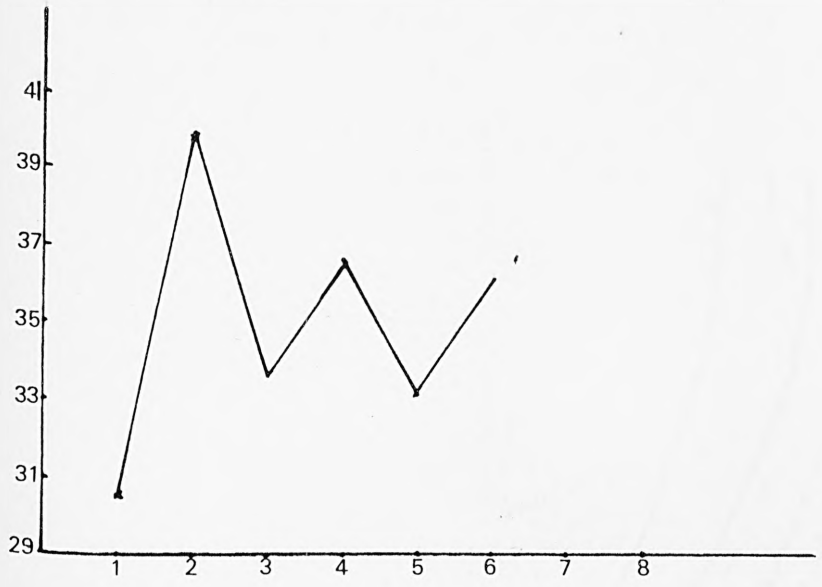

Run No.

Heart rate (bpm)

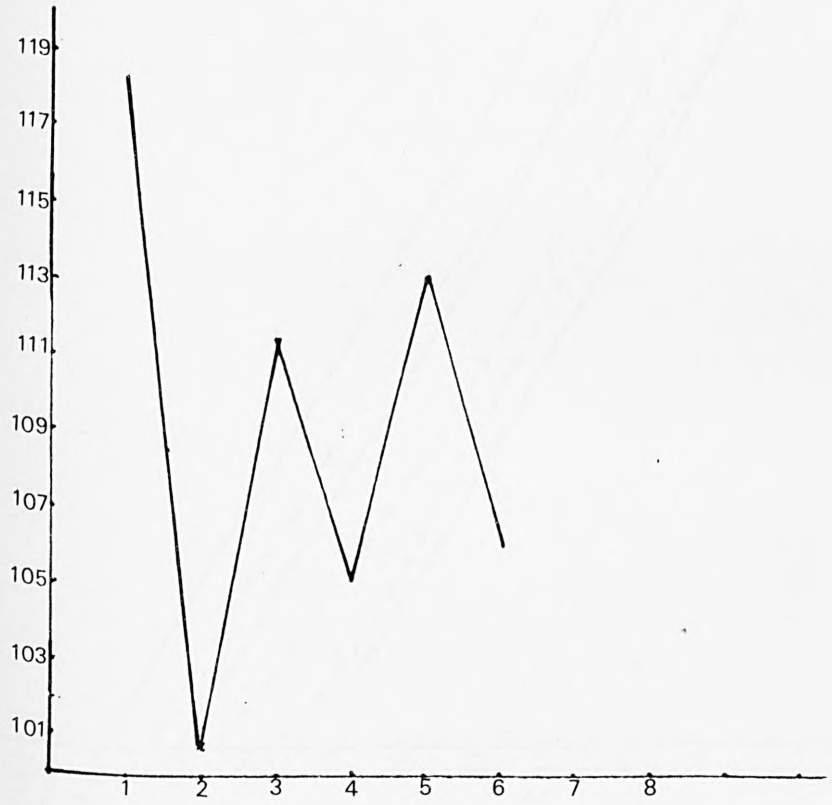

Run No.

Figure 7.12 The values of the main variables in each of the 6 simulations following the sudden removal of 500 ml of blood.

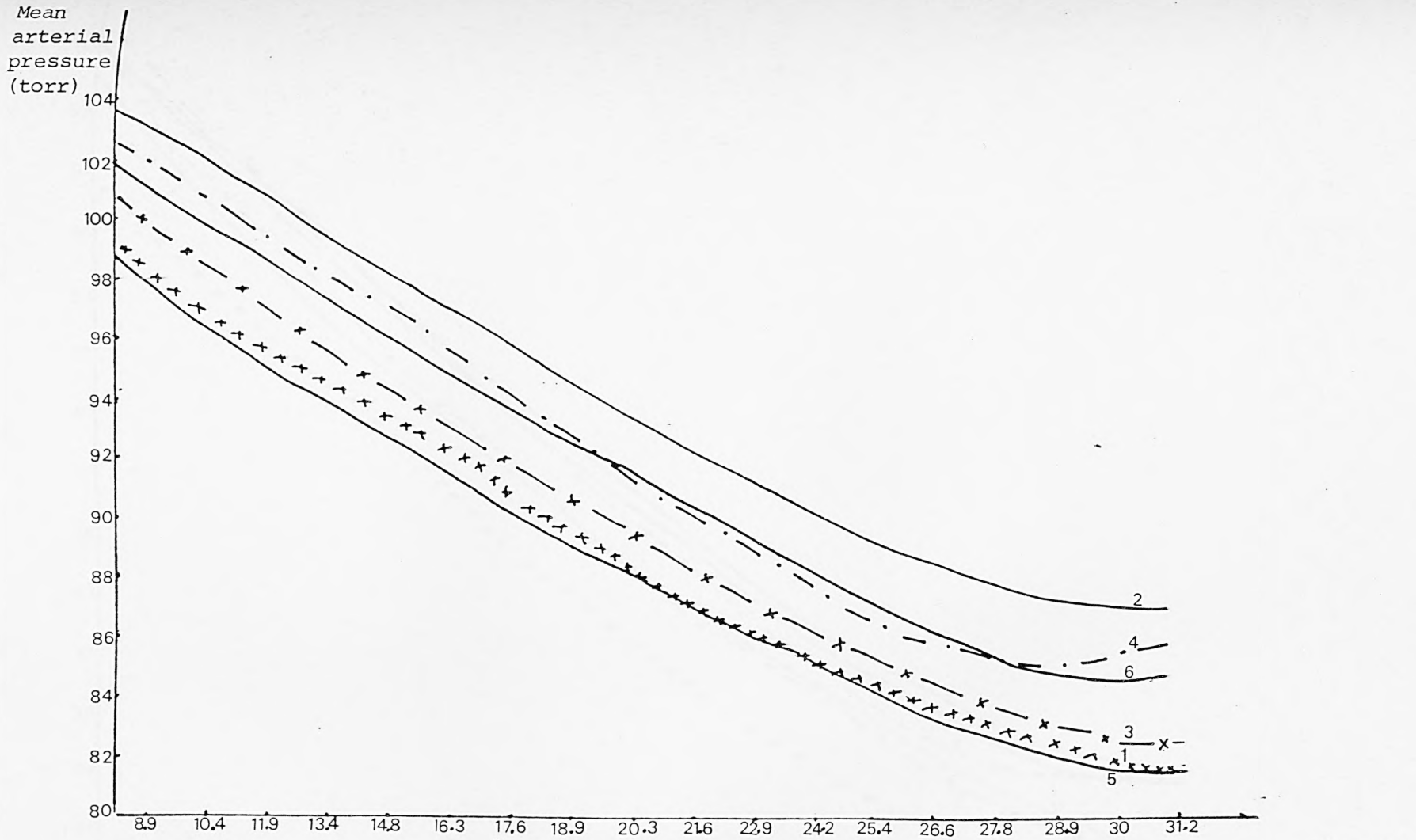

Figure 7.13a

Figure 7.13a-d The model responses following the sudden removal of 500 ml of blood obtained from 6 simulations using the Monte-Carlo approach.

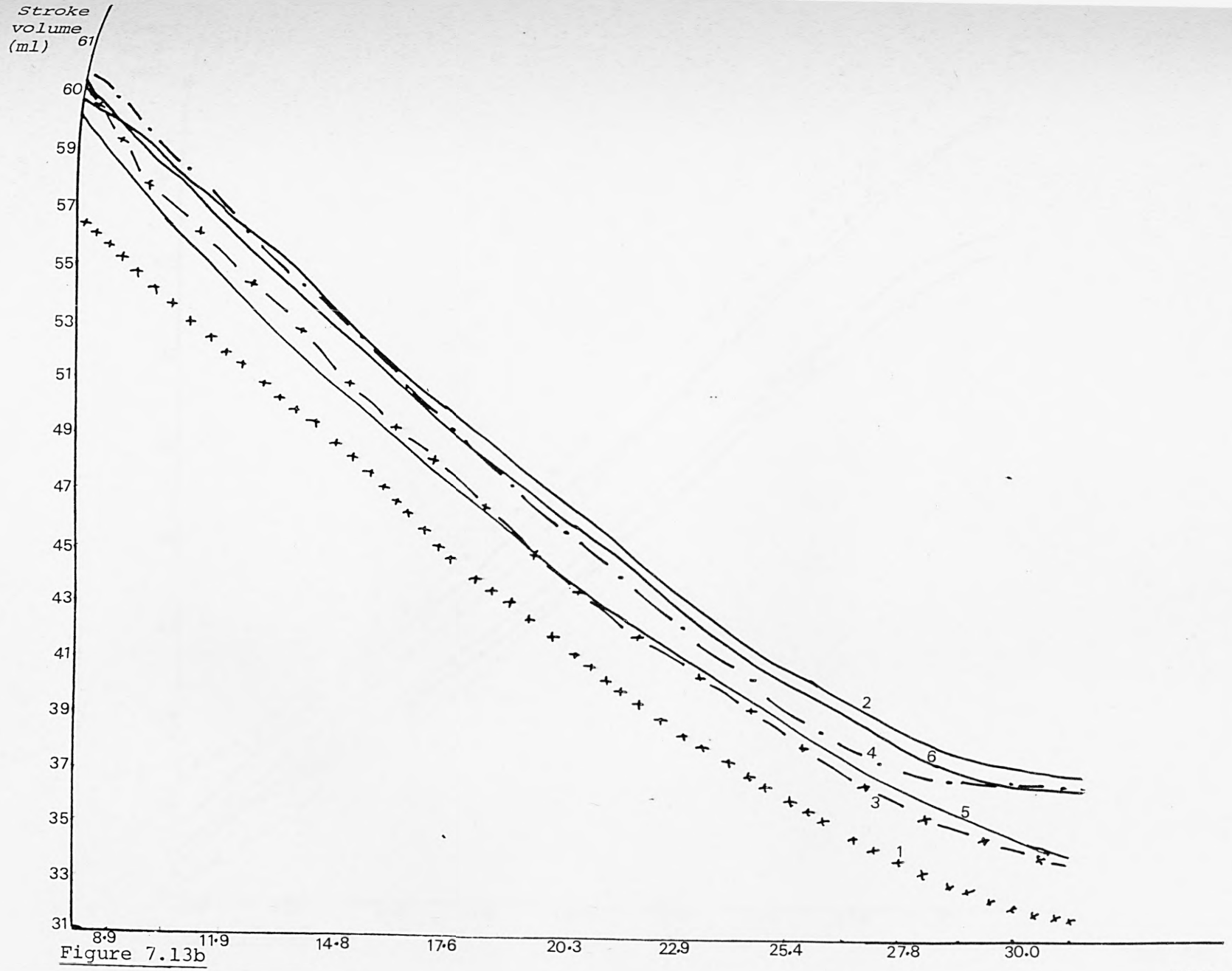
Stroke volume (ml)
61
60
59
57
55
53
51
49
47
45
43
41
39
37
35
33
31
8·9
11·9
14·8
17·6
20·3
22·9
25·4
27·8
30.0
Time (s)
1
2
3
4
5
6

Figure 7.13b

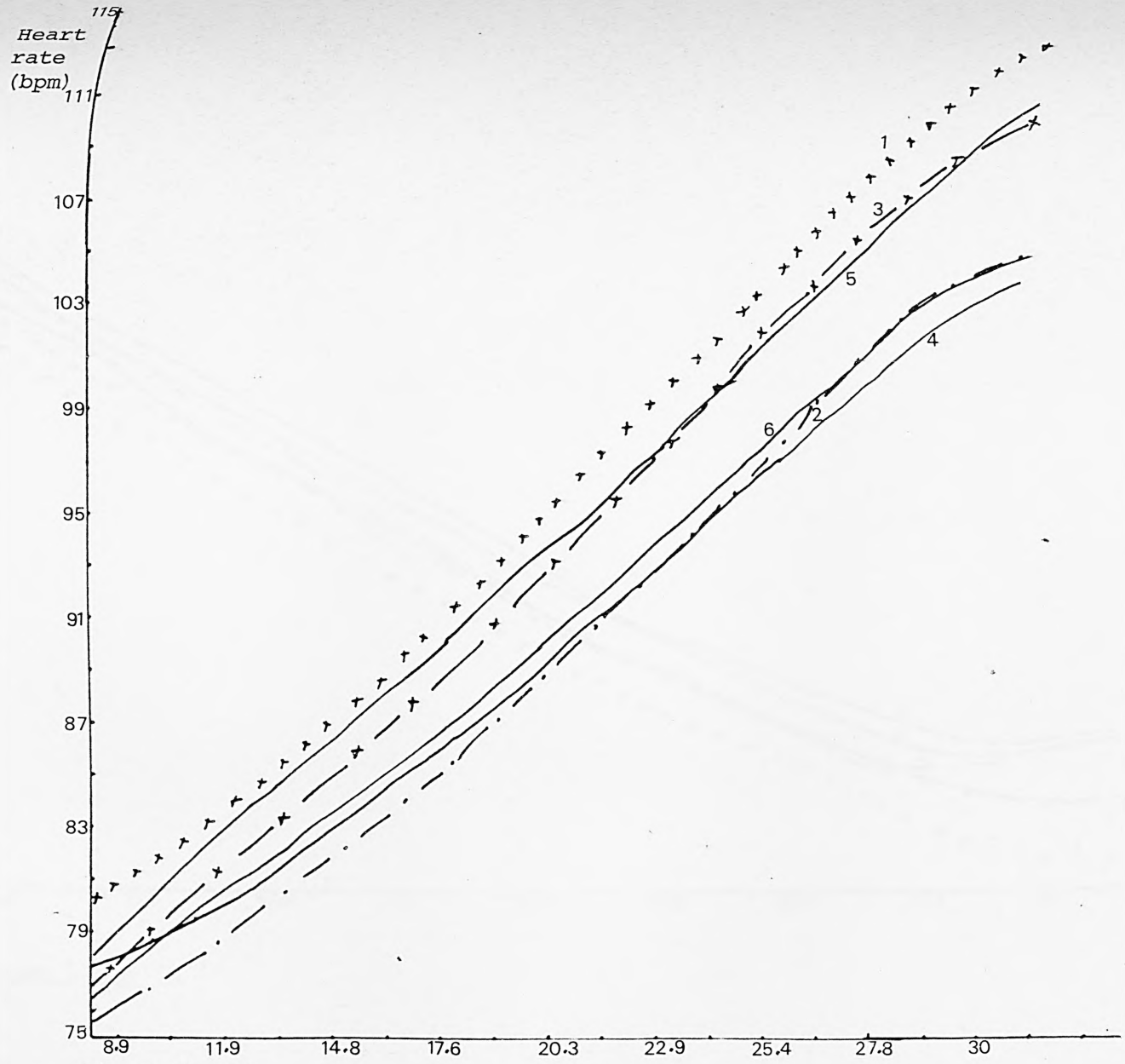
Heart rate (bpm)
115
111
107
103
99
95
91
87
83
79
75
8.9
11.9
14.8
17.6
20.3
22.9
25.4
27.8
30
Time (s)
1
2
3
4
5
6

Figure 7.13d

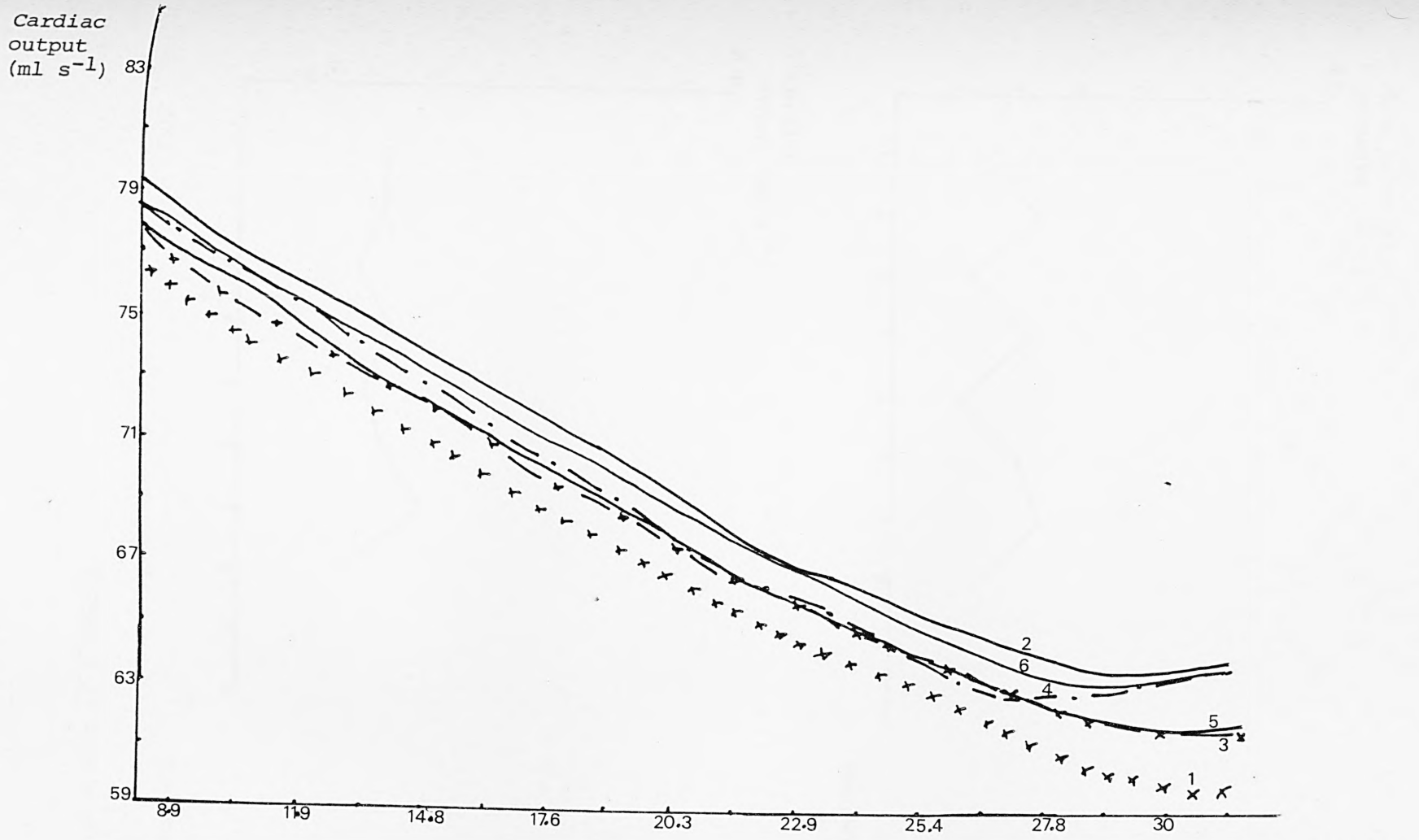
Cardiac output (ml s^{-1})
83
79
75
71
67
63
59
8.9
11.9
14.8
17.6
20.3
22.9
25.4
27.8
30
Time (s)
1
2
3
4
5
6

Figure 7.13c

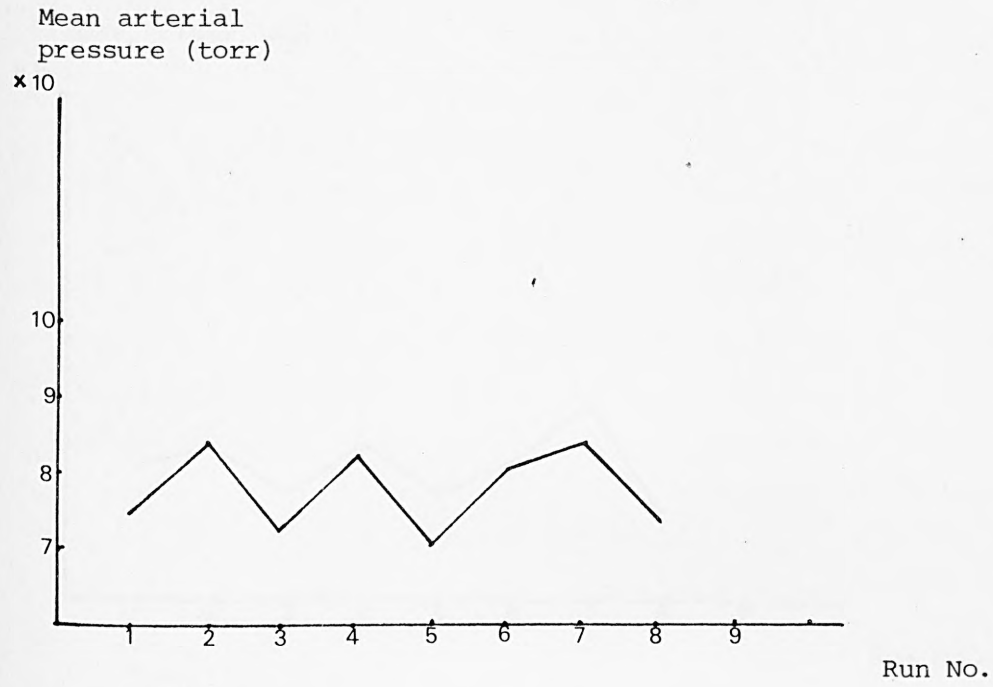

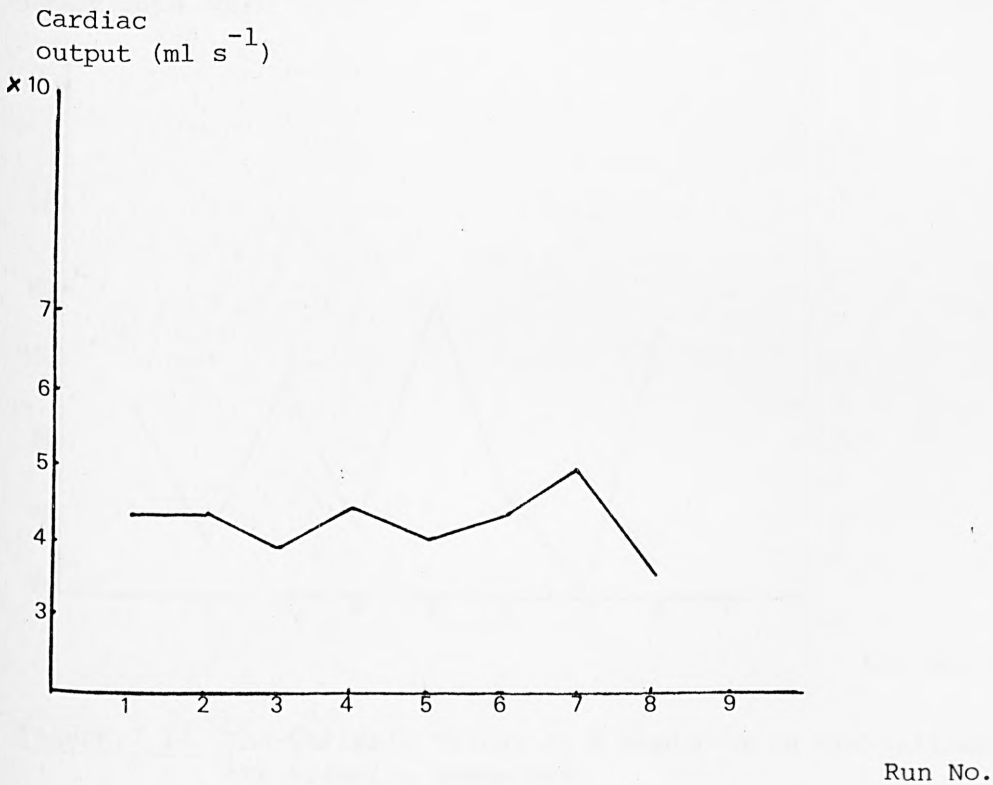

Figure 7.14 continued overleaf

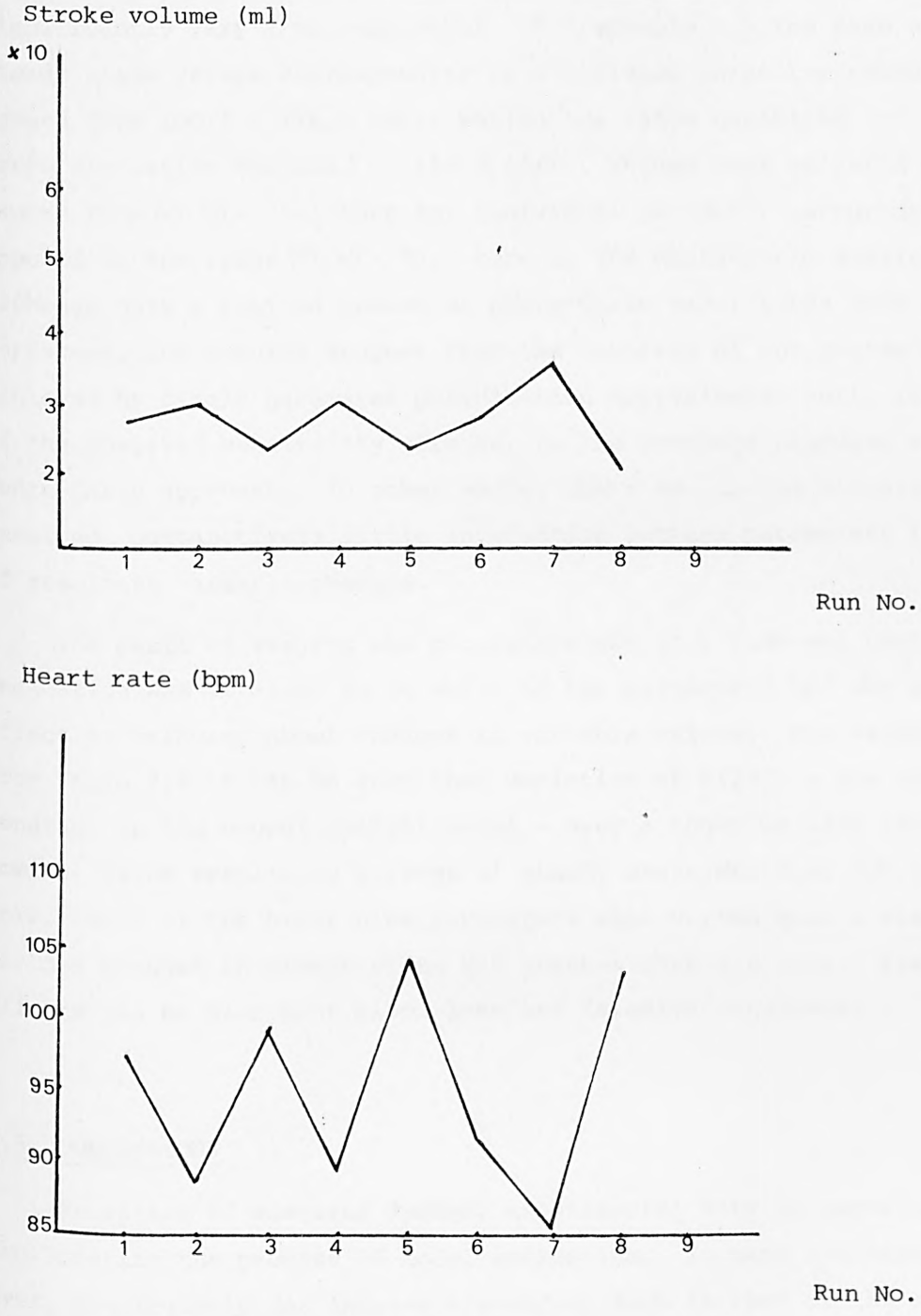

Figure 7.14 The variable values in 8 Monte-Carlo simulations of the Valsalva manoeuvre.

The range of values of the variables in the steady state and post blood loss and Valsalva manoeuvre for parameter variation, one at a time and for the Monte-Carlo simulations, is compared in Tables 7.6 - 7.9 for MAP, SV, CO and FH, respectively. In general, these ranges do not significantly vary from each other. For example, in the case of MAP, steady state values corresponding to individual parameter perturbation ranged from 100.1 - 116.8 torr, whilst the range exhibited in the Monte-Carlo simulation was 100.1 - 116.8 torr. Values post Valsalva manoeuvre ranged from 60.48 - 75.1 torr for individual parameter perturbation as opposed to the range 60.48 - 75.1 torr in the Monte-Carlo simulation. Although only a limited number of Monte-Carlo simulations have been performed, the results suggest that the coverage of the parameter space achieved by single parameter perturbation approximates well, in terms of the observed sensitivity effects, to the coverage produced by the Monte-Carlo approach. In other words, there is, in the situations examined, comparatively little interaction between parameters in terms of resultant variable changes.

The merit of varying the parameters one at a time was that a clear indication was obtained as to which of the parameters had the greatest effect in bringing about changes in variable values. For example, from Table 7.6 it can be seen that variation of P(137) - the threshold constant in the neural control model - over a range of $\pm$15% about its nominal value results in a range of steady state MAP from 100.1 - 116.8 torr. None of the other nine parameters when varied over a similar range yielded changes in steady state MAP greater than 4.2 torr. Similar effects can be seen post blood loss and Valsalva manoeuvre.

7.5 CONCLUSIONS

Provision of adequate dynamic experimental data is important in facilitating the process of model validation. In many situations, however, particularly for large-scale models such as that of the cardiovascular system considered in this thesis, data are comparatively scarce and thus such models clearly remain unidentifiable. For this class of model, one of the important techniques of validation is the use of sensitivity analysis. This chapter has described such an application of sensitivity analysis to the cardiovascular model which includes a 19-segment representation of the circulation.

Parameter in:		Pre-stimulus steady state		Post-stimulus value of MAP			
				Blood loss		Valsalva manoeuvre	
Computer program	Mathematical model	Min. value of MAP	Max. value of MAP	Min. value of MAP	Max. value of MAP	Min. value of MAP	Max. value of MAP
p(7)	P_{THN}	108.3	109.7	83.14	85.53	67.45	74.20
p(29)	a_{RAS}	108.4	109.5	83.69	84.90	66.67	67.2
p(30)	a_{RAD}	108.6	109.6	83.76	85.12	66.61	67.57
p(31)	V_{URA}	108.9	109.2	83.4	84.10	65.0	67.2
p(32)	R_{RARV}	109.1	109.0	84.25	84.38	67.0	67.31
p(34)	a_{RVS}	107.6	110.2	83.08	85.42	66.36	67.87
p(45)	V_{UPV}	106.8	111.0	80.71	87.75	65.4	69.16
p(53)	a_{LVS}	107.2	110.2	83.33	85.06	66.8	67.30
p(133)	K_{16}	108.7	109.3	83.81	85.16	64.81	69.98
p(137)	K_{18}	100.1	116.8	78.39	88.98	60.48	75.10

(a)

Pre-stimulus steady state		Post-stimulus value of MAP			
		Blood loss		Valsalva manoeuvre	
Min. value of MAP	Max. value of MAP	Min. value of MAP	Max. value of MAP	Min. value of MAP	Max. value of MAP
100.1	116.8	78.39	88.98	60.48	75.10

(b)

Table 7.6 Minimum and maximum values of mean arterial pressure (MAP) from the range of values obtained in the pre-stimulus steady state, at the lowest value post-removal of 500 ml blood, and at the end of the Valsalva manoeuvre from sensitivity analysis studies using (a) single parameter perturbation and (b) Monte-Carlo simulation.

Parameter in:		Pre-stimulus steady state		Post-stimulus value of SV			
				Blood loss		Valsalva manoeuvre	
Computer program	Mathematical model	Min. value of SV	Max. value of SV	Min. value of SV	Max. value of SV	Min. value of SV	Max. value of SV
p(7)	P_{THN}	68.82	70.43	34.46	36.38	27.67	28.17
p(29)	a_{RAS}	68.31	70.6	34.55	36.14	27.71	35.0
p(30)	a_{RAD}	68.56	71.06	34.69	36.48	25.68	27.33
p(31)	V_{URA}	69.2	69.89	35.12	36.0	26.4	29.0
p(32)	R_{RARV}	69.4	69.78	35.3	35.48	25.0	26.52
p(34)	a_{RVS}	66.5	72.20	33.7	36.95	26.21	27.39
p(45)	V_{UPV}	65.72	73.17	31.15	39.90	29.96	36.0
p(53)	a_{LVS}	66.62	71.90	34.0	36.57	28.33	35.2
p(133)	K_{16}	69.66	69.26	35.5	35.59	26.22	36.42
p(137)	K_{18}	60.02	77.62	30.61	39.45	20.52	33.61

(a)

Pre-stimulus steady state		Post-stimulus value of SV			
		Blood loss		Valsalva manoeuvre	
Min. value of SV	Max. value of SV	Min. value of SV	Max. value of SV	Min. value of SV	Max. value of SV
60.02	78.8	30.61	39.90	20.52	36.42

(b)

Table 7.7 Minimum and maximum values of stroke volume (SV) from the range of values obtained in the pre-stimulus steady state, at the lowest value post-removal of 500 ml blood and at the end of the Valsalva manoeuvre from sensitivity analysis studies using (a) single parameter perturbation and (b) Monte-Carlo simulation.

Parameter in:		Pre-stimulus steady state		Post-stimulus value of CO			
				Blood loss		Valsalva manoeuvre	
Computer program	Mathematical model	Min. value of CO	Max. value of CO	Min. value of CO	Max. value of CO	Min. value of CO	Max. value of CO
p(7)	P_{THN}	84.02	85.12	61.84	63.66	42.29	42.70
p(29)	a_{RAS}	83.73	85.3	62.06	63.34	42.56	53.4
p(30)	a_{RAD}	83.87	85.5	62.12	63.71	39.52	41.29
p(31)	V_{URA}	84.3	84.73	62.53	63.0	40.9	48.4
p(32)	R_{RARV}	84.50	84.68	62.67	62.82	40.78	54.4
p(34)	a_{RVS}	82.66	86.19	61.62	63.94	40.48	41.86
p(45)	V_{UPV}	82.29	86.72	59.53	66.02	44.57	55.0
p(53)	a_{LVS}	82.99	85.76	61.87	63.44	43.16	53.4
p(133)	K_{16}	84.45	84.76	62.44	63.2	40.48	42.92
p(137)	K_{18}	80.35	87.95	59.64	65.09	36.40	46.22

(a)

Pre-stimulus steady state		Post-stimulus value of CO			
		Blood loss		Valsalva manoeuvre	
Min. value of CO	Max. value of CO	Min. value of CO	Max. value of CO	Min. value of CO	Max. value of CO
80.35	88.7	59.53	66.02	36.04	55.0

(b)

Table 7.8 Minimum and maximum values of cardiac output (CO) from the range of values obtained in the pre-stimulus steady state, at the lowest value post removal of 500 ml blood and at the end of the Valsalva manoeuvre from sensitivity analysis studies using (a) single parameter perturbation and (b) Monte-Carlo simulation.

Parameter in:		Pre-stimulus steady state		Post-stimulus value of FH			
				Blood loss		Valsalva manoeuvre	
Computer program	Mathematical model	Min. value of FH	Max. value of FH	Min. value of FH	Max. value of FH	Min. value of FH	Max. value of FH
p(7)	P_{THN}	72.51	73.26	106.5	109.7	93.2	95.77
p(29)	a_{RAS}	72.4	73.5	106.9	109.5	95.0	96.84
p(30)	a_{RAD}	72.23	73.4	106.3	109.3	93.13	94.46
p(31)	V_{URA}	72.75	73.1	106.0	108.6	92.0	93.0
p(32)	R_{RARV}	72.81	73.1	107.6	108.2	93.0	95.25
p(34)	a_{RVS}	71.63	74.53	105.5	110.9	93.91	94.5
p(45)	V_{UPV}	71.13	75.2	100.8	116.2	90.57	96.0
p(53)	a_{LVS}	71.57	74.75	105.9	110.8	94.0	95.97
p(133)	K_{16}	73.0	73.16	103.0	108.7	93.7	95.71
p(137)	K_{18}	67.98	80.33	100.9	118.2	84.52	107.8

(a)

Pre-stimulus steady state		Post-stimulus value of FH			
		Blood loss		Valsalva manoeuvre	
Min. value of FH	Max. value of FH	Min. value of FH	Max. value of FH	Min. value of FH	Max. value of FH
67.5	88.33	100.8	118.2	84.52	107.8

(b)

Table 7.9 Minimum and maximum values of heart rate (FH) from the range of values obtained in the pre-stimulus steady state, at the highest value post-removal of 500 ml blood, and at the end of the Valsalva manoeuvre from sensitivity analysis studies using (a) single parameter perturbation and (b) Monte-Carlo simulation.

Two techniques have been adopted. The first involved perturbation of the parameters, one at a time, whilst the second involved Monte-Carlo simulation. From perturbation of the parameters one at a time, the results obtained indicated that parameter variation by $\pm$15% about the nominal value still yielded values of crucial physiological variables that were within the normal range. Such results are necessary if the model is to be deemed valid since parameter variability on this scale would be expected in a normal population. Equally, perturbation of parameters by 50%, corresponding to pathological conditions, did result in responses which were clearly abnormal.

Sensitivity analysis also revealed those parameters, change in which had the greatest effect upon system response. In all cases these are parameters which are very difficult to measure directly, if possible at all. Within this parameter set, the three having the greatest effects were K_{16} (the relative contribution of the baroreceptors to the control of the nervous system input), K_{18} (the neural gain threshold), where these are both related to the neural control system, and V_{UPV} (the unstressed pulmonary venous volume).

Uncertainty in this last parameter could give rise to uncertainty in dynamic effects associated with the filling of the left atrium. Since the other seven of the ten sensitive parameters included a number relating to elastance, uncertainty would also be expected in the model behaviour in relation to cardiac function properties.

The two most sensitive parameters K_{16} and K_{18} form a part of the neural control model which is itself highly empirical and hence one of the most uncertain areas of the whole cardiovascular system model. Model error in this neural control component is thus likely to have been the cause of a number of the non-physiological responses already described in Chapters 5 and 6. Further attention must therefore be given both to the estimation of uncertain parameters such as K_{16} and K_{18} and also to the structure of the neural control models.

The results obtained using Monte-Carlo simulation indicated that the coverage of parameter space achieved by single parameter perturbation approximated well, in terms of sensitivity effects, those yielded by this second approach, suggesting comparatively little parameter interaction.

Overall, the cardiovascular model containing the 19-segment circulatory component has been shown to have considerable heuristic validity.

Its complexity, however, renders it cumbersome for use in other than very short-term experiments. For use in a predictive mode , for example, a simpler realisation would be required. The problem of model reduction is considered in Chapter 8, after which a reduced model of cardiovascular system will be developed and tested.

CHAPTER 8

CARDIOVASCULAR MODEL REDUCTION

8.1 INTRODUCTION

Having undertaken in the previous chapters a comprehensive review of the validity of the cardiovascular system model incorporating the 19-segment circulatory component, it was clear that a large pulsatile model such as that had considerable heuristic potential. Its complexity, however, was such that it required very substantial computer time and hence could only be used for examining very short-term events. In order either to be capable of being run on a smaller computer or to facilitate longer term simulations, a more compact form of model would be required.

In this chapter the problem of model reduction is examined, first reviewing briefly available techniques for reduction and then examining their applicability to the large-scale cardiovascular system model already described. The aim was to achieve a more compact, yet still pulsatile, representation of the circulation and its control systems.

8.2 MODEL REDUCTION TECHNIQUES

Many sophisticated procedures have been developed for the reduction of high order models to lower order form.

The major types of technique used for model reduction are: dominant model reduction (e.g. Davison (1966)), continued fraction expansion, developed by Chen and Shieh (1968), projection methods (Anderson, 1967), simplification using moments (e.g. Bosley and Lees (1972)), and model reduction by time or frequency response matching (Sinha and Pille (1971)).

These techniques have been reviewed by Carson (1975) and Cesarcyzk (1981). In essence they involve either the reduction of full transfer function or state space representation to simpler forms or of the determination of the parameters of an equivalent reduced transfer function from the impulse, step or frequency response of the full model.

These methods are applicable either to linear systems or to non-linear systems for which linearised models are deemed appropriate.

However, the objectives of the reduction process vary according to the nature of the particular application. These may include the requirement that the reduced model should approximate the system in a specified sense according to the definition of adequacy chosen; that the risk or cost function should be less than a specified level or that the reduced model should satisfy certain constraints (Carson, 1975).

In the case of the cardiovascular system, those methods which simply produce a low order representation to describe available input/output data cannot be applied in the reduction process, since there is the requirement to preserve as far as possible a physiological structure and for that structure to have parameters whose values are physiologically meaningful. This requirement for the model to be "physiological", coupled with the essential non-linear nature of the cardiovascular system, means that it is inappropriate to apply any of the reduction techniques referred to above.

Approaches which are applicable here are increasing the step length adopted in the integration subroutine used to produce the model output, further aggregation of the compartmental representation and dynamic reduction. These approaches are described in the following section.

The other practicable approach is rather than producing a single reduced model, to develop a suite of compact models, each of which is capable of representing a limited number of aspects of system behaviour.

8.3 REDUCTION OF THE NINETEEN-SEGMENT CIRCULATORY MODEL

The detailed, pulsatile mathematical model of the human cardiovascular system and its control mechanisms, described earlier in Chapter 3, is appropriate for testing hypotheses regarding physiological function and short-term overall effects of drug administration.

If a model of the cardiovascular system is to be used as a teaching tool or for on-line patient-monitoring application, however, it must of necessity be sufficiently small in order that it may be implemented on a small computer and operate in or better than real-time. Thus a preliminary study has been carried out with a view to reducing the full model to a simpler form in which it would operate in close to real-time and yet still maintain physiologically meaningful parameters. Some of the results of the investigation are given below.

8.3.1 Integration Step Length

As reduction of the execution time of the simulation is one of the major objectives, increased integration step lengths have been tried. Limitations arise from the stiff nature of the differential equations if numerical instability is to be avoided. Nevertheless, the execution time of the 42nd order model of the controlled blood circulation has been successfully reduced from 39 seconds (Pullen, 1976) to 15 seconds on the CDC 7600 computer to reach t = 100 seconds in the solution without appreciable loss of accuracy (Al Dahan et al, 1979).

8.3.2 Aggregation of Segments

In view of the non-linearities involved, the degree of aggregation of segments that is possible in the model is limited. As a first stage of aggregation, the aortic arch and thoracic aorta were represented by an equivalent single segment. (In doing this, it was necessary to consider this aggregated segment as the aortic arch baroreceptor area for the determination of the baroreceptor output function in the neural control model.) The two venae cavae were grouped together as were the abdominal and leg arteries into a single compartment and similar treatment of the abdominal and leg veins. Thus the nineteen segments of the original model were reduced to fifteen.

Whilst simulation of this reduced model yielded results which were within acceptable physiological limits, no appreciable reduction in execution time was achieved. Further aggregation was therefore considered. This involved aggregating all three segments representing the aorta and considering the pressure in this segment as the arterial pressure. As in the model developed by Beneken (1965), the right atrium was lumped with the venae cavae and the left atrium with the pulmonary veins. This approach resulted in the reduction of the model to one comprising twelve segments. Little further reduction in execution time was achieved by this additional aggregation, however, and with the exception of the systolic arterial pressure, the critical physiological variables in the computer simulation were not within acceptable limits for an average human.

8.3.3 Dynamic Reduction

Given the unsatisfactory nature of aggregation of segments in seeking to reduce the model of the cardiovascular system, dynamic

reduction was then attempted. This would have the effect of reducing to pure gains very rapid time constants and neglecting the effects of dynamics, the time constants of which were long relative to the period 0 - 2 minutes which the full model was developed to simulate. The smallest time constants in the model were found to be variable, however, because of the non-linearities introduced by the pulmonary and aortic valves. Each of the time constants relating to flow through the pulmonary and aortic valves was found to have its minimum value only for a short period in each cardiac cycle when the flow reached its maximum value. Therefore it was not possible to neglect any fast dynamics. The slowest dynamics of the model were not longer than the time scale of the model. They were, however, found to be automatically neglected by the aggregation of segments.

8.3.4 Model of Neural Control

Dynamic reduction has also been applied to the model of the heart rate controller, reducing its dynamics from second to first order. The results of the use of only the aortic arch baroreceptor in the neural control model show that it can be made use of for the neural control of circulatory models which do not have a separate segment representing the upper parts arteries in which the carotid sinus baroreceptors are thought to be situated. There is, however, little appreciable reduction in execution time resulting from this procedure. Other controllers of the neural control model are not amenable to dynamic reduction.

8.4 ASPECT MODELS

Given the difficulties inherent in producing a generalised reduced model from the complex non-linear one developed by Pullen (1976), various reduced "aspect" models have been developed, each being appropriate as a representation of certain specific behavioural features of the cardiovascular system. Results obtained to date suggest that the most successful approach to the development of such reduced models is to start from the beginning by formulating a conceptual structural model for the well-defined purpose for which it is to be used and then developing the mathematical model making use of the approach used in the full model with appropriate modifications and simplifications wherever necessary. One example of such aspect models is given below.

8.4.1 Seven-Segment Lumped-Parameter Model of the Uncontrolled Circulation

A simple conceptual structural model of the cardiovascular system which possesses most of the essential anatomical and physiological features is the 7-segment representation shown in Figure 8.1. Neglecting the inertial properties of blood, each segment can be described by one differential and two algebraic equations. The complete mathematical model is then:

Right ventricle

$$\frac{dV_{RV}}{dt} = F_{VCRV} - F_{RVPA} \tag{8.1}$$

$$P_{RV} = a_{RV}.V_{RV} \tag{8.2}$$

$$F_1 = \left(P_{RV} - P_{PA}\right)/R_{RVPA} \tag{8.3}$$

$$F_{RVPA} = \begin{cases} F_1 , & F_1 > 0 \\ 0 , & F_1 \leq 0 \end{cases} \tag{8.4}$$

Pulmonary arteries

$$\frac{dV_{PA}}{dt} = F_{RVPA} - F_{PAPV} \tag{8.5}$$

$$P_{PA} = V_{PA}/C_{PA} \tag{8.6}$$

$$F_{PAPV} = \left(P_{PA} - P_{PV}\right)/R_{PAPV} \tag{8.7}$$

Pulmonary veins

$$\frac{dV_{PV}}{dt} = F_{PAPV} - F_{PVLV} \tag{8.8}$$

$$P_{PV} = V_{PV}/C_{PV} \tag{8.9}$$

$$F_2 = \left(P_{PV} - P_{LV}\right)/R_{PVLV} \tag{8.10}$$

$$F_{PVLV} = \begin{cases} F_2 , & F_2 > 0 \\ 0 , & F_2 \leq 0 \end{cases} \tag{8.11}$$

Left ventricle

$$\frac{dV_{LV}}{dt} = F_{PVLV} - F_{LVAO} \tag{8.12}$$

$$P_{LV} = a_{LV}.V_{LV} \tag{8.13}$$

$$F_3 = \left(P_{LV} - P_{AO}\right)/R_{LVAO} \tag{8.14}$$

$$F_{LVAO} = \begin{cases} F_3 & , \quad F_3 > 0 \\ 0 & , \quad F_3 \leq 0 \end{cases} \tag{8.15}$$

Aorta

$$\frac{dV_{AO}}{dt} = F_{LVAO} - F_{AOSC} \tag{8.16}$$

$$P_{AO} = V_{AO}/C_{AO} \tag{8.17}$$

$$F_{AOSC} = \left(P_{AO} - P_{SC}\right)/R_{AOSC} \tag{8.18}$$

Systemic circulation

$$\frac{dV_{SC}}{dt} = F_{AOSC} - F_{SCVC} \tag{8.19}$$

$$P_{SC} = V_{SC}/C_{SC} \tag{8.20}$$

$$F_{SCVC} = \left(P_{SC} - P_{VC}\right)/R_{SCVC} \tag{8.21}$$

Vena cava

$$\frac{dV_{VC}}{dt} = F_{SCVC} - F_{VCRV} \tag{8.22}$$

$$P_{VC} = V_{VC}/C_{VC} \tag{8.23}$$

$$F_4 = \left(P_{VC} - P_{RV}\right)/R_{VCRV} \tag{8.24}$$

$$F_{VCRV} = \begin{cases} F_4 & , \quad F_4 > 0 \\ 0 & , \quad F_4 \leq 0 \end{cases} \tag{8.25}$$

This model incorporates the time-varying elastances of the right and left ventricles as adopted in the full model described in Chapter 3 and also the increased diastolic compliance as in the case of the aggregated 12-segment model of Section 8.3.2 (Pullen, 1976). Data used in simulating this model are based on the studies of Benham (1972).

The selected simulation results presented in Figure 8.2 agree well with the general features of comparable physiological data, indicating that the assumptions made for the purpose of simplifying the model do not necessarily limit its effectiveness. A model of comparable complexity has been used by Rupeiks (1972) as a basic research and teaching tool for the simulation of congenital heart defects such as: ventricular septal defect, patent ductus arteriosus, stenosis and insufficiency of each of the four heart valves.

8.5 CONCLUSION

Having reviewed existing methods of model reduction, it is clear that most of them are inappropriate for application to complex physiological models such as are the subject of this thesis.

Two types of approach are applicable. The first involves taking a complex physiological model and systematically reducing it to a simpler form such that the relevant a priori physiological basis is still included, consistent with the purpose for which the model is intended. In doing this, results obtained from sensitivity analysis and other techniques of model validation may constitute a useful aid. The second approach is to begin afresh with a simple formulation, such that sufficient physiology is incorporated consistent with the model providing an adequate representation of specific aspects of behaviour.

Reduction procedures have been applied to the cardiovascular model which incorporates the 19-segment representation of the circulation. From the validation studies described in Chapters 4 - 6, it had been shown that short-term model behaviour was most sensitive to CNS control and to cardiac and pulmonary venous parameters. This suggested that the circulatory model could be greatly simplified by aggregating a number of the systemic arterial and venous compartments. An example of such aggregation resulting in a 7-segment model of the uncontrolled circulation has been presented.

In the next chapter an 8-segment model of the circulation, to which control loops and thermoregulatory and body-fluid components are added, is developed. This includes a reduced representation of neural control with a single pressure receptor and a single stretch receptor.

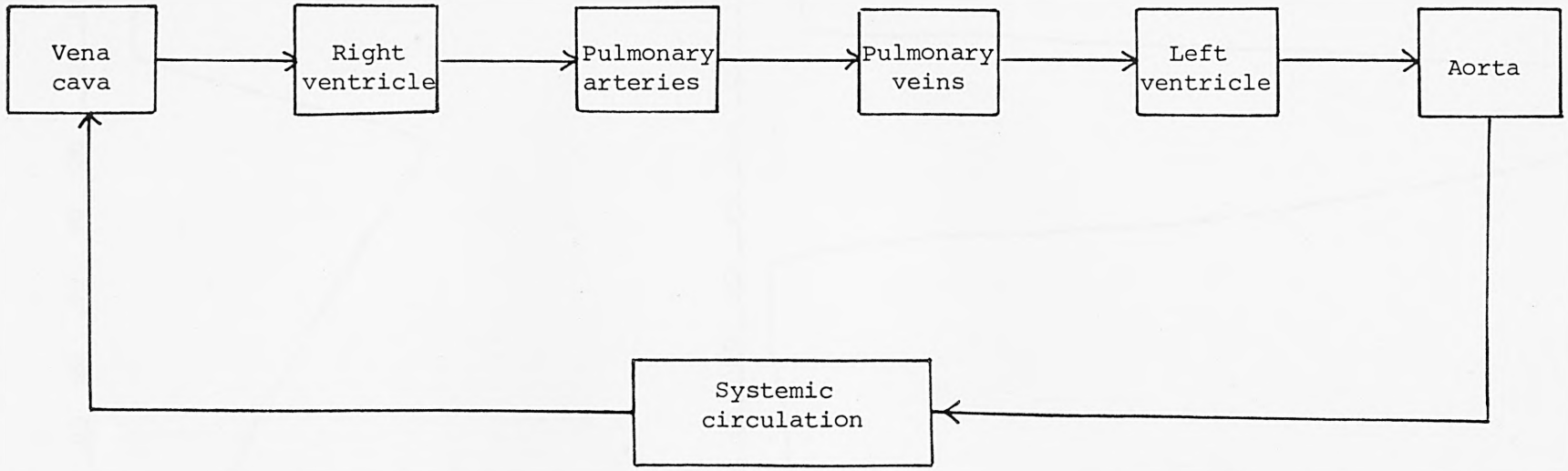

Figure 8.1 7-segment lumped parameter model.

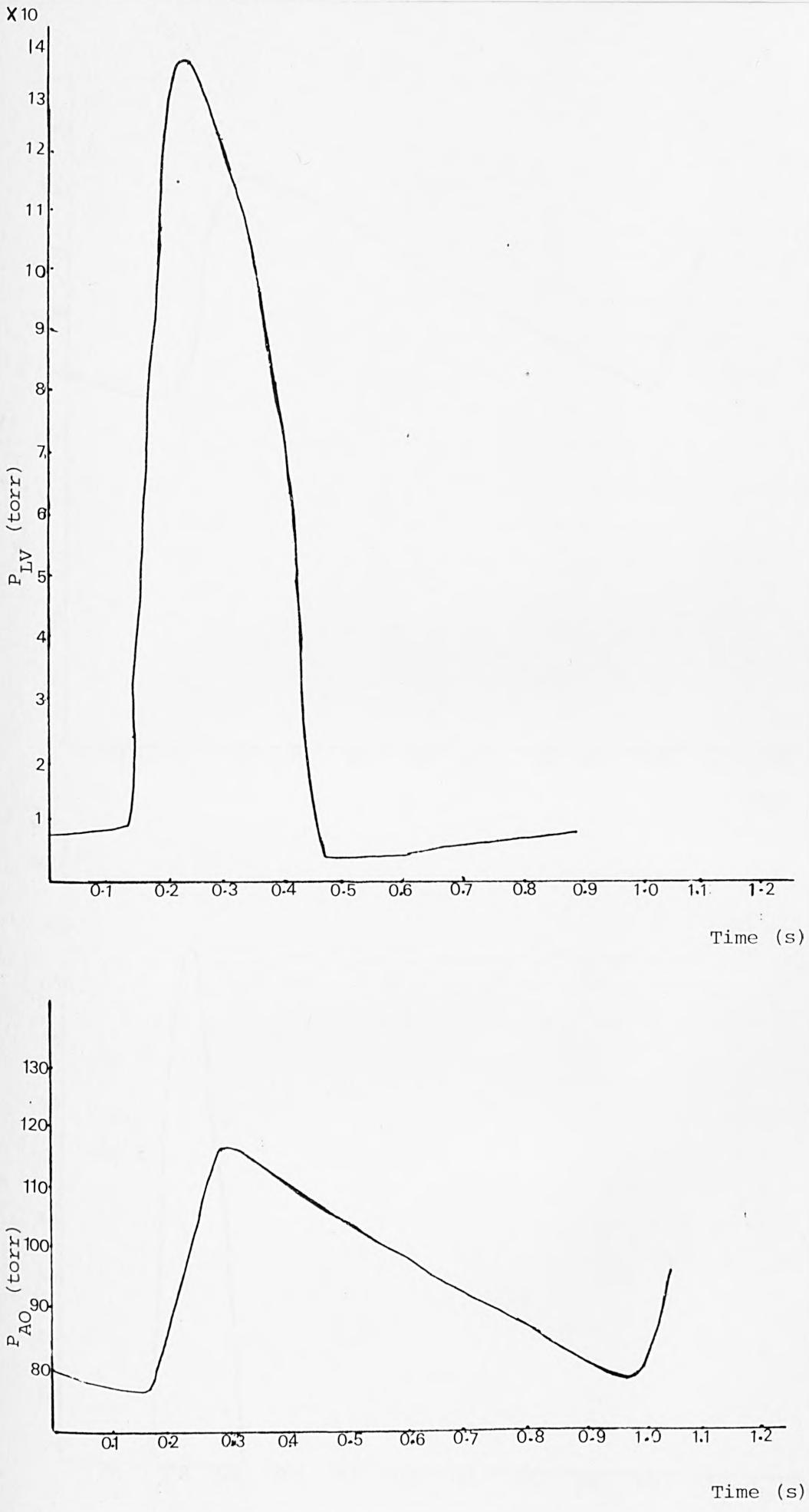

Figure 8.2a Waveforms of selected pressures during one cardiac cycle.

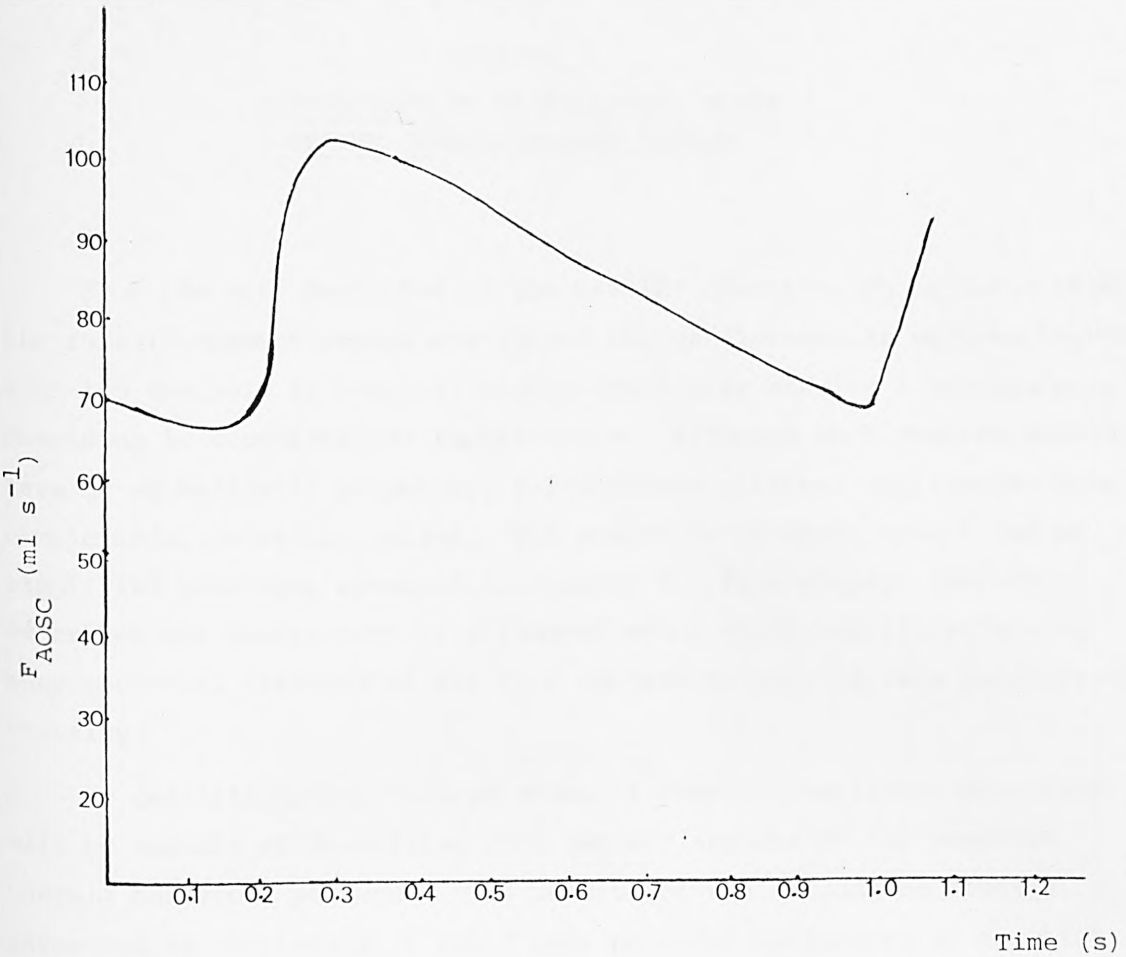

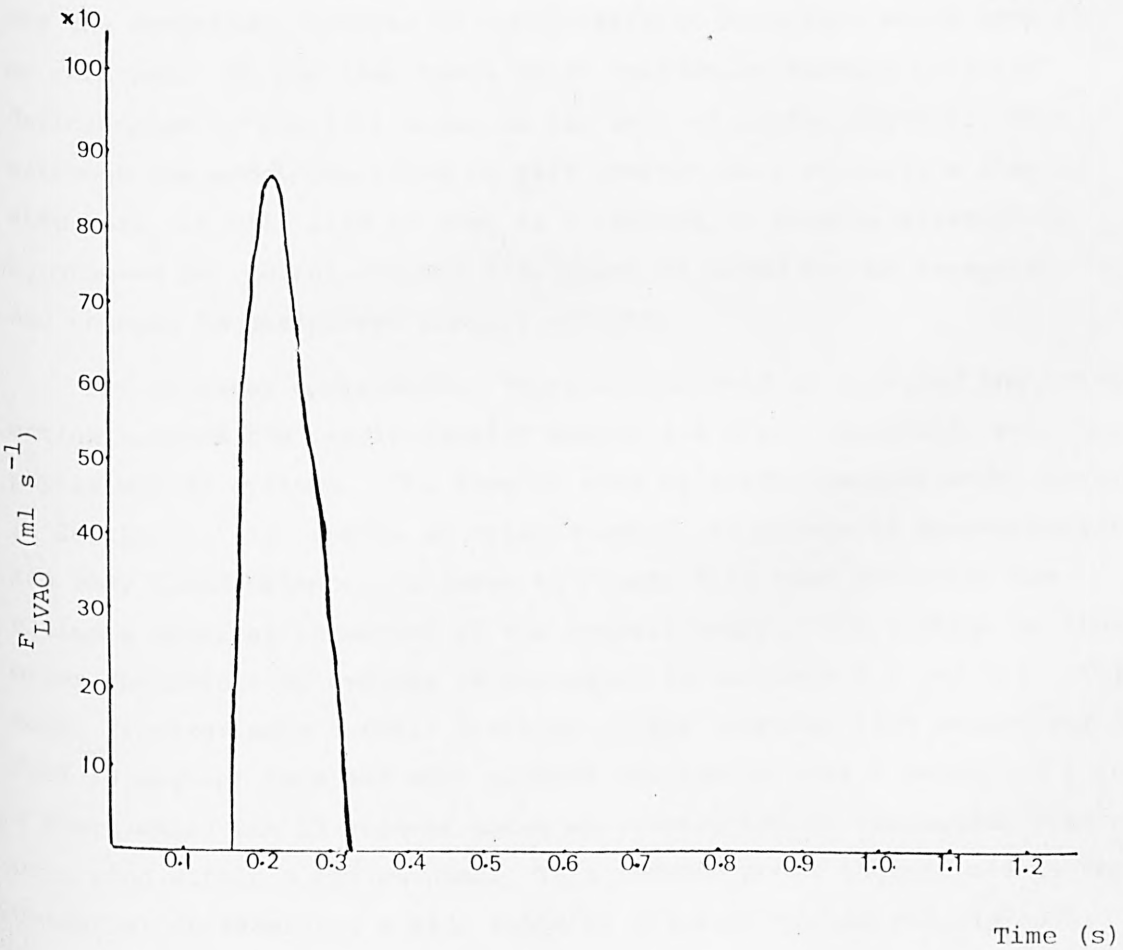

Figure 8.2b Waveforms of selected volumes during one cardiac cycle.

CHAPTER 9

DEVELOPMENT OF AN 8-SEGMENT MODEL OF THE CARDIOVASCULAR SYSTEM

From the work described in the earlier chapters, it is clear that the full 19-segment representation of the cardiovascular systems together with its controls is complex, highly non-linear and, as a consequence, demanding in computational requirements. Although such complex models have great heuristic potential, for ultimate clinical application more simple model forms are needed. The processes by which models can be simplified have been examined in Chapter 8. This chapter therefore describes the development of a reduced model which, whilst retaining many essential features of the full representation, is less computationally unwieldy.

By definition, any reduced model of complex non-linear processes will be capable of describing only certain aspects of the complete overall behaviour patterns. The results of the validation studies presented in Chapters 5, 6 and 7 have provided indicators as to which are the essential features of cardiovascular structure which need to be retained. At the same time, these validation studies revealed deficiencies in the full model in the area of neural control. Thus although the model described in this chapter has, overall, a simpler structure, it will also be used as a vehicle to examine alternative hypotheses for neural control (inclusion of blood volume receptors and changes in peripheral control effects).

For clinical application, there is the need to consider the interaction between the cardiovascular system and other important, relevant physiological systems. The simpler form of cardiovascular model developed in Section 9.1 is capable of being coupled to models of thermoregulation and body fluid balance, as shown in Figure 9.1, thus enhancing the ultimate clinical potential of the overall model. The linkage to these other physiological systems is described in Sections 9.2 and 9.3. This model requires only a small fraction of the computer time needed for the full 19-segment form and thus affords simulation over a period of 1 to 2 hours where the 19-segment model was restricted to simulating phenomena occurring within a few minutes. This reduced model thereby offers the potential of examining a wide range of clinical trends and, as such, complements the capability of the full pulsatile model described earlier.

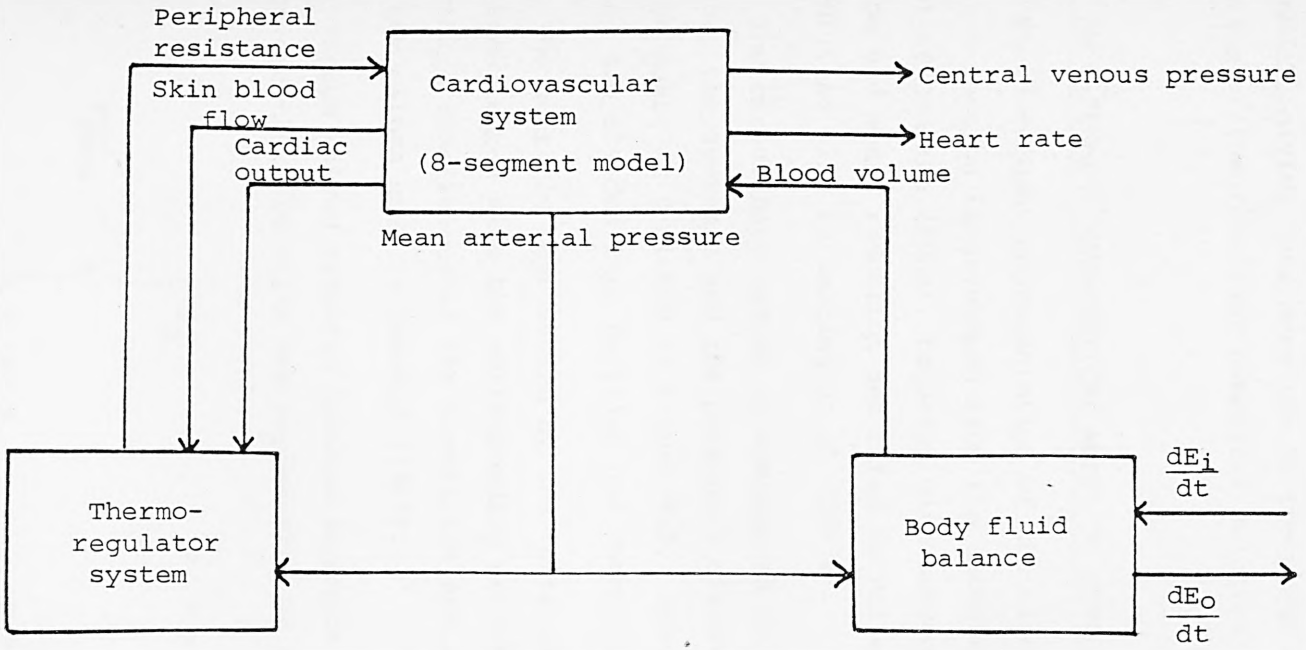

Figure 9.1 Interaction of a reduced circulatory system model with models of thermoregulation and body fluid balance.

Section 9.4 describes the modelling of central nervous control mechanisms in the reduced formulation, in particular testing a hypothesis relating to the effect of volume receptors in the controlling process. Sections 9.5 and 9.6 deal with the digital implementation of the model, giving consideration to the program structure and the accuracy of the resultant numerical solutions.

9.1 AN 8-SEGMENT MATHEMATICAL MODEL OF CIRCULATORY FLUID MECHANICS

The 8-segment representation of the circulatory system presented in this section is developed from the uncontrolled circulatory system model of Beneken (1965), together with subsequent work on model formulation and model reduction described in Pullen (1976) and Rajkumar (1978), and also in Leaning et al (1983b).

The circulatory system is considered to be subdivided into four parts: the systemic and the pulmonary circulation and the two sides of the heart as depicted in Figure 9.2. Systemic and pulmonary circulation are divided into arterial and venous segments.

The heart is represented by the ventricles only and the atria are each lumped with the corresponding neighbouring segment. The diastolic compliances of the ventricles are increased accordingly to the new values used by Beneken (1965).

Venous valves situated between segments representing systemic veins and thoracic veins are represented by the following equation:

$$F_{SVTV} = \begin{cases} F_2 & , \quad F_2 > 0 \\ 0.667\, F_2 & , \quad F_2 \leq 0 \end{cases} \tag{9.1}$$

where F_2 is the flow assuming no valve is present.

The mathematical model of the circulatory fluid mechanics, consisting of 11 first order differential equations, is given below:

Right ventricle

$$\frac{dV_{RV}}{dt} = F_{TVRV} - F_{RVPA} \quad , \quad V_{RV} \geq 0 \tag{9.2}$$

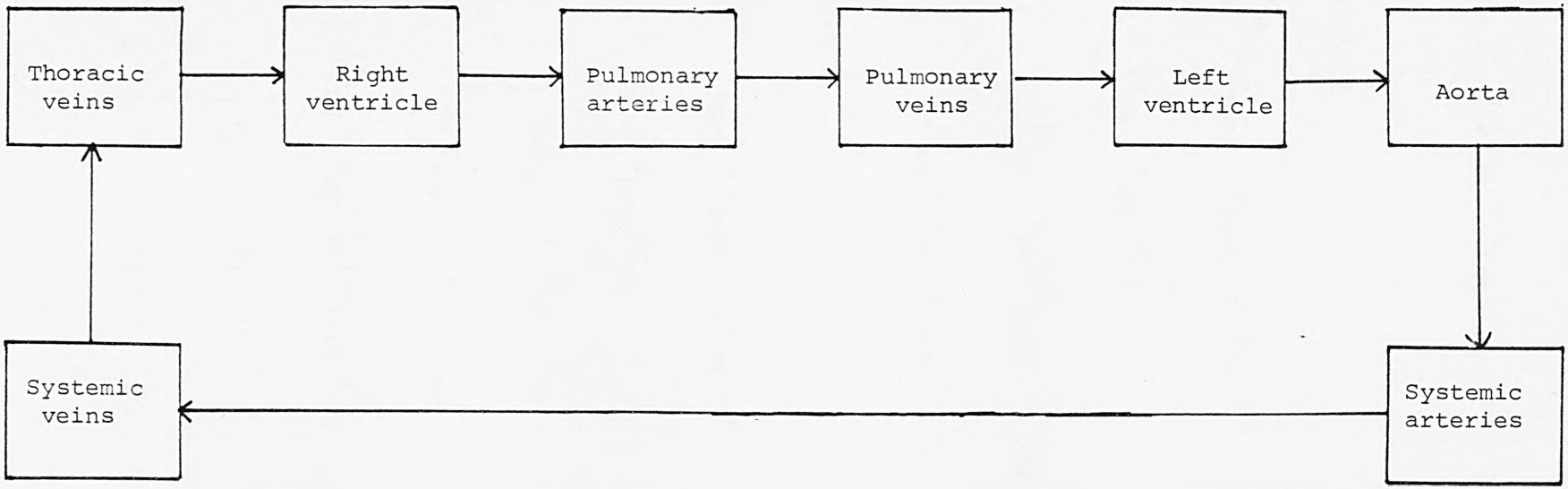

Figure 9.2 8-segment lumped parameter model.

$$\frac{dF_{RVPA}}{dt} = \frac{P_{RV} - P_{PA} - R_{RVPA}F_{RVPA} - \left(\frac{\rho}{2A_{PA}^2}\right) F_{RVPA}^2}{L_{RV}} \quad , \; F_{RVPA} \geq 0 \tag{9.3}$$

$$P_{RV} = a_{RV}\left(V_{RV} - V_{URV}\right) \tag{9.4}$$

Pulmonary arteries

$$\frac{dV_{PA}}{dt} = F_{RVPA} - F_{PAPV} \quad , \quad V_{PA} \geq 0 \tag{9.5}$$

$$P_{PA} = \left(V_{PA} - V_{UPA}\right)/C_{PA} \tag{9.6}$$

$$F_{PAPV} = \begin{cases} \left(P_{PA} - P_{PV}\right)/R_{LUNG} & , \; P_{PV} > P_{CC} \\ \left(P_{PA} - P_{CC}\right)/R_{LUNG} & , \; P_{PV} \leq P_{CC} \end{cases} \tag{9.7}$$

Pulmonary veins

$$\frac{dV_{PV}}{dt} = F_{PAPV} - F_{PVLV} \quad , \quad V_{PV} \geq 0 \tag{9.8}$$

$$P_{PV} = \left(V_{PV} - V_{UPV}\right)/C_{PV} \tag{9.9}$$

$$C_{PV} = \begin{cases} C_{PVN} & , \; V_{PV} > V_{UPV} \\ 20\, C_{PVN} & , \; V_{PV} \leq V_{UPV} \end{cases} \tag{9.10}$$

$$F_1 = \left(\left(P_{PV} - P_{LV}\right)V_{PV}^2\right)/R_{PVLV}\, V_{UPV}^2 \tag{9.11}$$

$$F_{PVLV} = \begin{cases} F_1 & , \; F_1 > 0 \\ 0 & , \; F_1 \leq 0 \end{cases} \tag{9.12}$$

Left ventricle

$$\frac{dV_{LV}}{dt} = F_{PVLV} - F_{LVAO} \quad , \quad V_{LV} \geq 0 \tag{9.13}$$

$$\frac{dF_{LVAO}}{dt} = \frac{P_{LV} - P_{AO} - R_{LVAO}F_{LVAO} - \left(\frac{\rho}{2A_{AO}^2}\right)F_{LVAO}^2}{L_{LV}} \quad , \quad F_{LVAO} \geq 0 \tag{9.14}$$

$$P_{LV} = a_{LV}\left(V_{LV} - V_{ULV}\right) \tag{9.15}$$

Aorta

$$\frac{dV_{AO}}{dt} = F_{LVAO} - F_{AOSA} \quad , \quad V_{AO} \geq 0 \tag{9.16}$$

$$\frac{dF_{AOSA}}{dt} = \left(P_{AO} - P_{SA} - R_{SA}F_{AOSA}\right)/L_{SA} \tag{9.17}$$

$$P_{AO} = \frac{V_{AO} - V_{UAO} + 0.04\left(F_{LVAO} - F_{AOSA}\right)}{C_{AO}} \tag{9.18}$$

Systemic arteries

$$\frac{dV_{SA}}{dt} = F_{AOSA} - F_{SASV} \quad , \quad V_{SA} \geq 0 \tag{9.19}$$

$$P_{SA} = \frac{V_{SA} - V_{USA} + 0.04\left(F_{AOSA} + \frac{P_{SV}}{R_{SYS}\ q_4}\right)}{C_{SA} + \left(\frac{0.04}{R_{SYS}\ q_4}\right)} \tag{9.20}$$

$$F_{SASV} = \left(P_{SA} - P_{SV}\right)/R_{SYS}\ q_4 \tag{9.21}$$

Systemic veins

$$\frac{dV_{SV}}{dt} = F_{SASV} - F_{SVTV} \quad , \quad V_{SV} \geq 0 \tag{9.22}$$

$$P_{SV} = d_3 \left(V_{SV} - V_{USV} \right) / C_{SV} \tag{9.23}$$

$$C_{SV} = \begin{cases} C_{SVN} & , \quad V_{SV} > V_{USV} \\ 20\ C_{SVN} & , \quad V_{SV} \leq V_{USV} \end{cases} \tag{9.24}$$

$$V_{USV} = \frac{V_{USVN}}{d_4} \tag{9.25}$$

$$F_2 = \left(\left(P_{SV} - P_{TV} \right) V_{SV}^2 \right) / R_{SV}\ V_{USVN}^2 \tag{9.26}$$

$$F_{SVTV} = \begin{cases} F_2 & , \quad F_2 > 0 \\ 0.667\ F_2 & , \quad F_2 \leq 0 \end{cases} \tag{9.27}$$

Thoracic veins

$$\frac{dV_{TV}}{dt} = F_{SVTV} - F_{TVRV} \quad , \quad V_{TV} \geq 0 \tag{9.28}$$

$$P_{TV} = \left(V_{TV} - V_{UTV} \right) / C_{TV} \tag{9.29}$$

$$C_{TV} = \begin{cases} C_{TVN} & , \quad V_{TV} > V_{UTV} \\ 20\ C_{TVN} & , \quad V_{TV} \leq V_{UTV} \end{cases} \tag{9.30}$$

$$F_3 = \left(\left(P_{TV} - P_{RV} \right) V_{TV}^2 \right) / R_{TVRV}\ V_{UTV}^2 \tag{9.31}$$

$$F_{TVRV} = \begin{cases} F_3 & , \quad F_3 > 0 \\ 0 & , \quad F_3 \leq 0 \end{cases} \tag{9.32}$$

The implementation of this model of the circulation, coupled to

the models of neural control, thermoregulation and body fluid balance, described in the sections which follow, is considered in Section 9.6.

9.2 THERMOREGULATORY SYSTEM MODEL

The thermoregulatory system model, which is to be coupled to the eight-segment circulatory system model described in the previous section, relies on the concepts of hypothalamic set-point theory for the control of deep body temperature. Control is effected by vasomotor adjustment of the rate of blood flow from the core to the surface of the body. Figure 9.3 shows the conceptual model of this set-point theory of thermoregulation. The temperatures in the core and at the surface of the body are sensed by thermoreceptors, and signals representing these temperatures are transmitted to the hypothalamus. These signals are compared with the hypothalamic 'set-point' temperatures, and signals representing the differences between the actual and set-point temperatures are transmitted to the vasomotor centre of the central nervous system. Appropriate sympathetic or parasympathetic stimulation causes a change in the rate of blood flow, and therefore heat transfer, from the core to the surface of the body. An increase in the rate of blood flow results in an increase in the temperature of the surface of the body and subsequently an increase in the rate of heat loss from the surface of the body to the environment. The converse is also true.

The overall thermoregulatory system model, based on the approach adopted by Uttamsingh et al (1977), is divided into two sections, a controlled thermoregulatory model and a thermoregulatory system controller.

9.2.1 Thermoregulatory Model (The Controlled System)

The model of the controlled thermoregulatory system consists of two compartments representing the human body as a core and surface system with heat transfer between core and surface and between surface and the environment, as shown in Figure 9.4. In this representation, it is assumed that the human body may be considered as two homogeneous concentric cylinders, each with uniformly distributed temperatures, where the surface cylinder represents the outer two-centimetre layer of the body, and the core cylinder represents the remainder.

The heat generation rate is simply the constant basal metabolic rate, and is totally assigned to the core. Heat transfer from the core to the surface is achieved by:

(i) conduction,

(ii) heat transfer due to blood flow from core to skin.

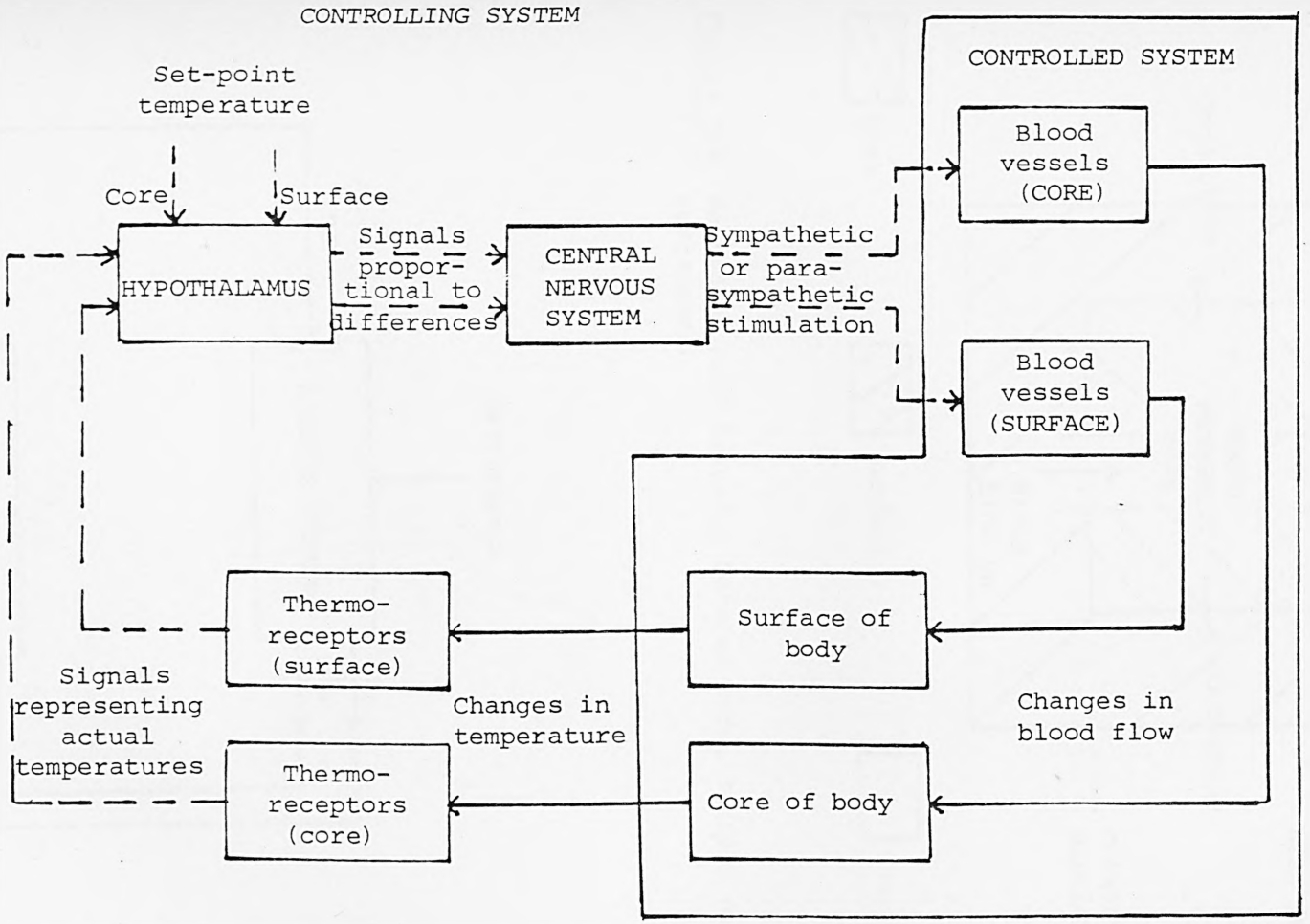

Figure 9.3 Diagram representing the "set-point" theory of the human thermoregulatory system.

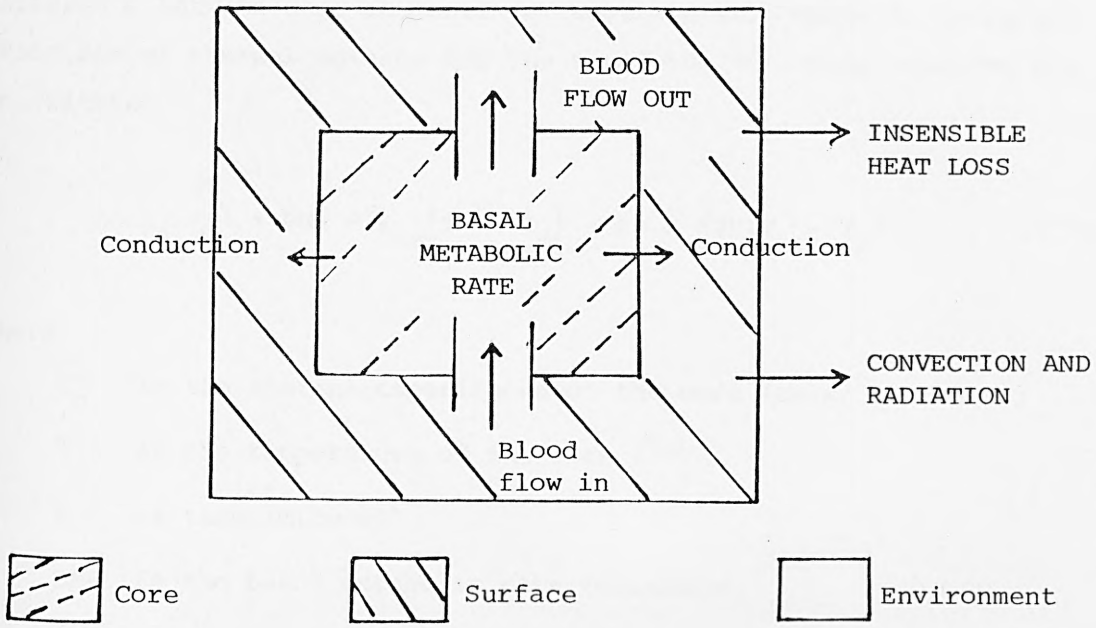

Figure 9.4 Method of heat transfer between core, surface and environment.

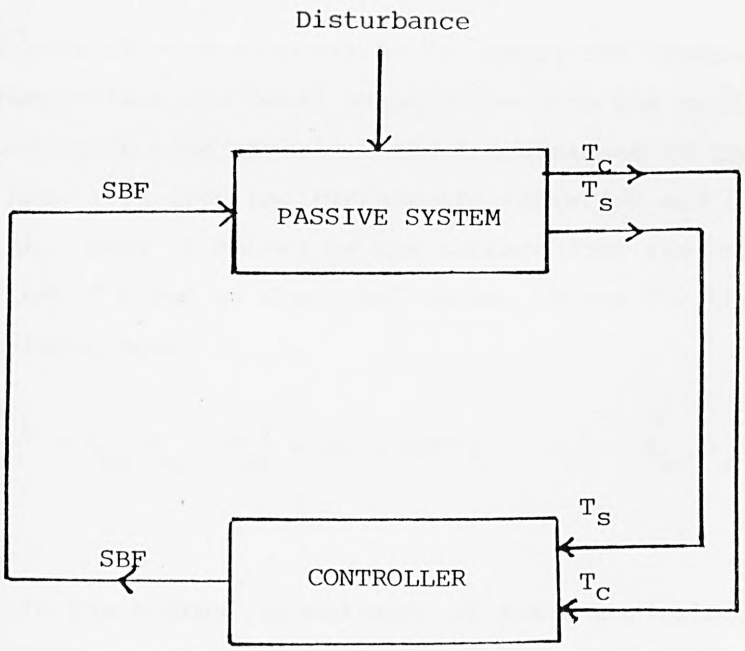

Figure 9.5 Configuration of the passive system and controller in the thermoregulatory model.

Blood temperature is assumed to be equal to core temperature so that in both cases heat transferred per unit time is proportional to the difference between core and surface temperatures. Hence in using the principle of thermal balance for the core, the following equation may be written:

$$C_c \frac{dT_c}{dt} = BMR - K_{cs}(T_c - T_s) - \rho c \times SBF(T_c - T_s) \qquad (9.33)$$

where

C_c is the thermal capacitance of the core (cals/^oC)

T_c is the temperature of the core (^oC)

t is time (minutes)

BMR is the basal metabolic rate (cals/min)

K_{cs} is the thermal conductance between core and skin (cals/min/^oC)

T_s is the temperature of the surface (^oC)

ρc is the product of density and specific heat of blood (cals/^oC)

SBF is skin blood flow calculated each minute by the controller (l/min).

Heat loss through evaporation is simply the insensible heat loss through respiration and basal evaporation from the skin, both of which are assumed to be time invariant and are assigned to the surface. Other forms of heat loss from the surface are radiation and convection to the environment. Heat is gained by the surface from the core by conduction and the flow of blood as described above. Hence for the body, the thermal balance equation is:

$$C_s \frac{dT_s}{dt} = K_{cs}(T_c - T_s) + \rho c \times SBF(T_c - T_s) - K_{sE}(T_s - T_E) - IHL \qquad (9.34)$$

where

C_s is the thermal capacitance of the surface (cals/^oC)

K_{sE} is the surface to environmental heat transfer coefficient accounting for radiation and convection (cals/^oC/min)

T_E is the environmental temperature (^oC)

IHL is the insensible heat loss (cals/min)

The values adopted for these parameters, derived by Uttamsingh et al (1977) from earlier work by Stolwijk et al (1966) are:

C_c	=	45040.0	cals/^oC
BMR	=	1167.0	cals/min
K_{cs}	=	405.67	cals/min/^oC
ρc	=	920.0	cals/^oC
C_s	=	12730.0	cals/^oC
K_{sE}	=	100.0	cals/min/^oC
IHL	=	300.0	cals/min

9.2.2 The Thermoregulatory System Controller

The passive (controlled) model of the thermoregulatory system as described above does not, by itself, exhibit control characteristics, but simply provides a transfer function relating surface blood flow or any disturbing input to the core and skin temperatures as outputs which, in turn, constitute the inputs to the controller, as shown in Figure 9.5. It is this controller which regulates the body temperature by adjusting the rate of blood flow from the core to the surface of the body.

As referred to earlier in the chapter, the hypothalamus receives signals from thermoreceptors in the body, some in the brain and spine, and some just under the surface of the body. These signals are compared with desired or set-point temperatures in the hypothalamus which then transmits signals proportional to the differences between actual and set-point temperatures in order to cause the central nervous system to constrict or dilate blood vessels so that the resultant blood flows cause the temperatures to tend towards their set-point values (see Figure 9.3).

When the body needs to dissipate heat (when core temperature rises above the set-point), peripheral blood vessels are caused to vasodilatate, permitting a larger flow of warm arterial blood to the surface of the body. Hence, the temperature at the surface of the body rises, and results in the increase in the rate of transfer of heat to the environment. Thus the temperature at the core of the body is returned towards the set-point. When the body needs to conserve heat, the converse effects are observed, brought about by vasoconstriction of the peripheral blood vessels (Uttamsingh et al, 1977).

Vasodilatation or vasoconstriction may be considered as the decrease or increase in the resistance to the flow of blood in the surface of the body.

Hence the blood flow is adjusted by changes in total peripheral resistance, which is also affected by other factors, such as concentration of pressor substances which, in turn, affect blood flow.

Figure 9.6 presents a simple electrical analogy of this concept. The pressure drop, MAP, forces blood through the resistances, R_c and R_s, representing the resistances to blood flow through the core and surface blood vessels, respectively. Hence, of the total rate of blood flow, CO, the rate at which blood flows through the surface blood vessels, SBF, is dependent on the relative values of the two resistances, R_c and R_s. For the development of the model for the controller in the human thermoregulatory system, the resistance to blood flow through the core of the body is assumed to be constant, whereas the resistance to blood flow through the surface blood vessels is considered to be a function of the passive thermoregulatory system model.

Using this analogy and assuming normal values of arterial pressure (100 torr), cardiac output (5.0 l/min) and normal surface blood flow (0.177 l/min) (Uttamsingh et al, 1977), normal values of core blood flow and resistances to blood flow through core and surface can be calculated as follows:

$$CBF = CO - SBF = 5.0 - 0.177 = 4.823 \text{ l/min}$$

$$R_c = \frac{MAP}{CBF} = \frac{100.0}{4.823} = 20.734 \text{ torr/l/min}$$

$$R_s = \frac{MAP}{SBF} = \frac{100.0}{0.177} = 565.0 \text{ torr/l/min.}$$

R_c is set to this constant value in the model.

If the core temperature rises above normal, the blood flow to the skin also rises by means of dilation of the appropriate blood vessels, causing a drop in R_s. This rise in skin blood flow causes the surface temperature to rise and thereby the body loses heat more rapidly to the environment. The converse is also true.

However, the relation between the deviation in temperature and resultant change in R_s is not known quantitatively, but from the extreme limits of skin blood flow (1.24 and 0.0177 l/min) (Uttamsingh et al, 1977), appropriate maximum and minimum values of R_s may be suggested as below. The resistance to blood flow through the core, R_c, and arterial pressure are assumed constant and equal to the normal values given above.

Thus,

$$R_{s\ max} = \frac{MAP}{SBF_{min}} \tag{9.35}$$

and

$$R_{s\ min} = \frac{MAP}{SBF_{max}} \tag{9.36}$$

Hence, $R_{s\ max}$ = 5650 torr/l/min, and $R_{s\ min}$ = 80.7 torr/l/min.

Figure 9.7 shows the relationship between core temperature and R_s between the points representing the extreme limits calculated above. This postulated relationship may be modified by a function relating skin temperature and resistance to skin blood flow, as shown in Figure 9.8. This applies only when the value of core temperature lies between 36.4 and 37.0^{o}C, as shown in Figure 9.7 (Uttamsingh et al, 1977).

Hence the controller inputs, core and skin temperatures yield a value for resistance to blood flow to the surface of the body approximately in accordance with known physiological facts of vasoconstriction and vasodilation due to thermal disturbances. It is then a simple matter to calculate skin blood flow which is the output of the controller.

$$SBF = \frac{MAP}{R_s} \tag{9.37}$$

where the value of arterial pressure, MAP, is obtained from the cardiovascular system model.

Since resistance to blood flow through the core, R_c, is assumed to be invariable to thermal disturbances, we may similarly write

$$CBF = \frac{MAP}{R_c} \tag{9.38}$$

The cardiac output may then be written as

$$CO = CBF + SBF \tag{9.39}$$

and the total peripheral resistance is then given by considering the two resistances in parallel, as shown in Figure 9.6.

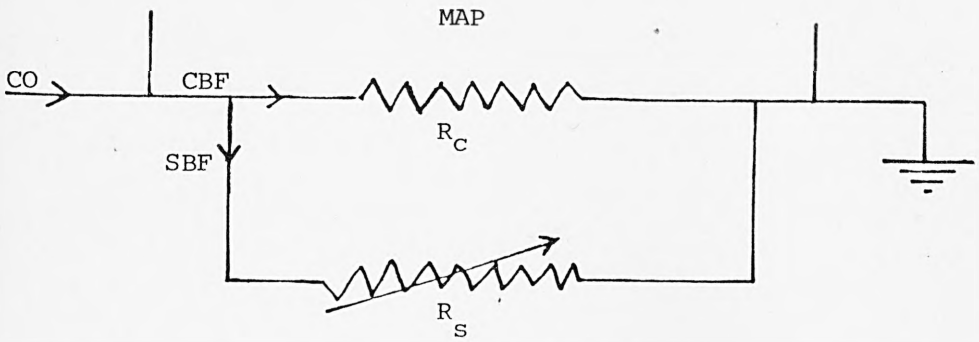

Figure 9.6 Electrical analogy for blood flow through core and surface of the body in thermoregulation.

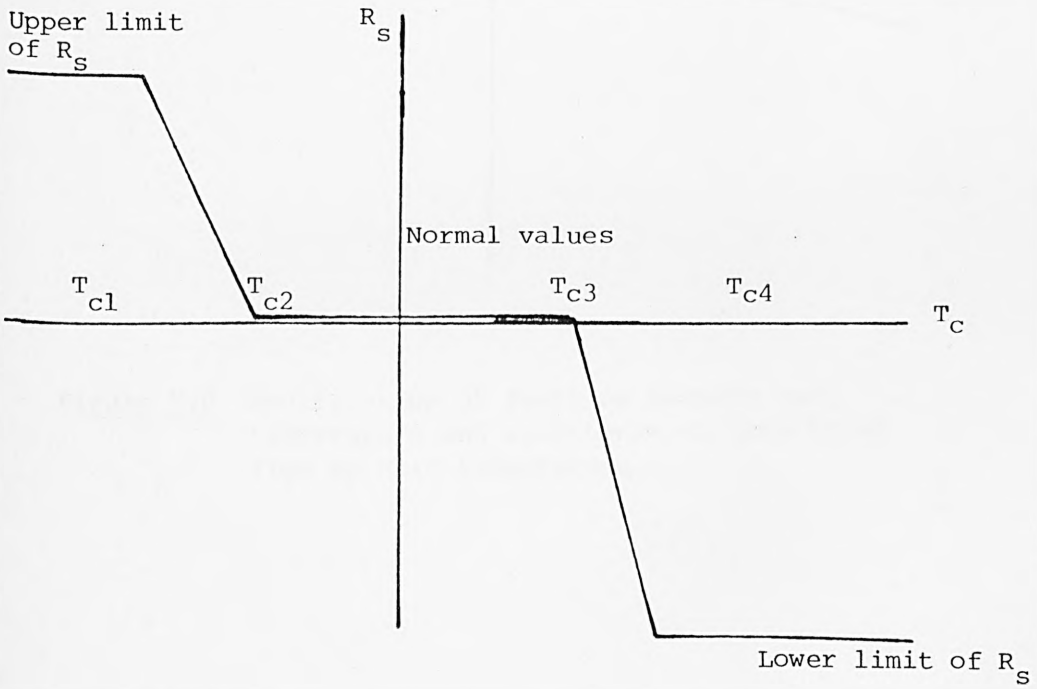

Figure 9.7 Postulate function between core temperature and resistance to blood flow.

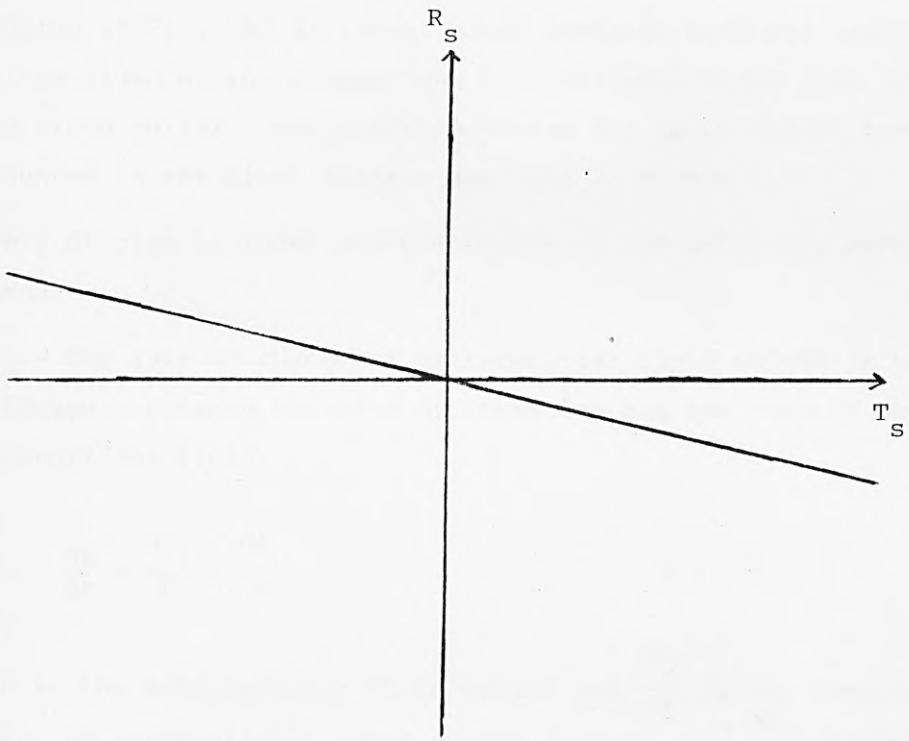

Figure 9.8 Modification of function between core temperature and resistance to skin blood flow by skin temperature.

$$TPR = \frac{R_c \times R_s}{R_c + R_s} \tag{9.40}$$

The linkage of this thermoregulatory model to the representation of the circulatory dynamics described in the previous section is achieved through (9.37) which relates skin blood flow, mean arterial pressure and skin resistance.

9.3 BODY FLUID BALANCE MODEL

The model of body fluid balance used in this work has been adapted from Guyton (1971). As is known, blood contains both extracellular fluid (the fluid of the plasma) and intracellular fluid (the fluid in the red blood cells). The basic mechanism for blood volume control is presented in the block diagram depicted in Figure 9.9.

This diagram includes representation of the following physiological phenomena:

Block 1 - The rate of change of extracellular fluid volume is equal to the difference between the rate of ingestion and the rate of excretion of extracellular fluid:

$$\frac{dE}{dt} = \frac{dE_i}{dt} - \frac{dE_o}{dt} \tag{9.41}$$

where E is the extracellular fluid volume and $\frac{dE_o}{dt}$ is the rate of excretion of extracellular fluid volume (l/min), and $\frac{dE_i}{dt}$ is the rate of ingestion of extracellular fluid volume (l/min).

Block 2 - The extracellular fluid volume is obtained by integrating the rate of change of extracellular fluid volume:

$$E = \int_o^t \frac{dE}{dt}\, dt \tag{9.42}$$

Block 3 - The blood volume (BV) is a fraction of the extracellular fluid volume (E):

$$BV = \frac{1}{3}.E \tag{9.43}$$

Block 4 - represents the linear relationship between blood volume, BV, and mean systemic pressure, MSP. This relationship is represented

quantitatively in the model by the function:

$$MSP = 3.5\ BV - 10.5 \tag{9.44}$$

Block 5 - If, for some reason, the right atrial pressure is not zero, the difference between the mean systemic pressure and the right atrial pressure gives the value of the pressure gradient for block flow through the venous system.

Block 6 - The resistance to blood flow through the venous system is a fraction of the total peripheral resistance and the venous return is equal to the pressure gradient divided by the resistance to venous return. Considering the fact that blood cannot be stored anywhere in the cardiovascular system, the venous return is exactly equal to the cardiac output (Starling's law of the heart).

Then the function of blocks 5 and 6 is:

$$CO = VR = \frac{MSP - RAP}{RVR} \tag{9.45}$$

Block 7 - represents the pressure-flow relationship between total peripheral resistance, cardiac output and arterial pressure:

$$MAP = CO \times TPR \tag{9.46}$$

Block 8 - The rate of excretion of fluid is related to the mean arterial pressure:

$$\frac{dE_o}{dt} = \frac{(0.023\ MAP - 1.38)}{1000.0} \quad \text{for MAP} < 90 \text{ torr}$$

$$\frac{dE_o}{dt} = \frac{(0.05\ MAP - 0.04)}{1000.0} \quad \text{for MAP} \geq 90 \text{ torr} \tag{9.47}$$

In the model simulation it is assumed that the extracellular fluid volume is equal to the sum of the interstitial volume and the blood volume:

$$E = V_{INT} + BV \tag{9.48}$$

Hence the model can be used to examine changes in blood volume (for

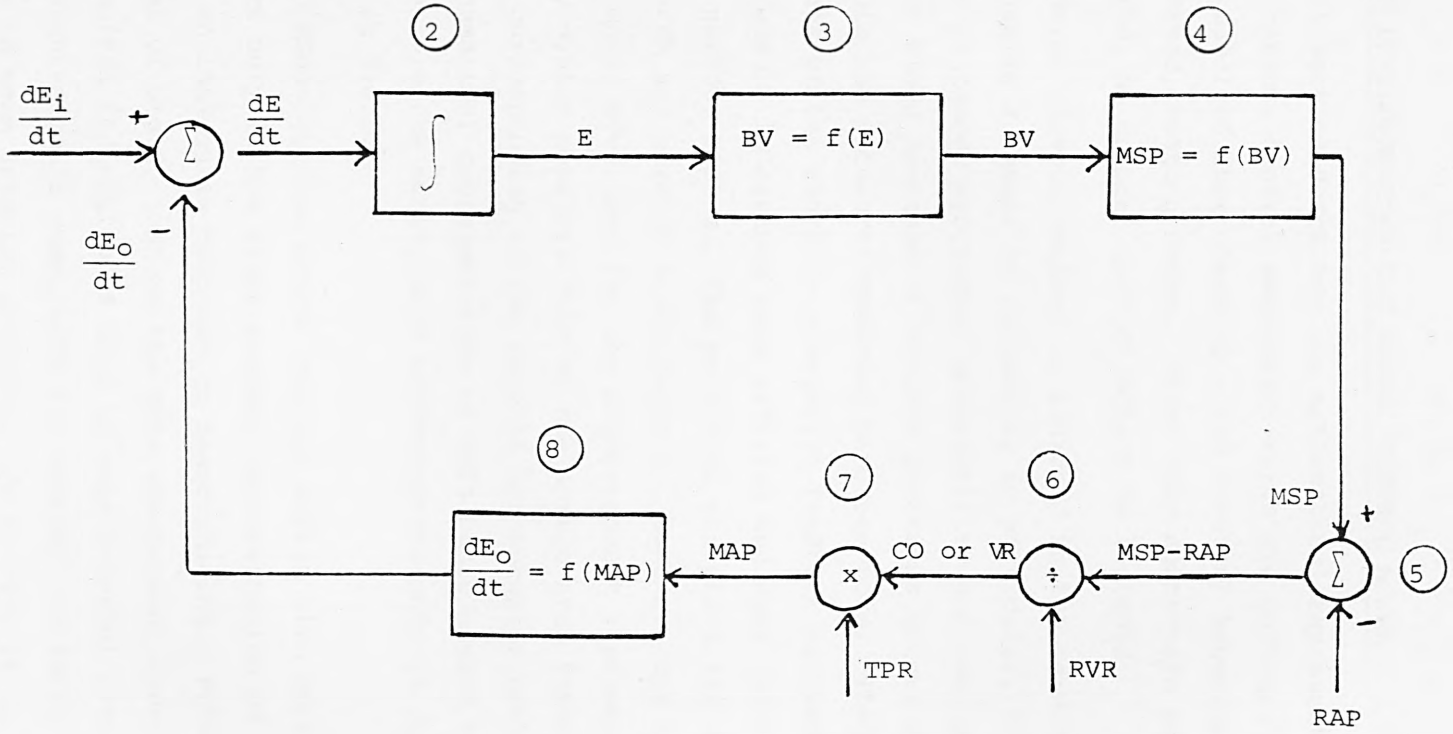

Figure 9.9 Block diagram representing the basic mechanism for blood volume control.

example due to haemorrhaging) as well as to calculate the mean system pressure using equation (9.44).

In the following section, developments in the representation of the neural control system are described.

9.4 THE DEVELOPMENT OF THE NEURAL CONTROL MODEL

This section describes the mathematical representation of the central nervous control mechanisms which are included and developed in this model of short-term (0 - 120 minutes) haemodynamics as applied to a relaxed, resting human. Since only short-term effects are being considered, no humoral control action is included.

Central nervous control is achieved in the cardiovascular system by changes in a number of variables, in particular, heart rate, peripheral resistance, myocardial contractility and venous tone. Information on blood pressure at various locations enters the central nervous system via the pressure-sensitive baroreceptors. These transducers are components of the short-term negative feedback mechanisms which monitor blood pressure in certain main arteries and send information to the central nervous system. The principal receptors are located in the aortic arch and carotid sinus regions. However, the original neural control model developed for the eight-segment representation of the circulatory system consists only of the aortic arch baroreceptor since no segment corresponding to the carotid baroreceptor area is included. The mathematical representation of this basic neural control action operating via the aortic arch baroreceptors only is described below in Section 9.4.1.

Implementing this neural control action with aortic arch baroreceptors only in the eight-segment representation of the circulation reveals an inadequate response to haemorrhaging. Following the removal of 500 ml of blood, just as the nineteen-segment model yielded a non-physiological indication of drop in mean arterial pressure (see Chapter 6), so the eight-segment model with its control similarly indicated a 22% decrease in mean arterial pressure. In reality it is known that for such a blood loss, the circulatory reflexes tend to result in effective compensation so that no such significant drop in blood pressure is apparent. This non-physiological response of the model indicated a deficiency in the control of peripheral resistance. As a first

modification, the control action of peripheral resistance was changed from bang-bang to continuous action. This is discussed in Section 9.4.3.

Since this change alone was found to be insufficient to bring about the required patterns of response in the model following 500 ml withdrawal of blood, further changes to the control of peripheral resistance were examined. This involved including the effects of volume receptors (stretch receptors), as described in Section 9.4.2.

The overall neural control model thus consists of empirical representations of the principal baroreceptors (aortic arch and stretch receptors), and the central nervous system control of heart rate, peripheral resistance, myocardial contractility and venous tone. The effects of the stretch receptors on the control of peripheral resistance and venous tone are considered in Sections 9.4.3 and 9.4.4, respectively.

9.4.1 The Aortic Arch Baroreceptor

A block diagram of the aortic arch receptor model is shown in Figure 9.10. (The general form of the receptor model was described earlier in Section 3.3).

The output function (B_{AO2}) of an aortic arch receptor is given by the linear combination of a dynamic estimate (S_C) of the positive pressure derivative (S_A) and the dynamic mean pressure estimate (S_B), together with a threshold pressure below which firing of the baroreceptors does not occur. Thus the linear combination of the mean and derivative estimates (as given in (9.52)), together with the constraint that the firing rate must be positive (9.53), gives the output function B_{AO2} for the aortic arch baroreceptor.

The equations for the baroreceptor area are thus as follows:

$$S_A = \begin{cases} \dfrac{dP_{AO2}}{dt} & , \quad \dfrac{dP_{AO2}}{dt} > 0 \\ 0 & , \quad \dfrac{dP_{AO2}}{dt} \leq 0 \end{cases} \tag{9.49}$$

$$\frac{dS_B}{dt} = \frac{P_{AO2} - S_B}{\tau_1} \tag{9.50}$$

$$\frac{dS_C}{dt} = \frac{S_A - S_C}{\tau_2} \tag{9.51}$$

$$S_D = S_B + K_C S_C - K_D \tag{9.52}$$

$$B_{AO2} = \begin{cases} S_D \ , & S_D > 0 \\ 0 \ , & S_D \leq 0 \end{cases} \tag{9.53}$$

where K_D is the threshold pressure below which firing does not occur. K_C is the average contribution of the positive pressure derivative term over one cardiac cycle and is estimated on the assumption that the average value of $K_C S_C$ over one cycle is 60,

i.e. $$\frac{1}{T_H} \int_{t_1}^{t_1+T_H} K_C S_C \, dt = 60 \tag{9.54}$$

giving $$K_C = \frac{60 \, T_H}{\int_{t_1}^{t_1+T_H} S_C \, dt} \tag{9.55}$$

The effective input for the central nervous system is assumed to be a static function of the output of the aortic arch baroreceptor (B_{AO2}).

Since only the aortic arch baroreceptors are included, the overall baroreceptor output function, B, is given by

$$B = B_{AO2} \tag{9.56}$$

9.4.2 Stretch Receptors

Cells sensitive to mechanical deformation exist in the walls of some blood vessels and produce afferent nerve impulses when the wall is stretched. Such receptors are known to exist in the atria and ventricles, in the pulmonary vessels and in the coronary artery.

In the situation of haemorrhage (one of the tests being used to examine model validity), the cardiovascular control systems respond primarily to the acute reduction in total blood volume, which is detected principally by atrial type β receptors (stretch receptors). A reflex sympathetic adrenergic discharge increases heart rate and myocardial contractility and produces peripheral arteriolar constriction and venoconstriction. Usually systemic arterial pressure is essentially insensitive to blood loss up to 10% of the total blood volume, but falls in response to a greater volume of blood loss. The venoconstriction produced by haemorrhage well illustrates the place occupied by venous capacity in cardiovascular control. Functionally, the increased venous tone in this situation tends to restore normal mean circulatory pressure in spite of decreased blood volume or, in other words, tends to match the total vascular capacity to the amount of blood available to fill it at physiological pressure (Mountcastle, 1974).

A block diagram of the operation of the volume (stretch) receptors is shown in Figure 9.11, where q_v is the output of the receptor.

In describing the control of peripheral resistance incorporating the effects of volume receptors, cardiac effects are neglected such that cardiac output is assumed to be directly proportional to the blood volume. The peripheral resistance now depends both on the output of the volume receptors as well as of the pressure receptors:

$$PR = PR_o . q_v . q_p \tag{9.57}$$

where PR_o is the normal peripheral resistance and q_v and q_p are dimensionless control multipliers as shown in Figure 9.12, where

$$q_v = \frac{1}{1 + k_v \frac{\Delta BV}{BV_o}} ; \tag{9.58}$$

$$q_p = \frac{1}{1 + k_p \frac{\Delta AP}{AP_o}} \tag{9.59}$$

Assuming $k_v \frac{\Delta BV}{BV_o}$ and $k_p \frac{\Delta AP}{AP_o}$ to be very much smaller than one,

$$q_v \simeq \left(1 - k_v \frac{\Delta BV}{BV_o}\right) \tag{9.60}$$

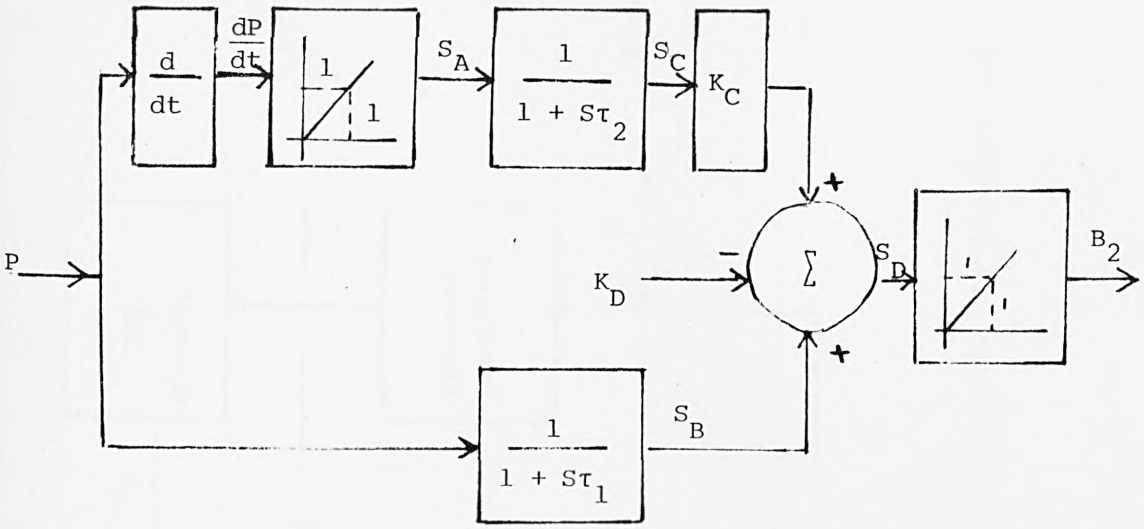

Figure 9.10 Block diagram of the baroreceptor.

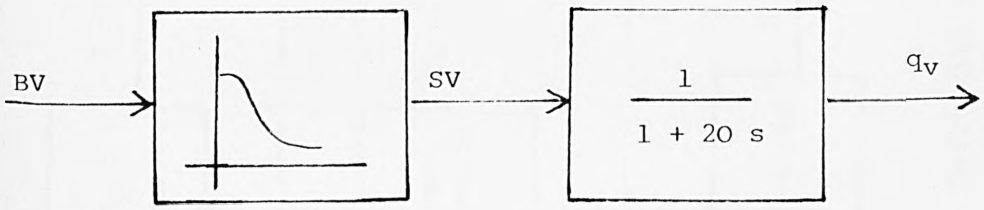

Figure 9.11 Block diagram of the volume receptor.

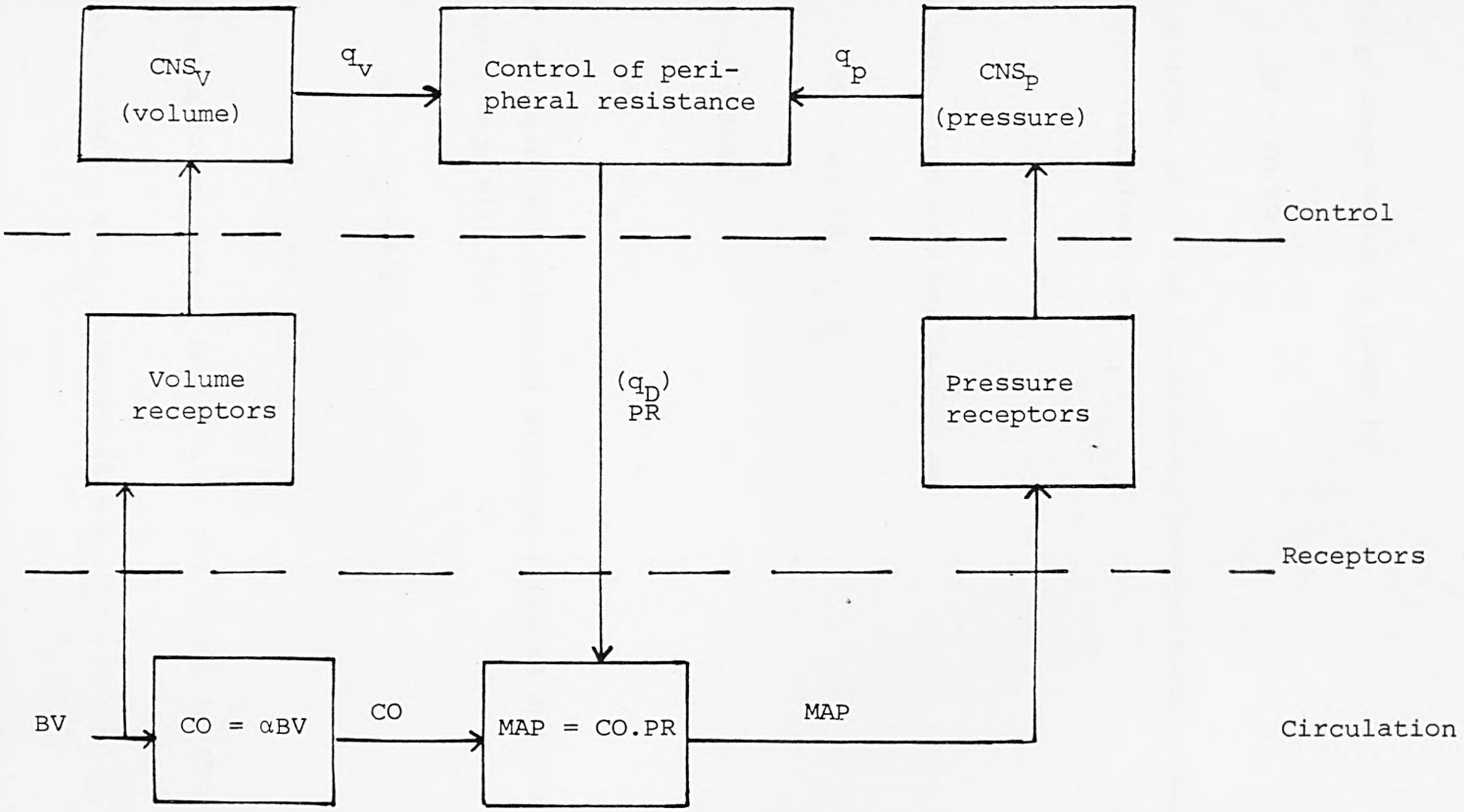

Figure 9.12 Peripheral resistance control of arterial pressure by pressure and volume receptors.

$$q_p \simeq \left(1 - k_p \frac{\Delta AP}{AP_o}\right) \tag{9.61}$$

Arterial pressure which is given by:

$$AP = CO.PR \tag{9.62}$$

can be written, using the relationship between cardiac output and blood volume described above, as:

$$AP = \alpha BV.PR \tag{9.63}$$

and in turn, incorporating (9.57), as:

$$AP = \alpha BV.PR_o\ q_v.q_p \tag{9.64}$$

For normal values

$$AP_o = \alpha BV_o.PR_o \tag{9.65}$$

so that the resultant values of arterial pressure and blood volume after any change will be:

$$AP = AP_o + \Delta AP \tag{9.66}$$

$$BV = BV_o + \Delta BV \tag{9.67}$$

Substituting for q_v and q_p from (9.58) and (9.59) in (9.64):

$$(AP_o + \Delta AP) = \alpha(BV_o + \Delta BV)PR_o\left(1 - k_v \frac{\Delta BV}{BV_o}\right)\left(1 - k_p \frac{\Delta AP}{AP_o}\right) \tag{9.68}$$

Assuming that any change in arterial pressure is negligible, (9.68) becomes:

$$AP_o = \alpha(BV_o + \Delta BV)PR_o\left(1 - k_v \frac{\Delta BV}{BV_o}\right) \tag{9.69}$$

Neglecting the effects of higher order terms, (9.69) can be rewritten as:

$$AP_o = \alpha PR_o(BV_o + \Delta BV - k_v\ \Delta BV) \tag{9.70}$$

Since, from (9.65) $BV_o = \frac{AP_o}{\alpha PR_o}$, combining this equation with (9.70):

$$BV_o = BV_o + \Delta BV - k_v \Delta BV \tag{9.71}$$

Thus $k_v = 1$ and hence, substituting in (9.60),

$$q_v = \frac{BV_o}{BV} \tag{9.72}$$

This expression is valid for small values of ΔBV only with q_v saturating at both high and low values of BV, as shown in Figure 9.13 (Leaning, 1981).

Returning to (9.68) for the case where ΔAP is not zero and neglecting higher order terms:

$$\Delta AP = \frac{\alpha PR_o (1 - k_v)}{(1 + k_p)} \Delta BV \tag{9.73}$$

Setting k_v and $k_p = 0$ gives the uncontrolled response

$$\Delta AP\Big|_o = \alpha PR_o \Delta BV \tag{9.74}$$

On the basis of the foregoing analysis it can be seen that it is possible to eliminate any steady state error, ΔAP, if there are volume receptors incorporated in the control of PR, as given by (9.72) with $k_v = 1$. Furthermore, without the volume receptors, ($k_v = 0$), as defined by (9.73), ΔAP will not be zero unless k_p is equal to infinity, which is clearly impossible.

Also from (9.73) it can be seen that if $k_v > 1$, a reduction of blood volume ($\Delta BV < 0$) can lead to an increase of arterial pressure. Thus, a prediction of the model incorporating volume (stretch) receptors is that if the given k_v of the volume control of peripheral resistance is sufficiently large ($k_v > 1$), a reduction of blood volume will lead to an increase of arterial pressure, and not a fall.

As a result, the following mathematical representation of the volume receptor control is included in the model:

$$\frac{d\, q_v}{dt} = \frac{s_v - q_v}{20} \tag{9.75}$$

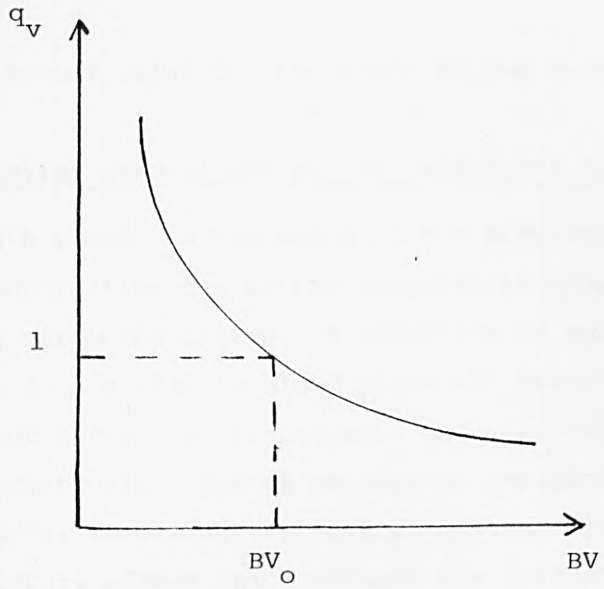

Figure 9.13 The relation between the stretch receptors output and the blood volume.

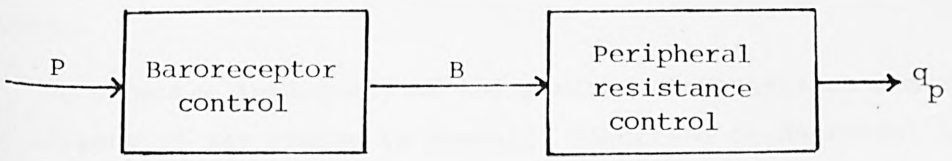

Figure 9.14 Model of the baroreceptors and the peripheral resistance control.

where

$$s_v = \frac{1}{1 + k_B \left(\frac{BV}{BV_o} - 1\right)} \qquad (9.76)$$

with the normal value for the blood volume being assumed to be 4.74 l.

9.4.3 Central Nervous Control of Peripheral Resistance

Smooth muscle in the walls of the arterioles is in a state of partial contraction due to the sympathetic tone originating from the medullary vasomotor centre. A reduction of sympathetic activity (i.e. resulting from a rise in blood pressure) leads to vasodilatation and a decrease of peripheral resistance, and vice-versa. In addition to this pressure controlling system regulating peripheral resistance, as described above, involving the central nervous system, there is a local autoregulatory effect which adjusts the perfusion of the vascular beds to meet the local demand for nutrition. This regulatory process, traditionally referred to as a flow controlling system, has almost no direct effect on heart action and cardiac output.

From the validation studies on the nineteen-segment model described in Chapter 6, a number of defects were apparent in the model responses. For example, the effect of a sudden blood loss (haemorrhage) of 500 ml resulted in a non-physiological drop of mean arterial pressure by 22%. This error could be traced to an inadequate increase of systemic resistance, and it is the modifications of the CNS control of peripheral resistance to remedy these defects which are described later in this section.

To show the inadequacy of the peripheral resistance controller, the effects of any change in pressure (increase or decrease) on q_p (the output of this controller) have been examined by separating out as a cascade the model of the baroreceptors and the peripheral resistance controller as shown in Figure 9.14. By inserting different values of P_{MAX} and PMIN (systolic and diastolic pressures) into the model equation, the results for q_p and B as shown in Table 9.1 are obtained. From this Table it is clear that the changes exhibited by q_p in response to substantial decreases in pressure are small and as such are not capable of leading to the maintenance of blood pressure which is observed experimentally following the loss of 500 ml of blood.

PMAX (torr)	PMIN (torr)	q_p	B
75	60	1.387	27.44
105	75	1.045	44.78
120	80	0.989	53.05
155	105	0.624	89.34
180	105	0.608	102.4

Table 9.1: Effects of pressure change on the output of the peripheral resistance controller

The first modification involved the replacement of the bang-bang control action, as incorporated in the nineteen-segment model, by a continuous control action. The input function B to the bang-bang controller represented all the systemic arterial baroreceptor activity and the output of the controller was a time-varying peripheral resistance, R, as described in Pullen (1976). The change to continuous control action parallels the work of Beneken and DeWit (1967) who assumed a first order transfer function relating the same input quantity B to the output of peripheral resistance. Thus the bang-bang relationship between q_A and B, as shown in Figure 9.15a, is replaced by the continuous relationship of Figure 9.15b:

$$q_A = f(B) \tag{9.77}$$

The particular form adopted is:

$$q_A = \frac{1}{1 + k\left(\frac{B}{BN} - 1\right)} \tag{9.78}$$

where B_N is the normal value of the input function B equal to 80 when evaluated using (9.79) derived by Beneken and DeWit (1967):

$$B_N = C\left\{\frac{S + D}{2} + \alpha(S - D) - \beta\right\} \tag{9.79}$$

where S and D are systolic and diastolic pressures, $\frac{(S + D)}{2}$ assumed the mean pressure, and C, α and β are respectively equal to 1, 1.5 and 80. In (9.78) k is equal to 0.5. The other components in the continuous

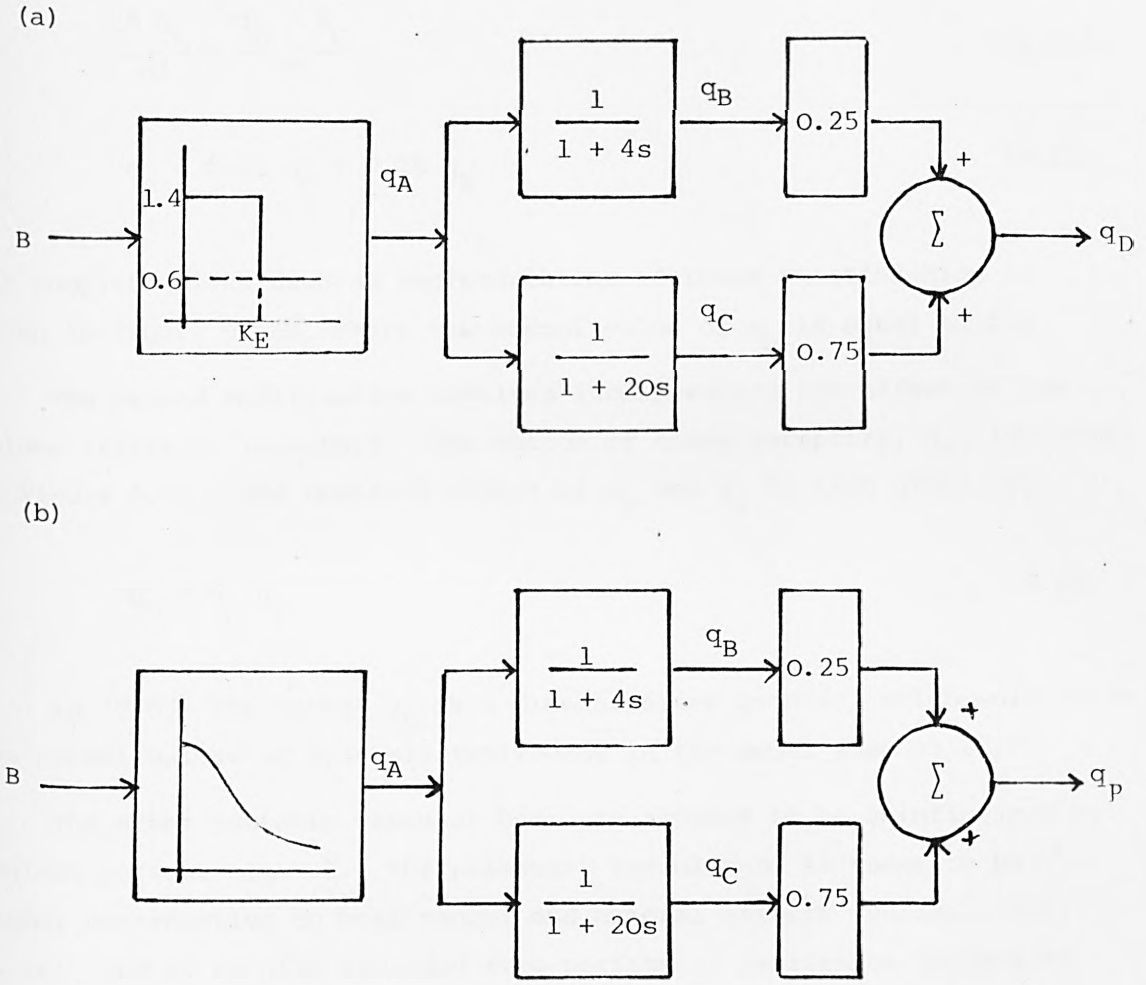

Figure 9.15 Block diagram of peripheral resistance controlled by pressure receptor, (a) with bang-bang control action, and (b) with continuous control action.

control action (Figure 9.15b) are identical to those for the bang-bang case (Figure 9.15a), namely:

$$\frac{d\,q_B}{dt} = \frac{q_A - q_B}{4} \tag{9.80}$$

$$\frac{d\,q_C}{dt} = \frac{q_A - q_C}{20} \tag{9.81}$$

$$q_p = 0.75\,q_C + 0.25\,q_B \tag{9.82}$$

The complete block diagram representation of these relationships is given in Figure 9.15b, where the normal value of q_p is equal to 1.0.

The second modification involves incorporating the effect of the volume (stretch) receptors. The output of these receptors, q_v, is shown in Figure 9.12. The combined effect of q_p and q_v is then given by:

$$q_D = q_p . q_v \tag{9.83}$$

In (9.83) the output q_D is a dimensionless quantity which multiplies the normal values of systemic resistance in the model (see (9.20)).

The other systemic vascular beds are assumed to be uninfluenced by central nervous control. The pulmonary vasculature is known to be highly non-reactive to both neural and humoral effects (Pullen, 1976, p. 66), and so is also excluded from peripheral resistance control in the model.

The negative feedback processes in the peripheral resistance control model are shown graphically in Figure 9.16.

9.4.4 Central Nervous Control of Venous Tone

Contraction or dilation of venules caused by variations of arterial pressure and mediated through the sympathetic nervous system is termed venous tone. Changes in venous tone are assumed to result in changes in the unstressed volumes and compliances of the lumped parameter venous segments. Mathematically, the control of venous tone is represented by the equations given below. These incorporate bang-bang control as adopted by Pullen (1976), but with modification to include the effects of volume (stretch) receptors:

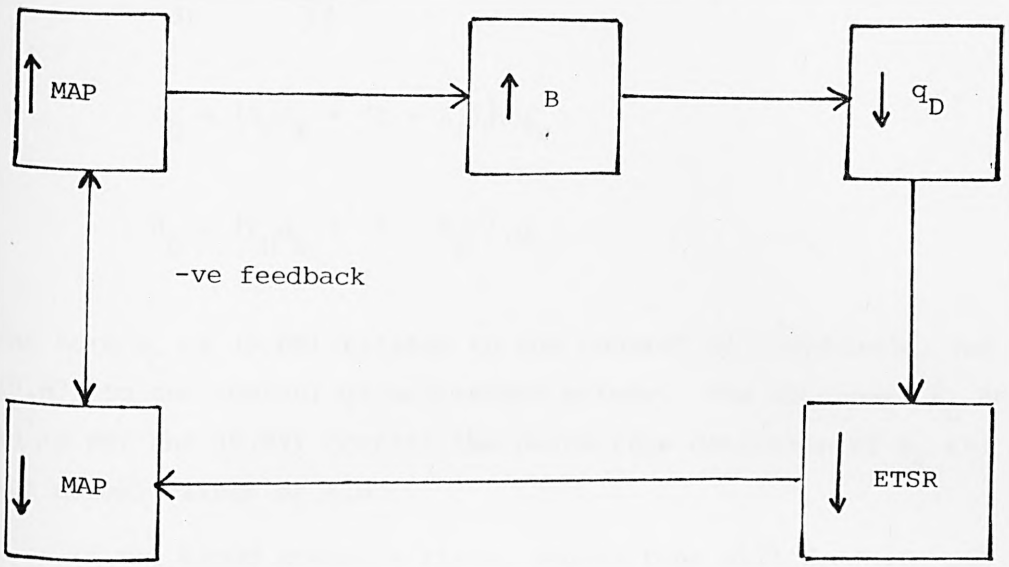

Figure 9.16 The negative feedback processes in the peripheral resistance control, while (↑) means increase and (↓) means decrease.

$$d_A = \begin{cases} 0.7 , & B > K_E \\ 1.6 , & B \leq K_E \end{cases} \tag{9.84}$$

$$\frac{d\, d_B}{dt} = \frac{d_A - d_B}{14} \tag{9.85}$$

$$d_C = \left(K_G d_B + (1 - K_G)\right).q_v \tag{9.86}$$

$$d_D = \left(K_H d_B + 1 - K_H)\right).q_v \tag{9.87}$$

The term d_C of (9.86) relates to the control of compliance, and d_D of (9.87) to the control of unstressed volume. The constants K_G and K_H in (9.86) and (9.87) control the percentage deviation of d_C and d_D from the normal values of 1.0.

If the blood pressure rises, venous tone will decrease and the venous compliance and unstressed volume will increase, thus lowering the venous pressure. This will result in reduced venous return and reduced cardiac output so that the original blood pressure rise will be limited. Equations for a typical systemic venous segment are modified as follows:

$$V_{U2} = \frac{V_{U2N}}{d_D} \tag{9.88}$$

$$P_2 = \frac{d_C}{C_2}\left(V_2 - V_{U2}\right) \tag{9.89}$$

$$C_2 = \begin{cases} C_{2N} , & V_2 > V_{U2} \\ 20\, C_{2N} , & V_2 \leq V_{U2} \end{cases} \tag{9.90}$$

A block diagram of the controller is given in Figure 9.17 and the negative feedback processes in the venous tone control model are shown graphically in Figure 9.18.

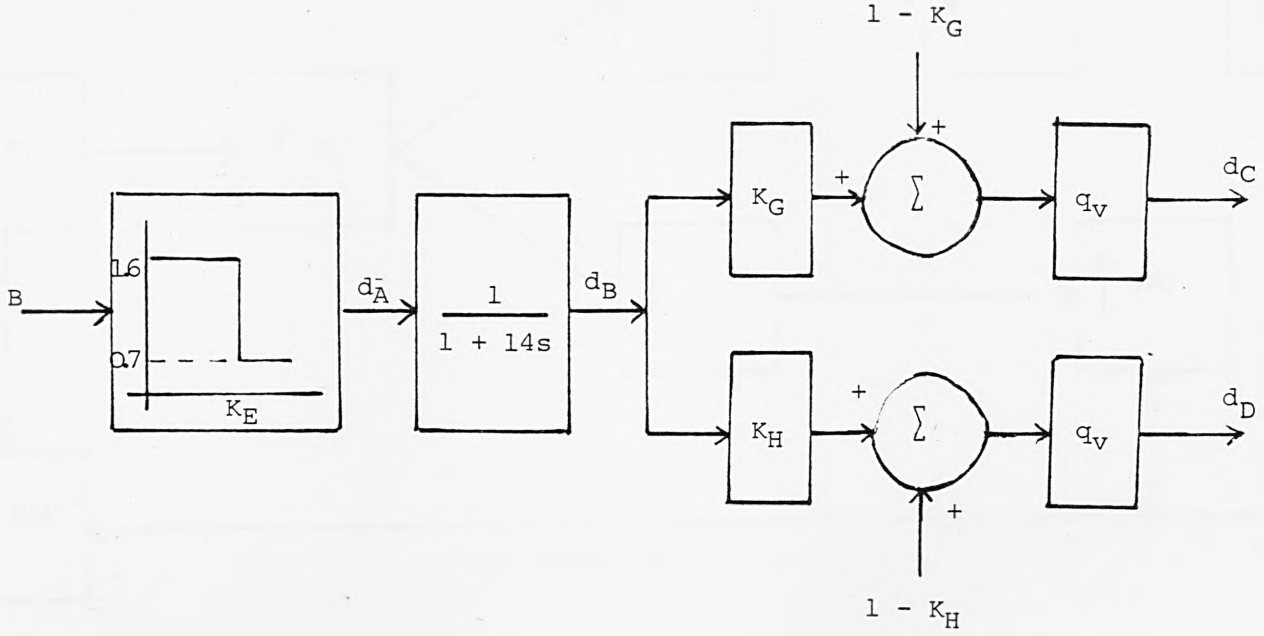

Figure 9.17 Block diagram of the venous tone controller.

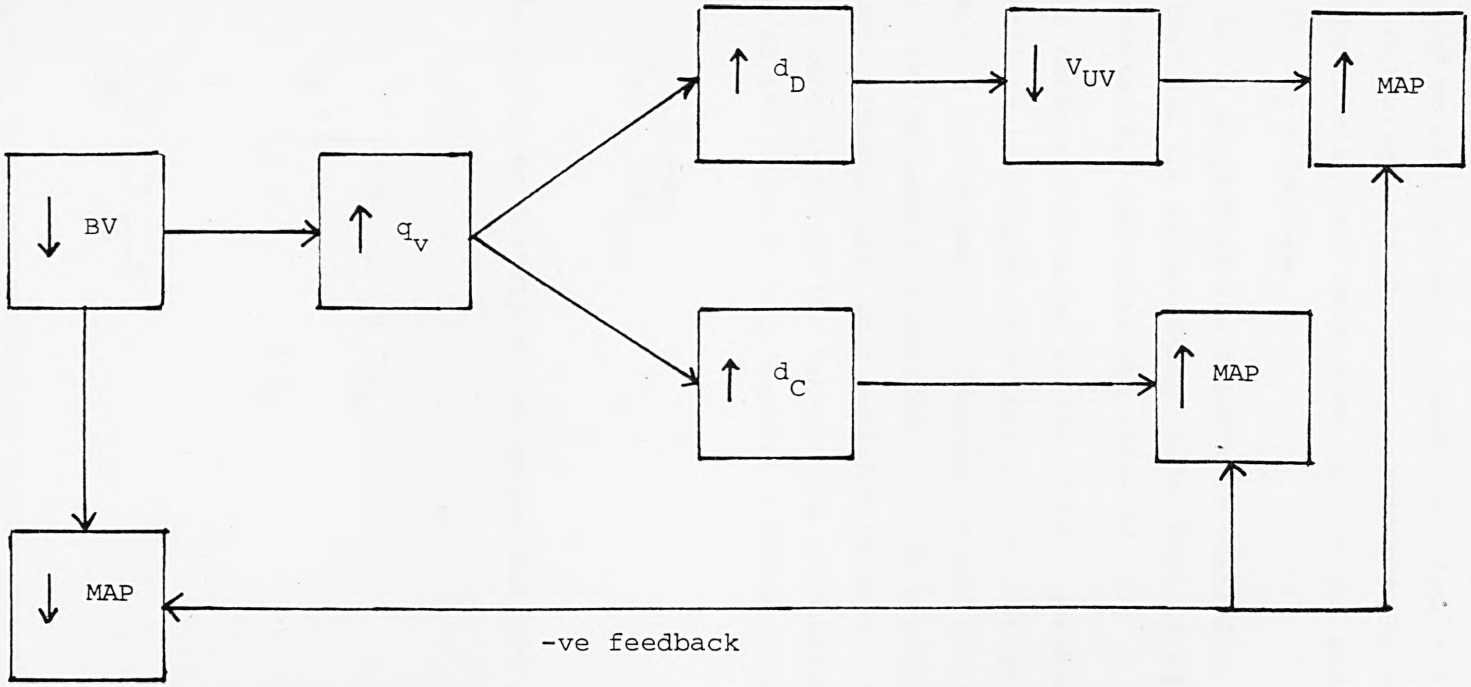

Figure 9.18 The negative feedback processes in the venous tone control model. while (↑) means increase and (↓) means decrease.

9.4.5 Central Nervous Controls of Heart Rate and Myocardial Contractility

A dynamic version of Katona's two-region model (1967) for the central nervous control of heart rate is adopted here, of the same form as that used in the nineteen-segment model (see Section 3.3.2). The two regions correspond to blood pressure greater and less than normal. The output of the controller sets the heart period for the next cardiac cycle, and is constrained so that heart rate (FH) in the model is limited to a range $30 \leq F_H \leq 200$ bpm.

A block diagram of the heart rate controller was shown in Figure 3.7. That for the eight-segment model here is identical, except that the parameter K_{14} now takes the value of 1.1.

The mathematical model of the central nervous control of myocardial contractility is adapted from that of the nineteen-segment model. The heart muscle has sympathetic innervation and increased sympathetic activity in the medullary centres (e.g. as a result of a fall in blood pressure). This results in a positive inotropic response, i.e. more powerful contraction of the ventricular musculature. Systolic elastance is used as the measure of myocardial contractility and is given by:

$$a_S = \left(\frac{dP}{dV}\right)_{max} \tag{9.91}$$

The equations describing the myocardial contractility controller are:

$$b_A = \begin{cases} 0.6 & , \quad B > K_E \\ 1.4 & , \quad B \leq K_E \end{cases} \tag{9.92}$$

$$\frac{d\, b_B}{dt} = \frac{b_A - b_B}{10} \tag{9.93}$$

The output b_B acts as a multiplier for the normal systolic elastances in ventricular chambers. A block diagram representation is given in Figure 9.19.

Figures 9.20a and 9.20b depict the signal flow diagrams for the eight-segment circulatory model and its controller.

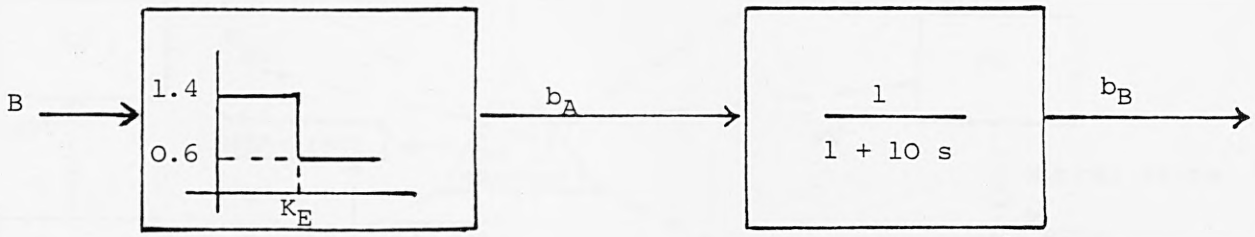

Figure 9.19 Block diagram of the myocardial contractility controller.

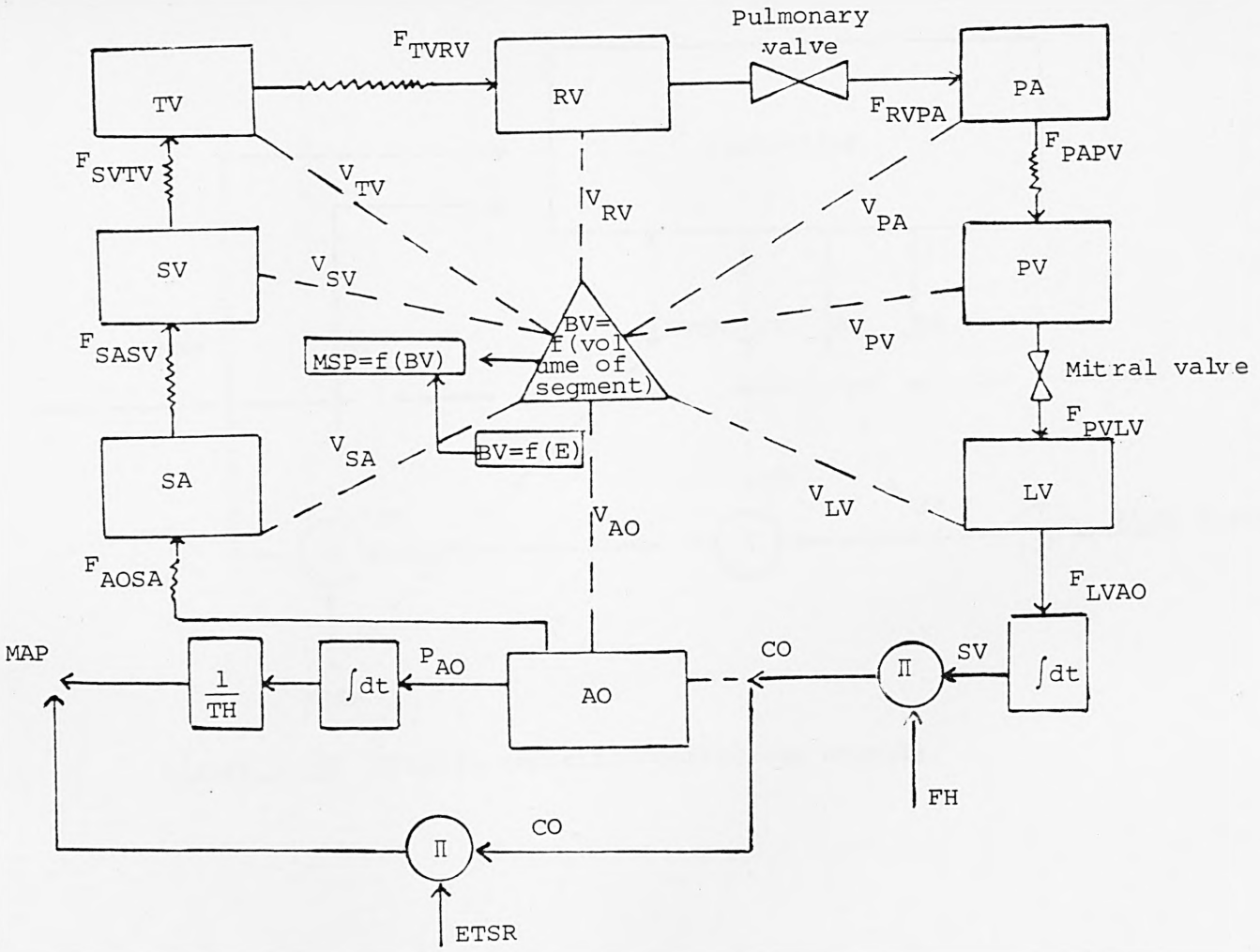

Figure 9.20a Signal flow diagram in the 8-segment model.

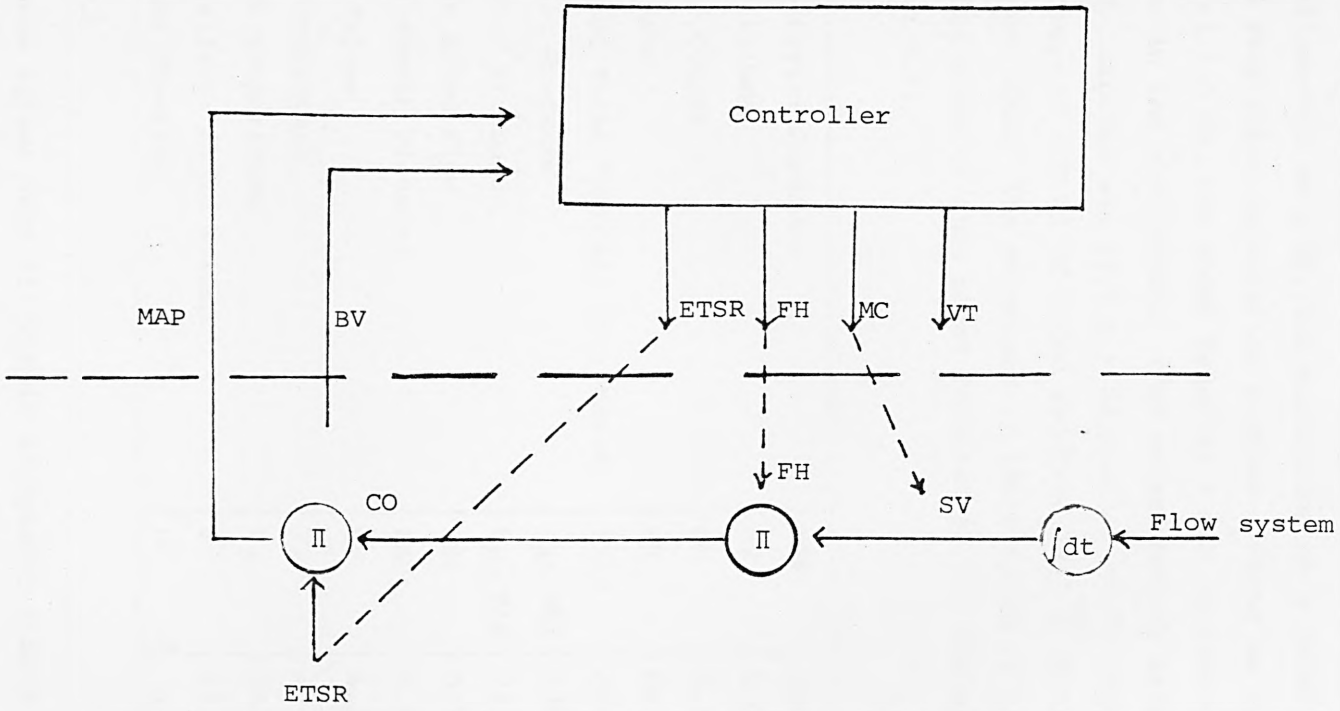

Figure 9.20b Diagram depicting controller signals.

9.5 DIGITAL COMPUTER IMPLEMENTATION OF THE MODEL

Figure 9.21 shows the interactions between the various subsystems which, together, form the complete model. This model, which is described by 26 first order differential equations and 56 algebraic equations (see Table 9.3), has been implemented as a digital simulation on a PRIME 550 computer using a fixed step Euler integration routine. Using an integration step length of 1.0 ms, the model required 9 min execution time to represent one hour in the simulation. (The corresponding execution time on the CDC 7600 computer was 14.5 s.) Simulation of 60 minutes of response to a haemorrhage of 420 ml of blood required 17.8 min on the PRIME and 29.1 s on the CDC 7600. The structure of the program is given in Appendix V.

Simulation of this model resulted in the steady state values listed in Table 9.2.

Mean Arterial Pressure	MAP	109.1	torr
Stroke Volume	SV	0.076	l
Cardiac Output	CO	5.36	l/min
Heart Rate	FH	69.95	bpm
Estimated Total Systemic Resistance	ETSR	20.35	torr min l^{-1}
Systolic Pressure	P_{AO} MAX	138.9	torr
Diastolic Pressure	P_{AO} MIN	93.6	torr
Surface Blood Flow	SBF	0.208	l min^{-1}
Mean Systemic Pressure	MSP	5.98	torr
Blood Volume	BV	4.7098	l
Core Temperature	T_C	36.6	^oC
Surface Temperature	T_S	34.7	^oC
Extracellular Fluid Volume	E	14.337	l
Ejection Fraction	EF	0.487	

Table 9.2

These values were all within acceptable limits for an average human subject. The "normal" arterial blood pressure for a young healthy adult is of the order of 120/75 torr, but these values vary with age, weight, sex, race, degree of fitness, etc. Typical variations with age are shown in Figure 9.22 (Rushmer, 1976). The mean arterial pressure is normally calculated as

$$MAP = \frac{1}{3}\left(P_{AO}\ MAX - P_{AO}\ MIN\right) + P_{AO}\ MIN$$

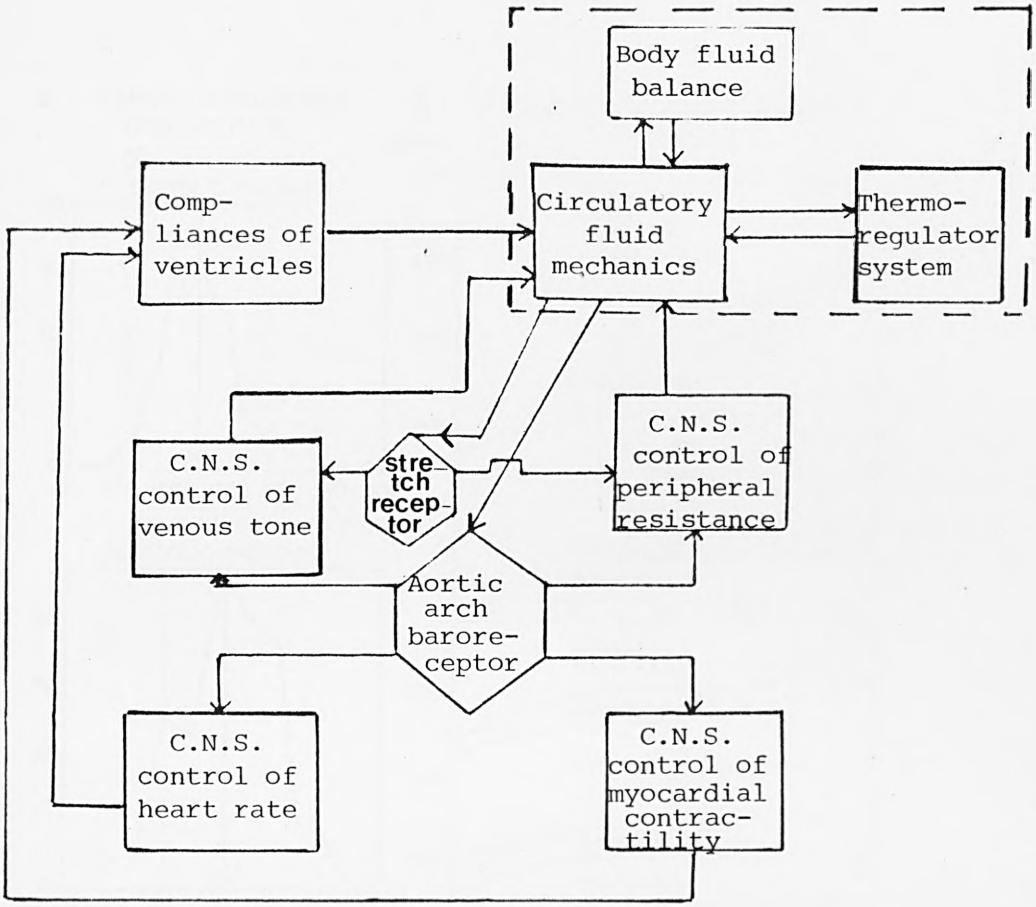

Figure 9.21 Interaction between subsystems in the model.

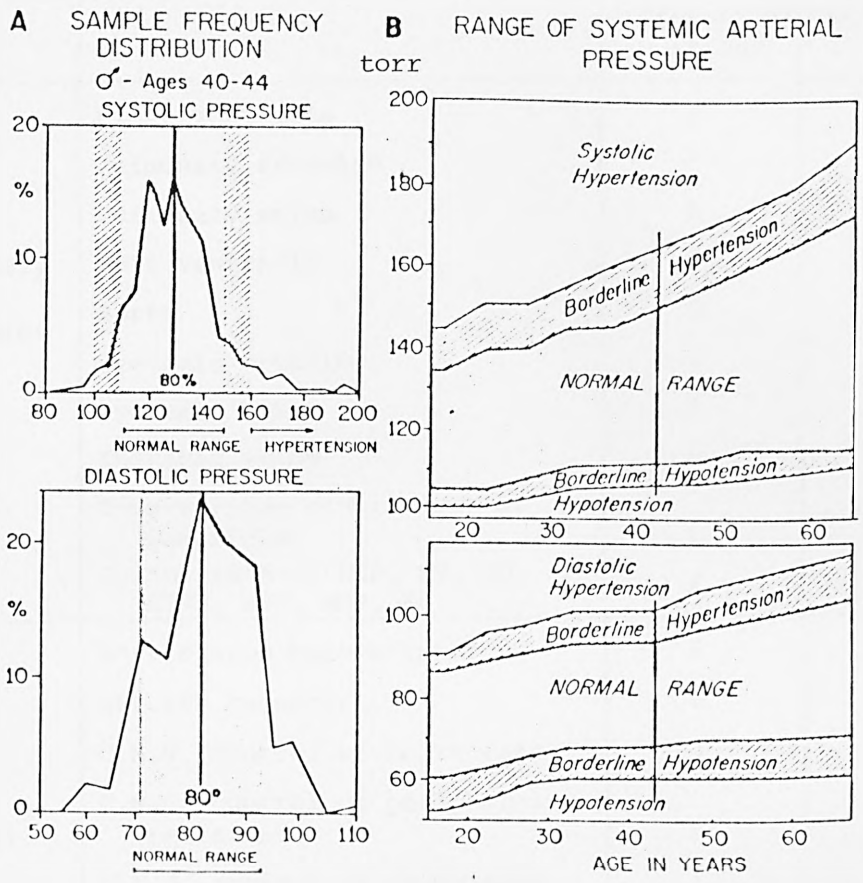

Figure 9.22 Range of normal arterial pressure.

A. In males aged 40 to 44, the normal arterial blood pressure is generally described in terms of range of values which will include a major portion of normal subjects (80 per cent in this graph). The "normal systolic pressure range" extends from 110 to 150 torr. Abnormal blood pressure is defined as extending above and below some borderline range.

B. Assembling the frequency distributions for various age groups demonstrates a distinct tendency for broadening of the normal systolic and diastolic pressure ranges and a tendency for higher pressures in older people. This fact must be considered in defining "high blood pressure" or hypertension. (Rushmer, 1967)

within the model, this value being 109.1 torr.

A detailed validation of the model is presented in Chapter 10.

Section	Subsection	Number of first order differential equations	Number of algebraic equations
Circulatory fluid mechanics model	Right ventricle	2	1
	Pulmonary arteries	1	2
	Pulmonary veins	1	4
	Left ventricle	2	1
	Aorta	2	1
	Systemic arteries	1	2
	Systemic veins	1	5
	Thoracic veins	1	4
	Time-varying compliances of ventricles	1	8
	Calculation of MAP, SV, CO, ETSR, SBF, MSP, EF	2	5
Neural control model	Aortic arch baroreceptor	2	4
	Stretch receptor	1	1
	C.N.S. control of heart rate	3	6
	C.N.S. control of peripheral resistance	2	3
	C.N.S. control of myocardial contractility	1	1
	C.N.S. control of venous tone	1	3
Thermoregulator system model		2	2
Body fluid balance model		0	3
	Total	26	56

Table 9.3: Number of equations in the digital computer implementation

9.6 CONCLUSION

In this chapter, the development of a reduced pulsatile model of the cardiovascular system and its digital implementation have been described; the resultant model consisting of 26 first order differential equations and 56 algebraic equations. With a view towards ultimate

clinical application, model segments have been included for thermo-regulation and body fluid balance.

The chapter describes a series of developments concerning the neural control system in order to remedy defects which were identified in Chapter 6 when seeking to identify the nineteen-segment model. These developments included replacement of bang-bang control action for the peripheral resistance controller by a continuous action and subsequent inclusion of a stretch receptor effect which was also incorporated in the controller of venous tone.

The programme of validation of this model, including sensitivity analysis, is presented in Chapter 10.

CHAPTER 10

THE VALIDATION OF THE 8-SEGMENT MODEL OF THE CARDIOVASCULAR SYSTEM

10.1 INTRODUCTION

In Chapter 9, the development of the 8-segment model of the cardiovascular system was described. The validation of this complete model is the subject of this chapter.

Section 10.2 examines model validity as evidenced by responses to changes in blood volume (haemorrhage and transfusion) in both qualitative and quantitative terms. This is followed in Section 10.3 by a comprehensive sensitivity analysis, examining the stability of the model, defining normal ranges for parameters and identifying those parameters whose values are most critical in determining the patterns of model response.

10.2 MODEL RESPONSE TO BLOOD VOLUME CHANGES

In this section, the validity of the model is assessed by examining its response to various changes in blood volume. These tests represent the effects of both haemorrhage and transfusion. Of particular importance is the ability of the model, with its modified neural control components, to provide a sufficient increase in peripheral resistance and thereby avoid the pronounced fall in aortic pressure when the 19-segment model was subjected to the effects of haemorrhaging.

10.2.1 Reduction in Blood Volume

The dynamic physiological processes occurring during haemorrhaging were described fully in Section 6.4.1. In essence, there is a reduction in the mean system filling pressure and venous return leading to reduced cardiac output. Arterial pressure is maintained by an increase in peripheral resistance, provided that the loss of blood is comparatively small.

There is, however, some disagreement in the literature as to the degree of haemorrhage which is necessary before any change in circulatory dynamics can be detected. For instance, McClintic (1978) indicates that changes can be observed with a loss in excess of 5%, whilst Guyton

(1981) suggests a threshold value of 10% or more before there is any appreciable drop in arterial pressure.

In this section, the empirical validity of the model is examined by comparison with the data on blood volume changes which were used in Chapter 6 in assessing the validity of the 19-segment model. These data were obtained at donor sessions in the North East Thames Regional Health Authority at Moor House, London, and the Regional Headquarters at Brentwood, Essex.

10.2.1.1 Comparison of model response with experiment data

The data obtained in these experimental studies followed the loss of 420 ml of blood from the systemic veins over a period of five minutes (the typical duration of a blood donation for an experienced volunteer). The data were described in Tables 6.7 - 6.9, repeated here for convenience as Tables 10.1 - 10.3.

The model response in simulating this loss of 420 ml of blood over a period of five minutes is shown in Figure 10.1. Cardiac output drops by approximately 19% and stroke volume by 2.7%, whilst the mean systemic pressure drops by 25%. Mean arterial pressure, however, drops by only 2% seven minutes after the start of bleeding and then is restored towards its normal value due to a 22% increase in peripheral resistance (vasoconstriction). This effective control of arterial pressure contrasts markedly with the results which were obtained for the 19-segment model (see Table 6.9b). Systolic pressure drops by 6% and diastolic pressure increases by 1%, while the heart rate is increased by 12% after seven minutes. Also from Figure 10.1 it can be seen that the ejection fraction is decreased by 13%, while the skin blood flow decreases by 21%. As expected, only small changes were observed in the thermal component (a 0.2% decrease in skin temperature and 0.1% increase in core temperature) and in the extracellular fluid volume.

A comparison can then be made between the experimental data presented in Tables 10.1 - 10.3 and the model response summarised in Table 10.4.

Six of the eight donors revealed only small or negligible changes in arterial pressure, consistent with the theory that for such a blood loss the compensatory mechanisms should be adequate to maintain arterial pressure (Mountcastle, 1974; Wright, 1955). Good agreement is thus obtained between model response, physiological theory and the majority of the experimental evidence in relation to arterial blood pressure.

Donor's No.	Age	Variable	Values of variables			
			Before bleeding	During bleeding	At the end of bleeding	10 minutes after the end of bleeding
(1)	30	Heart rate (bpm)	78	78	78	78
		Systolic pressure (torr)	120	140	150	130
		Diastolic pressure (torr)	75	75	80	75
(2)	24	Heart rate (bpm)	60	60	56	58
		Systolic pressure (torr)	120	120	120	120
		Diastolic pressure (torr)	70	70	70	70

Table 10.1 Heart rate and blood pressure data on two donors during the removal of 420 ml of blood over 5 and 8 minutes, respectively (Moor House data).

Donor's No.	Variables	Pre-stimulus values	Start of bleeding	End of bleeding	Sample values of variables taken during the 10-min period following the end of bleeding
BD1G (3)	(PMAX/PMIN) blood pressure	145/95	115/70	110/70	115/70
	Mean arterial pressure	111.66	85.00	83.33	85.00
	Heart rate (bpm)	60.87	85.13	82.87	70.41
	Index stroke volume	43.5	33.1	31.9	32.47
	Index cardiac output	44.07	46.92	44.01	37.87
BD2J (4)	(PMAX/PMIN) blood pressure	125/90	125/85	130/95	130/90
	Mean arterial pressure	101.6	98.33	106.66	103.33
	Heart rate (bpm)	120.4	93.29	112.6	100.87
	Index stroke volume	25.5	24.3	22.6	24.4
	Index cardiac output	51.14	37.83	42.43	41.04
BD3C (5)	(PMAX/PMIN) blood pressure	110/80	130/80	110/80	-
	Mean arterial pressure	90.0	96.66	90.0	-
	Heart rate (bpm)	84.76	82.81	82.67	81.32
	Index stroke volume	25.2	25.6	26.0	27.5
	Index cardiac output	35.31	35.35	35.86	37.22
BD5E (6)	(PMAX/PMIN) blood pressure	120/80	112/88	110/80	108/78
	Mean arterial pressure	93.33	96.0	90.0	88.0
	Heart rate (bpm)	89.46	96.6	79.04	86.07
	Index stroke volume	20.25	17.5	17.3	18.0
	Index cardiac output	30.2	28.15	22.8	25.77

Table 10.2 continued overleaf

Donor's No.	Variables	Pre-stimulus values	Start of bleeding	End of bleeding	Sample values of variables taken during the 10-min period following the end of bleeding
BD6F (7)	(PMAX/PMIN) blood pressure	125/70	125/70	120/80	127/75
	Mean arterial pressure	88.33	88.33	93.33	92.33
	Heart rate (bpm)	75.9	81.65	80.38	82.42
	Index stroke volume	19.45	18.2	15.5	18.75
	Index of cardiac output	24.52	24.73	20.75	25.38
BD7H (8)	(PMAX/PMIN) blood pressure	148.85	140/80	128/90	140/95
	Mean arterial pressure	106.0	100.0	102.66	110.0
	Heart rate (bpm)	82.61	82.39	75.68	82.94
	Index stroke volume	19.8	21.5	16.2	20.3
	Index cardiac output	27.27	29.47	20.43	28.17

Table 10.2 Effects of removal of 420 ml of blood from six donors (Regional Blood Transfusion Centre data).

Donor's No.	Percentage of change during removal of 420 ml of blood	
	FH (bpm)	MAP (torr)
1	0.0	+ 15.0
2	- 6.7	0.0
3	+ 36.0	- 25.3
4	- 6.4	+ 4.9
5	- 2.4	0.0
6	- 11.6	- 3.5
7	+ 5.9	+ 5.6
8	- 8.3	- 3.1

Table 10.3 Percentage of change of heart rate and mean arterial pressure for the eight donors obtained from removal of 420 ml of blood during 5 - 8 minutes.

Blood volume removed	Percentage change	
	FH (bpm)	MAP (torr)
420 ml	+ 12	- 2
500 ml	+ 14	- 3
1000 ml	+ 45	-12

Table 10.4 The change in heart rate (FH) and mean arterial pressure (MAP) two minutes after the end of a five-minute haemorrhage compared with the values at the start of bleeding, expressed as a percentage, for different volumes of blood loss.

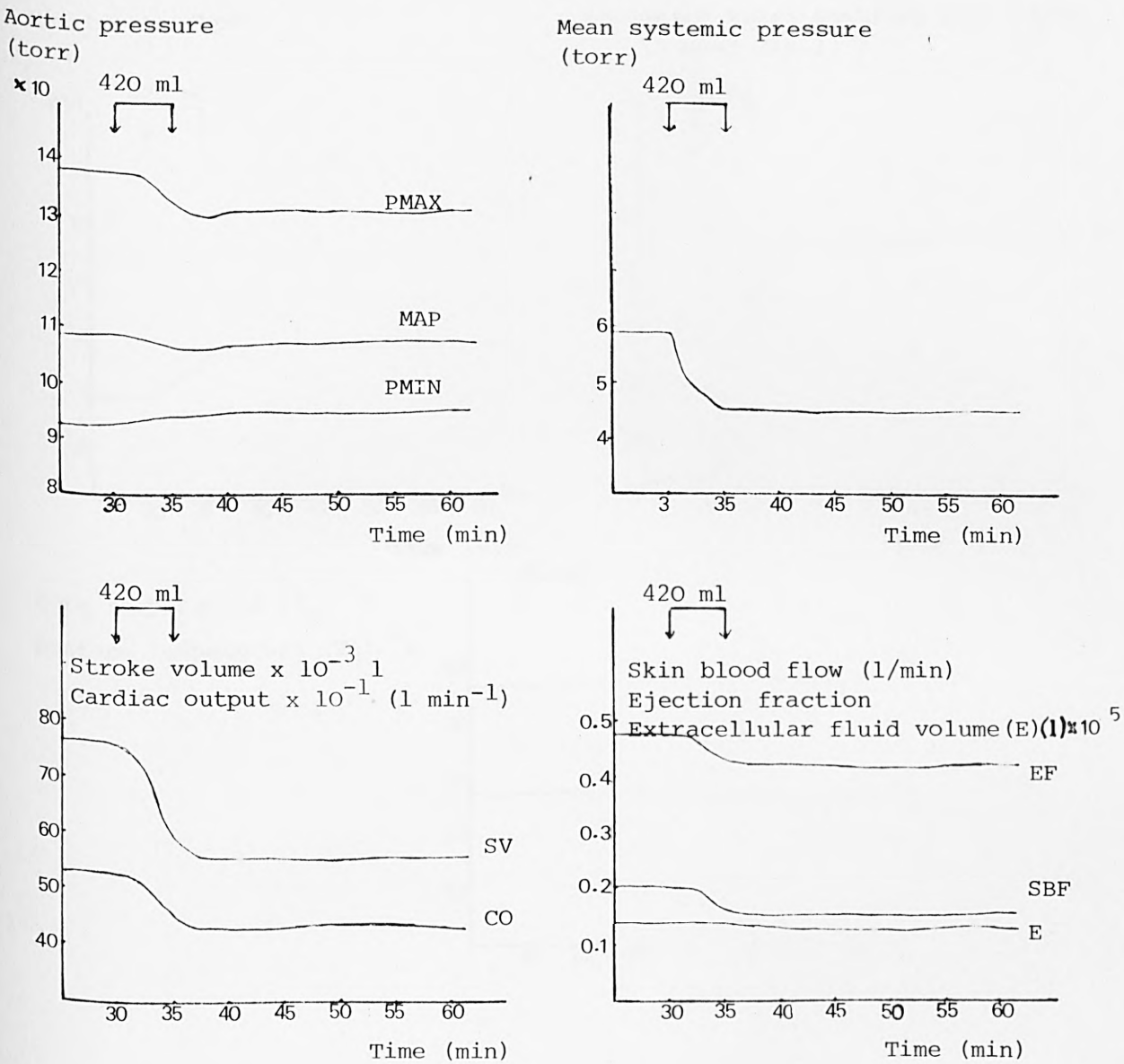

Figure 10.1 continued overleaf

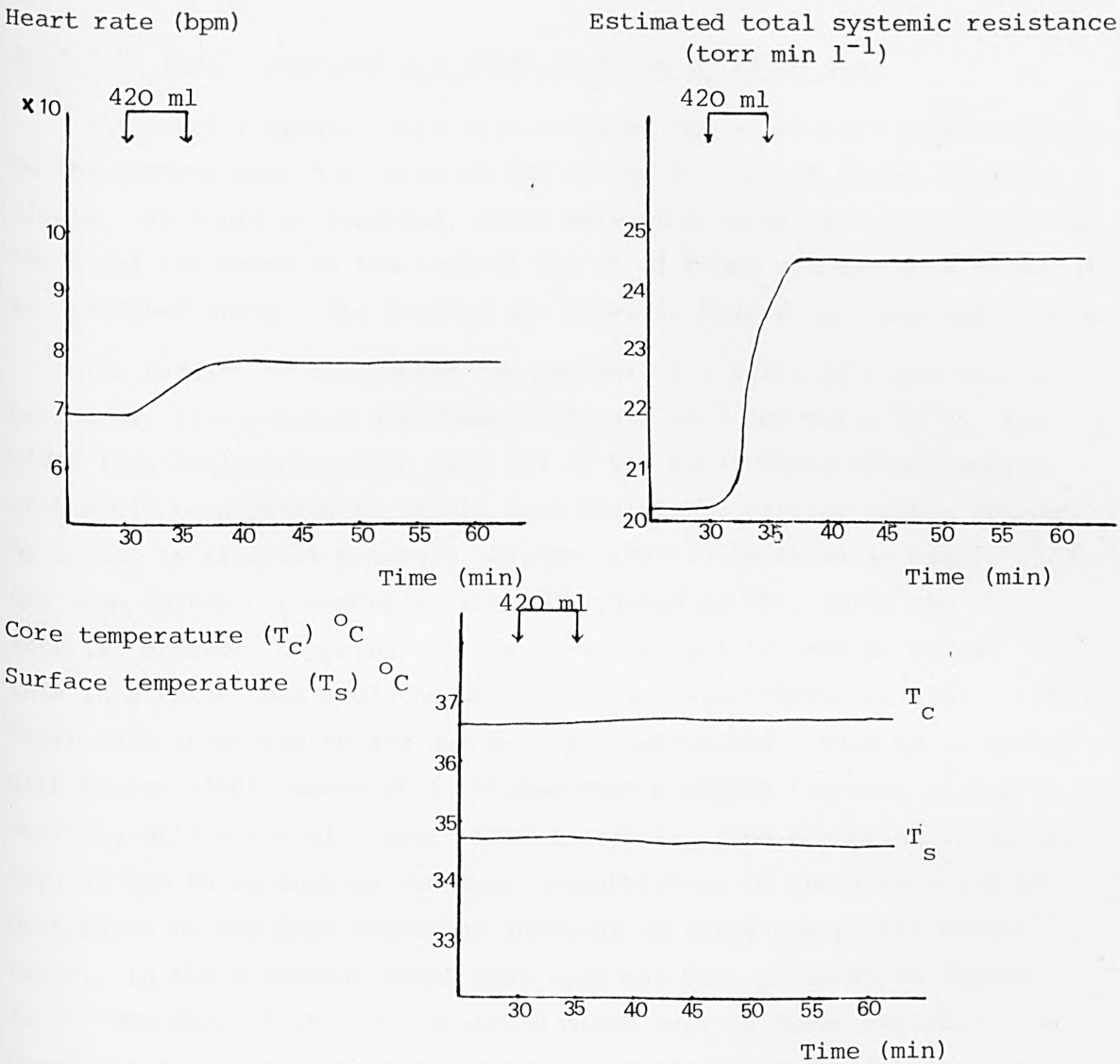

Figure 10.1 Dynamics following the removal of 420 ml of blood over a period of 5 minutes from the systemic veins segment, starting at t = 30 min.

In terms of heart rate, however, the position is less clear. The model predicted increase of 12% is in agreement with the data shown in Table 10.3, based on the effects of vasoconstriction. The eight subjects, on the other hand, exhibit a range of heart rate responses from which it is difficult to draw clear conclusions.

10.2.1.2 Model responses for other patterns of blood loss

The model responses were also examined for situations corresponding to the removal over 5 minutes of 500 ml and 1 litre of blood, respectively. As would be expected, there were only small differences between the model responses to the loss of 500 ml of blood and the loss of 420 ml as described above. The results are shown in Figure 10.2 and Table 10.4.

The results of simulating the removal of 1 litre of blood over a period of five minutes are shown in Figure 10.3 and Table 10.4. The blood loss constitutes more than 10% of the total blood volume and as such would be expected to result in a diminished cardiac output followed by a fall in arterial pressure (Guyton, 1981). As shown in Figure 10.3, the mean systemic pressure in the model drops by 58%, while the arterial pressure drops by 12% due to a 51% fall in cardiac output. This is greater than would be expected clinically (Bushman, 1982). The heart rate increased by 45% due to vasoconstriction. This is in accord with Guyton (1981) where it is stated that a marked increase in heart activity will occur with heart rate increasing from a resting value of, say, 72 bpm to as much as 200 bpm. Constriction of the arterioles in most parts of the body causes an increase in total peripheral resistance. In the 8-segment model this rise was 83%, as shown in Figure 10.3. The effects of this simulated blood loss on other variables are more marked than for the loss of 420 ml of blood, as would be expected. Skin blood flow is reduced by 53%, whilst the ejection fraction falls by 36%. The extracellular fluid volume falls by 7%. The changes in core and skin temperature are a rise of 0.2% and a drop by 0.6%, respectively.

No experimental data were available for this situation of the loss of 1 litre of blood, but the general pattern of behaviour evidenced by the model was broadly in agreement with known physiology. The greatest discrepancy was in relation to cardiac output as described above. What is clear, however, is that the modifications carried out to the neural control components of the model, as described in Chapter 9, have significantly enhanced the validity of the model in relation to blood loss

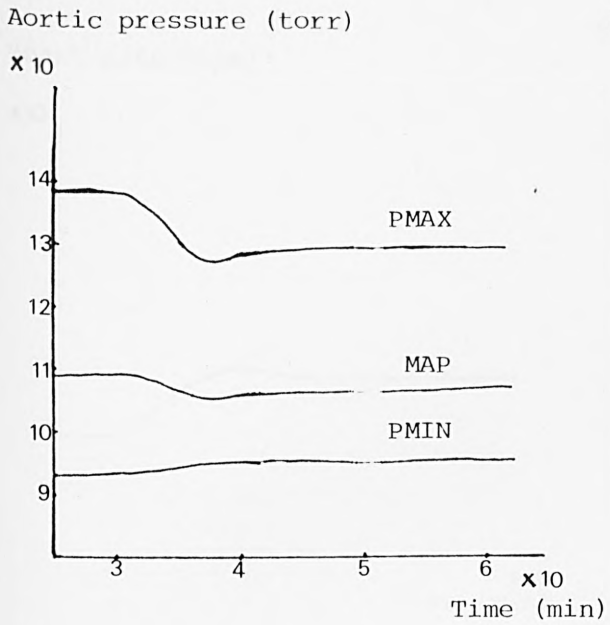

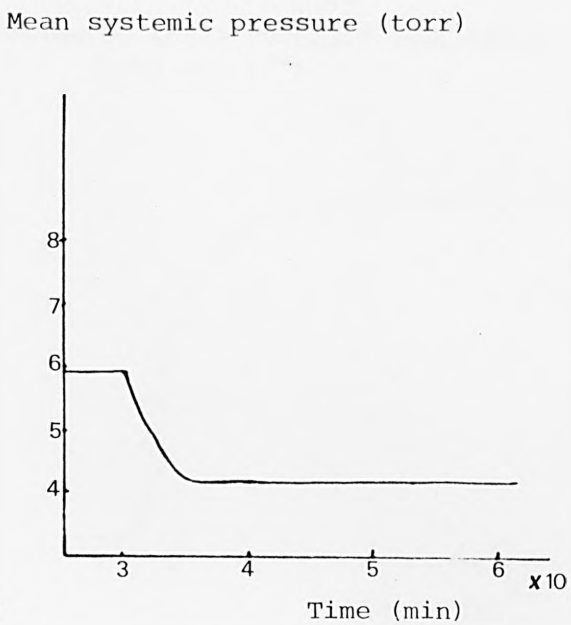

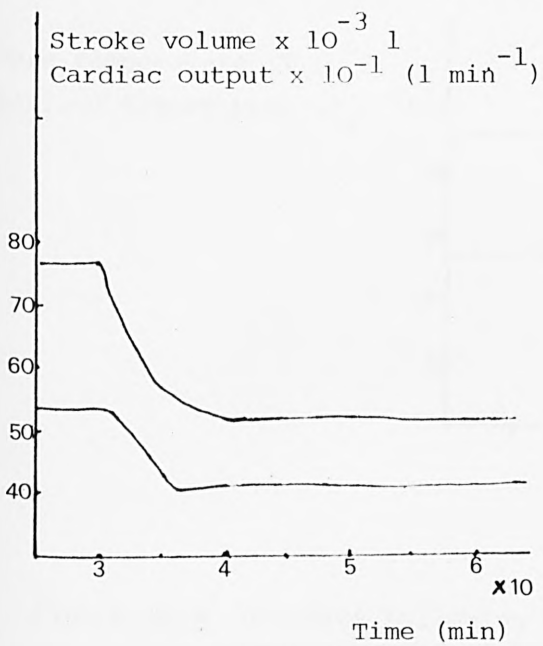

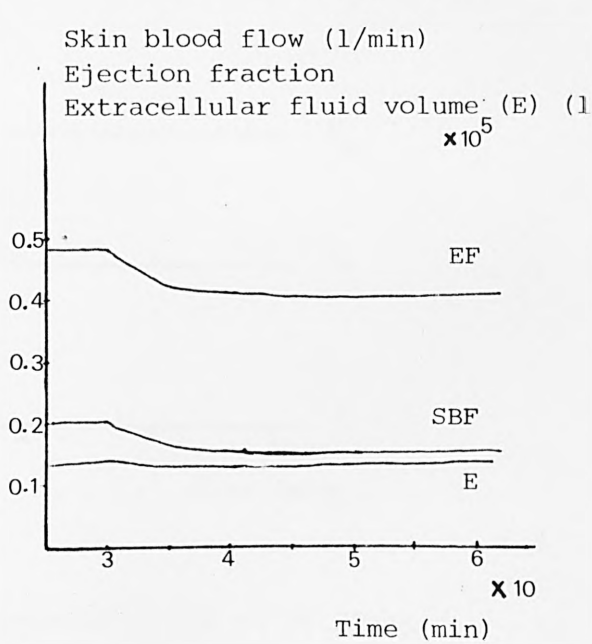

Figure 10.2 continued overleaf

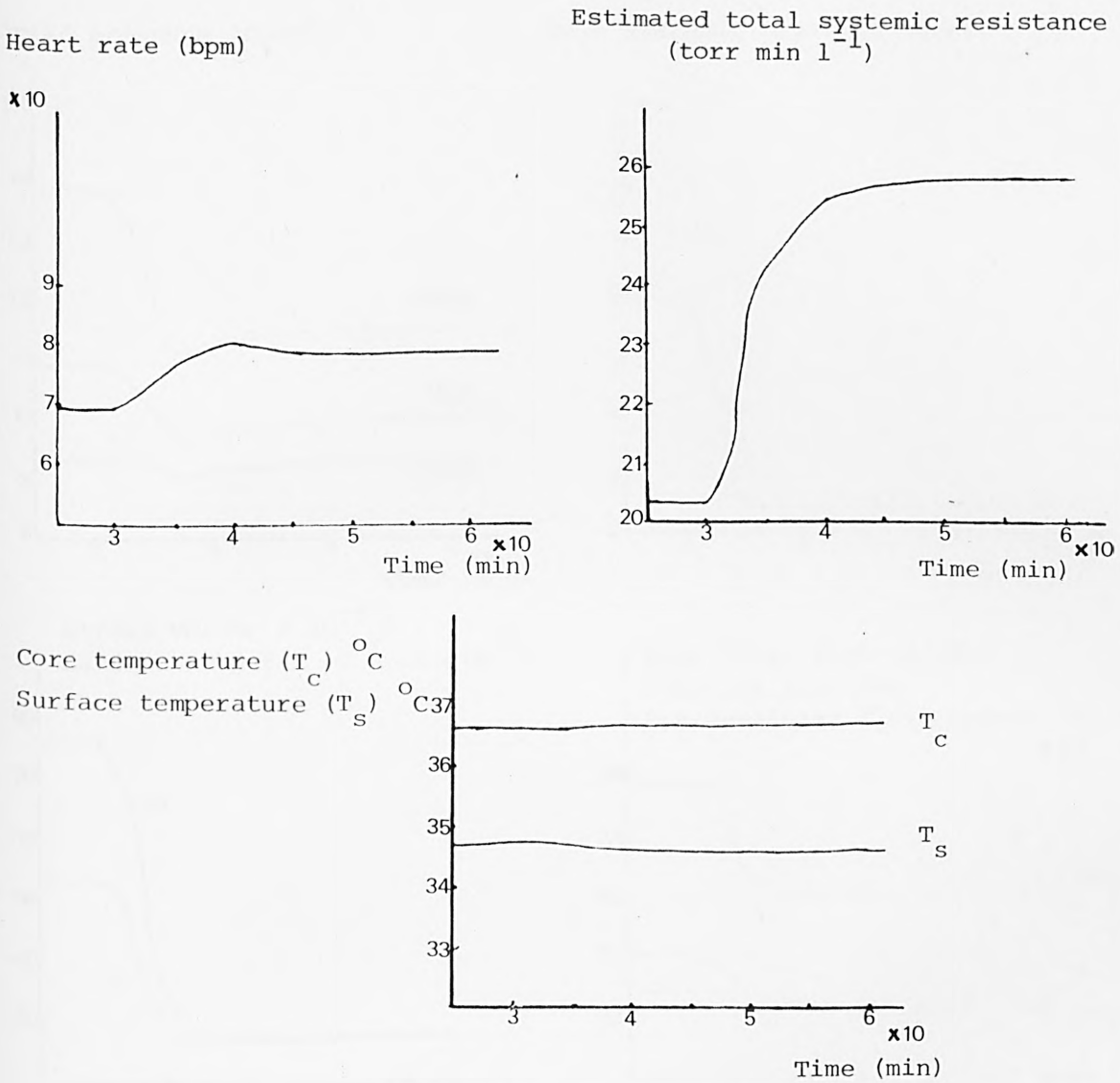

Figure 10.2 Dynamics following the removal of 500 ml of blood over a period of 5 minutes from the system veins segment, starting at t = 30 min.

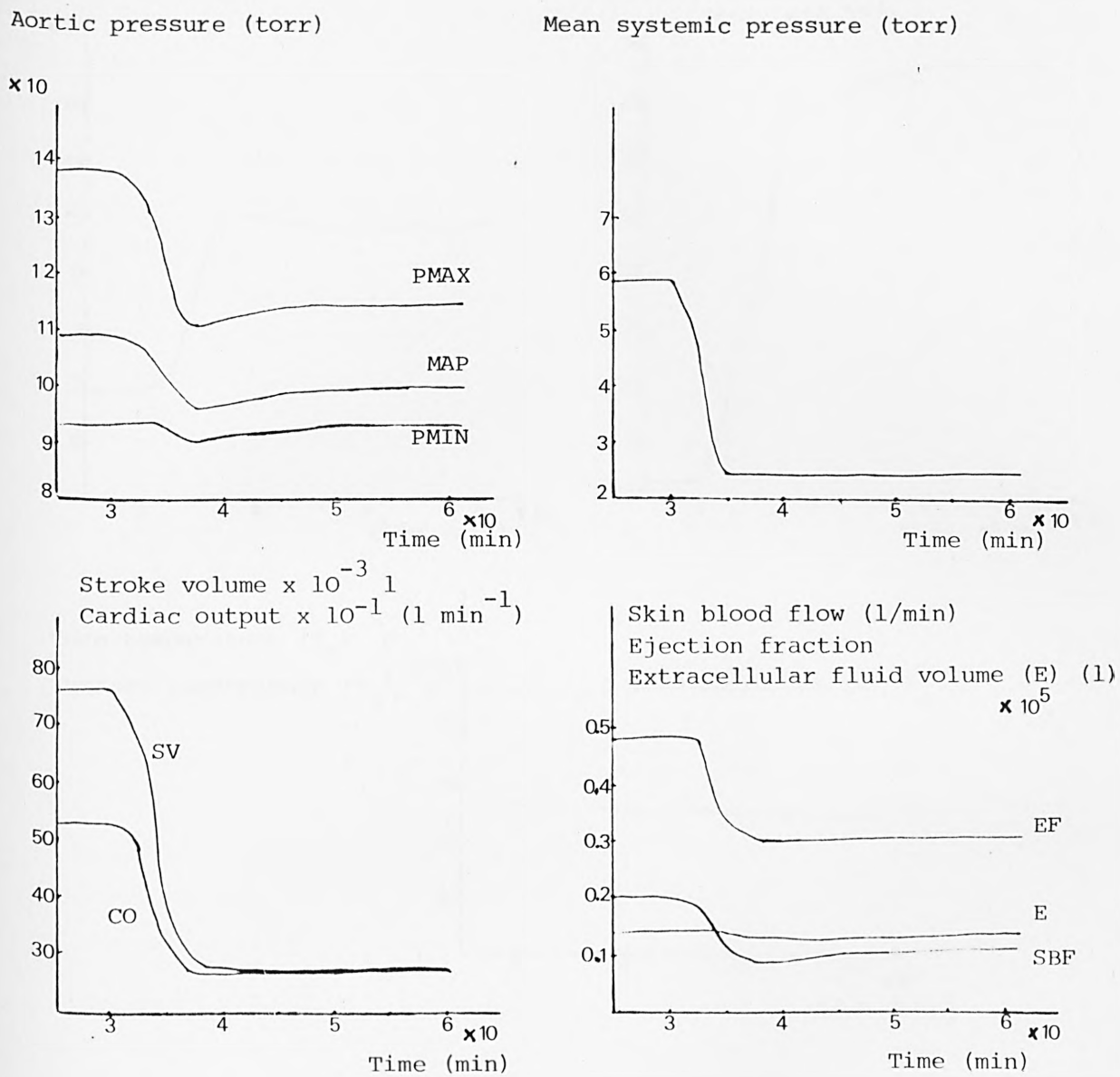

Figure 10.3 continued overleaf

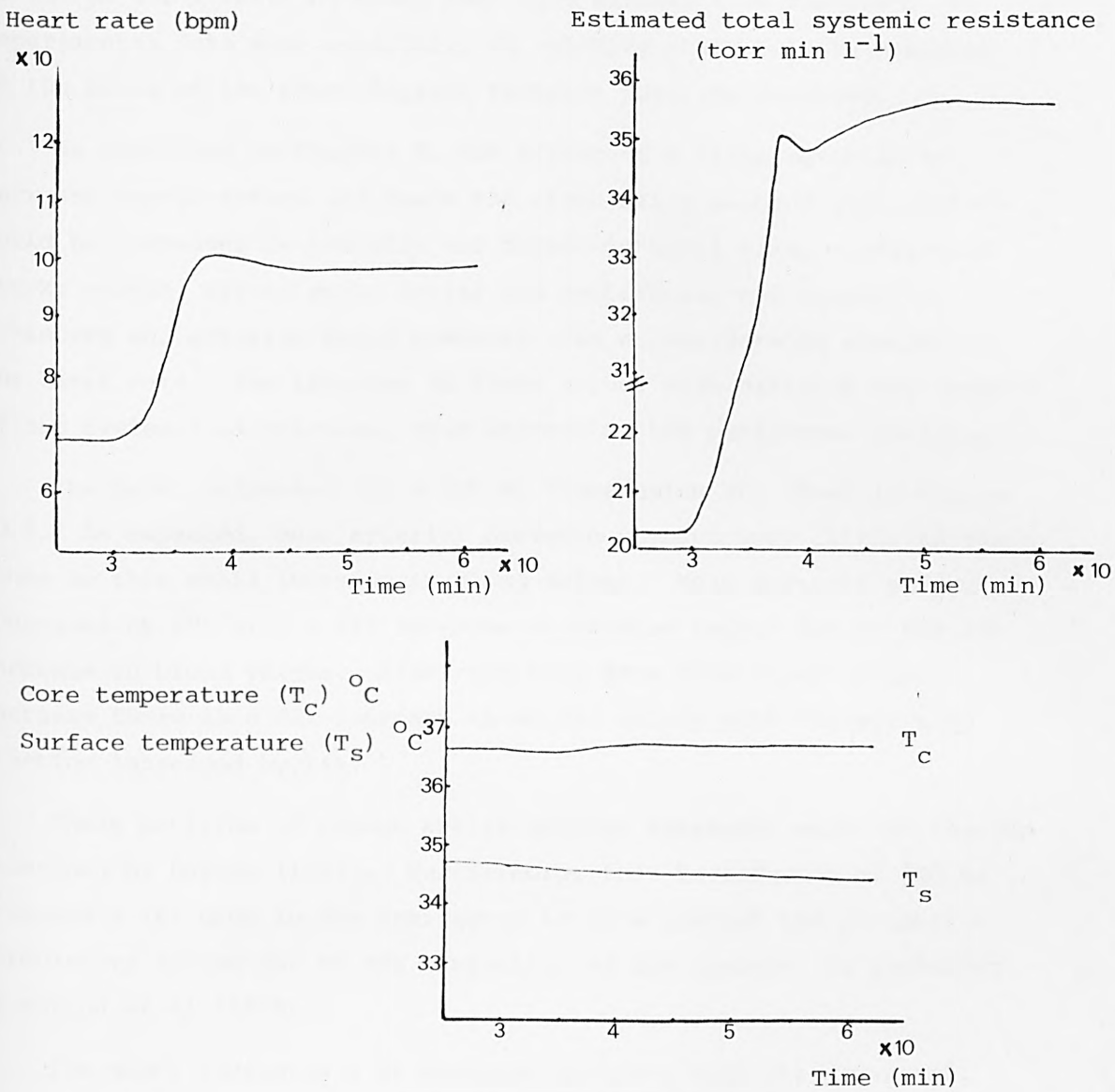

Figure 10.3 Dynamics following the removal of 1 litre of blood over a period of 5 minutes from the systemic veins segment, starting at t = 30 min.

as compared to the form incorporated in the 19-segment model.

10.2.2 Transfusion

As further tests of model validity, the responses to infusions of 500 ml and 1 litre of blood over five minutes were examined. No experimental data were available, so validity could only be assessed on the basis of the physiological response patterns produced.

As described in Chapter 6, the effect of a transfusion is to increase venous return and hence the circulating blood volume. There would be increases in systolic and diastolic heart size, ventricular stroke volume, stroke work, atrial and ventricular end diastolic pressures and arterial blood pressure with a considerable slowing of the heart rate. The increase in blood volume also distends the vessels of the systemic circulation, thus decreasing the peripheral resistance.

The model responses for a 500 ml transfusion are shown in Figure 10.4. As expected, mean arterial pressure changes very little in response to this small increase in blood volume. Mean systemic pressure increases by 29% with a 21% increase in cardiac output due to the 10% increase in blood volume. Also resulting from this blood volume increase there is a 32% increase in stroke volume with the ejection fraction increased by 11%.

These patterns of change are in general agreement with the changes described by Guyton (1981). Furthermore, this transfusion of 500 ml produces a 16% drop in the resistance to flow through the peripheral circulatory system due to the distention of the vessels, as explained by Guyton et al (1958).

The model indicated a 9% decrease in heart rate (bradycardia). This can be explained by the fact that the increase in blood volume increases arterial pressure which, in turn, initiates a reflex bradycardia due to stimulation of the cardio-inhibitory centre as a result of increased vagal tone (Ganong, 1975). The relation between heart rate and blood pressure (which is termed Marey's Law) is shown in Figure 10.5 (Bushman, 1983). The model also depicts a 3.5% increase in extracellular fluid volume, a core temperature decrease of 0.1% and a skin temperature rise of 0.3%.

The dynamic changes predicted by the model in response to a transfusion of 1 litre of blood over a period of five minutes are shown in Figure 10.6. The transfusion was administered to the segment representing

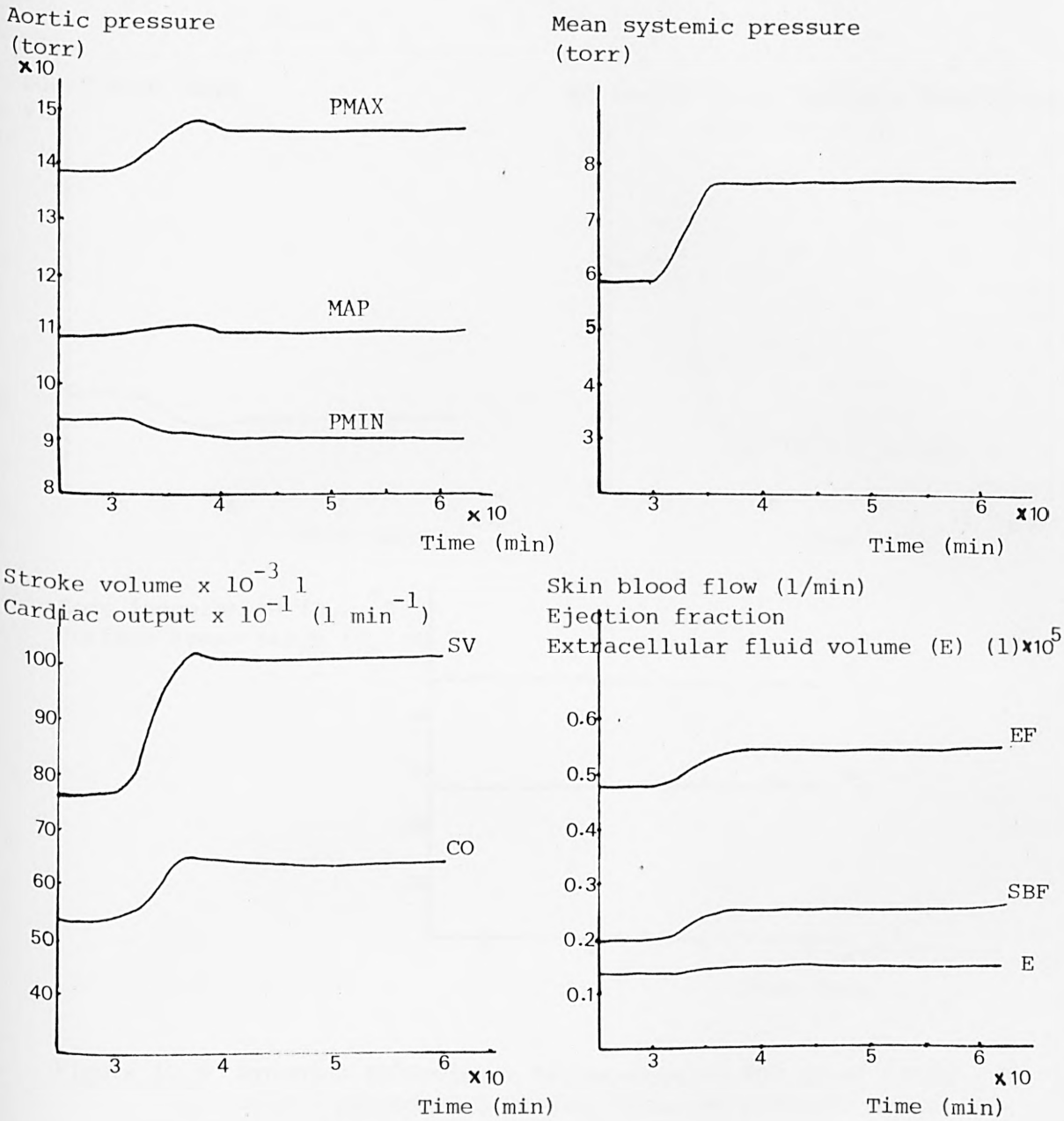

Figure 10.4 continued overleaf

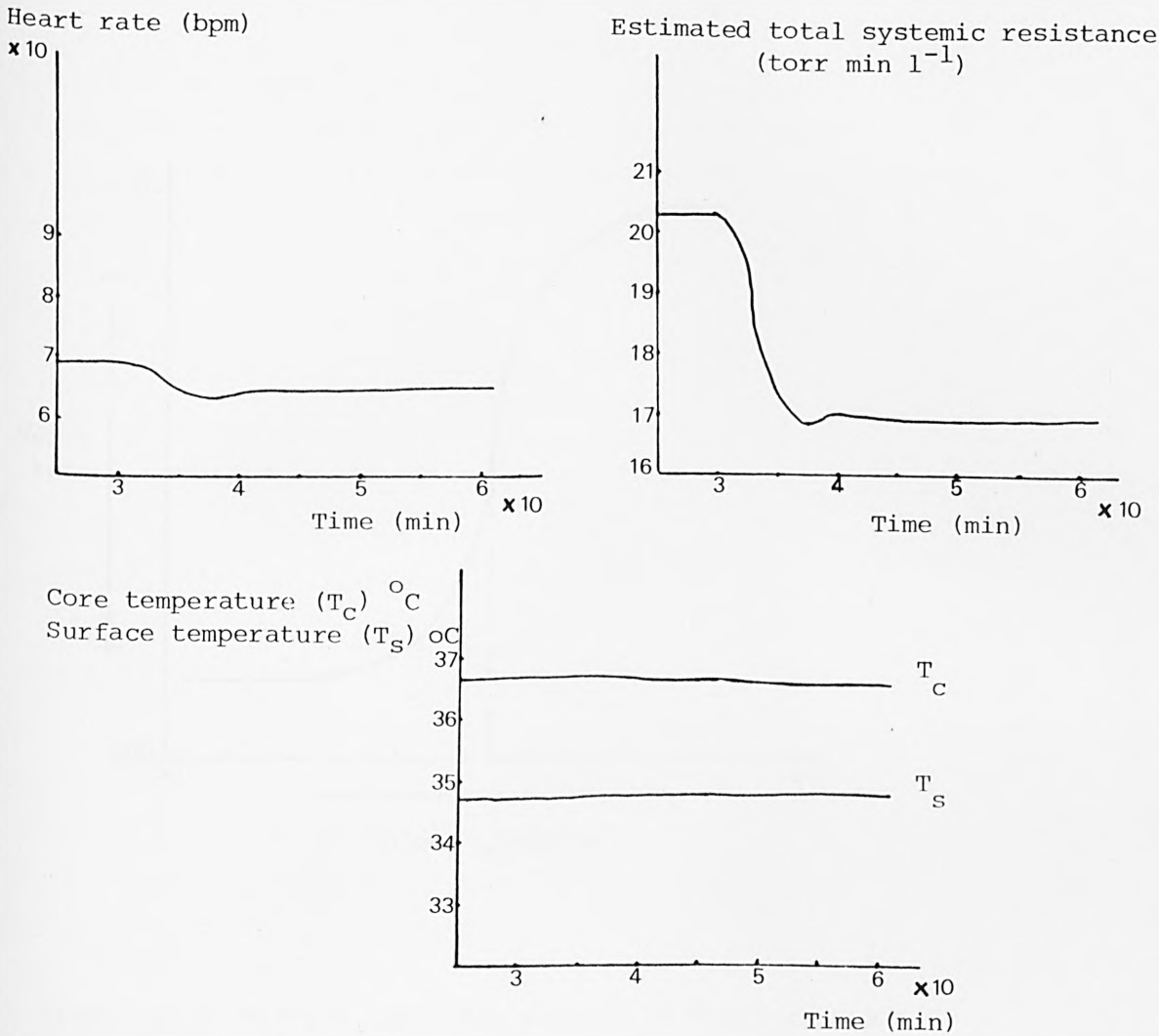

Figure 10.4 Dynamics following a transfusion of 500 ml of blood over a period of 5 minutes from the systemic veins segment, starting at t = 30 min.

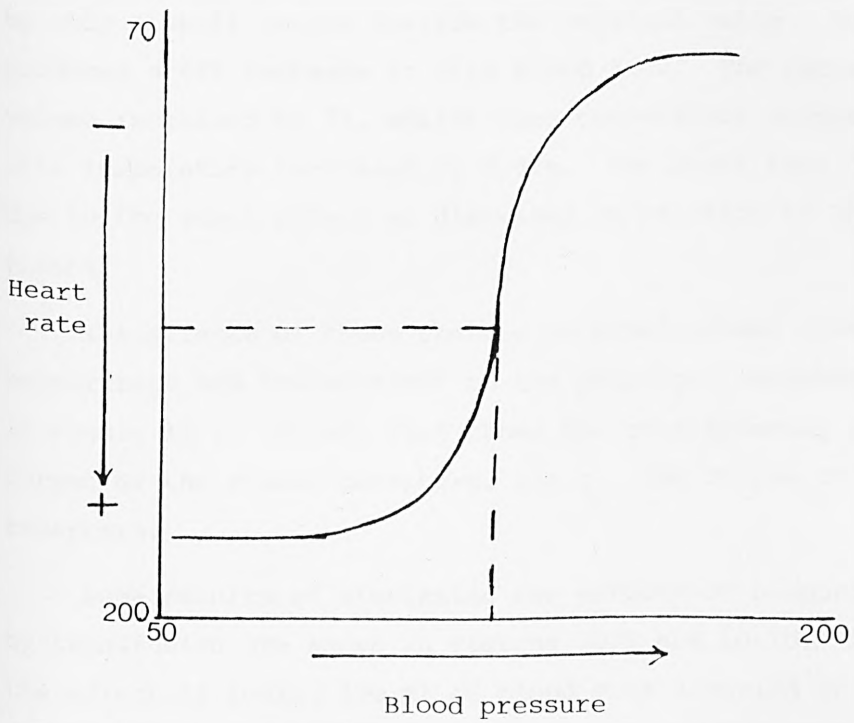

Figure 10.5 Marey's Law - the pattern of heart rate and blood pressure behaviour during transfusion (Bushman, 1983).

the systemic veins. Mean systemic pressure rises by 58% with increases of 39% and 65%, respectively, in cardiac output and stroke volume. Ejection fraction increased by 21%. Mean arterial pressure exhibits a 2% increase in value by the end of the five-minute transfusion before returning within the following five minutes essentially to its original value. Both systolic and diastolic pressures, however, are significantly changed as a result of the transfusion. Systolic pressure is increased by 10%, whilst the diastolic pressure is decreased by 5.4%. The effect of vasodilitation produces a sharp drop (by 29%) in the estimated total systemic resistance in the first six minutes followed by only a small return towards the original value. Vasodilitation also produces a 44% increase in skin blood flow. The extracellular fluid volume increased by 7%, whilst core temperature dropped by 0.14% and the skin temperature increased by 0.44%. The heart rate decreased by 15% due to the vagal effect as discussed in relation to the 500 ml transfusion.

The effects of these changes in blood volume (simulations of both haemorrhage and transfusion) on the principal variables are summarised in Figure 10.7. Figure 10.8 shows the corresponding effects on q_v, the output of the volume receptors, and q_p, the output of the pressure receptors.

Some results of simulating the effects of haemorrhage followed by transfusion are shown in Figures 10.9 and 10.10. Figure 10.9 shows the effect of losing 420 ml of blood over a period of five minutes, followed by its replacement at the same rate. This results in a return to the original steady state as would be expected. Figure 10.10 shows the effect of loss of 500 ml of blood over five minutes, followed by a transfusion of 1 litre.

10.3 SENSITIVITY ANALYSIS

In this section, the role of sensitivity analysis in examining the validity of the 8-segment model is described. Attention is given both to the effects of parameter variation on steady state values of the model variables as well as upon the dynamic responses observed following the loss of 500 ml of blood.

The form of analysis parallels that which was described for the full 19-segment model in Chapter 7. The effects of both individual parameter variation and Monte Carlo simulation are examined.

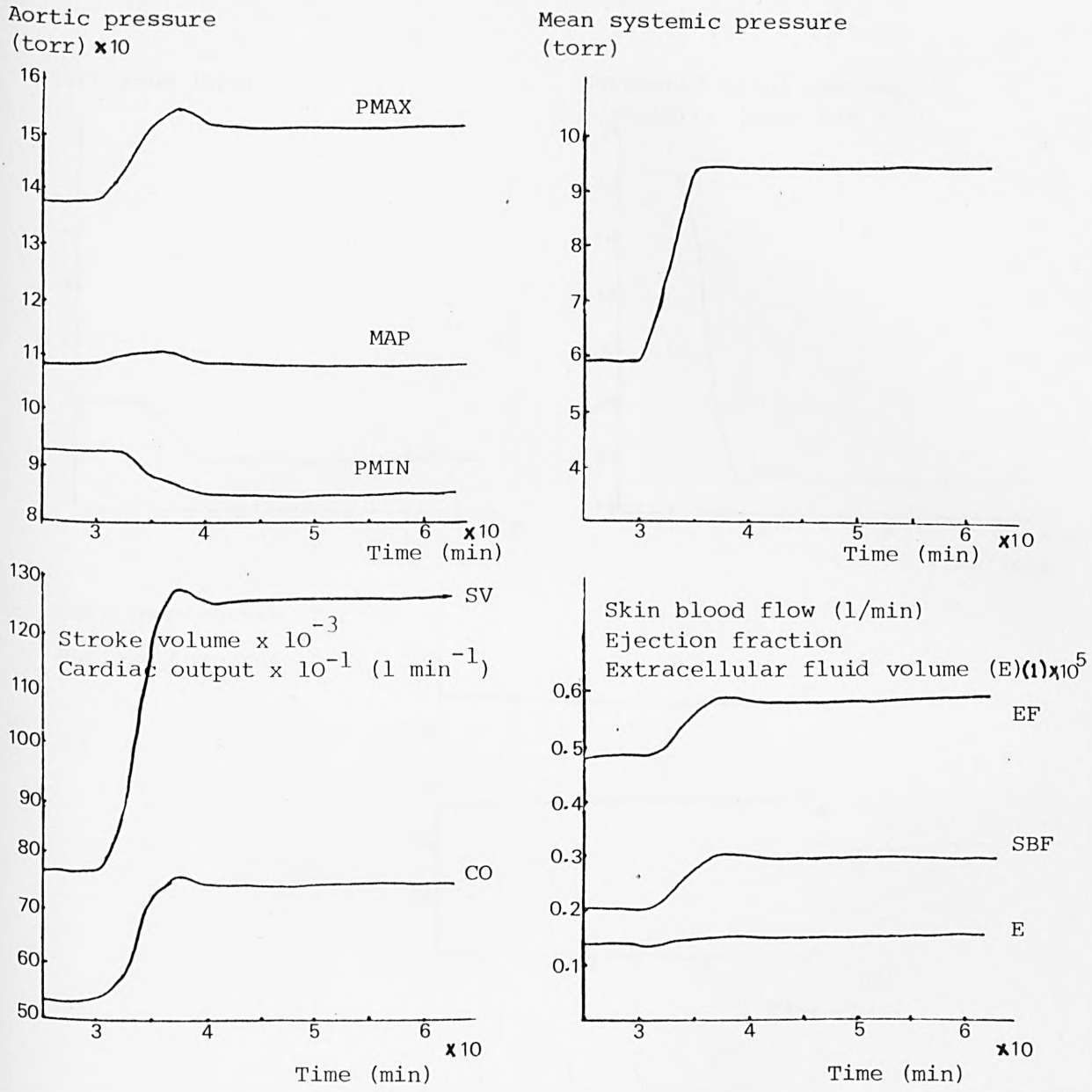

Figure 10.6 continued overleaf

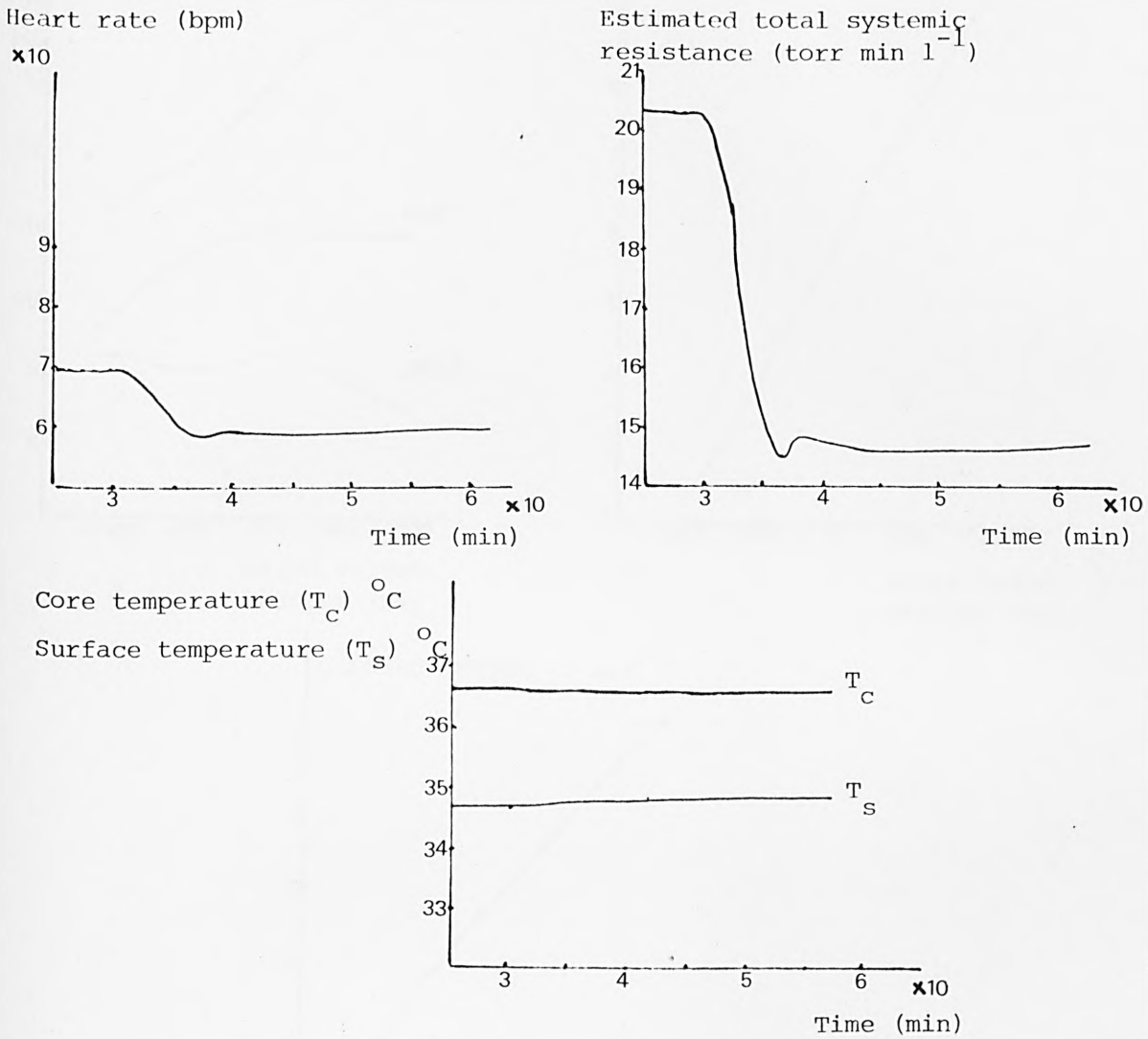

Figure 10.6 Dynamics following a transfusion of 1 litre of blood over 5 minutes to the systems veins segment, starting at t = 30 min.

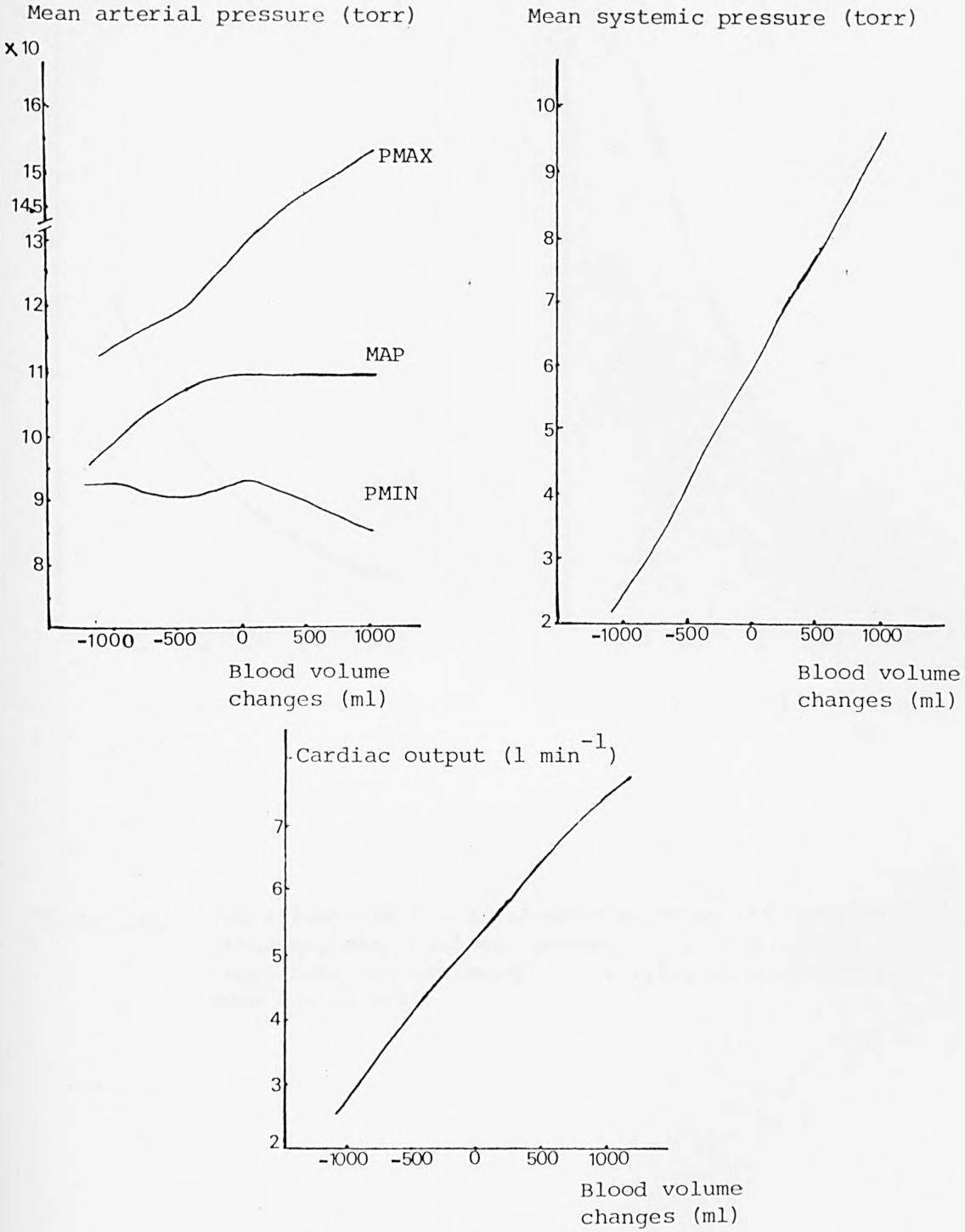

Figure 10.7 continued overleaf

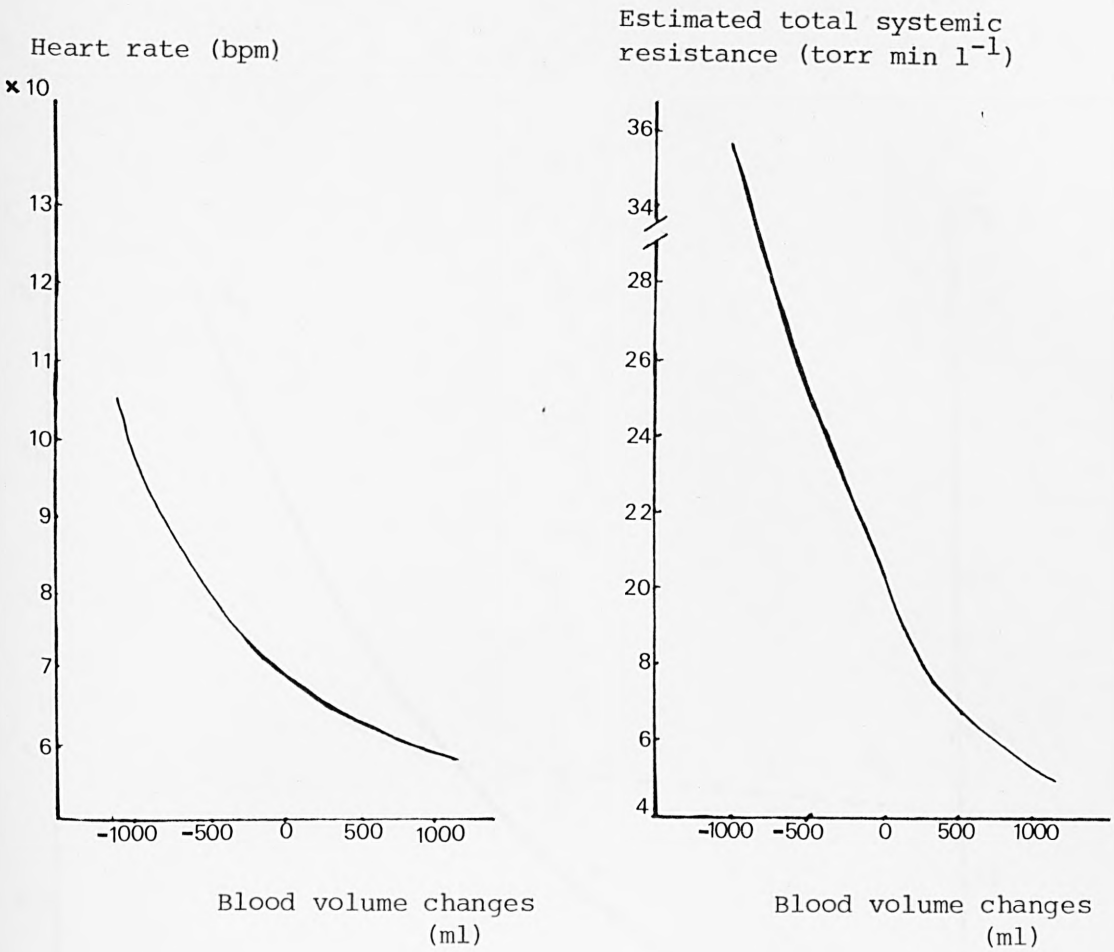

Figure 10.7 The effects of blood volume changes on the arterial pressure, mean systemic pressure, cardiac output, heart rate and estimated total systemic resistance, when t = 55 min.

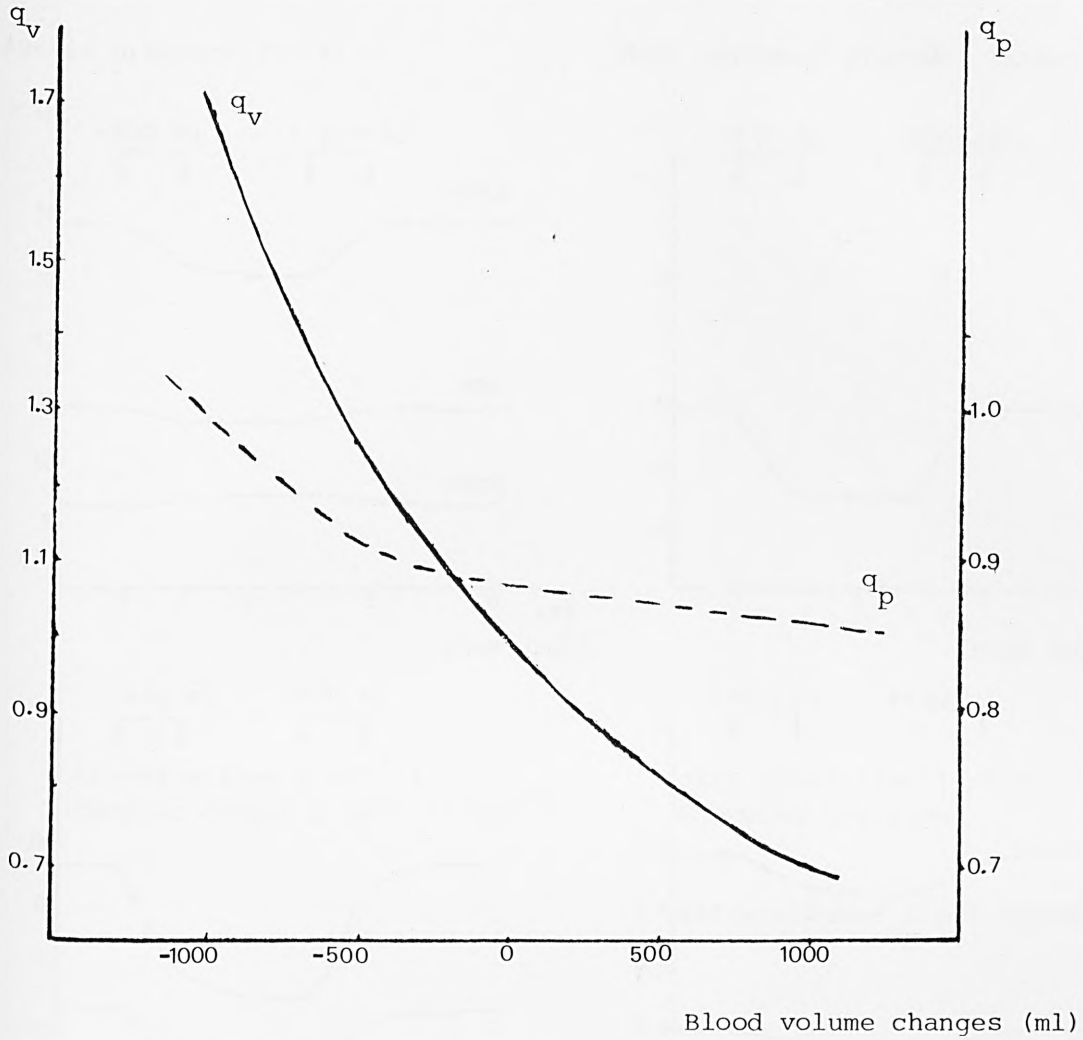

Figure 10.8 The relation between (q_v), the output of the volume receptors, and (q_p), the output of the pressure receptors, with the changes in blood volume.

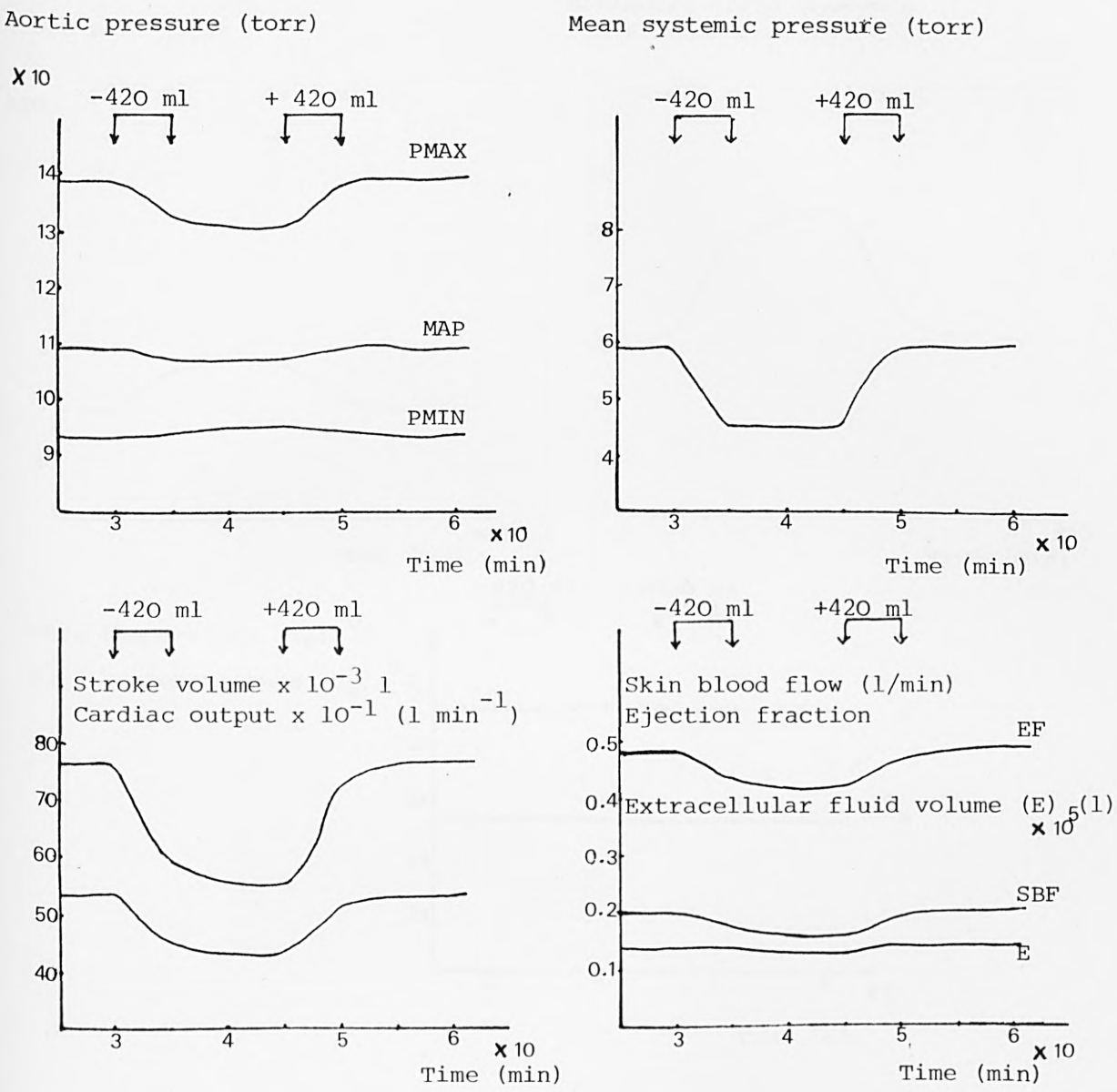

Figure 10.9 continued overleaf

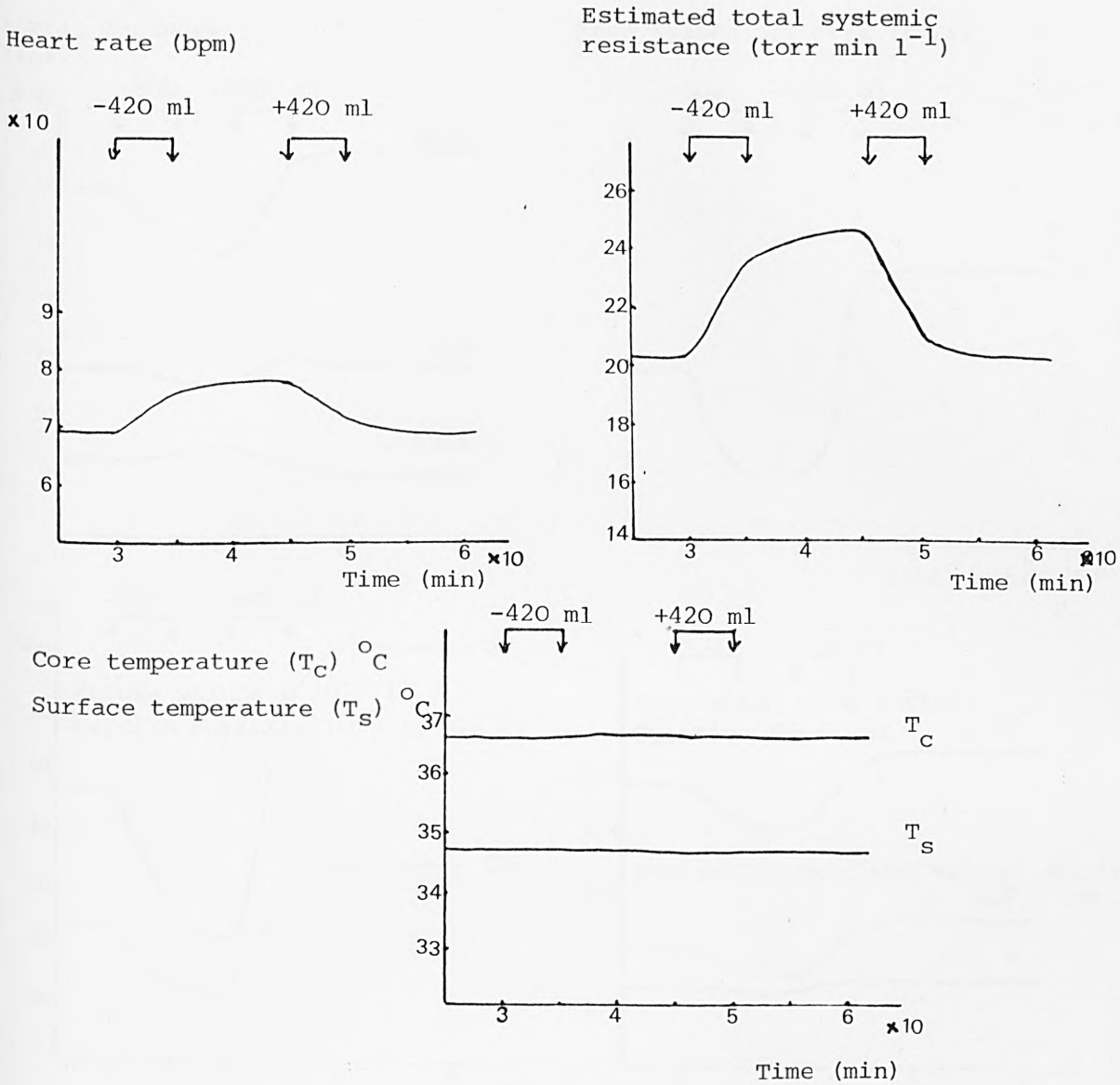

Figure 10.9 Dynamics following the removal of 420 ml of blood over a period of 5 minutes at t = 30 min, and regaining 420 ml of blood over a period of 5 minutes at t = 45 min in the systemic veins segment.

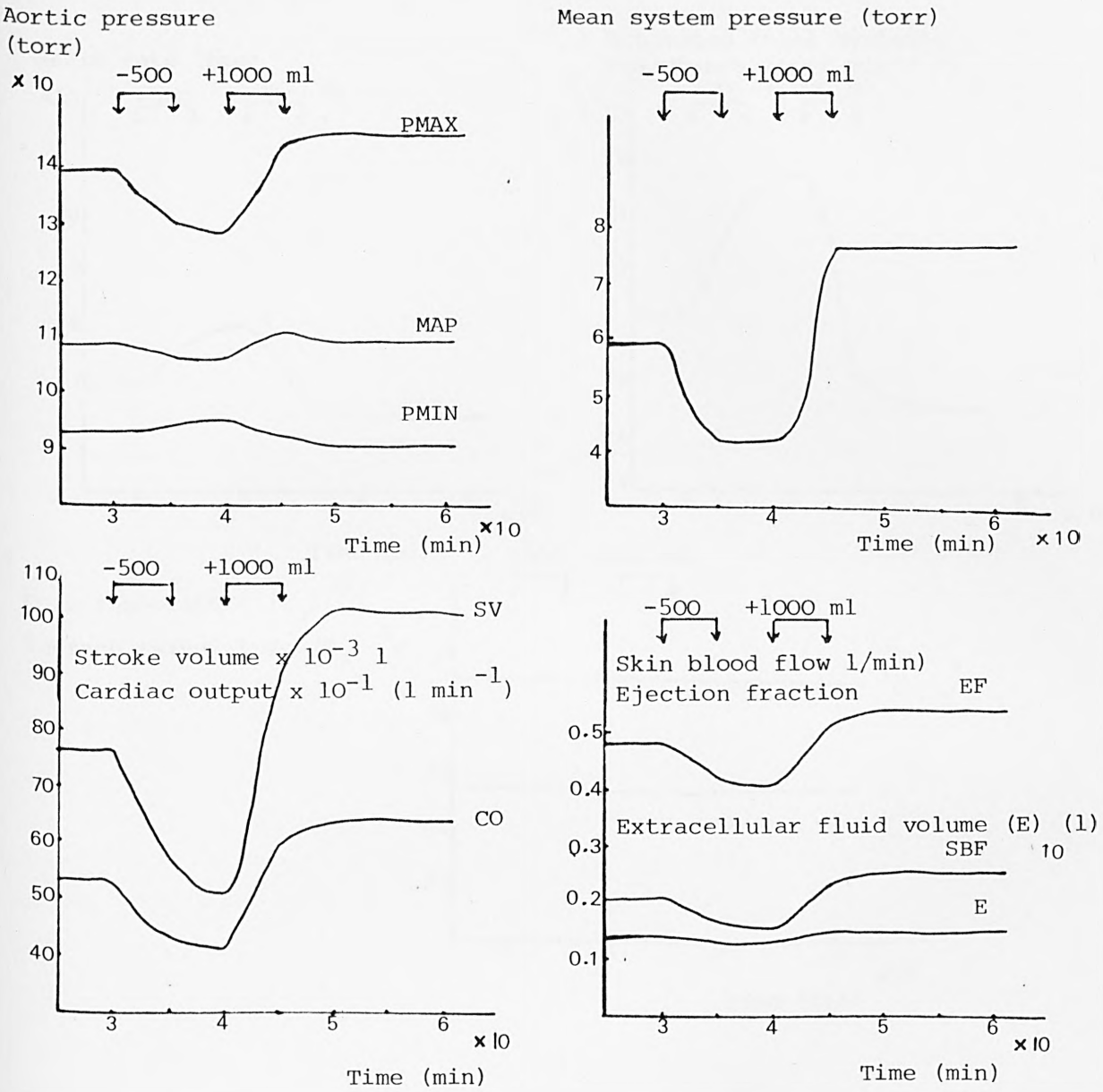

Figure 10.10 continued overleaf

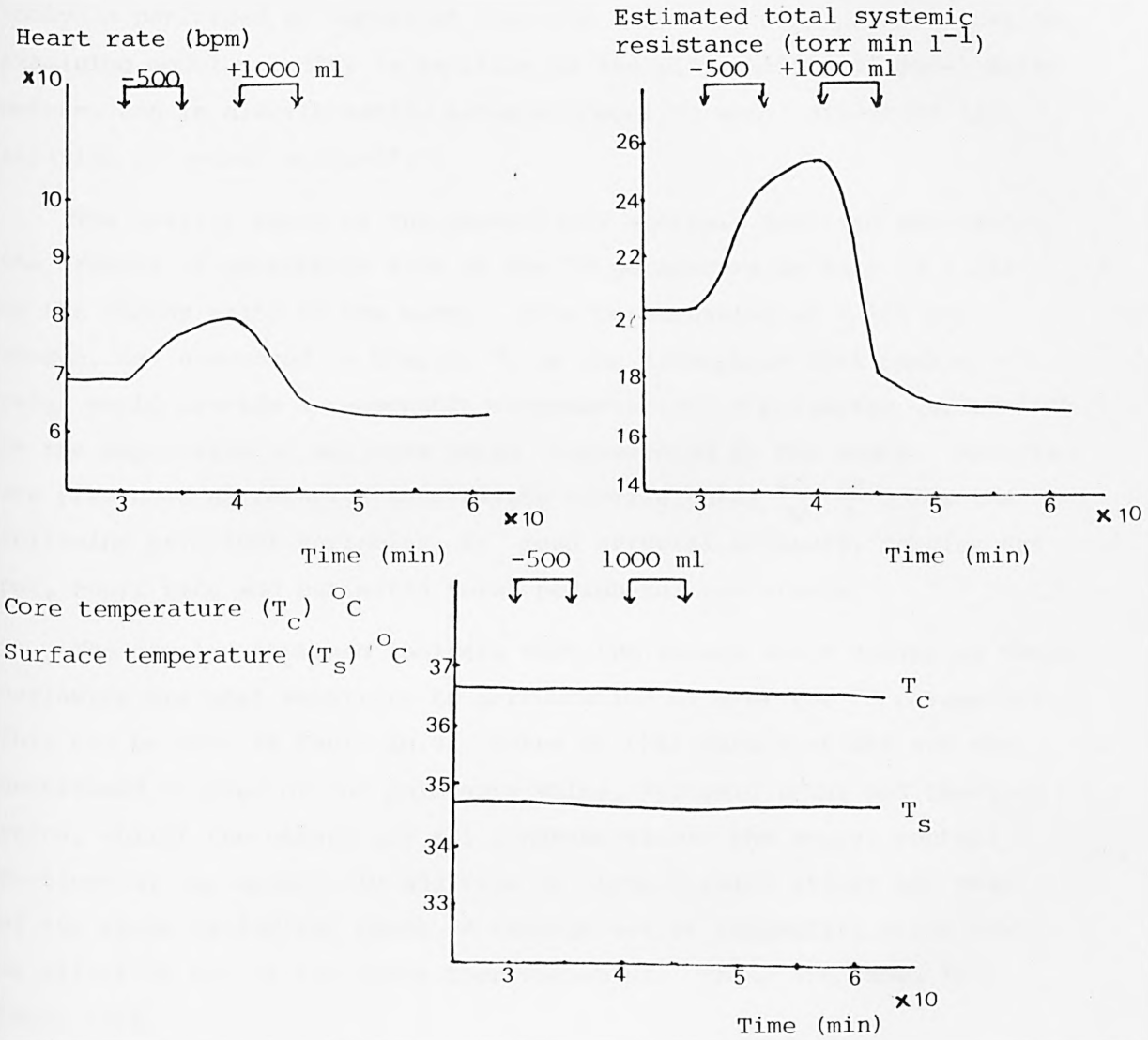

Figure 10.10 Dynamics response following the removal of 500 ml of blood at t = 30 min for 5 minutes, and regaining 1 litre of blood at t = 40 min for 5 minutes in the systemic veins segment.

10.3.1 Perturbation of Individual Parameters

Sensitivity analysis enables the effects of small changes in model structure, model parameters or inputs, including initial conditions, upon the overall model behaviour to be investigated. The 8-segment model includes 79 parameters, and in this case sensitivity analysis performed an important function in aiding model identification, examining model validity in relation to the plausibility of model parameters, and in discriminating between competing model structure (in relation to neural control).

The initial phase of the sensitivity analysis involved examining the effects of perturbing each of the 79 parameters in turn by $\pm$ 15% on the steady state of the model. This perturbation of $\pm$ 15% was chosen, as discussed in Chapter 7, on the assumption that such a range would provide a reasonable representation of parameter variability in the population of subjects being represented by the model. Results are presented as relative sensitivity coefficients, $\frac{\Delta X}{X} \Big/ \frac{\Delta P}{P}$, for the following principal variables, X: mean arterial pressure, cardiac output, heart rate and estimated total peripheral resistance.

The results obtained indicate that the steady state values of these variables are most sensitive to perturbation of 9 of the 79 parameters. This can be seen in Table 10.5. Three of this parameter set are the unstressed volumes of the pulmonary veins, systemic veins and thoracic veins, whilst the others are all constant within the neural control sections of the model. In addition to these 9 which affect all four of the above variables, there is another set of parameters which has an effect on two of the above four variables. These are shown in Table 10.6.

Tables 10.7 - 10.15 show the effects of perturbing the nine most sensitive parameters, one at a time, both on the steady state and also on the model response following the loss of 500 ml of blood. Values of the relative sensitivity coefficients for mean arterial pressure (MAP), cardiac output (CO), heart rate (FH) and estimated total systemic resistance (ETSR) corresponding to these nine parameters are listed both for the steady state and following the 500 ml blood loss. On the basis of their relative sensitivity coefficients, five of the parameters were seen to be substantially more sensitive than the other four. These are the unstressed volumes of the systemic veins and the thoracic veins (V_{USVN}, V_{UTV}) and the three neural control system constants K_{13}, K_{18} and $K_{21}\sigma_H$.

Parameter in computer program	Parameter in mathematical model	Nominal value	Interpretation
P(15)	V_{UPV}	430.0	Unstressed volume of the pulmonary veins
P(30)	V_{USVN}	1000.0	Normal unstressed volume of the systemic veins
P(32)	V_{UTV}	1300.0	Unstressed volume of thoracic veins
P(56)	K_{13}	1.0	Constant in the aortic arch baroreceptors
P(61)	K_{17}	1.0	Constant in central nervous system control
P(62)	K_{18}	80.0	
P(65)	$K_{21}\sigma_H$	0.006	
P(74)	K_{35}	1.4	
P(77)	K_{31}	1.6	

Table 10.5 The set of the nine most sensitive parameters in the 8-segment model.

Parameter in computer program	Parameter in mathematical model	Nominal value	Interpretation
P(26)	V_{USA}	370.0	Unstressed volume of systemic arteries
P(29)	C_{SVN}	59.0	Normal systemic veins compliance
P(51)	a_{LVD}	0.053	Elastance of the left ventricle during diastole
P(53)	a_{RVD}	0.027	Elastance of the right ventricle during diastole
P(55)	τ_2	0.1	Time constant in the aortic arch baroreceptor control model
P(57)	K_{14}	1.1	Constant in neural control system

Table 10.6 The set of the six next most sensitive parameters of the 8-segment model (having effects on at least two variables).

The results of applying similar procedures to the set of the six less sensitive parameters are shown in Tables 10.16 - 10.21.

10.3.2 Monte Carlo Simulation

In the previous section, sensitivity studies have been carried out on the basis of each parameter being varied in turn, that is all the parameters are kept at their nominal values except the parameter whose sensitivity is under investigation. This enabled the sub-set of the most sensitive parameters to be identified.

As a second stage of this validation procedure, the effects of varying all of these sensitive parameters together were examined using Monte Carlo simulation. The procedure was the same as that applied in seeking to validate the 19-segment model, which was reported earlier in Chapter 7. In essence, each of the nine sensitive parameters was assumed to lie within a $\pm$ 15% band about its nominal value, all values in this band being equally probable. Using a random number generator, values within this range were selected for each of the parameters and the simulation of the model using these values was performed. This procedure with different sets of "random" parameter values was repeated thirteen times, in order to obtain an adequate coverage of this uncertainty in the 9-parameter space. The values of the 9 parameters in each of these 14 simulations are shown in Table 10.22. The steady state values of mean arterial pressure, cardiac output, heart rate and estimated total systemic resistance for these 14 cases are given in Figure 10.11, these being presented in the form of a histogram in Figure 10.12. Figure 10.13 lists the corresponding values of these variables two minutes after the five-minute period during which the loss of 500 ml of blood had been simulated.

A similar Monte Carlo analysis was carried out using not only these nine parameters but also the six next most sensitive parameters, as defined above. Table 10.23 shows the values of these 15 parameters for ten simulation runs. The corresponding values of the four principal variables are shown in Figures 10.14 for the pre-stimulus steady state and 10.15 at two minutes after the end of the five-minute period during which 500 ml of blood was removed.

A comparison of results obtained from varying the parameters one at a time and those obtained from Monte Carlo simulation is given in Tables 10.24 - 10.27 for the nine most sensitive parameters. This

indicates first that the variation exhibited by the four variables is not unduly large. Secondly, the variation of the parameters one at a time produces variations nearly as great as those obtained from the limited number of Monte Carlo simulations which were performed.

10.4 CONCLUSIONS

This chapter has described the programme of validation which has been performed on the complete 8-segment model of the cardiovascular system.

In its complete form the model included the modifications to the structure of the neural control sub-system which were necessary in order to overcome the inadequacies revealed both in the 19-segment model, as reported in Chapter 6, and in the original version of the 8-segment model, as discussed in Chapter 9. These modifications involved including the effects of volume receptors and modifying the control of peripheral resistance so that the model was able to achieve the patterns of blood pressure change which are observed following the loss of a small quantity of blood.

Emphasis in this chapter has been placed upon empirical validity, examining the ability of the model to respond to both increase and decrease of blood volume. As discussed in Section 10.2, the model is generally able to reproduce the principal features expected over the range of test situations examined.

As has been discussed in earlier chapters, the chief limitation on examining the extent of model validity is the paucity of experimental data, a problem which is frequently encountered when dealing with complex, unidentifiable models in the observational sciences. Even having reduced the model from its original 19-segment form, this remains an overriding problem. Emphasis therefore has to be placed upon the role of sensitivity analysis in assessing model validity.

This was carried out in two stages, first examining the effects of individual parameter variation in order to identify those parameters, small variations in which would have an appreciable effect on both the steady-state and dynamic response of the model. Nine of the 79 parameters were thus identified on the basis of $\pm$ 15% variation about their nominal values, this variation being assumed to be an adequate

representation of the variability to be expected within a "normal" population. A set of the six next most sensitive parameters was revealed in a similar manner. This set was considered since it included parameter changes which can alter the patterns of heart rate, cardiac output and pressure response.

The second phase involved the use of Monte Carlo simulation, by which the effects of interactions between model parameters could be examined. From the analysis carried out the effects of interacting parameter changes were not generally very strong.

Two specific points do emerge. First, the majority of the most critical parameters form a part of the neural control section of the model. This implies that if the model was to be tuned to a specific subject or patient, additional data and/or knowledge in this area would be required if confidence was to be attached to the results of model prediction. Secondly, two of the most sensitive parameters, the unstressed volumes of the thoracic veins and the systemic veins, represent highly aggregated quantities. Clearly care needs to be taken when carrying out the reduction process (in this case from 19 to 8 segments for the circulation) in order to avoid any unnecessary increase in model uncertainty.

Variable	Pre-stimulus variable value			Post-stimulus (following haemorrhage) variable value			RSC for the steady state (pre-stimulus)		RSC post-stimulus	
	P(15) (nom)	P(15) +15%	P(15) -15%	P(15) (nom)	P(15) +15%	P(15) -15%	(+)	(-)	(+)	(-)
MAP	109.1	107.4	110.6	105.61	102.55	108.23	-0.103	0.091	-0.19	0.17
CO	5.36	5.23	5.47	4.13	3.97	4.27	-0.16	-0.136	-0.26	0.23
FH	69.95	71.58	68.62	80.08	83.38	77.35	0.155	0.126	0.27	+0.23
ETSR	20.35	20.5	20.21	25.57	25.80	25.3	0.049	0.045	0.06	+0.07

Table 10.7 Examination of the sensitivity of the four major model variables to perturbation of P(15) $\left(V_{UPV}\right)$, the unstressed volume of pulmonary veins, by ±15%. Pre-stimulus values and values at the end of the haemorrhage are presented, together with the relative sensitivity coefficients (RSC), evaluated for +15% (+) and -15% (-) parameter perturbation from the nominal (nom) value.

Variable	Pre-stimulus variable value			Post-stimulus (following haemorrhage) variable value			RSC for the steady state (pre-stimulus)		RSC post-stimulus	
	P(30) (nom)	P(30) +15%	P(30) -15%	P(30) (nom)	P(30) +15%	P(30) -15%	(+)	(-)	(+)	(-)
MAP	109.1	105.29	112.4	105.61	100.34	110.21	-0.232	-0.2	-0.33	-0.3
CO	5.36	5.075	5.62	4.13	3.84	4.401	0.354	-0.323	-0.47	-0.44
FH	69.95	73.91	66.84	80.08	86.16	75.37	0.377	0.29	0.51	0.39
ETSR	20.35	20.74	20.0	25.57	26.1	25.03	0.127	0.114	0.14	0.14

Table 10.8 Examination of the sensitivity of the four major model variables to perturbation of P(30) $\left(V_{USVN}\right)$, the unstressed volume of systemic veins, by ±15%. Pre-stimulus values and values at the end of the haemorrhage are presented, together with the relative sensitivity coefficients (RSC), evaluated for +15% (+) and -15% (-) parameter perturbation from the nominal (nom) value.

Variable	Pre-stimulus variable value			Post-stimulus (following haemorrhage) variable value			RSC for the steady state (pre-stimulus)		RSC post-stimulus	
	P(32) (nom)	P(32) +15%	P(32) -15%	P(32) (nom)	P(32) +15%	P(32) -15%	(+)	(-)	(+)	(-)
MAP	109.1	103.47	113.27	105.61	95.76	112.61	-0.34	-0.257	-0.62	-0.44
CO	5.36	4.967	5.66	4.13	3.63	4.51	-0.488	-0.37	-0.81	-0.61
FH	69.95	75.66	66.27	80.08	91.82	73.22	0.544	0.35	0.98	0.57
ETSR	20.35	20.83	19.98	25.57	26.37	24.91	0.157	0.12	0.21	0.17

Table 10.9 Examination of the sensitivity of the four major model variables to perturbation of P(32) (V_{UTV}), the unstressed volume of thoracic veins, by ±15%. Pre-stimulus values and values at the end of the haemorrhage are presented, together with the relative sensitivity coefficients (RSC), evaluated for +15% (+) and -15% (-) parameter perturbation from the nominal (nom) value.

Variable	Pre-stimulus variable value			Post-stimulus (following haemorrhage) variable value			RSC for the steady state (pre-stimulus)		RSC post-stimulus	
	P(56) (nom)	P(56) +15%	P(56) -15%	P(56) (nom)	P(56) +15%	P(56) -15%	(+)	(-)	(+)	(-)
MAP	109.1	102.26	117.26	105.61	100.2	111.86	-0.417	-0.49	-0.34	-0.39
CO	5.36	5.06	5.69	4.13	3.95	4.33	-0.37	-0.41	-0.29	-0.32
FH	69.95	65.86	75.74	80.08	74.57	87.53	-0.389	-0.55	-0.46	-0.62
ETSR	20.35	20.17	20.5	25.57	25.35	25.82	-0.058	-0.075	-0.06	-0.07

Table 10.10 Examination of the sensitivity of the four major model variables to perturbation of P(56) (K_{13}), the constant in the neural control system, by ±15%. Pre-stimulus values and values at the end of the haemorrhage are presented, together with the relative sensitivity coefficients (RSC), evaluated for +15% (+) and -15% (-) parameter perturbation from the nominal (nom) value.

Variable	Pre-stimulus variable value			Post-stimulus (following haemorrhage) variable value			RSC for the steady state (pre-stimulus)		RSC post-stimulus	
	P(61) (nom)	P(61) +15%	P(61) -15%	P(61) (nom)	P(61) +15%	P(61) -15%	(+)	(-)	(+)	(-)
MAP	109.1	108.77	109.33	105.61	105.84	105.16	-0.02	-0.014	0.015	0.03
CO	5.36	5.25	5.47	4.13	4.077	4.19	-0.136	0.136	-0.05	-0.1
FH	69.95	66.09	74.56	80.08	75.91	84.93	-0.36	-0.43	-0.35	-0.4
ETSR	20.35	20.69	19.97	25.57	25.95	25.09	0.111	0.12	0.1	0.13

Table 10.11 Examination of the sensitivity of the four major model variables to perturbation of P(61) (K_{17}), the constant in the central nervous control system, by ±15%. Pre-stimulus values and values at the end of the haemorrhage are presented, together with the relative sensitivity coefficients (RSC), evaluated for +15% (+) and -15% (-) parameter perturbation from the nominal (nom) value.

Variable	Pre-stimulus variable value			Post-stimulus (following haemorrhage) variable value			RSC for the steady state (pre-stimulus)		RSC post-stimulus	
	P(62) (nom)	P(62) +15%	P(62) -15%	P(62) (nom)	P(62) +15%	P(62) -15%	(+)	(-)	(+)	(-)
MAP	109.1	112.66	103.2	105.61	109.09	99.87	0.21	0.36	0.22	0.36
CO	5.36	5.595	4.97	4.13	4.30	3.86	0.28	0.48	0.27	0.44
FH	69.95	66.85	75.9	80.08	76.84	86.17	-0.29	-0.56	-0.27	-0.51
ETSR	20.35	20.13	20.72	25.57	25.36	25.86	-0.07	-0.12	-0.055	-0.08

Table 10.12 Examination of the sensitivity of the four major model variables to perturbation of P(62) (K_{18}), the constant in the central nervous control system, by ±15%. Pre-stimulus values and values at the end of the haemorrhage are presented, together with the relative sensitivity coefficients (RSC), evaluated for +15% (+) and -15% (-) parameter perturbation from the nominal (nom) value.

Variable	Pre-stimulus variable value			Post-stimulus (following haemorrhage) variable value			RSC for the steady state (pre-stimulus)		RSC post-stimulus	
	P(65) (nom)	P(65) +15%	P(65) -15%	P(65) (nom)	P(65) +15%	P(65) -15%	(+)	(-)	(+)	(-)
MAP	109.1	108.39	109.62	105.61	106.1	104.49	-0.043	-0.031	0.031	0.071
CO	5.36	5.146	5.61	4.13	3.99	4.27	-0.268	-0.31	-0.23	-0.23
FH	69.95	62.19	80.61	80.08	70.7	93.10	-0.739	-1.01	-0.78	-1.08
ETSR	20.35	21.06	19.53	25.57	26.54	24.42	0.23	-0.268	0.25	0.3

Table 10.13 Examination of the sensitivity of the four major model variables to perturbation of P(65) $(K_{21}\sigma_H)$, the constant in the central nervous control system, by ±15%. Pre-stimulus values and values at the end of the haemorrhage are presented, together with the relative sensitivity coefficients (RSC), evaluated for +15% (+) and -15% (-) parameter perturbation from the nominal (nom) value.

Variable	Pre-stimulus variable value			Post-stimulus (following haemorrhage) variable value			RSC for the steady state (pre-stimulus)		RSC post-stimulus	
	P(74) (nom)	P(74) +15%	P(74) -15%	P(74) (nom)	P(74) +15%	P(74) -15%	(+)	(-)	(+)	(-)
MAP	109.1	110.3	107.4	105.61	107.16	103.52	0.072	0.103	0.097	0.13
CO	5.36	5.458	5.23	4.13	4.22	4.01	0.111	0.161	0.145	0.19
FH	69.95	68.43	72.03	80.08	78.08	82.65	-0.144	0.198	-0.17	-0.21
ETSR	20.35	20.22	20.54	25.57	25.36	25.8	-0.042	-0.062	-0.055	-0.06

Table 10.14 Examination of the sensitivity of the four major model variables to perturbation of P(74) (K_{35}), the constant in the central nervous control system, by ±15%. Pre-stimulus values and values at the end of the haemorrhage are presented, together with the relative sensitivity coefficients (RSC), evaluated for +15% (+) and -15% (-) parameter perturbation from the nominal (nom) value.

Variable	Pre-stimulus variable value			Post-stimulus (following haemorrhage) variable value			RSC for the steady state (pre-stimulus)		RSC post-stimulus	
	P(77) (nom)	P(77) +15%	P(77) -15%	P(77) (nom)	P(77) +15%	P(77) -15%	(+)	(-)	(+)	(-)
MAP	109.1	111.4	105.7	105.61	108.68	101.2	0.14	0.2	0.19	0.28
CO	5.36	5.493	5.161	4.13	4.26	3.93	0.16	0.24	0.21	0.32
FH	69.95	67.99	73.09	80.08	77.13	84.69	-0.18	-0.29	-0.25	-0.38
ETSR	20.35	20.28	20.47	25.57	25.48	25.68	-0.02	-0.039	-0.02	-0.03

Table 10.15 Examination of the sensitivity of the four major model variables to perturbation P(77) (K_{31}), the constant in the central nervous control system, by ±15%. Pre-stimulus values and values at the end of the haemorrhage are presented, together with the relative sensitivity coefficients (RSC), evaluated for +15% (+) and -15% (-) parameter perturbation from the nominal (nom) value.

Variable	Pre-stimulus variable value			Post-stimulus (following haemorrhage) variable value			RSC for the steady state (pre-stimulus)		RSC post-stimulus	
	P(26) (nom)	P(26) +15%	P(26) -15%	P(26) (nom)	P(26) +15%	P(26) -15%	(+)	(-)	(+)	(-)
MAP	109.1	107.7	110.39	105.61	103.0	107.85	-0.085	-0.078	-0.164	-0.141
CO	5.36	5.25	5.45	4.13	3.995	4.25	-0.136	-0.111	-0.226	-0.19
FH	69.95	71.38	68.74	80.08	82.83	77.69	0.136	0.115	0.229	0.198
ETSR	20.35	20.49	20.23	25.57	25.79	25.33	0.045	0.039	0.057	0.062

Table 10.16 Examination of the sensitivity of the four major model variables to perturbation P(26) (V_{USA}), the unstressed volume of systemic arteries, by ±15%. Pre-stimulus values and values at the end of the haemorrhage are presented, together with the relative sensitivity coefficients (RSC) evaluated for +15% (+) and -15% (-) parameter perturbation from the nominal (nom) value.

Variable	Pre-stimulus variable value			Post-stimulus (following haemorrhage) variable value			RSC for the steady state (pre-stimulus)		RSC post-stimulus	
	P(29) (nom)	P(29) +15%	P(29) -15%	P(29) (nom)	P(29) +15%	P(29) -15%	(+)	(-)	(+)	(-)
MAP	109.1	107.69	110.55	105.61	103.82	107.34	-0.086	0.088	0.113	-0.11
CO	5.36	5.27	5.44	4.13	4.05	4.20	-0.111	0.099	-0.13	-0.113
FH	69.95	71.21	68.82	80.08	81.76	78.37	0.12	-0.107	0.139	0.14
ETSR	20.35	20.4	20.31	25.57	25.59	25.5	0.016	-0.013	0.005	0.018

Table 10.17 Examination of the sensitivity of the four major model variables to perturbation of P(29) (C_{SVN}), the normal systemic veins compliance, by ±15%. Pre-stimulus values and values at the end of the haemorrhage are presented, together with the relative sensitivity coefficients (RSC), evaluated for +15% (+) and -15% (-) parameter perturbation from the nominal (nom) value.

Variable	Pre-stimulus variable value			Post-stimulus (following haemorrhage) variable value			RSC for the steady state (pre-stimulus)		RSC post-stimulus	
	P(51) (nom)	P(51) +15%	P(51) -15%	P(51) (nom)	P(51) +15%	P(51) -15%	(+)	(-)	(+)	(-)
MAP	109.1	107.87	110.4	105.61	104.16	106.79	-0.075	-0.079	-0.09	-0.07
CO	5.36	5.26	5.458	4.13	4.06	4.19	-0.124	-0.121	-0.11	-0.099
FH	69.95	71.27	68.8	80.08	81.57	78.87	0.125	0.1	0.12	0.1
ETSR	20.35	20.48	20.22	25.57	25.65	25.47	0.042	0.042	0.021	0.026

Table 10.18 Examination of the sensitivity of the four major model variables to perturbation of P(51) (a_{LVD}), elastance of the left ventricle during diastole, by ±15%. Pre-stimulus values and values at the end of the haemorrhage are presented, together with the relative sensitivity coefficients (RSC), evaluated for +15% (+) and -15% (-) parameter perturbation from the nominal (nom) value.

Variable	Pre-stimulus variable value			Post-stimulus (following haemorrhage) variable value			RSC for the steady state (pre-stimulus)		RSC post-stimulus	
	P(53) (nom)	P(53) +15%	P(53) -15%	P(53) (nom)	P(53) +15%	P(53) -15%	(+)	(-)	(+)	(-)
MAP	109.1	107.77	110.42	105.61	103.96	107.22	-0.081	-0.08	-0.1	-0.1
CO	5.36	5.24	5.48	4.13	4.034	4.22	-0.149	-0.149	-0.16	-0.15
FH	69.95	71.44	68.6	80.08	81.8	78.31	0.142	0.128	0.14	0.15
ETSR	20.35	20.56	20.14	25.57	25.77	25.35	0.068	0.068	0.05	0.06

Table 10.19 Examination of the sensitivity of the four major model variables to perturbation of P(53) (a_{RVD}), elastance of the right ventricle during diastole, by ±15%. Pre-stimulus values and values at the end of the haemorrhage are presented, together with the relative sensitivity coefficients (RSC), evaluated for +15% (+) and -15% (-) parameter perturbation from the nominal (nom) value.

Variable	Pre-stimulus variable value			Post-stimulus (following haemorrhage) variable value			RSC for the steady state (pre-stimulus)		RSC post-stimulus	
	P(55) (nom)	P(55) +15%	P(55) -15%	P(55) (nom)	P(55) +15%	P(55) -15%	(+)	(-)	(+)	(-)
MAP	109.1	107.27	110.99	105.61	103.63	107.7	-0.111	-0.115	-0.124	-0.131
CO	5.36	5.31	5.4	4.13	4.088	4.17	-0.06	-0.049	-0.06	-0.064
FH	69.95	72.89	67.85	80.08	82.6	77.46	0.28	0.2	0.209	0.21
ETSR	20.35	20.2	20.53	25.57	25.34	25.77	-0.049	-0.05	-0.059	-0.052

Table 10.20 Examination of the sensitivity of the four major model variables to perturbation of P(55) (τ_2), the time constant in the aortic arch baroreceptor control, by ±15%. Pre-stimulus values and values at the end of the haemorrhage are presented, together with the relative sensitivity coefficients (RSC), evaluated for +15% (+) and -15% (-) parameter perturbation from the nominal (nom) value.

Variable	Pre-stimulus variable value			Post-stimulus (following haemorrhage) variable value			RSC for the steady state (pre-stimulus)		RSC post-stimulus	
	P(57) (nom)	P(57) +15%	P(57) -15%	P(57) (nom)	P(57) +15%	P(57) -15%	(+)	(-)	(+)	(-)
MAP	109.1	107.82	110.52	105.61	104.77	106.46	0.07	0.086	-0.053	-0.053
CO	5.36	5.25	5.46	4.13	4.07	4.19	0.13	0.124	-0.096	-0.097
FH	69.95	66.1	74.46	80.08	75.95	84.8	0.36	0.429	-0.344	-0.39
ETSR	20.35	20.5	20.22	25.57	25.7	25.36	-0.049	-0.04	0.033	0.055

Table 10.21 Examination of the sensitivity of the four major model variables to perturbation of P(57) (K_{14}), the constant in the central nervous control system, by ±15%. Pre-stimulus values and values at the end of the haemorrhage are presented, together with the relative sensitivity coefficients (RSC), evaluated for +15% (+) and -15% (-) parameter perturbation from the nominal (nom) value.

Run No.	1	2	3	4	5	6	7	8	9	10	11	12	13	14
P(15)	386.535	466.58	390.31	398.84	440.46	419.12	418.99	373.14	386.23	368.43	475.43	414.77	444.7	401.88
P(30)	1066.68	1046.07	1075.56	895.31	898.67	889.33	1114.5	950.73	946.37	1120.9	1132.6	1108.0	1043.3	857.02
P(32)	1242.85	1307.81	1279.65	1391.1	1200.67	1416.03	1205.9	1291.9	1412.9	1133.6	1149.0	1346.9	1127.9	1487.3
P(56)	0.919	1.044	1.09	1.035	0.9	0.886	0.86	1.005	1.02	1.026	0.998	0.94	1.089	1.02
P(61)	0.948	0.98	0.92	0.889	1.07	1.04	1.147	0.94	1.12	0.88	1.118	1.09	0.98	1.078
P(62)	82.32	73.05	82.57	77.35	68.16	73.67	90.73	82.16	89.08	79.03	87.11	71.9	81.59	73.27
P(65)	0.0062	0.006	0.0055	0.0063	0.0059	0.0062	0.0056	0.005	0.0063	0.0054	0.0057	0.0067	0.0056	0.0054
P(74)	1.218	1.26	1.35	1.47	1.285	1.34	1.238	1.2	1.57	1.31	1.536	1.52	1.599	1.23
P(77)	1.435	1.59	1.76	1.8	1.55	1.56	1.79	1.51	1.51	1.58	1.42	1.43	1.49	1.55

Table 10.22 The values of the nine most sensitive parameters obtained from fourteen Monte Carlo simulations.

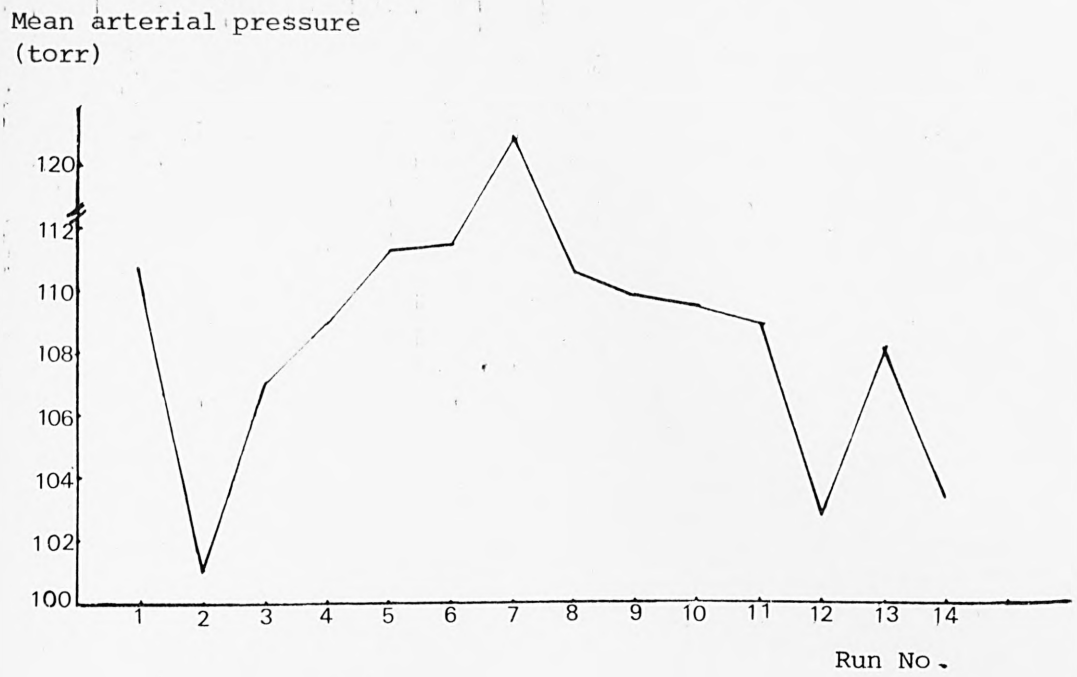

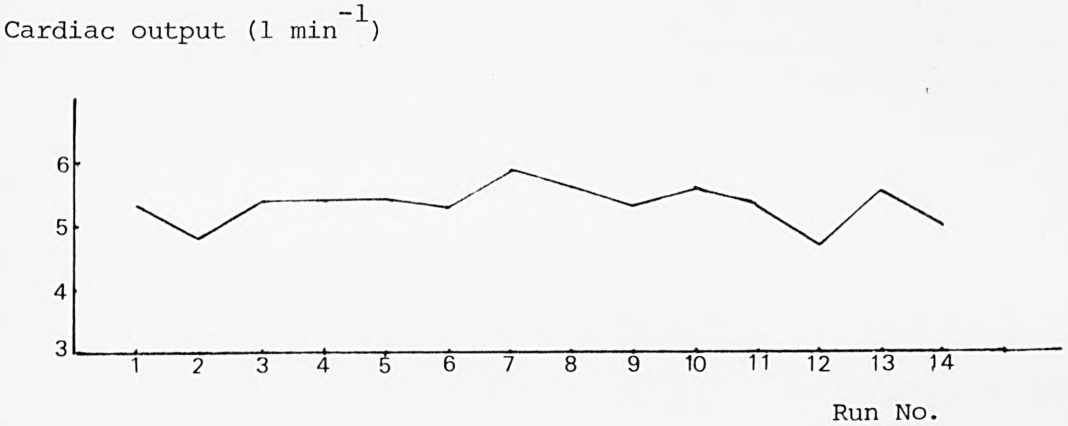

Figure 10.11 continued overleaf

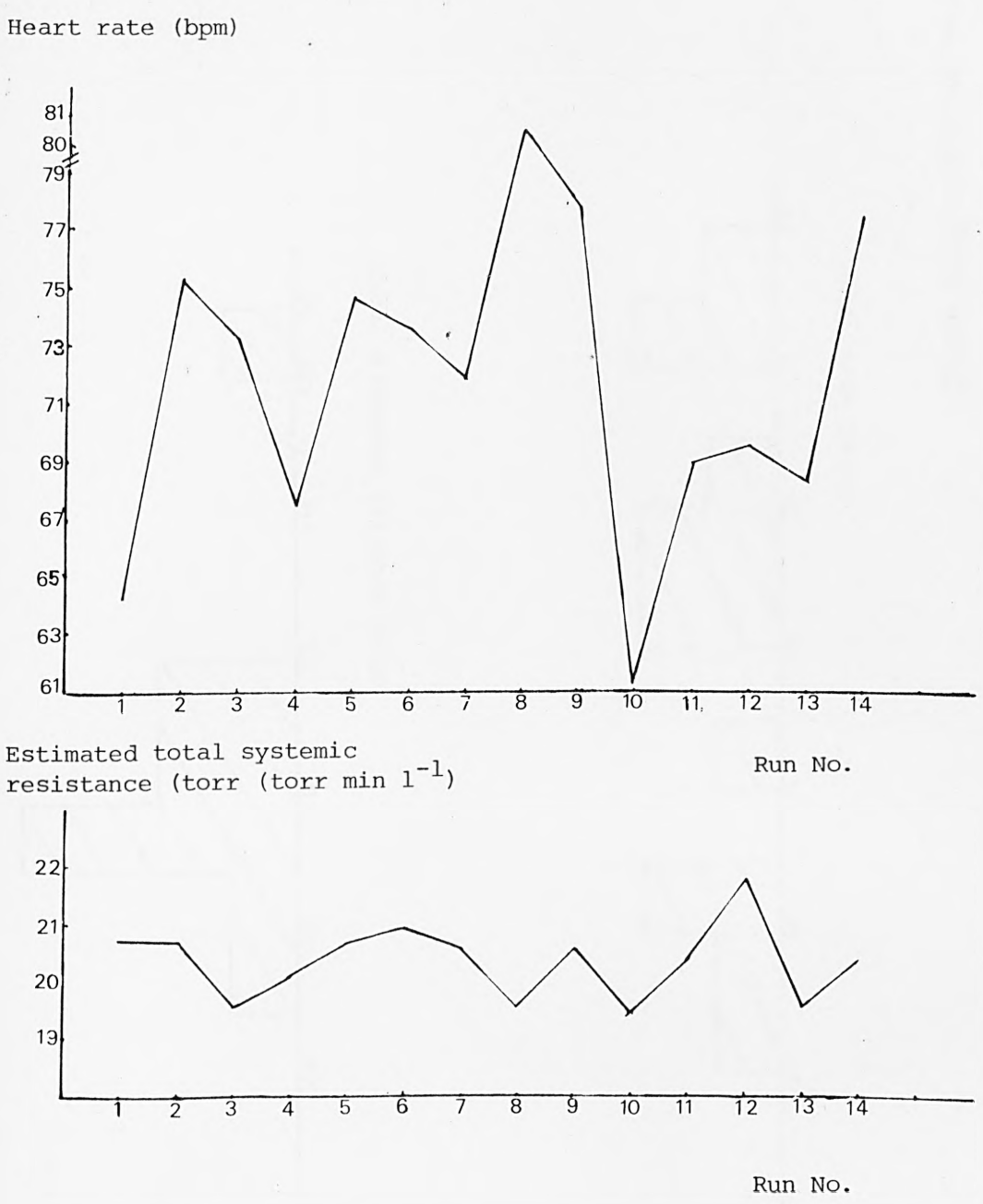

Figure 10.11 Variable values for fourteen simulations during the steady state by perturbation of the six most sensitive parameters together.

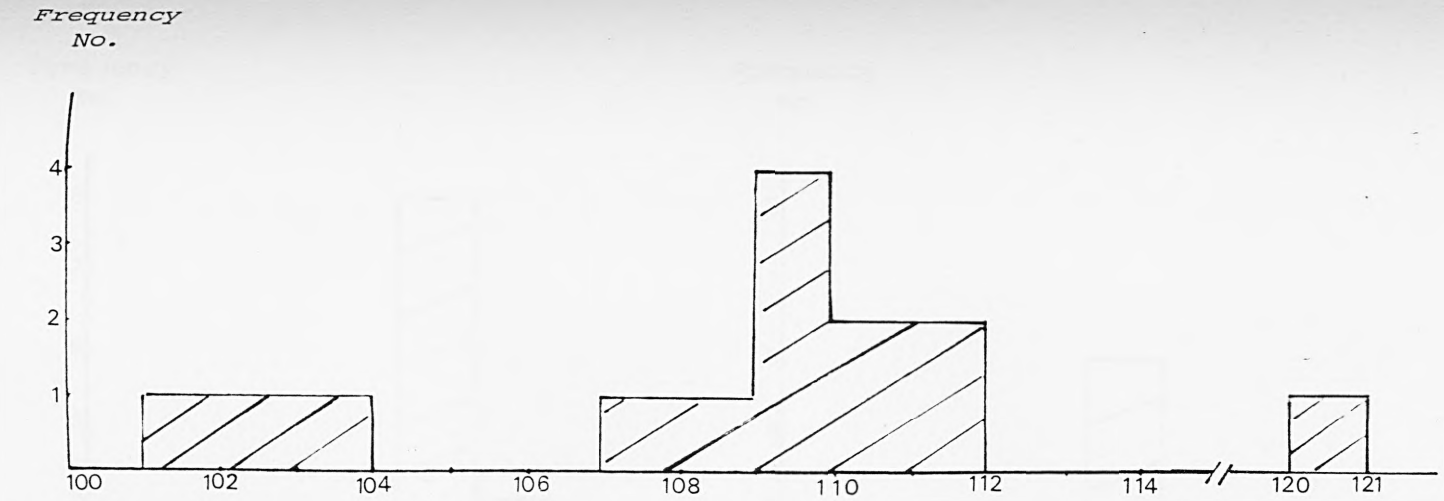

Frequency
No.

Mean arterial pressure (torr)

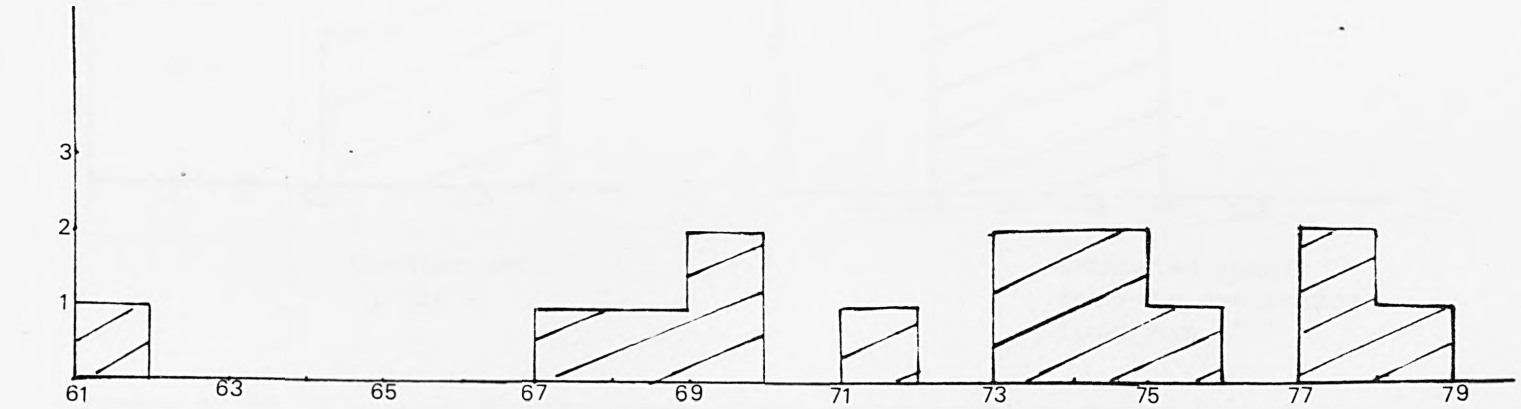

Heart rate (bpm)

Figure 10.12 continued overleaf

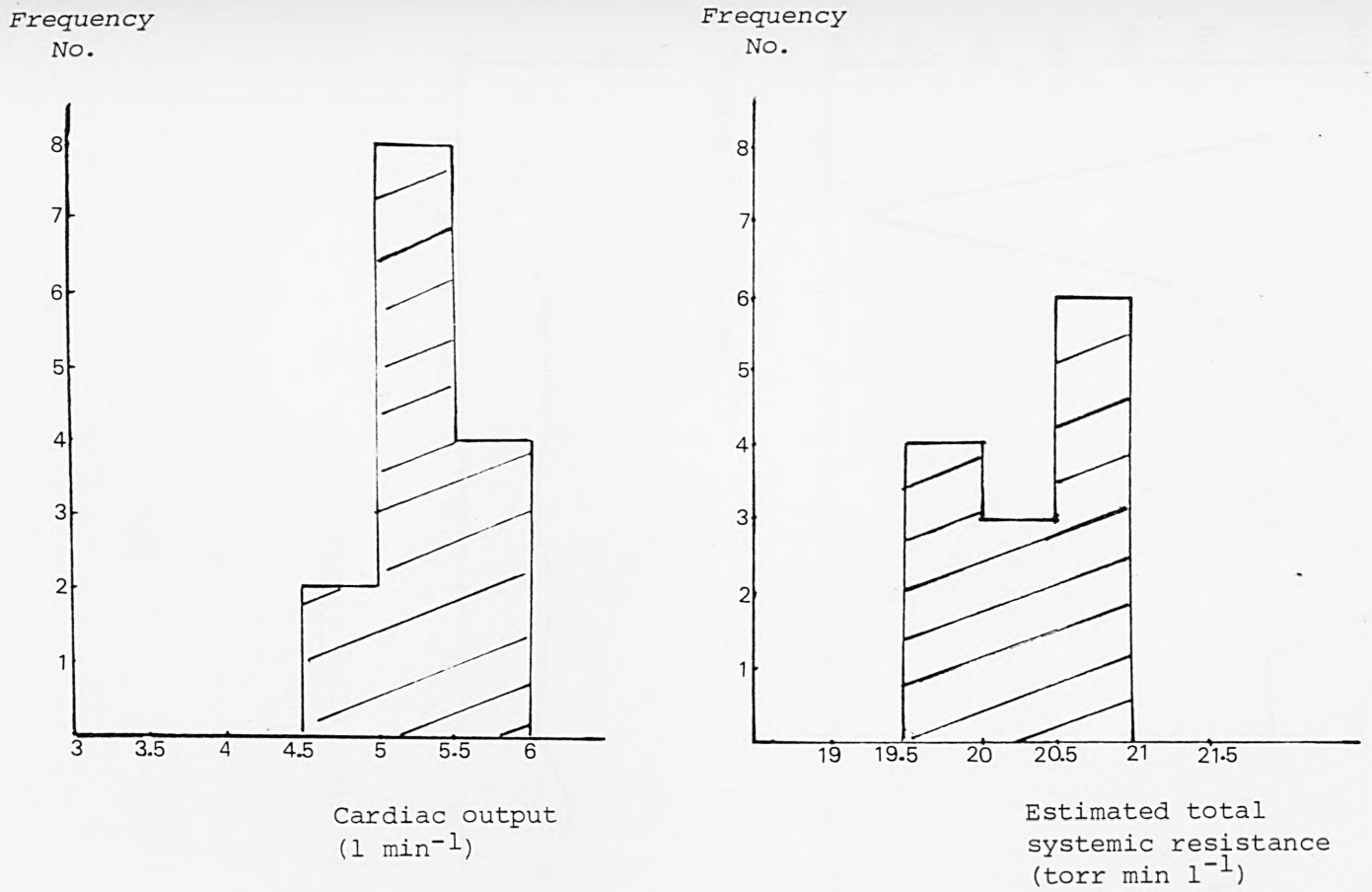

Figure 10.12 Histogram for the steady state variable values for the fourteen simulations of the nine most sensitive parameters.

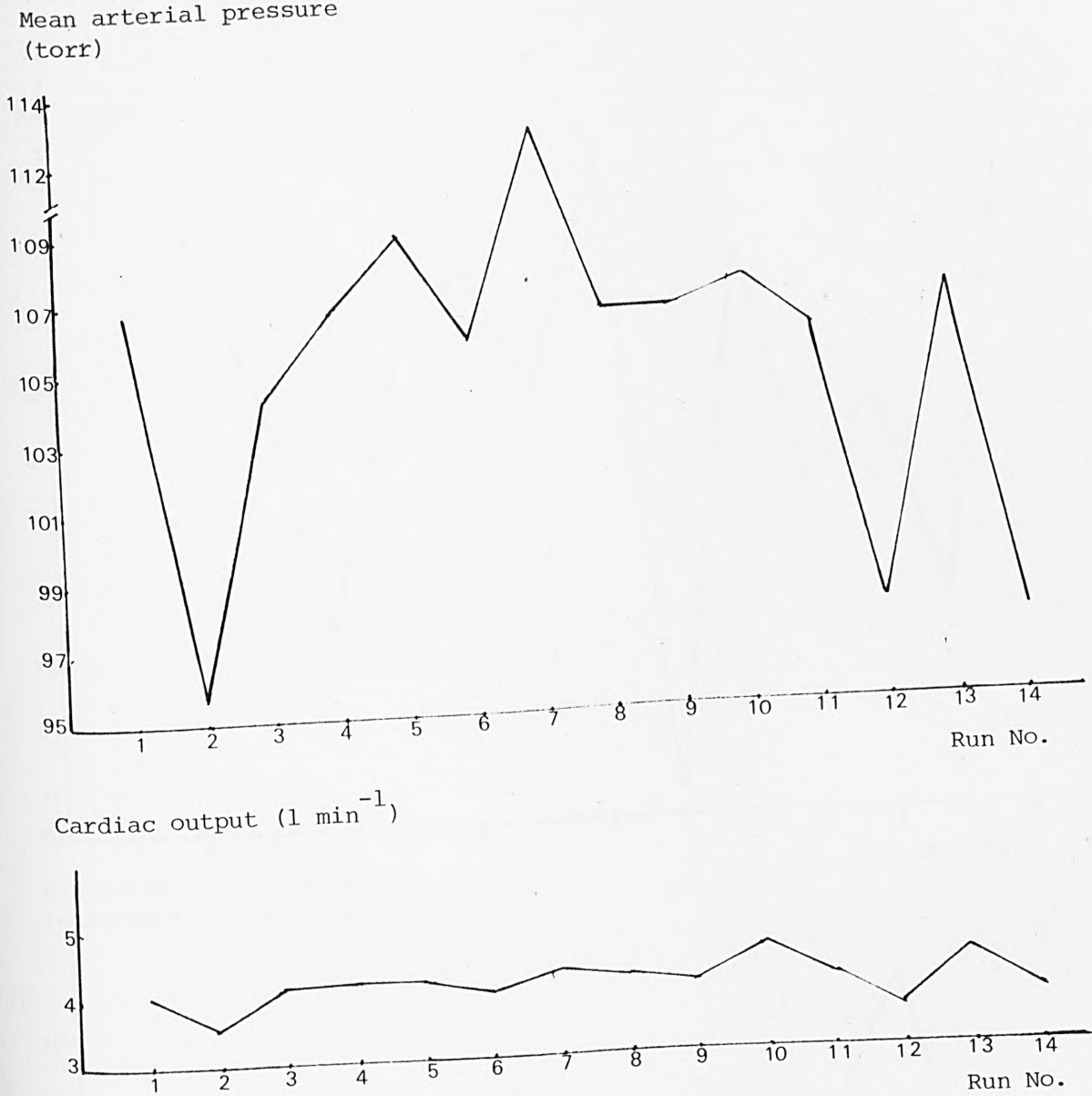

Figure 10.13 continued overleaf

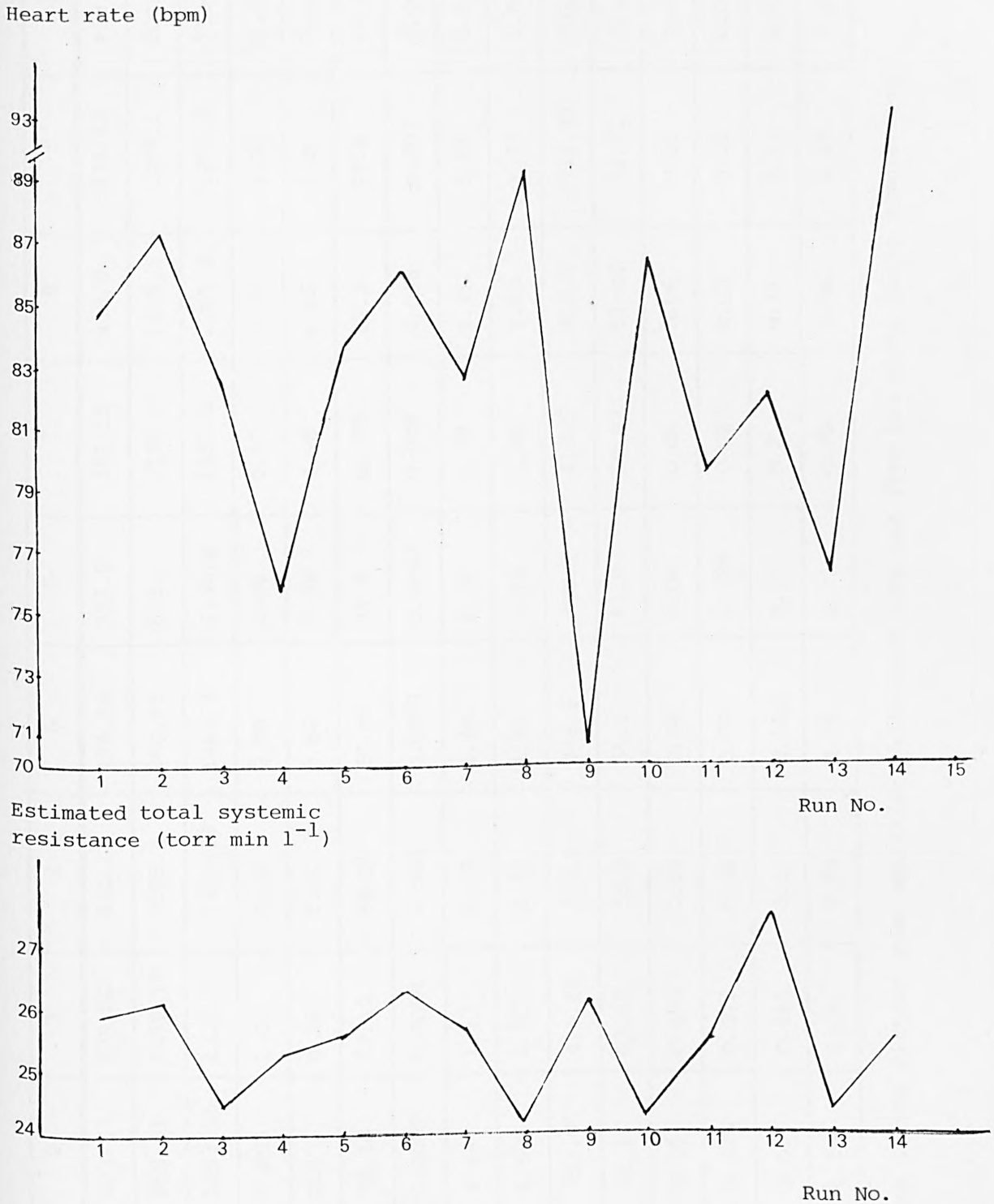

Figure 10.13 Variable values for 14 simulations following 500 ml loss of blood by perturbation of the 9 most sensitive parameters.

Run No.	1	2	3	4	5	6	7	8	9	10
P(15)	480.39	423.53	425.02	410.17	484.34	372.9	391.15	458.8	476.18	413.5
P(30)	1008.6	959.61	1059.17	1095.4	940.63	863.2	1134.1	1138.6	1099.1	1009.6
P(32)	1460.6	1253.16	1228.9	1180.38	1483.3	1144.6	1353.9	1205.3	1204.3	1304.86
P(56)	0.953	0.885	1.09	0.92	0.98	0.86	0.87	0.87	1.01	0.99
P(61)	1.134	1.1	0.86	1.04	0.86	0.99	0.98	1.05	1.06	0.91
P(62)	86.63	78.16	87.12	88.59	69.06	74.8	82.22	82.3	77.4	85.36
P(65)	0.0061	0.0069	0.0064	0.006	0.0057	0.0063	0.006	0.006	0.007	0.0058
P(74)	1.52	1.44	1.33	1.52	1.44	1.45	1.39	1.25	1.51	1.52
P(77)	1.5	1.626	1.57	1.58	1.61	1.54	1.68	1.83	1.77	1.81
P(26)	403.23	352.9	418.89	362.5	346.3	380.1	413.5	413.9	351.93	381.6
P(29)	52.26	61.1	63.87	58.0	61.1	51.8	59.83	57.04	51.72	57.4
P(51)	0.05	0.06	0.053	0.045	0.06	0.06	0.06	0.06	0.05	0.052
P(53)	0.029	0.024	0.023	0.024	0.03	0.028	0.027	0.03	0.02	0.026
P(55)	0.115	0.095	0.111	0.1	0.112	0.09	0.1	0.11	0.11	0.11
P(57)	0.95	1.2	1.04	0.94	0.94	1.11	0.96	0.96	1.24	1.23

Table 10.23 The values of the fifteen most sensitive parameters obtained from ten Monte Carlo simulations.

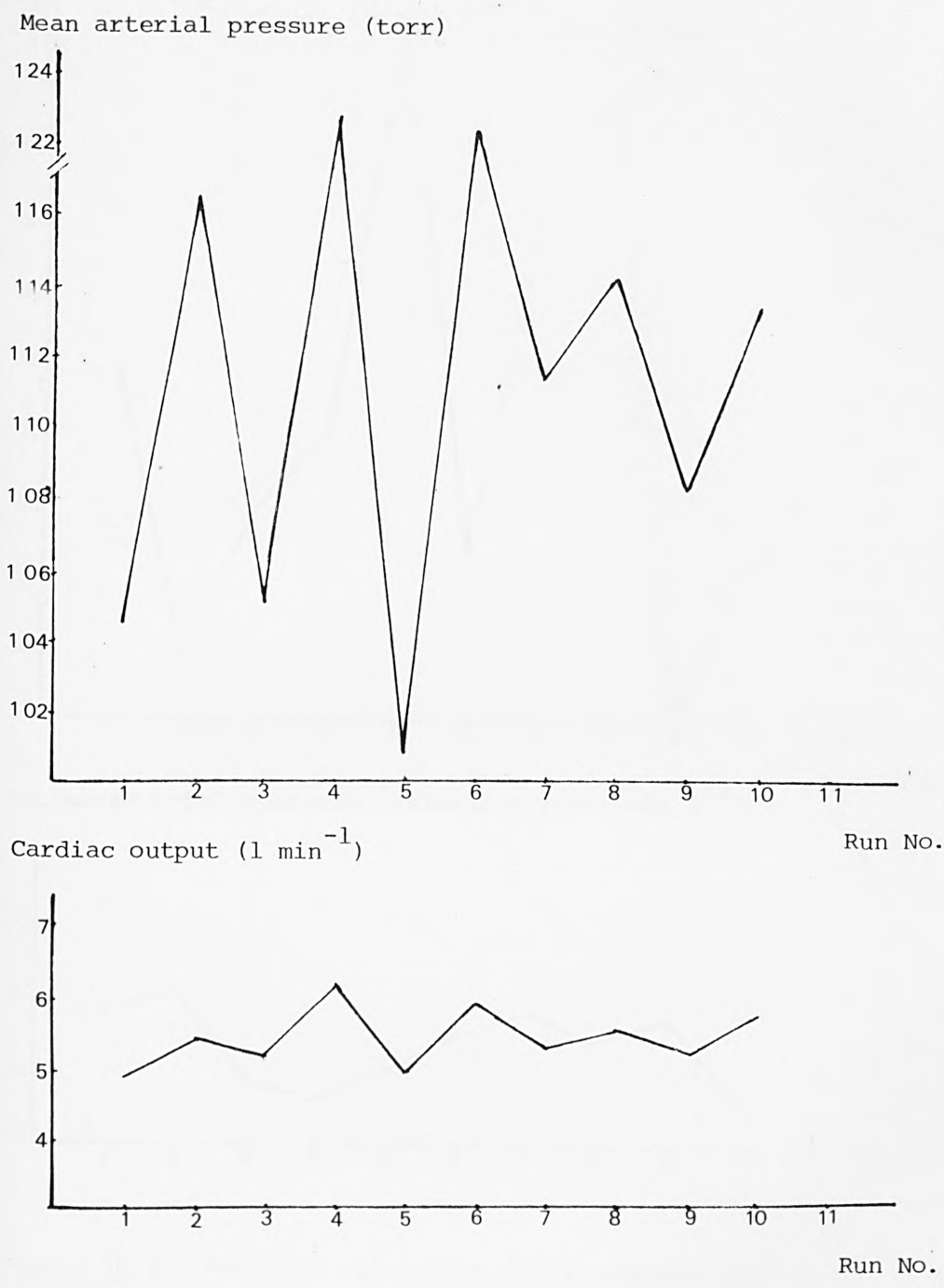

Figure 10.14 continued overleaf

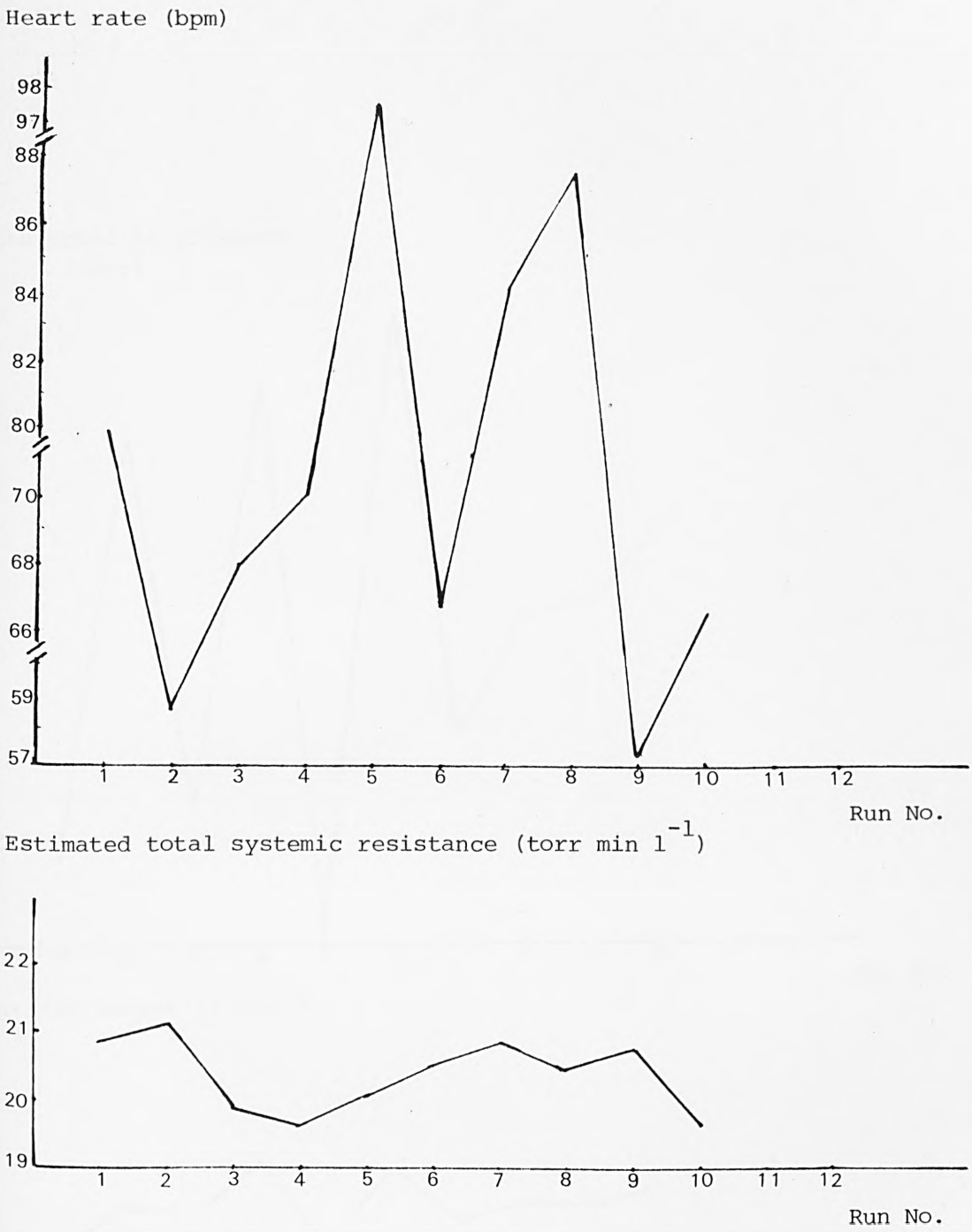

Figure 10.14 Variable values for 10 simulations during the steady state by perturbation of the 15 parameters together.

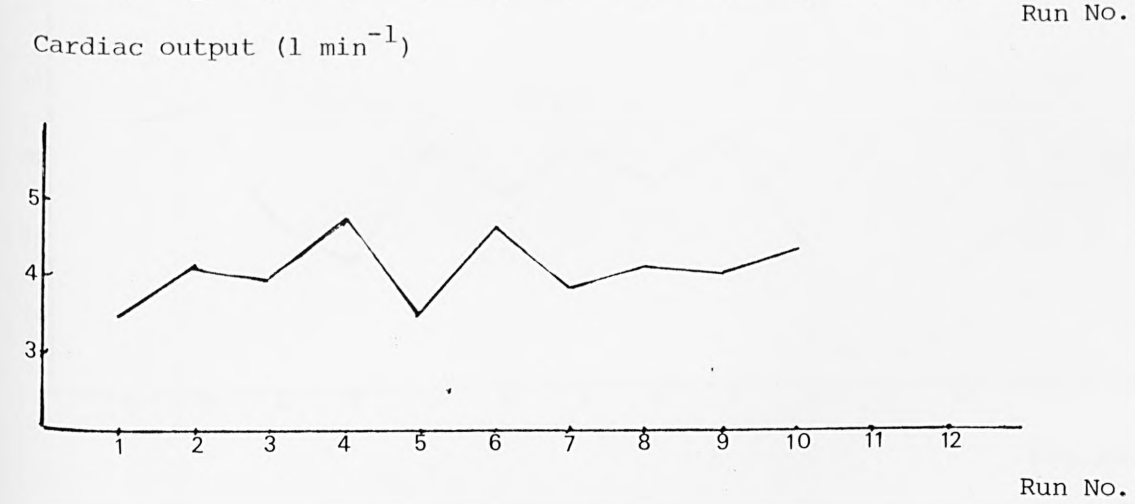

Figure 10.15 continued overleaf

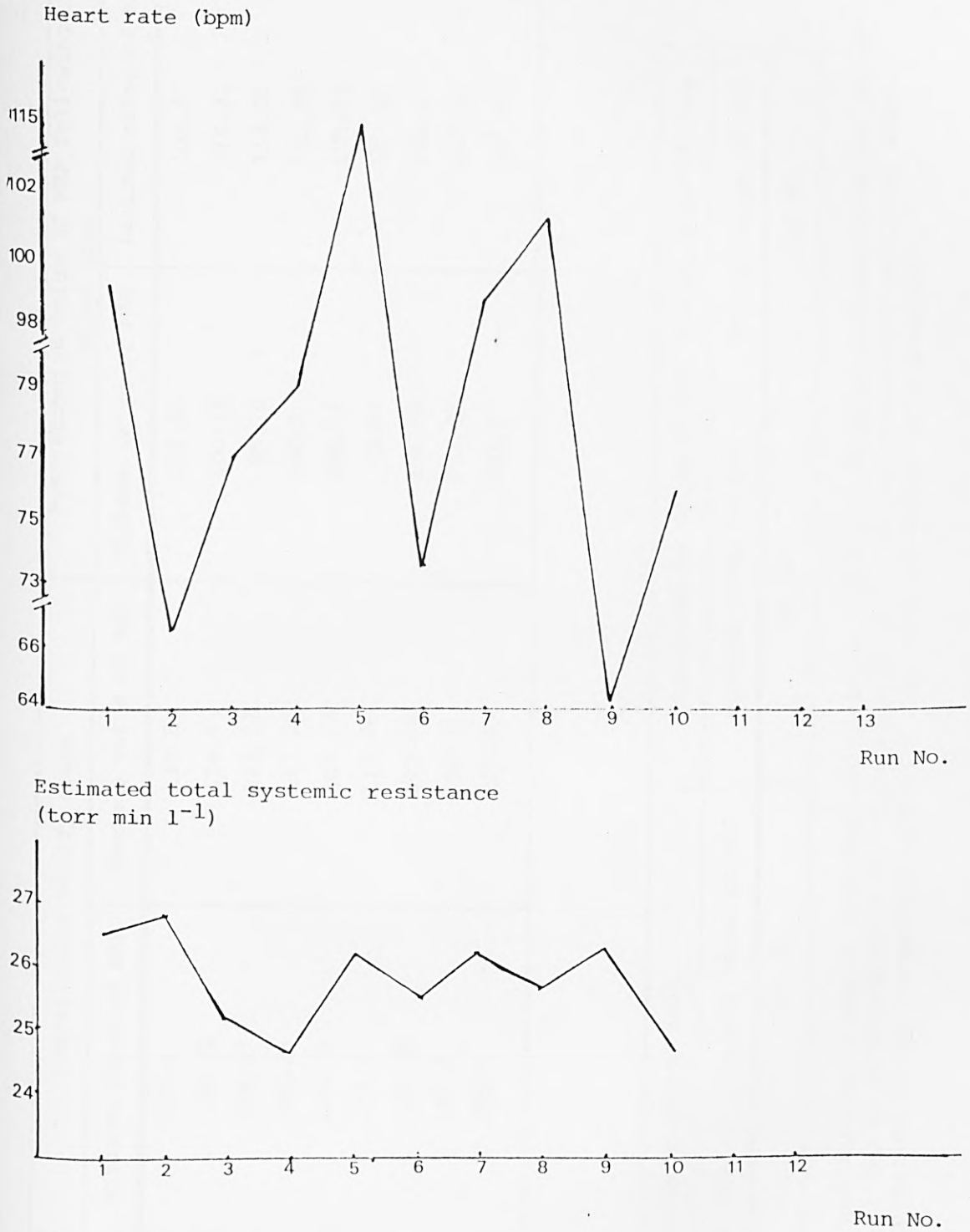

Figure 10.15 Variable values for ten simulations following 500 ml loss of blood by pertubation of the 15 parameters together.

(a)

Parameter in		Pre-stimulus steady state		Post-stimulus value of MAP following blood loss	
Computer program	Mathematical model	Minimum value of MAP	Maximum value of MAP	Minimum value of MAP	Maximum value of MAP
P(15)	V_{UPV}	107.4	110.6	102.55	108.2
P(30)	V_{USVN}	105.29	112.4	100.34	110.21
P(32)	V_{UTV}	103.47	113.27	95.76	112.61
P(56)	K_{13}	102.26	117.26	100.2	111.86
P(61)	K_{17}	108.77	109.33	105.16	105.84
P(62)	K_{18}	103.2	112.66	99.87	109.09
P(65)	$K_{21}\sigma_H$	108.39	109.62	104.49	106.1
P(74)	K_{35}	107.4	110.3	103.52	107.16
P(77)	K_{31}	105.7	111.4	101.2	108.68

(b)

Pre-stimulus steady state		Post-stimulus value of MAP following blood loss	
Minimum value of MAP	Maximum value of MAP	Minimum value of MAP	Maximum value of MAP
101.06	120.95	95.76	112.61

Table 10.24 Minimum and maximum values of mean arterial pressure (MAP) pre-stimulus and post-stimulus (after removal of 500 ml of blood) from the repeated simulations in the sensitivity analysis, using (a) perturbation of the parameters, one at a time, and (b) Monte Carlo analysis.

(a)

Parameter in		Pre-stimulus steady state		Post-stimulus value of CO following blood loss	
Computer program	Mathematical model	Minimum value of CO	Maximum value of CO	Minimum value of CO	Maximum value of CO
P(15)	V_{UPV}	5.23	5.47	3.97	4.27
P(30)	V_{USVN}	5.075	5.62	3.84	4.4
P(32)	V_{UTV}	4.967	5.66	3.63	4.51
P(56)	K_{13}	5.06	5.69	3.95	4.33
P(61)	K_{17}	5.25	5.47	4.077	4.19
P(62)	K_{18}	4.97	5.595	3.86	4.3
P(65)	$K_{21}\sigma_H$	5.146	5.61	3.99	4.27
P(74)	K_{35}	5.23	5.458	4.01	4.22
P(77)	K_{31}	5.161	5.493	3.93	4.26

(b)

Pre-stimulus steady state		Post-stimulus value of CO following blood loss	
Minimum value of CO	Maximum value of CO	Minimum value of CO	Maximum value of CO
4.71	5.89	3.56	4.546

Table 10.25 Minimum and maximum values of cardiac output (CO) pre-stimulus and post-stimulus (after removal of 500 ml of blood) from the repeated simulations in the sensitivity analysis, using (a) perturbation of the parameters, one at a time, and (b) Monte Carlo analysis.

(a)

Parameter in		Pre-stimulus steady state		Post-stimulus value of FH following blood loss	
Computer program	Mathematical model	Minimum value of FH	Maximum value of FH	Minimum value of FH	Maximum value of FH
P(15)	V_{UPV}	68.62	71.58	77.35	83.38
P(30)	V_{USVN}	66.84	73.91	75.37	86.16
P(32)	V_{UTV}	66.27	75.66	73.22	91.82
P(56)	K_{13}	65.86	75.74	74.57	87.53
P(61)	K_{17}	66.09	74.56	75.91	84.93
P(62)	K_{18}	66.85	75.9	76.84	86.17
P(65)	$K_{21}\sigma_H$	62.19	80.61	70.7	93.1
P(74)	K_{35}	68.43	72.03	78.08	82.65
P(77)	K_{31}	67.99	73.09	77.13	84.69

(b)

Pre-stimulus steady state		Post-stimulus value of FH following blood loss	
Minimum value of FH	Maximum value of FH	Minimum value of FH	Maximum value of FH
61.29	80.61	70.7	93.1

Table 10.26 Minimum and maximum values of heart rate (FH) pre-stimulus and post-stimulus (after removal of 500 ml of blood) from the repeated simulations in the sensitivity analysis, using (a) perturbation of the parameters, one at a time, and (b) Monte Carlo analysis.

(a)

Parameter in		Pre-stimulus steady state		Post-stimulus value of ETSR following blood loss	
Computer program	Mathematical model	Minimum value of ETSR	Maximum value of ETSR	Minimum value of ETSR	Maximum value of ETSR
P(15)	V_{UPV}	20.21	20.5	25.3	25.8
P(30)	V_{USVN}	20.0	20.74	25.03	26.1
P(32)	V_{UTV}	19.98	20.83	24.91	26.37
P(56)	K_{13}	20.17	20.5	25.35	25.82
P(61)	K_{17}	19.97	20.69	25.09	25.95
P(62)	K_{18}	20.13	20.72	25.36	25.86
P(65)	$K_{21}\sigma_H$	19.53	21.06	24.42	26.54
P(74)	K_{35}	20.22	20.54	25.36	25.8
P(77)	K_{31}	20.28	20.47	25.48	25.68

(b)

Pre-stimulus steady state		Post-stimulus value of ETSR following blood loss	
Minimum value of ETSR	Maximum value of ETSR	Minimum value of ETSR	Maximum value of ETSR
19.5	21.85	24.27	27.49

Table 10.27 Minimum and maximum values of estimated total systemic resistance (ETSR) pre-stimulus and post-stimulus (after removal of 500 ml of blood) from the repeated simulations in the sensitivity analysis, using (a) perturbation of the parameters, one at a time, and (b) Monte Carlo analysis.

CHAPTER 11

CONCLUSIONS

This thesis has described the application of a comprehensive method of model validation, within an overall integrated modelling framework, to large-scale models of complex dynamic processes. The focus of the study has been the human cardiovascular system, and the work described thus relates first and foremost to the relevant physiological processes and their representation in mathematical terms. At another level, however, this study of the cardiovascular system can be regarded as an exemplar of a complex, non-linear dynamic system, yielding general lessons on the application of the validation method.

The thesis makes contributions both to systems science and to physiology and anatomy. For systems science it provides a substantial test of the applicability of the methodology for validating complex (usually unidentifiable) models. It also provides a vehicle with which to examine procedures for model reduction when the models concerned are of high order and significant non-linearity. Specific details of these contributions are detailed below.

For physiology the crucial role of models in testing alternative hypotheses has been highlighted. For both physiology and anatomy the need for improved measurement and experimental design has been clearly revealed.

The earlier chapters of the thesis have been directed towards the validation of the large-scale model which incorporates a 19th order representation of the uncontrolled circulatory dynamics. Overall this model, with neural control, pharmacokinetic and local pharmacodynamic components, was of 61st order with 178 parameters.

One facet of the validation process involved examining the validity of data available regarding parameters and initial values of model variables. Despite extensive searching it was not possible to obtain reliable estimates of these quantities either from published literature or from discussions with clinicians, physiologists and anatomists. Where values did exist there were rarely measures of uncertainty specified, and even for standard anatomical measurements such as the dimensions of blood vessels the ranges of values corresponding to a "normal" population of human subjects were not well defined.

Knowledge of these ranges and degrees of uncertainty is essential for a comprehensive investigation of model validity. This work has thus revealed that current measurement procedures, although adequate for many conventional anatomical investigations, are not sufficient when the results are to be used in dynamic, model-based studies. This investigation thus highlights new fields of research for the anatomist. Similar arguments apply to measures of the resistive properties of the blood vessels and to the elastic properties of these vessels and the heart chambers. Substantial scope thus exists for greater collaboration between anatomist, physiologist and mathematical modeller to the potential benefit of all parties.

The empirical validity of the complete non-linear 19-segment model of the cardiovascular system was examined in order to define the adequacy and limitations of this model. This involved comparison of model response with the results of empirical tests, such as the Valsalva manoeuvre, blood volume changes, postural changes and drug effects.

Again, this programme of model testing highlighted the difficulty in obtaining adequate data for human studies, even for comparatively straightforward investigations such as the head-down tilt. This is of crucial importance since this experiment constituted one of the most critical tests of model validity. The relevant data revealed two distinct modes of heart rate response, in contrast to the single mode revealed in the model, thus indicating a potential defect in the model. More data are needed to confirm these findings which do not appear to have been previously reported.

Results of heart rate measurements obtained from both normal subjects and diabetics undergoing a Valsalva manoeuvre have provided evidence in support of the hypothesis that the principal difference, in relation to circulatory dynamics, is an increase in circulatory compliance in diabetics.

Model-based studies comparing a normal subject with a well-trained athlete have supported the hypotheses that the latter has both increased blood volume and decreased compliance.

The validation programme has revealed the heuristic potential of the model by highlighting areas of structural uncertainty in relation to both neural control and pharmacodynamics. One of the inadequacies of the neural control components is remedied in the reduced model by the successful incorporation of the effects of stretch receptors.

Despite its heuristic potential, the full model imposes considerable computational requirements and is limited by the lack of available experimental data. These difficulties were diminished by the development of the reduced model described in the later chapters of the thesis, a reduced form which can begin to offer a predictive capability at least in relation to short-term cardiovascular dynamics. Incorporation of volume (stretch) receptors in the neural control segment of this reduced model resolved the deficiency relating to control of peripheral resistance which had been highlighted in the model response to haemorrhage.

Substantial areas for future investigation have been revealed by these model-based investigations, particularly in seeking a greater understanding of the processes of neural control (including, for longer term studies, the effects of both baro- and chemoreceptors) and in attempting to develop the clinical potential of such models as decision-aids for the clinician. Further developments, however, must be dependent upon the availability of additional experimental data, both defining parameters as well as specifying the time course of major variables in both physiological and pharmacological investigations. This thesis has thus not only provided an exemplar of the methodology for validating complex physiological models, but has also indicated the need for closer inter-disciplinary collaboration if the full potential of such investigations is to be realised.

REFERENCES

Abel, F. L., Pierce, J. H., and Guntheroth, W. G. (1963), "Baroreceptor influence on postural changes in blood pressure and carotid blood flow", Am. J. Physiol., 205, 360-364.

Al-Dahan, M., Rajkumar, N., Pullen, H. E., Finkelstein, L., Hill, D. W., and Carson, E. R. (1979), "Mathematical modelling of the human cardiovascular system", Research Memorandum, DSS/MA-DNR-HEP-LF-DWH-ERC/188, Department of Systems Science, The City University, London.

American Physiological Society (1965), Handbook of Physiology, Section 2: Circulation.

Anderson, J. H. (1967), "Geometrical approach to reduction of dynamical systems", Proc. IEE., 114, 1014-1018.

Arenson, H. M. (1978), The Use of Impedance Techniques for the Assessment of Blood Flow during Anaesthesia, Ph.D. Thesis, Royal College of Surgeons, London.

Bendall, M., and Gray, D. C. (1978), "Sensitivity analysis of a pharmacokinetic system", Kybernetics, 7, 285-289.

Beneken, J. E. W. (1965a), A Mathematical Approach to Cardiovascular Function, Institute of Medical Physics TNO, Utrecht, The Netherlands, Report No. 2-4-5/6.

Beneken, J. E. W. (1965b), "A physical approach to cardiovascular function", Engineering in Medicine and Biology (Proceedings of the 18th Annual Conference), p. 77.

Beneken, J. E. W., and DeWit, B. (1967), "A physical approach to hemodynamic aspects of the human cardiovascular system", in E. B. Reeve and A. C. Guyton (eds.), Physical Bases of Circulatory Transport: Regulation and Exchange, W. B. Saunders, Philadelphia.

Beneken, J. E. W., and Rideout, V. C. (1968), "The use of multiple models in cardiovascular system studies: transport and perturbation methods", IEEE Trans. Biomed. Eng., BME-15, 281-289.

Benham, R. D. (1972), "An ISL-8 and ISL-15 study of the physiological simulation benchmark experiment", Simulation, 18, 152-156.

Bergel, D. H. (ed.) (1972), Cardiovascular Fluid Dynamics, Vol. 1, Academic Press, New York.

Blesser, W. B. (1969), A Systems Approach to Biomedicine, McGraw-Hill, New York.

Bogumil, R. J. (1980), "Sensitivity analysis of bio-system models", Fed. Proc., 39, 97-103.

Borst, C., Wieling, W., Van Brederode, J. F. M., Hond, A., De Rijk, L. G., and Dunning, A.J. (1982), "Mechanisms of initial heart rate response to postural change", Am. J. Physiol., 243, H676-H681.

Bosley, M. J., and Lees, F. P. (1972), "A survey of simple transfer function derivatives from high-order state-variable models", Automatica, 8, 765-775.

Bourdillon, P. (1981), Personal communication.

Boyers, D. G., Cuthbertson, J. G., and Luetscher, J. A. (1972), "Simulation of the human cardiovascular system: a model with normal responses to change of posture, blood loss, transfusion, and autonomic blockade", Simulation, 18(b), 197-205.

Brubakk, A. O., and Aaslid, R. (1978), "Use of a model for simulating individual aortic dynamics in man", Med. Biol. Eng. Comput., 16, 231-242.

Burgen, A. S. V., and Mitchell, J. F. (1978), Gaddum's Pharmacology, Eighth ed., Oxford University Press, London.

Bushman, J. (1980, 1982 and 1983), personal communication.

Caro, C. G., Pedley, T.J., and Seed, W. A. (1974), "Mechanics of the circulation", in A. C. Guyton and C. E. Jones (eds.), MTP International Review of Science, Physiology, Series One, Vol. 1, Cardiovascular Physiology, Butterworth, London.

Carson, E. R. (1975), Aspects of Dynamics Control and Identification of Metabolic Systems, Ph.D. Thesis, The City University, London.

Carson, E.R., and Finkelstein, L. (1982), "System identification in biology", Trans. Inst. M.C., 4, 171-176.

Carson, E. R., Cobelli, C., and Finkelstein, L. (1983), Mathematical Modeling of Metabolic and Endocrine Systems, Wiley, Chichester.

Carson, E. R., Cramp, D. G., Finkelstein, L., and Ingram, D. (1984), "Control system concepts and approaches in clinical medicine", in E. R. Carson and D. G. Cramp (eds.), Computers and Control in Clinical Medicine, Plenum, London.

Cesarcyzk, J. Z. J. (1981), Model Reduction and the Adequacy of Simple Models as Applied to the Design of Control Systems, Ph.D. Thesis, The City University, London.

Chen, C.F., and Shieh, L.S. (1968), "A novel approach to linear model simplification", Int. J. Control., 8, 561-570.

Cobelli, C., Carson, E. R., Finkelstein, L., and Leaning, M. S. (1984), "Validation of simple and complex models in physiology and medicine", Am. J. Physiol. 246, R259-R266.

Cole, P. (1982), Personal communication.

Cox, R. H. (1975), "Arterial wall mechanics and composition of the effects of smooth muscle activation", Am. J. Physiol., 229, 807-812.

Davison, E. J. (1966), "A method for simplifying linear dynamic systems", IEEE Trans. Automat. Contr., AC-11, 93-101.

Davson, H., and Segal, M. B. (1976), Introduction to Physiology, Vol. 3, Academic Press, London.

Dick, D. E., and Rideout, V. C. (1965), "Analog simulation of left heart and arterial dynamics", in Proc. 18th Annu. Conf. Eng. Biol. Med., Philadelphia, USA.

Dickinson, C. J., Ingram, D., and Shephard, P. (1971), "A digital computer model for teaching the principles of systemic haemodynamics (MacMan)", J. Physiol. (Lond.), 216, 9P-10P.

Finkelstein, L., and Carson, E. R. (1979), Mathematical Modeling of Dynamic Biological Systems, Wiley (Research Studies Press), Chichester.

Flessas, A. P., Kumar, S., Spodick, D.H. (1970), "Effect of the Valsalva manoeuvre on the cardiac systolic intervals: beat to beat versus timed analysis", Am. Heart J., 80, 522-531.

Folkow, B., and Neil, E. (1971), Circulation, Oxford University Press, New York.

Ganong, W. F. (1975), Review of Medical Physiology, Seventh ed., Lange Medical Publications.

Gold, H. J. (1977), Mathematical Modeling of Biological Systems: An Introductory Guidebook, Wiley, New York.

Goodman, L. S., and Gilman, A. (1965), The Pharmacological Basis of Theraputics, Third ed., Macmillan, New York.

Grande, F., and Taylor, H. L. (1965), "Adaptive changes in the heart, vessels and patterns of control under chronically high loads", in W. F. Hamilton and P. H. Dowleds. (eds.), Handbook of Physiology, Section 2: Circulation, Vol. 3, Ch. 74, American Physiological Society.

Green, H. D., Repela, C. E., and Conrad, M. C. (1963), "Resistance (conductance) and capacitance phenomena in terminal vascular beds", in W. F. Hamilton and P. H. Dowleds (eds.), Handbook of Physiology, Section 2, Vol. 2, Ch. 28, American Physiological Society.

Green, J. H. (1972), An Introduction to Human Physiology, Third ed., Oxford University Press, London.

Grodins, F. S. (1959), "Integrative cardiovascular physiology: a mathematical synthesis of cardiac and blood vessel haemodynamics", Quart. Rev. Biol., 34, 93.

Guyton, A. C. (1955),"Determination of cardiac output by equating venous return curves with cardiac response curves", Physiol. Rev., 35, 125-129.

Guyton, A. C., Lindsey, A. W., Kaufmann, B. N., and Abernathy, J. B. (1958), "Effect of blood transfusion and haemorrhage on cardiac output and on the venous return curve", Am. J. Physiol., 194, 265-267.

Guyton, A. C. (1959), Function of the Human Body, W. B. Saunders, Philadelphia.

Guyton, A. C., Coleman, T. G., and Granger, H. J. (1972), "Circulation: overall regulation", Annu. Rev. Physiol., 34, 13-46.

Guyton, A. C. (1979), Physiology of the Human Body, Fifth ed., W. B. Saunders, Philadelphia.

Guyton, A. C. (1981), A Textbook of Medical Physiology, Sixth ed., W. B. Saunders, Philadelphia.

Harreveld, A. van, Feigen, G. A., and Lerman, L. S. (1949), "Hemodynamics of aortic occlusion", Am. J. Physiol., 157, 168.

Harreveld, A. van, and Shadle, O. W. (1951), "On hemodynamics", Arch. Int. Physiol., 59, 165-182.

Harvey, W. (1628), The Circulation of the Blood (translated by K. J. Franklin (1958), Blackwell Scientific Publications, Oxford.

Hayashi, K., Handa, H., Nagsasawa, S., Okumura, A., and Moritake, K. (1980), "Stiffness and elastic behavior of human intracranial and extracranial arteries", J. Biomechan., 13, 175.

Hawker, R. W. (1979), Notebook of Medical Physiology. Cardiopulmonary aspects of clinical measurement, Churchill Livingstone, Edinburgh.

Hughes, R. (1971), "Continuous measurement of peripheral vascular resistance and circulatory function", Med. Biol. Eng., 9, 603-610.

Hyndman, B. W. (1970), A Digital Simulation of the Human Cardiovascular System and its Use in the Study of Sinus Arrhythmia, Ph.D. Thesis, Imperial College, London.

Katona, P. G., Jackson, W. D., and Barnett, G. O. (1965), "Computer simulation of the blood pressure control of heart period", in Proc. 18th Annu. Conf. Eng. Med. and Biol., 109, Philadelphia.

Katona, P. G., Barnett, G. O., and Jackson, W. D. (1967), "Computer simulation of the blood pressure control of heart period", in P. Kezdi (ed.), Baroreceptors and Hypertension, Pergamon, Oxford, 191-199.

Keele, C. A., Neil, E., and Joels, N. (1982), Samson Wright's Applied Physiology, Thirteenth ed., Oxford University Press, New York.

Kyriakou, K. (1980), Personal communication.

Last, R. J. (1978), Anatomy (Regional and Applied), Sixth ed., Churchill Livingstone, Edinburgh.

Leaning, M. S. (1980), The Validity and Validation of Mathematical Models, Ph.D. Thesis, The City University, London.

Leaning, M. S. (1981), Personal communication.

Leaning, M. S., Uttamsingh, R. J., Carson, E. R., Cobelli, C., and Finkelstein, L. (1982a), "Methodological aspects of model validation: A model of the human renal-artificial kidney system", in L. Troncale (ed.), A General Survey of Systems Methodology, International Federation for Systems Research, Louisville, Kentucky.

Leaning, M. S., Uttamsingh, R. J., Carson, E. R., and Finkelstein, L. (1982b), "System model of renal dialysis. Formulation, validation and identification", Proc. IEE, 129, Pt. A, 707-716.

Leaning, M. S., Pullen, H. F., Carson, E. R., Finkelstein, L. (1983a), "Modelling a complex biological system: the human cardiovascular system. I. Methodology and model description", Trans. Inst. M.C., 5, 71-86.

Leaning, M. S., Pullen, H. F., Carson, E. R., Al-Dahan, M., Rajkumar, N., Finkelstein, L. (1983b), "Modelling a complex biological system: the human cardiovascular system. II. Model validation, reduction and development", Trans. Inst. M.C., 5, 87-98.

Light, L. H., Hanson, G. C., Sequeira, R. F., and Cross, G. (1980), "Flow-orientated information on the central circulation by trans-cutaneous aortovelography", Proc. International Conference on Recent Advances in Biomedical Engineering, The Biological Engineering Society.

Lippold, O. C. J., and Winton, F. R. (1968), Human Physiology, Sixth ed., Churchill, London.

Lippold, O. C. J., and Winton, F. R. (1979), Human Physiology, Seventh ed., Churchill Livingstone, Edinburgh.

Mancia, G., Grassi, G., Pomidossi, G., Gregorini, L., Bertinieri, G., Parati, G., Ferrari, A., Zanchetti, A. (1983), "Effects of blood-pressure measurement by the doctor on patient's blood pressure and heart rate", The Lancet, 24th September.

McClintic, J. Robert (1978), Physiology of the Human Body, Second ed., Wiley, New York.

Milhorn, H. T. (1966), The Application of Control Theory to Physiological Systems", W.B. Saunders, Philadelphia.

Mountcastle, V.B. (1974), Medical Physiology, Vol. 2, Thirteenth ed., Mosby, St. Louis.

Nixon, J. V., Murray, G., Bryant, C., Johnson, R. L., Jr., Mitchell, J. H., Holland, O. B., Gromez-Sanchez, C., Vergne-Marini, P., and Blomqvist, C. G. (1979), "Early cardiovascular adaptation to simulated zero gravity", J. Appl. Physiol., 46, 541-548.

Noordergraaf, A. (1963), Development of an Analog Computer for the Human Systemic Circulatory System, in A. Noordergraaf, G.N. Jager and N. Westerhof (eds.), "Circulatory analog computers", North Holland Publishing Company, Amsterdam.

Noordergraaf, A., Verdoum, P. D., and Boom, H. B. K. (1963), "The use of an analog computer in a circulation model", University of Utrecht, Utrecht, The Netherlands, Progress in Cardiovascular Diseases, 5, 419-439.

Noordergraaf, A., Verdouw, P. D., Brummelen, A. G. W. van, and Wiegel, F. W. (1964), "Analog of the arterial bed", in E. O. Attinger (ed.), Pulsatile Blood Flow, McGraw-Hill, New York.

Noriaki Ikedia, Fumiaki Marumo, Masuo Shirataka, and Toshiro Sato (1979), "A model of overall regulation of body fluids", Ann. Biomed. Eng., 7, 135-166.

Patel, D. J., and Austen, W. G. (1964), "Impedance of certain large blood vessels in man", Ann. N.Y. Acad. Sci., 115, 1129-1139.

Pedley, T. J. (1980), The Fluid Mechanics of Large Blood Vessels, Cambridge University Press, Cambridge.

Pullen, H. E. (1976), Studies in the Modelling and Simulation of the Human Cardiovascular System with Application to the Effects of Drugs, Ph.D. Thesis, The City University, London.

Pullen, H. E., and Finkelstein, L. (1977), "A cybernetic model of the human cardiovascular system with application to the effects of drugs", in IFAC Symposium on Control Mechanisms in Bio- and Eco-Systems, Leipzig, Vol. 4, 23-30.

Rajkumar, N. (1978), Reduction of a Mathematical Model of the Human Cardiovascular System, M.Sc. Thesis, The City University, London.

Roberts, V. C. (1982), "Blood flow measurement in man", Trans. Inst. M. Co., 4, 59-60.

Rupeiks, I. (1972), "Computer-aided medical instruction using an interactive graphics model of the normal and congenitally defective heart", IEEE Trans. Biom. Eng., 19, 88-96.

Rushmer, R. F. (1976), Cardiovascular Dynamics, Fourth ed., W.B. Saunders, Philadelphia.

Salman, W. D. (1981), Personal communication.

Schwan, H. P. (1969), Biological Engineering, McGraw-Hill, New York.

Sharpey-Schafer, E. P. (1955), "Effects of Valsalva's manoeuvre on the normal and failing circulation", Brit. Med. J., 1, 693-695.

Sharpey-Schafer, E. P. (1965), "Effect of respiratory acts on the circulation", in Handbook of Physiology, Circulation III, Ch. 52, 1875-1886.

Sinha, N. K., and Pille, W. (1971), "A new method for reduction of dynamic systems", Int. J. Control, 14, 111-118.

Slate, J. B. (1980), Model-based Design of a Controller for Infusing Sodium Nitroprusside during Postsurgical Hypertension, Ph.D. Thesis, University of Wisconsin,Madison.

Slate, J. B. (1983), Personal communication.

Snyder, M. F., and Rideout, V. C. (1969), "Computer simulation studies of the venous circulation", IEEE Trans. Biomed. Eng., BME-16, 325-334.

Srinivasan, R., and Leonard, J. I. (1982), "Comparison of cardiovascular effects of space flight and its analogs using computer simulations", The Physiologist, 25, S-61 - S-62.

Stolwijk, J. A. J., and Hardy, J. D. (1966), "Temperature regulation in man - a theoretical study", Pflügers Archiv, 291, 129-162.

Tomovic, R. (1963), Sensitivity Analysis of Dynamic Systems, McGraw-Hill, New York.

ToMovic, R., and Vukobratovic, M. (1972), General Sensitivity Theory, Elsevier, New York.

Tuckman, J., and Shillingford, J. (1966), "Effect of different degrees of tilt on cardiac output, heart rate, and blood pressure in normal man", Brit. Heart J., 28, 32-39.

Tunstall-Pedoe, D. (1983), "Sports injuries, cardiological problems", Brit. J. of Hosp. Med., 29(3), 213-220.

Tunstall-Pedoe, D. (1984), Personal communication.

Uttamsingh, R. J., and Carson, E. R. (1977), A Mathematical Model of the Patient-Artificial Kidney System, Research Memorandum, DSS/RJU-ERC/122, Department of Systems Science, The City University, London.

Vander, A. T., Sherman, J. H., and Luciano, D. S. (1980), Human Physiology (The Mechanisms of Body Function), Third ed., McGraw-Hill, New York.

Wang, H. H., Liu, L. M., Katz, R. L. (1977), "A comparison of the cardiovascular effects of sodium nitroprusside and trimethaphan", Anaesthesiology, 46, 40-48.

Webster, K. E. W. (1980), Personal communication.

Weller, H., and Wiley, R. L. (1979), Basic Human Physiology, Van Nostrand, New York.

Westerhof, N., and Gessner, U. (1965), "Comparison of an electrical model of the human systemic arterial tree with measurements in humans", in Proc. 18th Annu. Conf. on Eng. in Med. and Biol., p. 35.

Westerhof, N., Bosman, F., Devries, C., and Noordergraaf, A. (1969), "Analog studies of the human systemic arterial tree", J. of Biochem., 2, 121-143.

Wilkins, R. W., Bradley, S. E., and Friedland, C. K. (1950), "The acute circulatory effects of the head-down position (negative G) in normal man, with a note on some measures designed to relieve cranial congestion in this position", J. Clin. Invest., 29, 940-949.

Williams, J. G. (1962), Sports Medicine, Edward Arnold, London.

Wright, G. P. (1955), Introduction to Pathology. Chapter 6, Haemorrhage and Haemostasis, Second ed., Longmans, London.

APPENDIX I

LIST OF PRINCIPAL SYMBOLS USED

Compartmental subscripts (19-segment circulatory representation) (after Beneken and DeWit, 1967)

AA	Abdominal arteries
AO1	Ascending aorta
AO2	Aortic arch
AO3	Thoracic aorta
AV	Abdominal veins
CA	Leg arteries
CV	Leg veins
IA	Intestinal arteries
IV	Intestinal veins
IVC	Inferior vena cava
LA	Left atrium
LV	Left ventricle
PA	Pulmonary arteries
PV	Pulmonary veins
RA	Right atrium
RV	Right ventricle
SVC	Superior vena cava
UA	Head and arm arteries
UV	Head and arm veins

Compartmental subscripts (8-segment circulatory representation) (after Beneken and DeWit, 1967)

AO	Aorta
LV	Left ventricle
PA	Pulmonary arteries
PV	Pulmonary veins
RV	Right ventricle
SA	Systemic arteries
SV	Systemic veins
TV	Thoracic veins

Other subscripts

ABD	Abdomen
BMR	Basal metabolic rate
BRONC	Bronchial
BV	Blood volume
CC	Critical closure
C_c	Thermal capacitance of the core of the body
C_s	Thermal capacitance of the surface of the body
CBF	Blood flow rate through the core of the body
CNS	Central nervous system
COR	Coronary
D	Diastolic
E	Extracellular fluid volume
E_i	Volume of fluid added to extracellular fluid through ingestion
EF	Ejection fraction
E_o	Volume of fluid removed from extracellular fluid by kidneys
H	Heart
HEAD	Head and arms
IE	Inhalation-exhalation
IHL	Insensible heat loss rate from the body
INT	Intestines
LEG	Legs
LUNG	Lungs
K_{cs}	Thermal conductance between the core and surface of the body
K_{sE}	Thermal conductance between the surface of the body and the environment
MAX	Maximum
MIN	Minimum
MSP	(PMSP) Mean systemic pressure
N	Normal
q_p	(QDP) The output of the pressure receptors
q_v	(Q_v) The output of the volume receptors
R	Respiratory
R_c	Resistance to blood flow through the core of the body
R_s	Resistance to blood flow through the surface of the body
$R_{s\ max}$	Maximum permitted value for resistance to blood flow through the surface of the body
$R_{s\ min}$	Minimum permitted value for resistance to blood flow through the surface of the body
RAP	Right atrial pressure

RVR	Resistance to venous return
SBF	Blood flow rate through the surface of the body
SBF_{max}	Maximum permitted value for blood flow rate through the surface of the body
SBF_{min}	Minimum permitted value for blood flow rate through the surface of the body
T	Total
T_c	Temperature of the core of the body
T_E	Temperature of the environment surrounding the body
T_s	Temperature of the surface of the body
TH	Thorax
U	Unstressed
V_{INT}	Interstitial volume
VR	Venous return
VT	Venous tone
MC	Myocardial contractility

List of principal symbols used

a	elastance (reciprocal compliance)
A	cross-sectional area
b	variable associated with myocardial contractility control
B	baroreceptor output
C	compliance
d	variable associated with venous tone control
f	frequency
F	flow
g	acceleration due to gravity
G	hydrostatic pressure difference
h	integration step length
k	constant
ℓ	length
L	inertance
m	mass
M	injected mass
n	number of g's of acceleration
P	pressure
q	variable associated with peripheral resistance control
r	radial coordinate
R	resistance
t	time
T	duration or period

u	variable associated with heart rate control
v	velocity
V	volume
ω	concentration
x	variable associated with time-varying compliance generation
y	variable associated with respiration
z	longitudinal coordinate
α	constant
θ	angular coordinate
μ	kinematic viscosity
ρ	density
σ	variable associated with drug effects
τ	time constant
ϕ	angle between the axis of a segment and a perpendicular to the direction of gravitational force
$\mathcal{L}$	Laplace transform

APPENDIX II

THE COMPLETE 19-SEGMENT MATHEMATICAL MODEL

A.II.1 The Circulatory Fluid Mechanics Model

Right atrium

$$\frac{dV_{RA}}{dt} = F_1 - F_{RARV} \quad , \quad V_{RA} \geq 0 \tag{AII.1}$$

$$P_{RA} = a_{RA}(V_{RA} - V_{URA}) \tag{AII.2}$$

$$F_{RARV} = \begin{cases} F_2 \quad , \quad F_2 > 0 \\ 0 \quad , \quad F_2 \leq 0 \end{cases} \tag{AII.3}$$

$$F_1 = F_{SVCRA} + F_{IVCRA} + F_{BRONC} + F_{COR} \tag{AII.4}$$

$$F_2 = (P_{RA} - P_{RV})/R_{RARV} \tag{AII.5}$$

Right ventricle

$$\frac{dV_{RV}}{dt} = F_{RARV} - F_{RVPA} \quad , \quad V_{RA} \geq 0 \tag{AII.6}$$

$$\frac{dF_{RVPA}}{dt} = \frac{P_{RV} - P_{PA} - R_{RVPA}F_{RVPA} - \left(\frac{\rho}{2A^2_{PA}}\right)F^2_{RVPA}}{L_{RV}} \quad , \quad F_{RVPA} \geq 0 \tag{AII.7}$$

$$P_{RV} = a_{RV}(V_{RV} - V_{URV}) \tag{AII.8}$$

Pulmonary arteries

$$\frac{dV_{PA}}{dt} = F_{RVPA} - F_{PAPV} \quad , \quad V_{PA} \geq 0 \tag{AII.9}$$

$$P_{PA} = (V_{PA} - V_{UPA})/C_{PA} \tag{AII.10}$$

$$F_{PAPV} = \begin{cases} (P_{PA} - P_{PV})/R_{LUNG} \quad , \quad P_{PV} > P_{CC} \\ (P_{PA} - P_{CC})/R_{LUNG} \quad , \quad P_{PV} \leq P_{CC} \end{cases} \tag{AII.11}$$

Pulmonary veins

$$\frac{dV_{PV}}{dt} = F_{PAPV} - F_{PVLA} \quad , \quad V_{PV} \geq 0 \tag{AII.12}$$

$$P_{PV} = (V_{PV} - V_{UPV})/C_{PV} \tag{AII.13}$$

$$C_{PV} = \begin{cases} C_{PVN} & , \quad V_{PV} > V_{UPV} \\ K_6 C_{PVN} & , \quad V_{PV} \leq V_{UPV} \end{cases} \tag{AII.14}$$

$$F_3 = \frac{(P_{PV} - P_{LA}) V^2_{PV}}{R_{PVLA} V^2_{UPV}} \tag{AII.15}$$

$$F_{PVLA} = \begin{cases} F_3 & , \quad F > 0 \\ K_1 F_3 & , \quad F_3 \leq 0 \end{cases} \tag{AII.16}$$

Left atrium

$$\frac{dV_{LA}}{dt} = F_{PVLA} - F_{LALV} \quad , \quad V_{LA} \geq 0 \tag{AII.17}$$

$$P_{LA} = a_{LA}(V_{LA} - V_{ULA}) \tag{AII.18}$$

$$F_4 = (P_{LA} - P_{LV})/R_{LALV} \tag{AII.19}$$

$$F_{LALV} = \begin{cases} F_4 & , \quad F_4 > 0 \\ 0 & , \quad F_4 \leq 0 \end{cases} \tag{AII.20}$$

Left ventricle

$$\frac{dV_{LV}}{dt} = F_{LALV} - F_{LVAO1} \quad , \quad V_{LV} \geq 0 \tag{AII.21}$$

$$\frac{dF_{LVAO1}}{dt} = \frac{P_{LV} - P_{AO1} - R_{LVAO1} F_{LVAO1} - \left(\frac{\rho}{2A^2_{AO1}}\right) F^2_{LVAO1}}{L_{LV}} \quad , \quad F_{LVAO1} \geq 0 \tag{AII.22}$$

$$P_{LV} = a_{LV}(V_{LV} - V_{ULV}) \qquad \text{(AII.23)}$$

Ascending aorta

$$\frac{dV_{AO1}}{dt} = F_{LVAO1} - F_{AO1AO2} - F_{COR} \text{ , } V_{AO1} \geq 0 \qquad \text{(AII.24)}$$

$$\frac{dF_{AO1AO2}}{dt} = \left(P_{AO1} - P_{AO2} - R_{AO2}F_{AO1AO2}\right)/L_{AO2} \qquad \text{(AII.25)}$$

$$P_{AO1} = \frac{1}{C_{AO1}}\left(V_{AO1} - V_{UAO1}\right) + \frac{K_8}{C_{AO1}} \cdot \frac{dV_{AO1}}{dt} \qquad \text{(AII.26)}$$

$$F_{COR} = (P_{AO1} - P_{RA})/R_{COR} \qquad \text{(AII.27)}$$

Aortic arch

$$\frac{dV_{AO2}}{dt} = F_{AO1AO2} - F_{AO2UA} - F_{AO2AO3} \text{ , } V_{AO2} \geq 0 \qquad \text{(AII.28)}$$

$$\frac{dF_{AO2UA}}{dt} = \frac{P_{AO2} + P_{TH} - P_{UA} - R_{UA}F_{AO2UA} - G_{AO2UA}}{L_{UA}} \qquad \text{(AII.29)}$$

$$\frac{dF_{AO2AO3}}{dt} = \frac{P_{AO2} - P_{AO3} - R_{AO3}F_{AO2AO3} + G_{AO2AO3}}{L_{AO3}} \qquad \text{(AII.30)}$$

$$P_{AO2} = \frac{1}{C_{AO2}}\left(V_{AO2} - V_{UAO2}\right) + \frac{K_8}{C_{AO2}} \cdot \frac{dV_{AO2}}{dt} \qquad \text{(AII.31)}$$

Head and arm arteries

$$\frac{dV_{UA}}{dt} = F_{AO2UA} - F_{UAUV} \text{ , } V_{UA} \geq 0 \qquad \text{(AII.32)}$$

$$P_{UA} = \frac{1}{C_{UA}}\left(V_{UA} - V_{UUA}\right) + \frac{K_8}{C_{UA}} \cdot \frac{dV_{UA}}{dt} \qquad \text{(AII.33)}$$

$$F_{UAUV} = \left(P_{UA} - P_{UV}\right)/\left(R_{HEAD}\sigma_{HEAD}\right) \qquad \text{(AII.34)}$$

Head and arms veins

$$\frac{dV_{UV}}{dt} = F_{UAUV} - F_{UVSUC} \quad , \quad V_{UV} \geq 0 \tag{AII.35}$$

$$P_{UV} = d_3(V_{UV} - V_{UUV})/C_{UV} \tag{AII.36}$$

$$C_{UV} = \begin{cases} C_{UVN} & , \quad V_{UV} > V_{UUV} \\ K_6 C_{UVN} & , \quad V_{UV} \leq V_{UUV} \end{cases} \tag{AII.37}$$

$$V_{UUV} = V_{UUVN}/d_4 \tag{AII.38}$$

$$F_5 = \frac{(P_{UV} - P_{SVC} - P_{TH} + G_{UVSVC})V^2_{UV}}{R_{UV}V^2_{UUVN}} \tag{AII.39}$$

$$F_{UVSVC} = \begin{cases} F_5 & , \quad F_5 > 0 \\ K_9 F_5 & , \quad F_5 \leq 0 \end{cases} \tag{AII.40}$$

Thoracic aorta

$$\frac{dV_{AO3}}{dt} = F_{AO2AO3} - F_{BRONC} - F_{AO3IA} - F_{AO3AA} \quad , \quad V_{AO3} \geq 0 \tag{AII.41}$$

$$\frac{dF_{AO3IA}}{dt} = \frac{P_{AO3} + P_{TH} - P_{IA} - P_{ABD} - R_{IA}F_{AO3IA} + G_{AO3IA}}{L_{IA}} \tag{AII.42}$$

$$\frac{dF_{AO3AA}}{dt} = \frac{P_{AO3} + P_{TH} - P_{AA} - P_{ABD} - R_{AA}F_{AO3AA} + G_{AO3AA}}{L_{AA}} \tag{AII.43}$$

$$P_{AO3} = \frac{1}{C_{AO3}}\left(V_{AO3} - V_{UAO3}\right) + \frac{K_8}{C_{AO3}} \cdot \frac{dV_{AO3}}{dt} \tag{AII.44}$$

$$F_{BRONC} = \frac{P_{AO3} - P_{RA} - G_{AO3RA}}{R_{BRONC} \cdot q_4 \cdot \sigma_{BRONC}} \tag{AII.45}$$

Intestinal arteries

$$\frac{dV_{IA}}{dt} = F_{AO3IA} - F_{IAIV} \quad , \quad V_{IA} \geq 0 \tag{AII.46}$$

$$P_{IA} = \frac{1}{C_{IA}} \left(V_{IA} - V_{UIA}\right) + \frac{K_8}{C_{IA}} \cdot \frac{dV_{IA}}{dt} \tag{AII.47}$$

$$F_{IAIV} = \left(P_{IA} - P_{IV}\right) / \left(R_{INT}\, \sigma_{INT}\, q_4\right) \tag{AII.48}$$

Intestinal veins

$$\frac{dV_{IV}}{dt} = F_{IAIV} - F_{IVIVC} \quad , \quad V_{IV} \geq 0 \tag{AII.49}$$

$$P_{IV} = d_3 \left(V_{IV} - V_{UIV}\right) / C_{IV} \tag{AII.50}$$

$$C_{IV} = \begin{cases} C_{IVN} & , \quad V_{IV} > V_{UIV} \\ K_6 C_{IVN} & , \quad V_{IV} \leq V_{UIV} \end{cases} \tag{AII.51}$$

$$V_{UIV} = V_{UIVN} / d_4 \tag{AII.52}$$

$$F_6 = \frac{\left(P_{IV} - P_{IVC} + P_{ABD} - P_{TH} - G_{IVCIV}\right) V^2_{IV}}{R_{IV}\, V^2_{UIVN}} \tag{AII.53}$$

$$F_{IVIVC} = \begin{cases} F_6 & , \quad F_6 > 0 \\ K_{10} F_6 & , \quad F_6 \leq 0 \end{cases} \tag{AII.54}$$

Abdominal arteries

$$\frac{dV_{AA}}{dt} = F_{AO3AA} - F_{AAAV} - F_{AACA} \quad , \quad V_{AA} \geq 0 \tag{AII.55}$$

$$\frac{dF_{AACA}}{dt} = \left(P_{AA} - P_{CA} + P_{ABD} - R_{CA} F_{AACA} + G_{AACA}\right) / L_{CA} \tag{AII.56}$$

$$P_{AA} = \frac{1}{C_{AA}} \left(V_{AA} - V_{UAA}\right) + \frac{K_8}{C_{AA}} \cdot \frac{dV_{AA}}{dt} \tag{AII.57}$$

$$F_{AAAV} = \left(P_{AA} - P_{AV}\right)/\left(R_{ABD} q_4 \sigma_{ABD}\right) \qquad \text{(AII.58)}$$

Abdominal veins

$$\frac{dV_{AV}}{dt} = F_{AAAV} + F_{CVAV} - F_{AVIVC} \quad , \quad V_{AV} \geq 0 \qquad \text{(AII.59)}$$

$$P_{AV} = d_3\left(V_{AV} - V_{UAV}\right)/C_{AV} \qquad \text{(AII.60)}$$

$$C_{AV} = \begin{cases} C_{AVN} & , \quad V_{AV} > V_{UAV} \\ K_6 C_{AVN} & , \quad V_{AV} \leq V_{UAV} \end{cases} \qquad \text{(AII.61)}$$

$$V_{UAV} = V_{UAVN}/d_4 \qquad \text{(AII.62)}$$

$$F_7 = \frac{\left(P_{AV} - P_{IVC} + P_{ABD} - P_{TH} - G_{IVCAC}\right) V^2_{AV}}{R_{AV} V^2_{UAVN}} \qquad \text{(AII.63)}$$

$$F_{AVIVC} = \begin{cases} F_7 & , \quad F_7 > 0 \\ K_{11} F_7 & , \quad F_7 \leq 0 \end{cases} \qquad \text{(AII.64)}$$

Leg arteries

$$\frac{dV_{CA}}{dt} = F_{AACA} - F_{CACV} \quad , \quad V_{CA} \geq 0 \qquad \text{(AII.65)}$$

$$P_{CA} = \frac{1}{C_{CA}}\left(V_{CA} - V_{UCA}\right) + \frac{K_8}{C_{CA}} \cdot \frac{dV_{CA}}{dt} \qquad \text{(AII.66)}$$

$$F_{CACV} = \left(P_{CA} - P_{CV}\right)/\left(R_{LEG} q_4 \sigma_{LEG}\right) \qquad \text{(AII.67)}$$

Leg veins

$$\frac{dV_{CV}}{dt} = F_{CACV} - F_{CVAV} \quad , \quad V_{CV} \geq 0 \qquad \text{(AII.68)}$$

$$P_{CV} = d_3\left(V_{CV} - V_{UCV}\right)/C_{CV} \qquad \text{(AII.69)}$$

$$C_{CV} = \begin{cases} C_{CVN} & , \quad V_{CV} > V_{UCV} \\ K_6 C_{VN} & , \quad V_{CV} \leq V_{UCV} \end{cases} \qquad \text{(AII.70)}$$

$$V_{UCV} = V_{UCVN}/d_4 \qquad \text{(AII.71)}$$

$$F_8 = \frac{\left(P_{CV} - P_{AV} - P_{ABD} - G_{AVCV}\right) V^2_{CV}}{R_{CV}\, V^2_{UCVN}} \qquad \text{(AII.72)}$$

$$F_{CVAV} = \begin{cases} F_8 & , \quad F_8 > 0 \\ K_{12} F_8 & , \quad F_8 \leq 0 \end{cases} \qquad \text{(AII.73)}$$

Inferior vena cava

$$\frac{dV_{IVC}}{dt} = F_{AVIVC} + F_{IVIVC} - F_{IVCRA} \quad , \quad V_{IVC} \geq 0 \qquad \text{(AII.74)}$$

$$P_{IVC} = \left(V_{IVC} - V_{UIVC}\right)/C_{IVC} \qquad \text{(AII.75)}$$

$$C_{IVC} = \begin{cases} C_{IVCN} & , \quad V_{IVC} > V_{UIVC} \\ K_6 C_{IVCN} & , \quad V_{IVC} \leq V_{UIVC} \end{cases} \qquad \text{(AII.76)}$$

$$F_9 = \frac{\left(P_{IVC} - P_{RA} - G_{IVCRA}\right) V^2_{IVC}}{R_{IVC}\, V^2_{UIVC}} \qquad \text{(AII.77)}$$

$$F_{IVCRA} = \begin{cases} F_9 & , \quad F_9 > 0 \\ K_5 F_9 & , \quad F_9 \leq 0 \end{cases} \qquad \text{(AII.78)}$$

Superior vena cava

$$\frac{dV_{SVC}}{dt} = F_{UVSVC} - F_{SVCRA} \quad , \quad V_{SVC} \geq 0 \qquad \text{(AII.79)}$$

$$P_{SVC} = \left(V_{SVC} - V_{USVC}\right)/C_{SVC} \qquad \text{(AII.80)}$$

$$C_{SVC} = \begin{cases} C_{SVCN} & , \quad V_{SVC} > V_{USVC} \\ K_6 C_{SVCN} & , \quad V_{SVC} \leq U_{USVC} \end{cases} \qquad \text{(AII.81)}$$

$$F_{1O} = \frac{\left(P_{SVC} - P_{RA} + G_{SVCRA}\right) V^2_{SVC}}{R_{SVC} \; V^2_{USVC}} \qquad \text{(AII.82)}$$

$$F_{SVCRA} = \begin{cases} F_{1O} & , \quad F_{1O} > O \\ K_5 F_{1O} & , \quad F_{1O} \leq O \end{cases} \qquad \text{(AII.83)}$$

Time-varying compliances of atria and ventricles

$$\frac{dU_{1O}}{dt} = 1.0 \; (U_{1O} \text{ set to zero at end of cardiac cycle}) \qquad \text{(AII.84)}$$

$$T_{AS} = K_{22} + K_{23} \; T_H \qquad \text{(AII.85)}$$

$$T_{AV} = T_{AS} - K_{24} \qquad \text{(AII.86)}$$

$$T_{VS} = K_{25} + K_{26} \; T_H \qquad \text{(AII.87)}$$

$$x_1 = \pi / T_{AS} \qquad \text{(AII.88)}$$

$$x_2 = \pi / T_{VS} \qquad \text{(AII.89)}$$

$$x_3 = \begin{cases} O & , \quad U_{1O} > T_{AS} \\ \sin\left(x_1 U_{1O}\right) & , \quad U_{1O} \leq T_{AS} \end{cases} \qquad \text{(AII.90)}$$

$$x_4 = \begin{cases} U_{1O} - T_{AV} & , \quad U_{1O} > T_{AV} \\ O & , \quad U_{1O} \leq T_{AV} \end{cases} \qquad \text{(AII.91)}$$

$$x_5 = \begin{cases} O & , \quad x_4 > T_{VS} \\ \sin\left(x_2 x_4\right) & , \quad x_4 \leq T_{VS} \end{cases} \qquad \text{(AII.92)}$$

$$a_{LA} = x_3\{b_2\ \sigma_{LA}\ a_{LAS} - a_{LAD}\} + a_{LAD} \quad \text{(AII.93)}$$

$$a_{LV} = x_5\{b_2\ \sigma_{LV}\ a_{LVS} - a_{LVD}\} + a_{LVD} \quad \text{(AII.94)}$$

$$a_{RA} = x_3\{b_2\ \sigma_{RA}\ a_{RAS} - a_{RAD}\} + a_{RAD} \quad \text{(AII.95)}$$

$$a_{RV} = x_5\{b_2\ \sigma_{RV}\ a_{RVS} - a_{RVD}\} + a_{RVD} \quad \text{(AII.96)}$$

Respiration

$$\frac{dy_2}{dt} = 1.0 \ (y_2 \text{ set to zero at end of respiratory cycle}) \quad \text{(AII.97)}$$

$$y_1 = \begin{cases} y_2 & , \ y_2 \leq T_{IE} \\ 0 & , \ y_2 > T_{IE} \end{cases} \quad \text{(AII.98)}$$

$$P_{TH} = K_1 + (K_2 - K_1)\sin(\pi y_1/T_{IE}) \quad \text{(AII.99)}$$

$$P_{ABD} = K_3 + (K_4 - K_3)\sin(\pi y_1/T_{IE}) \quad \text{(AII.100)}$$

Calculation of (MAP), (SV), (CO), (ETSR)

$$(MAP) = \frac{1}{TH} \int_{t_1}^{(t_1+T_H)} P_{AO1}\,dt \quad (t_1 = \text{start of a cardiac cycle}) \quad \text{(AII.101)}$$

$$(SV) = \int_{t_1}^{(t_1+T_H)} F_{LVAO1}\,dt \quad \text{(AII.102)}$$

$$(CO) = (SV)/T_H \quad \text{(AII.103)}$$

$$ETSR = (MAP/(CO) \quad \text{(AII.104)}$$

True total systemic resistance (TTSR)

$$R_A = R_{UA} + R_{HEAD}\sigma_{HEAD} + \frac{R_{UV}V^2_{UUVN}}{V^2_{UV}}\frac{R_{SVC}V^2_{USVC}}{V^2_{SVC}} \quad \text{(AII.105)}$$

$$R_B = q_4\sigma_{BRONC}R_{BRONC} \quad \text{(AII.106)}$$

$$R_C = R_{CA} + q_4R_{LEG}\sigma_{LEG} + R_{CV}V^2_{UCVN}/V^2_{CV} \quad \text{(AII.107)}$$

$$R_D = q_4R_{ABD}\sigma_{ABD} \quad \text{(AII.108)}$$

$$R_E = R_CR_D/(R_C + R_D) + R_{AA} + R_{AV}V^2_{UAVN}/V^2_{AV} \quad \text{(AII.109)}$$

$$R_F = R_{IA} + q_4\sigma_{INT}R_{INT} + R_{IV}V^2_{UIVN}/V^2_{IV} \quad \text{(AII.110)}$$

$$R_G = R_ER_F/(R_E + R_F) + R_{IVC}V^2_{UIVC}/V^2_{IVC} \quad \text{(AII.111)}$$

$$R_H = R_{AO3} + R_BR_G/(R_B + R_G) \quad \text{(AII.112)}$$

$$R_I = R_{AO2} + R_AR_H/(R_A + R_H) \quad \text{(AII.113)}$$

$$(TTSR) = R_{COR}R_I/(R_{COR} + R_I) \quad \text{(AII.114)}$$

A.II.2 The Neural Control Model

Aortic arch baroreceptors

$$\frac{dS_3}{dt} = (P_{AO2} - S_3)/\tau_1 \quad \text{(AII.115)}$$

$$\frac{dS_4}{dt} = (S_2 - S_4)/\tau_2 \quad \text{(AII.116)}$$

$$S_1 = \frac{dP_{AO2}}{dt} \quad \text{(AII.117)}$$

$$S_2 = \begin{cases} S_1 , & S_1 > 0 \\ 0 , & S_1 \leqslant 0 \end{cases} \quad \text{(AII.118)}$$

$$S_5 = K_{13}\left(S_3 + K_{14}S_4 - K_{15}\right) \tag{AII.119}$$

$$B_{AO2} = \begin{cases} S_5 , & S_5 > 0 \\ 0 , & S_5 \leq 0 \end{cases} \tag{AII.120}$$

Carotid sinus baroreceptors

$$\frac{dS_8}{dt} = (P_{UA} - S_8)/\tau_1 \tag{AII.121}$$

$$\frac{dS_9}{dt} = (S_7 - S_9)/\tau_2 \tag{AII.122}$$

$$S_6 = \frac{dP_{UA}}{dt} \tag{AII.123}$$

$$S_7 = \begin{cases} S_6 , & S_6 > 0 \\ 0 , & S_6 \leq 0 \end{cases} \tag{AII.124}$$

$$S_{10} = K_{13}\left(S_8 + K_{14}S_9 - K_{15}\right) \tag{AII.125}$$

$$P_{UA} = \begin{cases} S_{10} , & S_{10} > 0 \\ 0 , & S_{10} \leq 0 \end{cases} \tag{AII.126}$$

CNS input function

$$B = \left(1 - K_{16}\right)B_{AO2} + K_{16}B_{UA} \tag{AII.127}$$

CNS control of heart rate

$$\frac{dU_4}{dt} = (U_1 - U_4)/U_3 \tag{AII.128}$$

$$\frac{dU_6}{dt} = (U_5 - U_6)/\tau_3 \tag{AII.129}$$

$$\frac{dU_7}{dt} = (U_6 - U_7)/\tau_4 \qquad \text{(AII.130)}$$

$$U_1 = \begin{cases} K_{17}(B - K_{18}) & , \quad B > K_{18} \\ 0 & , \quad B \leq K_{18} \end{cases} \qquad \text{(AII.131)}$$

$$U_2 = \frac{dU_1}{dt} \qquad \text{(AII.132)}$$

$$U_3 = \begin{cases} K_{19} & , \quad U_2 > 0 \\ K_{20} & , \quad U_2 \leq 0 \end{cases} \qquad \text{(AII.133)}$$

$$U_5 = \begin{cases} K_{18} & , \quad B > K_{18} \\ B & , \quad B \leq K_{18} \end{cases} \qquad \text{(AII.134)}$$

$$U_9 = \begin{cases} 2.0 & , \quad U_8 \geq 2.0 \\ U_8 & , \quad 0.3 < U_8 < 2.0 \\ 0.3 & , \quad U_8 \leq 0.3 \end{cases} \qquad \text{(AII.135)}$$

$$U_8 = K_{21} \cdot \sigma_H(U_4 + U_7) \qquad \text{(AII.136)}$$

T_H is set to the value of U_9 at the end of the cardiac cycle.

CNS control of peripheral resistance

$$\frac{dq_2}{dt} = (q_1 - q_2)/\tau_5 \qquad \text{(AII.137)}$$

$$\frac{dq_3}{dt} = (q_1 - q_3)/\tau_6 \qquad \text{(AII.138)}$$

$$q_4 = K_{29}q_3 + (1 - K_{29})q_2 \qquad \text{(AII.139)}$$

$$q_1 = \begin{cases} K_{27} , & B > K_{18} \\ K_{28} , & B \leq K_{18} \end{cases} \qquad \text{(AII.140)}$$

CNS control of myocardial contractility

$$\frac{db_2}{dt} = (b_1 - b_2)/\tau_8 \qquad \text{(AII.141)}$$

$$b_1 = \begin{cases} K_{34} , & B > K_{18} \\ K_{35} , & B \leq K_{18} \end{cases} \qquad \text{(AII.142)}$$

CNS control of venous tone

$$\frac{dd_2}{dt} = (d_1 - d_2)/\tau_7 \qquad \text{(AII.143)}$$

$$d_1 = \begin{cases} K_{30} , & B > K_{18} \\ K_{31} , & B \leq K_{18} \end{cases} \qquad \text{(AII.144)}$$

$$d_3 = 1 + K_{32}(d_2 - 1) \qquad \text{(AII.145)}$$

$$d_4 = 1 + K_{33}(d_2 - 1) \qquad \text{(AII.146)}$$

A.II.3 The Pharmacokinetics Model

Right atrium

$$\frac{dm_{RA}}{dt} = \omega_{SVCRA}F_{SVCRA} + \omega_{COR}F_{COR} + \omega_{BRONC}F_{BRONC} + \omega_{IVCRA}F_{IVCRA} - \omega_{RARV}F_{RARV} - m_{RA}/\tau_9 \qquad \text{(AII.147)}$$

$$\omega_{RA} = m_{RA}/V_{RA} \qquad \text{(AII.148)}$$

Right ventricle

$$\frac{m_{RV}}{dt} = \omega_{RARV} F_{RARV} - \omega_{RVPA} F_{RVPA} - m_{RV}/\tau_9 \qquad \text{(AII.149)}$$

$$\omega_{RV} = m_{RV}/V_{RV} \qquad \text{(AII.150)}$$

Pulmonary arteries

$$\frac{dm_{PA}}{dt} = \omega_{RVPA} F_{RVPA} - \omega_{PAPV} F_{PAPV} - m_{PA}/\tau_9 \qquad \text{(AII.151)}$$

$$\omega_{PA} = m_{PA}/V_{PA} \qquad \text{(AII.152)}$$

Pulmonary veins

$$\frac{dm_{PV}}{dt} = \omega_{PAPV} F_{PAPV} - \omega_{PVLA} F_{PVLA} - m_{PV}/\tau_9 \qquad \text{(AII.153)}$$

$$\omega_{PV} = m_{PA}/V_{PV} \qquad \text{(AII.154)}$$

Left atrium

$$\frac{dm_{LA}}{dt} = \omega_{PVLA} F_{PVLA} - \omega_{LALV} F_{LALV} - m_{LA}/\tau_9 \qquad \text{(AII.155)}$$

$$\omega_{LA} = m_{LA}/V_{LA} \qquad \text{(AII.156)}$$

Left ventricle

$$\frac{dm_{LV}}{dt} = \omega_{LALV} F_{LALV} - \omega_{LVAO1} F_{LVAO1} - m_{LV}/\tau_9 \qquad \text{(AII.157)}$$

$$\omega_{LV} = m_{LV}/V_{LV} \qquad \text{(AII.158)}$$

Ascending aorta

$$\frac{dm_{AO1}}{dt} = \omega_{LVAO1} F_{LVAO1} - \omega_{AO1AO2} F_{AO1AO2} - \omega_{COR} F_{COR} - m_{AO1}/\tau_9 \qquad \text{(AII.159)}$$

$$\omega_{AO1} = m_{AO1}/V_{AO1} \qquad \text{(AII.160)}$$

Aortic arch

$$\frac{dm_{AO2}}{dt} = \omega_{AO1AO2} F_{AO1AO2} - \omega_{AO2UA} F_{AO2UA} - \omega_{AO2AO3} F_{AO2AO3} - m_{AO2}/\tau_9 \quad \text{(AII.161)}$$

$$\omega_{AO2} = m_{AO2}/V_{AO2} \quad \text{(AII.162)}$$

Head and arms arteries

$$\frac{dm_{UA}}{dt} = \omega_{AO2UA} F_{AO2UA} - \omega_{UAUV} F_{UAUV} - m_{UA}/\tau_9 \quad \text{(AII.163)}$$

$$\omega_{UA} = m_{UA}/V_{UA} \quad \text{(AII.164)}$$

Head and arms veins

$$\frac{dm_{UV}}{dt} = \omega_{UAUV} F_{UAUV} - \omega_{UVSVC} F_{UVSVC} - m_{UV}/\tau_9 + M\delta(t) \quad \text{(AII.165)}$$

(assuming mass M injected at t = 0)

$$\omega_{UV} = m_{UV}/V_{UV} \quad \text{(AII.166)}$$

Thoracic aorta

$$\frac{dm_{AO3}}{dt} = \omega_{AO2AO3} F_{AO2AO3} - \omega_{BRONC} F_{BRONC} - \omega_{AO3IA} F_{AO3IA} - \omega_{AO3AA} F_{AO3AA} - m_{AO3}/\tau_9 \quad \text{(AII.167)}$$

$$\omega_{AO3} = m_{AO3}/V_{AO3} \quad \text{(AII.168)}$$

Intestinal arteries

$$\frac{dm_{IA}}{dt} = \omega_{AO3IA} F_{AO3IA} - \omega_{IAIV} F_{IAIV} - m_{IA}/\tau_9 \quad \text{(AII.169)}$$

$$\omega_{IA} = m_{IA}/V_{IA} \quad \text{(AII.170)}$$

Intestinal veins

$$\frac{dm_{IV}}{dt} = \omega_{IAIV} F_{IAIV} - \omega_{IVIVC} F_{IVIVC} - m_{IV}/\tau_9 \quad \text{(AII.171)}$$

$$\omega_{IV} = m_{IV}/V_{IV} \quad \text{(AII.172)}$$

Abdominal arteries

$$\frac{dm_{AA}}{dt} = \omega_{AO3AA} F_{AO3AA} - \omega_{AAAV} F_{AAAV} - \omega_{AACA} F_{AACA} - m_{AA}/\tau_9 \quad \text{(AII.173)}$$

$$\omega_{AA} = m_{AA}/V_{AA} \quad \text{(AII.174)}$$

Abdominal veins

$$\frac{dm_{AV}}{dt} = \omega_{AAAV} F_{AAAV} + \omega_{CVAV} F_{CVAV} - \omega_{AVIVC} F_{AVIVC} - m_{AV}/\tau_9 \quad \text{(AII.175)}$$

$$\omega_{AV} = m_{AV}/V_{AV} \quad \text{(AII.176)}$$

Leg arteries

$$\frac{dm_{CA}}{dt} = \omega_{AACA} F_{AACA} - \omega_{CACV} F_{CACV} - m_{CA}/\tau_9 \quad \text{(AII.177)}$$

$$\omega_{CA} = m_{CA}/V_{CA} \quad \text{(AII.178)}$$

Leg veins

$$\frac{dm_{CV}}{dt} = \omega_{CACV} F_{CACV} - \omega_{CVAV} F_{CVAV} - m_{CV}/\tau_9 \quad \text{(AII.179)}$$

$$\omega_{CV} = m_{CV}/V_{CV} \quad \text{(AII.180)}$$

Inferior vena cava

$$\frac{dm_{IVC}}{dt} = \omega_{AVIVC} F_{AVIVC} + \omega_{IVIVC} F_{IVIVC} - \omega_{IVCRA} F_{IVCRA} - m_{IVC}/\tau_9 \quad \text{(AII.181)}$$

$$\omega_{IVC} = m_{IVC}/V_{IVC} \quad \text{(AII.182)}$$

Superior vena cava

$$\frac{dm_{SVC}}{dt} = \omega_{UVSVC} F_{UVSVC} - \omega_{SVCRA} F_{SVCRA} - m_{SVC}/\tau_9 \qquad \text{(AII.183)}$$

$$\omega_{SVC} = m_{SVC}/V_{SVC} \qquad \text{(AII.184)}$$

Concentrations appropriate to directions of flow

$$\omega_{SVCRA} = \begin{cases} \omega_{SVC} , & F_{SVCRA} > 0 \\ \omega_{RA} , & F_{SVCRA} \leq 0 \end{cases} \qquad \text{(AII.185)}$$

$$\omega_{COR} = \begin{cases} \omega_{AO1} , & F_{COR} > 0 \\ \omega_{RA} , & F_{COR} \leq 0 \end{cases} \qquad \text{(AII.186)}$$

$$\omega_{BRONC} = \begin{cases} \omega_{AO3} , & F_{BRONC} > 0 \\ \omega_{RA} , & F_{BRONC} \leq 0 \end{cases} \qquad \text{(AII.187)}$$

$$\omega_{IVCRA} = \begin{cases} \omega_{IVC} , & F_{IVCRA} > 0 \\ \omega_{RA} , & F_{IVCRA} \leq 0 \end{cases} \qquad \text{(AII.188)}$$

$$\omega_{RARV} = \begin{cases} \omega_{RA} , & F_{RARV} > 0 \\ \omega_{RV} , & F_{RARV} \leq 0 \end{cases} \qquad \text{(AII.189)}$$

$$\omega_{RVPA} = \begin{cases} \omega_{RV} , & F_{RVPA} > 0 \\ \omega_{PA} , & F_{RVPA} \leq 0 \end{cases} \qquad \text{(AII.190)}$$

$$\omega_{PAPV} = \begin{cases} \omega_{PA} , & F_{PAPV} > 0 \\ \omega_{PV} , & F_{PAPV} \leq 0 \end{cases} \qquad \text{(AII.191)}$$

$$\omega_{PVLA} = \begin{cases} \omega_{PV} , & F_{PVLA} > 0 \\ \omega_{LA} , & F_{PVLA} \leq 0 \end{cases} \qquad \text{(AII.192)}$$

$$\omega_{LALV} = \begin{cases} \omega_{LA} , & F_{LALV} > 0 \\ \omega_{LV} , & F_{LALV} \leq 0 \end{cases} \qquad \text{(AII.193)}$$

$$\omega_{LVAO1} = \begin{cases} \omega_{LV} , & F_{LVAO1} < 0 \\ \omega_{AO1} , & F_{LVAO1} \geq 0 \end{cases} \qquad \text{(AII.194)}$$

$$\omega_{AO1AO2} = \begin{cases} \omega_{AO1} , & F_{AO1AO2} < 0 \\ \omega_{AO2} , & F_{AO1AO2} \geq 0 \end{cases} \qquad \text{(AII.195)}$$

$$\omega_{AO2UA} = \begin{cases} \omega_{AO2} , & F_{AO2UA} > 0 \\ \omega_{UA} , & F_{AO2UA} \leq 0 \end{cases} \qquad \text{(AII.196)}$$

$$\omega_{AO2AO3} = \begin{cases} \omega_{AO2} , & F_{AO2AO3} > 0 \\ \omega_{AO3} , & F_{AO2AO3} \leq 0 \end{cases} \qquad \text{(AII.197)}$$

$$\omega_{UAUV} = \begin{cases} \omega_{UA} , & F_{UAUV} > 0 \\ \omega_{UV} , & F_{UAUV} \leq 0 \end{cases} \qquad \text{(AII.198)}$$

$$\omega_{UVSVC} = \begin{cases} \omega_{UV} , & F_{UVSVC} > 0 \\ \omega_{SVC} , & F_{UVSVC} \leq 0 \end{cases} \qquad \text{(AII.199)}$$

$$\omega_{AO3IA} = \begin{cases} \omega_{AO3} , & F_{AO3IA} > 0 \\ \omega_{IA} , & F_{AO3IA} \leq 0 \end{cases} \qquad \text{(AII.200)}$$

$$\omega_{AO3AA} = \begin{cases} \omega_{AO3} & , \quad F_{AO3AA} > 0 \\ \omega_{AA} & , \quad F_{AO3AA} \leq 0 \end{cases} \qquad \text{(AII.201)}$$

$$\omega_{IAIV} = \begin{cases} \omega_{IA} & , \quad F_{IAIV} > 0 \\ \omega_{IV} & , \quad F_{IAIV} \leq 0 \end{cases} \qquad \text{(AII.202)}$$

$$\omega_{IVIVC} = \begin{cases} \omega_{IV} & , \quad F_{IVIVC} > 0 \\ \omega_{IVC} & , \quad F_{IVIVC} \leq 0 \end{cases} \qquad \text{(AII.203)}$$

$$\omega_{AAAV} = \begin{cases} \omega_{AA} & , \quad F_{AAAV} > 0 \\ \omega_{AV} & , \quad F_{AAAV} \leq 0 \end{cases} \qquad \text{(AII.204)}$$

$$\omega_{AACA} = \begin{cases} \omega_{AA} & , \quad F_{AACA} > 0 \\ \omega_{CA} & , \quad F_{AACA} \leq 0 \end{cases} \qquad \text{(AII.205)}$$

$$\omega_{CVAV} = \begin{cases} \omega_{CV} & , \quad F_{CVAV} > 0 \\ \omega_{AV} & , \quad F_{CVAV} \leq 0 \end{cases} \qquad \text{(AII.206)}$$

$$\omega_{AVIVC} = \begin{cases} \omega_{AV} & , \quad F_{AVIVC} > 0 \\ \omega_{IVC} & , \quad F_{AVIVC} \leq 0 \end{cases} \qquad \text{(AII.207)}$$

$$\omega_{CACV} = \begin{cases} \omega_{CA} & , \quad F_{CACV} > 0 \\ \omega_{CV} & , \quad F_{CACV} \leq 0 \end{cases} \qquad \text{(AII.208)}$$

Effect of drug on heart rate

$$\sigma_H = \begin{cases} 1 + \sigma_2 \omega_{RA}, & \text{bradycardia} \\ \dfrac{1}{1 + \sigma_2 \omega_{RA}}, & \text{tachycardia} \end{cases} \qquad \text{(AII.209)}$$

Effect of drug on peripheral resistance

$$\sigma_{BRONC} = \begin{cases} 1 + \sigma_1 \omega_{AO3}, & \text{vasoconstriction} \\ \dfrac{1}{1 + \sigma_1 \omega_{AO3}}, & \text{vasodilatation} \end{cases} \qquad \text{(AII.210)}$$

$$\sigma_{INT} = \begin{cases} 1 + \sigma_1 \omega_{IA}, & \text{vasoconstriction} \\ \dfrac{1}{1 + \sigma_1 \omega_{IA}}, & \text{vasodilatation} \end{cases} \qquad \text{(AII.211)}$$

$$\sigma_{ABD} = \begin{cases} 1 + \sigma_1 \omega_{AA}, & \text{vasoconstriction} \\ \dfrac{1}{1 + \sigma_1 \omega_{AA}}, & \text{vasodilatation} \end{cases} \qquad \text{(AII.212)}$$

$$\sigma_{LEG} = \begin{cases} 1 + \sigma_1 \omega_{CA}, & \text{vasoconstriction} \\ \dfrac{1}{1 + \sigma_1 \omega_{CA}}, & \text{vasodilatation} \end{cases} \qquad \text{(AII.213)}$$

$$\sigma_{HEAD} = \begin{cases} 1 + \sigma_1 \omega_{UA}, & \text{vasoconstriction} \\ \dfrac{1}{1 + \sigma_1 \omega_{UA}}, & \text{vasodilatation} \end{cases} \qquad \text{(AII.214)}$$

Effect of drug on myocardial contractility

$$\sigma_{RA} = \begin{cases} 1 + \sigma_3 \omega_{RA}, & \text{positive inotropy} \\ \dfrac{1}{1 + \sigma_3 \omega_{RA}}, & \text{negative inotropy} \end{cases} \qquad \text{(AII.215)}$$

$$\sigma_{RV} = \begin{cases} 1 + \sigma_3 \omega_{RV} & , \quad \text{positive inotropy} \\ \dfrac{1}{1 + \sigma_3 \omega_{RV}} & , \quad \text{negative inotropy} \end{cases} \tag{AII.216}$$

$$\sigma_{LA} = \begin{cases} 1 + \sigma_3 \omega_{LA} & , \quad \text{positive inotropy} \\ \dfrac{1}{1 + \sigma_3 \omega_{LA}} & , \quad \text{negative inotropy} \end{cases} \tag{AII.217}$$

$$\sigma_{LV} = \begin{cases} 1 + \sigma_3 \omega_{LV} & , \quad \text{positive inotropy} \\ \dfrac{1}{1 + \sigma_3 \omega_{LV}} & , \quad \text{negative inotropy} \end{cases} \tag{AII.218}$$

APPENDIX III

VARIABLES AND CONSTANTS USED IN THE COMPUTER PROGRAM FOR THE 19-SEGMENT MODEL

The variables and constants given in the tables below are those referred to in the mathematical model of Appendix VII and the computer programme for the full model.

State Variables

State Variable in Computer Programme	State Variable in Mathematical Model	Initial Value of State Variable
X(1)	V_{RA}	153.63
X(2)	V_{RV}	132.32
X(3)	V_{PA}	114.86
X(4)	V_{PV}	536.52
X(5)	V_{LA}	104.02
X(6)	V_{LV}	131.27
X(7)	V_{AO1}	81.233
X(8)	V_{AO2}	90.243
X(9)	V_{UA}	146.39
X(10)	V_{UV}	546.85
X(11)	V_{AO3}	88.157
X(12)	V_{IA}	22.552
X(13)	V_{IV}	597.54
X(14)	V_{AA}	77.249
X(15)	V_{AV}	290.32
X(16)	V_{CA}	74.33
X(17)	V_{CV}	271.05
X(18)	V_{IVC}	534.04
X(19)	V_{SVC}	542.37
X(20)	F_{RVPA}	0.0
X(21)	F_{LVAO1}	0.0
X(22)	F_{AO1AO2}	6.8039
X(23)	F_{AO2UA}	-3.8444
X(24)	F_{AO2AO3}	25.669
X(25)	F_{AO3IA}	35.075
X(26)	F_{AO3AA}	-3.3266
X(27)	F_{AACA}	2.6994

State Variables (continued)

State Variable in Computer Programme	State Variable in Mathematical Model	Initial Value of State Variable
X(28)	y_2	0.0
X(29)	S_3	109.26
X(30)	S_4	1.4146
X(31)	S_8	104.93
X(32)	S_9	1.7048
X(33)	U_4	62.617
X(34)	U_6	75.268
X(35)	U_7	75.115
X(36)	U_{10}	0.0
X(37)	q_2	0.97272
X(38)	q_3	0.97109
X(39)	d_2	1.1178
X(40)	b_2	0.97153
X(41)	$\int P_{AO1} dt$	0.0
X(42)	$\int F_{LVAO1} dt$	0.0
X(43)	m_{RA}	0.0
X(44)	m_{RV}	0.0
X(45)	m_{PA}	0.0
X(46)	m_{PV}	0.0
X(47)	m_{LA}	0.0
X(48)	m_{LV}	0.0
X(49)	m_{AO1}	0.0
X(50)	m_{AO2}	0.0
X(51)	m_{UA}	0.0
X(52)	m_{UV}	0.0
X(53)	m_{AO3}	0.0
X(54)	m_{IA}	0.0
X(55)	m_{IV}	0.0
X(56)	m_{AA}	0.0
X(57)	m_{AV}	0.0
X(58)	m_{CA}	0.0
X(59)	m_{CV}	0.0
X(60)	m_{IVC}	0.0
X(61)	m_{SVC}	0.0

Other Numerical Variables

Variable in Computer Programme	Variable in Mathematical Model	Variable in Computer Programme	Variable in Mathematical Model
V(1)	P_{AA}	V(36)	F_{AAAV}
V(2)	a_{RA}	V(37)	P_{AV}
V(3)	dB_{AO2}/dt	V(38)	F_7
V(4)	F_1	V(39)	F_{AVIVC}
V(5)	F_2	V(40)	P_{CA}
V(6)	F_{AARV}	V(41)	F_{CACV}
V(7)	P_{RV}	V(42)	P_{CV}
V(8)	a_{RV}	V(43)	F_8
V(9)	P_{PA}	V(44)	F_{CVAV}
V(10)	F_{PAPV}	V(45)	P_{IVC}
V(11)	P_{PV}	V(46)	F_9
V(12)	F_3	V(47)	F_{IVCRA}
V(13)	F_{PVLA}	V(48)	P_{SVC}
V(14)	P_{LA}	V(49)	F_{10}
V(15)	a_{LA}	V(50)	F_{SVCRA}
V(16)	F_4	V(51)	S_1
V(17)	F_{LALV}	V(52)	S_2
V(18)	P_{LV}	V(53)	S_5
V(19)	a_{LV}	V(54)	B_{AO2}
V(20)	P_{AO1}	V(55)	S_6
V(21)	F_{COR}	V(56)	S_7
V(22)	P_{AO2}	V(57)	S_{10}
V(23)	P_{UA}	V(58)	B_{UA}
V(24)	F_{UAUV}	V(59)	B
V(25)	P_{UV}	V(60)	U_1
V(26)	F_5	V(61)	U_2
V(27)	F_{UVSVC}	V(62)	U_3
V(28)	P_{AO3}	V(63)	U_5
V(29)	F_{BRONC}	V(64)	U_8
V(30)	P_{IA}	V(65)	U_9
V(31)	F_{IAIV}	V(66)	T_H
V(32)	P_{IV}	V(67)	f_H
V(33)	F_6	V(68)	T_{AS}
V(34)	F_{IVIVC}	V(69)	T_{AV}
V(35)	P_{AA}	V(70)	T_{VS}

Other Numerical Variables (continued)

Variable in Computer Programme	Variable in Mathematical Model	Variable in Computer Programme	Variable in Mathematical Model
V(71)	x_1	V(106)	ω_{AV}
V(72)	x_2	V(107)	ω_{CA}
V(73)	x_3	V(108	ω_{CV}
V(74)	x_4	V(109)	ω_{IVC}
V(75)	x_5	V(110)	ω_{SVC}
V(76)	q_1	V(111)	$(P_{AO1})^{MAX}$
V(77)	q_4	V(112)	$(P_{AO1})^{MIN}$
V(78)	d_1	SRA	σ_{RA}
V(79)	d_3	SRV	σ_{RV}
V(80)	d_4	SLA	σ_{LA}
V(81)	b_1	SLV	σ_{LV}
V(82)	(MAP)	SHEAD	σ_{HEAD}
V(83)	(CO)	SBRONC	σ_{BRONC}
V(84)	(ETSR)	SINT	σ_{INT}
V(85)	(TTSR)	SABD	σ_{ABD}
V(86)	V_T	SLEG	σ_{LEG}
V(87)	(SV)	SHR	σ_H
V(88)	Y_1	PHI	ϕ
V(89)	P_{TH}		
V(90)	P_{ABD}		
V(91)	dB_{VA}/dt		
V(92)	ω_{RA}		
V(93)	ω_{RV}		
V(94)	ω_{PA}		
V(95)	ω_{PV}		
V(96)	ω_{LA}		
V(97)	ω_{LV}		
V(98)	ω_{AO1}		
V(99)	ω_{AO2}		
V(100)	ω_{UA}		
V(101)	ω_{UV}		
V(102)	ω_{AO3}		
V(103)	ω_{IA}		
V(104)	ω_{IV}		
V(105)	ω_{AA}		

Numerical constants

All constants are given in medical units (torr ml s) unless otherwise stated.

Constant in Computer Programme	Constant in Mathematical Model	Value
P(1)	$C_{PVN}K_6$	COMPUTED
P(2)	$R_{PVLA}V^2_{UPV}$	COMPUTED
P(3)	$C_{AO1} + \frac{K_8}{R_{COR}}$	COMPUTED
P(4)	$C_{UVN}K_6$	COMPUTED
P(5)	$C_{SVCN}K_6$	COMPUTED
P(6)	$R_{SVC}V^2_{USVC}$	COMPUTED
P(7)	P_{THN}	- 4.0
P(8)	P_{ABDN}	+ 4.0
P(9)	K_1	- 3.0
P(10)	K_2	- 6.0
P(11)	K_3	+ 3.0
P(12)	K_4	+ 6.0
P(13)	T_{IE}	4.0
P(14)	T_R	5.0
P(15)	n	1.0
P(16)	ϕ_N	90.0 degrees
P(17)	l_{AO2UA}	19.5 cm
P(18)	l_{AO2AO3}	10.0 cm
P(19)	l_{UVSVC}	18.0 cm
P(20)	l_{AO3IA}	8.0 cm
P(21)	l_{AO3AA}	16.0 cm
P(22)	l_{IVCIV}	8.0 cm
P(23)	l_{AACA}	48.0 cm
P(24)	l_{IVCAV}	16.0 cm
P(25)	l_{AVCV}	48.0 cm
P(26)	l_{IVCRA}	10.0 cm
P(27)	l_{SVCRA}	1.5 cm
P(28)	l_{AO3RA}	10.0 cm

Numerical constants (continued)

Constant in Computer Programme	Constant in Mathematical Model	Value
P(29)	a_{RAS}	0.15
P(30)	a_{RAD}	0.05
P(31)	V_{URA}	30.0
P(32)	R_{RARV}	0.003
P(33)	K_5	0.1
P(34)	a_{RVS}	0.3
P(35)	a_{RVD}	0.046
P(36)	V_{URV}	0.0
P(37)	R_{RVPA}	0.003
P(38)	A_{PA}	1.539 cm^2
P(39)	L_{RV}	0.00018
P(40)	C_{PA}	4.3
P(41)	V_{UPA}	50.0
P(42)	P_{CC}	7.0
P(43)	R_{LUNG}	0.11
P(44)	C_{PVN}	8.4
P(45)	V_{UPV}	460.0
P(46)	K_6	20.0
P(47)	R_{PVLA}	0.007
P(48)	K_7	0.1
P(49)	a_{LAS}	0.28
P(50)	a_{LAD}	0.12
P(51)	V_{ULA}	30.0
P(52)	R_{LALV}	0.003
P(53)	a_{LVS}	1.5
P(54)	a_{LVD}	0.067
P(55)	V_{ULV}	0.0
P(56)	R_{LVAO1}	0.003
P(57)	A_{AO1}	1.539 cm^2

Numerical constants (continued)

Constant in Computer Programme	Constant in Mathematical Model	Value
P(58)	L_{LV}	0.00022
P(59)	C_{AO1}	0.28
P(60)	V_{UAO1}	53.0
P(61)	K_8	0.04
P(62)	R_{COR}	12.0
P(63)	R_{AO2}	3.10×10^{-5}
P(64)	L_{AO2}	0.00043
P(65)	C_{AO2}	0.29
P(66)	V_{UAO2}	61.0
P(67)	R_{UA}	0.047
P(68)	L_{UA}	0.014
P(69)	R_{AO3}	0.0009
P(70)	L_{AO3}	0.0038
P(71)	G_{AO2UA}	COMPUTED
P(72)	G_{AO2AO3}	COMPUTED
P(73)	C_{UA}	0.33
P(74)	V_{UUA}	114.0
P(75)	R_{HEAD}	6.0
P(76)	C_{UVN}	9.4
P(77)	V_{UUVN}	552.0
P(78)	G_{UVSVC}	COMPUTED
P(79)	R_{UV}	0.226
P(80)	K_9	0.667
P(81)	C_{AO3}	0.29
P(82)	V_{UAO3}	59.0
P(83)	G_{AO3RA}	COMPUTED
P(84)	R_{BRONC}	12.0
P(85)	R_{IA}	0.0014
P(86)	L_{IA}	0.0027

Numerical constants (continued)

Constant in Computer Programme	Constant in Mathematical Model	Value
P(87)	G_{AO3IA}	COMPUTED
P(88)	R_{AA}	0.012
P(89)	L_{AA}	0.014
P(90)	G_{AO3AA}	COMPUTED
P(91)	C_{IA}	0.06
P(92)	V_{UIA}	17.0
P(93)	R_{INT}	2.3
P(94)	C_{IVN}	10.6
P(95)	V_{UIVN}	607.0
P(96)	G_{IVCIV}	COMPUTED
P(97)	R_{IV}	0.166
P(98)	K_{10}	1.0
P(99)	C_{AA}	0.21
P(100)	V_{UAA}	58.0
P(101)	R_{ABD}	57.0
P(102)	R_{CA}	0.18
P(103)	L_{CA}	0.031
P(104)	G_{AACA}	COMPUTED
P(105)	C_{AVN}	5.1
P(106)	V_{UAVN}	305.0
P(107)	G_{IVCAV}	COMPUTED
P(108)	R_{AV}	0.595
P(109)	K_{11}	1.0
P(110)	C_{CA}	0.12
P(111)	V_{UCA}	63.0
P(112)	R_{LEG}	15.0
P(113)	C_{CVN}	4.8
P(114)	V_{UCVN}	257.0
P(115)	G_{AVCV}	COMPUTED
P(116)	R_{CV}	0.3

Numerical constants (continued)

Constant in Computer Programme	Constant in Mathematical Model	Value
P(117)	K_{12}	0.0
P(118)	C_{IVCN}	8.3
P(119)	V_{UIVC}	488.0
P(120)	G_{IVCRA}	COMPUTED
P(121)	R_{IVC}	0.015
P(122)	$C_{IVCN}K_6$	COMPUTED
P(123)	C_{SVCN}	8.3
P(124)	V_{USVC}	488.0
P(125)	G_{SVCRA}	COMPUTED
P(126)	R_{SVC}	0.06
P(127)	$R_{IVC}V^2_{UIVC}$	COMPUTED
P(128)	τ_1	0.8
P(129)	τ_2	0.1
P(130)	K_{13}	1.0
P(131)	K_{14}	1.0
P(132)	K_{15}	40.0
P(133)	K_{16}	0.7
P(134)	$R_{UV}V^2_{UUVN}$	COMPUTED
P(135)	$C_{IVN}K_6$	COMPUTED
P(136)	K_{17}	1.0
P(137)	K_{18}	80.0
P(138)	$R_{IV}V^2_{UIVN}$	COMPUTED
P(139)	K_{19}	1.5
P(140)	K_{20}	4.5
P(141)	τ_3	1.0
P(142)	τ_4	2.0
P(143)	K_{21}	0.006
P(144)	$T_H(C)$	0.8264

Numerical constants (continued)

Constant in Computer Programme	Constant in Mathematical Model	Value
P(145)	K_{22}	0.1
P(146)	K_{23}	0.09
P(147)	K_{24}	0.04
P(148)	K_{25}	0.16
P(149)	K_{26}	0.2
P(150)	K_{27}	0.6
P(151)	K_{28}	1.4
P(152)	τ_5	4.0
P(153)	τ_6	20.0
P(154)	K_{29}	0.75
P(155)	T_{HN}	0.8
P(156)	K_{30}	0.7
P(157)	K_{31}	1.6
P(158)	τ_7	14.0
P(159)	K_{32}	1.0
P(160)	K_{33}	1.0
P(161)	K_{34}	0.6
P(162)	K_{35}	1.4
P(163)	τ_8	10.0
P(164)	$C_{AVN}K_6$	COMPUTED
P(165)	h	0.0005
P(166)	$R_{AV}V^2_{UAVN}$	COMPUTED
P(167)	$C_{CVN}K_6$	COMPUTED
P(168)	$R_{CV}V^2_{UCVN}$	COMPUTED
P(169)	τ_9	30.0
P(170)	$\rho/(2A^2_{PA})$	COMPUTED
P(171)	$\rho/(2A^2_{AOI})$	COMPUTED

Numerical constants (continued)

Constant in Computer Programme	Constant in Mathematical Model	Value
P(172)	π/T_{IE}	COMPUTED
P(173)	$K_2 - K_1$	COMPUTED
P(174)	M	70.0 µg
P(175)	σ_1	400.0 mℓ μg^{-1}
P(176)	σ_2	50.0 mℓ μg^{-1}
P(177)	σ_3	50.0 mℓ μg^{-1}
P(178)	$K_4 - K_3$	COMPUTED
PI	π	3.14159
ØRIF	$\rho/2$	0.0003978
RHØG	ρg	0.7807
DEGRAD	$\pi/180$	0.01745
NS	SIZE OF X-VECTOR	61
NP	SIZE OF P-VECTOR	178
NV	SIZE OF V-VECTOR	112
INJLØC	INJECTION LOCATION	52

Logical Variables

Logical variables are used to control the simulation.

'TRUE' is equivalent to 'ON' and 'FALSE' is equivalent to 'OFF'.

Logical variable in computer programme	Initial value	Comments
L(1)	TRUE	'ON' at t = 0; 'OFF' for t > 0
L(2)	FALSE	'ON' at the end of each cardiac cycle
L(3)	FALSE	Drug injection
L(4)	FALSE	Respiration
L(5)	FALSE	Orthostasis
L(6)	TRUE	Heart rate control
L(7)	TRUE	Peripheral resistance control
L(8)	TRUE	Venous tone control
L(9)	TRUE	Myocardial contractility control
L(10)	TRUE	'ON' = Tachycardia; 'OFF' = Bradycardia
L(11)	TRUE	'ON' = Vasoconstriction 'OFF' = Vasodilatation
L(12)	TRUE	'ON' = Positive inotropy 'OFF' = Negative inotropy
L(13)	FALSE	Drug transport
L(14)	FALSE	Drug action

APPENDIX IV

THE COMPLETE 8-SEGMENT MATHEMATICAL MODEL

A.IV.1 The Circulatory Fluid Mechanics Model

Right ventricle

$$\frac{dV_{RV}}{dt} = F_{TVRV} - F_{RVPA} \quad , \quad V_{RV} \geq 0 \tag{AIV.1}$$

$$\frac{dF_{RVPA}}{dt} = \frac{P_{RV} - P_{PA} - R_{RVPA} F_{RVPA} - \left(\frac{\rho}{2A^2_{PA}}\right) F^2_{RVPV}}{L_{RV}} \quad , \quad F_{RVPA} \geq 0 \tag{AIV.2}$$

$$P_{RV} = a_{RV}\left(V_{RV} - V_{URV}\right) \tag{AIV.3}$$

Pulmonary arteries

$$\frac{dV_{PA}}{dt} = F_{RVPA} - F_{PAPV} \quad , \quad V_{PA} \geq 0 \tag{AIV.4}$$

$$P_{PA} = \frac{V_{PA} - V_{UPA}}{C_{PA}} \tag{AIV.5}$$

$$F_{PAPV} = \begin{cases} \dfrac{P_{PA} - P_{PV}}{R_{LUNG}} & , \quad P_{PV} > P_{CC} \\ \dfrac{P_{PA} - P_{CC}}{R_{LUNG}} & , \quad P_{PV} \leq P_{CC} \end{cases} \tag{AIV.6}$$

Pulmonary veins

$$\frac{dV_{PV}}{dt} = F_{PAPV} - F_{PVLV} \quad , \quad V_{PV} \geq 0 \tag{AIV.7}$$

$$P_{PV} = \frac{V_{PV} - V_{UPV}}{C_{PV}} \tag{AIV.8}$$

$$C_{PV} = \begin{cases} C_{PVN} & , \quad V_{PV} > V_{UPV} \\ 20\ C_{PVN} & , \quad V_{PV} \leq V_{UPV} \end{cases} \tag{AIV.9}$$

$$F_1 = \frac{(P_{PV} - P_{LV}) V^2_{PV}}{R_{PVLV} V^2_{UPV}} \qquad \text{(AIV.10)}$$

$$F_{PVLV} \begin{cases} F_1 , & F_1 > 0 \\ 0 , & F_1 \leq 0 \end{cases} \qquad \text{(AIV.11)}$$

Left ventricle

$$\frac{dV_{LV}}{dt} = F_{PVLV} - F_{LVAO} , \quad V_{LV} \geq 0 \qquad \text{(AIV.12)}$$

$$\frac{dF_{LVAO}}{dt} = \frac{P_{LV} - P_{AO} - R_{LVAO} F_{LVAO} - \left(\frac{\rho}{2A^2_{AO}}\right) F^2_{LVAO}}{L_{LV}} , \quad F_{LVAO} \geq 0 \qquad \text{(AIV.13)}$$

$$P_{LV} = a_{LV}(V_{LV} - V_{ULV}) \qquad \text{(AIV.14)}$$

Aorta

$$\frac{dV_{AO}}{dt} = F_{LVAO} - F_{AOSA} , \quad V_{AO} \geq 0 \qquad \text{(AIV.15)}$$

$$\frac{dF_{AOSA}}{dt} = \frac{P_{AO} - P_{SA} - R_{SA} F_{AOSA}}{L_{SA}} \qquad \text{(AIV.16)}$$

$$P_{AO} = \frac{V_{AO} - V_{UAO} + 0.04 (F_{LVAO} - F_{AOSA})}{C_{AO}} \qquad \text{(AIV.17)}$$

Systemic arteries

$$\frac{dV_{SA}}{dt} = F_{AOSA} - F_{SASV} , \quad V_{SA} \geq 0 \qquad \text{(AIV.18)}$$

$$P_{SA} = \frac{V_{SA} - V_{USA} + 0.04 \left(F_{AOSA} + \frac{P_{SV}}{R_{sys} q_4}\right)}{C_{SA} + \frac{0.04}{R_{sys} q_4}} \qquad \text{(AIV.19)}$$

$$F_{SASV} = \frac{P_{SA} - P_{SV}}{R_{sys}\, q_4} \qquad \text{(AIV.20)}$$

Systemic veins

$$\frac{dV_{SV}}{dt} = F_{SASV} - F_{SVTV} \quad , \quad V_{SV} \geq 0 \qquad \text{(AIV.21)}$$

$$P_{SV} = \frac{d_3}{C_{SV}} \left(V_{SV} - V_{USV}\right) \qquad \text{(AIV.22)}$$

$$C_{SV} = \begin{cases} C_{SVN} & , \quad V_{SV} > V_{USV} \\ 20\, C_{SVN} & , \quad V_{SV} \leq V_{USV} \end{cases} \qquad \text{(AIV.23)}$$

$$V_{USV} = \frac{V_{USVN}}{d_4} \qquad \text{(AIV.24)}$$

$$F_2 = \frac{\left(P_{SV} - P_{TV}\right) V^2_{SV}}{R_{SV}\, V^2_{USVN}} \qquad \text{(AIV.25)}$$

$$F_{SVTV} = \begin{cases} F_2 & , \quad F_2 > 0 \\ 0.667\, F_2 & , \quad F_2 \leq 0 \end{cases} \qquad \text{(AIV.26)}$$

Thoracic veins

$$\frac{dV_{TV}}{dt} = F_{SVTV} - F_{TVRV} \quad , \quad V_{TV} \geq 0 \qquad \text{(AIV.27)}$$

$$P_{TV} = \frac{1}{C_{TV}} \left(V_{TV} - V_{UTV}\right) \qquad \text{(AIV.28)}$$

$$C_{TV} = \begin{cases} C_{TVN} & , \quad V_{TV} > V_{UTV} \\ 20\, C_{TVN} & , \quad V_{TV} \leq V_{UTV} \end{cases} \qquad \text{(AIV.29)}$$

$$F_3 = \frac{(P_{TV} - P_{RV}) V^2_{TV}}{R_{TVRV} V^2_{UTV}} \qquad \text{(AIV.30)}$$

$$F_{TVRV} = \begin{cases} F_3 & , \quad F_3 > 0 \\ 0 & , \quad F_3 \leq 0 \end{cases} \qquad \text{(AIV.31)}$$

Time-varying compliances of ventricles

$$\frac{dU_{1O}}{dt} = 1.0 \quad (U_{1O} \text{ set to zero at end of cardiac cycle} \qquad \text{(AIV.32)}$$

$$T_{AS} = K_{22} + K_{23} T_H \qquad \text{(AIV.33)}$$

$$T_{AV} = T_{AS} - K_{24} \qquad \text{(AIV.34)}$$

$$T_{VS} = K_{25} + K_{26} T_H \qquad \text{(AIV.35)}$$

$$X_1 = \frac{\pi}{T_{AS}} \qquad \text{(AIV.36)}$$

$$X_2 = \begin{cases} U_{1O} - T_{AV} & , \quad U_{1O} > T_{AV} \\ 0 & , \quad U_{1O} \leq T_{AV} \end{cases} \qquad \text{(AIV.37)}$$

$$X_3 = \begin{cases} 0 & , \quad X_2 > T_{VS} \\ \text{Sin}\,(X_1 X_2) & , \quad X_2 \leq T_{VS} \end{cases} \qquad \text{(AIV.38)}$$

$$a_{RV} = X_3 \left[b_2 (\sigma_{RV}\, a_{RVS}) - a_{RVD} \right] + a_{RVD} \qquad \text{(AIV.39)}$$

$$a_{LV} = X_3 \left[b_2 (\sigma_{LV}\, a_{LVS}) - a_{LVD} \right] + a_{LVD} \qquad \text{(AIV.40)}$$

Calculation of the output variables

$$MAP = \frac{1}{T_H} \int_{t_1}^{t_1+T_H} P_{AO}\, dt \quad (t_1 = \text{start of a cardiac cycle}) \tag{AIV.41}$$

$$SV = \int_{t_1}^{t_1+T_H} F_{LVAO}\, dt \tag{AIV.42}$$

$$CO = \frac{SV}{T_H} \tag{AIV.43}$$

$$ETSR = \frac{MAP}{CO} \tag{AIV.44}$$

$$SBF = \frac{MAP}{STPR.q_4} \tag{AIV.45}$$

$$MSP = (0.0035\ BV) - 10.5 \tag{AIV.46}$$

$$EF = \frac{SV}{EDV} \tag{AIV.47}$$

A.IV.2 The Neural Control Model

Aortic arch baroreceptors

$$\frac{dS_3}{dt} = \frac{P_{AO} - S_3}{\tau_1} \tag{AIV.48}$$

$$\frac{dS_4}{dt} = \frac{S_2 - S_4}{\tau_2} \tag{AIV.49}$$

$$S_1 = \frac{dP_{AO}}{dt} \tag{AIV.50}$$

$$S_2 = \begin{cases} S_1 , & S_1 > 0 \\ 0 , & S_1 \leq 0 \end{cases} \tag{AIV.51}$$

$$S_5 = K_{13}\left(S_3 + K_{14}S_4 - K_{15}\right) \tag{AIV.52}$$

$$B = \begin{cases} S_5 , & S_5 > 0 \\ 0 , & S_5 \leq 0 \end{cases} \qquad \text{(AIV.53)}$$

Stretch receptors

$$\frac{dq_v}{dt} = \frac{SV - q_v}{20} \qquad \text{(AIV.54)}$$

$$SV = \frac{1.0}{\left(1.0 + 2.0\left(\left(\frac{BV}{BV0}\right) - 1.0\right)\right)} \qquad \text{(AIV.55)}$$

C.N.S. control of heart rate

$$\frac{dU_4}{dt} = \frac{U_1 - U_4}{U_3} \qquad \text{(AIV.56)}$$

$$\frac{dU_6}{dt} = \frac{U_5 - U_6}{\tau_3} \qquad \text{(AIV.57)}$$

$$\frac{dU_7}{dt} = \frac{U_6 - U_7}{\tau_4} \qquad \text{(AIV.58)}$$

$$U_1 = \begin{cases} K_{17}\left(B - K_{18}\right) , & B > K_{18} \\ 0 , & B \leq K_{18} \end{cases} \qquad \text{(AIV.59)}$$

$$U_2 = \frac{dU_1}{dt} \qquad \text{(AIV.60)}$$

$$U_3 = \begin{cases} K_{19} , & U_2 > 0 \\ K_{20} , & U_2 \leq 0 \end{cases} \qquad \text{(AIV.61)}$$

$$U_5 = \begin{cases} K_{18} , & B > K_{18} \\ B , & B \leq K_{18} \end{cases} \qquad \text{(AIV.62)}$$

$$U_8 = K_{21}\sigma_H\left(U_4 + U_7\right) \qquad \text{(AIV.63)}$$

$$U_9 = \begin{cases} 2.0 & , \quad U_8 \geq 2.0 \\ U_8 & , \quad 0.3 < U_8 < 2.0 \\ 0.3 & , \quad U_8 \leq 0.3 \end{cases} \tag{AIV.64}$$

T_H is set to the value of U_9 at the end of the cardiac cycle.

C.N.S. control of peripheral resistance

$$\frac{dq_2}{dt} = \frac{q_1 - q_2}{\tau_5} \tag{AIV.65}$$

$$\frac{dq_3}{dt} = \frac{q_1 - q_3}{\tau_6} \tag{AIV.66}$$

$$q_p = K_{29}\, q_3 + \left(1 - K_{29}\right) q_2 \tag{AIV.67}$$

$$q_4 = q_p\, q_v \tag{AIV.68}$$

$$q_1 = \frac{1.0}{\left(1.0 + 0.5\left(\left(\frac{B}{BN} - 1.0\right)\right)\right)} \tag{AIV.69}$$

C.N.S. control of myocardial contractility

$$\frac{db_2}{dt} = \frac{b_1 - b_2}{\tau_8} \tag{AIV.70}$$

$$b_1 = \begin{cases} K_{34} & , \quad B > K_{18} \\ K_{37} & , \quad B \leq K_{18} \end{cases} \tag{AIV.71}$$

C.N.S. control of venous tone

$$\frac{dd_2}{dt} = \frac{d_1 - d_2}{\tau_7} \tag{AIV.72}$$

$$d_1 = \begin{cases} K_{30} & , \quad B > K_{18} \\ K_{31} & , \quad B \leq K_{18} \end{cases} \tag{AIV.73}$$

$$d_3 = \left(1 + K_{32}\left(d_2 - 1\right)\right)q_v \qquad \text{(AIV.74)}$$

$$d_4 = \left(1 + K_{33}\left(d_2 - 1\right)\right)q_v \qquad \text{(AIV.75)}$$

A.IV.3 The Thermoregulatory System Model

$$C_c \frac{dT_c}{dt} = BMR - K_{cs}\left(T_c - T_s\right) - \rho_c \times SBF\left(T_c - T_s\right) \qquad \text{(AIV.76)}$$

$$C_s \frac{dT_s}{dt} = K_{cs}\left(T_c - T_s\right) + \rho_c \times SBF\left(T_c - T_s\right) - K_{sE}\left(T_s - T_E\right) - IHL \qquad \text{(AIV.77)}$$

The thermoregulatory system controller

$$\left.\begin{array}{lll} STPR = 5650.0 & , & T_c < 35.0 \\ STPR = 3632.134\ T_c + 132775.0 & , & 35.0 \leq T_c < 36.4 \\ STPR = -322.773\ T_c + 12507.6 & , & 37.0 \leq T_c < 38.5 \\ STPR = 80.841 & , & T_c > 38.5 \\ STPR = 24.39\ T_s - 266.7 & , & T_s \leq 34.1 \\ STPR = 46.55\ T_s - 1022.41 & , & T_s > 34.1 \end{array}\right\} \qquad \text{(AIV.78)}$$

$$R_{sys} = \frac{R_c R_s}{R_c + R_s} \qquad \text{(AIV.79)}$$

Body fluid balance model

For each minute K = 1, 2, ..., where K is time.

$$V_{INT}(K + 1) = V_{INT}(K) + \left(E_i(K) - E_o(K)\right)\frac{V_{INT}(K)}{E(K)} \qquad \text{(AIV.80)}$$

$$BV(K + 1) = BV(K) + \left(E_i(K) - E_o(K)\right)\frac{BV(K)}{E(K)} \qquad \text{(AIV.81)}$$

$$E(K + 1) = V_{INT}(K + 1) + BV(K + 1) \qquad \text{(AIV.82)}$$

APPENDIX V

STRUCTURE OF THE DIGITAL SIMULATION PROGRAM

The complete 8-segment model is listed in Appendix IV. The model is run on a PRIME 550 computer, the compiled program requiring approximately (256 Kb) of main memory.

Arrays in the circulatory model are used rather than separate variable names to make the program listing more compact. The principal arrays are:

X(23) - state variables
D(23) - derivatives of state variables
V(53) - other numerical variables
P(79) - numerical constants
L(14) - logical variables (for control of the simulation).

The arrays V, P and L are placed in labelled common blocks to reduce the storage requirements, together with the thermoregulator system and body fluid variables.

The program consists of a main executive control segment together with 12 sub-programs. Details of these are given in the following sub-sections. Its design includes 3 main sub-routines for the cardiovascular, thermoregulatory and body fluid systems.

A.V.1 Executive Control Segment

This is the master segment which controls the execution of the simulation program. In the version listed in Appendix VI the values of selected variables are calculated at the end of each cardiac cycle. The other variables from the thermoregulatory and body fluid balance system are then printed at the end of each minute. The program is designed to start in a steady state with all neural controllers "switched on", but with the pharmacokinetics section "switched off" (it is not included in this 8-segment model). Any changes relating to the simulation period are introduced here. All these operations are illustrated in the flow diagram of Figure A.V.1.

A.V.2 Subroutine CVS (T, TMIN)

This subroutine controls the execution of the cardiovascular simulation program, calculating the selected variables at the end of each cardiac cycle.

A.V.3 Subroutine INTEG (D, T)

This subroutine performs one step of Euler's integration method when called by the executive control segment. The current state vector is replaced by the value of the state vector at the next integration step. The derivatives are obtained by a call of the subroutine MODEL. The volume controller vector, q_v, is replaced by its value at the next integration step, subject to its upper bound not being exceeded.

A.V.4 Subroutine MODEL (D)

This subroutine computes the derivatives of the state variables in (D) from the current state vector (X) and time (T), using the equations of the mathematical model. It is called by INTEG at each step and also once at t = 0 by the subroutine CVS.

A.V.5 Subroutine CYCLE (D)

This subroutine tests for the end of the cardiac cycle and, when detected, computes and records the systolic pressure, diastolic pressure and stroke volume during the cycle, computes the mean arterial pressure, cardiac output and estimated total systemic resistance, and sets the heart period to the value for the next cycle.

A.V.6 Subroutine PRELIM

This is used to compute some initial numerical constants required in the model. ORIF is the value of the subject's blood density.

A.V.7 Subroutine THERMO

This is the second main subroutine segment dealing with the simulation of the thermoregulatory system and, in particular, defining the

core and surface temperatures.

A.V.8 Subroutine TINTEG (TX)

This subroutine performs one step of Euler's integration method when called by the subroutine THERMO. The current state vector TX(J) is replaced by the value of this state vector at the next integration step. The derivatives are obtained by calling the subroutine TMODEL.

A.V.9 Subroutine TMODEL (DT, TX)

This subroutine computes the derivatives of the state variables in (DT) from the current state vector (TX) using the equations of the Thermoregulator model.

A.V.10 Subroutine CONTROL

This subroutine calculates the systemic total peripheral resistance. It is called once per minute from the Executive Control Segment.

A.V.11 Subroutine BFLUID (TMIN)

This is the third main subroutine segment, dealing with the body fluid balance system simulation. It calculates the blood volume and mean systemic pressure and is called once per minute from the Executive Control Segment.

A.V.12 Subroutine RESULT (TMIN)

At TMIN = 0, this subroutine prints a heading for the table of results. Thereafter values of the selected variables are printed whenever the subroutine is called by the Executive Control Segment. The variables to be printed are: TMIN, MAP, SV, CO, FH, ETSR, $(P_{AO1})MAX$, $(P_{AO1})MIN$, SBF, STPR, TC, TS, BV, MSP, E, EIN, EOUT, EF, QV and QDP.

A.V.13 BLOCK DATA

This subprogram is used by the compiler to initialise all the arrays and variables in Labelled Common blocks.

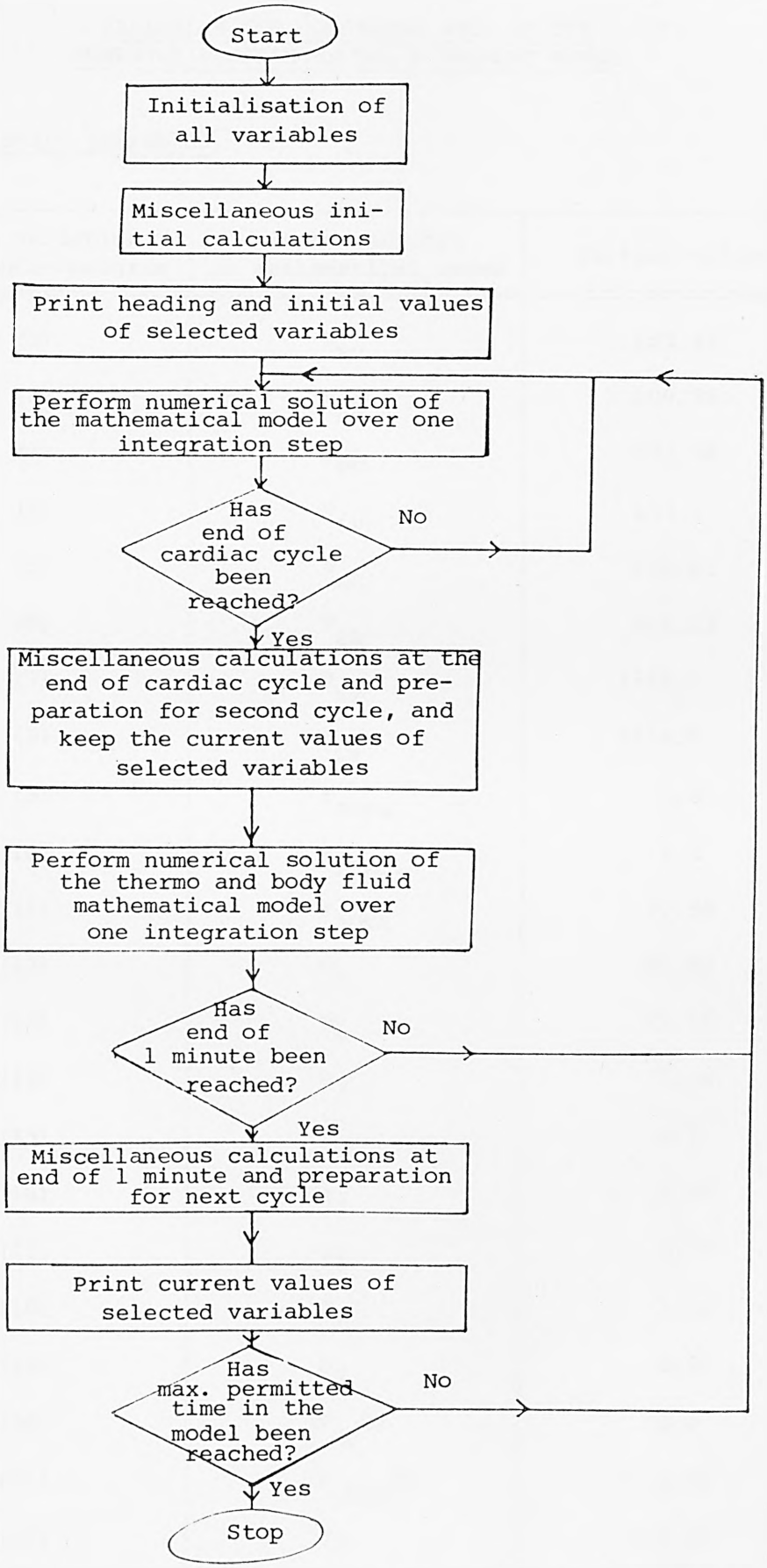

Figure AV.1 General flow diagram for this simulation program.

APPENDIX VI

VARIABLES AND CONSTANTS USED IN THE COMPUTER PROGRAM FOR THE 8-SEGMENT MODEL

A.VI.1 State Variables

State variable in computer program	State variable in mathematical model	Initial value
X (1)	V_{RV}	153.45
X (2)	V_{PA}	109.95
X (3)	V_{PV}	637.48
X (4)	V_{LV}	153.0
X (5)	V_{AO}	212.61
X (6)	V_{SA}	554.23
X (7)	V_{SV}	1345.0
X (8)	V_{TV}	1544.0
X (9)	F_{RVPA}	1.0
X(10)	F_{LVAO}	1.0
X(11)	F_{AOSA}	22.59
X(12)	U_4	63.64
X(13)	U_6	77.16
X(14)	U_7	77.04
X(15)	U_{10}	0.0
X(16)	q_2	0.97
X(17)	q_3	0.97
X(18)	d_2	1.12
X(19)	b_2	0.97
X(20)	$\int P_{AO} dt$	0.0
X(21)	$\int F_{LVAO} dt$	0.0
X(22)	S_3	112.03
X(23)	S_4	0.71

A.VI.2 Numerical Variables

Variable in computer model	Variable in mathematical model	Variable in computer model	Variable in mathematical model
V (1)	F_{TVRV}	V(28)	S_5
V (2)	P_{RV}	V(29)	B
V (3)	a_{RV}	V(30)	dB/dt
V (4)	P_{PA}	V(31)	U_1
V (5)	F_{PAPV}	V(32)	U_2
V (6)	P_{PV}	V(33)	U_3
V (7)	F_1	V(34)	U_5
V (8)	F_{PVLV}	V(35)	U_8
V (9)	P_{LV}	V(36)	U_9
V(10)	a_{LV}	V(37)	q_1
V(11)	P_{AO}	V(38)	q_4
V(12)	P_{SA}	V(39)	b_1
V(13)	F_{SASV}	V(40)	d_1
V(14)	P_{SV}	V(41)	d_3
V(15)	F_2	V(42)	d_4
V(16)	F_{SVTV}	V(43)	(MAP)
V(17)	P_{TV}	V(44)	(CO)
V(18)	F_3	V(45)	(ETSR)
V(19)	T_H	V(46)	(SV)
V(20)	T_{AS}	V(47)	PMAX
V(21)	T_{AV}	V(48)	PMIN
V(22)	T_{VS}	V(49)	f_H
V(23)	X_1	V(50)	U_4
V(24)	X_2	V(51)	U_7
V(25)	X_3	V(52)	S_3
V(26)	S_1	V(53)	S_4
V(27)	S_2		

A.VI.3 Numerical Constants

Constant in computer program	Constant in mathematical model	Value
P (1)	$20.0\ C_{PVN}$	Computed
P (2)	$R_{PVLV}\ V^2_{UPV}$	Computed
P (3)	$R_{TVRV}\ V^2_{UTV}$	Computed
P (4)	$20.0\ C_{SVN}$	Computed
P (5)	$R_{SV}\ V^2_{USVN}$	Computed
P (6)	$20.0\ C_{TVN}$	Computed
P (7)	$\rho/2A^2_{PA}$	Computed
P (8)	$\rho/2A^2_{AO}$	Computed
P (9)	R_{RVPA}	0.003
P(10)	L_{RV}	0.00018
P(11)	V_{URV}	0.0
P(12)	V_{UPA}	50.0
P(13)	C_{PA}	4.730
P(14)	R_{LUNG}	0.11
P(15)	V_{UPV}	430.0
P(16)	C_{PVN}	25.0
P(17)	R_{PVLV}	0.003
P(18)	P_{PC}	7.0
P(19)	R_{LVAO}	0.003
P(20)	L_{LV}	0.00022
P(21)	V_{ULV}	0.0
P(22)	V_{UAO}	140.0
P(23)	C_{AO}	0.77
P(24)	R_{SA}	0.06
P(25)	L_{SA}	0.00075
P(26)	V_{USA}	370.0
P(27)	C_{SA}	1.98
P(28)	R_{SYS}	1.0
P(29)	C_{SVN}	59.0
P(30)	V_{USVN}	1000.0
P(31)	R_{SV}	0.09

Constant in computer program	Constant in mathematical model	Value
P(32)	V_{UTV}	1300.0
P(33)	C_{TVN}	59.0
P(34)	R_{TVRV}	0.003
P(35)		20.0
P(36)	K_9	0.667
P(37)	K_8	0.04
P(38)	h	0.001
P(39)	A_{PA}	5.0
P(40)	A_{AO}	5.0
P(41)	K_{22}	0.1
P(42)	K_{23}	0.09
P(43)	K_{24}	0.04
P(44)	K_{25}	0.16
P(45)	K_{26}	0.2
P(46)	$T_H(O)$	0.8264
P(47)		0.8
P(48)		0.0
P(49)		0.0
P(50)	σ_{LV} a_{LVS}	1.5
P(51)	a_{LVD}	0.053
P(52)	σ_{RV} a_{RVS}	0.3
P(53)	a_{RVD}	0.027
P(54)	τ_1	0.8
P(55)	τ_2	0.1
P(56)	K_{13}	1.0
P(57)	K_{14}	1.1
P(58)	K_{15}	40.0
P(59)	τ_3	1.0
P(60)	τ_4	2.0
P(61)	K_{17}	1.0
P(62)	K_{18}	80.0
P(63)	K_{19}	1.5
P(64)	K_{20}	4.5
P(65)	K_{21} σ_H	0.006
P(66)		0.0
P(67)	τ_5	2.0

Constant in computer program	Constant in mathematical model	Value
P(68)	τ_6	10.0
P(69)	K_{29}	0.75
P(70)	K_{27}	0.6
P(71)	K_{28}	1.4
P(72)	τ_8	10.0
P(73)	K_{34}	0.6
P(74)	K_{35}	1.4
P(75)	τ_7	14.0
P(76)	K_{30}	0.7
P(77)	K_{31}	1.6
P(78)	K_{38}	1.0
P(79)	K_{33}	1.0
PI	π	3.14159
ϕRIF	$\rho/2$	0.0003978
NS	Size of X-Vector	23
NP	Size of P-Vector	81
NV	Size of V-Vector	57

A.VI.4 Logical Variables

Logical variables are used to control the simulation.

"TRUE" is equivalent to "ON" and "FALSE" is equivalent to "OFF".

Logical variable in computer program	Initial value	Comments
L (1)	TRUE	"ON" at t = 0; "OFF" for t > 0
L (2)	FALSE	"ON" at the end of each cardiac cycle
L (3)	FALSE	Drug injection
L (4)	FALSE	Respiration
L (5)	FALSE	Orthostasis
L (6)	TRUE	Heart rate control
L (7)	TRUE	Peripheral resistance control
L (8)	TRUE	Venous tone control
L (9)	TRUE	Myocardial contractility control
L(10)	TRUE	"ON" = Tachycardia; "OFF" = Bradycardia
L(11)	TRUE	"ON" = Vasoconstriction "OFF" = Vasodilation
L(12)	TRUE	"ON" = Positive inotropy "OFF" = Negative inotropy
L(13)	FALSE	Drug transport
L(14)	FALSE	Drug action

APPENDIX VII

COMPUTER PROGRAM FOR THE 19-SEGMENT MODEL

A.VII.1 Summary of the Program Structure

The program listed in Section A.VII.2 uses facilities available in most versions of FORTRAN IV to ensure portability. Free formats, mixed mode arithmetic and other features of extended FORTRAN IV are not used. In the program listing, the letter O is distinguished from the number O by placing a line through the letter thus: Ø.

The principal arrays in the program are:

(1) X(61) - vector of state variables
(2) D(61) - vector of derivatives of state variables
(3) V(112) - other numerical variables
(4) P(178) - numerical constants
(5) L(14) - logical variables (for control of the simulation)

The variables in the mathematical model corresponding to the program variables are given in Appendix VI.

Following the Executive Control Segment, the subprograms in order are:

(1) SUBROUTINE INTEG(D,X,T) - computes a new state vector after one integration step using Euler's method.
(2) SUBROUTINE MODEL(D,X,T) - computes the derivative of the current state vector from the mathematical model.
(3) SUBROUTINE ODDJOB(D,X,T) - performs miscellaneous tasks at t=O and once every cardiac cycle.
(4) SUBROUTINE CYCLE(D,X,T) - deals with respiration at each integration step, detects the end of the cardiac cycle and performs miscellaneous tasks at the end of the cardiac cycle.
(5) SUBROUTINE RESULT(D,X,T) - prints heading and results.
(6) SUBROUTINE PRELIM - preliminary calculation of frequently used constants.
(7) SUBROUTINE TTSR(X) - computes the true total systemic resistance.
(8) BLOCK DATA - initialises the arrays and variables in labelled COMMON blocks.

A.VII.2 The Program Listing

```
C
C   EXECUTIVE CØNTRØL SEGMENT
C
      LØGICAL L(14)
      DIMENSIØN X(61),D(61)
      CØMMØN /MISC/ NS,NP,NV,INJLØC,PMIN,PMAX
      CØMMØN /LØGIC/ L
      CØMMØN /PV/ P(178),V(112)
      CØMMØN /XIC/ XD(61)
C
C   SECØND PART ØF INITIALISATIØN (1ST PART IN BLØCK DATA SUBPRØGRAM)
C
      T=0.0
      DØ 1 I=1,NS
      D(I)=0.0
  1   X(I)=XD(I)
C
C-----------------------------------------------------------
C   ANY REQUIRED CHANGES IN STATE VARIABLES ØR NØN-CØMPUTED
C   CØNSTANTS BEFØRE THE RUN MAY BE INTRØDUCED AT THIS PØINT
C-----------------------------------------------------------
C
      CALL PRELIM
      CALL ØDDJØB(D,X,T)
      CALL MØDEL(D,X,T)
      CALL CYCLE(D,X,T)
      CALL RESULT(D,X,T)
C
C   DYNAMIC SECTIØN
C
      L(1)=.FALSE.
  2   CØNTINUE
      CALL INTEG(D,X,T)
      CALL CYCLE(D,X,T)
      IF(.NØT.L(2))GØ TØ 2
      CALL ØDDJØB(D,X,T)
      CALL RESULT(D,X,T)
      IF(T.GT.100.0)STØP
      L(2)=.FALSE.
      GØ TØ 2
      END
```

```
      SUBRØUTINE INTEG(D,X,T)
C
C   CØMPUTES NEW STATE VECTØR AFTER ØNE INTEGRATIØN
C   STEP USING EULER'S METHØD
C
      DIMENSIØN X(61),D(61)
      CØMMØN /PV/ P(178),V(112)
      CØMMØN /MISC/ NS,NP,NV,INJLØC,PMIN,PMAX
      H=P(165)
      DØ 1 I=1,NS
      X(I)=X(I)+H*D(I)
  1   CØNTINUE
      CALL MØDEL(D,X,T)
      T=T+H
      RETURN
      END
```

```
      SUBRØUTINE MØDEL(D,X,T)
C
C   CØMPUTES THE DERIVATIVE ØF THE STATE VECTØR FRØM THE
C   MATHEMATICAL MØDEL ØF THE HUMAN CARDIØVASCULAR SYSTEM
C
      LØGICAL L(14)
      DIMENSIØN X(61),D(61)
      CØMMØN /PV/ P(178),V(112)
      CØMMØN /MISC/ NS,NP,NV,INJLØC,PMIN,PMAX
      CØMMØN /LØGIC/ L
      CØMMØN /SIGMA/ SRA,SRV,SLA,SLV,SHEAD,SBRØNC,SINT,SABD,SLEG,SHR
      DATA PI/3.1415926536/
C
C   DECIDE IF DRUG ACTIØN IS REQUIRED
C
      IF(.NØT.L(14))GØ TØ 5
C
C   DIMENSIØNLESS FACTØRS FØR DRUG ACTIØN
C
      SIG1=P(175)
      SIG3=P(177)
      URA=1.0+SIG3*V(92)
      URV=1.0+SIG3*V(93)
      ULA=1.0+SIG3*V(96)
      ULV=1.0+SIG3*V(97)
      UHEAD=1.0+SIG1*V(100)
      UBRØNC=1.0+SIG1*V(102)
      UINT=1.0+SIG1*V(103)
      UABD=1.0+SIG1*V(105)
      ULEG=1.0+SIG1*V(107)
      UHR=1.0+P(176)*V(92)
      IF(.NØT.L(12))GØ TØ 1
C
C   PØSITIVE INØTRØPY
C
      SRA=URA
      SRV=URV
      SLA=ULA
      SLV=ULV
      GØ TØ 2
C
C   NEGATIVE INØTRØPY
C
1     SRA=1.0/URA
      SRV=1.0/URV
      SLA=1.0/ULA
      SLV=1.0/ULV
2     IF(.NØT.L(11))GØ TØ 3
C
C   VASØCØNSTRICTIØN
C
      SHEAD=UHEAD
      SBRØNC=UBRØNC
      SINT=UINT
      SABD=UABD
      SLEG=ULEG
      GØ TØ 4
C
C   VASØDILATATIØN
C
```

```
   3    SHEAD=1.0/UHEAD
        SBRØNC=1.0/UBRØNC
        SINT=1.0/UINT
        SABD=1.0/UABD
        SLEG=1.0/ULEG
C
C   BRADYCARDIA
C
   4    SHR=UHR
C
C   TACHYCARDIA
C
        IF(L(10))SHR=1.0/UHR
   5    CØNTINUE
C
C   SET INITIAL VALUE ØF HEART PERIØD
C
        IF(L(1))V(66)=P(144)
C
C   SET FIXED HEART PERIØD IF HEART RATE CØNTRØL ØFF
C
        IF(.NØT.L(6))V(66)=P(155)
C
C   TIME-VARYING CØMPLIANCE GENERATIØN
C
        V(68)=P(145)+P(146)*V(66)
        V(69)=V(68)-P(147)
        V(70)=P(148)+P(149)*V(66)
        V(71)=PI/V(68)
        V(72)=PI/V(70)
        V(73)=0.0
        IF(X(36).LE.V(68))V(73)=SIN(V(71)*X(36))
        V(74)=0.0
        IF(X(36).GT.V(69))V(74)=X(36)-V(69)
        V(75)=0.0
        IF(V(74).LE.V(70))V(75)=SIN(V(72)*V(74))
        V(2)=V(73)*(P(29)*X(40)*SRA-P(30))+P(30)
        V(8)=V(75)*(P(34)*X(40)*SRV-P(35))+P(35)
        V(15)=V(73)*(P(49)*X(40)*SLA-P(50))+P(50)
        V(19)=V(75)*(P(53)*X(40)*SLV-P(54))+P(54)
C
C   START ØF CIRCULATØRY FLUID MECHANICS AND NEURAL CØNTRØL MØDELS
C
        V(53)=P(130)*(X(29)+P(131)*X(30)-P(132))
        V(64)=P(143)*(X(33)+X(35))*SHR
        V(77)=P(154)*X(38)+(1.0-P(154))*X(37)
        IF(.NØT.L(7))V(77)=1.0
        V(79)=1.0+P(159)*(X(39)-1.0)
        V(80)=1.0+P(160)*(X(39)-1.0)
        V(1)=V(2)*(X(1)-P(31))
        V(7)=V(8)*(X(2)-P(36))
        V(5)=(V(1)-V(7))/P(32)
        V(6)=V(5)
        IF(V(5).LT.0.0)V(6)=0.0
        V(9)=(X(3)-P(41))/P(40)
        CPV=P(44)
        IF(X(4).LT.P(45))CPV=P(1)
        V(11)=(X(4)-P(45))/CPV
        V(10)=(V(9)-V(11))/P(43)
        IF(V(11).LT.P(42))V(10)=(V(9)-P(42))/P(43)
```

```
V(14)=V(15)*(X(5)-P(51))
V(12)=(V(11)-V(14))*X(4)*X(4)/P(2)
V(13)=V(12)
IF(V(12).LT.0.0)V(13)=V(12)*P(48)
V(18)=V(19)*(X(6)-P(55))
V(16)=(V(14)-V(18))/P(52)
V(17)=V(16)
IF(V(16).LT.0.0)V(17)=0.0
QA=X(7)-P(60)+P(61)*(X(21)-X(22)+V(1)/P(62))
V(20)=QA/P(3)
IF(V(20).GT.PMAX)PMAX=V(20)
IF(V(20).LT.PMIN)PMIN=V(20)
V(21)=(V(20)-V(1))/P(62)
QB=X(8)-P(66)+P(61)*(X(22)-X(23)-X(24))
V(22)=QB/P(65)
QC=X(10)-P(77)/V(80)
CUV=P(76)
IF(QC.LT.0.0)CUV=P(4)
V(25)=QC*V(79)/CUV
QHD=P(75)*SHEAD
QD=X(9)-P(74)+P(61)*(X(23)+V(25)/QHD)
DHD=P(73)+P(61)/QHD
V(23)=QD/DHD
V(24)=(V(23)-V(25))/QHD
QE=X(19)-P(124)
CSVC=P(123)
IF(QE.LT.0.0)CSVC=P(5)
V(48)=QE/CSVC
QF=(V(48)-V(1)+P(125))*X(19)*X(19)
V(49)=QF/P(6)
V(50)=V(49)
IF(V(49).LT.0.0)V(50)=V(49)*P(33)
QG=X(18)-P(119)
CIVC=P(118)
IF(QG.LT.0.0)CIVC=P(122)
V(45)=QG/CIVC
QH=(V(45)-V(1)-P(120))*X(18)*X(18)
V(46)=QH/P(127)
V(47)=V(46)
IF(V(46).LT.0.0)V(47)=V(46)*P(33)
QI=(V(25)-V(48)-V(89)+P(78))*X(10)*X(10)
V(26)=QI/P(134)
V(27)=V(26)
IF(V(26).LT.0.0)V(27)=V(26)*P(80)
QJ=V(77)*P(84)*SBRØNC
QK=X(11)-P(82)+P(61)*(X(24)-X(25)-X(26)+V(1)/QJ)
V(28)=QK/(P(81)+P(61)/QJ)
V(29)=(V(26)-V(1)-P(83))/QJ
QL=X(13)-P(95)/V(80)
CIV=P(94)
IF(QL.LT.0.0)CIV=P(135)
V(32)=QL*V(79)/CIV
QM=(V(32)-V(45)+V(90)-V(89)-P(96))*X(13)*X(13)
V(33)=QM/P(138)
V(34)=V(33)
IF(V(33).LT.0.0)V(34)=V(33)*P(98)
QN=V(77)*P(93)*SINT
QØ=X(12)-P(92)+P(61)*(X(25)+V(32)/QN)
V(30)=QØ/(P(91)+P(61)/QN)
```

```
      V(31)=(V(30)-V(32))/QN
      QP=X(15)-P(106)/V(80)
      CAV=P(105)
      IF(QP.LT.0.0)CAV=P(164)
      V(37)=QP*V(79)/CAV
      QQ=(V(37)-V(45)+V(90)-V(89)-P(107))*X(15)*X(15)
      V(38)=QQ/P(166)
      V(39)=V(38)
      IF(V(38).LT.0.0)V(39)=V(38)*P(109)
      QR=V(77)*P(101)*SABD
      QS=X(14)-P(100)+P(61)*(X(26)-X(27)+V(37)/QR)
      V(35)=QS/(P(99)+P(61)/QR)
      V(36)=(V(35)-V(37))/QR
      QT=X(17)-P(114)/V(80)
      CCV=P(113)
      IF(QT.LT.0.0)CCV=P(167)
      V(42)=QT*V(79)/CCV
      QU=(V(42)-V(37)-V(90)-P(115))*X(17)*X(17)
      V(43)=QU/P(168)
      V(44)=V(43)
      IF(V(43).LT.0.0)V(44)=V(43)*P(117)
      QV=V(77)*P(112)*SLEG
      QW=X(16)-P(111)+P(61)*(X(27)+V(42)/QV)
      V(40)=QW/(P(110)+P(61)/QV)
      V(41)=(V(40)-V(42))/QV
      V(4)=V(50)+V(47)+V(29)+V(21)
C
C     DECIDE IF DRUG TRANSPØRT IS REQUIRED
C
      IF(.NØT.L(13))GØ TØ 8
C
C     CØMPUTE DRUG CØNCENTRATIØNS IN EACH SEGMENT AND
C     SELECT CØNCENTRATIØNS APPRØPRIATE TØ DIRECTIØNS ØF FLØW
C
      DØ 6 I=1,19
      V(I+91)=X(I+42)/X(I)
    6 CØNTINUE
      GSVCRA=V(110)
      IF(V(50).LE.0.0)GSVCRA=V(92)
      GCØR=V(98)
      IF(V(21).LE.0.0)GCØR=V(92)
      GBRØNC=V(102)
      IF(V(29).LE.0.0)GBRØNC=V(92)
      GIVCRA=V(109)
      IF(V(47).LE.0.0)GIVCRA=V(92)
      GRARV=V(92)
      IF(V(6).LE.0.0)GRARV=V(93)
      GRVPA=V(93)
      IF(X(20).LE.0.0)GRVPA=V(94)
      GPAPV=V(94)
      IF(V(10).LE.0.0)GPAPV=V(95)
      GPVLA=V(95)
      IF(V(13).LE.0.0)GPVLA=V(96)
      GLALV=V(96)
      IF(V(17).LE.0.0)GLALV=V(97)
      GLVAØ1=V(97)
      IF(X(21).LE.0.0)GLVAØ1=V(98)
      GAØ12=V(98)
      IF(X(22).LE.0.0)GAØ12=V(99)
```

```
      GAØ2UA=V(99)
      IF(X(23).LE.0.0)GAØ2UA=V(100)
      GAØ23=V(99)
      IF(X(24).LE.0.0)GAØ23=V(102)
      GUAUV=V(100)
      IF(V(24).LE.0.0)GUAUV=V(101)
      GUVSVC=V(101)
      IF(V(27).LE.0.0)GUVSVC=V(110)
      GAØ3IA=V(102)
      IF(X(25).LE.0.0)GAØ3IA=V(103)
      GAØ3AA=V(102)
      IF(X(26).LE.0.0)GAØ3AA=V(105)
      GIAIV=V(103)
      IF(V(31).LE.0.0)GIAIV=V(104)
      GIVIVC=V(104)
      IF(V(34).LE.0.0)GIVIVC=V(109)
      GAAAV=V(105)
      IF(V(36).LE.0.0)GAAAV=V(106)
      GAACA=V(105)
      IF(X(27).LE.0.0)GAACA=V(107)
      GCVAV=V(108)
      IF(V(44).LE.0.0)GCVAV=V(106)
      GAVIVC=V(106)
      IF(V(39).LE.0.0)GAVIVC=V(109)
      GCACV=V(107)
      IF(V(41).LE.0.0)GCACV=V(108)
      HSVCRA=GSVCRA*V(50)
      HCØR=GCØR*V(21)
      HBRØNC=GBRØNC*V(29)
      HIVCRA=GIVCRA*V(47)
      HRARV=GRARV*V(6)
      HRVPA=GRVPA*X(20)
      HPAPV=GPAPV*V(10)
      HPVLA=GPVLA*V(13)
      HLALV=GLALV*V(17)
      HLVAØ1=GLVAØ1*X(21)
      HAØ12=GAØ12*X(22)
      HAØ2UA=GAØ2UA*X(23)
      HAØ23=GAØ23*X(24)
      HUAUV=GUAUV*V(24)
      HUVSVC=GUVSVC*V(27)
      HAØ3IA=GAØ3IA*X(25)
      HAØ3AA=GAØ3AA*X(26)
      HIAIV=GIAIV*V(31)
      HIVIVC=GIVIVC*V(34)
      HAAAV=GAAAV*V(36)
      HAACA=GAACA*X(27)
      HCVAV=GCVAV*V(44)
      HAVIVC=GAVIVC*V(39)
      HCACV=GCACV*V(41)
C
C     DRUG MASS DERIVATIVES IN PHARMACØKINETICS MØDEL
C
      D(43)=HSVCRA+HCØR+HBRØNC+HIVCRA-HRARV
      D(44)=HRARV-HRVPA
      D(45)=HRVPA-HPAPV
      D(46)=HPAPV-HPVLA
      D(47)=HPVLA-HLALV
      D(48)=HLALV-HLVAØ1
      D(49)=HLVAØ1-HAØ12-HCØR
```

```
      D(50)=HAØ12-HAØ2UA-HAØ23
      D(51)=HAØ2UA-HUAUV
      D(52)=HUAUV-HUVSVC
      D(53)=HAØ23-HBRØNC-HAØ3IA-HAØ3AA
      D(54)=HAØ3IA-HIAIV
      D(55)=HIAIV-HIVIVC
      D(56)=HAØ3AA-HAAAV-HAACA
      D(57)=HAAAV+HCVAV-HAVIVC
      D(58)=HAACA-HCACV
      D(59)=HCACV-HCVAV
      D(60)=HAVIVC+HIVIVC-HIVCRA
      D(61)=HUVSVC-HSVCRA
      DØ 7 I=43,61
C
C   INCLUSIØN ØF DRUG BREAKDØWN/ABSØRPTIØN
C
      D(I)=D(I)-X(I)/P(169)
C
C   ENSURES PØSITIVE DRUG MASSES IN VARIABLE STEP INTEGRATIØN RØUTINES
C
      IF(D(I).GT.0.0)GØ TØ 7
      SLØPE=-200.0*X(I)
      IF(D(I).LT.SLØPE)D(I)=SLØPE
7     CØNTINUE
8     CØNTINUE
      D(1)=V(4)-V(6)
      D(2)=V(6)-X(20)
      D(3)=X(20)-V(10)
      D(4)=V(10)-V(13)
      D(5)=V(13)-V(17)
      D(6)=V(17)-X(21)
      D(7)=X(21)-X(22)-V(21)
      D(8)=X(22)-X(23)-X(24)
      D(9)=X(23)-V(24)
      D(10)=V(24)-V(27)
      D(11)=X(24)-V(29)-X(25)-X(26)
      D(12)=X(25)-V(31)
      D(13)=V(31)-V(34)
      D(14)=X(26)-V(36)-X(27)
      D(15)=V(36)+V(44)-V(39)
      D(16)=X(27)-V(41)
      D(17)=V(41)-V(44)
      D(18)=V(39)+V(34)-V(47)
      D(19)=V(27)-V(50)
      D(20)=(V(7)-V(9)-X(20)*(P(37)+P(170)*X(20)))/P(39)
      D(21)=(V(18)-V(20)-X(21)*(P(56)+P(171)*X(21)))/P(58)
      DØ 9 I=1,21
C
C   ENSURES PØSITIVE VØLUMES AND PØSITIVE VENTRICULAR
C   ØUTFLØWS IN VARIABLE STEP INTEGRATIØN RØUTINES
C
      IF(D(I).GT.0.0)GØ TØ 9
      SLØPE=-200.0*X(I)
      IF(D(I).LT.SLØPE)D(I)=SLØPE
9     CØNTINUE
      D(22)=(V(20)-V(22)-X(22)*P(63))/P(64)
      D(23)=(V(22)+V(89)-V(23)-X(23)*P(67)-P(71))/P(68)
      D(24)=(V(22)-V(28)-X(24)*P(69)+P(72))/P(70)
      D(25)=(V(28)+V(89)-V(30)-V(90)-X(25)*P(85)+P(87))/P(86)
      D(26)=(V(28)+V(89)-V(35)-V(90)-X(26)*P(68)+P(90))/P(89)
```

```
      D(27)=(V(35)-V(40)+V(90)-X(27)*P(102)+P(104))/P(103)
      D(28)=1.0
C
C   NEURAL CØNTRØL SECTIØN
C
      D(29)=(V(22)-X(29))/P(126)
      V(51)=(D(8)+P(61)*(D(22)-D(23)-D(24)))/P(65)
      V(52)=V(51)
      IF(V(51).LT.0.0)V(52)=0.0
      V(55)=(D(9)+P(61)*(D(23)+V(79)*D(10)/(CUV*QHD)))/DHD
      V(56)=V(55)
      IF(V(55).LT.0.0)V(56)=0.0
      D(30)=(V(52)-X(30))/P(129)
      D(31)=(V(23)-X(31))/P(128)
      D(32)=(V(56)-X(32))/P(129)
      IF(V(53).LE.0.0)GØ TØ 10
      V(3)=P(130)*(D(29)+P(131)*D(30))
      V(54)=V(53)
      GØ TØ 11
10    V(54)=0.0
      V(3)=0.0
11    CØNTINUE
      V(57)=P(130)*(X(31)+P(131)*X(32)-P(132))
      IF(V(57).LE.0.0)GØ TØ 12
      V(91)=P(130)*(D(31)+P(131)*D(32))
      V(58)=V(57)
      GØ TØ 13
12    V(58)=0.0
      V(91)=0.0
13    CØNTINUE
      V(59)=(1.0-P(133))*V(54)+P(133)*V(58)
C
C   CØMPARE BARØRECEPTØR SYSTEM ØUTPUT WITH THRESHØLD
C   FØR BANG-BANG ACTIØN IN NEURAL CØNTRØLLERS
C
      IF(V(59).LE.P(137))GØ TØ 14
      V(60)=P(136)*(V(59)-P(137))
      V(63)=P(137)
      V(76)=P(150)
      V(78)=P(156)
      V(81)=P(161)
      V(61)=P(136)*((1.0-P(133))*V(3)+P(133)*V(91))
      GØ TØ 15
14    V(60)=0.0
      V(63)=V(59)
      V(76)=P(151)
      V(78)=P(157)
      V(81)=P(162)
      V(61)=0.0
15    CØNTINUE
      V(62)=P(139)
      IF(V(61).LE.0.0)V(62)=P(140)
      D(33)=(V(60)-X(33))/V(62)
      D(34)=(V(63)-X(34))/P(141)
      D(35)=(X(34)-X(35))/P(142)
      D(36)=1.0
      D(37)=(V(76)-X(37))/P(152)
      D(38)=(V(76)-X(38))/P(153)
      D(39)=(V(78)-X(39))/P(158)
      D(40)=(V(81)-X(40))/P(163)
```

```
C
C    IF VENOUS TONE OR MYOCARDIAL CONTRACTILITY CONTROL NOT REQUIRED,
C    SET DERIVATIVES OF CORRESPONDING STATE VARIABLES TO ZERO
C
       IF(.NOT.L(8))D(39)=0.0
       IF(.NOT.L(9))D(40)=0.0
C
C    PART OF MAP AND SV CALCULATION
C
       D(41)=V(20)
       D(42)=X(21)
       RETURN
       END
```

```
       SUBROUTINE ODDJOB(D,X,T)
C
C    MISCELLANEOUS TASKS AT T=0 AND ONCE EVERY CARDIAC CYCLE
C
       LOGICAL L(14)
       DIMENSION X(61),D(61)
       COMMON /PV/ P(178),V(112)
       COMMON /MISC/ NS,NP,NV,INJLOC,PMIN,PMAX
       COMMON /LOGIC/ L
       DATA RHOG,DEGRAD/0.7807,0.01745/
C
C    ORTHOSTASIS
C
       PHI=0.0
       IF(L(5))PHI=P(16)
       TILT=P(15)*RHOG*SIN(DEGRAD*PHI)
       P(71)=TILT*P(17)
       P(72)=TILT*P(18)
       P(78)=TILT*P(19)
       P(87)=TILT*P(20)
       P(90)=TILT*P(21)
       P(96)=TILT*P(22)
       P(104)=TILT*P(23)
       P(107)=TILT*P(24)
       P(115)=TILT*P(25)
       P(120)=TILT*P(26)
       P(125)=TILT*P(27)
       P(83)=TILT*P(28)
C
C    DRUG INJECTION
C
       IF(.NOT.L(3))GO TO 1
       X(INJLOC)=P(174)
       L(3)=.FALSE.
  1    CONTINUE
C
C    IF VENOUS TONE OR MYOCARDIAL CONTRACTILITY CONTROL NOT REQUIRED,
C    SET CORRESPONDING STATE VARIABLES TO UNITY
C
       IF(.NOT.L(8))X(39)=1.0
       IF(.NOT.L(9))X(40)=1.0
C
C    COMPUTE TOTAL BLOOD VOLUME
C
       VSUM=0.0
       DO 2 I=1,19
```

```
2       VSUM=VSUM+X(I)
        V(86)=VSUM
        RETURN
        END
```

```
        SUBRØUTINE CYCLE(D,X,T)
C
C   DEALS WITH RESPIRATIØN AT EACH INTEGRATIØN STEP
C   DETECTS END ØF CARDIAC CYCLE AND PERFØRMS
C   MISCELLANEØUS TASKS AT END ØF CARDIAC CYCLE
C
        LØGICAL L(14)
        DIMENSIØN X(61),D(61)
        CØMMØN /PV/ P(178),V(112)
        CØMMØN /MISC/ NS,NP,NV,INJLØC,PMIN,PMAX
        CØMMØN /LØGIC/ L
C
C   RESPIRATIØN
C
        IF(L(4))GØ TØ 1
        X(28)=0.0
        V(89)=P(7)
        V(90)=P(8)
        GØ TØ 2
  1     IF(X(28).GT.P(14))X(28)=0.0
        V(88)=X(28)
        IF(X(28).GT.P(13))V(88)=0.0
        Q=SIN(P(172)*V(88))
        V(89)=P(9)+P(173)*Q
        V(90)=P(11)+P(178)*Q
  2     CØNTINUE
C
C   TEST FØR END ØF CARDIAC CYCLE
C
        IF(X(36).LT.V(66))RETURN
C
C   VARIØUS CALCULATIØNS AT THE END ØF THE CARDIAC CYCLE
C
        L(2)=.TRUE.
        V(111)=PMAX
        V(112)=PMIN
        PMAX=-1.0E20
        PMIN=1.0E20
        V(87)=X(42)
        V(82)=X(41)/V(66)
        V(83)=V(87)/V(66)
        V(84)=V(82)/V(83)
        CALL TTOR(X)
C
C   UPDATE HEART PERIØD
C
        V(65)=V(64)
        IF(V(64).GT.2.0)V(65)=2.0
        IF(V(64).LT.0.3)V(65)=0.3
        IF(L(6))V(66)=V(65)
        V(67)=60.0/V(66)
        X(36)=0.0
        X(41)=0.0
        X(42)=0.0
        RETURN
        END
```

```
      SUBRØUTINE RESULT(D,X,T)
C
C   PRINT HEADING AND TABULATED RESULTS
C
      LØGICAL L(14)
      DIMENSIØN X(61),D(61)
      CØMMØN /PV/ P(178),V(112)
      CØMMØN /MISC/ NS,NP,NV,INJLØC,PMIN,PMAX
      CØMMØN /LØGIC/ L
      IF(.NØT.L(1))GØ TØ 1
      WRITE(2,100)
    1 WRITE(2,101)T,V(82),V(87),V(83),V(66),V(67),V(84),V(111),V(112)
      RETURN
  100 FØRMAT(1H1,6X,1HT,11X,3HHAP,9X,2HSV,10X,2HCØ,10X,
     A2HTH,10X,2HFH,10X,4HETSR,8X,4HPMAX,8X,4HPMIN/)
  101 FØRMAT(1H ,10E12.4)
      END
```

```
      SUBRØUTINE PRELIM
C
C   PRELIMINARY CALCULATIØN ØF FREQUENTLY USED CØNSTANTS
C
      CØMMØN /PV/ P(178),V(112)
      DATA PI,ØRIF/3.14159,0.0003978/
      P(1)=P(44)*P(46)
      P(2)=P(47)*P(45)*P(45)
      P(3)=P(59)+P(61)/P(62)
      P(4)=P(76)*P(46)
      P(5)=P(123)*P(46)
      P(6)=P(126)*P(124)*P(124)
      P(122)=P(118)*P(46)
      P(127)=P(121)*P(119)*P(119)
      P(134)=P(79)*P(77)*P(77)
      P(135)=P(94)*P(46)
      P(138)=P(97)*P(95)*P(95)
      P(164)=P(105)*P(46)
      P(166)=P(108)*P(106)*P(106)
      P(167)=P(113)*P(46)
      P(168)=P(116)*P(114)*P(114)
      P(170)=ØRIF/(P(38)*P(38))
      P(171)=ØRIF/(P(57)*P(57))
      P(172)=PI/P(13)
      P(173)=P(10)-P(9)
      P(178)=P(12)-P(11)
      RETURN
      END
```

```
      SUBRØUTINE TTSR(X)
C
C   CØMPUTES TRUE TØTAL SYSTEMIC RESISTANCE
C
      DIMENSIØN X(61)
      CØMMØN /PV/ P(178),V(112)
      CØMMØN /SIGMA/ SRA,SRV,SLA,SLV,SHEAD,SBRØNC,SINT,SABD,SLEG,SHR
      RA=P(67)+P(75)*SHEAD+P(134)/(X(10)*X(10))+P(6)/(X(19)*X(19))
      RB=V(77)*SBRØNC*P(84)
      RC=P(102)+V(77)*P(112)*SLEG+P(168)/(X(17)*X(17))
      RD=V(77)*P(101)*SABD
      RE=RC*RD/(RC+RD)+P(88)+P(166)/(X(15)*X(15))
      RF=P(85)+V(77)*SINT*P(93)+P(138)/(X(13)*X(13))
```

```
      RG=RE*RF/(RE+RF)+P(127)/(X(18)*X(18))
      RH=P(69)+RB*RG/(RB+RG)
      RI=P(63)+RA*RH/(RA+RH)
      V(85)=P(62)*RI/(P(62)+RI)
      RETURN
      END
```

```
      BLØCK DATA
C
C   FIRST PART ØF INITIALISATIØN
C
      LØGICAL L(14)
      CØMMØN /PV/ P(178),V(112)
      CØMMØN /XIC/ X(61)
      CØMMØN /MISC/ NS,NP,NV,INJLØC,PMIN,PMAX
      CØMMØN /LØGIC/ L
      CØMMØN /SIGMA/ SRA,SRV,SLA,SLV,SHEAD,SBRØNC,SINT,SABD,SLEG,SHR
      DATA P /0.0,0.0,0.0,0.0,0.0,0.0,-4.0,4.0,-3.0,
     A-6.0,3.0,6.0,4.0,5.0,1.0,90.0,19.5,10.0,18.0,
     B8.0,16.0,8.0,48.0,16.0,48.0,10.0,1.5,10.0,0.15,
     C0.05,30.0,0.003,0.1,0.3,0.046,0.0,0.003,1.539,0.00018,
     D4.3,50.0,7.0,0.11,8.4,460.0,20.0,0.007,0.1,0.28,
     E0.12,30.0,0.003,1.5,0.067,0.0,0.003,1.539,0.00022,0.28,
     F53.0,0.04,12.0,3.0E-5,0.00043,0.29,61.0,0.047,0.014,0.0009,
     G0.0038,0.0,0.0,0.33,114.0,6.0,9.4,552.0,0.0,0.226,
     H0.667,0.29,59.0,0.0,12.0,0.0014,0.0027,0.0,0.012,0.014,
     I0.0,0.06,17.0,2.3,10.6,607.0,0.0,0.166,1.0,0.21,
     J58.0,57.0,0.18,0.031,0.0,5.1,305.0,0.0,0.595,1.0,
     K0.12,63.0,15.0,4.8,257.0,0.0,0.3,0.0,8.3,488.0,
     L0.0,0.015,0.0,8.3,488.0,0.0,0.06,0.0,0.8,0.1,
     M1.0,1.0,40.0,0.7,0.0,0.0,1.0,80.0,0.0,1.5,
     N4.5,1.0,2.0,0.006,0.8264,0.1,0.09,0.04,0.16,0.2,
     Ø0.6,1.4,4.0,20.0,0.75,0.8,0.7,1.6,14.0,1.0,
     P1.0,0.6,1.4,10.0,0.0,0.0005,0.0,0.0,0.0,30.0,
     Q0.0,0.0,0.0,0.0,70.0,400.0,50.0,50.0,0.0/
      DATA V /112*0.0/
      DATA X /153.63,132.32,114.86,536.52,
     A104.02,131.27,81.233,90.243,146.39,
     B546.85,88.157,22.552,597.54,77.249,
     C290.32,74.33,271.05,534.04,542.37,
     D0.0,0.0,6.8039,-3.8444,25.669,
     E35.075,-3.3266,2.6994,0.0,109.26,
     F1.4146,104.93,1.7048,62.617,75.268,
     G75.115,0.0,0.97272,0.97109,1.1178,
     H0.97153,0.0,0.0,0.0,0.0,0.0,0.0,0.0,0.0,0.0,0.0,
     I0.0,0.0,0.0,0.0,0.0,0.0,0.0,0.0,0.0,0.0,0.0,
     J0.0,0.0/
      DATA NS,NP,NV,INJLØC,PMIN,PMAX/61,178,112,52,1.0E20,-1.0E20/
      DATA L/.TRUE.,.FALSE.,.FALSE.,.FALSE.,.FALSE.,.TRUE.,.TRUE.,
     A.TRUE.,.TRUE.,.TRUE.,.TRUE.,.TRUE.,.FALSE.,.FALSE./
      DATA SRA,SRV,SLA,SLV,SHEAD,SBRØNC,SINT,SABD,SLEG,SHR/10*1.0/
      END
```

APPENDIX VIII

COMPUTER PROGRAM FOR THE 8-SEGMENT MODEL

This Appendix lists the program for the complete model of the 8-segment cardiovascular system, with the thermoregulator and body fluid systems. This program is available on the Prime-550 at The City University.

```
      INTEGER*4 CPUTIM,TSTART,TEND,TACTUL
      IMPLICIT REAL*8(A-H,O-Z)
      DOUBLE PRECISION TMIN
C
C     HEART MODEL CONSISTS OF(EIGHT SEGMENT CARDIOVASCULAR SYSTEM(CVS),
C     THERMOREGULATOR SYSTEM(THERMO),BODY FLUID SYSTEM(BFLUID))
C
      COMMON /PV/ P(79),V(53)
      COMMON /MISC/ NS,NP,NV,PMIN,PMAX,EF
      COMMON /SFSR/ SBF,STPR
      COMMON /TEMP/ TC,TS
      COMMON /FLU/ E,BV,PMSP,EIN,EOUT
      COMMON /XIC/ X(23)
      COMMON /VQVD/ QV,DQV,QDP
      COMMON /LOGIC/ L
      LOGICAL L(14)
      TMIN=0.0
      CALL CTIMSA(CPUTIM)
      TSTART=CPUTIM
      CALL FDEL(4,'BODY',IERR)
      CALL FOPEN(5,4,'BODY',4,IERR)
      NMIN=60.0
      NRES=1
      N=NMIN/NRES
      DO 98 J=1,N
      DO 99 I=1,NRES
      WRITE(1,33)TMIN
      WRITE(5,33)TMIN
33    FORMAT(F6.3)
```

```
      WRITE(5,11)
11    FORMAT(' ')
      CALL CVS(T,TMIN)
      CALL THERMO
      CALL BFLUID(TMIN)
      CALL CONTRL
      TMIN=TMIN+1.0
99    CONTINUE
      CALL RESULT(TMIN)
98    CONTINUE
       CALL CTIM$A(CPUTIM)
      TEND=CPUTIM
      TACTUL=TEND-TSTART
      TACTUL=TACTUL/100.0
      WRITE(1,60)TACTUL
      WRITE(5,60)TACTUL
60    FORMAT('TACTUL IN SECS',I6)
      CALL FCLOSE(5,IERR)
      STOP
      END
C*************************
      SUBROUTINE CVS(T,TMIN)
      DIMENSION D(23)
      IMPLICIT REAL*8 (A-H,O-Z)
      COMMON /PV/P(79),V(53)
      COMMON /MISC/NS,NP,NV,PMIN,PMAX,EF
      COMMON /SFSR/SBF,STPR
      COMMON /TEMP/TC,TS
      COMMON /FLU/E,BV,PMSP,EIN,EOUT
      COMMON /LOGIC/ L
      COMMON /XIC/ X(23)
      COMMON /VQVD/QV,DQV,QDP
      LOGICAL L(14)
      DOUBLE PRECISION TMIN
      L(1)=.TRUE.
      T=0.0
```

```
      RC=20.734*6.0/100.0
      RS=STPR*6.0/100.0
      P(28)=RC*RS/(RC+RS)
      CALL PRELIM
      CALL MODEL(D)
      CALL CYCLE(D)
      L(1)=.FALSE.
1     CONTINUE
      CALL INTEG(D,T)
      CALL CYCLE(D)
      IF(.NOT.L(2))GO TO 1
      L(2)=.FALSE.
      IF(TMIN.GE.30.0.AND.TMIN.LT.36.0.OR.TMIN.GE.45.0.AND.
     1TMIN.LT.51.0)GO TO 3
      IF(T.GE.2.0)GO TO 2
      GO TO 1
3     IF(T.GE.30.0)GO TO 2
       GO TO 1
2     SBF=V(43)/(STPR*V(38))
      RETURN
      END
C***************
      SUBROUTINE INTEG(D,T)
      DIMENSION D(23)
      COMMON /PV/P(79),V(53)
      IMPLICIT REAL*8 (A-H,O-Z)
      COMMON /MISC/NS,NP,NV,PMIN,PMAX,EF
      COMMON /SFSR/SBF,STPR
      COMMON /TEMP/TC,TS
      COMMON /FLU/E,BV,PMSP,EIN,EOUT
      COMMON /XIC/ X(23)
      COMMON /LOGIC/ L
      COMMON /VQVD/QV,DQV,QDP
      LOGICAL L(14)
      H=P(38)
      DO 1 I=1,23
```

```
      X(I)=X(I)+H*D(I)
1     CONTINUE
      QV=QV+DQV*H
      IF(QV.GT.5.0)QV=5.0
      CALL MODEL(D)
      T=T+H
      RETURN
      END
C*****************
      SUBROUTINE MODEL(D)
      DIMENSION D(23)
      IMPLICIT REAL*8 (A-H,O-Z)
      COMMON /PV/P(79),V(53)
      COMMON /MISC/NS,NP,NV,PMIN,PMAX,EF
      COMMON /VQVD/QV,DQV,QDP
      COMMON /SFSR/SBF,STPR
      COMMON /TEMP/TC,TS
      COMMON /FLU/E,BV,PMSP,EIN,EOUT
      COMMON /LOGIC/ L
      COMMON /XIC/ X(23)
      LOGICAL L(14)
      DATA PI /3.1415926536/
      IF(L(1))V(19)=P(46)
      IF(.NOT.L(6))V(19)=P(47)
      V(20)=P(41)+P(42)*V(19)
      V(21)=V(20)-P(43)
      V(22)=P(44)+P(45)*V(19)
      V(23)=PI/V(22)
      V(24)=0.0
      IF(X(15).GT.V(21))V(24)=X(15)-V(21)
      V(25)=0.0
      IF(V(24).LE.V(22))V(25)=SIN(V(23)*V(24))
      V(3)=V(25)*(X(19)*P(52)-P(53))+P(53)
      V(10)=V(25)*(X(19)*P(50)-P(51))+P(51)
      V(28)=P(56)*(X(22)+P(57)*X(23)-P(58))
      V(35)=P(65)*(X(12)+X(14))
```

```
QDP =P(69)*X(17)+(1.0-P(69))*X(16)
V(38)=QDP*QV
V(41)=1.0+P(78)*(X(18)-1.0)
V(41)=V(41)*QV

V(42)=1.0+P(79)*(X(18)-1.0)
V(42)=V(42)*QV
QA=X(5)-P(22)+P(37)*(X(10)-X(11))
V(11)=QA/P(23)
IF(V(11).GT.PMAX)PMAX=V(11)
IF(V(11).LT.PMIN)PMIN=V(11)
CPV=P(16)
IF(X(3).LT.P(15))CPV=P(1)
V(6)=(X(3)-P(15))/CPV
V(2)=V(3)*(X(1)-P(11))
V(9)=V(10)*(X(4)-P(21))
V(4)=(X(2)-P(12))/P(13)
V(5)=(V(4)-V(6))/P(14)
IF(V(6).LE.P(18))V(5)=(V(4)-P(18))/P(14)
V(7)=(V(6)-V(9))*X(3)*X(3)/P(2)
V(8)=V(7)
IF(V(7).LT.0.0)V(8)=0.0
QF=X(8)-P(32)
CTV=P(33)
IF(QF.LE.0.0)CTV=P(6)
V(17)=QF/CTV
QD=X(7)-P(30)/V(42)
CSV=P(29)
IF(QD.LE.0.0)CSV=P(4)
V(14)=QD*V(41)/CSV
V(15)=(V(14)-V(17))*X(7)*X(7)/P(5)
V(16)=V(15)
IF(V(15).LE.0.0)V(16)=P(36)*V(15)
QE=P(28)*V(38)
QC=P(27)+P(37)/QE
QB=X(6)-P(26)+P(37)*(X(11)+V(14)/QE)
```

```
      V(12)=QB/QC
      V(13)=(V(12)-V(14))/QE
      V(18)=(V(17)-V(2))*X(8)*X(8)/P(3)
      V(1)=V(18)
      IF(V(18).LT.0.0)V(1)=0.0
      D(1)=V(1)-X(9)
      D(2)=X(9)-V(5)
      D(3)=V(5)-V(8)
      D(4)=V(8)-X(10)
      D(5)=X(10)-X(11)
      D(6)=X(11)-V(13)
      D(7)=V(13)-V(16)
      D(8)=V(16)-V(1)
      D(9)=(V(2)-V(4)-X(9)*(P(9)+P(7)*X(9)))/P(10)
      D(10)=(V(9)-V(11)-X(10)*(P(19)+P(8)*X(10)))/P(20)
      D(11)=(V(11)-V(12)-X(11)*P(24))/P(25)
      DO 9 I=1,11
      IF(D(I).GT.0.0)GO TO 9
      SLOPE=-200.0*X(I)
      IF(D(I).LT.SLOPE)D(I)=SLOPE
9     CONTINUE
      D(22)=(V(11)-X(22))/P(54)
      V(26)=(D(5)+P(37)*(D(10)-D(11)))/P(23)
      V(27)=V(26)
      IF(V(26).LT.0.0)V(27)=0.0
      D(23)=(V(27)-X(23))/P(55)
      V(30)=P(56)*(D(22)+P(57)*D(23))
      V(29)=V(28)
      IF(V(28).LE.0.0)V(29)=0.0
      IF(V(28).LE.0.0)V(30)=0.0
      IF(V(29).LE.P(62))GO TO 14
      V(31)=P(61)*(V(29)-P(62))
      V(34)=P(62)
      V(40)=P(76)
      V(39)=P(73)
      V(32)=P(61)*V(30)
```

```
      GO TO 15
14     V(31)=0.0
      V(34)=V(29)
      V(40)=P(77)
      V(39)=P(74)
      V(32)=0.0
15     CONTINUE
      BN=80.0
      V(37)=1.0/(1.0+0.5*((V(29)/BN)-1.0))
      V(33)=P(63)
      IF(V(32).LE.0.0)V(33)=P(64)
      D(12)=(V(31)-X(12))/V(33)
      D(13)=(V(34)-X(13))/P(59)
      D(14)=(X(13)-X(14))/P(60)
      D(15)=1.0
      D(16)=(V(37)-X(16))/P(67)
      D(17)=(V(37)-X(17))/P(68)
      D(18)=(V(40)-X(18))/P(75)
      D(19)=(V(39)-X(19))/P(72)
      D(20)=V(11)
      D(21)=X(10)
      BV0=4709.81
      SV=1.0/(1.0+2.0*((BV/BV0)-1.0))
      DQV=-QV/20.0+(SV/20.0)
      RETURN
      END
C**********************
      SUBROUTINE CYCLE(D)
      IMPLICIT REAL*8 (A-H,O-Z)
      DIMENSION D(23)
      COMMON /PV/P(79),V(53)
      COMMON /VQVD/QV,DQV,QDP
      COMMON /MISC/NS,NP,NV,PMIN,PMAX,EF
      COMMON /SFSR/SBF,STPR
      COMMON /TEMP/TC,TS
      COMMON /FLU/E,BV,PMSP,EIN,EOUT
```

```
      COMMON /LOGIC/ L
      COMMON /XIC/ X(23)
      LOGICAL L(14)
      IF(X(4).GT.X4MAX)X4MAX=X(4)
      IF(X(15).LT.V(19))RETURN
      L(2)=.TRUE.
      V(47)=PMAX
      V(48)=PMIN
      PMAX=-1.0E20
      PMIN=1.0E20
      V(46)=X(21)
      EF=V(46)/X4MAX
      V(43)=X(20)/V(19)
      V(44)=V(46)/V(19)
      V(45)=V(43)/V(44)
      V(36)=V(35)
      IF(V(35).GT.2.0)V(36)=2.0
      IF(V(35).LT.0.3)V(36)=0.3
      IF(L(6))V(19)=V(36)
      V(49)=60.0/V(19)
      X(15)=0.0
      X(20)=0.0
      X(21)=0.0
      V(50)=X(12)
      V(51)=X(14)
      V(52)=X(22)
      V(53)=X(23)
      X4MAX=0.0
      RETURN
      END
C*******************
      SUBROUTINE PRELIM
      IMPLICIT REAL*8 (A-H,O-Z)
      COMMON /PV/P(79),V(53)
      COMMON /VQVD/QV,DQV,QDP
      COMMON /MISC/NS,NP,NV,PMIN,PMAX,EF
```

```
      COMMON /SFSR/SBF,STPR
      COMMON /TEMP/TC,TS
      COMMON /FLU/E,BV,PMSP,EIN,EOUT
      COMMON /XIC/ X(23)
      COMMON /LOGIC/ L
      LOGICAL L(14)
      DATA PI,ORIF/3.14159,0.0003978/
      P(1)=P(16)*P(35)
      P(2)=P(17)*P(15)*P(15)
      P(3)=P(34)*P(32)*P(32)
      P(4)=P(35)*P(29)
      P(5)=P(31)*P(30)*P(30)
      P(6)=P(35)*P(33)
      P(7)=ORIF/(P(39)*P(39))
      P(8)=ORIF/(P(40)*P(40))
      RETURN
      END
C*******************
      SUBROUTINE THERMO
      IMPLICIT REAL*8 (A-H,O-Z)
      COMMON /PV/P(79),V(53)
      COMMON /VQVD/QV,DQV,QDP
      COMMON /MISC/NS,NP,NV,PMIN,PMAX,EF
      COMMON /SFSR/SBF,STPR
      COMMON /TEMP/TC,TS
      COMMON /FLU/E,BV,PMSP,EIN,EOUT
      COMMON /XIC/ X(23)
      COMMON /LOGIC/ L
      LOGICAL L(14)

      DIMENSION TX(2)
      TX(1)=TC
      TX(2)=TS
      CALL TINTEG(TX)
      TC=TX(1)
      TS=TX(2)
```

```
      RETURN
      END
C*******************
      SUBROUTINE TINTEG(TX)
      DIMENSION TX(2),DT(2)
      IMPLICIT REAL*8 (A-H,O-Z)
      COMMON /PV/P(79),V(53)
      COMMON /VQVD/QV,DQV,QDP
      COMMON /MISC/NS,NP,NV,PMIN,PMAX,EF
      COMMON /SFSR/SBF,STPR
      COMMON /TEMP/TC,TS
      COMMON /FLU/E,BV,PMSP,EIN,EOUT
      COMMON /XIC/ X(23)
      COMMON /LOGIC/ L
      LOGICAL L(14)
      H=1.0
      CALL TMODEL(DT,TX)
      DO 20 J=1,2
20    TX(J)=TX(J)+H*DT(J)
      RETURN
      END
C********************
      SUBROUTINE TMODEL(DT,TX)
      IMPLICIT REAL*8 (A-H,O-Z)
      COMMON /PV/P(79),V(53)
      COMMON /VQVD/QV,DQV,QDP
      COMMON /MISC/NS,NP,NV,PMIN,PMAX,EF
      COMMON /SFSR/SBF,STPR
      COMMON /TEMP/TC,TS
      COMMON /FLU/E,BV,PMSP,EIN,EOUT
      COMMON /XIC/ X(23)
      COMMON /LOGIC/ L
      LOGICAL L(14)
      DIMENSION TX(2),DT(2)
      DT(1)=(1167.0-405.67*(TX(1)-TX(2))-SBF*920.0*(TX(1)-TX(2)))
     1/45040.0
```

```
      DT(2)=(405.67*(TX(1)-TX(2))+SBF*920.0*(TX(1)-TX(2))-100.0*
     A(TX(2)-26.0)-300.0)/12730.0
      RETURN
      END
C***************
      SUBROUTINE CONTRL
      IMPLICIT REAL*8 (A-H,O-Z)
      COMMON /PV/P(79),V(53)
      COMMON /VQVD/QV,DQV,QDP
      COMMON /MISC/NS,NP,NV,PMIN,PMAX,EF
      COMMON /SFSR/SBF,STPR
      COMMON /TEMP/TC,TS
      COMMON /FLU/E,BV,PMSP,EIN,EOUT
      COMMON /XIC/ X(23)
      COMMON /LOGIC/ L
      LOGICAL L(14)
      IF(TC.LT.35.0)STPR=5650.0
      IF(TC.GE.35.0 .AND. TC.LT.36.4)
     1STPR=-3632.143*TC+132775.0
      IF(TC.GE.36.4 .AND. TC.LT.37.0)GO TO 999
      IF(TC.GE.37.0 .AND. TC.LT.38.5)
     1STPR=-322.773*TC+12507.6
      IF(TC.GE.38.5)STPR=80.841
      GO TO 100
999   IF(TS.LE.34.1)STPR=24.39*TS-266.7
      IF(TS.GT.34.1)STPR=46.55*TS-1022.41
100   CONTINUE
      RETURN
      END
C***************
      SUBROUTINE BFLUID(TMIN)
      DOUBLE PRECISION TMIN
      IMPLICIT REAL*8 (A-H,O-Z)
      COMMON /PV/P(79),V(53)
      COMMON /VQVD/QV,DQV,QDP
      COMMON /MISC/NS,NP,NV,PMIN,PMAX,EF
```

```
      COMMON /SFSR/SBF,STPR
      COMMON /TEMP/TC,TS
      COMMON /FLU/E,BV,PMSP,EIN,EOUT
      COMMON /XIC/ X(23)
      COMMON /LOGIC/ L
      LOGICAL L(14)
      DATA VINTS/9627.0/
      EIN=4.96
      EOUT=4.96
      IF(TMIN.NE.0.0)GO TO 8
      BV=0.0
      DO 7 I=1,8
7     BV=BV+X(I)
      BV1=BV
8     E=VINTS+BV
      VINTS=VINTS+(EIN-EOUT)*VINTS/E
      BV=BV+(EIN-EOUT)*BV/E
      DO 9 I=1,8
9     X(I)=X(I)*BV/BV1
      IF(TMIN.GE.30.0.AND.TMIN.LT.35.0)X(7)=X(7)-84.0
      IF(TMIN.GE.30.0.AND.TMIN.LT.35.0)BV=BV-84.0
      IF(TMIN.GE.45.0.AND.TMIN.LT.50.0)X(7)=X(7)+84.0
      IF(TMIN.GE.45.0.AND.TMIN.LT.50.0)BV=BV+84.0
      BV1=BV
      PMSP=(0.0035*BV)-10.5
      RETURN
      END
C***************
      SUBROUTINE RESULT(TMIN)
      IMPLICIT REAL*8 (A-H,O-Z)
      DOUBLE PRECISION TMIN
      COMMON /PV/P(79),V(53)
      COMMON /MISC/NS,NP,NV,PMIN,PMAX,EF
      COMMON /SFSR/SBF,STPR
      COMMON /TEMP/TC,TS
      COMMON /FLU/E,BV,PMSP,EIN,EOUT
```

```
      COMMON /XIC/ X(23)
      COMMON /LOGIC/ L
      COMMON /VQVD/QV,DQV,QDP
      LOGICAL L(14)
      V(46)=V(46)*0.001
      V(44)=V(44)*(60.0/1000.0)
      V(45)=V(45)*(1000.0/60.0)
      WRITE(1,987)
      WRITE(5,987)
1     WRITE(1,100)TMIN,V(43),V(46),V(44),V(49),V(45),V(47),V(48),
     ASBF,STPR
      WRITE(5,100)TMIN,V(43),V(46),V(44),V(49),V(45),V(47),V(48),
     ASBF,STPR
      WRITE(5,66)
66    FORMAT(' ')
22    FORMAT(F6.3)
      WRITE(1,988)
      WRITE(5,988)
      WRITE(1,100)TC,TS,BV,PMSP,E,EIN,EOUT,EF,QV,QDP
      WRITE(5,100)TC,TS,BV,PMSP,E,EIN,EOUT,EF,QV,QDP
      RETURN
987   FORMAT(6X,'TMIN',11X,'MAP',12X,'SV',10X,'CO',11X,'FH',10X,'ETSR',
     A8X,'PMAX',8X,'PMIN',11X,'SBF',11X,'STPR'/)
988   FORMAT(6X,'TC',11X,'TS',12X,'BV',10X,'PMSP',11X,'E',13X,'EIN',8X,
     A'EOUT',8X,'EF',11X,'QV',8X,'QDP'/)
100   FORMAT(20(6E13.5))
      RETURN
      END
C***************
      BLOCK DATA
      IMPLICIT REAL*8 (A-H,O-Z)
      COMMON /PV/P(79),V(53)
      COMMON /MISC/NS,NP,NV,PMIN,PMAX,EF
      COMMON /SFSR/SBF,STPR
      COMMON /TEMP/TC,TS
      COMMON /FLU/E,BV,PMSP,EIN,EOUT
```

```
      COMMON /XIC/ X(23)
      COMMON /LOGIC/ L
      COMMON /VQVD/QV,DQV,QDP
      LOGICAL L(14)
      DATA  BV/4740.6/
      DATA P /0.0,0.0,0.0,0.0,0.0,0.0,0.0,0.0,0.003,
     A0.00018,0.0,50.0,4.730,0.11,430.0,25.0,0.003,7.0,0.003,
     B0.00022,0.0,140.0,0.77,0.06,0.00075,370.0,1.98,1.0,59.0,
     C1000.0,0.09,1300.0,59.0,0.003,20.0,0.667,0.04,0.001,5.0,
     D5.0,0.1,0.09,0.04,0.16,0.2,0.8264,0.8,0.0,0.0,
     E1.5,0.053,0.3,0.027,0.8,0.1,1.0,1.1,40.0,1.0,
     F2.0,1.0,80.0,1.5,4.5,0.006,0.0,2.0,10.0,0.75,
     G0.6,1.4,10.0,0.6,1.4,14.0,0.7,1.6,1.0,1.0/
      DATA V/53*0.0/
      DATA X/153.54,109.95,637.48,153.0,
     A212.61,554.23,1345.0,1544.0,1.0,
     B1.0,22.59,63.64,77.16,77.04,
     C0.0,0.97,0.97,1.12,0.97,
     D0.0,0.0,112.03,0.71/
      DATA TC,TS,SBF,STPR,QV/36.7,34.67,0.19,591.5,1.0/
      DATA NS,NP,NV,PMIN,PMAX/23,31,57,1.0E20,-1.0E20/
      DATA L/.TRUE.,.FALSE.,.FALSE.,.FALSE.,.FALSE.,.TRUE.,.TRUE.,
     A.TRUE.,.TRUE.,.TRUE.,.TRUE.,.TRUE.,.FALSE.,.FALSE./
      END
```

OK,